UAlg
UNIVERSIDADE DO ALGARVE

UNIVERSIDADE DO ALGARVE

FACULDADE DE CIÊNCIAS E TECNOLOGIA

# EFFECTS OF NANOPARTICLES EXPOSURE IN THE MUSSEL *MYTILUS GALLOPROVINCIALIS*

Tânia Cristina Martins Gomes

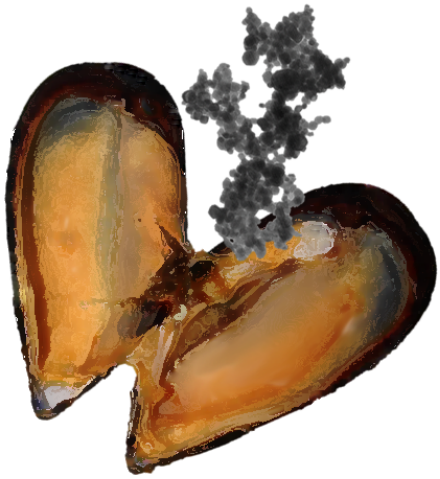

Dissertação apresentada na Universidade do Algarve

Doutoramento em Ciências do Mar, Terra e Ambiente

Ramo de Ciências e Tecnologias do Ambiente

Especialidade em Ecotoxicologia

Trabalho efectuado sobre a orientação da Professora Doutora Maria João Bebianno

2012

**Effects of nanoparticles exposure in the mussel *Mytilus galloprovincialis***

**Declaração de autoria de trabalho**

Declaro ser a autora deste trabalho, que é original e inédito. Autores e trabalhos consultados estão devidamente citados no texto e constam da listagem de referências incluída.

Tânia Gomes

---

This thesis was supported by the Portuguese Foundation for Science and Technology (fellowship BD/41605/2007).

# Acknowledgements

I wish to thank all the many people that helped me during the course of my PhD research. Without their support none of this would have been possible:

Professor Maria João Bebianno supervisor of my PhD thesis, for giving me the opportunity to dive in the fascinating (and nerve-wracking) area of nanotoxicology and for all her support, scientific advisement, research guidance and encouragement during these years.

Ibon Cancio, Margarida Ribau and Vânia Sousa for the kind and precious assistance with nanoparticles characterization. A special thanks to Professor José Paulo Pinheiro for the knowledge and guidance in the nanoparticle world.

All my friends from the Ecotoxicology and Environmental Chemistry Group (Angie, Bli, Carla, Catarina, Cátia, Maria, Professora Alexandra, Ruizito and Verinha) for all the enormous support, friendship and encouragement showed all these years. Thank you for all the kind words, welcome distractions, cocktails and fun when I needed it most. I would like to thank particularly to Catarina and Cátia for their precious help during my experimental assays and laboratory analysis. It was some crazy weeks dissecting mussels and reading samples in the spectrophotometer and I couldn't have done it without you girls! A huge thanks to my comet girls, Olinda e Rita.

My closest and dearest friends Armando, Cata, Isaurinha, João, Pirralha, Raquel, Ritinha, Sara, Susana and Suze for all the precious moments shared together, the laughs, the glasses of wine, the constant and interminable support and specially the patience for all the nano-drama.

My Family and especially my Parents, Lucinda and Manuel, and my Sister Joana for unconditional support and understanding and to whom I dedicate this thesis.

# General Abstract

Nanotechnology is rapidly developing and attracting attention due to the exploitation of the novel materials at the nanoscale for application within biomedical, cosmetic, electronic, energy production and environmental sectors. Increased production and widespread use of these nanomaterials result in their release into the environment; nevertheless, the knowledge of their behaviour in aquatic systems is scarce. Accordingly, this thesis assessed the effects of two commercially available nanoparticles, copper oxide (CuO NPs) and silver nanoparticles (Ag NPs), using mussels *Mytilus galloprovincialis* as bioindicators.

To understand the uptake, accumulation and effects of these NPs, mussels were exposed to a realistic environmental concentration of 10 $\mu g.L^{-1}$ of CuO (31 ± 10 nm) and Ag NPs (<100 nm) for 15 days, comparative to their ionic counterparts. NPs were characterized and biomarkers of oxidative stress, metal exposure, genotoxicity and neurotoxicity evaluated in mussel tissues. To identify pathways of NP exposure and detect new biomarkers, a proteomic approach was undertaken. Oxidative stress is the major NP-induced toxicity, but with distinct modes of action. Gills are more susceptible to oxidative stress while the digestive gland is the preferential site for NPs accumulation. The oxidative (enzymatic activation/inhibition, metallothionein induction and lipid peroxidation), genotoxic (DNA strand breaks) and neurotoxic (acetylcholinesterase inhibition) changes suggest that NPs toxicity is associated with ROS that induced a cascade of pathways (via nucleus and mitochondria) that ultimately lead to apoptosis but by different mechanisms. New biomarkers candidates were identified: caspase 3/7-1, cathepsin-L and zinc-finger protein for CuO NPs and precollagen-P, major vault protein and ras partial for Ag NPs exposure. Overall, these results show that even though oxidative stress and apoptosis are similar outcomes for NP toxicity, particle composition, size, solubility, aggregation and chemistry are key elements for determining their mode of action. This study contributed to understand the CuO and Ag NPs behaviour, bioavailability and toxicity in aquatic systems and their uptake and effects in filter-feeding organisms.

Keywords: *Mytilus galloprovincialis*, CuO NPs, Ag NPs, oxidative stress, proteomic analysis, biomarkers.

# Resumo geral

A nanotecnologia é uma indústria de grande rentabilidade mundial e em crescente desenvolvimento que consiste na produção ou alteração de substâncias à nanoescala (dimensão entre 1-100 nm) cujas características permitem uma crescente aplicação em diversos setores industriais e comerciais como a medicina, farmácia, cosmética, produção de energia, eletrónica e ambiente. O rápido desenvolvimento e uso generalizado destes nanomateriais torna inevitável a sua libertação para o ambiente e para o ambiente aquático em particular. No entanto, o conhecimento sobre o comportamento destes nanomateriais nos sistemas aquáticos, bem como a sua capacidade de acumulação nos organismos e consequente toxicidade é ainda escasso. Deste modo, esta dissertação teve como objetivo avaliar os efeitos ecotoxicológicos de duas nanopartículas metálicas com várias aplicações a nível comercial e industrial, nanopartículas de óxido de cobre (NPs CuO) e de prata (NPs Ag), utilizando o mexilhão *Mytilus galloprovincialis* como espécie bioindicadora.

Para compreender a biodisponibilidade, acumulação e efeitos destas nanopartículas, os mexilhões *M. galloprovincialis* foram expostos a uma concentração ambientalmente relevante de 10 $\mu g.L^{-1}$ de NPs CuO (31 ± 10 nm) e 10 $\mu g.L^{-1}$ de NPs Ag (<100 nm) durante 15 dias, e os efeitos comparados simultaneamente com as respetivas formas iónicas ($Cu^{2+}$ e $Ag^{+}$). As NPs foram caracterizadas em termos de forma e tamanho (diâmetro hidrodinâmico), carga superficial (potencial zeta), índice de poli-dispersidade e intensidade, utilizando suspensões em água ultrapura e água do mar. Foi utilizada uma bateria de biomarcadores nas brânquias e glândula digestiva dos mexilhões, nomeadamente biomarcadores de stress oxidativo (enzimas antioxidantes superóxido dismutase, catalase e glutationa peroxidase e peroxidação lípidica), de exposição metálica (metalotioninas), genotoxicidade (dano de ADN) e de neurotoxicidade (acetilcolinesterase). Para identificar possíveis mecanismos de ação das NPs e identificar novos biomarcadores de exposição e efeito foi também efetuada uma análise proteómica. A solubilidade das NPs e a libertação de iões metálicos ($Cu^{2+}$ e $Ag^{+}$) em conjunto com as propriedades inerentes às NPs são responsáveis pelos diferentes efeitos encontrados ao longo do tempo de exposição. Ambas as nanopartículas foram acumuladas nos dois tecidos ao longo do tempo de exposição, com exceção de um decréscimo de acumulação das NPs Ag nas brânquias no final da experiência. De um modo geral, as brânquias são mais suscetíveis a stress oxidativo (através dos iões metálicos que se dissolvem das NPs), enquanto a glândula digestiva é o tecido preferencial para a acumulação das NPs na forma de agregados. O comportamento dos biomarcadores foi diferente para cada uma das

nanopartículas, consoante o tecido considerado. Contudo, o stress oxidativo foi o mecanismo mais significativo de ação das NPs CuO e Ag, que difere do obtido para as correspondentes formas iónicas. Os dois tipos de nanopartículas alteraram o sistema de defesa antioxidante dos mexilhões através da indução/inibição da atividade das enzimas antioxidantes. Adicionalmente, foi também observada uma indução de metalotioninas nas brânquias e glândula digestivas expostas a ambas as NPs, diretamente relacionada com a sua acumulação nos dois tecidos. As glândulas digestivas dos mexilhões expostos a NPs Ag foram a exceção, já que neste tecido a Ag está maioritariamente associada a formas insolúveis nos lisossomas. As NPs CuO originaram peroxidação lipídica nos dois tecidos, enquanto que no caso das NPs Ag apenas foi detetada peroxidação lipídica nas brânquias. O potencial neurotóxico foi avaliado apenas nas brânquias expostas a NPs de CuO, onde foi observada uma inibição da atividade da acetilcolinesterase no final da experiência. Verificou-se ainda que tanto as NPs de CuO como de Ag têm efeitos genotóxicos nos hemócitos dos mexilhões (quebras nas cadeias de ADN), efeitos esses que parecem ser mediados pelo stress oxidativo. Os perfis de expressão proteica obtidos dependem do tecido e da forma de metal considerado (NP vs iónico), e permitiram identificar proteínas diferencialmente expressas (induzidas ou inibidas) associadas aos mecanismos de acumulação das NPs. A identificação de 15 destas proteínas confirmou o potencial oxidativo de ambas as NPs e permitiu perceber que a exposição a estas NPs origina várias cascatas de sinalização celular no núcleo e mitocôndria que em último caso podem originar apoptose. A análise proteómica permitiu também a identificação de alguns biomarcadores clássicos (proteínas de stress térmico, actina, glutationa s-transferase, ATP sintase), bem como novos biomarcadores moleculares resultantes da exposição de NPs de CuO (caspase 3/7-1, catepsina L e proteína de dedo de zinco) e Ag (pré-colagénio P, ribonucleo-proteína citoplasmática MVP e ras parcial). Os resultados obtidos demonstraram que apesar do stress oxidativo e a apoptose serem efeitos tóxicos semelhantes entre as duas NPs, a composição, tamanho e distribuição, solubilidade, aglomeração e química das partículas são elementos determinantes para decifrar o seu modo de ação. Deste modo, este estudo contribuiu para perceber a importância da solubilização, agregação, biodisponibilidade e toxicidade das NPs nos sistemas aquáticos bem como o seu comportamento, acumulação e efeitos em organismos filtradores.

Palavras-chave: *Mytilus galloprovincialis*, NPs CuO, Ag NPs, stress oxidativo, análise proteómica, biomarcadores.

# Index

# Figure Index

**Chapter 1. General Introduction**

**Chapter 3. Effects of silver nanoparticles exposure in the mussel *Mytilus galloprovincialis***



**Chapter 4. Genotoxicity of copper oxide and silver nanoparticles in the mussel *Mytilus galloprovincialis***

# Table Index

# Abbreviations

**-SH –** Sulfhydryl groups

**$^1O_2$ –** Singlet oxygen

**2-DE –** Two-dimensional electrophoresis

**4–HNE –** 4–hydroxyalkenals

**a.u. –** Arbritary units

**AAS –** Atomic absorption spectrophotometry

**AChE –** Acetylcholinesterase

**Ag –** Silver

**Ag NPs –** Silver nanoparticles

**$Ag^+$ –** Ionic silver

**ANOVA –** Analysis of variance

**ATP –** adenine triphosphate

**Au –** Gold

**$BaTiO_3$ –** Barium titanate

**BET –** Brunauer, Emmett, Teller method

**$Bi_2O_3$ –** Bismuth trioxide

**BLAST –** Basic Local Alignment Search Tool

**BSA –** Bovine serum albumin

**$Ca^{2+}$ –** Calcium

**CAT –** Catalase

**CatL –** Cathepsin L

**Cd –** Cadmium

**CdTe QD –** Cadmium telluride quantum dots

**$CeO_2$ –** Cerium oxide

**CHAPS –** 3-[(3-cholamidopropyl)dimethylamonio]-1-propanesulfonate

**CI –** Condition Index

**CNTs –** Carbon nanotubes

**Co –** Cobalt

**$CrO_2$ –** Chromium dioxide

**CT –** Control

**Cu –** Copper

**$Cu^{2+}$ –** Ionic copper

**CuO –** Copper oxide

**CuO NPs –** Copper oxide nanoparticles

**CV –** Coefficient of variation

**d.w. –** Dry weight

**DAPI –** 4,6-diamidino-2-phenylindole

**DLS –** Dynamic light scattering

**DNA –** Deoxyribonucleic acid

**DTT –** Dithiothreitol

**EDTA –** Ethylenediamine tetraacetic acid

**EDX –** Energy dispersive low spectrometry

**EELS –** Electron energy low spectrometry

**ELS –** Electrophoretic light scattering

**ENPs –** Engineered/manufactured nanoparticles

**Fe –** Iron

**$FeO/Fe_2O_3$ –** Iron oxide

**GPX –** Glutathione peroxidase

**GR –** Glutathione reductase

**GSH –** Glutathione

**GSSG –** Glutathione disulphide

**GST –** Glutatione s-transferase

**$H_2O$ –** Water

**$H_2O_2$ –** Hydrogen peroxide

**HCl –** Hydrochloric acid

**HEPES –** 4-(2-hydroxyethyl)-1-piperazineethanesulfonic acid

**Hg –** Mercury

**$HNO_3$ –** Nitric acid

**$HO_2^{\bullet}$ –** Hydroperoxyl radical

**HOCl –** Hypochlorous acid

**HSPs –** Heat-shock proteins

**ICP-MS –** Inductively coupled plasma mass spectrometry

**IEF –** Isoelectric focusing

**InSnO –** Indium tin oxide

**LH –** Polyunsaturated lipid

**$LiCoO_2$ –** Lithium cobalt dioxide

**LMA –** Low melting point agarose

**LO• –** Alkoxyl radicals

**$LOO^{\bullet}$ –** Lipid hydroperoxide

**LPO –** Lipid peroxidation

**MALDI-TOF –** Matrix-assisted laser desorption/ionization time-of-flight mass spectrometer

**MDA –** Malondialdehyde

**MgC1q60 –** Putative C1q domain containing protein

**$MoO_3$ –** Molybdenum trioxide

**MS/MS –** Tandem mass spectrometry

**MT –** Metallothionein

**MVP –** Major vault protein

**MW –** Molecular weight

**MWP –** Mussel watch project

**$N_2$ –** Nitrogen

**Na+/K+ ATPase –** Sodium-potassium adenosine triphosphatase

**NaCl –** Sodium chloride

**NADPH –** Reduced nicotinamide adenine dinucleotide phospate

**NAOH –** Sodium hydroxide

**NCB –** Nano carbon black

**NCBI –** National Centre for Biotechnology Information

**Ni –** Nickel

**NMA –** Normal melting point agarose

**NMs –** Nanomaterials

**$NO^{\bullet}$ –** Nitric oxide

**NPs –** Nanoparticles

**nZVI –** Nano scale zero valent iron

**$O^2$ –** Molecular oxygen

**$O_2^{-\bullet}$ –** Superoxide anion radical

**$O_3$ –** Ozone

**$OH^{\bullet}$ –** Hydroxyl radical

**OOHNO –** Peroxynitrite

**OTM –** Olive tail moment

**PCA –** Principal component analysis

**PEPs –** Protein expression profiles

**PESs –** Protein expression signatures

**p*I* –** Isoelectric point

**PMF –** Peptide mass fingerprint

**PMSF –** Phenylmethylsulfonyl fluoride

**ppb –** Parts per billion

**ppm –** Parts per million

**ppt –** Parts per trillion

**Precol-D –** Precollagen-D

**Precol-P –** Precollagen-P

**RNS –** Reactive nitrogen species

**$RO^{\bullet}$ –** Alcoxyl radical

**ROH –** Alcohols

**$ROO^{\bullet}$ –** Peroxyl radical

**ROOH –** Organic hydroperoxides

**ROS –** Reactive oxygen species

**SAED –** Selected area electron diffraction

**SDS –** Sodium dodecyl sulphate

**SDS-PAGE –** Sodium dodecyl sulphate polyacrylamide gel electrophoresis

**SEM –** Standard error of the mean

**$SiO_2$ –** Silicon dioxide

**SOD –** Superoxide dismutase

**Std –** Standard deviation

**TBARS –** Tiobarbituric acid reactive substances

**TEM –** Transmission electron microscopy

**$TiO_2$ –** Titanium dioxide

**UV-Vis –** Ultraviolet visible

**XRD –** X-Ray diffraction

**Zn –** Zinc

**ZnO –** Zinc oxide

# CHAPTER 1

## General Introduction

# 1. General introduction

## 1.1. Nanoparticles, an emerging environmental threat?

Natural occurring nanoparticles have been present on earth for millions of years (e.g. colloids, volcanic eruptions, forest fires) and organisms have found many ways to adapt to the presence of these nanoparticles. Anthropogenic activities also contributed to the generation of nano-scale materials, inadvertently formed as a by-product of industrial processes, as fumes generated during welding, metal smelting and automobile exhaust. Anthropogenic nanosized particles were also designed and produced for a specific purposes due to their particular characteristics being referred as engineered nanoparticles or manufactured nanoparticles (ENPs) (Nowach and Bucheli, 2007; Oberdörster *et al*., 2005). In recent years these ENPs attracted increasing attention due to their capacity to alter the physical and chemical properties of conventional materials and to their application into technological uses (nanotechnology).

Several definitions were attributed to nanotechnology, most of which are generally in agreement, nevertheless, no internationally formal definition of nanotechnology has yet been agreed. The Royal Academy of Engineering of the United Kingdom defines nanotechnology as the design, characterisation, production and application of structures, devices and systems by controlling shape and size at nanometre scale (Royal Society and Royal Academy of Engineering, 2004). Similar definitions were also proposed by The National Nanotechnology Initiative that defines nanotechnology as: (i) research and technology development involving structures with at least one dimension on the 1–100 nm range; (ii) creating/using structures, devices, systems that have novel properties and functions because of their nanometre scale dimensions and (iii) the ability to control or manipulate particles on the atomic scale (www.nano.gov). Other definitions are more specific, such as the one most commonly used by several authors, stating that nanotechnology is defined as the understanding and control of matter at dimensions of roughly 1-100 nm, where unique physical properties make novel applications possible (e.g. Borm *et al*., 2006; Handy *et al*., 2008a, b; Moore, 2006; Nowack and Bucheli, 2007). Therefore, any materials that have structures or components on their structure that are 100 nm or less in a least one dimension are examples of nanotechnology (Dowling *et al*., 2004; Nowack and Bucheli, 2007). Figure 1.1 puts in perspective the definition of a nanoscale object compared with cellular structures of the human body and a flea.

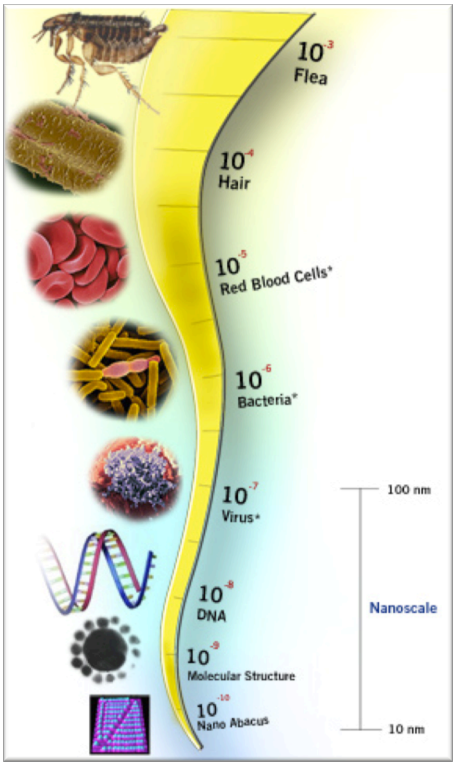


**Figure 1.1 –** Comparison of the size of biological molecules and structures in nanometre scale (adapted from http://www.discovernano.northwestern.edu).

Among these novel nanomaterials (NMs), nanoparticles (NPs) with 3 dimensions between 1 and 100 nm play a central role in the advance of nanotechnology (Ju-Nam and Lead, 2008). NPs production massively increased in the last decade and nowadays these materials are used in a wide range of different areas such as electronics, biomedical, pharmaceutical, cosmetic, energy, environmental, catalytic and material applications (Tiede *et al*., 2009). The importance and potential of NMs have catapulted nanotechnology as one of the most rentable and expanding technologies of the 21$^{th}$ century, with a worldwide increase in investment, research and development and with projections of nano-containing products to achieve sales in the order of trillions of dollars (Guzman *et al*., 2006). For example, levels of funding in nanotechnology research and development in 2008 reached $18.2 billion worldwide, with the United States and Japan at the top of the investment, and it is estimated that the annual revenue for all nanotechnology-related products will be $1 trillion by 2011–2015 (Lux Research, 2009; Roco, 2005). Accordingly, it is expected that the quantity of ENPs in use will increase rapidly over the next few years, with an estimated production rate of 58,000

metric tonnes per year between 2011-2020 (Fig. 1.2) (Maynard, 2006; Royal Society and Royal Academy of Engineering, 2004).

The development and increase in the production and use of NMs predicted for the following years makes it likely that human and environmental exposure to these materials will inevitably occur. As a result, NPs potential adverse effects are beginning to come to light and the discussion about their safety in terms of human health and the environment become a top priority for several governments, the private sector and the public all over the world (Nowack and Bucheli, 2007; Roco, 2005).

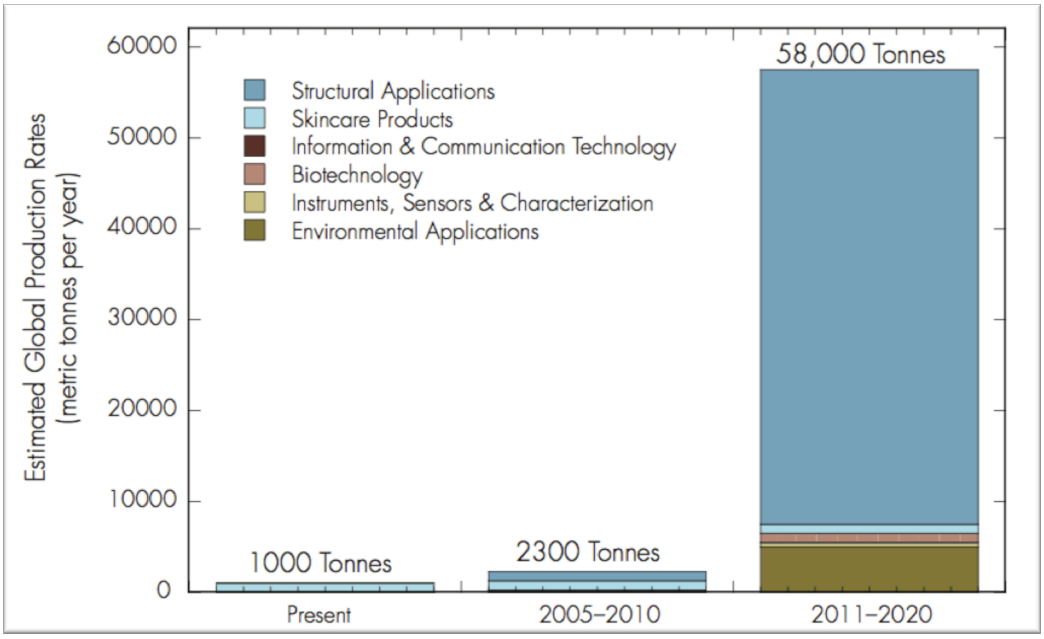


**Figure 1.2 –** Estimated annual global production rates for ENMs. Values are based on estimates in the 2004 Royal Social and Royal Engineering report on nanotechnologies of the United Kingdom (Maynard, 2006).

### 1.1.1. Nanoparticles properties

The increasing expansion of nanotechnology is directly related to the ability to exploit and manipulate molecules of exact specifications and properties allowing the creation of novel materials or the improvement of existing ones by making them more efficient. Materials can behave quite differently in the nano form to the way they do in bulk form because of their various physical and chemical characteristics, making them more attractive. Two important factors determine the different behaviour between nanomaterials and their bulk counterparts,

surface and quantum effects. Due to their decreased size, NPs have higher surface area/volume ratio, allowing higher number of atoms present at the surface of the NPs instead on the interior of the particle. This drastically increase in surface area will determine the reactivity of the NPs. An example of changes in the physical characteristics of gold particles (1 mg) as they are subdivided to approach, and reach, the nanoscale is illustrated in Figure 1.3. At the nanoscale, quantum effects are also significant, namely electron localization, binding energy shift, surface collective charge excitation, thus affecting mechanical, optical, electric and magnetic properties of NPs. Accordingly, these properties make NPs more appealing for new potential applications (Buzea *et al*., 2007; Castro *et al*., 2006; Dowling, 2004; Klaine *et al*., 2012; Nel, 2006). These differences in structure also contribute to other characteristics, for example reduction of melting point (Roduner, 2006). However, it also means that their behaviour/toxicity may be different from that of the micrometre or bulk form (Dowling, 2004).

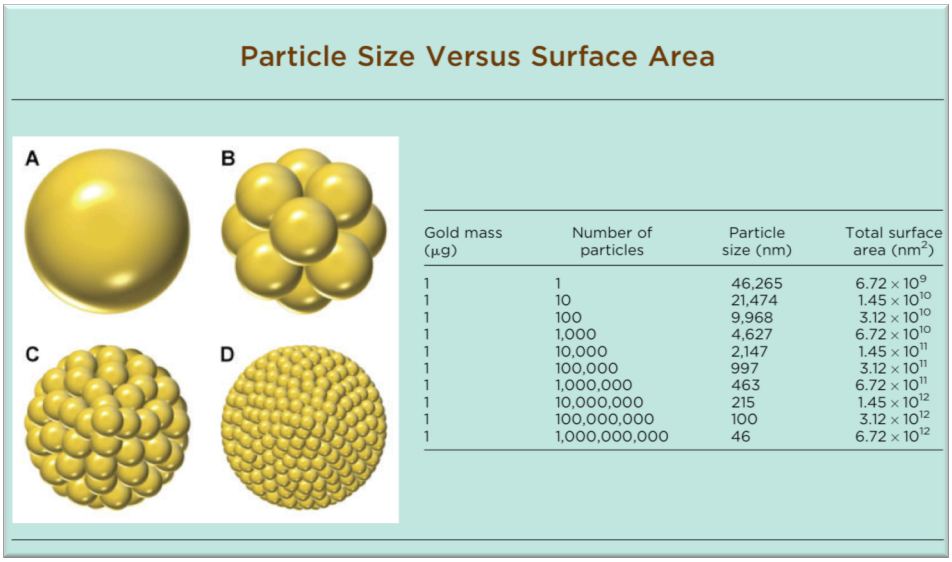


**Figure 1.3 –** Example of changes in the physical characteristics of gold particles of 1 mg as they are subdivided to reach the nanoscale: (A) 1 particle, (B) 10 particles, (C) 100 particles, and (D) 1,000 particles (Klaine *et al*., 2012).

### 1.1.2. Types of nanoparticles

The nanotechnology sector is extremely diverse given its potential to synthesize, manipulate and create a wide range of products/materials that have diverse technological uses. Given this

necessity for innovation, a wide range of ENPs with different composition, shape and size are currently being created and commercialized. They are produced using bottom-up (e.g. organic synthesis, self-assembly, colloidal aggregation) or top-down strategies (e.g. photolithography, laser-beam processing, mechanical techniques) (Borm *et al*., 2006; Dowling, 2004; Ju-Nam and Lead, 2008). Accordingly, the task of classifying these materials into groups or categories is difficult, as ENPs should be broken down into a series of classes and not considered as a single homogenous group (Christian *et al*., 2008; Ju-Nam and Lead, 2008). There are several ways of classifying ENPs being their chemical composition and properties the most commonly used. Other classifications and terminologies are also employed in the literature to refer to specific groups of NPs, based on their dimension, morphology, composition, uniformity, and agglomeration (Fig. 1.4) (Buzea *et al*., 2007; Ju-Nam and Lead, 2008).

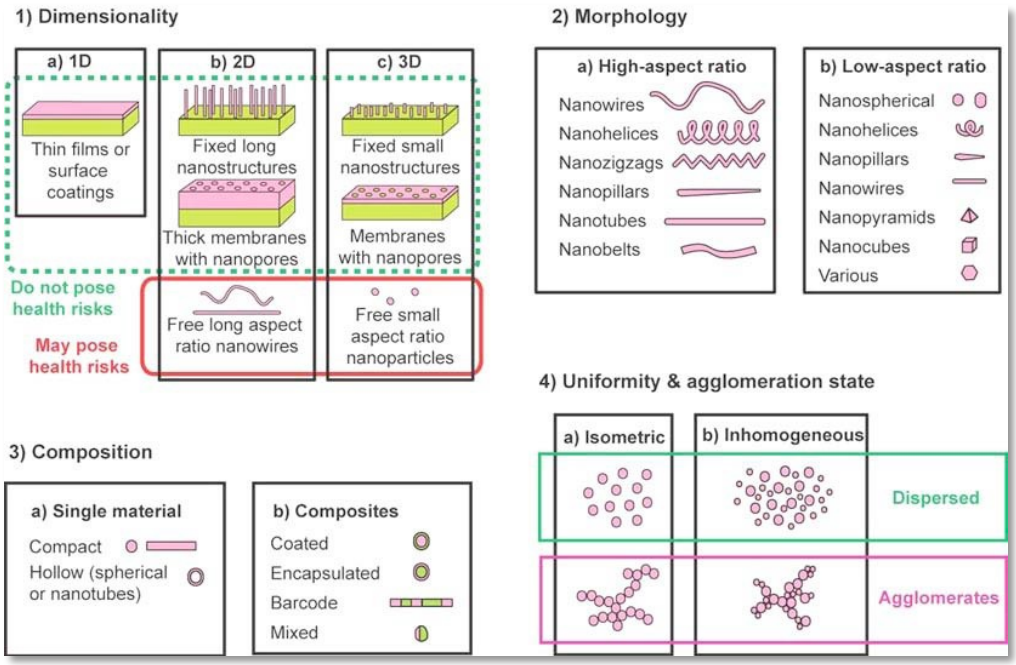


**Figure 1.4 –** Classification of nanostructured materials from the point of view of nanostructure dimension, morphology, composition, uniformity and agglomeration state (Buzea *et al*., 2007).

Regardless of how these materials are classified, the extensive variety of NPs even within a single chemical (e.g. size, specific surface area, shape) will result in different chemical reactivity, bioavailability and ecotoxicity (Handy *et al*., 2008b). Five main groups form the basis of chemical composition of ENPs, carbon based NPs, metal-containing NPs (including

metal oxides), quantum dots, zero-valent metals and dendrymers (Bhatt and Tripathi, 2011; Ju-Nam and Lead, 2008; Klaine *et al*., 2008). Nowadays, toxicological research has mainly focused on the effects of three of the five classes of NPs based on their composition: carbon-based NPs (e.g. carbon nanotubes (CNTs) and fullerenes) (e.g. Oberdörster, 2004; Smith *et al*., 2007) and metal or metal-oxide NPs (e.g. Ag NPs, CuO NPs, $TiO_2$) (e.g. Buffet *et al*., 2011; Heinlaan *et al*., 2008; Ringwood *et al*., 2010). The two classes consisting of metal and metal-oxide NPs will be more thoroughly addressed in this thesis.

#### *1.1.2.1. Metal-containing NPs*

Metal-containing NPs comprises the largest number of NPs, which includes oxides such as zinc oxide (ZnO), titanium dioxide ($TiO_2$), cerium dioxide ($CeO_2$), copper oxide (CuO), chromium dioxide ($CrO_2$), molybdenum trioxide ($MoO_3$), bismuth trioxide ($Bi_2O_3$) and binary oxides such as barium titanate ($BaTiO_3$), lithium cobalt dioxide ($LiCoO_2$) or indium tin oxide (InSnO) (Bhatt and Tripatti, 2011; Klaine *et al*., 2008). The synthesis of these NPs is very common and is achieved by hydrolysis of the transition metal ions (e.g. $TiO_2$ and ZnO) (Masala and Seshadri, 2004). Metal oxide NPs have received considerable attention and massively produced over the last years due to their extensive use in food, material, chemical and biological areas (Aitken *et al*., 2006). Amongst the metal oxides, CuO NPs are two of the most commonly used NPs mostly due to an elevated thermal and electrical conductivity. Cu NPs are intensively used as heat transfer fluid in machine tools (Chang *et al*., 2005), as well as in polymers and plastics, gas sensors (Li *et al*., 2007), wood preservation, conductive inks for printing electronic components (Lee *et al*., 2008) and coatings on integrated circuits and batteries (Dhas *et al*., 1998). Additionally, these Cu NPs are applied in several products as skin products, and textiles mainly due to their antimicrobial properties (Cioffi *et al*., 2005; Ren *et al*., 2008).

#### *1.1.2.2. Zero-valent metals*

The fourth class of NPs are made of zero-valent metals, iron (Fe), gold (Au) and silver (Ag) NPs. These NPs are typically made by reduction or co-reduction of metal salts (Li *et al*., 2006; Masala and Seshadri, 2004), whose physical properties are controlled by varying the reductant type and reduction conditions. These metal NPs have unique optical properties being largely implemented in electronics (Wang *et al*., 2008a, b), nevertheless other potential

applications have emerged like water, sediment, and soil remediation (zero-valent iron) (Zhang, 2003), catalysis industry (Au) (Kim *et al*., 2009), pharmaceuticals and drug delivery (Au and Ag) (Choi *et al*., 2007). From the variety of NPs that are currently being developed in nanotechnology, silver NPs (Ag NPs) have the highest degree of commercialization mainly due to their antibacterial properties. These particles have unique physico-chemical properties, including a high electrical and thermal conductivity, catalytic activity and chemical stability (e.g. Fabrega *et al*., 2011 and literature cited therein; Farkas *et al*., 2011; Luoma, 2008). Nevertheless, it is their antibacterial activity that makes them of common use in textiles, eating utensils, food storage, cosmetics and personal hygiene and household appliances (e.g. washing machines, vacuum cleaners) (www.nanoproject.org). Recently, Ag NPs have been used in medical equipment, such as catheters, infusion systems and medical textiles (Markarian, 2006; Simpson, 2003).

## 1.2. Nanoparticles and the environment

As nanotechnology industries start to come on line with larger scale production, it is inevitable that their products and by-products end up in the environment at quantities that will dramatically increase in a near future (Bhatt and Tripathi, 2011; Moore, 2006; Scown *et al*., 2010a). Although nano-sized particles have always occurred in nature, the latest developments in the use and production of ENPs have raised concern over their potential release and side effects not only in human health but also in the environment. In order to determine the fate and behaviour of NPs in the environment it is necessary to understand their potential risks: (i) do NPs retain some of their nominal properties (e.g. size, structure and reactivity) when they reach aquatic systems; (ii) will NPs interact and associates with other colloidal and particulate constituents; (iii) what will be the effects of solution and physical (e.g. flow) conditions of NPs behaviour (iv) in what way will NPs effects on aquatic and sedimentary biota differ from that of their larger counterparts; and (v) will biota (e.g. biofilms and invertebrates) interact and modify the behaviour of these particles? Accordingly, it is necessary to further improve the knowledge of NPs chemical behaviour, transport in and between environmental and biological compartments, ultimate environmental fate, mechanisms of biological uptake and toxic implications for living systems (Dowling *et al*., 2004; Ju-Nam and Lead, 2008; Klaine *et al*., 2008).

### 1.2.1. Inputs of nanoparticles to the environment

It is estimated that 50,000 kg/year of nano-sized materials are being produced through non-industrial and unintended proveniences, i.e. atmospheric emissions (e.g. waste combustion, diesel-exhaust and other combustion processes), leaching from NPs-containing products in landfills or soil-applied sewage sludge (Dowling *et al*., 2004; Klaine *et al*., 2008). Some will also enter the environment during the product's life cycle (e.g. by erosion of the materials, accidental spills), from production facilities (i.e. initial and downstream manufacturers) and wastewater treatment plants (Nowack and Bucheli, 2007; Oberdörster *et al*., 2005). Other types of sources resulting from the use of products that contain ENPs (e.g. paints, fabrics, and personal health care products) may be released in the environment proportionally to their use from both direct (e.g. bathing) and indirect (e.g. sewer) sources (Biswas and Wu, 2005; Zhang, 2003). Diffuse release associated with wear and erosion from general use is also possible (e.g. wear of car tires, urban air pollution), as well as intentional use in remediation of contaminated environmental media (soil and water) (e.g. use of iron NPs to remediate groundwater) (Bhatt and Thripathi, 2011; Zhang and Elliot, 2006). Independently of the source (water, soil or atmosphere), emitted particles will ultimately end up on land and waterways (e.g. drainage ditches rivers, lakes, estuaries and coastal waters) where they have the potential to contaminate soil, migrate into surface and ground waters, and interact with biota (Klaine *et al*., 2008; Moore, 2006; Nowack and Bucheli, 2007). All these routes will allow ENPs to disperse through the environment (Fig. 1.5); but the fate of each of these NPs will vary (Klaine *et al*., 2012).

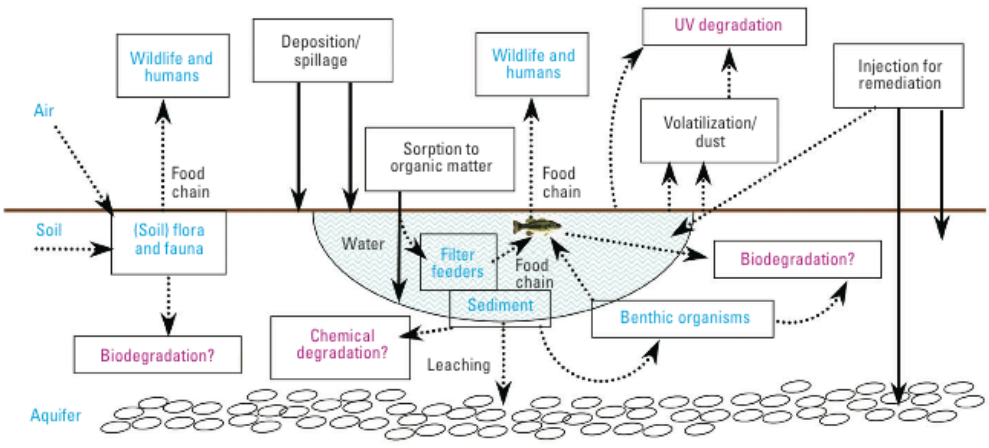


**Figure 1.5 –** Routes of exposure, uptake, distribution, and degradation of NPs in the environment. Solid lines indicate routes identified in the laboratory or in the field or that are

currently in use (remediation). Magenta lettering indicates possible degradation routes, and blue lettering indicates possible sinks and sources of NPs (Oberdörster *et al*., 2005).

The amount of NMs that may be found in the environment is difficult to predict, so, to ensure a sustainable development of nanotechnology, proper tools and methodologies for the measure and characterization of NPs in atmospheric, aquatic and terrestrial environments have to be applied to facilitate an accurate ecological risk assessment of these materials (Hasselöv *et al*., 2008; Klaine *et al*., 2008; Maynard, 2006). Nowadays the development of analytical methods to detect and quantify ENPs is still in its infancy and consequently little is know about their concentrations in the different environmental compartments (air, soils and water) or on their transport, fate and behaviour (Nowack and Bucheli, 2007; Scown *et al*., 2010a). Several challenges have emerged not only derived from their novel properties (e.g. size, shape, surface charge, composition, degree of dispersion) but also from the possible alterations (e.g. aging or weathering) and interactions during their environmental life cycle (Klaine *et al*., 2012). Classical exposure assessments are depended on the soluble fraction of a given contaminant and when dealing with NPs the chemical speciation concept used needs to include their physical forms (dissolved, colloidal, and particulate). The knowledge already gathered on colloidal behaviour is also very useful for the assessment of ENMs. Nevertheless, many of the well-established techniques for pure systems may not be appropriate to accurately detect NPs in complex environmental systems (Klaine *et al*., 2008, 2012).

Currently there are no standardized measures or methods to determine actual concentrations of ENPs in the environment, although some modelling approaches were undertaken to estimate the likely emission and load of ENPs in various environmental compartments including the aquatic environment (e.g. Boxall *et al*., 2008; Mueller and Nowack, 2008). These modelling approaches highlighted the uncertainties in the prediction of environmental concentrations and levels of ENPs based only on emission scenarios (from production volumes and life cycle assessments) and portioning parameters (fate and behaviour) where most of them require validation through measurements of actual environmental concentrations (Klaine *et al*., 2008).

### 1.2.2. Behaviour of nanoparticles in the aquatic environment

As soon as they enter the aquatic environment, NPs will interact with natural water components such as colloids and organic matter depending on a variety of physico- chemical conditions such as pH, ionic strength, hardness temperature or organic ligands, as well as light, oxidants or microorganisms. Little information about these interactions is yet available, specifically for the ENPs, and differences between pristine NPs and those actually released or altered after release are also highly significant for fate processes in the environment. Thus, what is already known for environmental colloids will significantly help the understanding of environmental impact of NPs (Hasselöv *et al*., 2008; Klaine *et al*., 2012; Nowack and Bucheli, 2007). These interactions between colloids and ENPs can lead to several chemical or biological modifications (e.g. size distribution, aggregation or disaggregation, charge and solubility, surface film formation, interaction with micropollutants and stabilization) or degradation of the particles that can strongly affect their behaviour in the water column. All these interactions are summarized in Figure 1.6 and described in detail elsewhere (Christian *et al*., 2008; Ju-Nam and Lead, 2007; Nowack and Bucheli 2007).

An example of the environmental significance of these interactions is the propensity of NPs to aggregate in natural waters. Changes in aggregation due to interaction between natural colloids and NPs and with other existing natural NPs or larger particles will have an effect in the potential transport of NPs in the water column, and consequently in the fate and toxicity of particles. The tendency of NPs to aggregate in the environment can lead to entrapment or elimination through sedimentation, where they are more likely to interact with sediment-dwelling and benthic organisms than with pelagic species. Nevertheless, the stabilization of NPs in the water column is also possible suggesting a potential uptake by aquatic organisms and transport within the water column with transportation to higher distance and rates. Disaggregation of NPs is also important, as the resulting small aggregates can be re-suspended and become mobile in the water column and beneficiate the co-transport of pollutants as well as nutrients (Baalousha *et al*., 2008; Christian *et al*., 2008; Nowack and Bucheli, 2007). Another example is the effect of humic and fulvic substances that have been shown to inhibit the aggregation of CNTs (Hyung *et al*., 2007) but also enhance the aggregation and stability of FeO NPs (Baalousha *et al*., 2008). Different environmental systems (e.g. seawater, freshwater) featuring different parameters (e.g. temperature, pH, ionic strength and organic complexation) can also affect the solubility of NPs and thus their dissolution kinetics (Tiede *et al*., 2009). Solubility is a significant factor in determining NPs

toxicity, especially in the case of metal-based NPs, as the release of soluble metal ions from the surface of the particles will determine the proportional exposure/bioavailability to organisms and increase the risk of metal toxicity (Fabrega et al., 2011; Scown et al., 2010a). Overall, the complex chemical and physical interactions and behaviour or NPs with other components in natural waters need further development to better understand the fate, behaviour, bioavailability and toxicity of these particles in aquatic systems (Klaine *et al*., 2008; Nowack and Bucheli 2007; Scown *et al*., 2010a).

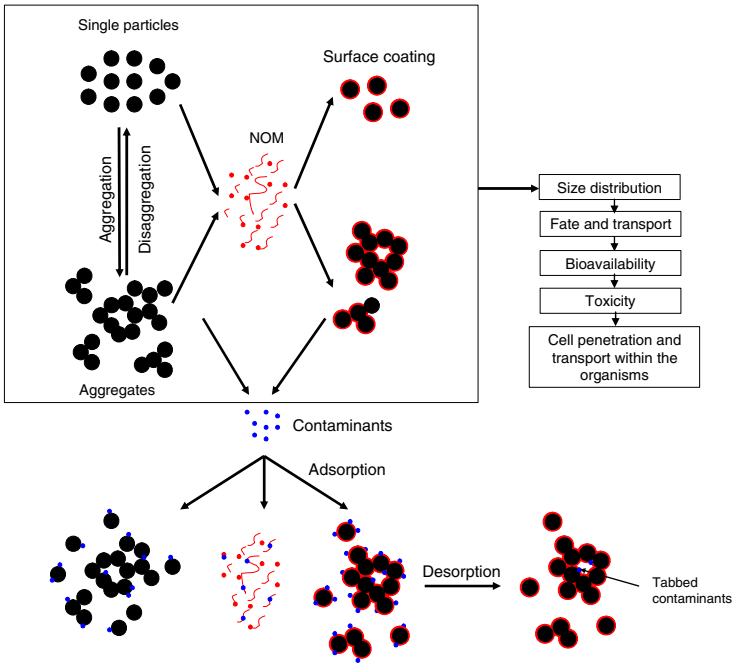


**Figure 1.6 –** Schematic representation of the interaction of engineered NPs with natural water components (Christian *et al*., 2008).

Considering the many factors that can influence NP–environment interactions, the use of multiple analytical techniques addressing a wide range of NPs properties (e.g. aggregation/agglomeration, size, dissolution/solubility, surface area and charge) are needed to measure the key parameters affecting NPs toxicity and behaviour (Hassellöv *et al*., 2008; Tiede *et al*., 2009). A wide range of methods is presently available for NP detection, identification and characterisation, including microscopy-based approaches (e.g. transmission electron microscopy), centrifugation, dynamic light scattering, voltammetry, and size separation methods (e.g. hydrodynamic chromatography) coupled to analytical instruments (e.g. inductively coupled plasma). Some of these methods, and analysis capabilities are presented below (Table 1.1).

**Table 1.1 –** Methods for analysis and characterization of NPs (Based on Hassellöv *et al*., 2008; Tiede *et al*., 2009).

| Analytical tool | Parameter | Particle type | Approximate size range (nm) | Limit of detection |
|---|---|---|---|---|
| **Atomic force microscopy** | Visualization, state of aggregation, shape | All types | 0.5 to > 1000 | ppb–ppm |
| **Centrifugation** | Size fractionation | All types | 10 to > 1000 | Detection dependant |
| **Dialysis** | Size fractionation | All types | 0.5–100 | Detection dependant |
| **Diffusive gradients in thin films** | Free metal ions, metal speciation | Metals | | Sensitivity depends on exposure time |
| **Dynamic light scattering** | Size distribution | All types | 3 to > 1000 | ppm |
| **Electron microscopy-EELS/EDX** | Visualization, state of aggregation, shape | Elements with high electron density (e.g. metals) | Analysis spot size: ~1 nm | ppm in single particle |
| **Electrophoretic mobility** | Zeta potential | All types | 3 to > 1000 | ppm |
| **Environmental scanning electron microscopy** | Visualization, state of aggregation, shape | Preferably elements with high electron density (e.g. metals) | 40 to > 1000 | ppb–ppm |
| **Field flow fractionation** | Size distribution, state of aggregation, shape | All types | Flow: 1–1000<br>Sedimentation: 50–1000 | Detection dependant; in combination with UV-Vis: ppm; fluorescence and ICP-MS: ppb |
| **Filtration** | Size fractionation | All types | Micro: 100 > 1000<br>Ultra: 1–30 | Detection dependant |
| **Hydrodynamic chromatography** | Size distribution | All types | 5–1200 | Detection dependant |

| | | | | |
|---|---|---|---|---|
| **Inductively coupled plasma mass spectrometry (ICP-MS)** | Elemental composition | Especially metals | Depends on fractionation | ppt-ppb |
| **Laser induced breakdown detection** | Size distribution, state of aggregation | All types | 5 to >1000 | ppt |
| **$N_2$ adsorption, BET** | Specific surface area, porosity | Powders | 1 to > 1000 | ~5 nm to several µm |
| **Nanoparticle tracking analysis** | Size distribution | All types | 10–1000 | ppb–ppm |
| **Scanning electron microscopy** | Size distribution, state of aggregation, shape | Preferably elements with high electron density (e.g. metals) | 10 to >1000 | ppb–ppm |
| **Selective laser sintering** | Size distribution, state of aggregation, shape | All types | 50 to >1000 | ppm |
| **Size exclusion chromatography** | Size distribution | All types | 0.5–10 | Detection dependant on pore size |
| **Transmission electron microscopy-SAED** | Surface chemical, structure analysis | Elements with high electron density (e.g. metals) | Analysis spot size: 1nm | - |
| **Turbidimetry** | Size distribution, state of aggregation | All types | 50 to >1000 | ppb–ppm |
| **Voltammetry** | Free metal ions, total substance concentration, metal speciation | Especially metals | | ng range |
| **X-ray diffraction** | Surface chemical, structure analysis | Powders | 0.5 > 1000 | Dry powder, µg to mg |

### 1.2.3 Exposure of aquatic organisms to nanoparticles

Although clear benefits are expected from the expansion of nanotechnology products, concern is growing about the potential toxicity and ecotoxicology associated with their unusual properties. The altered quantum effects and enhanced chemical reactivity that makes NPs so attractive and useful in numerous applications are also fundamental for their complex interactions and effects in the environment and their unpredictable/unknown effects in living organisms. Additionally, small particle size and high specific surface area will also benefit the passage across biological barriers of most organisms and enter cells through membranes and junctions between cells (Handy *et al*., 2008a; Scown *et al*., 2010a). Altogether, these properties give NPs the potential to induce adverse cellular effects and damage to living organisms. Most research on the ecotoxicity of NPs has focused on mammals, and various effects have been reported and debated (e.g. Colvin, 2003; Handy and Shaw, 2007; Handy *et al*., 2008a), while ecotoxicity of NPs in aquatic organisms is still emerging. Interaction of NPs with aquatic biota is a function of the physico-chemical properties of the particles (e.g. size, aggregation state, chemical composition), as well as of the biology of the target organisms. At least three primary biological targets can interact with NPs in the aquatic environment: (i) filter feeders, which can be exposed to high NPs concentrations present in surface waters; (ii) pelagic species (from phytoplankton to fish and mammals) exposed during vertical migration of the particles; and (iii) benthic species that are likely to interact to aggregated or adsorbed NPs or NPs deposited in sediment biofilms. A wide variety of parameters influence the fate and effects of NPs in cells and living organisms, and a given NP can have differing toxic effects depending on the particle properties (e.g. presence and type of coating), method of preparation (e.g. use of dispersants) or species sensitivity (Barber *et al*., 2009; Bhatt and Tripathi, 2011; Handy *et al*., 2008a; Matranga and Corsi, 2012). Most of the ecotoxicity of NPs directed towards aquatic organisms is centred on acute toxicity in species used for regulatory toxicology (i.e. short-term acute toxicity tests, chronic and life-cycle effects), namely in freshwater species as *Daphnia magna* and model fish species as *Danio rerio* (zebrafish), *Pimephales promelas* (fathead minnows) and *Oncorhynchus mykiss* (rainbow trout) (Baun *et al*., 2008; Cattaneo *et al*., 2009; Handy *et al*., 2008a). Despite the information given by acute experiments, they do not provide complete information about the interactions of NPs with other species that cover a wide range of trophic levels and there is a need to direct research towards invertebrates using long-term exposure to better understand NPs toxicity mechanisms (Baun *et al*., 2008; Griffitt *et al*., 2008; Heinlaan *et al*., 2008,

2011). NPs exposure induces a wide range of biological effects towards aquatic organisms. For example, carbon-based and metallic NPs are toxic to embryonic fish models, in terms of developmental abnormalities and mortality, as well as in invertebrate species (as *D. magna*), in terms of mortality, fertilization rates and reduced moulting success (e.g. Gaiser *et al*., 2011; Heinlaan *et al*., 2008; Oberdörster, 2004; Scown *et al*., 2010b). There are clearly still significant gaps in the knowledge about NPs toxicity, and the current knowledge on the fate, concentrations, behaviour and toxicity of these particles in the marine environment is mainly based on hypothesis rather than experimental information, in addition to a lack of an ecological and physiological endpoint of view in most laboratory studies. This is especially true for species living in estuarine and coastal areas that are major depositional areas for NPs. For example, in commercially harvested aquatic species, such as edible bivalves, such information is essential for the understanding of the potential transfer of NPs to humans (Canesi et al., 2012; Matranga and Corsi, 2012; Ward and Kach, 2009).

#### *1.2.3.1. Uptake, accumulation and bioavailability*

It is well known that because NPs have similar size to cellular proteins and components, they are able to cross some of the barriers of biologic systems. The cell membrane is selectively permeable and controls the movement of small and large molecules in and out the cell (Paur *et al*., 2011). Though the cellular uptake mechanisms of NPs are not fully understood, consistent evidence exist that these particles are taken up by a wide variety of cell types (prokaryotic and eukaryotic) and accumulate inside the cell (e.g. Canesi *et al*., 2012; Griffitt *et al*., 2008; Morones *et al*., 2005). This accumulation is dependent on their physicochemical properties (e.g. chemical composition, size/geometry, surface charge, coating/ligands and aggregation status), the exposed cell type (e.g. phagocytes, cancer cells), as well as the microenvironment (e.g. surfactant). The mechanisms of cellular uptake and intracellular trafficking described so far for NPs are phagocytosis (A), pinocytosis (B), endocytosis (C-E) and direct penetration (F) via disturbance of membrane components (Moore, 2006; Paur *et al*., 2011; Unfried *et al*., 2007; Ward and Kach, 2009) that are represented in Figure 1.7. To better understand the different mechanisms of NPs uptake, the letters between brackets in the following text refer to the letters in the figure.

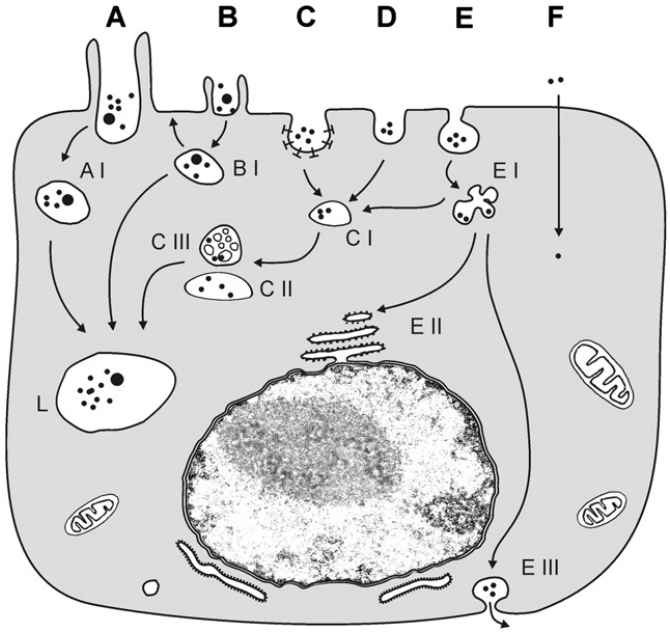


**Figure 1.7 –** Mechanisms of cellular uptake of NPs and related intracellular trafficking: (A) Phagocytosis, leading to phagosomes (AI) and phago-lysosomes (L). (B) Macropinocytosis, leading to macropinosomes (BI) which might be exocytosed or fuse with lysosomes (L). (C) Clathrin-mediated endocytosis, forming primary endosomes (CI) and late endosomes (CII) including multivesicular bodies (CIII). (D) Clathrin and caveolae independent endocytotic pathways. (E) Caveolae-mediated endocytosis, forming caveosomes (EI), which fuse with the ER (EII) or translocate through the cell (EIII). (F) Particle diffusion/transport through the membrane (Paur *et al*., 2011).

Phagocytosis (A) and macropinocytosis (B) are two processes by which larger particles (> 250 nm) can be interiorized by cells (Paur *et al*., 2011; Unfried *et al*., 2007), for example, the aggregates suspensions (> 100 nm) commonly formed by NPs. During phagocytosis (A), an actin-based mechanism, particles become engulfed via specific membrane receptors (e.g. scavenger receptors), leading to the formation of large vesicles called phagosomes (AI). The phagosomes go through a maturation stage for subsequent particle processing that results in the formation of a lysosome (L) in which the ingested particles will be broke down. Macropinocytosis (B) is also an actin-based mechanism that involves the internalization of larger areas of plasma membrane and significant amounts of fluid than a regular pinocytosis, via specific vesicles called macropinosomes (BI). Similarly to phagocytosis, macropinosomes undergo several maturation steps before formation into a lysosome (L) (Kirkham and Parton, 2005; Paur *et al*., 2011; Unfried *et al*., 2007).

As discussed by Moore (2006), most internalization of NPs will probably occur via endocytosis (particles up to 100 nm). Endocytosis is a complex mechanism that can occur through several pathways that can either lead to the endosomal and lysosomal compartments (clathrin- or non clathrin-mediated endocytosis) or else via caveolae-mediated endocytosis (cell-surface lipid raft associated domains) that avoids the degradation of material entering the endosomal/lysosomal system (Moore, 2006 and literature cited therein; Moore *et al*., 2009; Unfried *et al*., 2007). Clathrin mediated endocytosis (C) is the major route for endocytosis in most cells that is mediated by the molecule clathrin. The cellular uptake of particles takes place in clathrin-coated pits, followed by the formation of clathrin-coated vesicles. Particles will then be processed by primary endosomes (CI) and late endosomes (CII) including multivesicular bodies (CIII), before reaching the lysosome (L) stage for degradation. On the other hand, less is known about the specific mechanisms that form clathrin and caveolae independent endocytotic pathways, which may constitute a specialized pathway for lipids and fluids. Particles internalization are associated with rafts formed by lipids clustering from the cellular membrane, that ultimately result in the formation of intracellular vesicles, as endosomes (CI), that follow the same path as cathrin-mediated endocytosis (Kirkham and Parton, 2005; Paur *et al*., 2011; Unfried *et al*., 2007). Similarly to clathrin and caveolae independent endocytotic pathways, caveolae-mediated endocytosis (E) also occur as a result of the formation of lipid rafts, which then invaginate forming flask-shaped vesicles (diameter of 50–100 nm), caveosomes (EI) and can result in translocation and fusion with the endoplasmic reticulum (EII), Golgi or translocation through the cell (EIII) by trancytosis. Finally, NPs can also enter cells simply by diffusion/transport (F) through the membrane, resulting in particles located freely in the cytosol (Moore, 2006; Paur et al., 2011; Unfried et al., 2007).

This capacity of cells to internalize particles from sizes up to the mm range, suggests that both single NPs and aggregates present in the aquatic environment will be available for interaction with the cellular components after their uptake by an organism. So, it is very important to clarify the relationship between NPs uptake and subsequent translocation and accumulation into cells, nucleus and organelles, with the effects at cellular and molecular level (e.g. cytotoxicity, genotoxicity) along with signalling pathways (Unfried *et al*., 2007).

Accumulation of NPs by an organism is determined by the balance between uptake rate from the surrounding medium and the loss rate (detoxification/elimination) and dilution by growth, as well by as a direct way to evaluate the bioavailability of a given NP to penetrate into the organism. For most compounds, the balance between exposure, uptake, bioaccumulation and

elimination will determine the potential toxicity towards organisms. In the case of NPs, toxicity will be determined by the internally accumulated NP in each organism and whether or not its presence disrupts processes within cells. Nevertheless, several factors will influence the bioavailability of NPs present in an environment and the rate by which they will be accumulated: (i) the concentration of the NP in the environment, (ii) the physico-chemical properties of the NP (e.g. size, shape, chemical composition, solubility, and aggregation) (iii) the nature/characteristics of the environment (e.g. freshwater, marine, abiotic factors), (iv) the route of exposure (e.g. food, water, sediment), (v) the biology and functional ecology of the organism involved and (vi) exposure duration (Fabrega *et al*., 2011; Luoma and Rainbow 2005; Wang, 2011).

To study bioaccumulation, it is essential to be able to detect and quantify their uptake by organisms, as well as their distribution within tissues, cells and subcellular compartments. The amount of NPs accumulated in the organism has rarely been simultaneously quantified along with toxicological endpoints, rendering ambiguity in the interpretation of the results. This has also been aggravated by the fact that most of the available tools and techniques do not allow the accurately visualization, tracing and quantification of NPs in tissues, cells and sub-cellular components (Bhatt and Tripathi, 2011; Canesi *et al*., 2012; Scown *et al*. 2010a; Wang, 2011).

#### *1.2.3.2. Nanoparticles effects at the cellular level*

Even though several evidences exists on the toxicity and uptake of NPs, different experimental designs with diverse NPs sizes, coatings, concentrations, times of exposure, measured endpoints and cell types make it difficult to compare results and determine the mode of action by which these particles inflict damage to organisms (Handy *et al*., 2008a; Scown *et al*., 2010a). Particle uptake into cells by the mechanisms referred in the previous section has been demonstrated for a range of NPs types suggesting that the observed toxicity may result from both the interaction of the NPs with the cellular membrane and within the cytosol and sub-cellular compartments (Lapresta-Fernández *et al*., 2012; Unfried *et al*., 2007). Both *in vivo* and i*n vitro* exposure studies have shown that different types of NPs are capable of inducing various deleterious effects at different levels of cellular organization. Generation of reactive oxygen species (ROS) and free radicals have been observed and implicated in the cause of oxidative stress, namely in the form of antioxidant defence system activation/inhibition (e.g. depletion of glutathione), lipid peroxidation and DNA damage,

decreased mitochondrial activity, inflammatory processes and apoptosis in a wide variety of cell types (e.g. Ahamed *et al*., 2010; Canesi *et al*., 2012; Ivask *et al*., 2010; Yeo and Pak, 2008). While toxic mechanism have not yet been fully elucidated, possible mechanisms like disruption of membrane integrity and potential, destabilization and oxidation of proteins, genotoxicity, interruption of energy transduction, formation of ROS and release of harmful and toxic components (e.g. transition metal ions, organic components) have already been generalized (Klaine *et al*., 2008; Unfried *et al*., 2007). Some of these mechanisms are commonly accepted as the most important modes of action by which NPs exert toxicity and will be further discussed in the following sections.

#### *1.2.3.2.1. Oxidative stress and Reactive Oxygen Species*

The generation of ROS is considered one of the most harmful cellular effects induced by exposure to NPs. ROS-derived oxidative stress is the best developed paradigm to explain most of the cytotoxic effects exerted by NMs, which refers to a redox imbalance normally as a result of increased intracellular ROS and decreased antioxidants (Nel, 2006; Unfried *et al*., 2007). From a mechanistic perspective, three main hypotheses have been proposed on how NPs can induce intra- and extracellular ROS in organisms: (i) NPs inherent redox-active properties (e.g metal-containing NPs) or composition of surface properties (e.g. chemical reactivity), as well as of impurities present in particles preparation; (ii) physical interaction of NPs with cellular and sub-cellular components involved in the catalysis of redox processes; and (iii) NPs persistence in biological systems that can lead to continuous availability over time (by either disaggregate or dissolve) inducing site-specific ROS formation (Petersen and Nelson, 2010; Unfried *et al*., 2007).

The cellular metabolism in aerobic organisms is one of the most efficient forms of energy metabolism that involves the reduction of molecular oxygen ($O_2$). However, partial reduction of $O_2$ in endogenous reactions gives rise to the formation of both radical and non-radical ROS, which are highly toxic (Livingstone, 2001; Matés, 2000). These include superoxide anion radical ($O_2^{-\bullet}$), hydroxyl radical ($OH^{\bullet}$), peroxyl radical ($ROO^{\bullet}$), alcoxyl radical ($RO^{\bullet}$), hydroperoxyl radical ($HO_2^{\bullet}$) and nitric oxide ($NO^{\bullet}$), and non-radicals forms such as hydrogen peroxide ($H_2O_2$), singlet oxygen ($^1O_2$), ozone ($O_3$), hypochlorous acid (HOCl) and peroxynitrite (OOHNO) (Di Giulio *et al*., 1995; Livingstone, 2001). Most of these radicals have the potential to cause free-radical reactions, and when a free radical reacts with a non-

radical molecule, the target molecule is converted to a radical, which may further react with another molecule (Halliwell and Gutteridge, 1999).

The production of ROS is directly related to the concentration of molecular oxygen through simple oxidation and reduction processes (Unfried *et al*., 2007), being the mitochondria (namely the electron transport chain) the major site for ROS production in cells by consuming and reducing up to 90% of cellular oxygen. This reduction originates the reactive $O_2^{-\bullet}$ (Equation 1) that leads to the production of other higher reactive intermediates such as $H_2O_2$, $OH^{\bullet}$, and finally water ($H_2O$) (Finkel and Holbrook, 2000; Halliwell and Gutteridge 1999; Lesser, 2006; Unfried *et al*., 2007) through free-radical chain reactions.

$$O_2 + e^- \rightarrow O_2^{\cdot -} \quad (1)$$

Superoxide undergoes a dismutation to form $H_2O_2$ spontaneously or catalysed by the antioxidant enzyme superoxide dismutase (SOD) (Equation 2). The spontaneous dismutation rate of $O_2^{\cdot -}$ is slow, whereas the reaction catalysed by SOD is $10^4$ times faster (Halliwell and Gutteridge 1999; Lesser, 2006; Unfried *et al*., 2007).

$$2O_2^{\cdot -} + 2\,H^+ \rightarrow H_2O_2 + O_2 \quad (2)$$

Because $H_2O_2$ is uncharged and more stable than $O_2^{-\bullet}$ is able to diffuse through the plasma membrane. If not scavenged and fully reduced by catalase (CAT) (Equation 3) or glutathione peroxidase (GPX) (Equation 4) to form $H_2O$ and $O_2$, $H_2O_2$ can promote radical reactions far from its origin by producing the most reactive ROS, $OH^{\bullet}$ (Halliwell and Gutteridge 1999; Lesser, 2006; Unfried *et al*., 2007).

$$2\,H_2O_2 \rightarrow 2\,H_2O + O_2 \quad (3)$$

$$2\,GSH + H_2O_2 \rightarrow GSSG + 2H_2O \quad (4)$$

The production of the $OH^{\bullet}$ from $H_2O_2$ occurs through catalysis by redox active transition metals in their reduced form such as iron (II) and copper (I), the so-called Fenton reaction (Equation 5), or via metal-catalysed Haber-Weis reaction with $O_2^{\cdot -}$ as a reducing agent (Equation 6). While thermodynamically favourable, the Haber-Weiss reaction is kinetically slow, while the Fenton reaction facilitates OH• production (Di Giulio *et al*., 1995; Halliwell and Gutteridge 1999; Lesser, 2006; Unfried *et al*., 2007).

$$Fe^{2+} + H_2O_2 \rightarrow Fe^{3+} + OH^{\cdot} + OH^- \quad (5)$$

$$Metal\ (III)\ O_2^{\cdot -} + H_2O_2 \rightarrow O_2 + OH^{\cdot} + OH^- \quad (6)$$

Nevertheless, other sources of endogenous cellular ROS exist (Fig. 1.8), including oxidizing enzymes as NADPH oxidases, xanthine oxidase and cytochrome P450 reductase also responsible for the production of $O_2^{-\bullet}$, while other enzymes as guanyl cyclase and glucose oxidase are able to generate $H_2O_2$ (Unfried *et al*., 2007; Valavanidis *et al*., 2006). Exogenous sources can stimulate ROS production in biological systems, such as radiation (X- ray, gamma, ultraviolet light, or visible light in the presence of a sensitizer), particulate matter (asbestos, airborne material), nitrogen oxides, ozone, smoke of various forms, etc. Additionally, environmental pollutants as organic redox cycling compounds (e.g. quinones, nitroaromatics, nitroamines, bipyridyl herbicides), polycyclic aromatic and halogenated hydrocarbons (e.g. benzene, bromobenzene, polychlorinated biphenyls, lindane), dioxins and pentachorophenol, metals (e.g. aluminum, arsenic, nickel, copper, cadmium, chromium, mercury) and peroxides were also identified for their capacity to enhance oxyradicals production (Di Giulio *et al*., 1995; Lesser, 2006; Livingstone, 2001).

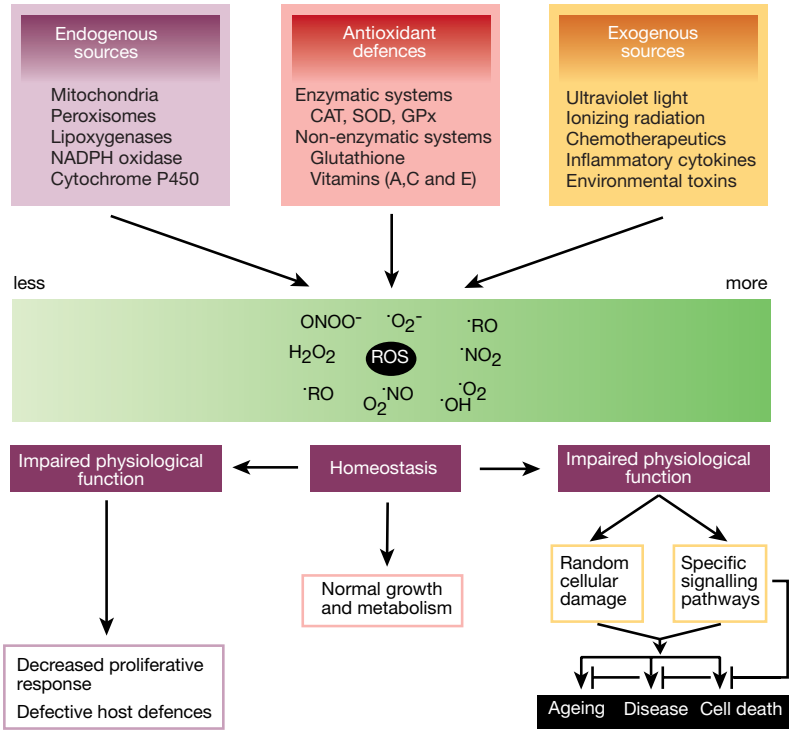


**Figure 1.8 –** Sources and cellular responses to ROS (Finkel and Holbrook, 2000).

As for NPs, several direct and indirect ROS-generating mechanisms may occur during interaction with biological cells leading to the production of ROS, where composition, purity,

chemical reactivity and surface properties seem to be preponderant factors (Unfried *et al*., 2007; Wilson *et al*., 2002). In single component NPs, as metal-containing NPs, one of the factors that could influence ROS formation is the release and dissolution of metal ions in their reduced form (e.g. $Cu^{2+}$ from Cu NPs) that can trigger the production of OH• free radical (Fenton and Haber-Weiss reactions, Equations 5 and 6, respectively). Additionally, the presence of transition metals partly derived from particle impurities (e.g. ultrafine particles and carbon nanotubes containing Fe and vanadium) or redox cycling organic compounds on the surface of NPs can also contribute to the production of ROS after released in the vicinity of the NPs and amplification of chemical changes in the NPs environment. Furthermore, transition metals are also involved in the redox cycling of quinones, a major organic species used in the coating of ultrafine NPs. ROS are also formed as a consequence of the interaction between particles and cellular components (e.g. endoplasmic reticulum, specific enzyme complexes on the cellular membrane and the mitochondria) or by directing its reactivity to subcellular compartments. For example, the physical contact between cells and metal containing-NPs causes changes in the vicinity of the contact area and increase the dissolution of metals (originating ROS by some of the reactions previously referred) or generate extracellular ROS. Finally, NPs discontinuous crystal planes, material defects, surface conductance and energy transfer properties (radiative light emission) also leads to the formation of ROS. In the case of photoactive NPs such as $TiO_2$, the presence of UV radiation can induce the generation of ROS and oxidative stress in cells (Nel, 2006; Unfried *et al*., 2007; Xia *et al*., 2009).

In Figure 1.9 the redox cycle is briefly described along with the generation of ROS by NPs, together with the antioxidant defence system and some of their known toxic consequences that will be further detailed in the following sections.

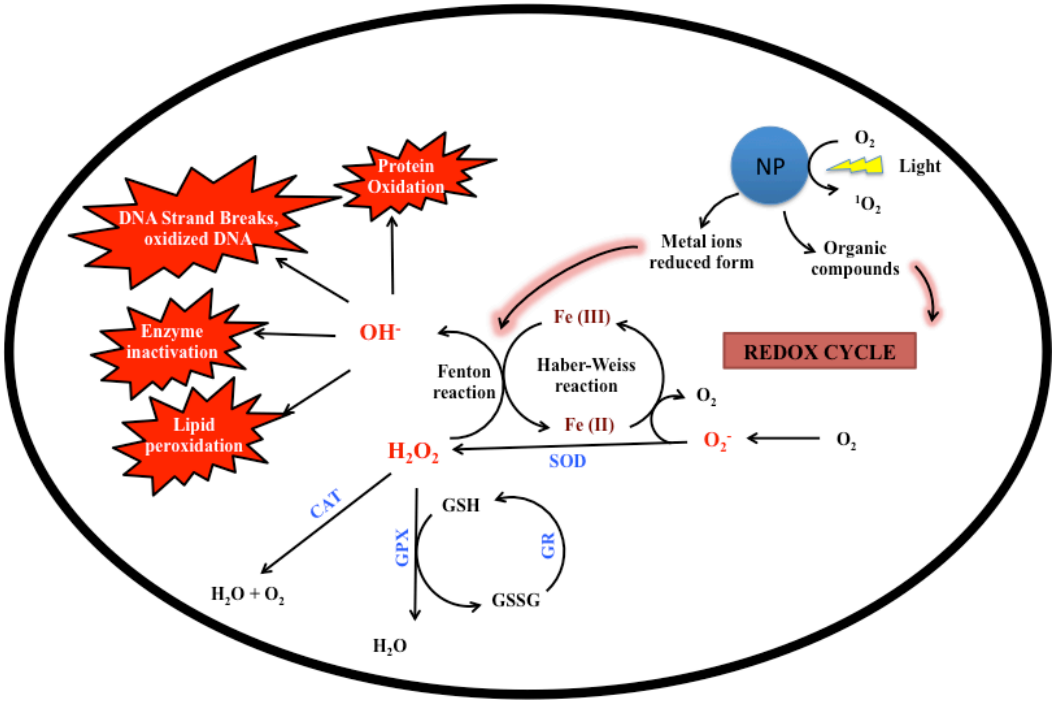


**Figure 1.9 –** ROS production, defence mechanisms and effects of free radicals on cells exposed to NPs. NP: Nanoparticle, $^1O_2$: singlet oxygen, $O_2^-$: superoxide anion radical, $OH^-$: hydroxyl radical, SOD: superoxide dismutase, $H_2O_2$: hydrogen peroxide, CAT: catalase, GPX: glutathione peroxidase, GSH: glutathione, GSSG: glutathione disulphide (oxidized form of GSH), GR: glutathione reductase (Adapted from Unfried *et al*., 2007).

To minimize ROS-oxidative damage to cellular components, biological systems have developed a complex antioxidant system, comprised of both enzymatic and non-enzymatic defence mechanisms. In normal metabolic conditions, free radicals production is strictly regulated by antioxidant defences (antioxidant enzymes and specific low molecular weight scavengers) to maintain a "redox homeostasis" within cells. Nevertheless, if an imbalance arises between ROS formation and the capacity of the organisms to neutralize or repair the resulting damage by enhancing intracellular generation of ROS and/or failure of antioxidant defences, oxidative stress occurs. These disturbances in the normal redox state of cells are very variable, depending on the cell type, duration of exposure and ROS levels inside the cell. The cellular response to the presence of ROS results in an increased cell proliferation for relatively low doses of ROS, an increased production of peroxides and free radicals that can damage all cellular components, as proteins, lipids and DNA and to a further extent to a disruption in normal mechanisms of cellular signalling and cellular death (Fig. 1.8 e 1.9). The production of damaging ROS are also associated to inflammation and immunity responses, since moderately low levels of ROS are involved in initiating the normal inflammatory

responses in organisms exposed to foreign compounds (Lesser, 2006; Livingstone, 2001; Valavanidis *et al*., 2006). The same responses were detected in organisms exposed to NPs. In this context, variations in the level or activity of specific components of the antioxidant system and consequent oxidative damage were proposed as biomarkers of oxidative stress (Di Giulio *et al.*, 1995; Regoli and Principato, 1995).

Biomarkers are defined as "specific biological responses (biochemical, cellular, molecular, physiological or behavioural) related to metabolism, detoxification or toxicity, measurable in cells, tissues or body fluids, or at the organism level, that are indicative of exposure to and/or effects of one or more contaminants. Biomarkers being rapidly activated give early 'early warning' signals of the stress in organisms. These rapid responses will allow the prediction of changes at higher levels of biological organization (i.e. population, community or ecosystem) in time for the initiation of bioremediation strategies before irreversible environmental damage of ecological consequences occurs (Cajaraville *et al*., 2000; Lam and Gray, 2003; Monserrat *et al*., 2007; van der Oost *et al*., 2003).

Biomarkers are different in their significance and terminology, being generally classified as biomarkers of exposure, effect and susceptibility. It is generally believed that exposure biomarkers indicate that the organism was exposed to contaminants or to its metabolites, by measuring their interaction with some specific target molecule or cell, even if not directly linked to harmful (toxic) effects. On the other hand, effect biomarkers should express the magnitude of the organisms' response (biochemical, physiological or other alterations) to the contaminant or associated metabolites before disturbances are detected at the population community or ecosystem levels. Biomarkers of susceptibility express the inherent or acquired ability of an organism to respond to the challenge of exposure to a specific contaminant. These biomarkers are indicators of the mechanistic processes that cause variability among the compartment between exposure and/or effect, including genetic factors and changes in receptors that alter the susceptibility of an organism to that exposure (Cajaraville *et al*., 2000; Lam and Gray, 2003; Schlenk, 1999; van der Oost *et al*., 2003)

Biomarkers indicating exposure to contaminants and their effects are increasingly applied in monitoring programs to assess the health of estuarine and marine ecosystems. Moreover, the assessment of the biological effects should be based on a battery of different biomarkers, since no single biomarker can unequivocally measure and reflect environmental stress (e.g. Dagnino *et al*., 2007; Galloway *et al*., 2004). The use of a suite of biomarkers at different levels of biological organization may therefore provide a clearer insight into the mechanisms of the environmental hazard (Lam and Gray, 2003; Schlenk, 1999; van der Oost *et al*., 2003).

Nevertheless, there is a limited number of well-established "core" biomarkers used routinely in marine environmental programs (Cajaraville *et al*., 2000; Viarengo *et al*., 2007) and still a need exists to develop new biomarkers that could be useful as diagnostic tools for specific types of responses or specific groups of existing and emerging contaminants (Porte *et al*., 2006), as the case of NPs.

Biomarkers are more sensitive indicators than traditional toxicity testing (e.g. survival) on the potential impact of NPs. Nevertheless, classic and recently developed endpoints of toxicity need to be investigated in different marine models exposed to different NPs (Handy *et al*., 2012; Matranga and Corsi, 2012). It is possible to select a group of biomarkers to identify overall NPs toxicity and to check for any specific modes of action that may not be detected by a general toxicity screen. In addition to immunotoxicity, genotoxicity or oxidative stress testing, the most applied endpoints so far in nanotoxicological studies, more specific assays related to cell surface defence or cellular biotransformation mechanisms (e.g. trans-membrane pumps or ATP-binding cassette ABC transporters, cytochrome P450 system) may help to understand the major toxic modes of action that could be relevant for different NP types, as well as point out similarities in toxic effects between macro- and nano- particles of similar substances (Crane *et al*., 2008; Matranga and Corsi, 2012). In fact, the application of a multi-biomarker approach was suggested to evaluate oxidative stress and toxicity of NPs and provide a more accurate characterization of their potential impact (Klaper *et al*., 2009).

Having in mind that one of the most common mechanism of toxic action of NPs is oxidative stress; it is possible to select a set of biomarkers to express the biological responses. These biomarkers include some of the known components of the antioxidant defence systems (as the enzymes CAT, SOD and GPX, and the metal-induced protein metallothionein) to test the antioxidant capacity of the organism against ROS formation due to NPs, and in case of antioxidant defence failure, the resulting oxidative damages (e.g. lipid peroxidation, DNA damage and acetylcholinesterase).

#### *1.2.3.2.2. Antioxidant defences*

Living organisms have evolved antioxidant defence mechanisms that prevent and intercept ROS to reduce their harmful effects in cells, along with repair mechanisms for oxidized components. Antioxidants are generally ubiquitous substances in animal species and different tissue-types widely found in aquatic organisms and whose presence, properties and other characteristics have been reviewed in literature throughout the years. The antioxidant systems

principally consist of three general classes that comprise biologically important compounds as intracellular antioxidant enzymes (e.g. SOD, CAT, GPX, glutathione reductase (GR) and glutathione S-transferase (GST)) and non-enzymatic defences as both the low molecular cytosolic water-soluble (ascorbic acid (vitamin C)), reduced glutathione (GSH), metallothionein (MT) and carotenenes (including ß-carotene) and membrane bound fat-soluble free radical scavengers (retinol (vitamin A) and α-tocopherol (vitamin E)), that are represented in Figure 1.10 ( e.g. de Almeida *et al*., 2007; Livingstone, 2001; Matés, 2000).

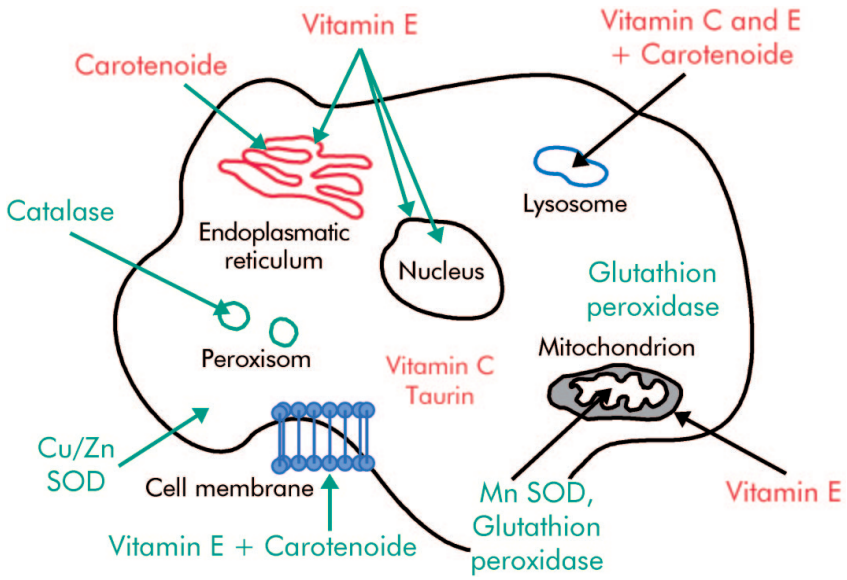


**Figure 1.10 –** Attack by and defence against free radicals; sites with antioxidant effect (red) and enzymes (green). SOD = superoxide dismutase (Simkó *et al*., 2011).

These various antioxidants can either directly or indirectly protect cells against the adverse effects of radical reactions by intercepting reagents and prevent ROS formation, by scavenging free reactive radicals to protect molecular targets against oxidative injury or by stimulating detoxification mechanisms within cells resulting in increased detoxification of ROS formation (Livingstone, 2001; Matés, 2000; Valavanidis *et al*., 2006). The levels of antioxidant enzymatic activities and scavengers vary according to various endogenous (e.g. age) and exogenous factors (e.g. reproductive cycle) and other pro-oxidants, where the balance between ROS production and antioxidant defences determines the degree of oxidative stress (Finkel and Holbrook, 2000; Livingstone, 2001). In this context, their induction under oxidative stress is an important indicator of contaminant-mediated oxidative stress, including NPs (de Almeida *et al*., 2007; Regoli and Principato, 1995).

Some of the most important antioxidant enzymes involved in the intricate antioxidant defence system in biological systems is SOD, CAT and GPX. An overproduction of ROS can be counteracted by the action of the antioxidant enzymes cascade initiated by SOD activity that metabolizes the highly reactive $O_2^{-\bullet}$ into less reactive species, $O_2$ and $H_2O_2$ (Equation 2). SOD plays a very important antioxidant role, being highly active not only in the presence of increased oxyradicals production but also upon exposure to redox-active contaminants. Hydrogen peroxide will in turn be transformed by CAT into $H_2O$ and $O_2$ (Equation 3). CAT is one of the most efficient enzymes that are turned on at high $H_2O_2$ concentrations, whereas at low rates of $H_2O_2$ generation only has a minor role in the catabolism of this radical. Finally, GPX reduces both organic hydroperoxides (ROOH) to their correspondent alcohols (ROH) and $H_2O_2$ to $H_2O$, associated to GSH oxidation (Equation 4) (Di Giulio *et al*., 1995; Halliwell and Gutteridge, 1984, Matés, 2000, Valavanidis *et al*., 2006). Accordingly, antioxidant enzymatic responses would be helpful to assess the oxidative status of organisms and reflect the biological effects of NPs capable to produce ROS.

MTs have high cysteine content (30%), low molecular weight, heat-stability, which may regulate the cellular metal homeostasis by binding and detoxifying metals such as Zn, Cu, Cd, Hg and Ag. MT is also known to have a protective role against oxidative damage caused by ROS by binding and sequestering transitions metals or scavenging oxyradicals as hydrogen peroxide (Amiard *et al*., 2006; Langston *et al*., 1998; Viarengo *et al*., 1999). So, this protein will probably have a valuable role as a biomarker as exposure to NPs, especially in the case of metal NPs.

#### *1.2.3.2.3. Oxidative damages*

When pro-oxidant forces overcome antioxidant defences, the imbalance or loss of cellular redox homeostasis results in oxidative stress, causing severe alterations and damage to virtually all biological molecules, including DNA, RNA, cholesterol, lipids, carbohydrates, proteins and antioxidants (Davies, 2005; de Almeida *et al*., 2007; Valavanidis *et al*., 2006). Increased levels of oxidative damage occur in organisms exposed to redox-active contaminants, as in the case of NPs, which stimulate ROS and other pro-oxidant production (Livingstone, 2001). However, it is also important to realize that increased ROS formation and oxidative damage also occur not because of direct pro-oxidant properties of NPs, but rather because of some organelle dysfunction caused by NPs (e.g. damage to mitochondria or endoplasmic reticulum) that can enhance the toxicity (Moore, 2006; Unfried *et al*., 2007).

Some of the most common examples of biochemical and physiological damages associated with oxidative stress are lipid peroxidation (LPO) (formation of malonaldehyde-like species and 4-hydroxyalkenals), protein oxidation (non-peptide carbonyl groups) and DNA damage (8-hydroxydeoxyguanosine and other oxidized bases) (Livingstone, 2001), that have been described as some of the mechanisms involved in the damage caused by NPs (Klaine *et al*., 2008; Unfried *et al*., 2007).

Membrane phospholipids of aerobic organisms are continually subjected to oxidant challenges from endogenous and exogenous sources, while peroxidised membranes and LPO products represent constant threats to cells. Lipids, particularly polyunsaturated fatty acids in phospholipids of both the cellular and mitochondria membrane are particularly prone to attack by ROS due to its double bonds between carbon atoms. This reaction is one of the most predominant mechanisms of cellular injury that is induced by $OH^{\bullet}$, which takes electrons from the polyunsaturated lipid (LH) causing a chain reaction during which the lipid will be further degraded into lipid hydroperoxide ($LOO^{\bullet}$). Peroxidised fatty acids can trigger reactions that generate other reactive species, including lipid alkoxyl radicals (LO•), aldehydes (e.g. malondyaldehyde, $HOC\text{-}CH_2\text{-}CHO$), alkanes, lipid epoxides and alcohols, that lead to more cell membrane and DNA damage (Fig. 1.11) (de Almeida *et al*., 2007; Halliwell and Gutteridge, 1984; Lesser, 2006; Valavanidis *et al*., 2006). The oxidation of the double bounds of fatty acid tails of membrane phospholipids is commonly known as LPO. LPO result in the formation of lipid-lipid, lipid-protein, protein-protein cross links which alter the structure and function of cellular membranes. As these reactions continue, ionic channels are affected, membrane transport proteins or enzymes inactivated, or the lipid bilayer become more permeable and fluid thereby disrupting ion homeostasis and making cells more susceptible to osmotic stress. In the mitochondria, the presence of lipid peroxides is particularly cytotoxic, with multiple effects on membrane properties, enzyme activity, respiration and oxidative phosphorylation and consequently ATP production, as well as on the initiation of apoptosis (Halliwell and Gutteridge, 1984; Klaine *et al*., 2008; Lesser, 2006; Viarengo and Nott, 1993). So, the determination of LPO levels (or its by-products) could be used as an indicator of oxidative damage and assess the overall efficiency of antioxidant system of organisms exposed to NPs.

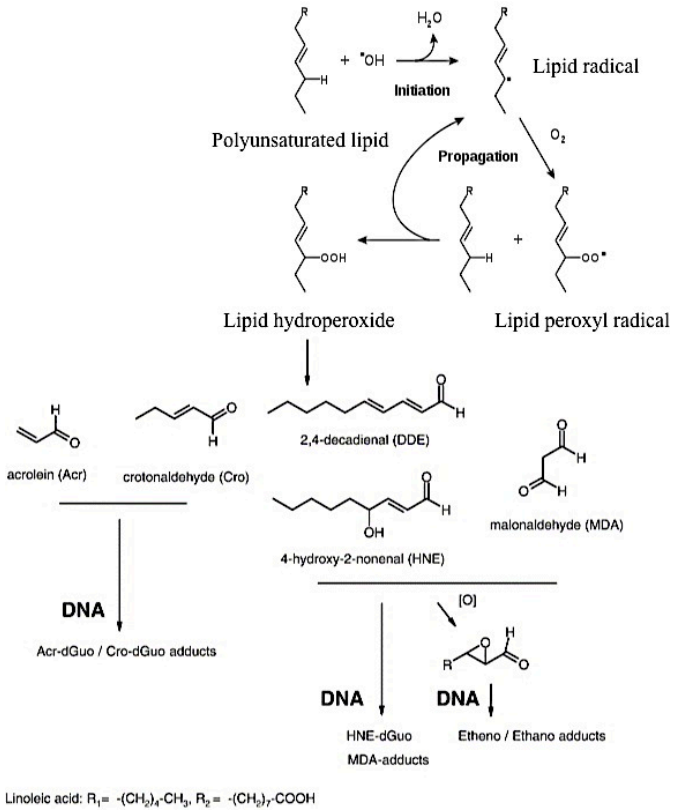


**Figure 1.11 –** Lipid peroxidation mediated by hydroxyl radical ($OH^{\bullet}$) and reactive aldehydes formed as by-products (adapted from Di Giulio *et al*., 1995 and de Almeida *et al*., 2007).

Proteins are one of the targets for oxidative stress as a result of their abundance in biological systems, and their high constants rates, making them highly susceptible to the adverse effects of NPs, either by NPs-protein physical interaction or to oxidative attacks by NPs producing ROS or other damaging radicals (Klaine *et al*., 2008). Oxidative stress can induce a wide range of reversible and irreversible modifications to proteins and their side chains (Davies, 2005; McDonagh and Sheehan, 2006). These oxidative stress-induced modification can result in site-specific modifications of amino acid side chains, peptide cleavage, reactions of peptides with lipids and carbohydrate oxidation products (e.g. peroxyl radicals formed during LPO), effects on disulphide patters (glutathionylation), altered electrical charge, increased susceptibility to removal and degradation, and formation of carbonyl derivatives of proteins (carbonylation) (Finkel and Holbrook, 2000; McDonagh and Sheehan, 2006; Valavanidis *et al*., 2006). The ratio of oxidative attack on proteins is dependent of a number of factors. Protein structure (primary, second or tertiary) along with existing different types of amino acids side-chains will determine the protein susceptibility for ROS attack and result in several potential reaction sites. Additionally, ROS forms also differ in potential reactivity giving rise

to limited and specific residue damage or to widespread non-specific damage. For many enzymes, the oxidation of sulfhydryl groups (e.g. methionine and cysteine) by ROS can activate or inactivate enzymatic function, while other amino acids, (e.g. arginine, lysine, threonine, proline and serine) form protein carbonyls, alcohols, and peroxides when oxidized, which have the ability to perturb the tertiary structure of proteins and lead to unfolded or misfolded proteins (Finkel and Holbrook, 2000; Lesser, 2006; Valavanidis *et al*., 2006). Most of these modifications lead to protein damage and inactivation (e.g. irreversible modifications) some protective of the protein's structural integrity and related to changes in the cellular redox status and consequent response to oxidative stress (e.g. glutathionylation and effects in disulfide bonds) (Davies, 2005; McDonagh and Sheehan, 2006). The consequent alteration on functional or structural integrity of proteins triggers a range of deleterious functional consequences that ultimately lead to cellular dysfunction and tissue damage.

#### *1.2.3.2.4. Genotoxicity*

DNA is another key cellular component highly susceptible to oxidative damage. NMs have unpredictable genotoxic properties with several mechanisms controlling their capacity to promote DNA damage (Fig. 1.12). Direct or indirectly, damage occur not only generated by direct particles influence through their reactivity and surface area and/or physical and chemical properties, by transition metals comprised or released from the particles (e.g. Cu, Fe, Cd) with the ability to produce ROS and generate oxidative stress, mechanical interference with cellular components or by direct interaction with DNA (Gonzalez *et al*., 2008; Karlsson, 2010; Singh *et al*., 2009; Unfried *et al*., 2007).

The main genotoxic effect of NPs comes from the production of ROS (e.g., $^1O_2$, $O_2^{-\bullet}$, $H_2O_2$ and $OH^\bullet$), either by the particles themselves, the induction of cellular responses or stimulation of target cells, presence of metallic contaminants or particle induced inflammatory processes. The presence and release/dissolution of transition metal ions (e.g. cadmium, copper, iron, nickel, titanium, zinc) from NPs can enhance ROS production by metal-catalysed Fenton and Haber-Weiss reactions (as previously described) and result in the formation of $OH^\bullet$, which are one of the primary DNA damaging species (Donaldson *et al*., 2010; Gonzalez *et al*., 2008; Singh *et al*., 2009). NPs or intracellular metal ions released from the particles can also enhance the permeability of the lysosomal membrane that lead to the release of DNase into the cytoplasm and passage to the nucleus, where it can cut DNA

(Karlsson, 2010). Other cellular components can indirectly enhance the production of ROS and consequently induce oxidative DNA damage, as mitochondria and membrane bound NADPH oxidases, in response to interactions with NPs and/or through depletion or impairment of the antioxidant defence system (e.g. GSH). In situations of chronic inflammation this can lead to persistent oxidative stress and to DNA damage in the form of chromosomal fragmentation, point mutations and DNA adducts, that if not repaired can ultimately lead to induction of DNA cell cycle arrest, carcinogenesis and apoptosis (Donaldson et al., 2010; Gonzalez *et al*., 2008; Lesser, 2006; Singh et al., 2009).

Direct NPs genotoxicity can be caused either by a direct interaction of the particles with DNA or with cellular constituents associated with DNA integrity. Cellular internalization and accumulation of NPs inside cells promote direct interaction with DNA inside the nucleus. NPs enter the nucleus either by direct passage across the membrane, transport through nuclear pore complexes or become trapped within the nucleus during mitosis when the nuclear membrane breaks down and they induce several DNA damages. Upon nuclear penetration, direct interaction between NPs and the DNA molecule or DNA-related proteins (e.g. nucleosomes, microtubules, actin filaments, centrosomes) lead to numerous physical or chemical interferences along with damage to the genetic material, as disturbed cellular trafficking and inhibition of replication, transcription and cell proliferation (Donaldson *et al*., 2010; Gonzalez *et al*., 2008; Singh *et al*., 2009 and literature cited therein). Other possible genotoxic effects of NPs are also referred by Gonzalez *et al*. (2008), as interaction with sulfhydryl groups and Zn-finger proteins, saturation of MTs, inhibition of key receptors/enzymes and changes in DNA methylation, nevertheless, less specific to NPs toxicity.

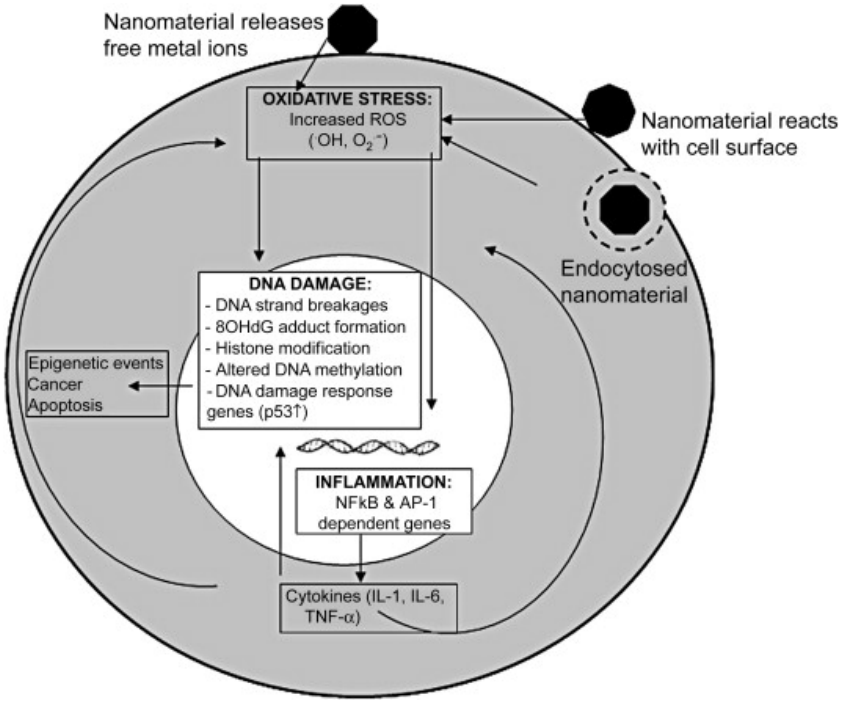


**Figure 1.12 –** Mechanisms that can lead to NPs genotoxicity. NMs result in oxidative stress or inflammatory responses with the potential to damage DNA and alter transcriptional patterns in cells (Singh *et al*., 2009).

Overall, many evidences suggest that NPs-induced toxicity is mediated through oxidative stress with several negative outcomes to cells, nevertheless, further research is required to fully understand their underlying mechanisms.

#### *1.2.3.2.5. Neurotoxicity*

The brain is also vulnerable to oxidative stress damage (high content of peroxidisable unsaturated fatty acids, high oxygen consumption rate and lack of antioxidant enzymes), and recent evidence suggests that different NPs can cross the blood-brain barrier and gain access to the central nervous system. As an important enzyme in the nervous system, NPs may bind to acetylcholinesterase (AChE) and affect its activity. This enzyme is responsible for the correct transmission of nerve impulses, by hydrolysing the neurotransmitter acetylcholine into choline and acetic acid in cholinergic synapses (Hu and Gao, 2010; Long *et al*., 2006; Wang *et al*., 2009). Many organophosphate and carbamate pesticides are effective AChE inhibitors and the inhibition of this enzyme was used to assess the biological effects of these compounds in the marine environment. However, AChE can be inhibited by a diverse range

of metals, including Cu (Cajaraville *et al*., 2000; Regoli and Principato, 1995). Therefore, this enzyme could be useful to assess the potential neurotoxic capacity of some NPs.

### 1.2.4. Proteomics and the identification of new biomarkers for nanoparticle exposure

Proteomics describes the study of the proteome, the total complement of proteins expressed by a genome within a cell, tissue or organism, under specific conditions. The proteome is very dynamic, where the protein content of cells varies in response to alterations in the environment, physiological state of the cell, drug administration, health and disease. Proteomics analysis is characterized by high-throughput methodologies that enable the high-resolution separation and display of the proteins in the tissue in a form that allows subsequent analysis and comparison. From the hundreds to thousands of proteins that can be obtained in a single experiment, those that are either expressed under a given condition or suppressed relative to the control specimen can subsequently be identified (Alban *et al*., 2003; Knigge *et al*., 2004; Liebler, 2002; Rabilloud, 2000; Snape *et al*., 2004).

Environmental proteomics (or ecotoxicoproteomics) aims to analyse the proteome of organisms and to identify variations in proteins induced by contaminants without the need for detailed knowledge of toxicity mechanisms. A comparison of proteomes from stress conditions (versus controls) has the potential to identify not only single protein markers, but also to generate protein patterns that react to a specific type and degree of stress, and consequently, differentiate exposure and/or effect to contaminants. Differential expression of proteins are compared among chemicals, concentrations or complex mixtures in different natural environments, and the obtained up- or down-regulated proteins combined within protein patterns that are specific to the stressor and the level of environmental stress. These alterations are identified as protein expression signatures (PESs), sets of proteins that potentially offer greater understanding of underlying toxic mechanisms of stress response (Knigge *et al*., 2004; Nesatyy and Sutter, 2007; Shepard and Bradley, 2000). In this context, proteomics has been extensively used in ecotoxicological research in the past few years, where field and laboratory studies showed that different PESs respond significantly to different kinds of contaminants, thus identifying candidate proteins for further study (e.g. Apraiz *et al*., 2006; López-Barea and Gómez-Ariza, 2006; Vioque-Fernández *et al*., 2009). Since PES itself constitutes a biomarker, the need to explicitly identify altered proteins is not indispensable to diagnose adverse environmental effects (Shepard and Bradley, 2000). This is specially useful when using bioindicator species whose genomes or proteomes were not yet

fully sequenced, as in the case of most bivalve species, being sufficient to show altered PES patterns to demonstrate contamination effects (López-Barea and Gómez-Ariza, 2006; Monsinjon *et al*., 2006). Nevertheless, as sequencing information becomes available, the identification of proteins from these non-model organisms (as bivalves) will provide greater understanding of the modes of action of toxic compounds and on how they affect affects organism and ecosystem quality (Monsinjon and Knigge, 2007; Nesatyy and Suter, 2008).

As referred previously, the use of conventional biomarkers were used in nanotoxicology studies; nevertheless, many of the toxic responses (e.g. oxidative stress, LPO, enzymatic activation/inhibition, genotoxicity) are common to several contaminants, including NPs ionic/bulk form (Handy *et al*., 2012). The use of conventional biomarkers present some disadvantages, as they are influenced by confounding factors (e.g. abiotic), highly dependent on the route of exposure, bioaccumulation tendency and detoxification mechanisms of chemicals, require a deep knowledge of the toxic mechanisms of contaminants and prevent a more comprehensive view of toxicity by focusing in only few proteins (Vioque-Fernández *et al*., 2009). Accordingly, there is a need to develop nano-specific biological measurements to differentiate nano-specific responses and mechanisms of action from their similar ionic/bulk counterparts. Proteomics-based methods therefore provide a more insightful view on the global changes in protein expression indicative of NPs exposure or effect by looking for specific molecular signatures (Amelina et al., 2007; López-Barea and Gómez-Ariza, 2006). These PESs can be quantified, identified and used as novel and unbiased biomarkers of NPs exposure and effect. These approaches have already successfully detected new biomarkers in response to conventional contaminants in bivalve species (e.g. Apraiz *et al*., 2006; López-Barea and Gómez-Ariza, 2006; Shepard and Bradley, 2000). Thus, proteomics applied to nanotoxicology may help to identify protein pathways affected by these particles, providing a deep understanding of the molecular mechanisms of NPs-induced stress syndrome in organisms, and help clarify and differentiate the toxic mode of action between macro- and nano- particles of similar substances.

## 1.3. Bivalves and their use in nanotoxicology

For several years, indicator or sentinel species were used to assess environmental quality and evaluate potential effects by contaminants. Accordingly, several monitoring programs were developed, including the “Mussel Watch” Project (MWP) initiated in 1986 using *Mytilus edulis*, to assess the current status and the long-term changes in environmental quality in US

estuarine and coastal waters. Nowadays, the "Mussel Watch" concept has spread worldwide, where several monitoring programs developed routine sampling using bivalve molluscs. More recently, biomarkers were integrated with chemical analyses to evaluate population, individual, tissue, molecular, biochemical and cellular effects induced by contaminants (Kimbrough *et al*., 2008; Livingstone, 1993; Phillips, 1986). Mussels were long recognized as valuable bioindicators of environmental contamination, and extensive background information exists on their biological responses (physiological, cellular and molecular) to a wide range of both inorganic and organic compounds, as well as trace metals (e.g. Cravo *et al*., 2009; Dagnino *et al*., 2007; Regoli and Principato, 1995). Mussels *Mytilus spp*. are the bivalve species more used worldwide that filter feeders and accumulate contaminants in their tissues well above that of surrounding waters (Cajaraville *et al*., 2000). Several other features make bivalves extensively used as sentinel organisms: (i) they are sessile, filter and accumulate particles from water, thus, measuring contaminant levels in their tissues is a good indicator of the contamination of the surrounding environment; (ii) they are relatively resistant to a wide variety of contaminants and environmental stress (e.g. salinity, temperature), thus, being able to survive in naturally stressed environments with different degrees of contamination; (iii) they are easily collected and maintained under well defined laboratory conditions; (iv) they are found in high densities in quite stable populations, allowing repeatedly sampling and time-integrated indication of environmental contamination throughout a sampling area; (v) they are widely distributed worldwide (both in freshwater and marine environments), allowing data comparison from different areas (Kimbrough *et al*., 2008; Livingstone, 1993; Viarengo and Canesi, 1991). For the above reasons, bivalves are therefore useful for characterizing the environmental impact of new and emerging contaminants in the aquatic environment, as NPs.

The use of *Mytilus spp*. as a relevant group of test organisms for investigating the effects of NPs was originally proposed by Moore (2006). They can filter contaminants and particulate matter directly from the water through the gills or indirectly through the digestive system. Particles trapped in the gills are subsequently transported to the labial palps and the mouth for ingestion, thus entering the gut for extracellular digestion by the crystalline style and the digestive gland for sorting and absorption (Baumard *et al*., 1999; Canesi *et al*., 2012; Ward *et al*., 1993). The digestive cells are highly adapted for endocytosis of large particles (>100 nm) for both intracellular digestion and nutrient storage (Moore, 2006; Moore *et al*., 2009). So, whether NMs reach the aquatic environment suspended or in an aggregated form, they will be taken up by these organisms and accumulate in their tissues. These endpoints will provide an

abundant database to compare nanotoxicological responses and decipher the mechanisms of action of NPs in aquatic organisms (Kádar *et al*., 2010a). Even though emissions of NMs to the aquatic environment may be low, their low degradability and unpredictable behaviour combined with the feeding habits of invertebrate species demands for research on the bioaccumulation behaviour and subsequent toxicity of NPs (Baun *et al*., 2008). Some toxicological data from NPs exposure to bivalves already exists, that support the hypothesis that these filter-feeding organisms are one of the major targets of NPs toxicity (see review by Canesi *et al*., 2012).

### 1.3.1. Nanoparticles uptake and effects in bivalve molluscs

For most aquatic organisms, direct ingestion or passage across epithelial boundaries such as gills (first organ in contact with surrounding water), olfactory organs or body wall and the epithelium of the digestive tract or the hepatopancreas (the site of nutrient absorption and storage in invertebrates) are the main routes of NP exposure (Barber *et al*., 2009; Moore, 2006). In the case of bivalve species, only a few studies exist on tissue localization, internal distribution and NPs uptake, accumulation, and toxic effects (Table 1.2). In *Mytilus edulis* exposed to NPs of glass wool (3-7 μm, 0.18-1 μm, 12h-16 days), uptake of NPs into gills occurred within 12 hours, either by diffusion (particles <5 nm) or by endocytosis (5-25 nm and larger fibres). Furthermore, the presence of larger fibrils in the gills suggests that materials are first sorted and transported at the gills before passing to the digestive gland (Koehler *et al*., 2008). On the other hand, the route of entry of NPs of sucrose polyester (1-100 $\mu g.L^{-1}$, 4h) was the digestive gland, where particles were taken up endocytotically by digestive cells and entered the lysosomal degradative compartment (Moore *et al*., 1997). Though evidence shows that some particles can be taken up across the epithelium of the gills and digestive gland, the major route for internal exposure and potential effects of NPs is via uptake by ingestion. In terms of bioavailability, the rate and ingestion dynamics of polystyrene NPs ($1.3x10^4$ $particles.mL^{-1}$, 100 nm, 6-72h.) in *M. edulis* and *Crassotrea virginica* indicate that NPs aggregates are more efficiently captured and ingested than those freely suspended. A longer gut retention time was also detected, suggesting that most of the NPs were directed into the tubules of the digestive gland and potentially taken up by the digestive cells via endocytosis, whereas some small fraction was rejected as pseudofeces (Ward and Kach, 2009). The capacity of mussels *Mytilus galloprovincialis* to filter particulate matter more efficiently than dissolved substances was confirmed by exposing

mussels to 1-10 mg.$L^{-1}$ of ZnO NPs (24 ± 3 nm) and $CeO_2$ NPs (67 ± 8 x 8 ± 31 nm) for 4 days. NPs were accumulated differentially in mussel tissues, with a strong preference for ZnO NPs, mostly likely due to $Zn^{2+}$ dissolution, whereas for $CeO_2$ NPs a higher retention in the gut was associated with a lower dissolution rate. A higher proportion of $CeO_2$ agglomerates were subsequently found in pseudofaeces (Montes *et al*., 2012). In the clam *Corbicula fluminea* exposed to 2-8 mg.$L^{-1}$ of BSA coated Au NPs (7, 15 and 46 nm) for 12-180h, NPs were mainly accumulated in the digestive gland in the nano form, with extended retention times in the gut indicative of extracellular digestion of the particles. Additional examination of faecal material indicated that dissolution or mechanical alterations of the particles could occur (resulting in nanoscale aggregated and individual particles) as a result of digestion and excretion (Hull *et al*., 2011).

**Table 1.2 –** Effects of different NPs in different species of bivalve molluscs.

| Species | NPs | | | | Observed effects | Reference |
|---|---|---|---|---|---|---|
| | Type | Concentration | Size | Duration | | |
| ***Corbicula fluminea*** | Au NPs | $1.6x10^3$-$1.6x10^5$ Au NPs/ cell | 10.0 ± 0.5 nm | 7 days | Accumulation in branchial and digestive epithelial cells. MT induction and oxidative stress in gills and visceral mass by genetic expression changes of CAT, SOD, GST and cytochrome C oxidase subunit-1. | Renault *et al*., 2008 |
| | BSA-coated Au NPs | 2-8 $mg.L^{-1}$ | 7.8, 15 and 46 nm | 12-180h | NPs accumulation in the digestive gland namely in the nano form. High retention times in the gut indicative of extracellular digestion. Mechanical alterations of the NPs as a result of digestion and excretion, resulting in nanoscale aggregated and individual particles. | Hull *et al*., 2011 |
| ***Elliptio complanata*** | Cd telluride quantum dots | 0-8 $mg.L^{-1}$ | - | 24h | High NPs aggregation and accumulation in tissues. Alterations in hemocytes immunocompetence (viability, number, phagocytic activity), high LPO in the gills and DNA damage in gills and digestive gland. Dose-response toxicity. | Gagné *et al*., 2008 |
| | | 0-8 $mg.L^{-1}$ | - | 24h | NPs accumulation in gills, digestive gland and gonads from NPs dissolution rather than uptake. Induction of MTs in digestive glands and gonad. MT decrease in the gills associated with oxidative stress by NPs or dissolved $Cd^{2+}$. | Peyrot *et al*., 2009 |
| ***Crassostrea virginica*** | C60 fullerenes | 1-500 $\mu g.L^{-1}$ | 10-100 nm | 4 days | NPs accumulation in digestive gland (namely lysosomes). Abnormal development in larvae, lysosomal membrane destabilization in digestive gland. No LPO. | Ringwood *et al*., 2009 |
| | Polysterene beads | $1.3x10^4$ particles.$mL^{-1}$ | 100 nm | 6-72h | NPs aggregates efficiently captured and ingested than those freely suspended. High gut retention time, with NPs directed into the digestive gland and taken up via endocytosis. NPs small fraction rejected as pseudofeces. | Ward and Kach, 2009 |

| | | | | | | |
|---|---|---|---|---|---|---|
| ***Crassostrea virginica*** | Ag NPs | 1.6-0.0016 µg.L$^{-1}$ | 15 ± 6 nm | 48h | Adverse effects on embryonic development and lysosomal integrity in adult oysters. High MTs induction in embryos compared to adults. | Ringwood *et al*., 2010 |
| ***Mytilus edulis*** | Sucrose polyester | 1-100 µg.L$^{-1}$ | - | 4h | NPs taken up endocytotically by digestive cells and the lysosomal degradative compartment. | Moore *et al*., 1997 |
| | Glass wool ($SiO_2$) | 3-7 µm | 0.18-1 µm | 12h-16 days | NPs uptake into gills by diffusion or endocytosis and into lysosomes and endocytic vesicles of digestive cells. Lysosomal destabilization and oxidative stress in the form of lipofuscin accumulation. Continuous NPs uptake followed by apoptosis. | Kohler *et al.*, 2008 |
| | Gold-citrate NPs | 750 µg.L$^{-1}$ | ~13 nm | 24h | NPs accumulation and oxidative stress in the digestive gland with higher ubiquitination of proteins and CAT induction. Gills with higher carbonylation and ubiquitination. | Tedesco *et al*., 2008 |
| | $Fe_2O_3$ NPs | 1 mg.L$^{-1}$ | 5-90 nm | 30 min-12h | High percentage of Fe lost in water associated with sedimentation and aggregation. Cellular uptake by pinocytosis (aggregates and small particles) linked to LPO in the gills. Impairment of lysosomal membrane stability in hemocytes. No neurotoxicity. | Kádar *et al*., 2010a |
| | Au NPs | 750 µg.L$^{-1}$ | 15.6 ± 5 nm | 24h | NPs accumulation, namely in the digestive gland. Decrease in reduced/oxidized GSH ratio and reduction in protein thiols in the digestive gland. No LPO or induction of thioredoxin reductase. | Tedesco *et al*., 2010a |
| | | 750 µg.L$^{-1}$ | 5.3 ± 1 nm | 24h | NPs accumulation, with high LPO and decreased thiol-containing proteins. Decrease in membrane lysosomal stability in hemocytes. Size a key factor in NPs toxicity. | Tedesco *et al*., 2010b |
| | Ag NPs | 0.7 µg.L$^{-1}$ | <40 nm | 3h30 min-72h | NPs uptake and higher concentrations in digestive gland. Hemocytes play an important role in Ag translocation in tissues. | Zuykov *et al*., 2011 |

| | | | | | | |
|---|---|---|---|---|---|---|
| ***Mytilus galloprovincialis*** | Nano carbon black | 1-10 µg.mL$^{-1}$ | 35 ± 12 nm | 30 min-4h | NPs taken up by hemocytes (concentration-dependent). High extracellular lysozyme release, extracellular oxyradical production and nitric oxide release. Changes in mitochondrial parameters (decrease mitochondrial mass/number and membrane potential). Early apoptotic processes at higher concentrations. | Canesi *et al*., 2008 |
| | C60-fullerenes, carbon nanotubes | 1-10 µg.L$^{-1}$ | | 60 min | Decrease in lysosomal membrane stability in hemocytes linked to the ingestion of NPs by phagocytosis and endocytosis and ROS formation. No effects by carbon nanotubes. | Moore *et al*., 2009 |
| | Polysterene beads | 1.3x10$^{4}$ particles.mL$^{-1}$ | 100 nm | 6-72h | NPs aggregates efficiently captured and ingested than those freely suspended. High gut retention time, with NPs directed into the digestive gland and taken up via endocytosis. NPs small fraction rejected as pseudofeces. | Ward and Kach, 2009 |
| | C60 fullerene, $TiO_2$ and $SiO_2$ | 0.7, 22 and 12 nm | 1-10 µg.mL$^{-1}$ | 30 min-4h | NPs aggregation and uptake by hemocytes. Release of lysosomal hydrolytic enzymes, oxidative burst and nitric oxide production, with different extent and time courses depending on NP concentration and type. No effects in lysosomal membrane stability. | Canesi *et al*., 2010a |
| | Nano carbon black, C60 fullerenes, $TiO_2$ NPs and $SiO_2$ NPs | 0.05-1.5 mg.mL$^{-1}$ | 30, 0.7, 22 and 12 nm | 24h | Changes in lysosomal parameters in the digestive gland, namely lysosomal membrane destabilization, lipofuscin and neutral lipid accumulation (except for C60). CAT induction by all NPs. Lysosomal membrane destabilization in hemocytes. GST stimulation by NCB and $TiO_2$ NPs. Lysosomal and oxidative stress biomarkers responses associated with the presence of large NPs aggregates in the digestive gland. | Canesi *et al*., 2010b |
| | $Fe_2O_3$ NPs | 0.1-10 mg.L$^{-1}$ | 40.1 ± 1.3 nm | 48h | No effects in larval development associated with NPs aggregation. | Kádar *et al*., 2010b |

| | | | | | | |
|---|---|---|---|---|---|---|
| ***Mytilus galloprovincialis*** | Zero-valent nanoiron | 0.1-10 $mg.L^{-1}$ | 50 nm | 48h | Disruption in embryos development (high mortality, decline in fertilization success and delay in development). DNA damage in sperm at higher concentrations. Toxicity linked to aggregation behaviour of NPs. | Kádar *et al*., 2011 |
| | $CeO_2$ and ZnO NPs | 1-10 $mg.L^{-1}$ | 67 ± 8 × 8 ± 31nm, 24±3 nm | 4 days | High accumulation of ZnO NPs due to $Zn^{2+}$ dissolution. High retention of $CeO_2$ NPs in the gut associated with a lower dissolution rate. Higher proportion of $CeO_2$ agglomerates in pseudofaeces, dependent of NP concentration. | Montes *et al*., 2012 |
| ***Mytilus spp.*** | C60 fullerenes | 0.1-1 $mg.L^{-1}$ | 100–200 nm | 3 days | NPs accumulation, namely in the digestive gland. Concentration-dependent increases in DNA strand breaks, with no evidence of DNA adduct formation. Abnormalities in the adductor muscle, digestive gland and gills, and alterations in clearance rate. Oxidative stress in the form of induction of total GSH content. | Al-Subiai *et al*., 2012 |
| ***Scrobicularia plana*** | CuO NPs | 10 $\mu g.L^{-1}$ | 40-500 nm | 16 days | High NPs aggregation and no particle dissolution. NPs accumulation in tissues. Impaired burrowing and feeding behaviours, induction of SOD, CAT and GST activities, and MT-like proteins, suggesting a specific NP effect. No neurotoxicity. | Buffet *et al*., 2011 |
| | $^{67}$ZnO NPs | 3 $mg.kg^{-1}$ sediment | 21-34 nm | 16 days | NPs accumulation in tissues. Induction of CAT activity and no effects in GST, SOD and MT. Impaired burrowing and feeding behaviours. | Buffet *et al*., 2012 |
| | Au NPs | 5, 15 and 40 nm | 100 $\mu g.L^{-1}$ | 16 days | NPs accumulation namely aggregates. MT induction and increase in AChE (overcompensation). Oxidative stress in the form of induction of CAT, SOD and GST activities. Impaired burrowing behaviour. | Pan *et al*., 2012 |

From the above examples, bivalve molluscs are able to ingest a variety of NPs, by an efficient filtration from the water column depending on particle diameter, accumulation in tissues and/or excretion in the form of pseudofeces (Hull *et al*., 2011; Montes *et al*., 2012; Ward and Kach, 2009;). Under natural conditions, aggregation of NPs into larger particle and incorporation into aggregated material (e.g. colloids) or other compounds (e.g. metals) will increase their bioavailability to suspension-feeding bivalves (Canesi *et al*., 2012; Ward and Kach, 2012). NP uptake will depend of the form in which the NPs are present (e.g. monodispersed, slightly aggregated or highly aggregated) and the capture efficiency of the bivalve species (e.g. NPs masses <5 μm will be captured and ingested with different efficiencies) (Ward and Kach, 2012). These processes influence the mass of NPs that will interact with bivalves, in both natural and experimental exposures, where the exposure levels might be much lower than those initially designed based on mass/number per volume of water delivered to the animals (Canesi *et al*., 2012; Ward and Kach, 2012). Nevertheless, there is still a lack of physiological data on the mode of uptake, ingestion or loss rate constants in different species, so whatever the exposure conditions and particle size (and other properties), the actual internal exposure concentration of NPs in bivalves is practically unknown (Canesi *et al*., 2012, Fabrega *et al*., 2011).

The accumulation and effects of different types of NPs have been evaluated in both freshwater and marine bivalves. In the freshwater clam *C. fluminea*, Au NPs (1-10 $1.6x10^3$-$1.6x10^5$ Au NPs/cell, 10.0 ± 0.5 nm, 7 days) accumulated in branchial and digestive epithelial cells and induced MT and oxidative stress in gills and visceral mass by altering the genetic expression of CAT, SOD, GST and cytochrome C oxidase subunit-1 (Renault *et al*., 2008). In the freshwater mussel *E. complanata*, cadmium telluride quantum dots (CdTe QDs, 0-8 $mg.L^{-1}$, 24h) were accumulated in tissues, with significant alterations in hemocytes immunocompetence (viability, number, phagocytic activity), together with LPO in the gills and DNA damage in gills and digestive gland (Gagné *et al*., 2008). In addition, exposure to CdTe QDs also led to induction of MTs in digestive glands, whereas in gills a decrease in MT levels was associated with the oxidation of this protein by the production of ROS at the surface of the QDs or by dissolved $Cd^{2+}$ (Peyrot *et al*., 2009). In oysters *C. virginica*, C60 fullerene (1-500 $\mu g.L^{-1}$, 10-100 nm, 4 days) accumulated *in vitro* in digestive gland cells (namely in lysosomes) and induced lysosomal membrane destabilization, whereas *in vivo* exposure induced abnormal development in larvae, digestive gland lysosomal membrane destabilization but no LPO in adults (Ringwood *et al*., 2009). Adverse effects of Ag NPs (16-0.0016 μg.L-1, 15 ± 6 nm, 48h) were observed on embryonic development and lysosomal

integrity in adult oysters despite the induction of MTs (Ringwood *et al*., 2010). In mussels *M. edulis*, exposure to glass wool (3-7 µm length, 0.18-1 µm, 12h-16 days) resulted in uptake in lysosomes and endocytic vesicles of digestive cells, associated with lysosomal destabilization and oxidative stress in the form of lipofuscin accumulation. Continuous uptake of NPs over time resulted in apoptosis (Koehler *et al*., 2008). Increased accumulation and oxidative stress were also reported in the digestive gland of *M. edulis* exposed to gold citrate NPs (750 $\mu g.L^{-1}$, 13 nm, 24h), with higher ubiquitination of proteins and CAT induction, when compared to the gills (higher carbonylation) (Tedesco *et al*., 2008). *M. edulis* exposed to the same Au NPs (~15 nm) showed a decrease in the reduced/oxidized glutathione ratio and a reduction in protein thiols, but without any changes on LPO or induction of thioredoxin reductase activity (Tedesco *et al*., 2010a). When using a smaller particle size (5.3 ± 1 nm), the same authors showed that Au NPs mainly accumulated in the digestive gland, where increased LPO and decreased thiol-containing proteins were observed, along with a decrease in membrane lysosomal stability in hemocytes. These results suggest that Au NP size is a key factor in biological responses (Tedesco et al., 2010b). In *M. edulis* exposed to $Fe_2O_3$ NPs (1 $mg.L^{-1}$, 5-90 nm, 30 min-12h), cellular uptake by pinocytosis was linked to oxidative stress in the form of LPO in the gills, along with impairment in lysosomal membrane stability in hemocytes, with similar responses between Fe forms (Kádar *et al*., 2010a). Mussels *M. edulis* exposed to radiolabelled Ag ($^{110m}Ag$, 0.7 $\mu g.L^{-1}$, 3h30min-72h) added to seawater in dissolved and nanoparticulate (<40 nm) phases also showed an important uptake and a similar Ag distribution with maximum concentrations in the digestive gland, where hemocytes seem to play an important role in Ag translocation in mussels tissues (Zuykov *et al*., 2011). Using the mussel *M. galloprovincialis*, *in vitro* alterations in hemocytes immune parameters were reported, in response to carbon black NPs (NCB, 35 ± 12 nm), C60-fullerenes (0.7 nm), $TiO_2$ (22 nm) and $SiO_2$ (12 nm) NPs. All particles were taken up by hemocytes (concentration-dependent), stimulating the release of lysosomal hydrolytic enzymes, oxidative burst and nitric oxide production, with different time courses (30 min-4h) depending on NP concentration (1-10 $\mu g.L^{-1}$) and type (Canesi *et al*., 2008, 2010a). At higher concentrations, NCB induced significant changes in mitochondrial parameters (decrease mitochondrial mass/number and membrane potential), suggesting early apoptotic processes (Canesi *et al*., 2008). Similar effects were reported by Moore *et al*. (2009) in the same species, characterized by decrease in lysosomal membrane stability in hemocytes linked to the ingestion of C60-fullerene suspensions by phagocytosis and endocytosis, in contrast to carbon nanotubes where no effects were detected. Following up the results obtained *in vitro*, Canesi *et al*.

(2010b) reported the possible effects of *in vivo* exposure of CNB (30 nm), C60-fullerenes (0.7 nm), $TiO_2$ (22 nm) and $SiO_2$ (12 nm) NPs in the mussel *M. galloprovincialis*. Exposure to all NPs (0.05-1.5 $mg.L^{-1}$, 24h) induced significant changes in lysosomal parameters in the digestive gland, namely lysosomal membrane destabilization, lipofuscin and neutral lipid accumulation (except for C60). Additionally, CAT induction was observed upon exposure to all NPs, along with GST stimulation by NCB and $TiO_2$ NPs. The significant changes in lysosomal and oxidative stress biomarkers observed in the digestive gland are associated with the presence of large particle aggregates over time of exposure (Canesi *et al*., 2010b). Exposure to $Fe_2O_3$ NPs (40.1 ± 1.3 nm) did not affect larval development in *M. galloprovincialis* (Kádar *et al*., 2010b), whereas zero valent nano-iron (nZVI, ~50 nm) caused serious disruption of development in mussels' embryos (mortality, fertilization success and delay in development), as well as DNA damage in sperm exposed to higher concentrations (Kádar *et al*., 2011). Finally, in *Mytilus spp.* exposed to C60-fullerenes (0.1-1$mg.L^{-1}$, 100-200 nm, 3 days), accumulation was observed in all organs, namely in the digestive gland, as well as concentration-dependent increases in DNA strand breaks, but with no evidence of DNA adduct formation. Furthermore, abnormalities in the adductor muscle, digestive gland and gills, and alterations in clearance rate were observed. Signs of oxidative stress were also detected, in the form of induction of total glutathione content (Al-Subiai *et al.*, 2012). In the marine clam *S. plana*, exposure to CuO NPs (10 $\mu g.L^{-1}$, 40-500 nm, 16 days) induced Cu accumulation, affected burrowing and feeding behaviours and increased SOD, CAT and GST enzymatic activities, along with MT-like protein induction, suggesting a specific NP effect (Buffet *et al*., 2011). In *S. plana* exposed to $^{67}ZnO$ NPs (3 $mg.Kg^{-1}$, 21-34 nm, 16 days) in sediments, NPs accumulated significantly in clam tissues but only CAT activity was induced, whereas GST, SOD and MT were not affected (Buffet *et al*., 2012). Accumulation of Au NPs (100 $\mu g.L^{-1}$, 5, 15 and 40 nm, 16 days) was observed in *S. plana* tissues (namely aggregates), where induction of MT, increase in AChE (overcompensation), CAT, SOD and GST activities (indicative of oxidative stress), along with impaired burrowing behaviour were observed (Pan *et al*., 2012).

Although NP uptake and toxicity occurs in freshwater and marine bivalves, it is unclear whether toxicity is induced following internalization of particulates, the release of soluble ions or extracellular/intracellular generation of ROS or to the specific physical characteristics of NPs. In this context, bivalves represent a major target for NPs toxicity and have proven its suitability as a model for investigating the effects and mechanisms of action underlying the potential toxicity of NPs.

Even though it is reported that metal and metal oxide NPs, which are among the most rapidly and commonly commercialized NMs, can cause toxicity to organisms, their fate in the environment and toxicity to aquatic organisms are not well understood. Cu and Ag NPs have been recognized as two potentially dangerous NPs for aquatic organisms, and their toxic effects will be discussed in the following sections.

## 1.4. Copper Nanoparticles

As previously referred, CuO NPs are one of the most commonly used NPs in nanotechnology nowadays, being industrially produced and commercially available in various applications (http://www.nanotechproject.org). The growing awareness of the possible toxic effects of these NPs towards organisms is related to what was already known of this metal in its ionic form. As a redox metal, $Cu^{2+}$ is capable of directly induce oxidative stress by catalysing the production of ROS via Haber-Weiss and Fenton type reactions that will potentially damage biological molecules (DNA, proteins, membrane lipids), interfere with cellular transport processes and change metabolites concentrations (Gaetke and Chow, 2003; Halliwell and Gutteridge, 1984; Stohs and Bagchi, 1995). The adverse effects and bioaccumulation of Cu ions towards aquatic organisms are well known (e.g. Bebianno *et al*., 2004; Maria and Bebianno, 2011; Regoli and Principato, 1995), nevertheless, less is known about the impact of this metal in the nano-form.

Environmental concentrations of CuO NPs have not been determined, but similarly to other NPs, CuO NPs are likely to enter the environment and interact with aquatic organisms via different sources as effluents, spillage during shipping and handling, consumer products and disposal, among others. Most of the studies on the potential toxicity of Cu NPs are focused on mammals (such as mice and rats) and/or on different types of human cell cultures. For instance, Karlsson *et al*. (2008) showed that CuO NPs are highly toxic when compared to the bulk form of CuO, in human alveolar epithelial cell line A549, especially in terms of oxidative damage and ROS production. Toxicity data for nano-sized CuO in aquatic organisms are rare, especially concerning effects of long-term exposure, and the only existing data are on bacteria (e.g. Yoon *et al*., 2007), crustaceans (e.g. Heinlaan *et al*., 2008) and algae (e.g. Aruoja *et al*., 2009), showing a cytotoxic effect in all these species. A review on the uptake, accumulation and toxic effects of Cu NPs in aquatic organisms is summarized in Table 1.3. The antimicrobial characteristics of Cu NPs on several bacterial species showed that, for example, *Escherichia coli* and *Bacillus subtilis* are highly susceptible to Cu NPs (24

h exposure), with different strain specificity possibly associated with the structure of the bacterial membrane (presence of amines and carboxyl groups). Both size (7-100 nm) and dose (10-300 $\mu g.mL^{-1}$) also showed to affect Cu NPs antibacterial properties (Yoon *et al*., 2007; Ruparelia *et al*., 2008). Ivask *et al*. (2010) demonstrated the ROS-generating potential of CuO NPs ($40g.L^{-1}$, 30 nm) in recombinant *E. coli* strains exposed for 24h, using high-throughput luminescent bacterial tests. Oxidative stress is one of the possible effects of these NPs (0-20 $g.L^{-1}$,~30 nm, 72h) in *D. magna*, *Vibrio fisheri* and *Thamnocephalus platyurus* using traditional ecotoxicological methods combined with metal-specific recombinant biosensors (Heinlaan *et al*., 2008). In this case intimate contact between cells (bacteria cell wall or crustacean gut) and NPs are of extreme importance in terms of toxicity and transmission electron microscopy (TEM) showed the ingestion of CuO NPs (0.5-4 $mg.L^{-1}$,~30 nm, 48h) in the midgut cells of *D. magna*, where ultrastrutural changes in the midgut were associated with nanosize-related adverse effects (Heinlaan *et al*., 2011). In the algae *Pseudokirchneriella subcapitata* and the protozoa *Tetrahymena thermophile*, the toxicity of CuO NPs (0.1-500 $mg.L^{-1}$, ~30 nm, 4-72h) in terms of shading effect, algae growth and cell viability was also explained by soluble Cu ions as proved by recombinant bacterial and yeast Cu-sensors (Aruoja *et al*., 2009; Mortimer *et al*., 2010), and dependent on particle size (when compared to bulk Cu). In zebrafish (*D. rerio*) exposed to Cu NPs for 48h (0.25-1.5 $mg.L^{-1}$, 80 nm), gills is the primary target for NPs with damage to the lamellae and inhibition of $Na^+/K^+$-ATPase activity (Griffitt *et al*., 2007), in addition to different gene expression patterns for both Cu NPs (100 $\mu g.L^{-1}$, 26.7 ± 7.1 nm) and soluble Cu, suggesting different biological mechanisms (combination between dissolution and particulate effect) (Griffitt *et al*., 2009). In rainbow trout (*O. mykiss*) gills were also a preferential site for Cu NPs (20-100 $\mu g.L^{-1}$, 87 ± 27 nm, 4-10 days) accumulation. Changes to plasma and tissue concentrations along with $Na^+/K^+$-ATPase activity in several tissues were detected, along with effects in the antioxidant capacity, characterized by alterations in TBARS (damage thibarbyturic acid reactive substances) (Shaw *et al*., 2012). In polychaetes *Hediste diversicolor* exposed to 10 $\mu g.L^{-1}$ of CuO NPs (40-500 nm) for 16 days, alterations in antioxidant defences, namely CAT and GST were detected but with no signs of neurotoxicity (AChE) and damage (TBARS). Despite similar Cu body burden, biological responses were more important in polychaetes exposed to CuO NPs, whereas $Cu^{2+}$ lead to a decrease in burrowing capacity, suggesting a specific NP effect (Buffet *et al*., 2011). A parallel experiment with *S. plana* exposed to the same CuO NPs is the only available information on the effects of these particles in bivalve species, confirming the oxidative potential of the particles towards aquatic organisms.

**Table 1.3 –** Effects of Cu NPs in different species.

| Species | Nanoparticles | | | | Observed effects | Reference |
|---|---|---|---|---|---|---|
| | Type | Concentration | Size | Duration | | |
| **Bacteria** | | | | | | |
| ***Escherichia coli* + *Bacillus subtilis*** | Cu | 10-100 µg.mL$^{-1}$ | 7-100 nm | 24h | Susceptibility affected by particle size and concentration (compared to bulk Cu). | Yoon *et al*., 2007 |
| | Cu | 20-300 µg.mL$^{-1}$ | 9 nm | 24h | Different strain susceptibility associated with the structure of the bacterial membrane (presence of amines and carboxyl groups). | Ruparelia *et al*., 2008 |
| ***Escherichia coli*** | CuO | 40 g.L$^{-1}$ | 25-70 nm | 30 min-24h | ROS-generating potential caused by solubilized $Cu^{2+}$. | Ivask *et al*., 2010 |
| ***Vibrio fischeri*** | CuO | Concentrations up to 20 g.L$^{-1}$ | 30 nm | 72h | Oxidative stress by soluble $Cu^{2+}$. Contact between bacteria cell wall and NPs important for toxicity. | Heinlaan *et al*., 2008 |
| **Protozoa** | | | | | | |
| ***Tetrahymena thermophila*** | CuO | 31.25-500 mg.L$^{-1}$ | 30 nm | 4-24h | Cell viability dependent on particle size and NP soluble fraction. | Mortimer *et al*., 2010 |
| **Algae** | | | | | | |
| ***Pseudokirchneriella subcapitata*** | CuO | 0.1-100 mg.L$^{-1}$ | ~30 nm | 24-72h | Toxicity on shading effect and algae growth by soluble $Cu^{2+}$. | Aruoja *et al*., 2009 |
| **Crustaceans** | | | | | | |
| ***Thamnocephalus platyurus*** | CuO | Concentrations up to 20 g.L$^{-1}$ | 30 nm | 24h | Oxidative stress by soluble $Cu^{2+}$. Contact between gut environment and NPs important for toxicity. | Heinlaan *et al*., 2008 |
| ***Daphnia magna*** | CuO | Concentrations up to 20 g.L$^{-1}$ | 30 nm | 48h | Oxidative stress not fully explained by soluble $Cu^{2+}$. Ingestion of NPs increased bioavailability due to gut physiology. | Heinlaan *et al*., 2008 |

| | | | | | | |
|---|---|---|---|---|---|---|
| ***Daphnia magna*** | CuO | 0.5-4 mg.$L^{-1}$ | ~30 nm | 48h | Ingestion in midgut cells. Ultrastrutural changes in the midgut associated with nanosize-related adverse effects. | Heinlaan *et al*., 2011 |
| | | | | **Fish** | | |
| ***Danio rerio*** | Cu | 0.25-1.5 mg.$L^{-1}$ | 80 nm | 48h | NPs aggregation and dissolution with time. High Cu concentration in gills. Concentration-dependent damage to the lamellae and inhibition of $Na^+/K^+$-ATPase activity. Different gene expression patterns compared to $Cu^{2+}$. Cu dissolution from NPs not sufficient to explain toxicity. | Griffitt *et al*., 2007 |
| | Cu | 100 µg.$L^{-1}$ | 26.7 ± 7.1 nm | 24-48h | High concentrations in gills mainly $Cu^{2+}$ from the NPs. High mean gill filament. Different global gene expression in gills for CuO NPs and $Cu^{2+}$, due to a combination between dissolution and particulate effect. CuO NPs genes involved in apoptosis, cell proliferation and differentiation. | Griffitt *et al*., 2009 |
| ***Oncorhynchus mykiss*** | Cu NPs | 20-100 µg.$L^{-1}$ | 87 ± 27 nm | 4-10 days | NPs accumulation namely in gills. Changes to plasma and tissue concentrations along with $Na^+/K^+$-ATPase activity in several tissues, similar to $Cu^{2+}$. Alterations in TBARS (damage thiobarbituric acid reactive substances), more significant in trout exposed to $Cu^{2+}$. Toxic mechanisms and bioavailability dependent on the Cu form. | Shaw *et al*., 2012 |
| | | | | **Polychaetes** | | |
| ***Hediste diversicolor*** | CuO | 10 µg.$L^{-1}$ | 40-500 nm | 16 days | High NPs aggregation and no particle dissolution. Enhanced CAT and GST activities. No neurotoxicity (AChE) and oxidative damage (TBARS). Similar Cu whole body burdens. Biological responses more important in CuO NPs, suggesting a specific NP effect. | Buffet *et al*., 2011 |

The above examples raise the uncertainty of CuO NPs toxicity. The effects of CuO NPs in contrast to its bulk and ionic forms are contradictory; nevertheless, evidence exists of different mechanisms of action dependent on the Cu form (e.g. Griffitt *et al*., 2007; Shaw *et al*., 2012). Most of the NP toxicity was attributed to the dissolution of $Cu^{2+}$ from the particles; nevertheless, the great extent of the effects mainly derives from the inherent particle properties (e.g. Griffitt *et al*., 2009; Heinlaan *et al*., 2011). However, the mechanisms by which these particles induce toxic responses are still poorly understood and there is a severe lack of information on the potential effects of CuO NPs in aquatic organisms (as bivalve species), as well as its behaviour in aquatic environments.

## 1.5. Silver Nanoparticles

From the variety of NPs that are currently being developed in nanotechnology, Ag NPs have the highest degree of commercialization mainly due to their antibacterial properties (www.nanoproject.org). Given the capacity of Ag NPs to release $Ag^{+}$ ions (Navarro *et al*., 2008) it seems inevitable that these particles can easily enter cells, interact and perturb any thiol group-containing enzymes or proteins (Bar-Ilan *et al*., 2009; Lapresta-Fernández *et al*., 2012) leading to the disruption of target structures, in addition to the effects caused by the NPs specific properties. Ionic silver ($Ag^{+}$) is a known environmental stressor due to its persistence and accumulation in the environment (water, sediments and organisms). The toxicity of this metal ion is significant to both freshwater and marine organisms, even at low levels ($\mu g.L^{-1}$ range) (e.g. Fabrega *et al*., 2011; Luoma, 2008; Wang and Rainbow, 2005). Its strong affinity with sulfhydryl, amino and phosphate groups and the capacity to induce ROS production can lead to inhibition/inactivation of enzymes, damage to essential components of the cell (such as membranes and mitochondria), and eventually to significant oxidant stress (Bar-Ilan *et al*., 2009 and literature cited therein; Lapresta-Fernández *et al*., 2012). In aquatic organisms its effects are well documented but less is known about the mechanism by which Ag in the nano form exerts toxicity to organisms, namely to invertebrate species. In this context, it seems critical to expand the information about Ag NPs presence and behaviour in the marine environment as well as their consequences in marine organisms.

The rapid devolvement nano-products containing Ag NPs increase their probability to end up in the aquatic environment and interact to aquatic organisms. The majority of Ag NPs-containing products can release, directly or indirectly, considerable amounts of Ag particles or $Ag^{+}$ ions (dissolved from the particles) into sewage treatment plants from where they

could be further release into the aquatic environment (Benn and Westerhoff, 2008; Blaser *et al*., 2008; Farkas *et al*., 2011). Environmental concentrations of Ag NPs have not been determined but in 2010 up to 15% of the total silver released in European waters came from biocidal plastics and textiles containing Ag NPs (Blaser *et al*., 2008). Predicted concentrations of Ag NPs in natural waters using simplified models range from 0.03 to 500 $ng.L^{-1}$ (Luoma, 2008), with values around 0.03 $\mu g.L^{-1}$ based on a life-cycle perspective of NPs-containing products (washing, abrasion and run-off) (Mueller and Nowack, 2008) and 0.01 $\mu g.L^{-1}$ derived from consumer products and assessment of exposure routes in the United Kingdom (Boxall *et al*., 2008). Benn and Westerhoff (2008) and Geranio *et al*. (2009) also demonstrated leaching of silver (ionic and nanoparticulate) from socks impregnated with Ag NPs into water after washing that end up in the aquatic environment at concentrations up to 377 $\mu g.g^{-1}$. Accordingly, diverse aquatic species are at risk to be exposed to Ag NPs. The environmental effects of Ag NPs and Ag ions dissolved from the particles and consequent toxicity towards aquatic organisms was recently reviewed by Fabrega *et al*. (2011) and Lapresta-Fernández *et al*. (2012). In general, Ag NPs is taken in, adhere and accumulate in aquatic organisms, with several examples evidencing the toxic effects of both Ag NPs and $Ag^{+}$. Apart from the toxic effects caused by the release of $Ag^{+}$ from the particles, other mechanisms for Ag NPs toxicity based on oxidative reactions were suggested. A review on the uptake, accumulation and toxic effects of Ag NPs in aquatic organisms is summarized in Table 1.4.

The capacity of Ag ions to interact with sulphur groups of vital enzymes and proteins, affecting cellular respiration, transport of ions across membranes and culminating in cell death, was more intensely investigated in terms of toxicity to microbes that to invertebrate and vertebrate species (Fabrega *et al*., 2011; Luoma, 2008). Direct interaction of Ag NPs (10-100 $\mu g.cm^{-3}$, 12 nm) with cell membranes, subsequent accumulation and Ag NPs ROS-generating potential was associated to the formation of 'pits' in *E. coli* cells treated with Ag NPs for 24h (0.2-33 mM, 13.5 ± 2.6 nm) (Kim *et al*., 2007; Sondi and Salopek-Sondi, 2004) and bacterial accumulation of intracellular ROS (40 $g.L^{-1}$, <100 nm) (Ivask *et al*., 2010). In algae *Chlamydomonas reinhardtii*, Ag NPs (10-100,000 nM, ~40nm, 1-5h) toxicity indicated a potential NP-mediated effect due to an interaction with the algae cell (Navarro *et al*., 2008). In *D. magna*, Ag NPs (0-10 $mg.L^{-1}$, 35 nm, 96h-21 days) affected growth, moulting and survival, not only related to particle size and solubility but also to aggregation (Gaiser *et al*., 2011). Additionally, DNA damage characterized by DNA strand breaks was found along with an increase in mortality, suggesting higher-level consequences in organisms by Ag NPs

(0-50 μg.$L^{-1}$, <50 nm, 24h) (Park and Choi, 2010). Exposure of zebrafish (*D. rerio*) embryos to Ag NPs (5-46 nm, 24 to 120h) induce different types of abnormalities, as hatching delay, spinal cord deformities, slow blood flow, cardiac arrhythmia and survival (Asharani *et al*., 2008; Lee *et al*., 2007). In terms of accumulation, Ag NPs (0.071 mM) are transported in and out the chorion pore channels and exhibit Brownian diffusion (Lee *et al*., 2007), as well as distributed in the brain, heart, yolk, blood (5-100 μg.$mL^{-1}$) (Asharani *et al*., 2008) and gills (1000 μg.$mL^{-1}$) (Griffitt *et al*., 2009). Oxidative stress (induction of GSH, decrease of CAT an GPX and high levels of LPO), DNA damage (induction of the p53 gene and double strand breaks) and apoptosis (e.g. caspase genes 3 and 9) was also been associated with Ag NPs (0.4 μg.$L^{-1}$ to 120 mg.$L^{-1}$, 5-20 nm) in zebrafish exposed for 24 to 52h (Choi *et al*., 2010, Yeo and Pak, 2008). In rainbow trout (*O. mykiss*), Ag NPs (10-100 μg.$L^{-1}$, 10-35 nm, 10 days) were accumulated in the gills and liver tissue, affecting the capacity to cope with low oxygen levels and inducing oxidative stress (Scown *et al*., 2010b). Ag NPs coated with citrate or polyvinylpyrrolidone (0.1-10 mg.$L^{-1}$, ~12nm, 48h) also accumulated in rainbow trout primary gill cells, reducing membrane integrity and originating high levels of oxidative stress in the form of reduced GSH, highly dependent on particle size and coating (Farkas *et al*., 2011). In japonese medaka (*Oryzias latipes*) exposed to Ag NPs (1-25 μg.$L^{-1}$, 49.6 nm, 1-4 days), expression of several stress-related genes showed cellular and DNA damage, carcinogenic and oxidative stresses, induction of metal detoxification/metabolism regulation and radical scavenging action, suggesting an apoptotic effect associated with ROS formed by the NPs. Lower stress responses were obtained with $Ag^{+}$, with induction of inflammatory response (e.g. transferrin) and metal detoxification (e.g. MT) (Chae *et al*., 2009). In *N. diversicolor*, Ag NPs (250 ng.$g^{-1}$, 30 ± 5 nm, 10 days) were internalized by endocytosis into the gut epithelia, mainly in the form of aggregates, as denoted by a large number of endosomes and large vesicles near the cellular membrane. Ag NPs and $Ag^{+}$ have separate routes of cellular internalization and fates, with Ag NPs predominantly associated with inorganic granules, organelles and heat-denatured proteins, while $Ag^{+}$ is mostly associated with MT, suggesting that Ag is predominantly accumulated in the nano form (García-Alonso *et al*., 2011). Only two experiments addressed the effects of Ag NPs in bivalves species (Table 1.4), with oysters *C. virginica* (16-0.0016 μg.$L^{-1}$, 15 ± 6 nm, 48h) and mussels *M. edulis* ($^{110m}$Ag, 0.7 μg.$L^{-1}$, 3h30min-72h), confirming the capacity of these particles to be taken up, accumulate and cause adverse effects in bivalve tissues (Ringwood *et al*., 2010; Zuykov *et al*., 2011).

**Table 1.4 –** Effects of Ag NPs in different species.

| Species | Nanoparticles | | | | Observed effect | Reference |
|---|---|---|---|---|---|---|
| | Type | Concentration | Size | Duration | | |
| **Bacteria** | | | | | | |
| ***Escherichia coli*** | Ag | 0-100 $\mu g.mL^{-1}$ | 16 ± 8 nm | 30 min | NPs accumulation inside cells and attached to the membrane. Size dependent bactericidal effect and associated with dissolution of $Ag^{+}$ from the NPs. | Morones *et al*., 2005 |
| | Ag | 10-100 $\mu g.cm^{-3}$ | 12 nm | 24h | Direct interaction of particles with cell membranes. NPs accumulation associated to the formation of 'pits' in the cell wall. | Sondi and Salopek-Sondi, 2004 |
| | Ag | 0.2-33 mM | 13.5 ± 2.6 nm | 24h | NPs ROS-generating potential affect regulation (disruption of the ion efflux systems) and transport though the membrane. | Kim *et al*., 2007 |
| | Ag | 40 $g.L^{-1}$ | <100 nm | 30 min-24h | Accumulation of intracellular ROS (namely superoxide anions) by $Ag^{+}$ dissolution in combination to NPs specific properties. | Ivask *et al*., 2010 |
| **Algae** | | | | | | |
| ***Chlamydomonas reinhardtii*** | Ag | 10-100,000 nM | ~40nm | 1-5h | Higher toxicity in Ag NPs than $Ag^{+}$ by a NP-mediated effect due to an interaction with the algae cell. | Navarro *et al*., 2008 |
| **Crustaceans** | | | | | | |
| ***Daphnia magna*** | Ag | 0- 10 $mg.L^{-1}$ | 35 nm | 96h-21 days | Mortality, inhibition of growth and moulting, related to particle size, solubility, aggregation and interactions with food matter. Mode of action of Ag NPs different from $Ag^{+}$. | Gaiser *et al*., 2011 |
| | Ag | 0-50 $\mu g.L^{-1}$ | <50 nm | 24h | DNA strand breaks along with an increase in mortality. | Park and Choi (2010) |

| Fish | | | | | | |
|---|---|---|---|---|---|---|
| ***Danio rerio*** | Ag | 0-0.71 mM | 5-46 nm | 24-120h | Dose-dependent hatching delay, spinal cord deformities, slow blood flow, cardiac arrhythmia and survival. Transport in and out the chorion pore channels and Brownian diffusion. | Lee *et al*., 2007 |
| | Ag capped with BSA | 5-100 $\mu g.mL^{-1}$ | 5-20 nm | 72h | Mortality, hatching delay, spinal cord deformities, slow blood flow and cardiac arrhythmia, dose-dependent. NPs distributed in brain, heart, yolk and blood. | Asharani *et al*., 2008 |
| | Ag | Concentrations up to 10 $mg.L^{-1}$ | 26.6 ± 8.8 nm | 48h | $Ag^{+}$ 300 times more toxic than Ag NPs. Ag dissolution (<1%) not sufficient to explain the obtained mortality. | Griffitt *et al*., 2008 |
| | Ag | 1000 $\mu g.L^{-1}$ | 26.6 ± 8.8 nm | 24-48h | Whole body burdens higher in Ag NPs than $Ag^{+}$ (namely NPs). Ag NPs associated with the gill tissue but no thickening of the gill filament. Different gene expression between Ag NPs and $Ag^{+}$, not solely attributed to the release of silver ion. | Griffitt *et al*., 2009 |
| | Ag | 0.4-4 $\mu g.L^{-1}$ | ~10-20nm | 48-52h | Mitochondrial damage and inflammation, infiltration in all organelles (including the nucleus), large mitochondria with empty matrices and accumulation in blood vessels. Alteration in expression of the p53 gene pathway related to apoptosis, including caspase genes 3 and 9. | Yeo and Pak, 2008 |
| | Ag | 30-120 $mg.L^{-1}$ | 5-20 nm | 24h | Induction of MT and GSH, decrease of CAT and GPX and high levels of LPO, DNA damage (induction of the p53 gene and double strand breaks) and apoptosis in liver tissue. | Choi *et al*., 2010 |
| ***Oncorhynchus mykiss*** | Ag | 10-100 $\mu g.L^{-1}$ | 10-35 nm | 10 days | Accumulation in the gills and liver tissue (dissolved and NPs aggregates). Affected capacity to cope with low oxygen levels and oxidative stress (expression of *cyp1a2*), depended on particle size. No LPO due to low uptake rates. | Scown *et al*. 2010b |

| | | | | | | |
|---|---|---|---|---|---|---|
| ***Oncorhynchus mykiss*** | Ag coated with citrate or polyvinylpyrroli-done | 0.1-10 mg.$L^{-1}$ | 3-40 nm | 48h | Accumulation in gills with silver transport trough epithelial layers dependent on epithelial tightness and particle size. Reduced membrane integrity and high levels of oxidative stress in the form of reduced GSH. Different behaviour associated with different coatings. | Farkas *et al*., 2011 |
| ***Oryzias latipes*** | Ag | 1-25 µg.$L^{-1}$ | 49.6 nm | 1-4 days | Cellular and DNA damage and repair, carcinogenic and oxidative stresses, induction of metal detoxification/ metabolism regulation and radical scavenging action (e.g. GST, Cytochrome 1A, heat-shock protein 70 and p53 genes) by Ag NPs, suggesting an apoptotic effect by ROS. Lower induction of inflammatory response (e.g. transferrin) and metallic detoxification (e.g. MT) by $Ag^{+}$. | Chae *et al*., 2009 |
| | | | **Polychaetes** | | | |
| ***Nereis diversicolor*** | Citrate capped Ag | 250 ng.$g^{-1}$ sediment | 30 ± 5 nm | 10 days | Direct internalization of aggregates into gut epithelia. High number of endosomes and large vesicles near the cellular membrane associated with NPs endocytosis. Ag NPs associated with inorganic granules, organelles and heat-denatured proteins. $Ag^{+}$ associated with MT fraction. | García-Alonso *et al*., 2011 |

As found with Cu NPs, a conclusion cannot be drawn about the toxicity of Ag NPs via aqueous exposure, as contradictory results were detected in terms of the most toxic Ag form (NP vs ionic). Accordingly, it is still not clear if its enhanced toxicity is derived from the properties inherent to the particles, the release of $Ag^{+}$ or a combination of both (Asharani *et al*., 2008; Fabrega *et al*., 2011; Griffitt *et al*., 2009). Even though there is some evidence on the bioaccumulation and toxicity of Ag NPs, there is still a lack of information on the uptake, tissue distribution and their potential toxicity towards marine organisms.

## 1.6. Aims and outline

The aquatic environment is continuously subjected to the input of anthropogenic contaminants arising from human activities. Nanotechnology industry is no exception. Its rapid expansion and large-scale production is resulting in the frequent release of NMs and their by-products into the environment, thus becoming an emergent threat to the aquatic environment. Knowledge of the potential adverse effects of NPs in aquatic organisms and marine organisms in particular is crucial to understand the associated risks to the aquatic environment. Accordingly, bioavailability, mechanisms of uptake, fate and behaviour of NPs in aquatic organisms must be clarified in order to understand their full potential. Even though much information exists of bivalve molluscs as bioindicator species not only in field but also in laboratory experiments with a wide range of contaminants, their use in nanotoxicological studies is still scarce.

Therefore, the main objective of this thesis was to fill this gap by studying the effects of two commercially available NPs used in a wide number of industrial applications and consumer products, CuO and Ag NPs, using mussels *M. galloprovincialis* as bioindicators. A comparison was made regarding the uptake and bioaccumulation of CuO and Ag NPs with their ionic counterparts ($Cu^{2+}$ and $Ag^{+}$) in mussels tissues, together with their biological effects, namely through the use of conventional biomarkers (antioxidant enzymes, MTs, LPO, AChE and DNA damage) and high-throughput proteomic-based approaches. Furthermore, the patterns of distribution and modes of action of both NPs were also compared with those of $Cu^{2+}$ and $Ag^{+}$. To achieve this purpose, this thesis is divided in seven chapters that are outlined below.

**Chapter 1:** General introduction

This first Chapter reviews the subject of NPs as an emerging environmental threat, including its main properties, a brief description of the existing types of NPs and the emissions and behaviour of these particles in the environment. The uptake, accumulation and bioavailability of NPs to living organisms were also discussed, along with the processes of ROS production and oxidative stress, the importance of antioxidant defence systems and their main consequences, and neurotoxic and genotoxic effects in biological systems. Furthermore, the application of conventional biomarkers in nanotoxicology, together with the importance of proteomics for the discovery of new biomarkers was also reviewed. This general introduction also describes the known effects of Cu and Ag NPs exposure to aquatic organisms and the uncertainty surrounding their mechanisms of action. The use of bivalve species in nanotoxicology was also characterized, focusing on uptake and toxic effects.

**Chapter 2:** Effects of CuO NPs in the mussel *M. galloprovincialis*.

The aim of this Chapter was to address the bioavailability, uptake, accumulation and effects of CuO NPs in mussels *M. galloprovincialis* and to identify target organs of CuO NPs toxicity. For this purpose, the effects of CuO NPs were studied in the gills (Subchapter 2.1) and digestive glands (Subchapter 2.2) of mussels exposed to an environmental realistic concentration (10 $\mu g.L^{-1}$) of CuO NPs for 15 days and compared to that of $Cu^{2+}$. Knowing that oxidative stress and neurotoxic effects were identified as possible effects of NPs exposure, the responses of biomarkers of oxidative stress (antioxidant enzymes SOD, CAT and GPX), damage (LPO), metal exposure (MT) and neurotoxicity (AChE) were evaluated. Transmission electron microscopy and dynamic light scattering were also used to characterize the NPs and relate their behaviour in the aquatic environment with the biological effects observed.

**Chapter 3:** Effects of Ag NPs in the mussel *M. galloprovincialis*.

With the intent to also elucidate the mechanisms of uptake, target tissues and toxicity of Ag NPs in mussels *M. galloprovincialis*, an assay using an environmental realist concentration of Ag (10 $\mu g.L^{-}1$; in the nanoparticulate and ionic form) was conducted. The same approach of Chapter 2 was used, where the oxidative potential of Ag NPs was evaluated in mussels'

tissues using biomarkers of oxidative stress, damage and metal exposure in comparison to $Ag^{+}$. Particle size (hydrodynamic diameter), shape, surface charge (zeta potential), polydispersity index, intensity and solubility in natural seawater were also determined to understand and interpret the toxic effects of Ag NPs.

**Chapter 4:** Genotoxicity of CuO and Ag NPs in the mussel *M. galloprovincialis*.

Given that one of the possible effects of NPs exposure is DNA damage, the genotoxic potential of CuO and Ag NPs were investigated in this Chapter and compared to that of $Cu^{2+}$ and $Ag^{+}$ using mussels *M. galloprovincialis*. To do so, mussels were exposed to CuO and Ag NPs for 15 days with the same concentrations of Chapters 2 and 3, and DNA damage (DNA strand breaks) was assessed in hemocytes using the Comet assay.

**Chapter 5:** Proteomic analysis in mussels *M. galloprovincialis* exposed to CuO NPs and $Cu^{2+}$.

Assuming that accumulation of NPs can induce changes at a protein expression level, a proteomics approach was applied to mussels *M. galloprovincialis* to identify crucial proteins that were affected by CuO NPs exposure. Accordingly, the different responses in protein expression profiles were assessed in mussels tissues (gills and digestive gland) exposed to CuO NPs and $Cu^{2+}$ (10 $\mu gCu.L^{-1}$) for 15 days. Unique sets of tissue-specific protein expression signatures were identified for CuO NPs and $Cu^{2+}$, along with groups of proteins that varied commonly between the Cu copper forms and new candidate molecular biomarkers to assess CuO NPs and $Cu^{2+}$ toxicity were proposed.

**Chapter 6:** Differential protein expression in mussels *M. galloprovincialis* exposed to nano and ionic Ag.

Similarly to Chapter 5, differences in protein expression profiles of gills and digestive gland of mussels *M. galloprovincialis* exposed to Ag NPs and $Ag^{+}$ (10 $\mu g.L^{-1}$) for a period of 15 days were investigated. Protein expression profiles were compared using proteomic analysis to discriminate differentially expressed protein patterns for Ag NPs and $Ag^{+}$. Different tissue-specific patterns of protein expression were obtained together with unique sets of protein

expression signatures affected by each or both Ag forms, aiming at the identification of potentially novel molecular biomarkers for Ag NPs and $Ag^+$ exposure.

**Chapter 7:** General discussion

Finally, this last Chapter presents a general discussion that gathers all the results obtained in the previous Chapters and discusses the possible mechanisms of toxic action of CuO NPs and Ag NPs. Perspectives for future research are also considered.

## 1.7. References

Ahamed, M.; Posgai, R.; Gorey, T.J.; Nielsen, M.; Saber, M.H.; Rowe, J.J. (2010). Silver nanoparticles induce heat shock protein 70, oxidative stress and apoptosis in *Drosophila melanogaster*. *Toxicology and Applied Pharmacology*. **242:** 263–269.

Aitken, R.J.; Chaudhry, M.Q.; Boxall, A.B.A.; Hull, M. (2006). Manufacture and use of nanomaterials: current status in the UK and global trends. *Occupational Medicine*. **56:** 300–306.

Al–Subiai, S.N.; Moody, A.J.; Mustafa, S.A.; Jha, A.N. (2011). A multiple biomarker approach to investigate the effects of copper on the marine bivalve mollusc, *Mytilus edulis*. *Ecotoxicology and Environmental Safety*. **74:** 1913–1920.

Alban, A.; David, S.O.; Jorkesten, L.; Andersson, C.; Sloge, E.; Lewis, S.; Currie, I. (2003). A novel experimental design for comparative difference gel electrophoresis incorporating a pooled intern standard. *Proteomics*. **3:** 36–44.

Amelina, H.; Apraiz, I.; Sun, W.; Cristobal, S. (2007). Proteomics–based method for the assessment of marine pollution using liquid chromatography coupled with two–dimensional electrophoresis. *Journal of Proteome Research*. **6:** 2094–2104.

Amiard, J.–C.; Amiard–Triquet, C.; Barka, S.; Pellerin, J.; Rainbow, P.S. (2006). Metallothioneins in aquatic invertebrates: Their role in metal detoxification and their use as biomarkers. *Aquatic Toxicology*. **76:** 160–202.

Apraiz, I.; Mi, J.; Cristobal, S. (2006). Identification of proteomic signatures of exposure to marine pollutants in mussels (*Mytilus edulis*). *Molecular and Cellular Proteomics*. **5(7):** 1274–1285.

Aruoja, V.; Dubourguier, H.–C.; Kasemets, K.; Kahru, A. (2009). Toxicity of nanoparticles of CuO, ZnO and $TiO_2$ to microalgae *Pseudokirchneriella subcapitata*. *Science of the Total Environment.* **407(4):** 1461–1468.

Asharani, P.V.; Wu, Y.L.; Gong, Z.; Valiyaveettil, S. (2008). Toxicity of silver nanoparticles in zebrafish models. *Nanotechonoly*. **19:** 255102.

Baalousha, M.; Manciulea, A.; Cumberland, S.; Kendall, K.; Lead, J.R. (2008). Aggregation and surface properties of iron oxide nanoparticles: Influence of pH and natural organic matter. *Environmental Toxicology and Chemistry*. **27:** 1875–1882.

Bar–Ilan, O.; Albrecht, R.M.; Fako, V.E.; Furgeson, D.Y. (2009). Toxicity assessments of multisized gold and silver nanoparticles in zebrafish embryos. *Small*. **5(16):** 1897–1910.

Barber, D.S.; Denslow, N.D.; Griffitt, R.J.; Martyniuk, C.J. (2009). Sources, fate and effects of engineered nanomaterials in the aquatic environment. In: Sahu, S.C.; Casciano, D.A. (Eds.). Nanotoxicity. John Wiley and Sons, Ltd, Chichester, UK, pp. 227–246.

Baumard, P.; Budzinski, H.; Garrigues, P.; Dizer, H.; Hansen, P.D. (1999). Polycyclic aromatic hydrocarbons in recent sediments and mussels (*Mytilus edulis*) from the Western Baltic Sea: occurrence, bioavailability and seasonal variations. *Marine Environmental Research*. **47:** 17–47.

Baun, A.; Hartmann, N.B.; Grieger, K.; Kusk, K.O. (2008). Ecotoxicity of engineered nanoparticles to aquatic invertebrates: a brief review and recommendations for future toxicity testing. *Ecotoxicology*. **17:** 387–395.

Bebianno, M.J.; Géret, F.; Hoarau, P.; Serafim, M.A.; Coelho, M.R.; Gnassia–Barelli, M.; Roméo, M. (2004). Biomarkers in *Ruditapes decussatus*: a potential biondicator species. *Biomarkers*. ***9*(4–5):** 305–330.

Benn, T.M.; Weterhoff, P. (2008). Nanoparticle silver release into water from commercially available sock fabrics. *Environmental Science and Technology*. **42:** 4133– 4139.

Bhatt, I.; Tripathi, B.N. (2011). Interaction of engineered nanoparticles with various components of the environment and possible strategies for their risk assessment. *Chemosphere*. **82(3):** 308–317.

Biswas, P.; Wu, P. (2005). Nanoparticles and the environment. *Journal of the Air and Waste Management Association.* **55:** 708–746.

Blaser, S.A.; Scheringer, M.; MacLeod, M.; Hungerbühler, K. (2008). Estimation of cumulative aquatic exposure and risk due to silver: Contribution of nano–functionalized plastics and textiles. *Science of the Total Environment*. **390:** 396–409.

Borm, P. J. A.; Robbins, D.; Haubold, S.; Kuhlbusch, T., Fissan, H., Donaldson, K.; Schins, R.; Stone, V.; Kreyling, W.; Lademann, J.; Krutmann, J., Warheit, D.; Oberdorster, E. (2006). The potential risks of nanomaterials: a review carried out for ECETOC. *Particle and Fibre Toxicology*. **3:**11.

Boxall, A.B.A.; Chaudhry, Q.; Sinclair, C.; Jones, A.; Aitken, R.; Jefferson, B.; Watts, C. (2008). Current and future predicted environmental exposure to engineered nanoparticles. Report by Central Science Laboratory for Department for Environment, Food and Rural Affairs, Her Majesty's Government, UK.

Buffet, P.–E.; Amiard–Triquet, C.; Dybowska, A.; Faverney, C.R.–d.; Guibbolini, M.; Valsami–Jones, E.; Mouneyrac, C. (2012). Fate of isotopically labeled zinc oxide nanoparticles in sediment and effects on two endobenthic species, the clam *Scrobicularia plana* and the ragworm *Hediste diversicolor*. *Ecotoxicology and Environmental Safety*. **84:** 191–198.

Buffet, P.E.; Tankoua, O.F.; Pan, J.F.; Berhanu, D.; Herrenknecht, C.; Poirier, L.; Amiard–Triquet, C.; Amiard, J.C.; Bérard, J.B.; Risso, C.; Guibbolini, M.; Roméo, M.; Reip, P.; Valsami–Jones, E.; Mouneyrac, C. (2011). Behavioural and biochemical responses of two marine invertebrates *Scrobicularia plana* and *Hediste diversicolor* to copper oxide nanoparticles. *Chemosphere*. **84:** 166–174.

Buzea, C.; Blandino, I. P.; Robbie, K. (2007). Nanomaterials and nanoparticles: Sources and toxicity. *Biointerphases*. **2(4):** MR17–MR172.

Cajaraville, M.P.; Bebianno, M.J.; Blasco, J.; Porte, C.; Sarasquete, C.; Viarengo, A. (2000). The use of biomarkers to assess the impact of pollution in coastal environments of the Iberian Peninsula: a practical approach. *The Science of the Total Environment*. **247:** 295–311.

Canesi, L.; Ciacci, C.; Betti, M.; Fabbri, R.; Canonico, B.; Fantinati, A.; Marcomini, A.; Pojana, G. (2008). Immunotoxicity of carbon black nanoparticles to blue mussel hemocytes. *Environment International*. **34:** 1114–1119.

Canesi, L.; Ciacci, C.; Fabbri, R.; Marcomini, A.; Pojana, G.; Gallo, G. (2012). Bivalve molluscs as a unique target group for nanoparticle toxicity. *Marine Environmental Research*. **76:** 16–21.

Canesi, L.; Ciacci, C.; Vallotto, D.; Gallo, G.; Marcomini, A.; Pojana, G. (2010a). In vitro effects of suspensions of selected nanoparticles (C60 fullerene, $TiO_2$, $SiO_2$) on *Mytilus* hemocytes. *Aquatic Toxicology*. **96:** 151–158.

Canesi, L.; Fabbri, R.; Vallotto, D.; Marcomini, A.; Pojana, G. (2010b). Biomarkers in *Mytilus galloprovincialis* exposed to suspensions of selected nanoparticles (Nano carbon black, C60 fullerene, Nano–$TiO_2$, Nano–$SiO_2$). *Aquatic Toxicology*. **100:** 168–177.

Castro, A. T.; Cuéllar, E. L.; Méndez, U. O.; Yacamán, M. J. (2006). Advances in developing TiNi nanoparticles. *Materials Science and Engineering A*. **438–440:** 411–413.

Cattaneo, A.G.; Gornati, R.; Chiriva–Internati, M.; Bernardini, G. (2009). Ecotoxicology of nanomaterials: the role of invertebrate testing. *Invertebrate Survival Journal*. **6:** 78–97.

Chae, Y.J.; Pham, C.H.; Lee, J.; Bae, E.; Yi, J.; Gu, M.B. (2009). Evaluation of the toxic impact of silver nanoparticles on Japanese medaka (*Oryzias latipes*). *Aquatic toxicology*. **94(4):** 320–327.

Chang, H.; Jwo, C.; Lo, C.; Tsung, T.; Kao, M.; Lin, H. (2005). Rheology of CuO nanoparticle suspension prepared by ASNSS. *Reviews on Advanced Material Science*. **10:** 128–132.

Choi, J.E.; Kim, S.; Ahn, J.H.; Youn, P.; Kang, J.S.; Park, K.; Yi, J.; Ryu, D.–Y. (2010). Induction of oxidative stress and apoptosis by silver nanoparticles in the liver of adult zebrafish. *Aquatic Toxicology*. **100:** 151–159.

Choi, M.–R.; Stanton–Maxey, K.J.; Stanley, J.K.; Levin, C.S.; Bardhan, R.; Akin, D.; Badve, S.; Sturgis, J.; Robinson, J.P.; Bashir, R. (2007). A cellular trojan horse for delivery of therapeutic nanoparticles into tumors. *Nano Letters.* **7(12):** 3759–3765.

Christian, P.;Von der Kammer, F.; Baalousha, M.; Hofmann, Th. (2008). Nanoparticles: structure, properties, preparation and behavior in environmental media. *Ecotoxicology*. **17:** 326–343.

Cioffi, N.; Ditaranto, N.; Torsi, L.; Picca, R.A.; De Giglio, E.; Sabbatini, L.; Novello, L.; Tantillo, G.; Bleve–Zacheo, T.; Zambonin, P.G. (2005). Synthesis, analytical characterization and bioactivity of Ag and Cu nanoparticles embedded in poly–vinyl–methyl–ketone films. *Analytical and Bioanalytical Chemistry*. **382:** 1912–1918.

Colvin, V.L. (2003) The potential environmental impact of engineered nanomaterials. *Nature Biotechnology*. **21:** 1166–1170.

Crane, M.; Handy, R.D.; Garrod, J.; Owen, R. (2008). Ecotoxicity test methods and environmental hazard assessment for engineered nanoparticles. *Ecotoxicology*. **17:** 421–37.

Cravo, A.; Lopes, B.; Serafim, A.; Company, R.; Barreira, L.; Gomes, T.; Bebianno, M.J. (2009). A multibiomarker approach in *Mytilus galloprovincialis* to assess environmental quality. *Journal of Environmental Monitoring*. **11:** 1673–1686.

Dagnino, A.; Allen, J.I.; Moore, M.N.; Broeg, K.; Canesi, L.; Viarengo, A. (2007). Development of an expert system for the integration of biomarker responses in mussels into an animal health index. *Biomarkers*. **12:** 155–172.

Davies, M.J. (2005). The oxidative environment and protein damage. *Biochimica et Biophysica Acta*. **1703:** 93–109.

de Almeida, E.A.; Bainy, A.C.D.; Loureiro, A.P.d.M.; Martinez, G.R.; Miyamoto, S.; Onuki, J.; Barbosa, L.F.; Garcia, C.C.M.; Prado, F.M.; Ronsein, G.E.; Sigolo, C.A.; Brochini, C.B.; Martins, A.M.G.; de Medeiros, M.H.G.; Mascio, P.D. (2007). Oxidative stress in *Perna perna* and other bivalves as indicators of environmental stress in the Brazilian marine environment: Antioxidants, lipid peroxidation and DNA damage. *Comparative Biochemistry and Physiology, Part A*. **146:** 588–600.

Dhas, N.A.; Raj, C.P.; Gedanken, A. (1998). Synthesis, characterization, and properties of metallic copper nanoparticles. *Chemical Materials.* **10:** 1446–1452.

Di Giulio, R.T.; Benson, W.H.; Sanders, B.M.; Van Held, P.A. (1995). Biochemical mechanisms: metabolism, adaptation and toxicity. *In*: Rand, G.M. (Ed). Fundamentals of aquatic toxicology. Effects, environmental fate, and risk assessment. Taylor and Francis. pp. 523–561.

Donaldson, K.; Poland, C.A.; Schins, R.P.F. (2010). Possible genotoxic mechanisms of nanoparticles: Criteria for improved test strategies. *Nanotoxicology*. **4(4):** 414–420.

Dowling, A.P. (2004). Development of nanotechnologies. *Materials Today*. **7:** 30–35.

Fabrega, J.; Luoma, S.N.; Tyler, C.R.; Galloway, T.M.; Lead, J.R. (2011). Silver nanoparticles: Behaviour and effects in the aquatic environment. *Environmental International*. **37(2):** 517–531.

Farkas, J.; Christian, P.; Gallego–Urrea, J.A.G.; Roos, N.; Hassellöv, M.; Tollefsen, K.E.; Thomas, K.V. (2011). Uptake and effects of manufactured silver nanoparticles in rainbow trout (*Oncorhynchus mykiss*) gill cells. *Aquatic toxicology*. **101:** 117–125.

Finkel, T; Holbrook, N.J. (2000). Oxidants, oxidative stress and the biology of ageing. *Nature*. **408:** 239–247.

Gaetke, L.M.; Chow, C.K. (2003). Copper toxicity, oxidative stress, and antioxidant nutrients. *Toxicology*. **189:** 147–163.

Gagné, F.; Auclair, J.; Turcotte, P.; Fournier, M.; Gagnona, C.; Sauvé, S.; Blaise, C. (2008). Ecotoxicity of CdTe quantum dots to freshwater mussels: Impacts on immune system, oxidative stress and genotoxicity. *Aquatic Toxicology*. **86:** 333–340.

Gaiser, B.K.; Biswas, A.; Rosenkranz, P.; Jepson, M.A.; Lead, J.R.; Stone, V.; Tyler, C.R.; Fernandes, T.F. (2011). Effects of silver and cerium dioxide micro– and nano–sized particles on *Daphnia magna*. *Journal of Environmental Monitoring*. **13:** 1227–1235.

Galloway, T.S.; Brown, R.J.; Browne, M.A.; Dissanayake, A.; Lowe, D.; Jones, M.B.; Depledge, M.H. (2004). A multibiomarker approach to environmental assessment. *Environmental Science and Technology*. **38:** 1723–1731.

García–Alonso, J.; Khan, F.R.; Misra, S.K.; Turmaine, M.; Smith, B.D.; Rainbow, P.S.; Luoma, S.N.; Valsami–Jones, E. (2011). Cellular internalization of silver nanoparticles in gut epithelia of the estuarine polychaete *Nereis diversicolor*. *Environmental Science and Technology*. **45:** 4630–4636.

Geranio, L.; Heuberger, M.; Nowack, B. (2009). The behavior of silver nanotextiles during waching. *Environmental Science and Technology*. **43:** 8113–8118.

Gonzalez, L.; Lison, D.; Kirsch–Volders, M. (2008). Genotoxicity of engineered nanomaterials: A critical review. *Nanotoxicology*. **2(4):** 252–273.

Griffitt, R.J.; Hyndman, K.; Denslow, N.D.; Barber, D.S. (2009). Comparison of molecular and histological changes in zebrafish gills exposed to metallic nanoparticles. *Toxicological Sciences*. **107(2):** 404–415.

Griffitt, R.J.; Luo, J.; Gao, J.; Bonzongo, J.C.; Barber, D.S. (2008). Effects of particle composition and species on toxicity of metallic nanomaterials in aquatic organisms. *Environmental Toxicology and Chemistry*. **27(9):** 1972–1978.

Griffitt, R.J.; Weil, R.; Hyndman, K.A.; Denslow, N.D.; Powers, K.; Taylor, D.; Barber, S.D. (2007). Exposure to copper nanoparticles causes gill injury and acute lethality in zebrafish (*Danio rerio*). *Environmental Science and Technology*. **41:** 8178–8186.

Guzman, K.A.D.; Taylor, M.R.; Banfield, J.F. (2006). Environmental risks of nanotechnology: national nanotechnology initiative funding, 2000–2004. *Environmental Science and Technology*. **40:** 1401–1407.

Halliwell, B.; Gutteridge, J.M.C. (1984). Oxygen toxicity, oxygen radicals, transition metals and disease. *Biochemical Journal*. **219:** 1–14.

Halliwell, B.; Gutteridge, J.M.C. (1999). Free Radicals in Biology and Medicine. New York: Oxford Univ. Press. 936 pp.

Handy, R.D.; Shaw B.J. (2007). Toxic effects of nanoparticles and nanomaterials: Implications for public health, risk assessment and the public perception of nanotechnology. *Health, Risk and Society*. **9(2):** 125–144.

Handy, R. D.; Owen, R.; Valsami–Jones, E. (2008a). The ecotoxicology of nanoparticles and nanomaterials: current status, knowledge gaps, challenges, and future needs. *Ecotoxicology*. **17:** 315–325.

Handy, R.D.; Cornelis, G.; Fernandes, T.; Tsyusko, O.; Decho, A.; Sabo–Attwood, T.; Metcalfe, C.; Steevens, J.A.; Klaine, S.J.; Koelmans, A.A.; Horn, N. (2012). Ecotoxicity test methods for engineered nanomaterials: Practical experiences and recommendations from the bench. *Environmental Toxicology and Chemistry*. **31(1):** 15–31.

Handy, R.D.; Kammer, F.; Lead, J.R.; Hassellöv, M.; Owen, R.; Crane, M. (2008b). The ecotoxicology and chemistry of manufactured nanoparticles. *Ecotoxicology*. **17:** 287–314.

Hassellöv, M.; Readman, J. W.; Ranville, J. F.; Tiede, K. (2008). Nanoparticle analysis and characterization methodologies in environmental risk assessment of engineered nanoparticles. *Ecotoxicology*. **17:** 344–361.

Heinlaan, M.; Ivask, A.; Blinova, I.; Dubourguier, H.C.; Kahru, A. (2008). Toxicity of nanosized and bulk ZnO, CuO and $TiO_2$ to bacteria *Vibrio fischeri* and crustaceans *Daphnia magna* and *Thamnocephalus platyurus*. *Chemosphere.* **71:** 1308–1316.

Heinlaan, M.; Kahru, A.; Kasemets, K.; Arbeille, B.; Prensier, G.; Dubourgier, H.–C. (2011). Changes in the *Daphnia magna* midgut upon ingestion of copper oxide nanoparticles: A transmission electron microscopy study. *Water Research*. **45:** 179–190.

http://discovernano.northwestern.edu Using nanotechnology (2005). Northwestern University, Evanston, IL, USA. Accessed July 2012.

http://www.luxresearchinc.com. Sizing Nanotechnology's Value Chain (2004). Lux Research Inc. New York, USA. Accessed October 2009.

http://www.nano.gov. National Nanotechnology Initiative (NNI) (2007). Accessed February 2008.

http://www.nanotechproject.org The project on emerging nanotechnologies (2012). Woodrow Wilson International Center for Scholars, Washington, DC, USA. Accessed March 2012.

Hu, Y.–L.; Gao, J.–Q. (2010). Potential neurotoxicity of nanoparticles. *International Journal of Pharmaceutics*. **394:** 115–121.

Hull, M.S.; Chaurand, P.; Rose, J.; Auffan, M.; Bottero, J.–Y.; Jones, J.C.; Schultz, I.R.; Vikesland, P.J. (2011). Filter–feeding bivalves store and biodeposit colloidally stable gold nanoparticles. *Environmental Science and Technology*. **45:** 6592–6599.

Hyung, H.; Fortner, J.D.; Hughes, J.B.; Kim, J.H. (2007). Natural organic matter stabilizes carbon nanotubes in the aqueous phase. *Environmental Science and Technology*. **41:** 179–184.

Ivask, A.; Bondarenko, O.; Jepihhina, N.; Kahru, A. (2010). Profiling of the reactive oxygen species–related ecotoxicity of CuO, ZnO, TiO2, silver and fullerene nanoparticles using a set of recombinant luminescent *Escherichia coli* strains: differentiating the impact of particles and solubilised metals. *Analytical and Bioanalytical Chemistry*. **398:** 701–716.

Ju–Nam, Y.; Lead, J.R. (2008). Manufactured nanoparticles: An overview of their chemistry, interactions and potential environmental implications. *Science of the Total Environment*. **400:** 396–414.

Kádar, E.; Lowe, D.M.; Solé, M.; Fisher, A.S.; Jha, A.N.; Readman, J.W.; Hutchinson, T.H. (2010a). Uptake and biological responses to nano–Fe versus soluble $FeCl_3$ in excised mussel gills. *Analytical and Bioanalytical Chemistry*. **396:** 657–666.

Kádar, E.; Simmance, F.; Martin, O.; Voulvoulis, N.; Widdicombe, S.; Mitov, S.; Lead, J. R.; Readman, J. W. (2010b). The influence of engineered $Fe_2O_3$ nanoparticles and soluble ($FeCl_3$) iron on the developmental toxicity caused by $CO_2$–induced seawater acidification. *Environmental Pollution*. **158**: 3490–3497.

Kádar, E.; Tarran, G.A.; Jha, A.N.; Al–Subiai, S.N. (2011). Stabilization of engineered zero–valent nanoiron with Na–acrylic copolymer enhances spermiotoxicity. *Environmental Science and Technology*. **45:** 3245–3251.

Karlsson, H.L. (2010). The comet assay in nanotoxicology research. *Analytical and Bioanalytical Chemistry*. **398:** 651–666.

Karlsson, H.L.; Cronholm, P.; Gustafsson, J.; Möller, L. (2008). Copper oxide nanoparticles are highly toxic: a comparison between metal oxide nanoparticles and carbon nanotubes. *Chemical Research in Toxicology*. **21:** 1726–1732.

Kim, J.S.; Kuk, E.; Yu, K.N.; Kim, J.–H.; Park, S.J.; Lee, H.J.; Kim, S.H.; Park, Y.K.; Park, Y.H.; Hwang, C.–Y.; Kim, Y.K.; Lee, Y.–S.; Jeong, D.H.; Cho, M.–H. (2007). Antimicrobial effects of silver nanoparticles. Nanomedicine: *Nanotechnology, Biology and Medicine*. **3:** 95–101.

Kim, S.; Bae, S.W.; Lee, J.S.; Park, J. (2009). Recyclable gold nanoparticle catalyst for the aerobic alcohol oxidation and C–C bond forming reaction between primary alcohols and ketones under ambient conditions. *Tetrahedron*. **65(7):** 1461–1466.

Kimbrough, K.L.; Johnson, W.E.; Lauenstein, G.G.; Christensen, J.D.; Apeti, D.A. (2008). An assessment of two decades of contamination monitoring in the nation's coastal zone. Silver Spring, MD. NOAA Technical Memorandum NOS NCCOS 44. 105pp.

Kirkham, M.; Parton, R.G. (2005). Clathrin–independent endocytosis: new insights into caveolae and non–caveolae lipid raft carriers. *Biochimica et Biophysica Acta*. **1746(3):** 349–363.

Klaine, S. J.; Alvarez, P. J. J.; Batley, G. E.; Fernandes, T. F.; Handy, R. D.; Lyon, D. Y.; Mahendra, S.; McLaughlin, M. J.; Lead, J. R. (2008). Nanomaterials in the environment: behavior, fate, bioavailability and effects. *Environmental Toxicology and Chemistry*. **27(9):** 1825–1851.

Klaine, S.J.; Koelmans, A.A.; Horne, N.; Carley, S.; Handy, R.D.; Kapustka, L.; Nowack, B.; von der Kammer, F. (2012). Paradigms to assess the environmental impact of manufactured nanomaterials. *Environmental Toxicology and Chemistry*. **31(1):** 3–14.

Klaper, R.; Crago, J.; Barr, J.; Arndt, D.; Setyowati, K.; Chen, J. (2009). Toxicity biomarker expression in daphnids exposed to manufactured nanoparticles: Changes in toxicity with functionalization. *Environmental Pollution*. **157:** 1152–1156.

Knigge, T., Monsinjon, T., Andersen, O.K. (2004). Surface–enhanced laser desorption/ ionization–time of flight–mass spectrometry approach to biomarker discovery in blue mussels (*Mytilus edulis*) exposed to polyaromatic hydrocarbons and heavy metals under field conditions. *Proteomics.* **4**: 2722–2727.

Koehler, A.; Marx, U.; Broeg, K.; Bahns, S.; Bressling, J. (2008). Effects of nanoparticles in *Mytilus edulis* gills and hepatopancreas – a new threat to marine life? *Marine Environmental Research*. **66(1):** 12–14.

Lam, P.K.S.; Gray, J.S. (2003). The use of biomarkers in environmental monitoring programmes. *Marine Pollution Bulletin*. **46:** 182–186.

Langston, W.J.; Bebianno, M.J.; Burt, G.R. (1998). Metal handling strategies in molluscs. In: Langston, W.J.; Bebianno, M.J. (Eds.). Metal Metabolism in Aquatic Environments. Chapman and Hall, London, pp. 219–283.

Lapresta–Fernández, A.; Fernández, A.; Blasco, J. (2012). Nanoecotoxicity effects of engineered silver and gold nanoparticles in aquatic organisms. *Trends of Analytical Chemistry*. **32:** 40–59.

Lee, K. J.; Nallathamby, P. D.; Browning, L. M.; Osgood, C. J.; Xu, X. N. (2007). In *vivo* imaging of transport and biocompatibility of single silver nanoparticles in early development of zebrafish embryos. *ACS Nano*. **1(2):** 133–143.

Lee, Y.; Choi, J.R.; Lee, K.J.; Stott, N.E.; Kim, D. (2008). Large–scale synthesis of copper nanoparticles by chemically controlled reduction for applications of inkjet–printed electronics. *Nanotechnology*. **19:** 7.

Lesser, M.P. (2006). Oxidative stress in marine environments: Biochemistry and physiology ecology. *Annual Reviews in Physiology*. **68:** 253–278.

Li, A.Q.; Elliot, D.W.; Zhang, W.X. (2006). Zero–valent iron nanoparticles for abatement of environmental pollutants: materials and engineering aspects. *Critical Reviews in Solid State and Materials Science*. **31:** 111–122.

Li, Y.; Liang, J.; Tao, Z.; Chen, J. (2007). CuO particles and plates: Synthesis and gas–sensor applications. *Materials Research Bulletin*. **43:** 2380–2385.

Liebler, D.C. (2002). Proteomic approaches to characterize protein modifications: new tools to study the effects of environmental exposures. *Environmental Health Perspectives.* **110(1)**: 3–9.

Livingstone, D.R. (1993). Biotechnology and pollution monitoring: Use of molecular biomarkers in the aquatic environment. *Journal of Chemical and Technical Biotechnology*. **57:** 195–211.

Livingstone, D.R. (2001). Contaminant–stimulated reactive oxygen species production and oxidative damage in aquatic organisms. *Marine Pollution Bulletin.* **42**: 656–666.

Long, T. C.; Saleh, N.; Tilton, R. D.; Lowry, G. V.; Veronesi, B. (2006). Titanium Dioxide (P25) Produces Reactive Oxygen Species in Immortalized Brain Microglia (BV2): Implications for Nanoparticle Neurotoxicity. *Environmental Science and Technology*. **40(14):** 4346–4352.

López–Barea, J.; Gómez–Ariza, J.L. (2006). Environmental proteomics and metallomics. *Proteomics*. **6:** S51–S62.

Luoma, S.N. (2008). Silver Nanotechnologies and the Environment: Old Problems or New Challenges. Project on Emerging Nanotechnologies. Publication 15. Woodrow Wilson International Centre for Scholars and PEW Charitable Trusts, Washington, DC.

Luoma, S.N.; Rainbow, P.S. (2005). Why is metal bioaccumulation so variable? Biodynamics as a unifying concept. *Environmental Science and Technology*. **39:** 1921–1931.

Maria, V.L.; Bebianno, M.J. (2011). Antioxidant and lipid peroxidation responses in *Mytilus galloprovincialis* exposed to mixtures of benzo(a)pyrene and copper. *Comparative Biochemistry and Physiology Part C: Toxicology and Pharmacology*. **154(1):** 56–63.

Markarian J. (2006). Steady growth predicted for biocides. *Plastics, Additives and Compounding*. **8(1):** 30–3.

Masala, O.; Seshadri, R. (2004). Synthesis routes for large volumes of nanoparticles. *Annual Review of Materials Research*. **34:** 41–81.

Matés, J.M. (2000). Effects of antioxidant enzymes in the molecular control of reactive oxygen species toxicology. *Toxicology*. **153:** 83–104.

Matranga, V.; Corsi, I. (2012). Toxic effects of engineered nanoparticles in the marine environment: Model organisms and molecular approaches. *Marine Environmental Research*. **76:** 32–40.

Maynard, A. (2006). Nanotechnology: a research strategy for addressing risk. Project on Emerging Nanotechnologies. Publication 3. Woodrow Wilson International Centre for Scholars and PEW Charitable Trusts, Washington, DC.

McDonagh, B.; Sheehan, D. (2006). Redox proteomics in the blue mussel *Mytilus edulis*: Carbonylation is not a pre–requisite for ubiquitination in acute free radical–mediated oxidative stress. *Aquatic Toxicology*. **79(4):** 325–333.

Monserrat, J.M.; Martínez, P.E.; Geracitano, L.A.; Amado, L.L.; Martins, C.M.G.; Pinho, G.L.L.; Chaves, I.S.; Ferreira–Cravo, M.; Ventura–Lima, J.; Bianchini, A. (2007). Pollution biomarkers in estuarine animals: critical review and new perspectives. *Comparative Biochemistry and Physiology C.* **146:** 221–234.

Monsinjon, T.; Andersen, O.K.; Leboulenger, F.; Knigge, T. (2006). Data processing and classification analysis of proteomic changes: a case study of oil pollution in the mussel, *Mytilus edulis*. *Proteome Science.* **4(17):** 1–13.

Monsinjon, T.; Knigge, T. (2007). Proteomic applications in ecotoxicology. *Proteomics*. **7(16):** 2997–3009.

Montes, M.O.; Hanna, S.K.; Lenihan, H.S.; Keller, A.A. (2012). Uptake, accumulation, and biotransformation of metal oxide nanoparticles by a marine suspension–feeder. *Journal of Hazardous Materials*. **225–226:** 139–45.

Moore, M.N. (2006). Do nanoparticles present ecotoxicological risks for the health of the aquatic environment? *Environmental International*. **32:** 967–976.

Moore, M.N.; Lowe, D.M.; Soverchia, C.; Haigh, S.D.; Hales, S.G. (1997). Uptake of a non–calorific, edible sucrose polyester oil and olive oil by marine mussels and their influence on uptake and effects of anthracene. *Aquatic Toxicology*. **39:** 307–20.

Moore, M.N.; Readman, J.A.J.; Readman, J.W.; Lowe, D.M.; Frickers, P.E.; Beesley, A. (2009). Lysosomal cytotoxicity of carbon nanoparticles in cells of the molluscan immune system: an in vitro study. *Nanotoxicology*. **3(1):** 40–45.

Morones, J.R.; Elechiguerra, J.L.; Camacho, A.; Holt, K.; Kouri, J.B.; Ramírez, J.T.; Yacaman, J.M. (2005). The bactericidal effect of silver nanoparticles. *Nanotechnology*. **16:** 2346–2353.

Mortimer, M.; Kasemets, K.; Kahru, A. (2010). Toxicity of ZnO and CuO nanoparticles to ciliated protozoa *Tetrahymena thermophila*. *Toxicology*. **269(2–3):** 182–189.

Mueller, N.C.; Nowack, B. (2008). Exposure modelling of engineered nanoparticles in the environment. *Environmental Science and Technology*. **42(12):** 4447–4453.

Navarro, E.; Baun, A.; Behra, R.; Hartmann, N.B.; Filser, J.; Miao, A.; Quigg, A.; Santschi, P.H.; Sigg, L. (2008). Environmental behavior and ecotoxicity of engineered nanoparticles to algae, plants and fungi. *Ecotoxicology*. **17:** 372–386.

Nel, A. (2006). Toxic Potential of Materials at the Nanolevel. *Science.* **311:** 622–627.

Nesatyy, V.J.; Suter, M.J.–F. (2007). Proteomics for the analysis of environmental stress responses in organisms. *Environmental Science and Technology*. **41(20):** 6891–6900.

Nowack , B.; Bucheli, T.D. (2007). Occurrence, behavior and effects of nanoparticles in the environment. *Environmental Pollution*. **150:** 5–22.

Oberdörster, G.; Oberdörster, E.; Oberdörster, J. (2005). Nanotoxicology: An Emerging Discipline Evolving from Studies of Ultrafine Particles. *Environmental Health Perspective*. **113**(7): 823–839.

Oberdörster. E. (2004). Manufactured Nanomaterials (Fullerenes, C60) Induce Oxidative Stress in the Brain of Juvenile Largemouth Bass. *Environmental Health Perspectives*. **112(10)**: 1058–1062

Pan, J.–F.; Buffet, P.–E.; Poirier, L.; Amiard–Triquet, C.; Gilliland, D.; Joubert, Y.; Pilet, P.; Guibbolini, M.; de Faverney, C.R.; Roméo, M.; Valsami–Jones, E.; Mouneyrac, C. (2012). Size dependent bioaccumulation and ecotoxicity of gold nanoparticles in an endobenthic invertebrate: The Tellinid clam *Scrobicularia plana*. *Environmental Pollution*. **168:** 37–43.

Park, S.–Y.; Choi, J. (2011). Geno– and ecotoxicity evaluation of silver nanoparticles in freshwater crustacean *Daphnia magna*. *Environmental Engineering Research*. **15(1):** 23–27.

Paur, H.–R.; Cassee, F.R.; Teeguarden, J.; Fissan, H.; Diabate, S.; Aufderheide, M.; Kreyling, W.G.; Hänninen, O.; Kasper, G.; Riediker, M.; Rothen–Rutishauser, B.; Schmid, O. (2011). In–vitro cell exposure studies for the assessment of nanoparticle toxicity in the lung—A dialog between aerosol science and biology. *Journal of Aerosol Science*. **42:** 668–692.

Petersen, E.J.; Nelson, B.C. (2010). Mechanisms and measurements of nanomaterial–induced oxidative damage to DNA. *Analytical and Bioanalytical Chemistry*. **398:** 613–650.

Peyrot, C.; Gagnon, C.; Gagné, F.; Willkinson, K. J.; Turcotte, P.; Sauvé, S. (2009). Effects of cadmium telluride quantum dots on cadmium bioaccumulation and metallothionein production to the freshwater mussel, *Elliptio complanata*. *Comparative Biochemistry and Physiology C*. **150:** 246–251.

Phillips, D.J.H. (1986). The use of bio–indicators in monitoring conservative contaminants. Program design imperatives. *Marine Pollution Bulletin.* **17:** 10–17.

Porte, C.; Janer, G.; Lorusso, L.C.; Ortiz–Zarragoitia; M.; Cajaraville, M.P.; Fossi, M.C.; Canesi, L. (2006). Endocrine disruptors in marine organisms: Approaches and perspectives. *Comparative Biochemistry and Physiology, Part C*. **143:** 303–315.

Rabilloud, T. (2000). Proteome research: Two–Dimensional Gel Electrophoresis and Identification Methods. Springer Verlag, Heidelberg. 244 pp.

Regoli, F.; Principato, G. (1995). Glutathione, glutathione–dependent and antioxidant enzymes in mussel, *Mytilus galloprovincialis*, exposed to metals under field and laboratory conditions: implications for the use of biochemical biomarkers. *Aquatic Toxicology*. **31:** 143–164.

Ren, G.; Hu, D.; Cheng, E.W.C.; Vargas–Reus, M.A.; Reip, P.; Allaker, R.P. (2008). Characterisation of copper oxide nanoparticles for antimicrobial applications. *International Journal of Antimicrobial Agents*. **33:** 587–590.

Renault, S.; Baudrimont, M.; Mesmer– Dudons, N.; Gonzalez, P.; Mornet, S.; Brisson, A. (2008). Impacts of gold nanoparticle exposure on two freshwater species: a phytoplanktonic alga (*Scenedesmus subspicatus*) and a benthic bivalve (*Corbicula fluminea*). *Gold Bulletin*. **41(2):** 116–126.

Ringwood, A.H.; Levi–Polyachenko, N.; Carroll, D.L. (2009). Fullerene exposures with oysters: embryonic, adult and cellular responses. *Environmental Science and Technology*. **43:** 7136–7141.

Ringwood, A.H.; McCarthy, M.; Bates, T.C.; Carroll, D.L. (2010). The effects of silver nanoparticles on oyster embryos. *Marine Environmental Research*. **69(1):** 549–551.

Roco, M.C. (2005) Environmentally responsible development of nanotechnology. *Environmental Science and Technology*. **39:** 106A–112A.

Roduner, E. (2006) Size matters: why nanomaterials are different? *Chemical Society Reviews*. **35:** 583–592.

Royal Society and Royal Academy of Engineering (2004) Nanoscience and nanotechnologies: opportunities and uncertainties. RS policy document 19/04. London. 113 pp.

Ruparelia, J.P.; Chatterjee, A.K.; Duttagupta, S.P.; Mukherji, S. (2008). Strain specificity in antimicrobial activity of silver and copper nanoparticles. *Acta Biomaterialia*. **4(3):** 707–716.

Schlenk, D. (1999). Necessity of defining biomarkers for use in ecological risk assessments. *Marine Pollution Bulletin*. **39(1–12):** 48–53.

Scown, T.M.; Aerle, R.V.; Tyler, C.R. (2010a). Review: do engineered nanoparticles pose a significant threat to the aquatic environment? *Critical Reviews in Toxicology*. **40(7):** 653–670.

Scown, T.M.; Santos, E.M.; Johnston, B.D.; Gaiser, B.; Baalousha, M.; Mitov, S.; Lead, J.R.; Stone, V.; Fernandes, T.F.; Jepson, M.; van Aerle, R.; Tyler, C.R. (2010b). Effects of aqueous exposure to silver nanoparticles of different sizes in rainbow trout. *Toxicological Sciences*. **115(2):** 521–534.

Shaw, B.J.; Al–Bairuty, G.; Handy, R.D. (2012). Effects of waterborne copper nanoparticles and copper sulphate on rainbow trout, (*Oncorhynchus mykiss*): Physiology and accumulation. *Aquatic Toxicology*. **116–117:** 90–101.

Shepard, J.L.; Bradley, B.P. (2000). Protein expression signatures and lysosomal stability in *Mytilus edulis* exposed to graded copper concentrations. *Marine Environmental Research*. **50:** 457–463.

Simkó, M.; Gazsó, A.; Fiedeler, U.; Nentwich, M. (2011). Nanoparticles, free radicals and oxidative stress. *Nano Trust Dossier*. 12: 1–3.

Simpson, K. (2003). Using silver to fight microbial attack. *Plastics, Additives and Compounding*. **5:** 32–35.

Singh, N.; Manshian, B.; Jenkins, G.J.S.; Griffiths, S.M.; Williams, P.M.; Maffeis, T.G.G.; Wrigh, C.J.; Doak, S.H. (2009). NanoGenotoxicology: The DNA damaging potential of engineered nanomaterials. *Biomaterials*. **30:** 3891–3914.

Smith, C.J.; Shaw, B.J.; Handy, R.D. (2007). Toxicity of single walled carbon nanotubes to rainbow trout, (*Oncorhynchus mykiss*): Respiratory toxicity, organ pathologies, and other physiological effects. *Aquatic Toxicology*. **82**: 94–109.

Snape, J.R.; Maund, S.J.; Pickford, D.B.; Hutchinson, T.H. (2004). Ecotoxicogenomics: the challenge of integrating genomics into aquatic and terrestrial ecotoxicology. *Aquatic Toxicology*. **67:** 143–154.

Sondi, I.; Salopek–Sondi, B. (2004). Silver nanoparticles as antimicrobial agent: case study on *E. coli* as a model for Gram–negative bacteria. *Journal of Colloid and Interface Science*. **275:** 177–82.

Stohs, S.J.; Bagchi, D. (1995). Oxidative mechanisms in the toxicity of metal ions. *Free Radical Biology and Medicine*. **8(2)**: 321–336.

Tedesco, S.; Doyle, H.; Blasco, J.; Redmond, G.; Sheehan, D. (2010b). Oxidative stress and toxicity of gold nanoparticles in *Mytilus edulis*. *Aquatic Toxicology*. **100:** 178–186.

Tedesco, S.; Doyle, H.; Blasco, J.; Redmond, G.; Sheehan, D. (2010a). Exposure of the blue mussel, *Mytilus edulis*, to gold nanoparticles and the pro–oxidant menadione. *Comparative Biochemistry and Physiology, Part C*. **151:** 167–174.

Tedesco, S.; Doyle, H.; Redmond, G.; Sheehan, D. (2008). Gold nanoparticles and oxidative stress in *Mytilus edulis*. *Marine Environmental Research*. **66:** 131–133.

Tiede, K.; Hassellöv, M.; Breitbarth, E.; Chaudhry, Q.; Boxall, A.B.A. (2009). Considerations for environmental fate and ecotoxicity testing to support environmental risk assessments for engineered nanoparticles. *Journal of Chromatography A*. **1216(3):** 503–509.

Unfried, K.; Albrecht, C.; Klotz, L.; Mikecz, A.V.; Grether–Beck, S.; Schins, R.P.F. (2007). Cellular responses to nanoparticles: target structures and mechanisms. *Nanotoxicology.* **1(1):** 52–71.

Valavanidis, A.; Vlahogianni, T.; Dassenakis, M.; Scoullos, M. (2006). Molecular biomarkers of oxidative stress in aquatic organisms in relation to toxic environmental pollutants. *Ecotoxicology and Environmental Safety*. **64:** 178–189.

van der Oost, R.; Beyer, J.; Vermeulen, N.P.E. (2003). Fish bioaccumulation and biomarkers in environmental risk assessment: a review. *Environmental Toxicology and Pharmacology*. **13:** 57–149.

Viarengo, A.; Burlando, B.; Cavaletto, M.; Marchi, B.; Ponzano, E.; Blasco, J. (1999). Role of metallothionein against oxidative stress in the mussel *Mytilus galloprovincialis*. *American Journal of Physiology: Regulatory, Integrative and Comparative Physiology*. **277:** R1612–R1619.

Viarengo, A.; Lowe, D.; Bolognesi, C.; Fabbri, E.; Koehler, A. (2007). The use of biomarkers in biomonitoring: A 2–tier approach assessing the level of pollutant–induced stress syndrome in sentinel organisms. *Comparative Biochemistry and Physiology, Part C*. **146:** 281–300.

Viarengo, A.; Nott, J.A. (1993). Mechanisms of heavy metal cation homeostasis in marine invertebrates. *Comparative Biochemistry and Physiology*. **104C(3):** 355–372.

Viarengo, A.M.; Canesi, L. (1991). Mussels as biological indicators of pollution. *Aquaculture*. **94(2–3):** 225–243.

Vioque–Fernández, A. de Almeida, E.A.; López–Barea, J. (2009). Assessment of Doñana National Park contamination in *Procambarus clarkii*: Integration of conventional biomarkers and proteomic approaches. *Science of the Total Environment*. **407:** 1784–1797.

Wang, C.; Hu, Y.J.; Lieber, C.M.; Sun, S.H. (2008a). Ultrathin Au nanowires and their transport properties. *Journal of the American Chemical Society*. **130(28):** 8902–8903.

Wang, H.–T.; Nafday, O.A.; Haamheim, J.R.; Tevaarwerk, E.; Amro, N.A.; Sanedrin, R.G.; Chang, C.–Y.; Ren, F.; Pearton. S.J. (2008b). Toward conductive traces: Dip Pen

Nanolithography® of silver nanoparticle–based inks. *Applied Physics Letters*. **93(14):** 143105.

Wang, W.–X. (2011). Incorporating exposure into aquatic toxicological studies: An imperative. *Aquatic Toxicology*. **105(3–4):** 9–15.

Wang, W.–X.; Rainbow, P.S. (2005). Influence of metal exposure history on trace metal uptake and accumulation by marine invertebrates. *Ecotoxicology and Environmental Safety*. **61:** 145–159.

Wang, Z.; Zhao, J.; Li, F.; Gao, D.; Xing, B. (2009). Adsoprtion and inhibition of acetylcholinesterase by different nanoparticles. *Chemosphere.* **77(1):** 67–73.

Ward, J.E.; Kach, D.J. (2009). Marine aggregates facilitate ingestion of nanoparticles by suspension–feeding bivalves. *Marine Environmental Research.* **68:** 137–142.

Ward, J.E.; Macdonald, B.A.; Thompson, R.J.; Beninger, P.G. (1993). Mechanisms of suspension–feeding in bivalved–resolution of current controversies by means of endoscopy. *Limnology and Oceanography*. **38:** 265–272.

Wilson, M.R.; Lightbody, J.H.; Donaldson, K.; Sales, J.; Stone V. (2002). Interactions between ultrafine particles and transition metals in vivo and in vitro. *Toxicology and Applied Pharmacology*. **184:**172–179.

Xia, T.; Li, N.; Nel, A.E. (2009). Potential health impact of nanoparticles. *Annual Review of Public Health*. **30:** 137–150.

Yeo, M.–K.; Pak, S.–W. (2008). Exposing zebrafish to silver nanoparticles during caudal fin regeneration disrupts caudal fin growth and p53 signaling. *Molecular and Cellular Toxicology*. **4(4):** 311–317.

Yoon, K.Y.; Byeon, J.H.; Park, J.H.; Hwang, J. (2007). Susceptibility constants of *Escherichia coli* and *Bacillus subtilis* to silver and copper nanoparticles. *Science of the Total Environment*. **373:** 572–575.

Zhang, W. (2003). Nanoscale iron particles for environmental remediation: An overview. *Journal of Nanoparticle Research.* **5:** 323–332.

Zhang, W.–X.; Elliott, D.W. (2006). Applications of iron nanoparticles for groundwater remediation. *Remediation.* **16:** 7–21.

Zuykov, M.; Pelletier, E.; Demers, S. (2011). Colloidal complexed silver and silver nanoparticles in extrapallial fluid of *Mytilus edulis*. *Marine Environmental Research*. **71(1):** 17–21.

# CHAPTER 2

## Effects of copper nanoparticles exposure in mussels *Mytilus galloprovincialis*

# 2.1

# EFFECTS OF COPPER OXIDE NANOPARTICLES IN THE MUSSEL *MYTILLUS GALLOPROVINCIALIS*

*Tânia Gomes[1], José P. Pinheiro[2], Ibon Cancio[3], Catarina G. Pereira[1], Cátia Cardoso[1], Maria João Bebianno[1]*

[1]CIMA, Faculty of Science and Technology, University of Algarve, Campus de Gambelas, 8005–139 Faro, Portugal

[2]CBME, Faculty of Science and Technology, University of Algarve, Campus de Gambelas, 8005–139 Faro, Portugal

[3]Department of Zoology & Animal Cell Biology, Scholl of Science and Technology, University of the Basque Country, E–48080 Bilbao, Spain

Environmental Science and Technology 45: 9356–9362

## Abstract

CuO NPs are widely used in various industrial and commercial applications. However, little is known about their potential toxicity or fate in the environment. In this study the effects of copper nanoparticles were investigated in the gills of mussels *Mytilus galloprovincialis*, comparative to $Cu^{2+}$. Mussels were exposed to 10 μgCu.$L^{-1}$ of CuO NPs and $Cu^{2+}$ for 15 days, and biomarkers of oxidative stress, metal exposure and neurotoxicity evaluated. Results show that mussels accumulated copper in gills and responded differently to CuO NPs and $Cu^{2+}$, suggesting distinct modes of action. CuO NPs induced oxidative stress in mussels by overwhelming gills antioxidant defence system, while for $Cu^{2+}$ enzymatic activities remained unchanged or increased. CuO NPs and $Cu^{2+}$ originated lipid peroxidation in mussel despite different antioxidant efficiency. Moreover, an induction of MT was detected throughout the exposure in mussels exposed to nano and ionic Cu, more evident in CuO NPs exposure. Neurotoxic effects reflected as AChE inhibition were only detected at the end of the exposure period for both forms of copper. In overall, these findings show that filter–feeding organisms are significant targets for nanoparticle exposure and need to be included when evaluating the overall toxicological impact of nanoparticles in the aquatic environment.

Keywords: *Mytilus galloprovincialis*, CuO NPs, oxidative stress, gills

### 2.1.1. Introduction

Nanotechnology is a rapid growing field that comprises the research and development of particles <100 nm. As nanotechnology start to come on line with larger scale production and increasing applications, it is inevitable that nanomaterials and their by–products end up in the aquatic environment where they can induce short and long term effects in aquatic organisms (Baun *et al*., 2008; Moore, 2006).

Copper is an essential metal, with a role as a co–factor in numerous enzymes (cytochrome oxidase, superoxide dismutase, among others) that is toxic when present in higher concentrations than those necessary for organisms (Bebianno *et al*., 2004; da Silva and Williams, 2001; Maria and Bebianno, 2011; Regoli and Principato, 1995). Soluble forms of Cu have been extensively investigated on its bioavailability and effects in aquatic organisms (e.g.Bebianno *et al*., 2004; Maria and Bebianno, 2011; Regoli and Principato, 1995). In the nanoform, copper is increasingly used in various applications such as air and liquid filtration, wood preservation, bioactive coatings and coatings on integrated circuits and batteries and thermal and electrical conductivity. Additionally, these Cu nanoparticles are applied in several products as inks, skin products and textiles manly due to their bactericide properties (Aruoja *et al*., 2009; Fahmy and Cormier, 2009; Griffitt *et al*., 2007; Heinlaan *et al*., 2008; Yoon *et al*., 2007). The toxicity of copper oxide nanoparticles (CuO NPs) was assessed in several test organisms, namely, bacteria (*Vibrio fischeri, Escherichia coli, Staphylococcus aureus, Bacillus subtilis*), protozoa (*Tetrahymena thermophila*), crustaceans (*Daphnia magna*, *Thamnocephalus platyurus*, *Daphnia pulex* and *Ceriodaphnia dubia*), algae (*Pseudokirchneriella subcapitata*) and zebrafish (*Danio rerio*), showing a cytotoxic effect in all these species (Aruoja *et al*., 2009; Griffitt *et al*., 2007, 2008, 2009; Heinlaan *et al*., 2008,2011; Mortimer *et al*., 2010; Ruparelia *et al*., 2008; Yoon *et al*., 2007). However, there is a severe lack of information on the potential effects of CuO NPs in bivalve species, as well as its behaviour in aqueous environments.

Despite the rapid emerging literature on the production of reactive oxygen species (ROS) and oxidative stress as main effects of NPs exposure, its mechanisms of toxicity need further clarification in invertebrate species (Baun *et al*., 2008; Moore, 2006; Unfried *et al*., 2007; Xia *et al*., 2006). Recent studies have suggested that oxidative stress may be the cause of CuO NPs cytotoxicity in bacteria, daphnids, zebrafish as well as in human lung cells (Fahmy and Cormier, 2009; Griffitt *et al*., 2007, 2009; Heinlaan *et al*., 2008, 2011). Biomarkers that have been used as early warning signals of the presence of contaminants in aquatic environments

are important tools to assess the toxic effects of nanomaterials in aquatic organisms (Bebianno *et al*., 2004; Heinlann *et al*., 2008; Moore, 2006; Regoli and Principato, 1995). Filter–feeding molluscs such as *Mytilus sp.* are a target group for the uptake of nanoparticles present in the aquatic environment. They have been widely used in the assessment of water quality due to their ability to accumulate conventional contaminants in the dissolved or the suspended form (Baun *et al*., 2008; Griffitt *et al*., 2007; Langston *et al*., 1998; Moore, 2006). Due to their filter feeding habits, bivalves gill epithelium is the main interface between the organism and the surrounding environment, being the primary pathway of exposure to environmental contaminants. In bivalves exposed to nanoparticles, gills seem to be the first targeted organ, either by direct passage or particle uptake (e.g. Baun *et al*., 2008; Griffitt *et al*., 2007, 2009; Moore, 2006). Therefore, in this work, the toxic effects of CuO NPs in gills of mussels *Mytilus galloprovincialis* were evaluated using as end points biomarkers of oxidative stress (antioxidant enzymes SOD, CAT and GPX and lipid peroxidation), metal exposure (MT) and neurotoxicity (AChE). These effects were compared with mussels exposed to ionic Cu since the mode of action of Cu accumulation in this species is well understood.

## 2.1.2. Materials and methods

### 2.1.2.1.Nanoparticles characterization

Copper oxide nanoparticles (<50 nm) stock solution was prepared in ultrapure water, sonicated for 30 minutes and kept in constant shaking to reach a concentration of 10 μgCu.$L^{-1}$. Ionic copper stock solution ($Cu^{2+}$) was prepared identically but not sonicated. The particles size was characterized using Transmission Electron Microscopy (TEM) and Dynamic Light Scattering (DLS). For TEM analysis, CuO NPs were diluted in ultrapure water and sonicated to keep the particles in solution and avoid aggregation. A drop of the dilution at 32 ppm was allowed to dry on a Ni grid cover and examined at 80 KV. The range of particles sizes was determined through analysis of 250 NPs randomly selected. Images were recorded using a JEOL JEM–1230 TEM equipped with a digital camera Model 785 ES1000W Erlangshen CCD. Additionally, particle size and agglomerates, as well as behaviour in natural seawater during 12 hours were followed using DLS. The hydrodynamic radii of the nanoparticles were determined using an ALV apparatus with Ar Ion Lased (514.5 nm). Diluted particle dispersions (100 μg.$l^{-1}$ CuO NPs) were measured at 90º and intensity fluctuations analyzed automatically and in a single run by an ALV–7000 digital correlator. The temperature was

controlled (20 ± 0.1 ºC) using a Haake Phoenix–II heater/circulator with a C30P cooling bath, with Haake Sil 180 mineral oil. The temperature was read directly from the decalin bath using a Platinum Pt100 temperature sensor.

### 2.1.2.2. Laboratory exposure

Mussels *Mytilus galloprovincialis* (61.7 ± 8.4 mm) were collected in South of Portugal and acclimated during 7 days in natural seawater at constant temperature and aeration. Afterwards, fifty mussels were placed in tanks filled with seawater in a triplicate design (around 2.5 mussels/L) and exposed to 10 μgCu.$L^{-1}$ of CuO NPs and $Cu^{2+}$ along with a control group kept in clean seawater, for a period of 15 days. The copper concentration selected was environmentally relevant (Bebianno *et al*., 2004; Damiens *et al*., 2006). Water was changed every 12 hours (to avoid nanoparticles aggregation) with re–dosing after each change. Temperature (17.8 ± 1.1ºC), salinity (36.3 ± 0.2), oxygen saturation (97.8 ± 4.9%) and pH (7.8 ± 0.1) were measured daily. Mussels were collected from controls, CuO NPs and $Cu^{2+}$ in the beginning of the experiment and after 3, 7 and 15 days of exposure. No mortality was detected during the exposure period. After sampling, gills were dissected and immediately frozen in liquid nitrogen and stored at –80ºC until further use.

### 2.1.2.3. Metal analysis

Copper concentrations were determined in water samples from CuO NPs and $Cu^{2+}$ exposures after a period of 12 hours before water renewal and re–dosing. Total copper concentrations from both exposures were determined after acid digestion with 2% nitric acid ($HNO_3$), while dissolved copper from CuO NPs exposure was determined after water filtration (0.02 μm filter, Anotop 25, Whatman) and acid digestion (Griffitt *et al*., 2009). Cu in all water samples and on dried (80ºC) mussel of gills after wet digested with $HNO_3$ were analysed by graphite furnace atomic absorption spectrometry (AAS AAnalyst 800 – Perkin Elmer). Quality assurance was checked using a standard reference material (Lobster Hepatopancreas) provided by the National Research Council, Canada – TORT II. The mean±standard deviation (106.8 ± 2.5 μg.$g^{-1}$) was similar to the certificated value (106.0 ± 10.0 μg.$g^{-1}$). Quality assurance was checked using a standard reference material (Lobster Hepatopancreas) provided by the National Research Council, Canada – TORT II. The mean±standard deviation (106.8 ± 2.5 μg.$g^{-1}$) was similar to the certificated value (106.0 ± 10.0 μg.$g^{-1}$).

### 2.1.2.4. Enzymatic activities

Superoxide dismutase, catalase and glutathione peroxidase activities were measured in the gills cytosolic fraction. Superoxide dismutase activity (SOD) was determined by the absorption of the reduction of cytochrome c by the xanthine oxidase/hypoxanthine system at a wavelength of 550 nm (McCord and Fridovich, 1969). Catalase activity (CAT) was a result of the decrease of the absorbance at 240 nm due to hydrogen peroxide consumption, using a molar extinction coefficient of 40 $M^{-1}$ $cm^{-1}$ (Greenwald, 1985). Total glutathione peroxidase (GPX) was measured following NADPH oxidation at 340 nm in the presence of excess glutathione reductase, reduced glutathione and cumene hydroperoxide as substrate (Lawrence and Burke, 1976).

### 2.1.2.5. Metallothioneins

Gills were homogenised in three volumes of Tris–HCl buffer (0.02 M, pH 8.6) and centrifuged at 30,000 *g* for 45 minutes (4ºC). The supernatant was separated from the pellet, and two aliquots were used for lipid peroxidation and total protein determination. The remaining supernatant was heat–treated at 80ºC and re–centrifuged at 30,000 *g* for 45 minutes (4ºC). An aliquot of the heat–treated cytosol was used for the quantification of MT concentration by Differential Pulse Polarography (Bebianno and Langston, 1989).

### 2.1.2.6. Acetylcholinesterase

Gills were homogenized on ice in five volumes of a Tris–HCl buffer (100 mM, pH 8.0) containing 10% Triton and centrifuged at 12,000 *g* for 30 minutes (4ºC). This calorimetric method is based on the coupled enzyme reaction of acetylthiocholine as the specific substrate for AChE and 5,5'–dithio–bis–2–nitrobenzoate as an indicator for the enzyme reaction at 450 nm (Ellman *et al*., 1961).

### 2.1.2.7. Lipid peroxidation

Lipid peroxidation (LPO) was assessed by determining malondialdehyde (MDA) and 4–hydroxyalkenals (4–HNE) concentrations upon the decomposition by polyunsaturated fatty acid peroxides using malondialdehyde bis–(tetrametoxypropan) as a standard (Erdelmeier *et al*., 1998).

#### 2.1.2.8. Total protein concentration

Total protein content of gills was measured by the Lowry method (Lowry *et al*., 1951) using Folin's Reagent and Bovine Serum Albumin (BSA) as a standard.

#### 2.1.2.9. Statistical analysis

The data obtained was tested using one–way analysis of variance (ANOVA) or the Kruskal–Wallis One Way Analysis of Variance on Ranks. If significant, pairwise multiple–comparison procedures were conducted, using the Tukey test or the Dunn's method. Linear regression was also applied, to verify existing relationships between variables. Statistical significance was set at $p<0.05$ and analyses were performed using SigmaPlot10®.

Principal Component Analysis (PCA) was applied to evaluate the relationship between copper concentrations, antioxidant enzymes activities, MT concentrations, AChE activity and LPO levels in the gills of control and exposed mussels along the period of exposure. Computations were performed using XLStat2009®.

### 2.1.3. Results and Discussion

To our knowledge this is the first study that focused on the effects of CuO NPs in the gills of *M. galloprovincialis*. The nanoparticles used are spherical in shape and not strongly aggregated, with a mean diameter of 31 ± 10 nm (Figure 2.1.1A–B). The particles size distributions of CuO NPs obtained by DLS showed polydisperse aggregates (polydispersity index between 0.26 and 0.48) characterized by single particles with sizes from 30–40 nm to aggregates ranging from 238–338 nm. The higher size of CuO NPs suspended in seawater obtained by DLS compared to TEM is due to the propensity of these particles to aggregate in aqueous state. This finding is supported by other studies that used CuO NPs, some of which from the same manufacturer (Griffitt *et al*., 2007, 2008, 2009; Heinlaan *et al*., 2011; Karlsson *et al*., 2008).

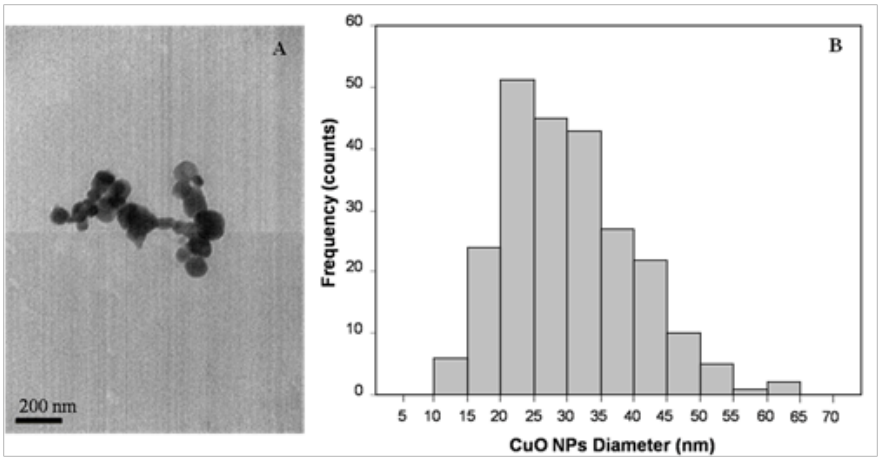


**Figure 2.1.1 –** A) Transmission electron microscopic image of CuO nanoparticles at 32 ppm in Milli–Q water. (B) Particle size distribution histogram of CuO NPs obtained from TEM images. (C) Copper concentrations in gills of mussels *M. galloprovincialis* from controls and exposed to CuO NPs and $Cu^{2+}$ for 15 days in a dry weight tissue basis (average ± Std). Capital and lower letters represent statistical differences between treatments in each exposure day and for each treatment during the exposure duration, respectively ($p$<0.05).

As the number of CuO NPs applications increase, it is likely that they will end up into the environment, and in significant quantities. However, emissions of NPs to the aquatic environment are difficult to detect and quantify, and no available data exists on CuO NPs. In our study, more than 50% of the nominal concentration of 10μgCu.$L^{-1}$ added in the nano or ionic form was removed from the water column after the 12–hour exposure (53% for CuO NPs and 66% for $Cu^{2+}$). The lost of this amount of copper may be due either to the presence of the mussels, copper dissolution or nanoparticles aggregation and sedimentation (Griffitt *et al*., 2008, 2009). Of the total Cu concentration (4.8 ± 01 μgCu.$L^{-1}$) obtained from the CuO NPs exposure, less than 1% of the initial added dose is present in the dissolved form, indicating that most of the Cu present in solution is in the nanoparticulate form. Other authors using CuO NPs also showed lower dissolution from nanocopper, suggesting that Cu toxicity is mainly due to CuO NPs (Griffitt *et al*., 2007, 2008, 2009; Heinlaan *et al*., 2011).

The bioaccumulation of NPs in invertebrates provides valuable knowledge on NPs bioavailability and allows more realistic toxicity information (Baun *et al*., 2008; Moore, 2006; Ward and Kach, 2009). Data about internal exposure concentrations and accumulation of NPs in various tissues on chronic exposure of aquatic organisms is practically inexistent (Baun *et al*., 2008; Ward and Kach, 2009). In this study, the exposure to CuO NPs resulted in a significant accumulation of copper in mussel gills with time (9.8 ± 1.9 to 12.5 ± 1.4 μg.$g^{-1}$ dw, Figure 2.1.2). In mussels exposed to $Cu^{2+}$, accumulation only occurred in the first week

(16.9 ± 2.4 and 15.5 ± 2.4 μg.g$^{-1}$ dw, $p$<0.05), followed by a decrease at the end of the experiment, to levels similar to control ($p$>0.05, Figure 2.1.2). This decrease is indicative of the elimination rate of Cu in bivalves through detoxification processes (da Silva and Williams, 2001; Langston *et al*., 1998), while in those exposed to CuO NPs the elimination rate is slower than its accumulation. Mussels accumulated more copper from $Cu^{2+}$ than CuO NPs in the first week of exposure, suggesting a higher copper bioavailability from $Cu^{2+}$. Mussel gills are a target organ for nanoparticles exposure, being more sensitive to metal dissociation from NPs than its internalization (Baun *et al*., 2008; Griffitt *et al*., 2007, 2009; Moore, 2006; Peyrot *et al*., 2009); nevertheless, no distinction was made between dissolved and incorporated copper particles. Several studies have shown copper accumulation in bivalves tissues (e.g. Bebianno *et al*., 2004; Regoli and Principato, 1995; Serafim and Bebianno, 2009), however, no data exists on the accumulation of copper from NPs exposure.

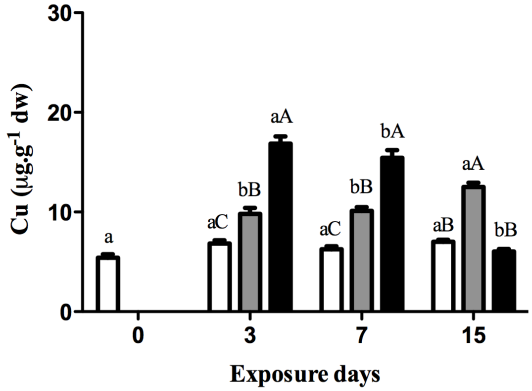


**Figure 2.1.2 –** Copper concentrations in gills of mussels *M. galloprovincialis* from controls and exposed to CuO NPs and $Cu^{2+}$ for 15 days in a dry weight tissue basis (average ± Std). Capital and lower letters represent statistical differences between treatments in each exposure day and for each treatment during the exposure duration, respectively ($p$<0.05).

Chemical reactivity, as well as specific surface characteristics confers nanomaterials the capacity to generate ROS by mere interaction with subcellular structures and by directing its reactivity to subcellular compartments. In the case of metal nanoparticles, the physical contact between cells and particles may cause changes in the vicinity of the contact area and increase the dissolution of metals or generate extracellular ROS (Griffitt *et al*., 2007; Heinlaan *et al*., 2008; Unfried *et al*., 2007). Copper, being a redox active metal, has the capacity to produce ROS through Fenton–type reactions leading to the production of

oxyradicals that activate/inhibit several antioxidant enzymes (Bebianno *et al*., 2004; da Silva and Williams, 2001; Griffitt *et al*., 2007; Heinlaan *et al*., 2008; Maria and Bebianno, 2011; Regoli and Principato, 1995; Yoon *et al*., 2007). The activities of SOD, CAT and GPX were used along with lipid peroxidation to assess the oxidative status of mussel gills exposed to CuO NPs and $Cu^{2+}$ (Figures 2.1.3 and 2.1.4).

SOD, CAT and GPX activities changed after exposure to CuO NPs, showing that these NPs have also potent redox properties with the capacity to generate ROS (Figure 2.1.3). In CuO NPs exposed mussels, SOD activity increased linearly (7.5 $U.mg^{-1}prot.d^{-1}$, $r$=0.99, $p$<0.05) in the first 7 days, indicative of the formation of superoxide anions. CAT was only induced after 3 days of NPs exposure (43%) while GPX activity remained unchanged and similar to unexposed mussels ($p$>0.05). The induction of GPX after a week of NPs exposure (15.8 ± 3.1 to 21.3 ± 1.7 $nmol.min.mg^{-1}prot$) suggests the detoxification of hydroperoxides possibly associated with increased levels of hydroxyl radicals originated by CuO NPs, whereas at the beginning SOD and CAT levels may have been sufficient to counteract the overproduction of ROS. The SOD and CAT similar antioxidant efficiencies were supported by the PCA analysis (Figure 2.1.5A) that shows a significant correlation in the first week of exposure. After two weeks, both SOD and CAT activities decreased (38 and 33 % of inhibition, $p$<0.05) in mussels exposed to CuO NPs, whereas GPX continued to increase. These inhibitory effects suggest an overproduction of ROS that could have lead to the degeneration of the enzymes. These ROS can be available to react with $Cu^{2+}$ from CuO NPs dissolution, leading to the formation of hydroxyl radicals generated from $H_2O_2$ under $Cu^{+}$ exposure through the Fenton and Haber Weiss reactions, possibly leading to SOD and CAT inactivation (Bebianno *et al*., 2004; Maria and Bebianno, 2011). These data are in line with recent observations that show that CuO NPs cytotoxicity is mediated by oxidative stress, altering the antioxidant capacity of cells against ROS. In human lung epithelial cells, CuO NPs (80 $\mu g.cm^{-2}$, 4 hours, 30 nm) blocked the antioxidant defences by inhibiting CAT and GR activities and increasing GPX or SOD and CAT activities after exposure to 10, 25 and 50 $\mu g.mL^{-1}$ for 24 hours (52.5 ± 10.2 nm) (Ahamed *et al*., 2010; Fahmy and Cormier, Karlsson *et al*., 2008). In bivalves, the only existing data on antioxidant efficiency are to $Cu^{2+}$ exposure.

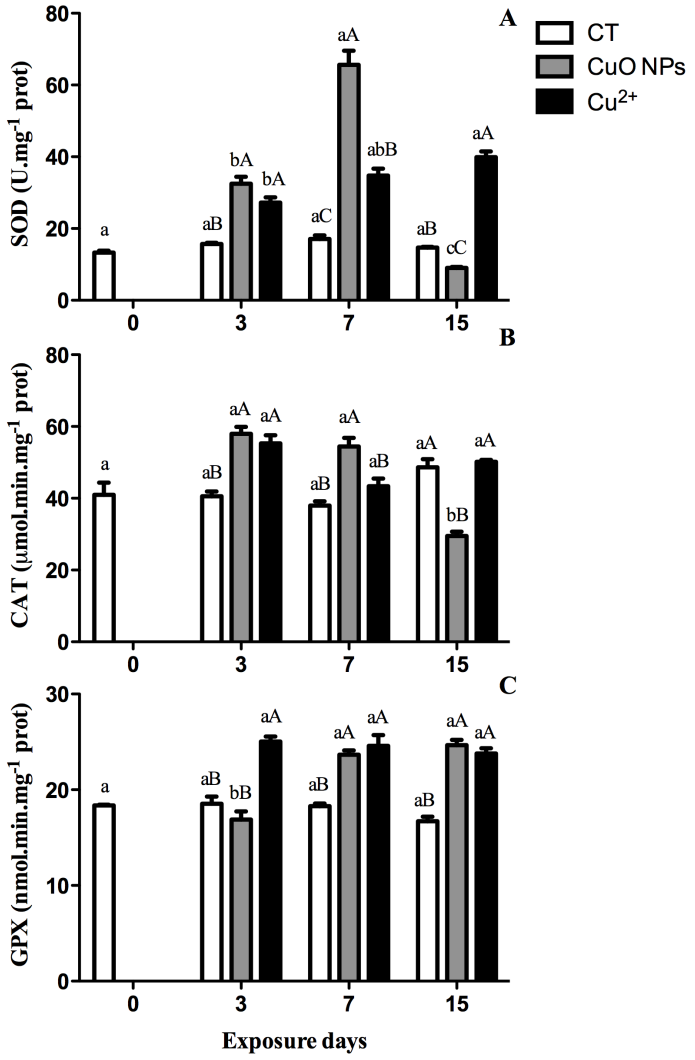


**Figure 2.1.3 –** Superoxide dismutase (A), catalase (B) and glutathione peroxidase (C) activities in gills of mussels *M. galloprovincialis* from control and exposed to CuO NPs and $Cu^{2+}$ for 15 days (average ± Std). Capital and lower letters represent statistical differences between treatments in each day of exposure and for each treatment during the exposure duration, respectively ($p$<0.05).

Mussels exposed to $Cu^{2+}$ showed different antioxidant responses with the enzymatic activities unchanged or increased (Figure 2.1.3). SOD activity was activated during the whole experiment (171% increase by day 15) resulting in the formation of superoxide radicals. CAT activity only increased after 3 days of exposure (36%) and remained unchanged from day 7 until the end of the experiment, at levels similar to controls ($p$>0.05). As mentioned above, this result can be associated with the involvement of Cu in Fenton and Haber Weiss reactions, leaving no substrate available for CAT activation, or to the induction of other

components of the antioxidant defence system (Bebianno *et al*., 2004; Maria and Bebianno, 2011). Like for CAT, GPX activity was induced in the first 3 days of exposure (25.0±1.7 nmol.min.mg$^{-1}$prot, $p$<0.05) remaining unchanged until the end of the experiment, always higher than that in control. This increase in GPX activity suggests a further detoxification of ROS combined with the action of MT; either by ROS scavenging (day 7) or Cu detoxification (day 15), justifying CAT unaltered activities. The PCA analysis shows a clear association between GPX activity and $Cu^{2+}$–exposed mussels, validating the enhancement of this enzyme activity to neutralize ROS (Figure 2.1.5A). Similar results were detected in mussels exposed to 60µgCu.L$^{-1}$ (Regoli and Principato, 1995) for 3 weeks and in the clam *R. decussatus* exposed to 0.5 and 2.5 µgCu.L$^{-1}$ Cu for 3 days (Bebianno *et al*., 2004).

Metallothioneins are low–molecular weight cysteine–rich proteins induced by metals that can also act as an oxygen species scavengers, participating in antioxidant processes protecting cells from oxidative stress (Damiens *et al*., 2006; Langston *et al*., 1998; Serafim and Bebianno, 2009). Although information on MT behaviour upon exposure to CuO NPs is non–existent, the role of MT in ionic/soluble Cu detoxification mechanisms is well understood in bivalves, either by controlling its intracellular availability or by detoxifying excessive metal concentrations (Bebianno *et al*., 2004; Damiens *et al*., 2006; Lehtonen *et al*., 2003; Regoli and Principato, 1995; Serafim and Bebianno, 2009). In mussels exposed to CuO NPs, MT increased linearly with time of exposure, with an induction rate of 0.3 mg.g$^{-1}$prot.d$^{-1}$ ($r$=0.99, $p$<0.05), reflecting not only the role of this protein in Cu homeostasis and detoxification (Figure 2.1.4A), but also a possible involvement in gills antioxidant defence system that can explain the absence of SOD and CAT responses (day 15). Only two studies addressed the role of MT in bivalve species, in *C. virginica* exposed to silver nanoparticles (16 µg.L$^{-1}$–1.6 ng.L$^{-1}$, 15 ± 6 nm) an increase in MT expression was associated with silver metabolism or to the increase of oxyradicals and in *C. fluminea* exposed to gold nanoparticles ($1.6x10^3$–$1.6x10^5$ Au NP/cell, 10 nm) to protect cells against gold–induced oxidative stress (Renault *et al*., 2008; Ringwood *et al*., 2010).

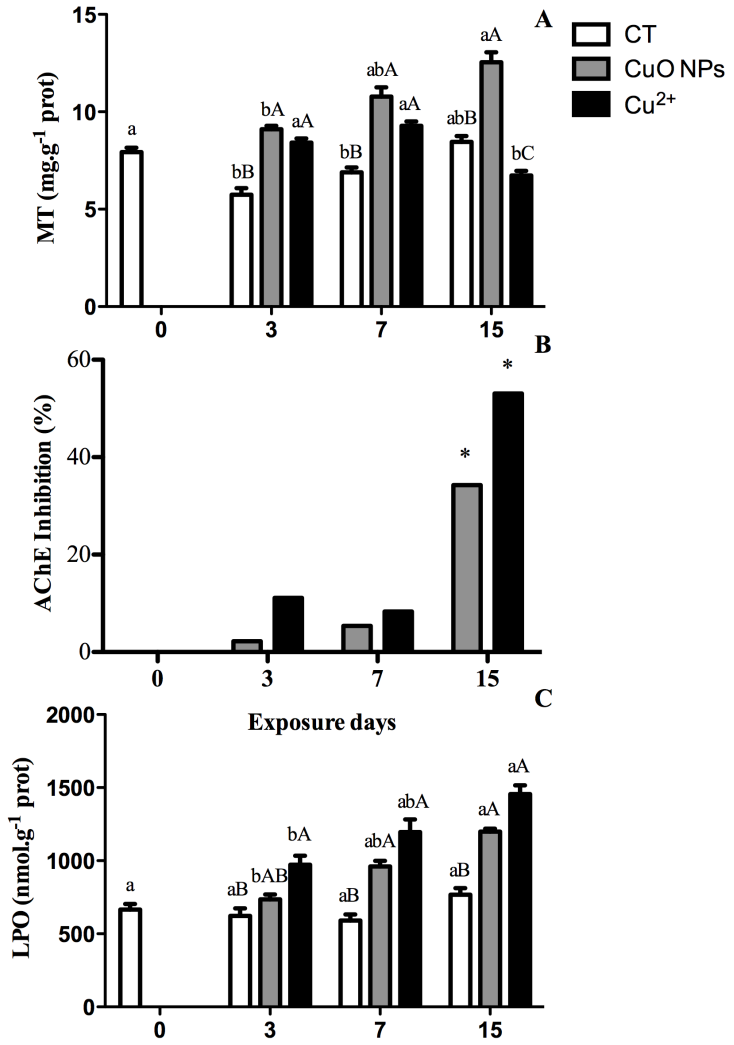


**Figure 2.1.4 –** Metallothionein concentrations (A), inhibition of acetycholinesterase activity (B) and lipid peroxidation (C) in gills of mussels *M. galloprovincialis* from controls and exposed to CuO NPs and $Cu^{2+}$ for 15 days (average ± Std). Capital and lower letters represent statistical differences between treatments in each exposure day and for each treatment during the exposure duration, respectively ($p$<0.05). Asterisks represent statistical differences between control and exposed mussels ($p$<0.05).

In mussels exposed to $Cu^{2+}$, MT levels also increased in the first week of exposure with a lower induction rate (0.2 $mg.g^{-1}prot.d^{-}1$, $r$=0.99, $p$<0.05) when compared to CuO NPs (Figure 2.1.4A), denoting its importance in Cu metabolism, as also seen by the close association between Cu concentrations and MT in the PCA (Figure 2.1.5). Contrarily to the response for CuO NPs, MT decreased in the gills of mussels exposed to $Cu^{2+}$ at the end of the experiment (6.7 $mg.g^{-1}prot$), suggesting a role of MT in copper detoxification, which is in

agreement with the copper accumulation results in mussel gills (Figure 2.1.2). Cu can bind to MT to form insoluble Cu–MT complexes that precipitate into lysosomes and are eliminated by exocytosis (Damiens *et al*., 2006; da Silva and Williams, 2001; Serafim and Bebianno, 2009). Similar results were detected in *R. decussatus* (Serafim and Bebianno, 2009) and *Crassostrea gigas* (Damiens *et al*., 2006) exposed to 50 $\mu gCu.L^{-1}$ and 0.5–5 $\mu gCu.L^{-1}$, respectively.

Acetylcholinesterase is a biomarker of exposure to organo–phosphorous pesticides that can also be inhibited by a diverse range of metals, including copper (Bebianno *et al*., 2004; Lethonen *et al*., 2003; Regoli and Principato, 1995). A dose–dependent decrease of this enzyme after $Cu^{2+}$exposure is well established in bivalve species, as in *R. decussatus* (75 $\mu gCu.L^{-1}$, 5 days) (Bebianno *et al*., 2004) and mussels (40 $\mu g.L^{-1}$ and 60 $\mu g.L^{-1}$, 1 and 3 weeks) (Lethonen *et al*., 2003; Regoli and Principato, 1995). In this study, inhibition of AChE was observed in CuO NPs and $Cu^{2+}$ exposed mussels (Figure 2.1.4B) only at the end of the experiment, with a 34% and 53% inhibition, respectively ($p<0.05$), also confirmed by the PCA (Figure 2.1.5). The high affinity of Cu to sulphur donor groups can cause AChE inhibition by binding to its thiol residues, as in MT (Bebianno *et al*., 2004). These results confirm the specificity of AChE response to Cu exposure, either in the nano or ionic form. The neurotoxic effects of nanoparticles in *M. edulis* exposed to 1 $mg.L^{-1}$ Fe NPs (5–90 nm, 12 hours) showed no significant differences in AChE activity (Kádar *et al*., 2010). Nevertheless, one study showed that AChE has the potential to be used as a biomarker for CuO NPs (25 nm), because of its strong AChE inhibition (76%) and low median inhibitory concentration (4 $mg.L^{-1}$) (Wang et al., 2009).

Significant variations of enzymatic activities exist between control and Cu–exposed mussels throughout the experimental period suggesting that gills responded differently to both forms of copper (Figure 2.1.3). The overall PCA analysis (Figure 2.1.5) indicates a clear separation between control and Cu–exposed mussels. Unexposed mussels, as well as those exposed to $Cu^{2+}$ are closely associated at different times of exposure (day 3, 7 and 15) showing similar biomarker tendency. As for CuO NPs exposed mussels, a clear separation of the sampling periods occurred, suggesting a marked different behaviour between mussel gills response with time of exposure. Failure of antioxidant defences to counteract ROS produced by both forms of Cu either by being inhibited or overwhelmed can interrupt the balance between the antioxidant/prooxidant system in mussels leading to oxidative damage of biomolecules (Bebianno *et al*., 2004; Maria and Bebianno, 2011; Regoli and Principato, 1995). One of the best known effects of excess Cu is the peroxidative damage to membrane lipids, triggered by

the reaction of lipid radicals and oxygen to form peroxyl radicals that can alter membranes fluidity and permeability or attack other intracellular molecules (Bebianno *et al*., 2004; Maria and Bebianno, 2011; Regoli and Principato, 1995). Despite different antioxidant efficiency, LPO increased linearly with time in mussels exposed to CuO NPs and $Cu^{2+}$ (Figure 2.1.4C), with induction rates of 36.8 $nmol.g^{-1}prot.d^{-1}$ ($r$=0.99; $p$<0.05) and 49.7 $nmol.g^{-1}prot.d^{-1}$ ($r$=0.97, $p$<0.05), respectively. In the first three days of CuO NPs exposure, SOD and CAT activities proved to be antioxidant efficient and prevent deleterious effects in lipids of cellular membranes, confirmed by the relative proximity of these mussels to the control group in the PCA analysis (Figure 2.1.5A). In the remaining period, CuO NPs seems to continuously increase ROS production activating the combined action of antioxidant defences (SOD, CAT, GPX and MT) until a point where the antioxidant capacity was overwhelmed causing SOD and CAT inactivation and a continuous MT and GPX increase. Although GPX and MT can remove most of the ROS by increasing its activities, they cannot compete with hydroxyl radicals' generation via the Fenton reaction thereby causing an increase in LPO levels. In mussels exposed to $Cu^{2+}$, antioxidant enzymes were activated during the whole exposure period (except CAT) along with an increase in MT levels leading to a detoxification process by the end of the exposure, nevertheless, not enough to prevent LPO. These results are in agreement with the PCA that shows a clear association between copper concentrations in gills and LPO levels, as well as with MT and GPX (Figure 2.1.5). In human cells and *E. coli* exposed to CuO NPs (30–50 nm) their toxicity was related to oxidative stress, mediated by lipid peroxidation, oxidative lesions and increase of intracellular ROS (Ahamed *et al*., 2010; Fahmy and Cormier, 2009; Griffitt *et al*., 2009; Heinlaan *et al*., 2011; Karlsson *et al*., 2008). Evidence that LPO occurs after Cu exposure was also observed in several bivalve species, as clams and mussels (Bebianno *et al*., 2004; Maria and Bebianno, 2011; Regoli and Principato, 1995).

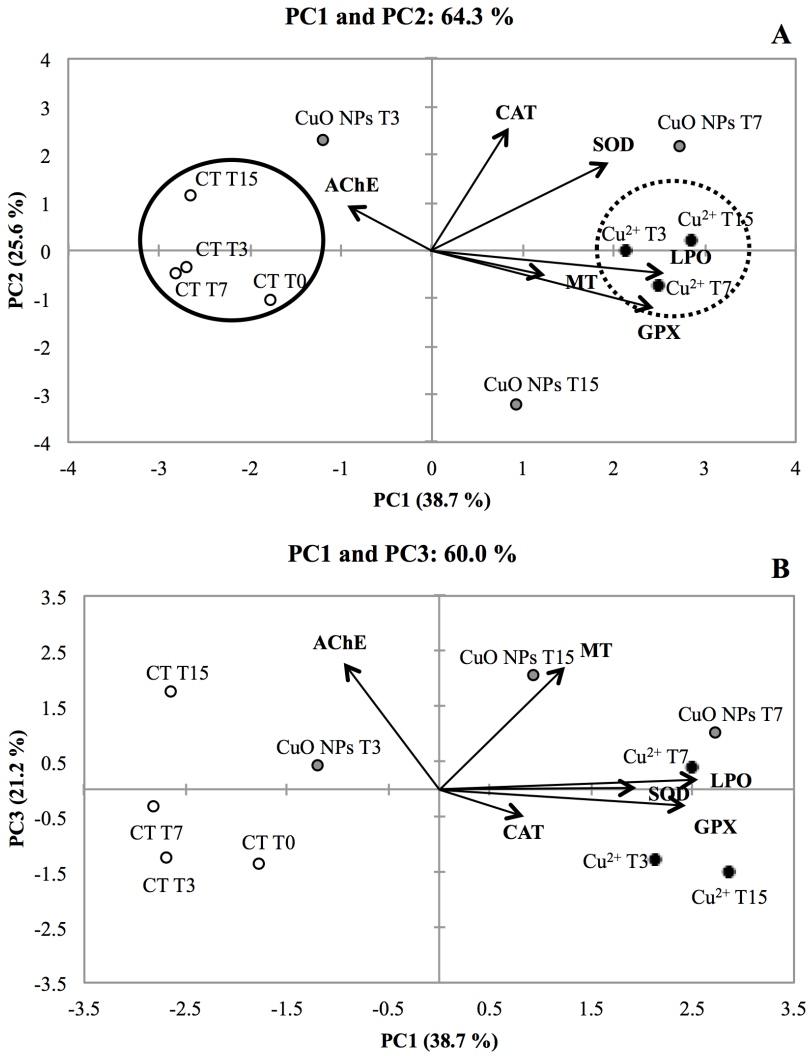


**Figure 2.1.5 –** Principal Component Analysis (PCA) of copper accumulation and the battery of biomarkers in gills of mussels *M. galloprovincialis* from controls and exposed to CuO NPs and $Cu^{2+}$ for 15 days. A – PC1 vs PC2; B – PC1 vs PC3.

Altogether, our results support the conclusion that oxidative stress is a significant mechanism of toxicity for CuO NPs (Ahamed *et al*., 2010; Fahmy and Cormier, 2009; Griffitt *et al*., 2007; Heinlaan *et al*., 2008, 2011; Studer *et al*., 2010) and that its mode of action appears distinct from $Cu^{2+}$. In other aquatic organisms (*V. fisheri, D. magna, T. platyurus, P. subcapitata, T. thermophila*) CuO NPs (~30 nm) showed a higher toxicity when compared to its ionic/soluble form, associated with Cu ions dissolution (Aruoja *et al*., 2009; Heinlaan *et al*., 2008; Mortimer *et al*., 2010). Nevertheless, the dissolution of Cu ions do not fully explain the toxicity of CuO NPs in zebrafish (Griffitt *et al*., 2007, 2009), human cell cultures

(Ahamed *et al*., 2010; Fahmy and Cormier, 2009; Karlsson *et al*., 2008) or daphnids (Heinlaan *et al*., 2011) exposed to particles with similar size (30–50 nm), where other mechanisms derived from the particle effect had to be considered (e.g. oxidative stress due to ROS formation). In our study, a combination of the particle effect and ions dissolution can account for the differences in the toxic effects exerted by CuO NPs along the exposure period. Mussel gills can be taking up dissolved Cu released from the particles combined with a cellular uptake of nanoparticles aggregates. CuO NPs can pass the cellular membrane, enter inside the cell, dissolve rapidly and release high concentrations of ions sufficient to disrupt Cu homeostasis and generate radicals (Griffitt *et al*., 2009; Karlsson *et al*., 2008; Moore, 2006; Studer *et al*., 2010). This NPs mechanism of toxicity named "Trojan horse–type mechanism" was identified in cell cultures (Limbach *et al*., 2007; Studer *et al*., 2010). The increasing copper concentrations in mussel gills can be indicative of an increasing rate of exposure that leads to a continuous release of Cu from the NPs. The reaction time of gills cells is slower than the particle dissolution and uptake leading to enzymatic breakdown and to a continuous increase in MT levels, while in mussels exposed to $Cu^{2+}$, this metal is eliminated more rapidly via MT detoxification pathway. Another fraction of the CuO NPs can be taken up by endocytosis and their toxicological response controlled by surface processes (ROS, adsorption) (Baun *et al*., 2008; Moore, 2006; Studer *et al*., 2010). The presence of CuO NPs aggregates in suspension (as seen by DLS) facilitate a continuous source of NPs that can either be dissolved or incorporated, leading to a continuous ROS generation (intra and/or extracellular), that increases with time of exposure. A correlation between formation of larger aggregates and biomarker responses with increasing time of exposure was suggested in *M. galloprovincialis* exposed to nano carbon black, C60 fullerenes, nano–$TiO_2$ and nano–$SiO_2$ (Canesi *et al*., 2010). A more efficient and rapid capture and ingestion of NPs in aggregated form was also observed in mussels and oysters exposed to polystyrene NPs when compared to those in suspension (Koehler *et al*., 2008). As for *M. edulis*, NPs from glass wool and Fe are taken up by gills epithelial cells as pathways of uptake by diffusion or by endocytosis, independently of the size of the aggregates (Kádar *et al*., 2010; Koehler *et al*., 2008). Aggregation has a crucial role in nanoparticles toxicity, and the cumulative effects of the dissociation of metal ions, size and surface–area properties of these particles cannot be discarded and need further clarification in CuO NPs mechanisms (Baun *et al*., 2008; Canesi *et al*., 2010; Moore, 2006; Ringwood *et al*., 2010; Ward and Kach, 2009).

Despite the information given by acute experiments, they do not provide complete information about the interactions of nanomaterials with classical test species and there is a need to direct research towards invertebrate tests using long–term exposure to better understand NPs toxicity mechanisms (Baun *et al*., 2008; Griffitt *et al*., 2009; Heinlaan *et al*., 2008, 2011). As for CuO NPs, most of the data available concerns on acute toxicity across a wide spectrum of aquatic species (Aruoja *et al*., 2009; Griffitt *et al*., 2007, 2008, 2009; Heinlaan *et al*., 2008, 2011; Mortimer *et al*., 2010; Ruparelia *et al*., 2008; Yoon *et al*., 2007), and this study is one of the first to address long term effects of these NPs in this species. Overall our results show that mussels represent a target for environmental exposure to nanoparticles where exposure duration may be a contributing factor in NPs mediated toxicity. In summary, long term exposure to CuO NPs cause oxidative stress in gills of mussels as evidenced by the breakdown of the antioxidant defence system and lipid peroxidation, as well as acetylcholinesterase inhibition and metallothionein induction. Nevertheless the underlying mechanisms associated with biomarkers responses are still uncertain, and the observed oxidative stress may due to an association between the nanoparticle effect and the dissociation of copper ions from the nanoparticles. Future research is required to understand the mechanisms of CuO NPs toxicity in aquatic organisms, where the uptake and accumulation of CuO NPs in other mussel tissues should be considered, as well as the importance of bioavailability and particle aggregation for long periods of time.

## 2.1.4. References

Ahamed, M.; Siddiqui, M.A.; Akhtar, M.J.; Ahmad, I.; Pant, A.B. (2010). Genotoxic potential of copper oxide nanoparticles in human lung epithelial cells. *Biochemical and Biophysical Research Communications*. **396:** 578–583.

Aruoja, V.; Dubourguier, H.–C.; Kasemets, K.; Kahru, A. (2009). Toxicity of nanoparticles of CuO, ZnO and $TiO_2$ to microalgae *Pseudokirchneriella subcapitata*. *Science of the Total Environment.* **407(4):** 1461–1468.

Baun, A.; Hartmann, N.B.; Grieger, K.; Kusk, K.O. (2008). Ecotoxicity of engineered nanoparticles to aquatic invertebrates: a brief review and recommendations for future toxicity testing. *Ecotoxicology*. **17:** 387–395.

Bebianno, M.J.; Géret, F.; Hoarau, P.; Serafim, M.A.; Coelho, M.R.; Gnassia–Barelli, M.; Roméo, M. (2004). Biomarkers in *Ruditapes decussatus*: a potential biondicator species. *Biomarkers*. ***9*(4–5):** 305–330.

Bebianno, M.J.; Langston W.J. (1989). Quantification of metallothioneins in marine invertebrates using differential pulse polarography. *Portugaliae Electrochimica Acta*. ***7*:** 59–64.

Canesi, L.; Fabbri, R.; Vallotto, D.; Marcomini, A.; Pojana, G. (2010). Biomarkers in *Mytilus galloprovincialis* exposed to suspensions of selected nanoparticles (Nano carbon black, C60 fullerene, Nano–$TiO_2$, Nano–$SiO_2$). *Aquatic Toxicol*ogy. **100:** 168–177.

da Silva, J.J.R.F.; Williams, R.J.P. (2001). *The Biological Chemistry of the Elements: The Inorganic Chemistry of Live*, 2nd ed.; Oxford University Press: New York.

Damiens, G.; Mouneyrac, C.; Quiniou, F.; His, E.; Gnassia–Barelli, M.; Roméo, M. (2006). Metal bioaccumulation and metallothionein concentrations in larvae of *Crassostrea gigas*. *Environmental Pollution*. **140:** 492–499.

Ellman, G.L.; Courtney, K.O.; Anders, V.; Featherstone, R.M. (1961). A new and rapid colorimetric determination of acetylcholinesterase activity. *Biochemical Pharmacology*. **7:** 88–95.

Erdelmeier, I.; Gerard–Monnier, D.; Yadan J.C.; Acudiere J. (1998). Reactions of N–methyl–2–phenylindole with malondialdehyde and 4–hydroxyalkenals. Mechanistic aspects of the colorimetric assay of lipid peroxidation. *Chemical Research in Toxicol*ogy. **11:** 1184–1194.

Fahmy, B.; Cormier, S.A. (2010). Copper oxide nanoparticles induce oxidative stress and cytotoxicity in airway epithelial cells. *Toxicology In Vitro*. **23:** 1365–1371.

Greenwald, R.A. (1985). Handbook of methods for oxygen radical research. CRC Press: Boca Raton, Florida, United States of America.

Griffitt, R.J.; Weil, R.; Hyndman, K.A.; Denslow, N.D.; Powers, K.; Taylor, D.; Barber, S.D. (2007). Exposure to copper nanoparticles causes gill injury and acute lethality in zebrafish (*Danio rerio*). *Environmental Science and Technology.* **41:** 8178–8186.

Griffitt, R.J.; Luo, J.; Gao, J.; Bonzongo, J.C.; Barber, D.S. (2008). Effects of particle composition and species on toxicity of metallic nanomaterials in aquatic organisms. *Environmental Toxicology and Chemistry*. **27(9):** 1972–1978.

Griffitt, R.J.; Hyndman, K.; Denslow, N.D.; Barber, D.S. (2009). Comparison of molecular and histological changes in zebrafish gills exposed to metallic nanoparticles. *Toxicological Sciences.* **107(2):** 404–415.

Heinlaan, M.; Ivask, A.; Blinova, I.; Dubourguier, H.C.; Kahru, A. (2008). Toxicity of nanosized and bulk ZnO, CuO and $TiO_2$ to bacteria *Vibrio fischeri* and crustaceans *Daphnia magna* and *Thamnocephalus platyurus*. *Chemosphere.* **71:** 1308–1316.

Heinlaan, M.; Kahru, A.; Kasemets, K.; Arbeille, B.; Prensier, G.; Dubourgier, H.–C. (2011). Changes in the *Daphnia magna* midgut upon ingestion of copper oxide nanoparticles: A transmission electron microscopy study. *Water Research*. **45:** 179–190.

Kádar, E.; Lowe, D.M.; Solé, M.; Fisher, A.S.; Jha, A.N.; Readman, J.W.; Hutchinson, T.H. (2010). Uptake and biological responses to nano–Fe versus soluble $FeCl_3$ in excised mussel gills. *Analytical and Bioanalytical Chemistry*. **396:** 657–666.

Karlsson, H.L.; Cronholm, P.; Gustafsson, J.; Möller, L. (2008). Copper oxide nanoparticles are highly toxic: a comparison between metal oxide nanoparticles and carbon nanotubes. *Chemical Research in Toxicology.* **21:** 1726–1732.

Koehler, A.; Marx, U.; Broeg, K.; Bahns, S.; Bressling, J. (2008). Effects of nanoparticles in *Mytilus edulis* gills and hepatopancreas – a new threat to marine life? *Marine Environmental Research*. **66(1):** 12–14.

Langston, W.J.; Bebianno, M.J.; Burt, G.R. (1998). Metal handling strategies in molluscs. In: Langston, W.J.; Bebianno, M.J. (Eds.). Metal Metabolism in Aquatic Environments. Chapman and Hall, London, pp. 219–283.

Lawrence, R.A.; Burk, R.F. (1976). Glutathione peroxidase activity in selenium–deficient rat liver. *Biochemical and Biophysical Research Communications.* **71:** 952–958.

Lehtonen, K.K.; Leiniö, S. (2003). Effects of exposure to copper and malathion on metallothionein levels and acetylcholinesterase activity of the mussel *Mytilus edulis* and the clam *Macoma balthica* from the Northern Baltic Sea. *Bulletin of Environmental Contamination and Toxicology.* **71:** 489–496.

Limbach, L.K.; Wick, P.; Manser, P.; Grass, R.N.; Bruinink, A.; Stark, W.J. (2007). Exposure of engineered nanoparticles to human lung epithelial cells: influence of chemical composition and catalytic activity on oxidative stress. *Environmental Science and Technology*. **41:** 4158–4163.

Lowry, O.H.; Rosenbrough, N.J.; Farr, A.L.; Randall, R.J. (1951). Protein measurement with the Folin phenol reagent. *Journal of Biological Chemistry*. **193:** 265–275.

Maria, V.L.; Bebianno, M.J. (2011). Antioxidant and lipid peroxidation responses in *Mytilus galloprovincialis* exposed to mixtures of benzo(a)pyrene and copper. *Comparative Biochemistry and Physiology Part C: Toxicology and Pharmacology*. **154(1):** 56–63.

McCord, J.M.; Fridovich, I. (1969). Superoxide dismutase: an enzymatic function for erythrocuprein (hemocuprein). *Journal of Biological Chemistry*. **244(22):** 6049–6955.

Moore, M.N. (2006). Do nanoparticles present ecotoxicological risks for the health of the aquatic environment? *Environmental International*. **32:** 967–976.

Mortimer, M.; Kasemets, K.; Kahru, A. (2010). Toxicity of ZnO and CuO nanoparticles to ciliated protozoa *Tetrahymena thermophila*. *Toxicology*. **269(2–3):** 182–189.

Peyrot, C.; Gagnon, C.; Gagné, F.; Willkinson, K. J.; Turcotte, P.; Sauvé, S. (2009). Effects of cadmium telluride quantum dots on cadmium bioaccumulation and metallothionein production to the freshwater mussel, *Elliptio complanata*. *Comparative Biochemistry and Physiology C*. **150:** 246–251.

Regoli, F.; Principato, G. (1995). Glutathione, glutathione–dependent and antioxidant enzymes in mussel, *Mytilus galloprovincialis*, exposed to metals under field and laboratory conditions: implications for the use of biochemical biomarkers. *Aquatic Toxicology*. **31:** 143–164.

Renault, S.; Baudrimont, M.; Mesmer– Dudons, N.; Gonzalez, P.; Mornet, S.; Brisson, A. (2008). Impacts of gold nanoparticle exposure on two freshwater species: a phytoplanktonic alga (*Scenedesmus subspicatus*) and a benthic bivalve (*Corbicula fluminea*). *Gold Bulletin*. **41(2):** 116–126.

Ringwood, A.H.; McCarthy, M.; Bates, T.C.; Carroll, D.L. (2010). The effects of silver nanoparticles on oyster embryos. *Marine Environmental Research*. **69(1):** 549–551.

Ruparelia, J.P.; Chatterjee, A.K.; Duttagupta, S.P.; Mukherji, S. (2008). Strain specificity in antimicrobial activity of silver and copper nanoparticles. *Acta Biomaterialia*. **4(3):** 707–716.

Serafim, A.; Bebianno, M.J. (2009). Metallothionein role in the kinetic model of copper accumulation and elimination in the clam *Ruditapes decussatus*. *Environmental Research*. **109:** 390–399.

Studer, A.M.; Limbach, L.K.; Duc, L.V.; Krumeich, F.; Athanassiou, E.K.; Gerber, L.C.; Moch, H.; Stark, W.J. (2010). Nanoparticle cytotoxicity depends on intracellular solubility: Comparison of stabilized copper metal and degradable copper oxide nanoparticles. *Toxicologica Letters*. **197:** 169–174.

Unfried, K.; Albrecht, C.; Klotz, L.; Mikecz, A.V.; Grether–Beck, S.; Schins, R.P.F. (2007). Cellular responses to nanoparticles: target structures and mechanisms. *Nanotoxicology.* **1(1):** 52–71.

Wang, Z.; Zhao, J.; Li, F.; Gao, D.; Xing, B. (2009). Adsoprtion and inhibition of acetylcholinesterase by different nanoparticles. *Chemosphere.* **77(1):** 67–73.

Ward, J.E.; Kach, D.J. (2009). Marine aggregates facilitate ingestion of nanoparticles by suspension–feeding bivalves. *Marine Environmental Research.* **68:** 137–142.

Xia, T.; Kovochich, M.; Brant, J.; Hotze, M.; Sempf, J.; Oberley, T.; Sioutas, C.; Yeh, J.I.; Wiesner, M.R.; Nel, A.E. (2006). Comparison of the abilities of ambient and manufactured nanoparticles to induce cellular toxicity according to an oxidative stress paradigm. *Nano Letters.* **6(8):** 1794–1807.

Yoon, K.Y.; Byeon, J.H.; Park, J.H.; Hwang, J. (2007). Susceptibility constants of *Escherichia coli* and *Bacillus subtilis* to silver and copper nanoparticles. *Science of the Total Environment*. **373:** 572–575.

# 2.2.

# ACCUMULATION AND TOXICITY OF COPPER OXIDE NANOPARTICLES IN THE DIGESTIVE GLAND OF *MYTILLUS GALLOPROVINCIALIS*

*Tânia Gomes[1], Catarina G. Pereira[1], Cátia Cardoso[1], José P. Pinheiro[2], Ibon Cancio[3], Maria João Bebianno[1]*

[1]CIMA, Faculty of Science and Technology, University of Algarve, Campus de Gambelas, 8005–139 Faro, Portugal

[2]CBME, Faculty of Science and Technology, University of Algarve, Campus de Gambelas, 8005–139 Faro, Portugal

[3]Department of Zoology & Animal Cell Biology, Scholl of Science and Technology, University of the Basque Country, E–48080 Bilbao, Spain

Aquatic Toxicology 118–119: 72–79

## Abstract

Given the wide use of CuO nanoparticles in various industrial and commercial applications they will inevitably end up in the aquatic environment. However, little information exists on their biological effects in bivalve species. Accordingly, mussels *Mytilus galloprovincialis* were exposed to 10 μgCu.$L^{-1}$ as CuO nanoparticles and $Cu^{2+}$ for 15 days, and biomarkers of oxidative stress (superoxide dismutase, catalase and glutathione peroxidase), damage (lipid peroxidation) and metal exposure (metallothionein) were determined along with Cu accumulation in mussels digestive glands. Cu was linearly accumulated with time of exposure in mussels exposed to CuO nanoparticles, while in those exposed to $Cu^{2+}$ elimination was significant by day 15. Both forms of Cu cause oxidative stress with distinct modes of action. Exposure to CuO nanoparticles induces lower SOD activity in mussels digestive glands compared to those exposed to $Cu^{2+}$, while CAT was only activated after 7 days of exposure to nano and ionic Cu, with contradictory effects after 15 days of exposure and GPX levels were similar. Lipid peroxidation levels increased in both Cu forms despite different antioxidant efficiency. Moreover, a linear induction of metallothionein was detected with time in mussels exposed to CuO nanoparticles, directly related to Cu accumulation, whereas in those exposed to $Cu^{2+}$ was only induced after 15 days of exposure. Since only a small fraction of soluble Cu fraction was released from CuO nanoparticles, the observed effects seem to be related to the nano form of Cu, with aggregation as a key factor. Overall, our results show that the digestive gland is susceptible to CuO nanoparticles related oxidative stress, being also the main tissue for their accumulation.

Keywords: *Mytilus galloprovincialis*, CuO NPs, Oxidative stress, Digestive gland

## 2.2.1. Introduction

The large–scale production and application of nanoparticles in several industries led to its frequent release into the environment. Nonetheless, to date it is still unclear how, at which concentrations and in what forms nanoparticles (NPs) are released, as well as their fate and interaction with the various compartments of the environment, including biota (Bhatt and Tripathi, 2011; Moore, 2006). As the ultimate sink for most conventional contaminants, the aquatic environment is highly susceptible to NPs exposure and aquatic organisms (e.g. filter–feeding molluscs) can represent a target group for NPs uptake and effects (Canesi *et al*., 2012; Moore, 2006; Scown *et al*., 2010).

When compared to other metal oxide NPs, the toxicity of copper oxide nanoparticles (CuO NPs) is still poorly understood, which is a cause of concern given its increased use in several industrial and commercial applications (e.g. electronic circuits and batteries, gas sensors, polymers) mainly due to its thermal and electrical conductive efficiency (Buffet *et al*., 2011; and literature cited therein, Griffitt *et al*., 2009 and literature cited therein). Such usage may increase the potential risk of these particles to end up in the environment in significant quantities. NPs are potentially more toxic than their bulk and ionic counterparts mostly due to their amplified surface area and reactivity, which may lead to increased bioavailability and toxicity (Bhatt and Tripathi, 2011; Scown *et al*., 2010). The toxicity of copper ions towards aquatic organisms is well known and as a redox metal, Cu participates in Fenton and Haber–Weiss reactions, facilitating the formation of reactive oxygen species (ROS) and oxidative stress (Bebianno *et al*., 2004; Maria and Bebianno, 2011; Regoli and Principato, 1995). The known effects of CuO NPs in contrast to its bulk and ionic forms are contradictory regarding the highest toxic form of Cu; nevertheless, evidence exists of different mechanisms of action dependent on the Cu form (Chapter 2.1; Griffitt *et al*., 2007; Karlsson *et al*., 2008). CuO NPs have not only antibacterial properties (Ruparelia *et al*., 2008; Yoon *et al*., 2007), but also cytotoxic and genotoxic effects. ROS–derived oxidative stress (Buffet *et al*., 2011; Chapter 2.1; Ivask *et al*., 2010; Fahmy and Cormier, 2009), DNA damage and oxidative lesions (Ahamed *et al*., 2010; Chapter 4; Karlsson *et al*., 2008) were observed not only in human cell cultures but also in freshwater and marine organisms. Most of the NPs toxicity has been attributed to the dissolution of $Cu^{2+}$ from the particles; nevertheless, the great extent of the effects mainly derives from the inherent particle properties (e.g. Fahmy and Cormier, 2009; Griffitt *et al*., 2009; Heinlaan *et al*., 2011). Less information exists on the biological effects of CuO NPs in bivalve species, but given its the capacity to generate oxidative stress it is not

surprising that mussels exposed to these particles for two weeks (10 μgCu.$L^{-1}$, 31 ± 10 nm) presented failure of the antioxidant defence system, lipid peroxidation, metallothionein induction, as well as neurotoxic impairment in the gills and DNA damage in hemolymph cells (Chapters 2.1 and 4). Additionally, the knowledge of NPs bioaccumulation is essential to detect and quantify the NPs uptake by organisms as well as their distribution within tissues, cells and sub–cellular compartments (Bhatt and Tripathi, 2011; Canesi *et al*., 2012; Scown *et al*., 2010). The preferential sites of NPs accumulation also explain the toxicological effects in organisms and allow the clarification of its modes of action. Bivalve molluscs have the capacity to uptake and accumulate several types of NPs in their tissues (see Canesi *et al*., 2012, Chapter 2.1), but little information exists on the cellular uptake of CuO NPs as well as its actual internal concentration and distribution. CuO NPs were ingested in *Daphnia magna* midgut cells (Heinlaan *et al*., 2011), food vacuoles of the protozoa *Tetrahymena thermophila* (Mortimer *et al*., 2009) and accumulated in zebrafish (Griffitt *et al*., 2007), polychaetes *Nereis diversicolor*, clams *Scrobicularia plana* (Buffet *et al*., 2011) and mussels *Mytilus galloprovincialis* gills (Chapter 2.1). Even though evidence exists on the toxicity and uptake of CuO NPs, different experimental designs with diverse NPs sizes, coatings, concentrations, times of exposure, measured endpoints and cell types make it difficult to compare results and determine the mode of action by which these particles inflict damage to organisms. Accordingly, the objective of this study was to compare the accumulation of nano and ionic forms of Cu in the digestive gland of *M. galloprovincialis* after exposure to an environmental realistic concentration (10μgCu.$L^{-1}$) (Bebianno *et al*., 2004; Bryan and Langston, 1992), as well as the potential of the NPs to induce cellular oxidative stress. For this purpose, biomarkers of oxidative stress (superoxide dismutase–SOD, catalase–CAT and glutathione peroxidase–GPX), damage (lipid peroxidation–LPO) and metal exposure (metallothionein–MT) were measured along with Cu concentrations in mussels' digestive glands.

## 2.2.2. Materials and methods

### 2.2.2.1. Preparation and characterization of CuO NPs

CuO NPs (<50 nm) stock solution was prepared in ultrapure water and characterized as previously described in Chapter 2.1. The size distribution of 250 CuO NPs (32 ppm in ultrapure water) was determined by transmission electron microscopy (TEM) using a JEOL JEM–230 TEM equipped with a digital camera model 785 ES1000 W. The hydrodynamic size and polydispersity index of CuO NPs (100 μg.$L^{-1}$ in filtered seawater) during a cycle of

12 hours (corresponding to the period between water change and NPs redosing) were determined by dynamic light scattering (DLS) using an ALV apparatus with Ar ion lased (515.5 nm). The results of CuO NPs characterization are summarised in Table 2.2.1 and Figure 2.2.1.

### 2.2.2.2. CuO NPs exposure

Mussels *Mytilus galloprovincialis* of similar shell length (61.7 ± 8.4 mm) were collected in the Ria Formosa Lagoon (southern coast of Portugal), transported alive to the laboratory and acclimated for 7 days in natural seawater at constant temperature and aeration, as previously described in Chapter 2.1. After acclimation, fifty mussels were placed in 25L tanks filled with 20L of seawater (2.5 mussels/L) in a triplicate design (3 tanks per treatment): 10 $\mu gCu.L^{-1}$ of CuO NPs, 10 $\mu gCu.L^{-1}$ of $Cu^{2+}$, and a control group kept in clean seawater for a period of 15 days. Fifty mussels were collected from each treatment at four different times: 0, 3, 7 and 15 days. To avoid nanoparticle aggregation, water in tanks was renewed every 12 hours with redosing of Cu solutions after each change. During the experimental period, seawater quality was confirmed daily in each tank by measuring temperature, salinity, oxygen saturation and pH (17.8 ± 1.1ºC; 36.3 ± 0.2; 97.8 ± 4.9% and 7.8 ± 0.1, respectively). Mussels were not fed during the experiment and no mortality was registered. Collected mussels were dissected and digestive glands immediately frozen in liquid nitrogen and stored at –80ºC until further use.

### 2.2.2.3. Metal analysis

Copper was analysed in water samples collected 12 hours before water renewal and re–dosing from the CuO NPs and $Cu^{2+}$ exposure groups, as previously described in Chapter 2.1. Cu was also determined in dried (80ºC) mussels' digestive glands after wet digestion with $HNO_3$ followed by graphite furnace atomic absorption spectrometry (AAS AAnalyst 800 – Perkin Elmer). Accuracy of the analytical procedure was assured with certified reference material (TORT–II, Lobster Hepatopancreas) from the National Research Council (Canada). Results agreed with the certified values (samples: 106.8 ± 2.5 $\mu g.g^{-1}$; certified value: 106.0 ± 10.0 $\mu g.g^{-1}$). Metal levels are expressed as $\mu g.g^{-1}$ of dry weight.

### 2.2.2.4. Enzymatic activities

To determine SOD, CAT and GPX enzymatic activities, digestive glands were homogenized in five volumes of Tris–HCl buffer (20mM, pH 7.6), containing 1mM of EDTA, 0.5M of saccharose, 0.15M of potassium chloride and 1mM of DTT, in an ice bath for 2 minutes. The homogenate was centrifuged at 500 *g* for 15 minutes at 4ºC to precipitate large particles. The supernatant was separated from the pellet and centrifuged at 12,000 *g* for 45 minutes at 4ºC to precipitate the mitochondrial fraction, and the cytosolic fraction was purified on a Sephadex G–25 gel column (PD10, Pharmacia) to remove the low molecular weight proteins. Enzymatic activities were measured in the cytosolic fraction. To determine SOD activity, the reduction of cytochrome c by the system xanthine oxidase/hypoxanthine was measured at 550 nm (McCord and Fridovich, 1969) and results expressed in $U.mg^{-1}$ total protein concentration. CAT activity was determined by the decrease in absorbance at 240 nm due to $H_2O_2$ consumption, with a molar extinction coefficient of 40 $M^{-1}$ $cm^{-1}$ (Greenwald, 1985) and results expressed as $\mu mol.min^{-1}.mg^{-1}$ of total protein concentration. GPX activity was measured through NADPH oxidation in the presence of excess glutathione reductase, reduced glutathione and hydroperoxide as substrate, at 340 nm (Lawrence and Burk, 1976) and results expressed as $nmol.min^{-1}.mg^{-1}$ of total protein concentration.

### 2.2.2.5. Metallothioneins

Digestive glands were homogenised in three volumes of Tris–HCl buffer (0.02 M, pH 8.6) in an ice bath. The homogenate was centrifuged at 30,000 *g* for 45 minutes at 4ºC. The supernatant was separated from the pellet, and two aliquots were used for lipid peroxidation and total protein determination. The remaining supernatant was heat–treated at 80ºC for 10 min to precipitate the high molecular weight proteins and re–centrifuged at 30,000 *g* for 45 minutes at 4ºC. An aliquot of the heat–treated cytosol was used for the quantification of MT concentration by differential pulse polarography according to the method described by Bebianno and Langston (1989). In the absence of a mussel MT standard, quantification of MT in the cytosol was based on rabbit liver metallothionein, MT–I (10 $mg.L^{-1}$), using the standard additions method. MT concentrations are expressed as a $milligram.g^{-1}$ of total protein concentration.

### 2.2.2.6. Lipid peroxidation

LPO was assessed by determining malondialdehyde (MDA) and 4–hydroxyalkenals (4–HNE) concentrations upon the decomposition by polyunsaturated fatty acid peroxides, following the method described by Erdelmeier *et al*. (1998). This procedure is based on the reaction of two moles of *N*–methyl–2–phenylindole, a chromogenic reagent, with one mole of either MDA or 4–HNE at 45ºC for 60 min to yield a stable chromophore that has a maximal absorbance at 586 nm, using malondialdehyde bis–(tetrametoxypropan) as a standard. Lipid peroxidation is expressed as nmols MDA+4–HNE.$g^{-1}$ of total protein.

### 2.2.2.7. Total protein concentration

Total protein content was determined in the cytosolic fraction of digestive glands according to Lowry's method (Lowry *et al*., 1951) and Bovine Serum Albumin (BSA) was used as standard material.

### 2.2.2.8. Statistical analyses

Statistical analyses were performed using SigmaPlot10® and XLStat2009®. Results are presented as mean ± standard deviation. Significant differences between biomarkers and copper concentrations were studied using one–way analysis of variance (ANOVA) or Kruskal–Wallis One Way Analysis of Variance on Ranks. If significant, the following pairwise multiple–comparison tests were applied: Tukey's or Dunn's, accordingly. Additionally, linear regression was applied to confirm existing relationships between variables and multiple correlations were conducted between all data. Principal Component Analysis (PCA) was used to evaluate the influence of copper concentrations (nano and ionic) in the determined biomarkers in control and exposed mussels along the period of exposure and assess the overall results. Another PCA was performed between the results obtained in this study and the ones obtained in the gills of the same mussels exposed to CuO NPs and $Cu^{2+}$ (Chapter 2.1) in order to differentiate responses and modes of action of both forms of copper in the two tissues. The statistical significance level was set at $p<0.05$.

## 2.2.3. Results

### 2.2.3.1. Nanoparticles characterization

The size and shape of CuO NPs were determined by TEM and DLS analysis (Table 2.2.1) and the characterization is described in detail in Chapter 2.1. The size of CuO NPs reported by the manufacturer is < 50 nm (Table 2.2.1), which is in agreement with the size obtained by TEM (31 ± 10 nm). The mean particle size was also determined in seawater during a 12 hours cycle using DLS. The hydrodynamic size obtained ranges from approximately 238 nm to 338 nm (Table 2.2.1, 284 ± 21 nm) that increases with time (Fig. 2.2.1). A high polydispersity index was also observed by DLS (Table 2.2.1, 0.35 ± 0.03), suggesting that under the exposure conditions, CuO NPs tends to aggregate producing suspensions with both small and large aggregates.

**Table 2.2.1 –** Characterization of CuO nanoparticles using different techniques. Values are mean ± std.

| Particle characterization | Method | CuO NPs |
|---|---|---|
| Particle size (nm) | TEM | <50[a] |
| Primary particle size distribution (nm) | TEM | 31 ± 10[b] |
| Polydispersity index | DLS | 0.35 ± 0.03[c] |
| Mean particle diameter (nm) | DLS | 284 ± 21[c] |
| Specific surface area ($m^2/g$) | – | 29[a] |
| Dissolution after 12h in natural seawater (% mass) | AAS | <1[d] |

[a]Information from the manufacturer Sigma–Aldrich
[b]CuO NPs dispersed in ultrapure water. Average diameter of 250 particles.
[c]CuO NPs dispersed in natural seawater during a 12 hours cycle.
[d]Described in Chapter 1.

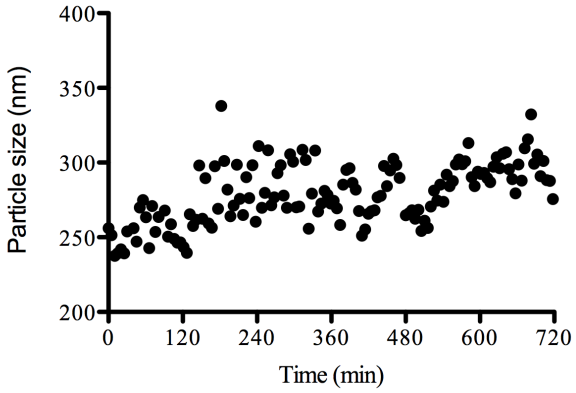


**Figure 2.2.1 –** Particle size distribution (nm) during a 12 hours cycle by dynamic light scattering using a concentration of 100 µg.$L^{-1}$.

### 2.2.3.2. Metal analysis

Digestive glands of mussels accumulated significantly higher Cu concentrations along the exposure period when compared to unexposed mussels (Fig. 2.2.2, $p$<0.05). In those exposed to CuO NPs, copper was linearly accumulated with time with an accumulation rate of 1.02 µg.$g^{-1}d^{-1}$ (r=0.94, $p$>0.05). As for those exposed to $Cu^{2+}$, the accumulation was higher than in CuO NPs exposed mussels in the first week of exposure (28.9 ± 2.8 µg.$g^{-1}$ dw), followed by a decrease by the end of the experiment (22.4 ± 2.8 µg.$g^{-1}$ dw) reaching levels similar to CuO NPs exposed mussels ($p$<0.05).

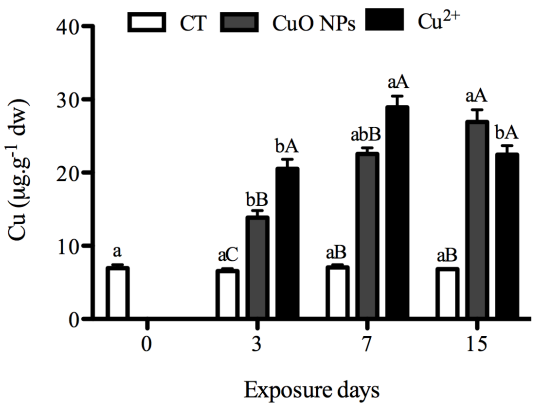


**Figure 2.2.2 –** Copper concentrations (µg.$g^{-1}$ dry weight) in digestive gland of mussels *M. galloprovincialis* from controls and exposed to CuO NPs and $Cu^{2+}$ for 15 days (mean ± Std).

Lower and capital letters represent statistical differences for each treatment during the exposure period and between treatments in each day of exposure, respectively ($p<0.05$).

### 2.2.3.3. Enzymatic activities

Enzymatic activities (Fig. 2.2.3) of unexposed mussels did not vary over time ($p>0.05$). Antioxidant responses of mussels exposed to CuO NPs and $Cu^{2+}$ were different. In mussels exposed to CuO NPs, SOD activity (Fig. 2.2.3A) increased 1.8–fold over the first week, remaining unchanged until the end of the exposure period ($p>0.05$). In $Cu^{2+}$ exposed mussels, SOD activity (Fig. 2.2.3A) was induced (1.7–fold) after the first three days and remained unchanged throughout the exposure period, but higher than those of CuO NPs exposure, except after a week (no significant differences, $p>0.05$). As for CAT activity (Fig. 2.2.3B), exposure to CuO NPs resulted in a 1.6–fold increase after a week of exposure ($p<0.05$) that decreased afterwards to levels similar to controls ($p>0.05$). In $Cu^{2+}$ exposed mussels, CAT activity increased with time of exposure, reaching a 1.8–fold increase by the end of the experiment to levels significantly higher than CuO NPs ($p<0.05$). As for GPX (Fig. 2.2.3C), no significant differences were detected between the two forms of copper over the exposure period. A significant increase in GPX was detected in exposed mussels by the $7^{th}$ day of exposure (1.4–fold for CuO NPs and 1.6–fold for $Cu^{2+}$) that continued to increase in the case of CuO NPs ($18.6 \pm 1.6$ nmol.min.mg$^{-1}$ prot $p<0.05$) to levels similar to those exposed to $Cu^{2+}$ ($18.6 \pm 2.3$ nmol.min.mg$^{-1}$ prot $p>0.05$). Correlation analysis revealed that there was only a significant relationship between SOD and CAT activities in mussels exposed to $Cu^{2+}$ ($r=0.99$, $p=0.011$).

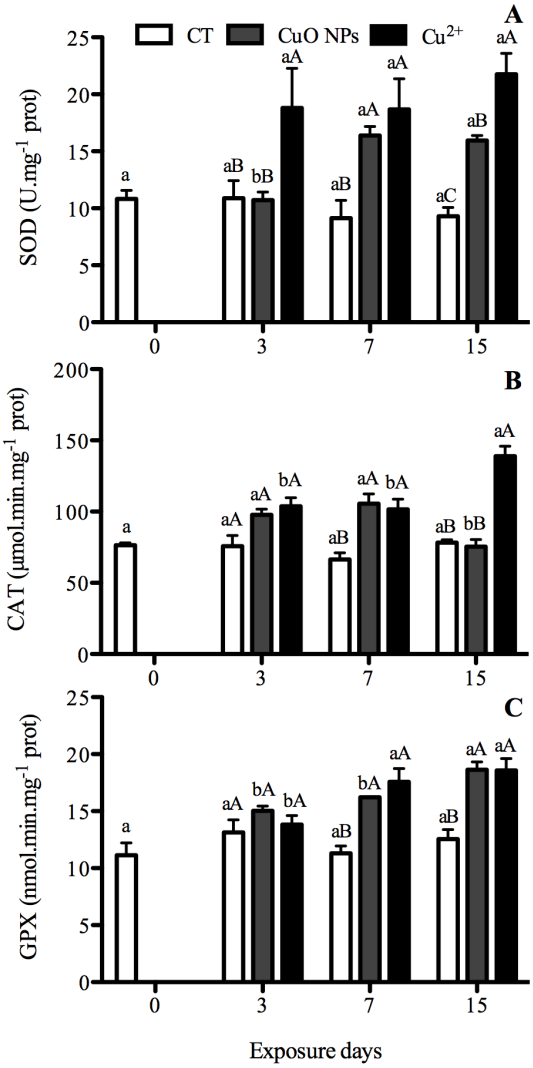


**Figure 2.2.3** – Superoxide dismutase (A), catalase (B) and glutathione peroxidase (C) activities in the digestive gland of mussels *M. galloprovincialis* from control and exposed to CuO NPs and $Cu^{2+}$ for 15 days (mean ± Std). Lower and capital letters represent statistical differences for each treatment during the exposure period and between treatments in each day of exposure, respectively ($p$<0.05).

### 2.2.3.4. Metallothionein

MT levels of unexposed mussels remained unchanged along the exposure period (Fig. 2.2.4A). In mussels exposed to CuO NPs, MT levels increased linearly over time, with an induction rate of 0.28 $mg.g^{-1}d^{-1}$ prot ($r$=0.97, $p$<0.05). As for mussels exposed to $Cu^{2+}$, MT was only induced at the end of the experiment (1.5–fold), to levels similar to CuO NPs exposed ones (8.4 ± 1.1 $mg.g^{-1}$ prot, $p$<0.05). Statistical analysis revealed that copper

concentrations in mussels exposed to CuO NPs are directly related with MT (r=0.99, $p$<0.034), while in $Cu^{2+}$ exposed ones, SOD and CAT activities are related to MT (r=0.99, $p$=0.022 and r=0.99, $p$=0.033, respectively).

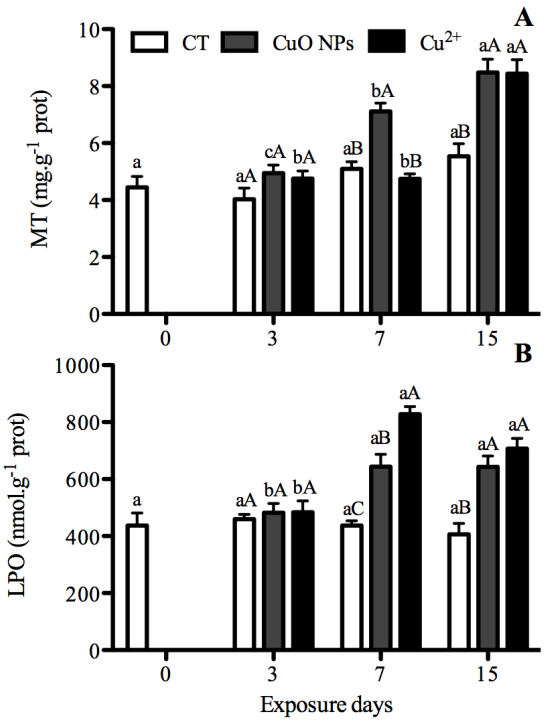


**Figure 2.2.4 –** Metallothionein concentrations (A) and lipid peroxidation (B) in the digestive gland of mussels *M. galloprovincialis* from controls and exposed to CuO NPs and $Cu^{2+}$ for 15 days (average ± Std). Lower and capital letters represent statistical differences for each treatment during the exposure period and between treatments in each day of exposure, respectively ($p$<0.05).

### 2.2.3.5. Lipid peroxidation

In control mussels (Fig. 2.2.4B) no significant changes were detected in LPO levels during the exposure period ($p$>0.05). Exposure of mussels to CuO NPs caused a 1.5–fold increase in LPO levels following 7 days of exposure ($p$<0.05), reaching a steady state by the end of the experiment ($p$>0.05). $Cu^{2+}$ exposed mussels presented a similar trend to CuO NPs exposed ones, with higher levels after a week of exposure (643.6 ± 97.8 nmol.$g^{-1}$ prot and 827.9 ± 59.3 nmol.$g^{-1}$ prot, respectively, $p$<0.05). Only in mussels exposed to CuO NPs, LPO is directly related with SOD activity (r=0.98 $p$=0.043).

### 2.2.3.6. Principal component analysis (PCA)

A PCA was applied to all the data obtained for the digestive glands to help explain the effects of both forms of Cu (NPs and ionic) on biomarkers response (Fig. 2.2.5A). The two principal components represent 86.6% of total variance, with PC1 representing 75.5% and PC2 11.1%. The overall PCA indicates a clear separation between control and Cu exposed mussels. Unexposed mussels are closely associated in PC1 showing homogenous biomarker variance with time. As for Cu–exposed mussels (CuO NPs and $Cu^{2+}$), a clear separation of the sampling periods occurred (after 3 and 15 days), suggesting a specific response of mussel digestive glands due to the type of exposure. Mussels exposed to CuO NPs after 3 days showed a relative proximity to the control group, reflecting the effectiveness of the antioxidant system and the absence of oxidative damage. Copper concentrations in the digestive gland is clearly associated with LPO levels and enzymatic activities in mussels, namely those exposed to CuO NPs after 7 days and $Cu^{2+}$ exposed mussels, reflecting a significant relationship between mussels antioxidant efficiency to counteract Cu exposure. On the other hand, MT levels in PC2 were more affected by CuO NPs after 7 and 15 days of exposure, as well as $Cu^{2+}$ for 15 days.

Another PCA was obtained incorporating the data for the digestive gland of mussels, as well as for the gills (data shown in Chapter 2.1) to differentiate responses and modes of action of both forms of copper in the two mussel tissues (Fig. 2.2.5B). The two principal components represent 78.9% of total variance, where PC1 represents 53.0% and PC2 25.9%. The overall PCA shows distinct responses of mussel tissues. Similar responses were obtained between control groups, for gills (PC1) and digestive gland (PC2), closely associated with mussels exposed to CuO NPs after 3 days. The antioxidant defence system (namely SOD and GPX) combined with MT induction (7 and 15 days of exposure) seem to be more important in the gills, while in the digestive gland copper accumulation (more evident after 15 days) associated with CAT induction (more evident at the end of the exposure) are the more pronounced responses.

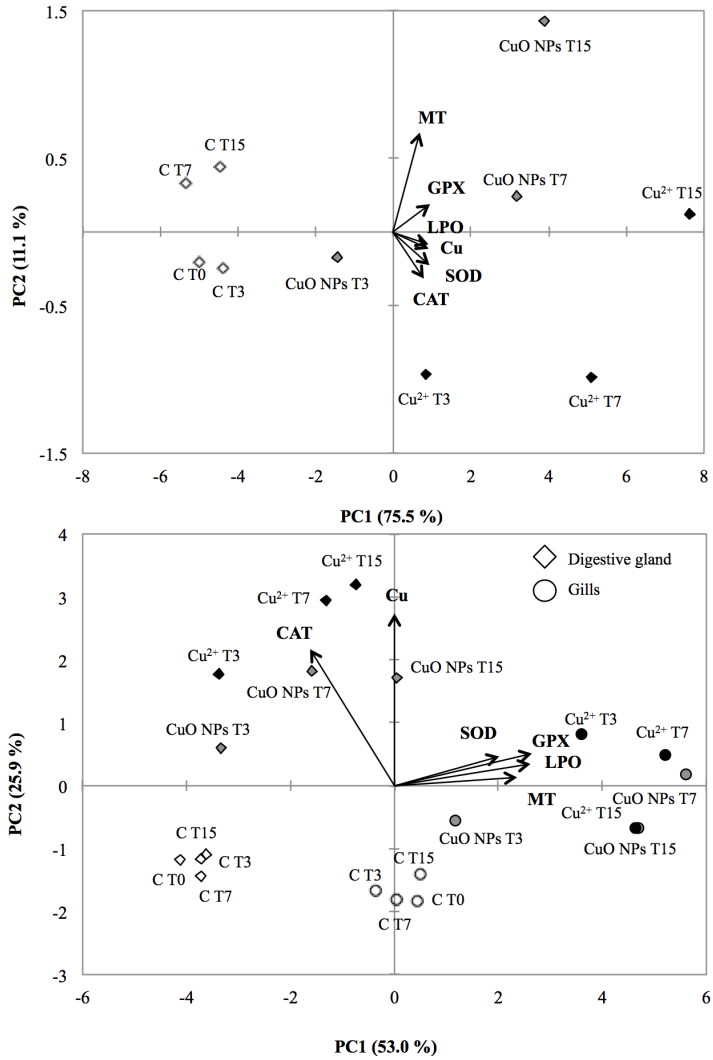


**Figure 2.2.5 –** Principal component analysis (PCA) of copper accumulation and the battery of biomarkers in the digestive gland of mussels *M. galloprovincialis* from controls and exposed to CuO NPs and $Cu^{2+}$ for 15 days (A); PCA of copper accumulation and biomarkers levels in the gills and digestive gland of control and exposed mussels.

## 2.2.4. Discussion

The bioavailability, uptake, accumulation and consequent toxicity of nanoparticles towards aquatic organisms are dependent on several physico–chemical properties as particle size/shape, surface charge and structure, particle chemistry and solubility and aggregation state (Bhatt and Tripathi, 2011; Scown *et al*., 2010).

The bioaccumulation results showed that both nano and ionic Cu accumulated in mussels' digestive glands (Fig. 2.2.2). Even though Cu concentrations in the digestive gland were

higher in $Cu^{2+}$ exposed mussels than in those exposed to CuO NPs in the first week of exposure, Cu accumulation decreased at the end of the experiment, which is in accordance with the role of the digestive gland in the detoxification of $Cu^{2+}$ (e.g. Viarengo *et al*., 1981; 1990; Regoli and Principato, 1995). On the other hand, Cu was linearly accumulated with time in CuO NPs exposure (Fig. 2.2.2), showing a higher accumulation rate, as seen in gills and total edible tissues of mussels exposed to the same nanoparticles (Chapters 2.1 and 4). Based on what is already known for CuO NPs accumulation in gills (Chapter 2.1), the increase of Cu concentrations in the digestive gland (twice that of the gills) indicate that there was uptake and transport of CuO from the NPs that cannot be explained by the dissolution of Cu alone. A selective handling of NPs seems to occur in the gills, where NPs aggregates are sorted and broken down into smaller particles followed by their transport to the digestive system where they can either accumulate or be transferred to the haemolymph and other tissues (Canesi *et al*., 2010; Moore *et al*., 2009; Peyrot *et al*., 2009; Ward and Kach, 2009). The digestive cells are highly adapted for endocytosis of large particles (<100 nm) for intra–cellular digestion and nutrient storage (Canesi *et al*., 2012; Moore, 2006; Moore *et al*., 2009) and have a key role in the metabolism of essential metals (Langston *et al*., 1998, Viarengo *et al*., 1981, 1990). Some studies with bivalve species have shown that nanoparticles are easily taken up by cells, especially those incorporated into aggregates (see Canesi *et al*., 2012; Ward and Kach, 2009) and even though gills seem to be the primary target for NPs toxicity, the digestive gland is the main tissue for their accumulation (Canesi *et al*., 2010; Koehler *et al*., 2008; Moore, 2006; Ringwood *et al*., 2010). For example, polystyrene nanoparticles translocate to the digestive gland of mussels and are taken up in the digestive cells possibly by endocytosis with longer gut retention times, promoted by the presence of aggregates (Ward and Kach, 2009). The translocation and extent of NPs uptake seems to be size and tissue dependent and in these experimental conditions, the existence of aggregates in suspension (Table 2.2.1, Figure 2.2.1) increases CuO NPs bioavailability to mussels, enhancing their uptake and internal exposure as well as a high retention time in cells (gills and digestive gland). Aggregation is therefore a key factor in determining the exposure and uptake of NPs in aquatic organisms, being also determinant in CuO NPs toxicity (Canesi *et al*., 2010; Chapter 2.1, Koehler *et al*., 2008; Ward and Kach, 2009).

The results of antioxidant enzymes showed responses in the digestive gland of exposed mussels dependent on the form of Cu, reflecting the capacity of both CuO NPs and $Cu^{2+}$ to generate ROS (Fig. 2.2.3). SOD activity was induced after 3 and 7 days of exposure to $Cu^{2+}$ and CuO NPs, respectively, suggesting the production of superoxide anions by both forms of

Cu (Fig 2.2.3A). Exposure to CuO NPs resulted in lower SOD activities than in $Cu^{2+}$ exposed mussels throughout the exposure period, suggesting a lower superoxide anions formation. The generation of hydrogen peroxide by SOD in the first week of exposure by both nano and ionic Cu does not seem to be counteracted by either CAT or GPX (Figs 2.2.3B–C) in CuO NPs exposure (activities similar to the beginning of the experiment), while in mussels exposed to $Cu^{2+}$ GPX activities increased to detoxify $H_2O_2$. With increasing time of exposure, CAT activity decreased (to levels similar to control) in CuO NPs exposed mussels, suggesting either a minimal increase of $H_2O_2$ or their use in Fenton reactions. On the other hand, in mussels exposed to $Cu^{2+}$ CAT was activated possibly by an excess of $H_2O_2$ originated by SOD or by hydroxyl radical formation via Fenton reaction. GPX activity was also triggered after exposure for 15 days to both forms of Cu (no significant differences) to further remove hydroperoxides accumulated by a reduced CAT activity (in the case of CuO NPs) or by an overproduction of hydroxyl radicals (in the case of $Cu^{2+}$). As a known redox cycling metal, $Cu^{2+}$ is capable of producing ROS by Fenton reactions that generally increases SOD, CAT and GPX activities in bivalves to prevent oxidative damage (Bebianno *et al*., 2004; Maria and Bebianno, 2011; Regoli and Principato, 1995). The capacity of CuO NPs to originate oxidative stress was also described, suggesting that they may lead to the alteration of the antioxidant capacity of the cells against the generation of ROS and consequently enzymatic activation or inhibition (Ahamed *et al*., 2010; Buffet *et al*., 2011; Chapter 2.1 Fahmy and Cormier, 2009; Karlsson *et al*., 2008).

Different mechanisms are involved in the uptake, toxicity and body burden of mussels exposed to nano or ionic forms of Cu not only due to different routes of exposure and uptake, different behaviour in the experimental medium, concentrations but also to different detoxification mechanisms (Chapters 2.1 and 4). Mussels are able to control $Cu^{2+}$ levels in their tissues using mechanisms of sequestration and elimination as the induction of metal binding proteins like metallothioneins or other detoxification pathways as membrane–limited vesicles or lipofuscin granules (Langston *et al*., 1998; Viarengo *et al*., 1981, 1990). The decrease in copper concentrations in digestive gland after 15 days of exposure to $Cu^{2+}$ suggest that mussels' detoxification mechanism was triggered. On the other hand, in mussels exposed to CuO NPs, MT induction was directly related to Cu accumulation suggesting that MT was playing a detoxifying role, nevertheless, with no clear signs of Cu elimination in digestive glands. Regardless of the tissue exposed (gills, or in this case digestive gland), the accumulation of these nanoparticles is always time dependent and higher than its elimination, in contrast to $Cu^{2+}$, where the metal is easily eliminated (Chapters 2.1 and 4). No detailed

information exists on NPs detoxification in bivalve species, only the suggestion of MT induction as a detoxification pathway for CuO NPs, Au NPs and Ag NPs (Chapter 2.1; Renault *et al*., 2008; Ringwood *et al*., 2010). Since MT plays an important role in controlling $Cu^{2+}$ availability and detoxification in the digestive gland (Langston *et al*., 1998; Maria and Bebianno, 2011; Viarengo *et al*., 1981, 1990), it is assumed that this metalloprotein will also participate in the sequestration and elimination of CuO NPs. In digestive gland cells, MT can bind to Cu and form Cu–MT complexes that accumulate into lysosomes in an insoluble form and are subsequently eliminated via exocytosis (Viarengo *et al*., 1981, 1990). However, this does not seem to be the case with CuO NPs. With increasing time of exposure and accumulation of higher quantities of Cu in the digestive gland, a linear induction of MT levels was detected in mussels exposed to CuO NPs, reflecting the MT role in the metabolism of these NPs (Fig. 2.2.4A) but not its participation in this metal elimination via formation of Cu–MT complexes. MT can also be a part of the antioxidant defence system by capturing harmful oxidant radicals (e.g. superoxide and hydroxyl radicals) in response to enzymes unaltered or inhibited activities (Viarengo *et al*., 1999). The role of MTs in oxidative stress originated by NPs was also proposed in *M. galloprovincialis* gills exposed to these CuO NPs (Chapter 2.1), in the clams *Scrobicularia plana* and *Corbicula fluminea* exposed to CuO NPs (10 µgCu.$L^{-1}$, 40–500 nm) and Au NPs ($1.6x10^3$–$1.610^5$ Au NP/cell, 10 nm), respectively (Buffet *et al*., 2011; Renault *et al*., 2008), the oyster *Crassostrea virginica* exposed to Ag NPs (16 µg $L^{-1}$–1.6 ng.$L^{-1}$, 15 ± 6 nm) (Ringwood *et al*., 2010) and the freshwater mussel *Elliptio complanata* exposed to CdTe quantum dots (1.6, 4, 8 mgCd.$L^{-1}$) (Peyrot *et al*., 2009). Contrarily, in mussels exposed to $Cu^{2+}$, MT was only induced after 15 days of exposure (Fig. 2.2.4A), which is in accordance with a decrease in Cu concentrations in the digestive glands, corroborating the active function of MT in Cu homeostasis and detoxification as well its scavenger activities (significant correlations with SOD and CAT activities) (Chapter 2.1; Langston *et al*., 1998; Maria and Bebianno, 2011; Viarengo *et al*., 1981). Accordingly, the exact detoxification mechanisms by which mussels eliminate CuO NPs, whether they differ between nano or ionic Cu, how and how long after exposure they are triggered and in what form this metal will be eliminated needs further investigation.

Lipid peroxidation results (Fig. 2.2.4B) indicated that the production of ROS overwhelmed the antioxidant efficiency of cells to maintain redox balance, resulting in peroxidative damage of membrane lipids. Lipid peroxidation was only detected after one week in mussels exposed to both forms of copper (CuO NPs and $Cu^{2+}$). During the initial exposure period, the cell defence mechanisms (enzymatic activities and MT levels) may have been sufficient to

counteract the presence of Cu and prevent LPO, as corroborated by the PCA (Fig. 2.2.5A) In the remaining period, both forms of Cu caused lipid peroxidation despite the efforts of the antioxidant defence system to counteract ROS production. Only mussels exposed to $Cu^{2+}$ showed a slight decrease in LPO levels (not significant, Fig. 2.2.4B) by the end of the experiment probably related to the beginning of detoxification processes while in CuO NPs exposed mussels, LPO maintained its levels. These results confirm the hypothesis that one of CuO NPs main toxic mechanism is mediated by oxidative stress leading to significant damage in the cells that changes over time. CuO NPs have also been shown to cause oxidative stress in gills and haemocytes of mussels in the form of lipid peroxidation and DNA damage (Chapters 2.1 and 4), as well as lipid peroxidation, oxidative lesions and increase of intracellular ROS in human cell cultures and *E. coli* (Ahmed *et al*., 2010; Fahmy and Cormier, 2009; Ivask *et al*., 2010; Karlsson *et al*., 2008). The dissimilar antioxidant capacity, MT induction and lipid peroxidation presented by mussels are dependent on time of exposure and form of copper (Figs. 2.2.3 and 2.2.4), as also confirmed by PCA (Fig. 2.2.5A). The levels of free Cu ions can be determinant to the different mode of action of the antioxidant system of mussels, as suggested by Maria and Bebianno (2011), explaining the results obtained for both forms of Cu. Nevertheless, other factors than the release of soluble $Cu^{2+}$ from the dissolution of the NPs (e.g. metal reactivity or physical contact) seem to contribute to the toxicity of CuO NPs, which is consistent with other studies (Ahamed *et al*., 2010; Buffet *et al*., 2011; Chapter 2.1; Fahmy and Cormier, 2009; Griffitt *et al*., 2007; Heinlaan *et al*., 2011). In fact, the CuO NPs used have poor solubility in the exposure medium (<1% dissolved Cu) and a great tendency to form large aggregates with increasing time of exposure (Table 2.2.1, Figure 2.2.1), with agglomeration state affecting biomarkers response with time of exposure (Chapter 2.1). Due to their small size, large surface area and oxidative stress damaging potential, CuO NPs may be internalized by the digestive system and release higher damaging concentrations of $Cu^{2+}$ within the cells. This mechanism of toxic action of nanoparticles has been entitled Trojan horse mechanism and has been suggested on mussel gills (Chapter 2.1), as well as in human cell cultures (Karlsson *et al*., 2008; Studer *et al*., 2010). The particles can also be retained in the extracellular compartment where other mechanisms of toxicity as the direct contact between particles and cellular membranes or other surface processes can also inflict damage due to the nanoparticle effect (Griffitt *et al*., 2009; Heinlaan *et al*., 2011; Studer *et al*., 2010).

The PCA applied to the data obtained for the gills and digestive gland of mussels exposed to both forms of Cu (Fig. 2.2.5B) shows different biomarker responses and accumulation

patterns that reflect the distinct physiological and metabolic functions of the two tissues. Gills seem to be more susceptible to oxidative stress than the digestive gland, as inhibition of antioxidants (especially SOD and CAT) is more pronounced (Chapter 2.1). As the main tissue involved in filtration, gills are in direct contact with the nanoparticles, especially $Cu^{2+}$ dissolved from the NPs. The digestive gland is also an important target for Cu (namely in the form of aggregates), with high enzymatic activities attributed to oxidative stress caused by either nano or ionic Cu. Nevertheless, Cu accumulation is the more pronounced response in the digestive gland (Fig. 2.2.5B), with levels 2–fold higher than those accumulated in the gills. This result also highlights the importance of the digestive gland in CuO NPs accumulation suggesting that particle uptake by mussels may help to explain the responses seen upon exposure to CuO NPs.

The digestive gland of mussels is a susceptible tissue to CuO NPs toxicity probably related to the presence of CuO NPs aggregates that are taken up and accumulated more significantly in this tissue than in the gills. Oxidative stress was detected in the form of activated antioxidant enzymatic activities and lipid peroxidation of membrane lipids, as well as MT induction. MT is also an important detoxifying mechanism for CuO NPs in this tissue. Nevertheless, the exact mechanism responsible for the oxidative stress is unclear though it appears to be mediated by the significant CuO NPs accumulation with increasing time of exposure. Further research is required to understand not only the mechanisms inherent to CuO NPs–related oxidative stress but also their uptake pathways and subsequent detoxification mechanisms from tissues.

## 2.2.5. References

Ahamed, M.; Siddiqui, M.; Akhtar, M.J.; Ahmad, I.; Pant, A.B.; Alhadlaq, H.A. (2010). Genotoxic potential of copper oxide nanoparticles in human lung epithelial cells. *Biochemical and Biophysical Research Communications*. **396:** 578–583.

Bebianno, M.J.; Langston, W.J. (1989). Quantification of metallothioneins in marine invertebrates using differential pulse polarography. *Portugaliae Electrochimica Acta*. **7:** 59–64.

Bebianno, M.J.; Géret, F.; Hoarau, P.; Serafim, M.A.; Coelho, M.R.; Gnassia–Barelli, M.; Roméo, M. (2004). Biomarkers in *Ruditapes decussatus*: a potential biondicator species. *Biomarkers*. **9(4–5):** 305–330.

Bhatt, I.; Tripathi, B.N. (2011). Interaction of engineered nanoparticles with various components of the environment and possible strategies for their risk assessment. *Chemosphere*. **82(3):** 308–317.

Bryan, G.W.; Langston, W.J. (1992). Bioavailability, accumulation and effects of heavy metals in sediments with special reference to United Kingdom estuaries: a review. *Environmental Pollution*. **76:** 89–131.

Buffet, P.E.; Tankoua, O.F.; Pan, J.F.; Berhanu, D.; Herrenknecht, C.; Poirier, L.; Amiard–Triquet, C.; Amiard, J.C.; Bérard, J.B.; Risso, C.; Guibbolini, M.; Roméo, M.; Reip, P.; Valsami–Jones, E.; Mouneyrac, C. (2011). Behavioural and biochemical responses of two marine invertebrates *Scrobicularia plana* and *Hediste diversicolor* to copper oxide nanoparticles. *Chemosphere*. **84:** 166–174.

Canesi, L.; Fabbri, R.; Vallotto, D.; Marcomini, A.; Pojana, G. (2010). Biomarkers in *Mytilus galloprovincialis* exposed to suspensions of selected nanoparticles (Nano carbon black, C60 fullerene, Nano–$TiO_2$, Nano–$SiO_2$). *Aquatic Toxicology*. **100:** 168–177.

Canesi, L.; Ciacci, C.; Fabbri, R.; Marcomini, A.; Pojana, G.; Gallo, G. (2012). Bivalve molluscs as a unique target group for nanoparticle toxicity. *Marine Environmental Research*. **76:** 16–21.

Erdelmeier, I.; Gerard–Monnier, D.; Yadan, J.C.; Acudiere, J. (1998). Reactions of N–methyl–2–phenylindole with malondialdehyde and 4–hydroxyalkenals. Mechanistic aspects of the colorimetric assay of lipid peroxidation. *Chemical Research in Toxicology*. **11:** 1184–1194.

Fahmy, B.; Cormier, S.A. (2009). Copper oxide nanoparticles induce oxidative stress and cytotoxicity in airway epithelial cells. *Toxicology In Vitro*. **23:** 1365–1371.

Greenwald, R.A. (1985). Handbook of Methods for Oxygen Radical Research. CRC Press, Boca Raton, FL.

Griffitt, R.J.; Weil, R.; Hyndman, K.A.; Denslow, N.D.; Powers, K.; Taylor, D.; Barber, S.D. (2007). Exposure to copper nanoparticles causes gill injury and acute lethality in zebrafish (*Danio rerio*). *Environmental Science and Technology*. **41:** 8178–8186.

Griffitt, R.J.; Hyndman, K.; Denslow, N.D.; Barber, D.S. (2009). Comparison of molecular and histological changes in zebrafish gills exposed to metallic nanoparticles. *Toxicological Sciences*. **107(2):** 404–415.

Heinlaan, M.; Kahru, A.; Kasemets, K.; Arbeille, B.; Prensier, G.; Dubourguier, H.C. (2011). Changes in *Daphnia magna* midgut upon ingestion of copper oxide nanoparticles: a transmission electron microscopy study. *Water Research*. **45:** 179–190.

Ivask, A.; Bondarenko, O.; Jepihhina, N.; Kahru, A. (2010). Profiling of the reactive oxygen species–related ecotoxicity of CuO, ZnO, $TiO_2$, silver and fullerene nanoparticles using a set of recombinant luminescent *Escherichia coli* strains: differentiating the impact of particles and solubilised metals. *Analytical and Bioanalytical Chemistry*. **398:** 701–716.

Karlsson, H.L.; Cronholm, P.; Gustafsson, J.; Möller, L. (2008). Copper oxide nanoparticles are highly toxic: a comparison between metal oxide nanoparticles and carbon nanotubes. *Chemical Research in Toxicology*. **21:** 1726–1732.

Koehler, A.; Marx, U.; Broeg, K.; Bahns, S.; Bressling, J. (2008). Effects of nanoparticles in *Mytilus edulis* gills and hepatopancreas – a new threat to marine life? *Marine Environmental Research*. **66(1):** 12–14.

Langston, W.J.; Bebianno, M.J.; Burt, G.R. (1998). Metal handling strategies in molluscs. In: Langston, W.J.; Bebianno, M.J. (Eds.). Metal Metabolism in Aquatic Environments. Chapman and Hall, London, pp. 219–283.

Lawrence, R.A.; Burk, R.F. (1976). Glutathione peroxidase activity in selenium deficient rat liver. *Biochemical and Biophysical Research Communications*. **71:** 952–958.

Lowry, O.H.; Rosenbrough, N.J.; Farr, A.L.; Randall, R.J. (1951). Protein measurement with the Folin phenol reagent. *Journal of Biological Chemistry*. **193:** 265–275.

Maria, V.L.; Bebianno, M.J. (2011). Antioxidant and lipid peroxidation responses in *Mytilus galloprovincialis* exposed to mixtures of benzo(a)pyrene and copper. *Comparative Biochemistry and Physiology Part C: Toxicology and Pharmacology*. **154(1):** 56–63.

McCord, J.M.; Fridovich, I. (1969). Superoxide dismutase: an enzymatic function for erythrocuprein (hemocuprein). *Journal of Biological Chemistry*. **244(22):** 6049–6055.

Moore, M.N. (2006). Do nanoparticles present ecotoxicological risks for the health of the aquatic environment? *Environment International*. **32:** 967–976.

Moore, M.N.; Readman, J.A.J.; Readman, J.W.; Lowe, D.M.; Frickers, P.E.; Beesley, A. (2009). Lysosomal cytotoxicity of carbon nanoparticles in cells of the molluscan immune system: an in vitro study. *Nanotoxicology*. **3(1):** 40–45.

Mortimer, M.; Kasemets, K.; Kahru, A. (2010). Toxicity of ZnO and CuO nanoparticles to ciliated protozoa *Tetrahymena thermophila*. *Toxicology*. **269(2–3):** 182–189.

Peyrot, C.; Gagnon, C.; Gagné, F.; Willkinson, K.J.; Turcotte, P.; Sauvé, S. (2009). Effects of cadmium tulleride quantum dots on cadmium bioaccumulation and metallothionein production to the freshwater mussel, *Elliptio complanata*. *Comparative Biochemistry and Physiology C*. **150:** 246–251.

Regoli, F.; Principato, G. (1995). Glutathione, glutathione–dependent and antioxidant enzymes in mussel, *Mytilus galloprovincialis*, exposed to metals under field and laboratory conditions: implications for the use of biochemical biomarkers. *Aquatic Toxicology*. **31:** 143–164.

Renault, S.; Baudrimont, M.; Mesmer–Dudons, N.; Gonzalez, P.; Mornet, S.; Brisson, A. (2008). Impacts of gold nanoparticle exposure on two freshwater species: a phytoplanktonic algae (*Scenedesmus subspicatus*) and a benthic bivalve (*Corbicula fluminea*). *Gold Bulletin*. **41(2):** 116–126.

Ringwood, A.H.; McCarthy, M.; Bates, T.C.; Carroll, D.L. (2010). The effects of silver nanoparticles on oyster embryos. *Marine Environmental Research*. **69(1):** 549–551.

Ruparelia, J.P.; Chatterjee, A.K.; Duttagupta, S.P.; Mukherji, S. (2008). Strain specificity in antimicrobial activity of silver and copper nanoparticles. *Acta Biomaterialia*. **4(3):** 707–716.

Scown, T.M.; Aerle, R.V.; Tyler, C.R. (2010). Review: do engineered nanoparticles pose a significant threat to the aquatic environment? *Critical Reviews in Toxicology*. **40(7):** 653–670.

Studer, A.M.; Limbach, L.K.; Duc, L.V.; Krumeich, F.; Athanassiou, E.K.; Gerber, L.C.; Moch, H.; Stark, W.J. (2010). Nanoparticle cytotoxicity depends on intracellular solubility: comparison of stabilized copper metal and degradable copper oxide nanoparticles. *Toxicology Letters*. **197:** 169–174.

Viarengo, A.; Zanicchi, G.; Moore, M.N.; Orunesu, M. (1981). Accumulation and detoxification of copper by the mussel *Mytilus galloprovincialis* Lam: a study of subcellular distribution in the digestive gland cells. *Aquatic Toxicology*. **1:** 147–157.

Viarengo, A.; Canesi, L.; Pertica, M.; Poli, G.; Moore, M.N.; Orunesu, M. (1990). Heavy metal effects on lipid peroxidation in the tissues of *Mytilus galloprovincialis* Lam.

*Comparative Biochemistry and Physiology Part C: Comparative Pharmacology*. **97(1):** 37–42.

Viarengo, A.; Burlando, B.; Cavaletto, M.; Marchi, B.; Ponzano, E.; Blasco, J. (1999). Role of metallothionein against oxidative stress in the mussel *Mytilus galloprovincialis*. *American Journal of Physiology: Regulatory, Integrative and Comparative Physiology*. **277:** R1612–R1619.

Ward, J.E.; Kach, D.J. (2009). Marine aggregates facilitate ingestion of nanoparticles by suspension–feeding bivalves. *Marine Environmental Research*. **68:** 137–142.

Yoon, K.Y.; Byeon, J.H.; Park, J.H.; Hwang, J. (2007). Susceptibility constants of *Escherichia coli* and *Bacillus subtilis* to silver and copper nanoparticles. *The Science of the Total Environment*. **373:** 572–575.

# CHAPTER 3

## Effects of silver nanoparticles exposure in the mussel *Mytilus galloprovincialis*

# 3.

# EFFECTS OF SILVER NANOPARTICLES EXPOSURE IN THE MUSSEL *MYTILLUS GALLOPROVINCIALIS*

*Tânia Gomes, Olinda Araújo, Rita Pereira, Ana C. Almeida, Alexandra Cravo, Maria João Bebianno*

[1]CIMA, Faculty of Science and Technology, University of Algarve, Campus de Gambelas, 8005–139 Faro, Portugal

[2]CENSE and University of Algarve, Faculty of Sciences and Technology, Campus de Gambelas, 8005–139 Faro, Portugal

[3]CBME, Faculty of Science and Technology, University of Algarve, Campus de Gambelas, 8005–139 Faro, Portugal

[4]Department of Zoology & Animal Cell Biology, Scholl of Science and Technology, University of the Basque Country, E–48080 Bilbao, Spain

Submitted to Nanotoxicology

## Abstract

Silver NPs have emerged as one of the most important currently used NPs in a wide range of industrial and commercial applications. This has caused increasing concern about their fate and toxicity in the environment as well as uptake and potential toxicity towards aquatic invertebrates. Accordingly, mussels *Mytilus galloprovincialis* were exposed to 10 μgAg.$L^{-1}$ as Ag NPs and $Ag^{+}$ for 15 days, and SOD, CAT, GPX, LPO and MT were determined along with Ag accumulation in gills and digestive gland. Accumulation results show that Ag NPs and $Ag^{+}$ accumulated in both tissues with similar patterns except in the digestive gland. Enzymatic activities in gills were significantly higher in Ag NPs–exposed mussels while in those exposed to $Ag^{+}$ decreased with time. In digestive gland, enzymatic activities remained unchanged or decreased. Moreover, induction of MTs was detected in exposed gills, directly related to Ag accumulation. On the other hand, differences in Ag accumulation in the digestive gland may result from Ag binding in an insoluble detoxified form, with little role played by MT. LPO was higher in gills exposed to Ag NPs, whereas in the digestive gland only $Ag^{+}$ induced LPO. Ag NPs and $Ag^{+}$ cause oxidative stress with distinct modes of action and it's not clear if for Ag NPs the observed effects are attributed to free $Ag^{+}$ ions associated with the nanoparticle effect. Overall, our results show that gills are more susceptible to oxidative stress originated by Ag NPs and $Ag^{+}$, whereas the digestive gland constitutes the main storage organ.

Keywords: *Mytilus galloprovincialis*, Ag NPs, oxidative stress, gills, digestive gland

## 3.1. Introduction

Silver nanoparticles (Ag NPs) are one of the most commonly NPs used in the nanotechnology industry mainly due to their antibacterial properties (e.g. Fabrega et al., 2011 and literature cited therein; Farkas *et al*., 2011; Luoma, 2008). Ag NPs are used in a broad range of products such as medical equipment, consumer products (e.g. textiles, eating utensils, food storage, cosmetics and personal hygiene) and household appliances (e.g. washing machine, vacuum cleaners) (www.nanoproject.org). The majority of products containing Ag NPs can release considerable amounts of Ag particles or $Ag^+$ ions into sewage treatment plants from where they could be further release via wastewater discharge into the aquatic environment (Benn and Westerhoff, 2008; Blaser *et al*., 2008; Farkas *et al*., 2011). For example, Benn and Westerhoff (2008) and Geranio *et al*. (2009) demonstrated leaching of silver (ionic and nanoparticulate) from socks impregnated with Ag NPs into water after washing. Environmental concentrations of Ag NPs have not been determined but it is estimated that by 2010, more than 15% of silver released in European waters will come from biocidal plastics and textiles containing Ag NPs (Blaser *et al*., 2008). Predicted concentrations of Ag NPs in natural waters range from 0.03 to 500 $ng.L^{-1}$ (Luoma, 2008), with values around 0.03 $\mu g.L^{-1}$ based on a life–cycle perspective of nanomaterials (Mueller and Nowack, 2008) and 0.01 $\mu g.L^{-1}$ derived from consumer products (Boxall *et al*., 2008). Due to the rapid development of commercialized nano–products, future discharge of Ag NPs into the environment will increase, where aquatic organisms are likely to be exposed.

Many factors influence the behaviour of NPs in the environment, being their physico–chemical properties the most important ones. Particle composition, size, agglomeration, mobility, complexation, adsorption, concentration, charge and interactions with organic material and natural colloids are key elements for determining the environmental fate, ecotoxicity and bioavailability to organisms (Bhatt and Tripathi, 2011; Scown *et al*., 2010a). Solubility is another important factor to be considered, since the release of $Ag^+$ ions from Ag NPs may be determinant for its relative toxicity. Silver is one of the most toxic metals to both freshwater and marine organisms (e.g. Wang and Fisher, 1999; Wang and Rainbow, 2005), highly persistent in the environment and with a great capacity to accumulate in water, sediments and organisms (Fabrega *et al*., 2011; Luoma, 2008). On the other hand, there is limited knowledge about the possible adverse effects that Ag NPs can exert to aquatic organisms. Ag NPs have not only antibacterial action (Kim *et al*., 2007; Morones *et al*., 2005), but also cytotoxic and genotoxic properties. ROS–derived oxidative stress (Choi *et al*.,

2010; Hussain *et al*., 2005), biomembrane damage (Arora *et al*., 2008; Farkas *et al*., 2010), DNA damage (Asharani *et al*., 2009; Park and Choi, 2010) and bioaccumulation (Farkas et *al*., 2011; Scown *et al*., 2010b; Zuykov *et al*., 2011) were observed not only in mammalian cells but also in freshwater and marine organisms. Nevertheless, some difficulty arises in interpreting results due to a wide range of Ag NPs sizes and shapes, exposure routes (saltwater, freshwater, sediment), concentrations (majority environmentally irrelevant), time of exposure (normally short–term) and differences within and among species (high variety of species) (e.g. Baun *et al*., 2008; Canesi *et al*., 2012). The exact mechanism of action of Ag NPs has not yet been determined and it is still not clear if its enhanced toxicity is derived from the properties inherent to the particles, the release of $Ag^{+}$ or a combination of both (Asharani *et al*., 2008; Fabrega *et al*., 2011; Griffitt *et al*., 2009). Though there is some evidence on the bioaccumulation and toxicity of Ag NPs, there is a lack of information on the uptake, tissue distribution and their potential toxicity towards aquatic invertebrates, namely bivalve molluscs. Filter–feeding molluscs such as *Mytilus* sp. are a target group for NPs toxicity due to their capacity to filter large volumes of water and capture particulate matter and xenobiotics in suspension that are subsequently distributed through their organs and cellular compartments (Baun *et al*., 2008; Moore, 2006). Therefore, the aim of this study was to identify target tissues for Ag NPs accumulation and toxic effects using mussels *M. galloprovincialis* and to compare the patterns of distribution and modes of action with those of ionic silver (same Ag mass). The effects were assessed in terms of oxidative stress, through the determination of the activities of the antioxidant enzymes superoxide dismutase (SOD), catalase (CAT) and glutathione peroxidase (GPX), lipid peroxidation (LPO) and metallothioneins (MTs) in mussels' gills and digestive glands along with Ag accumulation.

## 3.2. Materials and methods

### 3.2.1. Preparation and characterization of Ag NPs

Silver nanoparticles (Ag NPs) were obtained from Sigma–Aldrich (Germany) with the particle size specified as <100 nm, surface area as 5.0 $m^2.g^{-1}$ and density 10.5 $g.cm^3$. A stock solution of 10 $\mu gAg.L^{-1}$ was prepared in ultrapure water (18 MΩ/cm), sonicated for 1 hour (45 kHz frequency) and kept in constant shaking to breakdown particles aggregates before adding to the exposure tanks. Ionic silver stock solution ($Ag^{+}$) was prepared identically but not sonicated.

The size (z–average hydrodynamic diameter) and surface charge (zeta potential) of Ag NPs were determined by dynamic light scattering (DLS) and electrophoretic light scattering (ELS), respectively, using a Zetasizer Nano ZS analyzer (Malvern Instruments Inc., UK). Suspensions of 100 $mg.L^{-1}$ of Ag NPs were prepared in ultrapure water (18 MΩ/cm), ultrapure water with 100 and 1000 mM of NaCl, as well as in natural seawater, and sonicated for 15 minutes (USC500TH, VWR International) immediately prior to analysis. A He–Ne laser with fixed wavelength of 633 nm was used as a light source and the intensity of scattered light was measured by a detector at 90°. NPs size was determined as the z–average hydrodynamic diameter using the Stokes–Einstein equation. For each size measurement 1 mL of the suspension was introduced into a disposable polystyrene cuvette and, at minimum, three replicates were made. The used concentration of suspended Ag NPs was adequate to create sufficient scattered intensity. All measurements were conducted at 25°C.

The hydrodynamic size, polydispersity index and intensity of Ag NPs in natural seawater during 12 hours (period between water renewals) were also determined using an ALV apparatus with Ar Ion Lased (514.5 nm) by DLS. Particle dispersions (100 $\mu g.L^{-1}$ Ag NPs) were measured at 90º and intensity fluctuations analyzed by an ALV–7000 digital correlator, automatically and in a single run. The temperature was controlled (20 ± 0.1 ºC) using a Haake Phoenix–II heater/circulator with a C30P cooling bath, with Haake Sil 180 mineral oil. The temperature was read directly from the decalin bath using a Platinum Pt100 temperature sensor. The shape and size of Ag NPs were also investigated by transmission electron microscopy (TEM) using a JEOL JEM–1230 TEM equipped with a digital camera Model 785 ES1000W Erlangshen CCD. Ag NPs were diluted in ultrapure water and sonicated to keep the particles in solution and avoid aggregation. A drop of the dilution at 32 $mg.L^{-1}$ was allowed to dry on a Ni grid cover and examined by TEM at 80 KV. Ag NPs were also characterized by X–Ray diffraction (XRD). X–ray diffraction patterns were obtained in a Panalytical X'Pert Pro diffractometer using CuKα radiation filtered by Ni and X'Celerator detector. The measurements were made using a step–scanning program with 0.167° per step and acquisition time of 100 s per step. The HighScore Plus software with the ICDD PDF–2 database was used for peak analysis and crystalline phase identification.

### 3.2.2. Laboratory assay

Mussels *M. galloprovincialis* (63.2 ± 5.8 mm) were collected in the Ria Formosa Lagoon (South of Portugal) and acclimated for 7 days at constant temperature and aeration. Mussels

were divided between 25L tanks (around 2.5 mussels/L), filled with 20 litters of natural seawater in a triplicate design. Mussels in three tanks were exposed to 10 μgAg.$L^{-1}$ by adding Ag NPs, other three tanks to 10 μgAg.$L^{-1}$ by adding $Ag^{+}$ ($AgNO_3$) and three other tanks were used as control. Silver exposure (Ag NPs and $Ag^{+}$) was maintained for 15 days during which time the water was renewed every 12 hours, with the fresh water being re–dosed with Ag NPs and $Ag^{+}$ stock solutions. Before each renewal, Ag NPs solution was sonicated for 30 minutes (45 kHz frequency) to break down the size of aggregates. Water in control tanks was also replaced every 12 hours. During the exposure period, water quality was checked in all tanks by measuring temperature (17.6 ± 0.3ºC), salinity (36.3 ± 0.1), percentage of oxygen saturation (96.9 ± 3.3%) and pH (7.8 ± 0.05). The Ag concentration used is environmentally relevant and reported for several aquatic systems (Fabrega *et al*., 2009; Luoma, 2008; Scown *et al*., 2010b). Mussels were not fed and no mortality was detected during the exposure. Unexposed and Ag (NPs and ionic) exposed mussels were collected after 3, 7 and 15 days, after which mussels were collected and biotic parameters measured. Collected mussels were dissected and gills and digestive glands separated and immediately frozen in liquid nitrogen and stored at –80ºC until further use.

### 3.2.3. Condition index

To assess the physiological status of control and exposed mussels to Ag NPs and $Ag^{+}$ during the course of the experiment, the soft tissues and shells of ten individuals were weighted and the condition index (CI) estimated as the percentage of the ratio between the drained weight of soft tissues (g) and the total weight (g).

### 3.2.4. Ag in experimental medium

Silver was analysed in water samples from control and exposure groups collected immediately after addition of Ag NPs and $Ag^{+}$ stock solution and 12 hours after water renewal and re–dosing from the Ag–exposure groups. Total silver concentrations were determined after nitric acid (2%) digestion and dissolved silver from the nanoparticle exposure group was determined after water filtration (0.02 μm filter, Anotop 25, Whatman) and acid digestion (Griffitt *et al*., 2009). Silver was analysed by graphite furnace atomic absorption spectrometry (Analyst 800 – Perkin Elmer).

### 3.2.5. Ag in mussel tissues

For each experimental condition (control, Ag NPs and $Ag^{+}$) five pools of ten gills and digestive glands were used to determine silver concentrations. Dried (80ºC) tissues were submitted to wet digestion with $HNO_3$ and silver analysed by graphite furnace atomic absorption spectrometry (Analyst 800 – Perkin Elmer).

### 3.2.6. Antioxidant enzymes

Antioxidant enzymatic activities were determined in the gills and digestive gland of mussels from control and exposed to Ag NPs and $Ag^{+}$ after homogenization with Tris–HCl buffer (20mM, pH 7.6), containing 1mM of EDTA, 0.5M of saccharose, 0.15M of potassium chloride and 1mM of DTT, in an ice bath for 2 minutes. The homogenates were centrifuged at 500 *g* for 15 minutes at 4ºC to precipitate large particles and centrifuged again at 12,000 *g* for 45 minutes at 4ºC to precipitate the mitochondrial fraction. The cytosolic fraction obtained was purified on a Sephadex G–25 gel column (PD10, Pharmacia) to remove the low molecular weight proteins that can interfere with enzymatic activity analysis. Enzymatic activities were measured in the purified cytosolic fraction.

To determine SOD activity (EC 1.15.1.1), the reduction of cytochrome c by the system xanthine oxidase/hypoxanthine was measured at 550 nm (McCord and Fridovich, 1969). One unit of SOD is defined as the amount of enzyme that inhibits the reduction of cytochrome c by 50%. SOD activity is expressed in $U.mg^{-1}$ total protein concentration. CAT activity (EC 1.11.1.6) was determined by the decrease in absorbance at 240 nm due to $H_2O_2$ consumption, with a molar extinction coefficient of 40 $M^{-1}$ $cm^{-1}$ (Greenwald, 1985) and results are expressed as $\mu mol.min^{-1}.mg^{-1}$ of total protein concentration. GPX activity was measured through NADPH oxidation in the presence of excess glutathione reductase, reduced glutathione and hydroperoxide as substrate, at 340 nm (Lawrence and Burk, 1976) and results expressed as $nmol.min^{-1}.mg^{-1}$ of total protein concentration.

### 3.2.7. Metallothioneins

Metallothionein (MT) concentrations were determined in aliquots of the heat–treated cytosol (S2 fraction) from gills and digestive gland of mussels according to the method described by Bebianno and Langston (1989). In the absence of a mussel MT standard, quantification of MT was based on rabbit liver metallothionein, MT–I (10 $mg.L^{-1}$), using the standard

additions method. MT concentrations are expressed as a milligram.$g^{-1}$ of total protein concentration.

### 3.2.8. Lipid peroxidation

Lipid peroxidation (LPO) was assessed in the cytosol (S1 fraction) of gills and digestive gland of unexposed and exposed (Ag NPs and $Ag^{+}$) mussels by determining malondialdehyde (MDA) and 4–hydroxyalkenals (4–HNE) concentrations upon the decomposition by polyunsaturated fatty acid peroxides (Erdelmeier *et al*., 1998). This procedure is based on the reaction of two moles of *N*–methyl–2–phenylindole, a chromogenic reagent, with one mole of either MDA or 4–HNE at 45ºC for 60 min to yield a stable chromophore that has a maximal absorbance at 586 nm, using malondialdehyde bis–(tetrametoxypropan) as a standard. Lipid peroxidation is expressed as nmols of MDA+4–HNE.$g^{-1}$ of total protein.

### 3.2.9. Total protein concentration

Total protein content was determined in the cytosolic fraction (S1 fraction) of gills and digestive glands of unexposed and Ag exposed mussels (NPs and ionic) according to Lowry's method (Lowry *et al*., 1951) for MT and LPO concentrations or to Bradford method (Bradford, 1976) for antioxidant enzymes activities. For both procedures bovine serum albumin (BSA) was used as a standard.

### 3.2.10. Statistical analyses

Statistical analyses were performed using SigmaPlot10® and XLStat2009®. Results are presented as mean ± standard deviation. Significant differences between biomarkers and silver concentrations were detected using one–way analysis of variance (ANOVA) or Kruskal–Wallis One Way Analysis of Variance on Ranks and only $p<0.05$ was accepted as significant. Whenever significant, the pairwise multiple–comparison tests Tukey's or Dunn's were applied. Additionally, linear regression was applied to confirm existing relationships between variables.

Principal Component Analysis (PCA) was used to evaluate the influence of silver concentrations (nano and ionic) in biomarkers of control and exposed mussels along the period of exposure and assess the overall results, as well as to differentiate responses and modes of action of both forms of silver in the gills and digestive glands.

## 3.3. Results

### 3.3.1. Nanoparticles characterization

The size, shape and zeta potential of the Ag NPs particles were characterized by TEM and DLS analysis (Fig. 3.1). Ag NPs are mainly spherical in shape and polysdiperse (Fig. 3.1A). The size of Ag NPs reported by the manufacturer (< 100nm) is in agreement with the size obtained by TEM (Fig. 3.1A). DLS results show an average size of Ag NPs higher than the average reported by the manufacturer (<100 nm) and in the presence of salts the NPs size is much higher due to NPs aggregation. Zeta potential measurements of Ag NPs in both ultrapure water and natural seawater suggest that these NPs have a propensity to aggregate, corroborating the results obtained by the hydrodynamic diameter of particles. Zeta potential tends to increase in the presence of salts (become less negative) due to the increase in ionic strength. A typical XRD pattern of Ag nanoparticles is shown in Figure 3.1B, from which the phase and the crystal structure were analysed. Ag NPs have a single–phase with monocubic structure. The intensity and position of the diffraction peaks of the Ag NPs are in good agreement with the reported values (JCPDS #01–087–0718) and no peaks of impurities were found in XRD pattern. The lattice parameters are: $a$ = 4.077 Å, $b$ = 4.077 Å and $c$ = 4.077 Å. The mean particle size was also determined during a cycle of 12 hours using DLS, showing a wide size distribution ranging from approximately 97.0 to 690.4 nm (Table 3.1, 144.2 ± 39.2 nm) that increases with time (Fig. 3.1C). On the other hand, Ag NPs intensity (Fig. 3.1D) decreased during the 12–hour period, indicative of particles dissolution or settlement with time. A high polydispersity index was also observed by DLS (Table 3.1, 0.44 ± 0.03), suggesting that under the exposure conditions, Ag NPs tends to aggregate producing suspensions with the presence of both small and large aggregates.

**Table 3.1 –** Characterization of Ag nanoparticles using different techniques. Values are mean ± std.

| Particle characterization | Method | Manufacturer specifications | Ultrapure water | Ultrapure water + 100 nM NaCl | Ultrapure water + 1000 nM NaCl | Natural seawater |
|---|---|---|---|---|---|---|
| Particle size (nm) | TEM | <100 | – | – | – | – |
| Specific surface area ($m^2.g^{-1}$) | – | 5.0 | – | – | – | – |
| Density ($g.cm^{-3}$) | – | 10.49 | | | | |
| Z–average (nm)[a] | DLS | – | 141.1 ± 3.2 | 758.2 ± 61.1 | 666.9 ± 111.0 | 895.5 ± 83.9 |
| Zeta potential (mV)[a] | ELS | – | –42.5 ± 1.3 | –15.1±1.9 | –9.8 ± 5.5 | –10.2 ± 1.2 |
| Mean particle diameter (nm)[b] | DLS | – | – | – | – | 144.2 ± 39.2 |
| Polydispersity index | DLS | – | – | – | – | 0.44 ± 0.03 |
| pH | – | – | 7.02 | 5.33 | 6.00 | 8.08 |

[a] 100 $mg.L^{-1}$ of Ag NPs dispersed in ultrapure and natural seawater.
[b] 100 $\mu g.L^{-1}$ of Ag NPs dispersed in natural seawater during a 12 hours cycle.

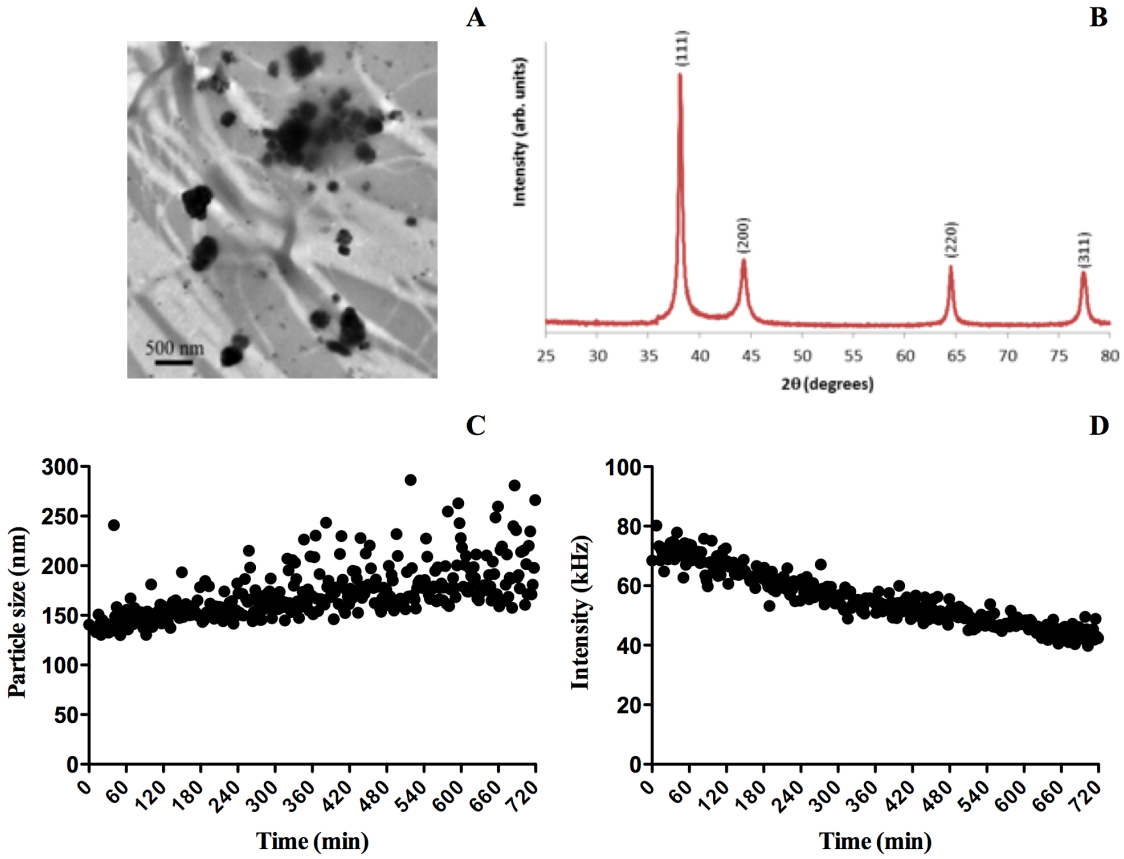


**Figure 3.1 –** Characterization of Ag NPs. (A) Transmission electron microscopic image of Ag NPs at 32 ppm in Milli–Q water. (B) XRD patterns of Ag NPs. (C) Particle size distribution (nm) during a cycle of 12 hours by dynamic light scattering using a concentration of 100 µg.L$^{-1}$. (D) Intensity (kHz) during a cycle of 12 hours by dynamic light scattering using a concentration of 100 µg.L–1.

### 3.3.2. Condition index

The condition index of unexposed and Ag NPs and $Ag^{+}$ exposed mussels was similar throughout the exposure period, ranging from 16.0 ± 2.6 to 22.2 ± 4.2 ($p$>0.05).

### 3.3.3. Ag in experimental medium

Silver analysis of water samples taken from control tanks show that Ag concentrations were below the detection limit (<1 µg.L$^{-1}$). Immediately after dosing, the Ag concentration in the exposure tanks was 41.3% and 39.4% lower than the nominal concentration of 10µgAg.L$^{-1}$ for Ag NPs and $Ag^{+}$, respectively. After the 12h period between water change and redosing,

more than 80% of the initial added dose of 10μgAg.$L^{-1}$ added in the nano or ionic form was removed from the water column (84.2% for Ag NPs and 89.1% for $Ag^{+}$). Of the total Ag concentrations on the Ag NPs exposure (4.13 ± 0.1 μg.$L^{-1}$), around 24.5% of the initial added dose is present in the dissolved form, indicating that most of the Ag in solution is in the nanoparticulate form. The percentage of total dissolved silver from the Ag NPs increased to 44.2 % after 12 hours indicating that these particles tend to dissolve in seawater with increasing time of exposure.

### 3.3.4. Ag bioaccumulation in mussel tissues

The exposure to Ag NPs and $Ag^{+}$ resulted in higher Ag accumulation ($p$<0.05) in mussel tissues (Fig. 3.2A–B) compared to control mussels, with higher concentrations in the digestive gland (Fig. 3.2B) than in gills (Fig. 3.2A). In the gills, the same pattern of accumulation was detected in Ag NPs and $Ag^{+}$ exposed mussels. However, in $Ag^{+}$ exposed mussels' gills accumulated higher levels than in those exposed to Ag NPs (1.6±0.4 μg.$g^{-1}$ dw and 2.5±0.4 μg.$g^{-1}$ dw, respectively) in the first 3 days, while in the remaining exposure period no significant differences exist ($p$>0.05). After the first week, Ag continued to accumulate in the gills with a 11–fold and 7–fold increase, followed by a 2 and 3–fold decrease by the end of the experiment for Ag NPs and $Ag^{+}$ exposed mussels, respectively.

As in gills, mussels exposed to $Ag^{+}$ accumulated higher Ag levels in the digestive gland (Fig. 3.2B) than in Ag NPs–exposed ones after 3 days of exposure (8.4±2.2 μg.$g^{-1}$ dw and 14.8±3.0 μg.$g^{-1}$ dw, respectively). After a week of exposure, Ag levels continued to increase 3–fold in Ag NPs and 2–fold in $Ag^{+}$–exposed mussels, reaching similar levels ($p$>0.05). By the end of the experiment, Ag concentrations reached a steady state in Ag NPs exposed mussels ($p$>0.05) while in those exposed to $Ag^{+}$ levels decreased 2–fold ($p$<0.05).

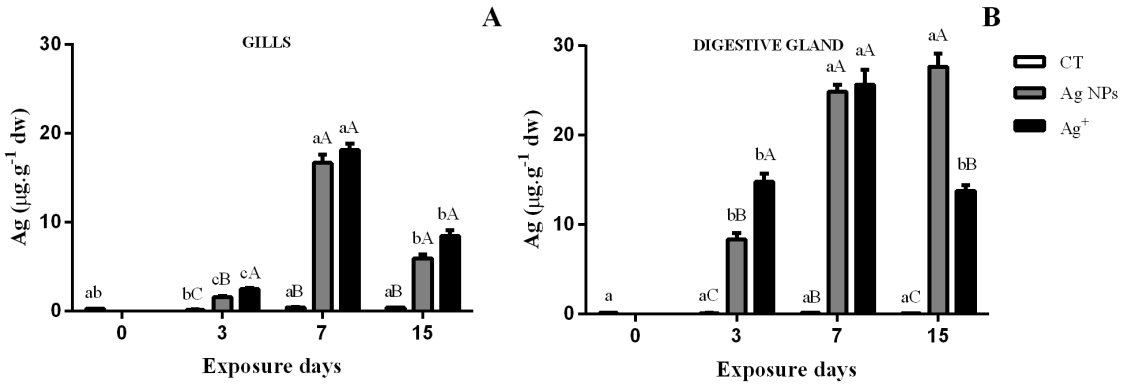


**Figure 3.2 –** Ag concentrations (µg.g$^{-1}$ dry weight) in gills (A) and digestive glands (B) of mussels *M. galloprovincialis* unexposed and exposed to Ag NPs and $Ag^+$ for 15 days (mean ± Std). Capital and lower letters represent statistical differences between treatments in each exposure day and for each treatment during the exposure duration, respectively ($p$<0.05).

### 3.3.4. Enzymatic activities

Mussels exposed to Ag NPs and $Ag^+$ presented different antioxidant responses in both gills and digestive gland with enzymatic activities that varied throughout the exposure period, generally higher in mussels exposed to Ag NPs than in those exposed to $Ag^+$ (Fig. 3.3). On the other hand, the enzymatic activities of unexposed mussels did not vary over time ($p$>0.05). In Ag NPs–exposed gills, SOD activity (Fig. 3.3A) increased significantly with time (1.2–fold increment in the first 3 days of exposure compared to control) reaching 2.8–fold by the end of exposure period. Contrarily, in $Ag^+$ exposure, SOD had a higher increase in the first 3 days (1.8–fold) but decreased afterwards (1.6 and 1.4–fold after 7 and 15 days of exposure, respectively). On the other hand, after one week of exposure to Ag NPs, CAT activity in the gills decreased 2.1–fold (Fig. 3.3C) following a 2.1–fold increase (compared to controls) by day 3 that increased again 1.6–fold by the end of the exposure. In $Ag^+$ exposed mussels, CAT activities (Fig. 3.3C) were similar during the first week of exposure (1.7–fold higher than controls), decreasing 1.4–fold afterwards to levels similar to unexposed mussels ($p$>0.05). As for GPX activity (Fig. 3.3E), a linear increase was detected with time after exposure to Ag NPs (induction rate of 7.0 nmol.min.mg$^{-1}$d$^{-1}$ prot, r=0.99, $p$<0.05), while in $Ag^+$ exposure GPX decreased with time, reaching a 2.5–fold decrease by the end of exposure period (compared to controls).

In the digestive gland of Ag NPs–exposed mussels, SOD activities (Fig. 3.3B) were similar between exposure times ($p$>0.05) after a 1.6–fold increase following 3 days (compared to control mussels, $p$<0.05). On the other hand, exposure to $Ag^+$ resulted in a linear decrease in

SOD activity (Fig. 3.3B) with time of exposure (decreasing rate of 3.0 $U.mg^{-1}d^{-1}$ prot, r=0.99, $p<0.05$), even after a higher increase (compared to NPs) following 3 days of exposure. As for CAT, a linear decrease was detected following exposure to Ag NPs with increasing time of exposure, with a decreasing rate of 10.3 $\mu mol.min.mg^{-1}d^{-1}$ prot (r=0.99, p<0.05), while in mussels exposed to $Ag^{+}$, CAT activities did not vary over time (from 48.6 ± 5.9 $\mu mol.min.mg^{-1}$ prot to 50.9 ± 10.3 $\mu mol.min.mg^{-1}$ prot, $p>0.05$). GPX activities (Fig. 3.3F) of Ag NPs–exposed mussels increased after 3 days of exposure and remained unchanged in the remaining period ($p>0.05$). As for mussels exposed to $Ag^{+}$, a 1.5–fold increase in GPX activity (Fig. 3.3F) was detected following 7 days of exposure (compared to controls) that decreased to levels similar to unexposed mussels by the end of exposure (5.2 ± 0.1 $nmol.min.mg^{-1}$ prot and 5.8 ± 1.1 $nmol.min.mg^{-1}$ prot, respectively, $p<0.05$).

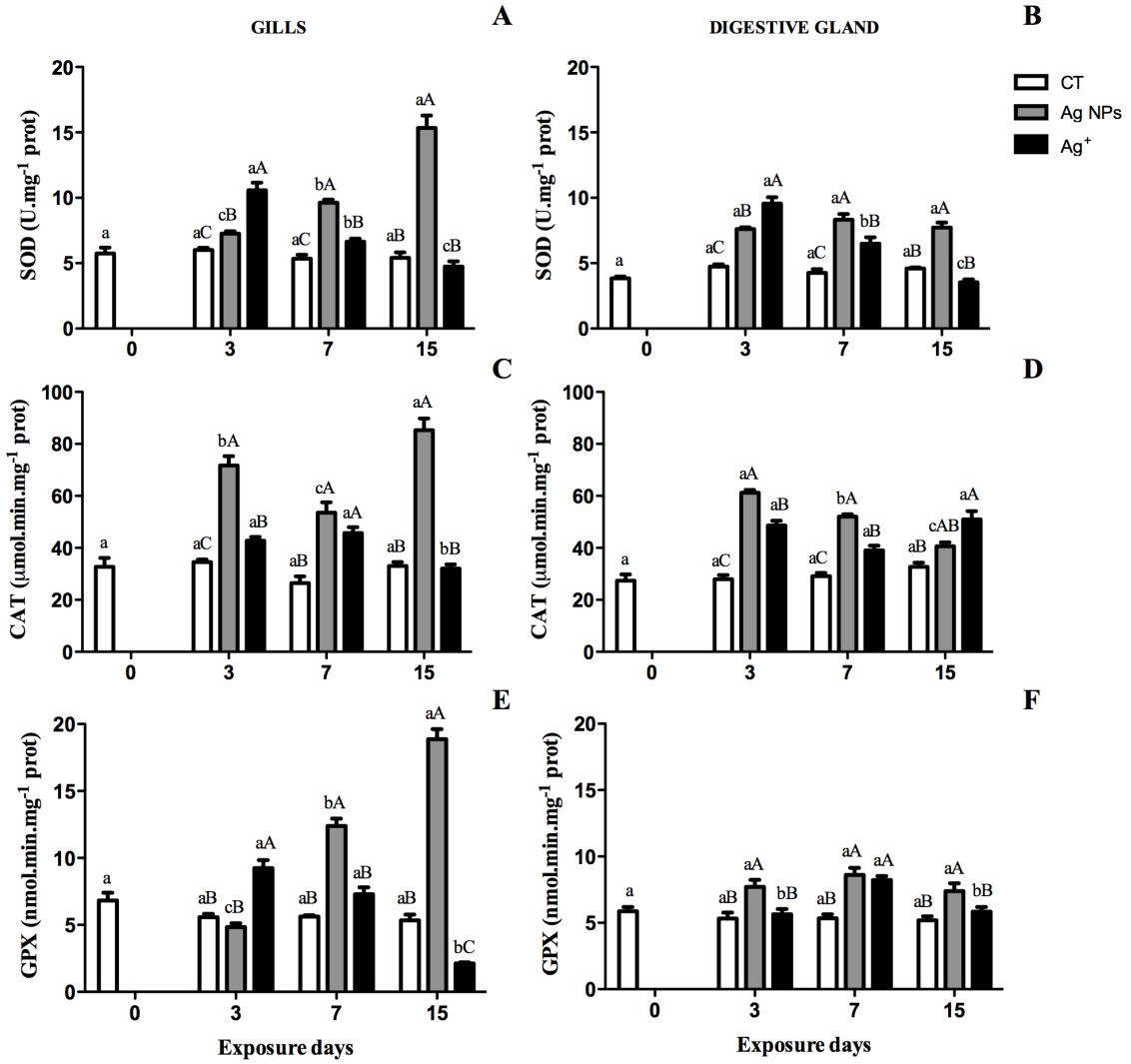


**Figure 3.3 –** SOD in the gills (A) and digestive glands (B), CAT in the gills (C) and digestive glands (D) and GPX activities in the gills (E) and digestive gland (F) of mussels *M.*

*galloprovincialis* from control and exposed to Ag NPs and $Ag^+$ for 15 days (average ± Std). Capital and lower letters represent statistical differences between treatments in each day of exposure and for each treatment during the exposure duration, respectively ($p$<0.05).

### 3.3.5. Metallothioneins

MTs in control and Ag exposed mussels are in Figure 3.4A–B for gills and digestive glands, respectively. MT concentrations were significantly lower in the digestive gland compared with the gills, but always higher in exposed mussels than in unexposed ones. In control mussels (Fig. 3.4B) MT concentrations only decreased slightly in the digestive gland after 3 days of exposure but remained unaltered in the rest of the exposure period ($p$>0.05).

Mussels exposed to both forms of Ag exhibited a similar pattern of MT induction. In the gills (Fig. 3.4A), MT was induced in the first 3 days of exposure (1.5–fold for Ag NPs and 1.6–fold for $Ag^+$) that remained unchanged following a week of exposure (no differences between Ag forms). By the end of the experiment, MT increase was significantly higher upon exposure to $Ag^+$ when compared to Ag NPs (3.6–fold and 2.5–fold, respectively) ($p$<0.05). As for the digestive gland (Fig. 3.4B), MT was induced at the beginning of the experiment (2.1–fold), to levels similar to Ag NP–exposed ones (6.3 ± 1.2 $mg.g^{-1}$ prot; p>0.05), remaining unchanged over time, where in $Ag^+$ exposed mussels MT levels were only higher at day 7 (5.4 ± 0.5 $mg.g^{-1}$ prot compared to 9.2 ± 1.8 $mg.g^{-1}$; prot $p$<0.05).

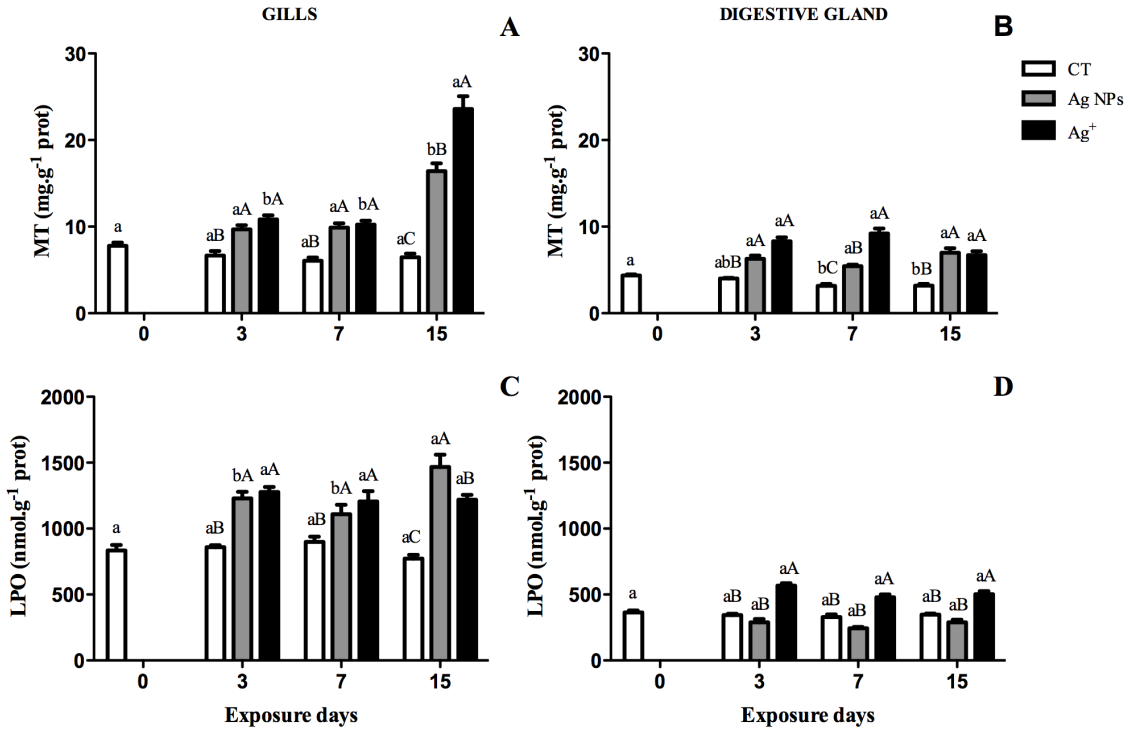


**Figure 3.4 –** MTs in the gills (A) and digestive glands (B) and LPO in the gills (C) and digestive gland (D) of mussels *M. galloprovincialis* unexposed and exposed to Ag NPs and $Ag^{+}$ for 15 days (average ± Std). Capital and lower letters represent statistical differences between treatments in each exposure day and for each treatment during the exposure duration, respectively ($p$<0.05). Asterisks represent statistical differences between unexposed and exposed mussels ($p$<0.05).

### 3.3.6. Lipid peroxidation

As for MTs, LPO levels (Fig. 3.4C–D) where significantly higher in gills than in digestive gland for all exposure groups ($p$<0.05). In unexposed mussels LPO levels did not vary over time in both gills and digestive gland ($p$>0.05).

In Ag NPs–exposed gills LPO levels were about 1.4–fold higher than controls and similar to $Ag^{+}$ on the 3$^{rd}$ and 7$^{th}$ days, increasing afterwards 1.9–fold to levels higher than in mussels exposed to $Ag^{+}$ ($p$<0.05). In mussels exposed to $Ag^{+}$, LPO increased 1.5–fold over the first 3 days, remaining unchanged until the end of the exposure period ($p$>0.05).

In the digestive gland, no LPO was detected upon exposure to Ag NPs ($p$>0.05), whereas in $Ag^{+}$ a 1.6–fold increase was detected at the beginning of the experiment that remained unchanged with time (higher than controls; $p$>0.05).

### 3.3.7. Principal component analysis (PCA)

Principal component analyses were applied to all the data obtained for the gills (Fig. 3.5A) and digestive gland (Fig. 3.5B) to help to explain the effects of both forms of Ag (NPs and ionic) on biomarkers response. The overall PCA indicates a clear separation between controls and Ag–exposed gills (Fig. 3.5A), where PC1 represents 52.6% and PC2 19.4% (72% of total variance). Unexposed mussels are closely associated in PC1 showing homogenous biomarker variance with time. As for Ag–exposed mussels (Ag NPs and $Ag^{+}$), a clear separation of the sampling periods occurred, suggesting a specific response of mussel gills due to the type and time of exposure. Ag concentrations in the gills are clearly associated with LPO levels and enzymatic activities in mussels exposed to Ag NPs and after 7 and 15 days and in $Ag^{+}$–exposed mussels after 3 and 7 days of exposure, reflecting a significant relationship between mussels antioxidant efficiency to counteract Ag exposure. On the other hand, MT levels in PC2 were more affected by Ag NPs after 3 days of exposure, as well as $Ag^{+}$ for 15 days. Mussels exposed to both Ag NPs and $Ag^{+}$ after 15 days are the more separated groups, suggesting a marked difference between mussel gills response to both forms of Ag probably related to different modes of action. As for the digestive gland (Fig. 3.5B), the principal components represent 70.4% of total variance, where PC1 represents 50.2% and PC2 20.2%. Similarly to the gills, the overall PCA indicates a clear separation between unexposed and Ag–exposed mussels, showing dissimilar biomarker tendency. PC1 clearly divides mussels exposed to Ag NPs and $Ag^{+}$, showing a dissimilarity of biomarkers response during the course of the experiment, dependent on the Ag form used. The group formed by mussels exposed to Ag NPs is closely related (namely 3 and 15 days of exposure) showing a similarity of biomarkers response during the course of the experiment. On the other hand, those exposed to $Ag^{+}$ are further apart, suggesting distinct differences between digestive glands responses with time of exposure. In PC1, CAT and SOD and GPX activities are closely associated to Ag concentrations in mussels' digestive glands, showing a significant correlation between their antioxidant efficiency to counteract Ag NPs exposure. On the other hand, mussels exposed to $Ag^{+}$ for 15 days are directly related to LPO levels, as is clearly evident in PC2, with MT also showing a relative proximity to the $Ag^{+}$ exposure group.

Another PCA was obtained incorporating all the data for the gills and digestive gland of mussels to help differentiate responses and modes of action of both forms of Ag (Fig. 3.5C). The two principal components represent 65.7% of total variance, where PC1 represents 46.2% and PC2 19.5%. The overall PCA shows distinct responses of mussel tissues and

forms of Ag, namely after 15 days of exposure. Similar responses were obtained between control groups, for gills (PC2) and digestive gland (PC1). The antioxidant defence system (7 days of exposure) combined with LPO and MT induction (3 days of exposure) seem to be more important in the gills, while in the digestive gland Ag accumulation is the more pronounced response.

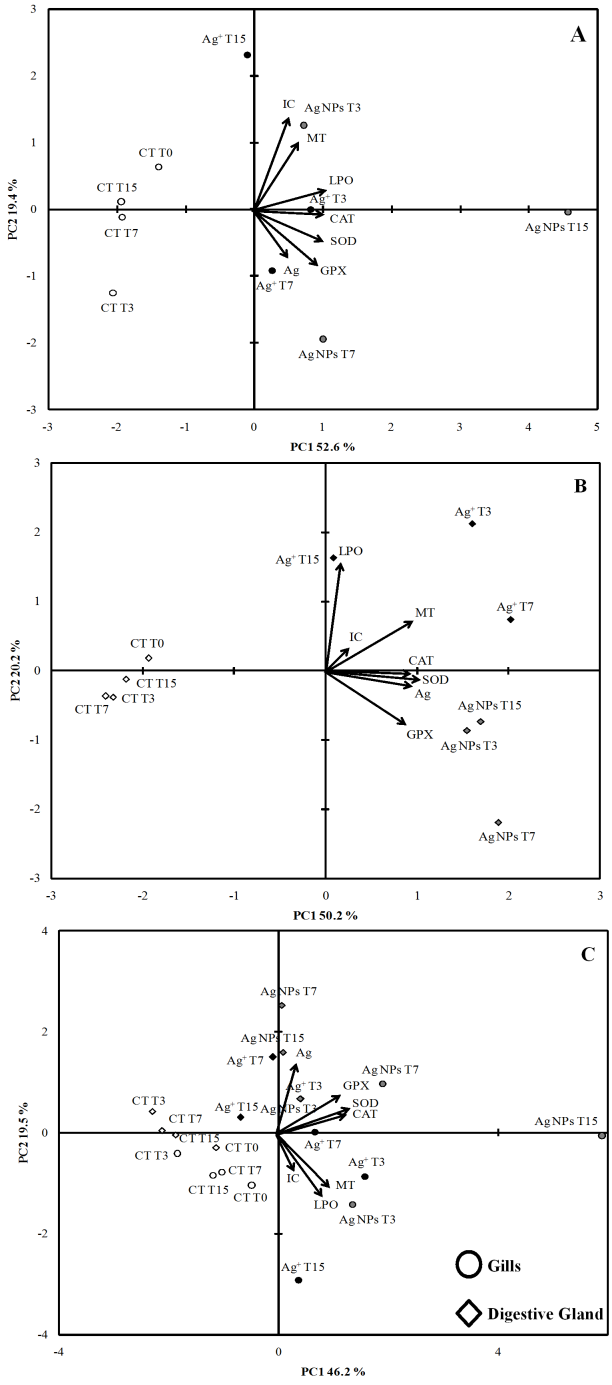


**Figure 3.5 –** PCA of Ag accumulation and battery of biomarkers in mussels *M. galloprovincialis* unexposed and exposed to Ag NPs and $Ag^{+}$ for 15 days. (A) Gills; (A) Digestive gland; (C) Both tissues combined.

## 3.4. Discussion

Several factors influence the behaviour of NPs in dispersion media, being their physico–chemical properties the most important ones (e.g. size, agglomeration, solubility). Preparation, dosing and maintenance of NPs within a test medium are important factors when investigating the potential toxic effects of NPs exposure. Furthermore, an accurate characterization of nanoparticles is essential to ensure a better understanding and interpretation of the toxic effects of NPs in relation to their properties (Bhatt and Tripathi, 2011; Scown *et al*., 2010a).

In this study, size distribution and zeta potential of Ag NPs was determined in the different exposure media (ultrapure water and seawater) using TEM and DLS. The TEM image (Fig. 3.1A) demonstrates that Ag NPs are spherical and polydisperse with sizes within and higher than the defined size range by the manufacturer (< 100nm). The results obtained (Table 3.1) on hydrodynamic diameter (895.5 ± 83.9 nm) and zeta potential (–10.2 ± 1.2 mV) by DLS show that Ag NPs tends to aggregate while suspended in seawater (Fig. 3.1C), with sizes increasing with time of exposure (12 hours cycle) and the presence of both small and large aggregates (144.2 ± 39.2 nm). The zeta potential on the surface of NPs has been shown to influence agglomeration behaviour, with values closer to zero point charge (0 mV) leading to increased aggregation (Fang *et al*., 2009). The tendency of these particles to aggregate while in suspension have been previously established by other authors using these particles, some of which from the same manufacturer (e.g. Choi *et al*., 2010; Farkas *et al*., 2010; Park and Choi, 2010; Scown *et al*., 2010b). The capacity of NPs for aggregation, sedimentation and solubility in water can limit the transport within the water column and reduce bioavailability of most nanoparticles to organisms (Baalousha *et al*., 2008). The silver concentrations in water samples collected from the tanks immediately after Ag NPs and $Ag^{+}$ dosing gradually decreased over the 12–hour period between water change and Ag redosing. In fact, 84.2 % of the initial mass of Ag NPs was removed from the water column after the 12 hours exposure. The lost of this amount of silver suggest aggregation, sedimentation and dissolution of the particles in the exposure media that resulted in a lower Ag NPs concentration in the water column (reduce bioavailability to mussels) compared with the nominal Ag concentration (Griffitt *et al*., 2009; Scown *et al*., 2010b) The results obtained by DLS on Ag NPs intensity (Fig. 3.1D) showed a decreased during a 12–hour period, indicative of particles dissolution or settlement with time. Of the total Ag NPs added to the exposure medium, 24.5% of the initial dose is present in the dissolved form, indicating that most of Ag NPs added to the exposure

tanks are in the nanoparticulate form, which dissolves with time of exposure (44.2% after 12 hour period). A few studies hypothesized that NPs solubility can increase in the presence of organisms and their contact with the NPs, thus affecting the percentage of solubilized Ag NPs when compared to the percentage quantified at the beginning of the experiment (Fabrega *et al*., 2009; Navarro *et al*., 2008). The inherent instability of Ag NPs by release of free $Ag^+$ ions and agglomeration in aqueous environments may contribute to its toxicity and be a major concern in toxicity studies (Choi *et al*., 2010).

Mussels accumulated Ag in both gills and digestive gland, regardless of the Ag form used (Fig. 3.2). $Ag^+$–exposed mussels accumulated more Ag (1.6–fold) in the first 3 days of exposure in the gills than those exposed to Ag NPs, whereas after one week both Ag forms accumulated similarly in the gills, followed by a decrease by the end of the experiment (Fig. 3.2A). This decrease detected in mussels' gills after 15 days of exposure may be indicative of an elimination of $Ag^+$ and Ag NPs through detoxification processes. A higher Ag bioavailability from $Ag^+$ from the surrounding water seems to exist in the beginning of the experience while the bioavailability of Ag NPs seems to increase with time of exposure. This strongly suggests that an important incorporation of $Ag^+$ occurred through the dissolved pathway. In fact, in marine filter–feeder bivalves, gills are well known to play a key role in dissolved metal accumulation (Rainbow, 1990). Knowing that only 24.5 to 44.2 % of Ag NPs are in the soluble form in the exposure media (along 12 hour period), accumulation of Ag cannot be solely explained by $Ag^+$ dissolution and uptake of dissolved Ag, indicating that some uptake of Ag NPs may have occurred. Contrasting to what was found in the gills, in the digestive gland of Ag NPs exposed mussels Ag was accumulated with increasing time of exposure (Fig. 3.2B). As for $Ag^+$ exposed mussels, the same pattern was found where Ag was accumulated significantly in the first week of exposure, decreasing afterwards at the end of the experiment. This difference in Ag accumulation in the digestive gland suggests that the nanoparticles themselves are contributing to the Ag concentrations whereas on the $Ag^+$ exposure $Ag^+$ ions are easily eliminated. In fact, it is well known that the translocation of the $Ag^+$ can occur from the tissues in direct contact with seawater (gills) towards the digestive gland, where the $Ag^+$ ions can be detoxified and/or stored (Rainbow, 1990). Furthermore, the level of Ag in the digestive gland was two to five–fold higher than that of the gills for exposed mussels, reflecting the key role of this tissue in the Ag bioaccumulation and detoxification, as well as different uptake routes and subsequent transport for Ag NPs (Langston *et al*., 1998, Scown *et al*., 2010b; Viarengo *et al*., 1990). The high retention time of Ag NPs in the digestive gland cells when compared to the gills and $Ag^+$ exposure is

probably related to the presence of Ag NPs aggregates. It has been described that mussels can incorporate nanoparticles presented either in the form of agglomerates in suspension or dissolved particles through direct ingestion or across the gills. In fact, a selective handling of NPs seems to occur in the gills, where NPs aggregates are broken down into smaller particles that are transported to the digestive system to be accumulated or transferred to other tissues (Canesi *et al*., 2012; Moore *et al*., 2009; Ward and Kach, 2009). Ward and Kach (2009) demonstrated that in mussels exposed to polystyrene nanoparticles, the presence of aggregates promotes the transport of NPs to the digestive gland where they are taken up by digestive cells possibly via endocytosis with longer gut retention times. Differences in uptake rates have been previously reported in several organisms (including mussels) with maximum concentrations in the digestive gland not only for Ag NPs (Scown *et al*., 2010b; Zuykov *et al*., 2011) but also for other NPs (Chapter 2.1) associated with the presence of aggregates. Nevertheless, it is still unclear how agglomeration can affect the cytotoxicity of Ag NPs.

Mussels antioxidant system is based on the cascade action of SOD, CAT and GPX to counteract the overproduction of reactive oxygen species (ROS) by metals (or other oxidizing agents) and minimize oxidative damage to cellular components (Halliwell and Gutteridge, 1984; Matés, 2000; Valavanidis *et al*., 2006). Ag NPs induced an overall increase in the antioxidant enzymes in the gills, whereas in $Ag^{+}$ exposed mussels enzymatic activities tended to decrease with time of exposure (Fig. 3.3). SOD is the first enzyme to be induced, being responsible for catalysing superoxide anions into hydrogen peroxide. Exposure to Ag NPs resulted in an induction of SOD activities in the gills with increasing time of exposure, suggesting the production of superoxide anions by these NPs (Fig. 3.3A). On the other hand, SOD decreased with time (to levels similar to control) as a result to exposure to $Ag^{+}$ even after a higher induction of SOD in the first 3 days of exposure. The increase of CAT and GPX activities upon exposure to Ag NPs suggests a further detoxification of hydrogen peroxide (or other hydroperoxides) originated as a by–product of SOD (Fig. 3.3C–E). Contrarily, a higher availability of free ROS levels (superoxide anions and hydroxyl radicals) originated by $Ag^{+}$ and the reduction of SOD may have lead to the catalytic impairment (decrease in enzymatic activities) of CAT and GPX (Fig. 3.3A–C–E). $Ag^{+}$ is known to interact with thiol–groups that are found in many antioxidants that when disrupted can result in the inhibition/inactivation of enzymes (SOD, CAT and peroxidases) and lead to significant oxidant stress (Bar–Ilan *et al*., 2009; Lapresta–Fernández *et al*., 2012). The effects of Ag NPs and $Ag^{+}$ in mussels' digestive gland are slightly different from those observed in the gills (Fig 3.3B–D–F). In the first 3 days of exposure to Ag NPs all enzymatic activities were

enhanced as a result of ROS formation. However, SOD and GPX activities remain unchanged in the remaining exposure period, while CAT was inhibited suggesting a minimal increase of $H_2O_2$. As for $Ag^+$, a reduction on SOD activity was also observed with time of exposure (as in gills), nevertheless, CAT and GPX activities (in general) remained unchanged with time and where lower than Ag NPs. The observed results suggest differential and less pronounced responses by these cellular defence mechanisms in the digestive glands compared to the gills, especially for Ag NPs exposed mussels, suggesting a lower effect of ROS in this tissue. The combined action of antioxidant enzymes to neutralize ROS formation originated either by Ag NPs and $Ag^+$ was supported by the PCA (Fig. 3.5) that shows significant correlations between their activities and Ag accumulation in both tissues that was time and Ag form dependent. Oxidative stress seems to mediate the mode of action of Ag NPs and $Ag^+$–induced toxicity where ROS seem to be mostly generated by free $Ag^+$. However, $Ag^+$ dissolution from Ag NPs may not account for the different antioxidant defence responses and effects related to the inherent particle properties cannot be discarded. There are no studies concerning either the effect of $Ag^+$ or Ag NPs in mussels antioxidant system, however different and transitory responses of antioxidant activities and consequent oxidative stress were already reported in other species. Exposure to Ag NPs reduced levels of CAT and GPX in zebrafish liver tissues (5–20 nm; 30–120 $mg.L^{-1}$) (Choi *et al*., 2010), increased hydrogen peroxide and superoxide production (6–20 nm, 2, 5 and 50 $\mu g.mL^{-1}$) (Asharani *et al*., 2009) and decreased SOD (7–20 nm, 0.76–50 $\mu g.mL^{-1}$) in human cells (Arora *et al*., 2008) and increased SOD and CAT activities in *Drosophila melanogaster* (10 nm, 50 and 100 $\mu g.mL^{-1}$) (Ahamed *et al*., 2010), all contributing to oxidative stress. Other enzymes besides those measured in this study (e.g. GST, GSH) have shown to alter their expression after exposure to Ag NPs thus playing an important role in the defence against or detoxification of these NPs (Chae *et al*., 2009; Choi *et al*., 2010; Arora *et al*., 2008). Overall, Ag NPs seem to modulate antioxidant enzymes at transcription and translation levels, resulting in the accumulation of oxyradicals, which cause oxidative damage.

Detoxification mechanisms of metals in marine invertebrates mainly involve the precipitation or co–precipitation of metals on insoluble granules, the compartmentalization within membrane–limited vesicles (lysosomes) and the binding to specific soluble proteins (e.g. MTs) (Langston *et al*., 1998; Viarengo and Nott 1993; Viarengo *et al*., 1990). MTs are low molecular weight proteins (6–7kDa) with high cysteine content (30%), which may regulate the cellular metal homeostasis by binding and detoxifying metals such as Zn, Cu, Cd, Hg and

Ag (Amiard *et al*., 2006; Lansgton *et al*., 1998; Viarengo and Nott, 1993). MTs are also efficient scavengers of hydroxyl radicals, contributing to protect tissues against oxidative injuries (Amiard *et al*., 2006; Langston *et al*., 1998). A similar patter of MT induction was detected in mussels' gills upon exposure to Ag NPs and $Ag^+$ (Fig. 3.4A), with a significant increase along the exposure period (especially by $Ag^+$ at day 15), supporting the hypothesis of the role of this protein in Ag homeostasis and detoxification (Amiard *et al*., 2006; Lansgton *et al*., 1998; Viarengo and Nott, 1993), which is corroborated by Ag accumulation patterns and the close association between Ag concentrations and MT levels in the PCA (Fig. 3.5A). It is well documented in bivalves that $Ag^+$ display high affinity to –SH groups, which are abundant in the cysteine residues of MTs that contributes significantly to its detoxification (Geffard *et al*., 2004; Langston *et al*., 1998; Ng and Wang, 2004). So, it is plausible to assume that Ag NPs and $Ag^+$ released from the NPs are able to bind specifically to MTs to regulate silver metabolism, detoxify Ag ions or scavenge ROS generated by these particles (Chae *et al*., 2009; Choi *et al*., 2010; Ringwood *et al*., 2010). Only Ringwood *et al*. (2010) addressed the role of MT in *C. virginica* exposed to Ag NPs (16 $\mu g.L^{-1}$–1.6 $ng.L^{-1}$, 15±6 nm) where an increase in MT expression was associated with Ag metabolism or to the increase of oxyradicals. Additionally, in zebrafish and medaka liver tissues exposed to 30–120 $mg.L^{-1}$ Ag NPs (5–20 nm) and 1.25 $\mu g.L^{-1}$ Ag NPs (49.6 nm), respectively, MT was induced suggesting either release of $Ag^+$ from Ag NPs or Ag NPs–generated free radicals (Chae *et al*., 2009; Choi *et al*., 2010). As for the digestive glands, MT levels remained unchanged after a significant induction in the first 3 days of exposure for both Ag forms (NPs and $Ag^+$), with concentrations significantly lower than in the gills (Fig. 3.4B). The decrease in $Ag^+$ concentrations in digestive glands after the 15 days of exposure suggests that mussel' detoxification mechanisms were triggered, probably by the induction of MT. As for Ag NPs, no clear signs of detoxification were detected in exposed digestive glands even after MT induction, suggesting that the accumulation of these nanoparticles in this tissue is time dependent and higher that its elimination, in contrast to $Ag^+$, as already seen with CuO NPs in mussels tissues (Chapter 2). Given the high Ag accumulation in mussels' digestive glands (2 to 5–fold higher than that of the gills) it would be expected that the concentrations of MT concentrations should be higher in this tissue. Accordingly, other mechanisms of detoxification may be responsible for Ag detoxification (Ag NPs and $Ag^+$) with MTs only slightly contributing to Ag sequestration and detoxification (small fraction of Ag associated with MT). This is in agreement with previously observations indicating that, in the digestive gland of bivalves, no clear relationships exist between Ag concentrations and MT where $Ag^+$

is mainly associated with insoluble forms mainly of Ag–sulphide in lysosomes, which is are very stable, thus able to detoxify Ag in tissues (Berthet *et al*., 1992; Geffard *et al*., 2004; Shi *et al*., 2003). In polychaetes *Nereis diversicolor*, subcellular fractionation showed that Ag NPs accumulate in inorganic granules, organelles and heat–denatured proteins while $Ag^{+}$ is mainly located in the MT fraction (García–Alonso *et al*., 2011). Since Ag may be strongly bound with sulphides; this complex may not be easily depurated by mussels, especially in the presence of Ag NPs aggregates, being responsible to the higher retention rate seen in mussels' digestive glands exposed to these particles. The central importance of the gills and digestive gland in metal bioaccumulation has been highlighted many times, particularly for toxic metals such as Ag (e.g. Langston *et al*., 1998; Rainbow, 1990), nevertheless, the detoxification processes occurring after exposure to NPs remains poorly understood. No fate, storage or excretion of NPs has yet been identified in mussels, but the induction of MT has been suggested as the main detoxification mechanism of NPs (CuO NPs, Au NPs and Ag NPs) in bivalve species (Chapter 2; Renault *et al*., 2008; Ringwood *et al*., 2010). More research is required to determine the main detoxification mechanisms of Ag NPs exposed mussels and the involvement of MTs, whether they differ between Ag forms and tissues and in what form Ag will be eliminated from tissues.

The strong affinity of silver ions with sulfhydryl, amino and phosphate groups and the capacity to induce ROS production can lead to damage of essential components of the cell, such as membranes (Bar–Ilan *et al*., 2009; Lapresta–Fernández *et al*., 2012). A possible mechanism for membrane–related toxicity is by peroxidation of lipid components of membranes as a result of oxyradicals, that can change the fluidity and permeability of the membrane or attacking directly DNA and other intracellular molecules (Halliwell and Gutteridge, 1984; Matés, 2000; Valavanidis *et al*., 2006). The results obtained in this study showed that Ag NPs and $Ag^{+}$ caused lipid peroxidation in the gills of exposed mussels as a result of ROS formation (Fig. 3.4C). In the first 3 days of exposure both Ag NPs and $Ag^{+}$ increased LPO (no differences between Ag forms) despite the efforts of the antioxidant defence system to counteract ROS production. In the remaining period, $Ag^{+}$ continuously increased ROS production to a point where gills antioxidant capacity was overwhelmed; nevertheless, LPO levels were similar throughout the exposure period. On the other hand, mussels exposed to Ag NPs showed an increase in LPO levels by the end of the experiment (higher than $Ag^{+}$) even though a decrease in Ag levels was detected in addition to the induction of MT and activation of antioxidant enzymes (also reflected in the PCA). This strongly suggests a higher ROS formation by Ag NPs exposure than $Ag^{+}$, probably related to

a higher availability of free silver ions released from the particles combined with the intrinsic effect of Ag NPs that were not efficiently removed by the combined action of antioxidant defences. It has been suggested that NPs act as Trojan horse–type carriers that enable the transport of metal ions into cells (Limbach *et al*., 2007). In fact, surface oxidation of Ag NPs after contact with proteins in the cytoplasm liberates $Ag^+$ ions that could amplify their toxicity (Asharani *et al*., 2009). In addition to the release of $Ag^+$ ions from NPs, it seems that there are other mechanisms by which these NPs can originate toxicity on a cellular level. If not taken up by cells Ag NPs could mediate toxicity by attaching to the cellular membrane surface and release $Ag^+$ compromising cell integrity and permeability or originate extracellular ROS and oxidative stress by surface processes due to the nanoparticle effect (Farkas *et al*., 2010; Morones *et al.*, 2005; Navarro *et al*., 2008). In the digestive gland $Ag^+$ presented a similar trend to the gills, whereas for Ag NPs no LPO was detected (Fig. 3.4D). The lack of LPO in the digestive gland of mussels exposed to Ag NPs, despite a large accumulation of Ag, is an unexpected finding and diverge with the assumption of the ROS–generating potential of these NPs and subsequent oxidative stress. This could result from an intensification of the antioxidant system of mussels, including MT induction, or to the induction of other components of the antioxidant defence system (e.g. GR, GST) that was sufficient to counteract ROS production in this tissue. The PCA also shows a relationship between mussels' antioxidant efficiency (SOD, CAT, GPX and MT) to counteract Ag exposure (Fig. 3.5B). Additionally, the mechanism of storage/detoxification of Ag NPs as non–toxic, insoluble silver–sulphide precipitates (e.g. Berthet *et al*., 1992; Geffard *et al*., 2004; Shi *et al*., 2003) could inhibit the potentially deleterious effects of these NPs, which are mainly accumulated in this tissue in the form of aggregates. Thus, the different capacity of the two forms of Ag to originate ROS and consequently lipid peroxidation can be related to the presence of Ag NPs mainly in the form of aggregates, whereas $Ag^+$ has the capacity to produce more ROS in this tissue. It was demonstrated in several cell types that Ag NPs have the capacity to generate ROS (Hussain *et al*., 2005; Park *et al*., 2010) and cause membrane damage by increased lipid peroxidation in zebrafish (30–120 $mg.L^{-1}$; 5–20 nm) (Choi *et al*., 2010), *D. melanogaster* (10 nm, 50 and 100 $\mu g.mL^{-1}$) (Ahamed *et al*., 2010) and human cellular lines (7–20 nm, 0.76–50 $\mu g.mL^{-1}$ (Arora *et al*., 2008), as well as oxidative stress through DNA damage in hemocytes of mussels (Chapter 4). The dissimilar antioxidant capacity, MT induction and LPO obtained for exposed mussels confirm the hypothesis that one of Ag NPs main toxic mechanism is mediated by oxidative stress leading to significant

damage in cells, especially in the gills of exposed mussels, that differs from that of $Ag^+$, as referred by other authors (Asharani *et al*. 2008; Chae et a., 2009; Griffitt *et al*., 2009) and highlighted in the PCA (Fig. 3.5C). Nevertheless, an issue of uncertainty regarding the toxicity of Ag NPs is whether it is a function of the release of dissolved Ag from the particles or a combined effect with the toxicity of the particles themselves.

In summary, Ag NPs exhibited toxic effects in mussels with a potency comparable to that of $Ag^+$ ions primarily attributed to oxidative stress. The distinct antioxidant efficiency, MT induction and lipid peroxidation in the gills and digestive gland of exposed mussels are dependent on the Ag form used, reflecting the dissimilar physiological and metabolic function of the two tissues. Gills seem to be more susceptible to oxidative stress (from $Ag^+$ ions or $Ag^+$ dissolved from the NPs) than the digestive gland, as alterations of enzymatic activities were more pronounced while the digestive gland is the main tissue for Ag accumulation especially in the case of Ag NPs (presence of aggregates). MTs seem to be the main detoxification mechanism of both Ag NPs and $Ag^+$ in the gills, while in the digestive gland Ag may be predominantly in insoluble detoxified forms, with little role for MT. Despite the significant accumulation of Ag in digestive glands, there was no obvious lipid peroxidation in this tissue as a result of Ag NPs exposure, although some low damage level was noted in the mussels exposed to $Ag^+$. Overall, these results suggest that Ag NPs–induced toxicity need to more thoroughly addressed to fully understand if the observed oxidative stress is solely attributed to the free $Ag^+$ ions dissolved from the NPs or to a combination with the intrinsic effects of NPs. Additionally, further research is also required to unravel Ag NPs uptake pathways, interactions with subcellular components and detoxification mechanisms.

## 3.5. References

Ahamed, M.; Siddiqui, M.; Akhtar, M.J.; Ahmad, I.; Pant, A.B.; Alhadlaq, H.A. (2010). Genotoxic potential of copper oxide nanoparticles in human lung epithelial cells. *Biochemical and Biophysical Research Communications*. **396:** 578–583.

Amiard, J.–C.; Amiard–Triquet, C.; Barka, S.; Pellerin, J.; Rainbow, P.S. (2006). Metallothioneins in aquatic invertebrates: Their role in metal detoxification and their use as biomarkers. *Aquatic Toxicology*. **76:** 160–202.

Arora, S.; Jain, J.; Rajwade, J.M.; Paknikar, K.M. (2008). Cellular responses induced by silver nanoparticles: In vitro studies. *Toxicology Letters*. **179:** 93–100.

Asharani, P.V.; Wu, Y.L.; Gong, Z.; Valiyaveettil, S. (2008). Toxicity of silver nanoparticles in zebrafish models. *Nanotechonoly*. **19:** 255102.

Asharani, P.V.; Mun, G.L.K.; Hande, M.P.; Valiyaveettil, S. (2009). Cytotoxicity and genotoxicity of silver nanoparticles in human cells. *ACS Nano*. **3(2):** 279–290.

Baalousha, M.; Manciulea, A.; Cumberland, S.; Kendall, K.; Lead, J.R. (2008). Aggregation and surface properties of iron oxide nanoparticles: Influence of pH and natural organic matter. *Environmental Toxicology and Chemistry*. **27:** 1875–1882.

Bar–Ilan, O.; Albrecht, R.M.; Fako, V.E.; Furgeson, D.Y. (2009). Toxicity assessments of multisized gold and silver nanoparticles in zebrafish embryos. *Small*. **5(16):** 1897–1910.

Baun, A.; Hartmann, N.B.; Grieger, K.; Kusk, K.O. (2008). Ecotoxicity of engineered nanoparticles to aquatic invertebrates: a brief review and recommendations for future toxicity testing. *Ecotoxicology*. **17:** 387–395.

Bebianno, M.J.; Langston, W.J. (1989). Quantification of metallothioneins in marine invertebrates using differential pulse polarography. *Portugaliae Electrochimica Acta*. **7:** 59–64.

Benn, T.M.; Weterhoff, P. (2008). Nanoparticle silver release into water from commercially available sock fabrics. *Environmental Science and Technology*. **42:** 4133– 4139.

Berthet, B.; Amiard, J.C.; Amiard–Triquet, C.; Martoja, M.; Jeantet, A.Y. (1992) Bioaccumulation, toxicity and physico–chemical speciation of silver in bivalve molluscs: ecotoxicological and health consequences. *Science of the Total Environment*. **125:** 97–122.

Bhatt, I.; Tripathi, B.N. (2011). Interaction of engineered nanoparticles with various components of the environment and possible strategies for their risk assessment. *Chemosphere*. **82(3):** 308–317.

Blaser, S.A.; Scheringer, M.; MacLeod, M.; Hungerbühler, K. (2008). Estimation of cumulative aquatic exposure and risk due to silver: Contribution of nano–functionalized plastics and textiles. *Science of the Total Environment*. **390:** 396–409.

Boxall, A.B.A.; Chaudhry, Q.; Sinclair, C.; Jones, A.; Aitken, R.; Jefferson, B.; Watts, C. (2008). Current and future predicted environmental exposure to engineered nanoparticles. Report by Central Science Laboratory for Department for Environment, Food and Rural Affairs, Her Majesty's Government, UK.

Bradford, M. (1976). A rapid and sensitive method for the quantitation of microgram quantities of protein utilizing the principle of protein–dye binding. *Analytical Biochemistry*. **72:** 248–254.

Canesi, L.; Ciacci, C.; Fabbri, R.; Marcomini, A.; Pojana, G.; Gallo, G. (2012). Bivalve molluscs as an unique target group for nanoparticle toxicity. *Marine Environmental Research*. **76:** 16–21.

Chae, Y.J.; Pham, C.H.; Lee, J.; Bae, E.; Yi, J.; Gu, M.B. (2009). Evaluation of the toxic impact of silver nanoparticles on Japanese medaka (*Oryzias latipes*). *Aquatic toxicology*. **94(4):** 320–327.

Choi, J.E.; Kim, S.; Ahn, J.H.; Youn, P.; Kang, J.S.; Park, K.; Yi, J.; Ryu, D.–Y. (2010). Induction of oxidative stress and apoptosis by silver nanoparticles in the liver of adult zebrafish. *Aquatic Toxicology*. **100:** 151–159.

Erdelmeier, I.; Gerard–Monnier, D.; Yadan, J.C; Acudiere, J. (1998). Reactions of N–methyl–2–phenylindole with malondialdehyde and 4–hydroxyalkenals. Mechanistic aspects of the colorimetric assay of lipid peroxidation. *Chemical Research in Toxicology*. **11:** 1184–1194.

Fabrega, J.; Fawcett, S.R.; Renshaw, J.C.; Lead, R.L. (2009). Silver nanoparticles: Impact on bacterial growth: Effect of pH, concentration, and organic matter. *Environmental Science and Technology*. **43:** 7285–7290.

Fabrega, J.; Luoma, S.N.; Tyler, C.R.; Galloway, T.M.; Lead, J.R. (2011). Silver nanoparticles: Behaviour and effects in the aquatic environment. *Environmental International*. **37(2):** 517–531.

Fang, J.; Shan, X.Q.; Wen, B.; Lin, J.M.; Owens, G. (2009). Stability of titania nanoparticles in soil suspensions and transport in saturated homogeneous soil columns. *Environmental Pollution*. **157:** 1101–1109.

Farkas, J.; Christian, P.; Urrea, J.A.G.; Roos, N.; Hassellöv, M.; Tollefsen, K.E.; Thomas, K.V. (2010). Effects of silver and gold nanoparticles on rainbow trout (*Oncorhynchus mykiss*) hepatocytes. *Aquatic toxicology*. **96(1):** 44–52.

Farkas, J.; Christian, P.; Gallego–Urrea, J.A.G.; Roos, N.; Hassellöv, M.; Tollefsen, K.E.; Thomas, K.V. (2011). Uptake and effects of manufactured silver nanoparticles in rainbow trout (*Oncorhynchus mykiss*) gill cells. *Aquatic toxicology*. **101:** 117–125.

García–Alonso, J.; Khan, F.R.; Misra, S.K.; Turmaine, M.; Smith, B.D.; Rainbow, P.S.; Luoma, S.N.; Valsami–Jones, E. (2011). Cellular internalization of silver nanoparticles in gut epithelia of the estuarine polychaete *Nereis diversicolor*. *Environmental Science and Technology*. **45:** 4630–4636.

Geffard, A.; Jeantet, A.Y.; Amiard, J.C.; Pennec, M.L.; Ballan–Dufrançais, C.; Amiard–Triquet, C. (2004). Comparative study of metal handling strategies in bivalves *Mytilus edulis* and *Crassostrea gigas*: a multidisciplinary approach. *Journal of Marine Biological Association of the United Kingdom*. **84:** 641–650.

Geranio, L.; Heuberger, M.; Nowack, B. (2009). The behavior of silver nanotextiles during waching. *Environmental Science and Technology*. **43:** 8113–8118.

Greenwald, R.A. (1985). Handbook of methods for oxygen radical research. CRC Press: Boca Raton, Florida, United States of America.

Griffitt, R.J.; Hyndman, K.; Denslow, N.D.; Barber, D.S. (2009). Comparison of molecular and histological changes in zebrafish gills exposed to metallic nanoparticles. *Toxicological Sciences*. **107(2):** 404–415.

Halliwell, B.; Gutteridge, J.M.C. (1984). Oxygen toxicity, oxygen radicals, transition metals and disease. *Biochemical Journal*. **219:** 1–14.

Hussain, S.M.; Hess, K.L.; Gearhart, J.M.; Geiss, K.T.; Schlager, J.J. (2005). In vitro toxicity of nanoparticles in BRL 3A rat liver cells. *Toxicology in Vitro*. **19(7):** 975–983.

Kim, J.S.; Kuk, E.; Yu, K.N.; Kim, J.–H.; Park, S.J.; Lee, H.J.; Kim, S.H.; Park, Y.K.; Park, Y.H.; Hwang, C.–Y.; Kim, Y.K.; Lee, Y.–S.; Jeong, D.H.; Cho, M.–H. (2007). Antimicrobial effects of silver nanoparticles. Nanomedicine: *Nanotechnology, Biology and Medicine*. **3:** 95–101.

Langston, W.J.; Bebianno, M.J.; Burt, G.R. (1998). Metal handling strategies in molluscs. In: Langston, W.J.; Bebianno, M.J. (Eds.). Metal Metabolism in Aquatic Environments. Chapman and Hall, London, pp. 219–283.

Lapresta–Fernández, A.; Fernández, A.; Blasco, J. (2012). Nanoecotoxicity effects of engineered silver and gold nanoparticles in aquatic organisms. *Trends of Analytical Chemistry*. **32:** 40–59.

Lawrence, R.A.; Burk, R.F. (1976). Glutathione peroxidase activity in selenium–deficient rat liver. *Biochemical and Biophysical Research Communications*. **71:** 952–958.

Limbach, L.K.; Wick, P.; Manser, P.; Grass, R.N.; Bruinink, A.; Stark, W.J. (2007). Exposure of engineered nanoparticles to human lung epithelial cells: Influence of chemical composition and catalytic activity on oxidative stress. *Environmental Science and Technology*. **41:** 4158–4163.

Lowry, O.H.; Rosenbrough, N.J.; Farr, A.L.; Randall, R.J. (1951). Protein measurement with the Folin phenol reagent. *Journal of Biological Chemistry*. **193:** 265–275.

Luoma, S.N. (2008). Silver Nanotechnologies and the Environment: Old Problems or New Challenges. Project on Emerging Nanotechnologies. Publication 15. Woodrow Wilson International Centre for Scholars and PEW Charitable Trusts, Washington, DC.

Matés, J.M. (2000). Effects of antioxidant enzymes in the molecular control of reactive oxygen species toxicology. *Toxicology*. **153:** 83–104.

McCord, J.M.; Fridovich, I. (1969). Superoxide dismutase: an enzymatic function for erythrocuprein (hemocuprein). *Journal of Biological Chemistry*. **244(22):** 6049–55.

Moore, M.N. (2006). Do nanoparticles present ecotoxicological risks for the health of the aquatic environment? *Environmental International*. **32:** 967–976.

Moore, M.N.; Readman, J.A.J.; Readman, J.W.; Lowe, D.M.; Frickers, P.E.; Beesley, A. (2009). Lysosomal cytotoxicity of carbon nanoparticles in cells of the molluscan immune system: An in vitro study. *Nanotoxicology*. **3(1):** 40–45.

Morones, J.R.; Elechiguerra, J.L.; Camacho, A.; Holt, K.; Kouri, J.B.; Ramírez, J.T.; Yacaman, J.M. (2005). The bactericidal effect of silver nanoparticles. *Nanotechnology*. **16:** 2346–2353.

Mueller, N.C.; Nowack, B. (2008). Exposure modelling of engineered nanoparticles in the environment. *Environmental Science and Technology*. **42(12):** 4447–4453.

Navarro, E.; Baun, A.; Behra, R.; Hartmann, N.B.; Filser, J.; Miao, A.; Quigg, A.; Santschi, P.H.; Sigg, L. (2008). Environmental behavior and ecotoxicity of engineered nanoparticles to algae, plants and fungi. *Ecotoxicology*. **17:** 372–386.

Ng, T.Y.–T.; Wang, W.–X. (2004). Detoxification and effects of Ag, Cd, and Zn pre–exposure on metal uptake kinetics in the clam *Ruditapes philippinarum*. *Marine Ecology Progressive Series*. **268:** 161–172.

Park, S.–Y.; Choi, J. (2011). Geno– and ecotoxicity evaluation of silver nanoparticles in freshwater crustacean *Daphnia magna*. *Environmental Engineering Research*. **15(1):** 23–27.

Park, E.–J.; Yi, J.; Kim, Y.; Choi, K.; Park, K. (2010). Silver nanoparticles induce cytotoxicity by a Trojan–horse type mechanism. *Toxicology in Vitro*. **24:** 872–878.

Rainbow, P.S. (1990). Heavy metal concentration in marine invertebrates. In: Furness, R.W.; Rainbow, P.S., eds. Heavy metals in the marine environment. CRC Press, Boca Raton, 67–79.

Renault, S.; Baudrimont, M.; Mesmer–Dudons, N.; Gonzalez, P.; Mornet, S.; Brisson, A. (2008). Impacts of gold nanoparticle exposure on two freshwater species: a phytoplanktonic alga (*Scenedesmus subspicatus*) and a benthic bivalve (*Corbicula fluminea*). *Gold Bulletin*. **41(2):** 116–126.

Ringwood, A.H.; McCarthy, M.; Bates, T.C.; Carroll, D.L. (2010). The effects of silver nanoparticles on oyster embryos. *Marine Environmental Research*. **69(1):** 549–551.

Scown, T.M.; van Aerle, R.; Tyler, C.R. (2010a). Review: Do engineered nanoparticles pose a significant threat to the aquatic environment? *Critical Review in Toxicology*. **40(7):** 653–670.

Scown, T.M.; Santos, E.M.; Johnston, B.D.; Gaiser, B.; Baalousha, M.; Mitov, S.; Lead, J.R.; Stone, V.; Fernandes, T.F.; Jepson, M.; van Aerle, R.; Tyler, C.R. (2010b). Effects of aqueous exposure to silver nanoparticles of different sizes in rainbow trout. *Toxicological Sciences*. **115(2):** 521–534.

Shi, D.; Blackmore, G.; Wang, W.–X. (2003). Effects of aqueous and dietary pre–exposure and resulting tissue concentration on silver biokinetics in the green mussel *Perna viridis*. *Environmental Science and Technology*. **37:** 936–943.

Valavanidis, A.; Vlahogianni, T.; Dassenakis, M.; Scoullos, M. (2006). Molecular biomarkers of oxidative stress in aquatic organisms in relation to toxic environmental pollutants. *Ecotoxicology and Environmental Safety*. **64:** 178–189.

Viarengo, A.; Nott, J.A. (1993). Mechanisms of heavy metal cation homeostasis in marine invertebrates. *Comparative Biochemistry and Physiology*. **104C(3):** 355–372.

Viarengo, A.; Canesi, L.; Pertica, M.; Poli, G.; Moore, M.N.; Orunesu, M. (1990). Heavy metal effects on lipid peroxidation in the tissues of *Mytilus galloprovincialis* Lam. *Comparative Biochemistry and Physiology Part C: Comparative Pharmacology*. **97(1):** 37–42.

Wang, W.–X.; Fisher, N.S. (1999). Delineating metal accumulation pathways for marine invertebrates. *Science of the Total Environment*. **237/238:** 459–472.

Wang, W.–X.; Rainbow, P.S. (2005). Influence of metal exposure history on trace metal uptake and accumulation by marine invertebrates. *Ecotoxicology and Environmental Safety*. **61:** 145–159.

Ward, J.E.; Kach, D.J. (2009). Marine aggregates facilitate ingestion of nanoparticles by suspension–feeding bivalves. *Marine Environmental Research*. **68:** 137–142.

Zuykov, M.; Pelletier, E.; Demers, S. (2011). Colloidal complexed silver and silver nanoparticles in extrapallial fluid of *Mytilus edulis*. *Marine Environmental Research*. **71(1):** 17–21.

# CHAPTER 4

## Genotoxicity of copper oxide and silver nanoparticles in the mussel *Mytilus galloprovincialis*

# 4.

# GENOTOXICITY OF COPPER OXIDE AND SILVER NANOPARTICLES IN THE MUSSEL *MYTILLUS GALLOPROVINCIALIS*

*Tânia Gomes, Olinda Araújo, Rita Pereira, Ana C. Almeida, Alexandra Cravo, Maria João Bebianno*

CIMA, Faculty of Science and Technology, University of Algarve, Campus de Gambelas, 8005–139 Faro, Portugal

Submitted to Marine Environmental Research

## Abstract

Though there is some information on cytotoxicity of copper nanoparticles and silver nanoparticles on human cell lines, there is no information their genotoxic and cytotoxic behaviour in bivalve molluscs. The aim of this study was to investigate the genotoxic impact of copper oxide and silver nanoparticles using mussels *Mytilus galloprovincialis*. Mussels were exposed to 10 $\mu g.L^{-1}$ of CuO nanoparticles and $Cu^{2+}$ and Ag nanoparticles and $Ag^{+}$ for 15 days to assess genotoxic effects in hemocytes using the comet assay. The results obtained indicate that copper and silver forms (nanoparticles and ionic) induce DNA damage in hemolymph cells and a time–response effect was evident when compared to unexposed mussels. Ionic forms presented higher genotoxicity than nanoparticles, suggesting different mechanisms of action that may be mediated through oxidative stress. DNA strand breaks proved to be a useful biomarker of exposure to genotoxic effects of CuO and Ag nanoparticles in marine molluscs.

Keywords: CuO NPs, Ag NPs, DNA damage, comet assay, oxidative stress, *Mytilus galloprovincialis*

## 4.1. Introduction

Nanoparticles exhibit novel electrical, catalytic, chemical and magnetic properties that can be applied in several commercial and industrial applications that have led to its increased production and use. Inevitably these particles will end up in the environment, accumulate and interact with the biota and their potential genotoxic effects could have short and long–term consequences in aquatic organisms (Handy *et al*., 2008; Moore, 2006; Singh *et al*., 2009).

Copper nanoparticles (CuO NPs) are commonly used in many industrial and consumer applications mostly because of its antimicrobial properties, as well as for its elevated thermal and electrical conductive efficiency. These nanoparticles are used in air and liquid filtration, in coatings on integrated circuits and batteries, catalysts, microelectronics and cosmetics, among others (Ahamed *et al*., 2010; Fahmy and Cormier, 2009; Griffitt *et al*., 2007; Karlsson *et al*., 2008). The use of silver nanoparticles (Ag NPs) incorporated in consumer products has become common in the last years because of the antimicrobial and antibacterial effect of the silver ion (e.g. Luoma, 2008). Industry makes use of this new technology in food contact applications, in building materials, wound dressings, socks, and other textiles, air filters, medical equipment and textiles, toothpaste, baby products, vacuum cleaners and washing machines (www.nanoproject.org). Accordingly, these NPs may already exist in the environment, but at present there is no information regarding its levels in the aquatic compartment.

Overproduction of reactive oxygen species (ROS) is commonly considered the major source of genotoxicity that has been observed after exposure to many types of NPs that have been found to cause DNA–strand breaks, point mutations, oxidative DNA adducts, and chromosomal fragmentation (Bhatt and Tripathi, 2011; Handy *et al*., 2008; Karlsson, 2010; Singh *et al*., 2009). CuO NPs possess redox cycling properties with the capacity to generate intra– and extracellular generation of ROS due to a combination between the particle effect and the dissociation of copper ions from the NPs (Chapter 2; Fahmy and Cormier, 2009; Griffitt *et al*., 2009). Ag NPs have also generates ROS resulting from the release of silver ions, NPs properties (e.g. size and/or shape) or a combination of both (Asharani *et al*., 2008; Fabrega *et al*., 2011; Griffitt *et al*., 2009). Oxidative stress is a significant mechanism of toxicity of CuO and Ag NPs, but the underlying mechanism of action of these NPs are still uncertain (Ahamed *et al*., 2010; Asharani *et al*., 2009; Chapters 2 and 3; Fahmy and Cormier, 2009). Organisms have developed enzymatic and non–enzymatic antioxidant defence mechanisms to prevent and intercept ROS, as well as repair systems for oxidized

components. When the rate of ROS production exceeds the antioxidant defences and repair mechanisms, oxidative stress occurs leading to oxidation of key cellular components as proteins, DNA, lipids and carbohydrates (Halliwell and Gutteridge, 1984; Valavanidis *et al*., 2006). In mussel gills and digestive glands, oxidative stress after long–term exposure to CuO NPs and Ag NPs was evidenced by induction or reduction of the antioxidant defence system, lipid peroxidation, as well as metallothionein induction (Chapters 2 and 3). Given the capacity of both CuO and Ag NPs to generate oxidative stress and oxidative damage, it becomes imperative to address the genotoxic potential of these particles, principally in bivalve species where scarce information exists. Though there is some information on cytotoxicity of Cu and Ag NPs on human cell lines, the information on genotoxic and cytotoxic behaviour of these nanoparticles in aquatic organisms is scarce (e.g. Ahamed *et al*., 2010; Asharani *et al*., 2009; Fahmy and Cormier, 2009; Park and Choi, 2010). Only Gagné *et al*. (2008) and Kádar *et al*. (2011) addressed DNA damage in the mussels *Elliptio complanata* and *Mytilus galloprovincialis* after exposure to cadmium telluride quantum dots and nano iron, respectively. DNA strand breaks (single and double) represent one of the major oxidative damage to DNA via oxidative stress that is generally assessed by the Comet assay. This methodology has been extensively used to evaluate the genotoxic effects of contaminants (as metals) in bivalves' hemocytes (e.g. Almeida *et al*., 2011; Al–Subiai *et al*., 2011; Steinert, 1995; Valavanidis *et al*., 2006) that are a potential target for nanoparticles genotoxicity (Canesi *et al*., 2010, 2012; Gagné *et al*., 2008; Kádar *et al*., 2011; Moore *et al*., 2009).

The main goal of the current work was to assess of the genotoxic potential of CuO NPs and Ag NPs in the mussel *M. galloprovincialis* exposed to 10 $\mu g.L^{-1}$ either in nano or in the ionic form. The comet assay was applied to detect DNA damage (single and double strand breaks) in hemolymph cells (hemocytes) of mussels.

## 4.2. Materials and methods

### 4.2.1. Nanoparticles preparation and characterization

CuO and Ag nanoparticles were obtained from Sigma–Aldrich (Germany) with the particle size specified as <50 nm and <100 nm, respectively. NPs stock solutions (CuO NPs and Ag NPs) were prepared in bi–distilled water (10 $\mu g.L^{-1}$), sonicated for 30 minutes and kept in constant shaking. Ionic stock solution ($Cu^{2+}$ and $Ag^{+}$; 10 $\mu g.L^{-1}$) were prepared identically but not sonicated. NPs were characterized in terms of particle size, aggregation behaviour in

natural seawater using Transmission Electron Microscopy (TEM) (JEOL JEM–1230) equipped with a digital camera (model 785 ES1000W) and by Dynamic Light Scattering (DLS) using an ALV apparatus with Ar ion lased (514.5 nm). More details on the characterization methods are described in Chapters 2 and 3.

### 4.2.2. Experimental design

Mussels *M. galloprovincialis* (Cu exposure: 61.7 ± 8.4 mm and Ag exposure: 63.2 ± 5.8 mm) were collected in the Ria Formosa Lagoon (South of Portugal) and acclimated for 7 days in natural seawater at constant temperature and aeration. Mussels were placed in 25L aquaria, filled with 20L of natural seawater in a triplicate design (around 2.5 mussels/L) and exposed to 10 $\mu g.L^{-1}$ of CuO NPs and Ag NPs and corresponding ionic form, along with a control group for a period of 15 days. The Cu and Ag concentrations chosen are environmentally relevant and reported for several aquatic systems (Bryan and Langston, 1992; Luoma, 2008). Water and copper and silver solutions were renewed every 12 hours to avoid nanoparticles aggregation. Before each renewal, CuO and Ag NPs solutions were sonicated for 30 minutes to break down the size of aggregates. Physico–chemical parameters were measured daily for Cu exposure: temperature (17.8 ± 1.1ºC), salinity (36.3 ± 0.2), percentage of oxygen saturation (97.8 ± 4.9%) and pH (7.8 ± 0.07); and Ag exposure: temperature (17.6 ± 0.3ºC), salinity (36.3 ± 0.1), percentage of oxygen saturation (96.9 ± 3.3%) and pH (7.8 ± 0.05). Multiple sampling was performed (3, 7 and 15 days) where mussels were collected and biotic parameters measured. Mussels were not fed and no mortality was detected during the exposure period.

### 4.2.3. Metal analysis

Copper and silver were analysed in water samples collected 12 hours before water renewal and re–dosing from the NPs and ionic exposure groups, as previously described in Chapters 2 and 4. Copper and silver concentrations in total edible tissues of mussels were also determined on dried samples (80ºC) after wet digestion with nitric acid by atomic absorption spectrophotometry (AAS Analyst 800, Perkin–Elmer).

### 4.2.4. Condition index

To assess the physiological status of control and exposed mussels to CuO and Ag NPs and $Cu^{2+}$ and $Ag^{+}$ during the course of the experiment, the soft tissues and shells of ten individuals were weighted and the condition index (CI) estimated as the percentage of the ratio between the drained weight of soft tissues (g) and the total weight (g).

### 4.2.5. DNA damage using the Comet Assay

Hemolymph of ten mussels collected after 0, 3, 7 and 15 days of exposure to CuO and Ag NPs and corresponding ionic forms was extracted from the posterior adductor muscle with a sterile hypodermic syringe. DNA damage was estimated using the comet assay in a slightly modified version of that by Singh *et al*. (1988) and described in Almeida *et al*. (2011). Briefly, microscopic slides were coated with 0.65% normal melting point agarose (NMA) in Tris–acetate EDTA. After collection, hemolymph cells for each mussel were centrifuged at 3,000 *rpm* for 3 minutes (4ºC) and the pellets with isolated cells suspended in 0.65% low melting point agarose (LMA, in Kenny's salt solution) and casted on the microscope slides. Afterwards, the slides with the embedded cells were immersed in a lysis buffer (2.5 M NaCl, 100 mM EDTA, 10 mM Tris, 1% Triton X–100, 10% Dimethylsulfoxide, 1% Sarcosil, pH 10, 4ºC) for 1 hour, for the diffusion of cellular components and DNA immobilization in agarose. Following the lysis step, slides were gently placed in an electrophoresis chamber containing electrophoresis buffer (300 mM NaOH, 1 mM EDTA, adjusted at pH 13, 4 ºC). The slides were gently submerged and left in this solution for 15 min to permit DNA unwinding. The electrophoresis was carried out for 5 minutes at 25V and 300 mA. Once the electrophoresis concluded, the slides were removed and immersed in neutralizing solution (0.4 mM Tris, pH 7.5), rinsed with bi–distilled water and left to dry overnight. Afterwards, slides were stained with 4,6–diamidino–2–phenylindole (DAPI, 1 $\mu g.mL^{-1}$) and the presence of comets was analysed using an optical fluorescence microscope (Axiovert S100) coupled to a camera (Sony). The Komet 5.5 image analysis system (Kinetic Imaging Ltd) was used to score 50 randomly chosen cells for each slide (25 in each gel from each individual mussel) at a total magnification of x400. Different parameters of the comet, including the olive tail moment (product of comet tail length and proportion DNA in comet tail), comet tail length (in micrometres, measured from the edge of the comet head) and amount of DNA in the comet tail (proportion based on tail intensity) were used. Results are expressed as mean ± SEM. Cells were also categorized for grade of damage (using tail % DNA) based on the

criteria referred in Almeida *et al*. (2011): grade of damage: zero or minimal 10% tail, low damage 10–25%, mid damage 25–50%, high damage 50–75%, and extreme damage >75%. During the entire procedure, great care was taken to avoid exposing cells and slides to light and heat.

### 4.2.6. Statistical analysis

One–way analysis of variance (ANOVA) was applied to the comet parameters and metal concentrations, as variances were homogeneous and distribution normal, followed by the Tukey pair–wise multiple comparison test, in order to evaluate differences between control and exposed mussels. Linear regression analysis was also applied to verify existing relationships between variables. Statistical significance was defined at $p<0.05$ and analysis performed with SigmaPlot10.

## 4.3. Results

### 4.3.1. Nanoparticles characterization

The distribution, size and shape of CuO NPs and Ag NPs were obtained by TEM analysis and DLS analysis (Table 4.1, Fig. 4.1). CuO NPs are spherical in shape and present a mean size of 31 ± 10 nm (Fig. 4.1A, Chapter 2). Ag NPs are mainly spherical in shape and polysdiperse (Fig. 4.1B). The size of Ag NPs reported by the manufacturer (< 100nm) is broadly in agreement with the sizes obtained by TEM. The mean particle size was also determined using DLS, confirming the formation of CuO NPs (284 ± 21 nm) and Ag NPs (144.2 ± 39.2 nm) large aggregates in seawater that increase with time of exposure (Fig. 4.1C–D). Additionally, high polydispersity indexes were observed for CuO NPs (0.35 ± 0.03) and Ag NPs (0.44 ± 0.03), suggesting that under the exposure conditions, both nanoparticles tendency to aggregate produces suspensions with the presence of both single particles and large aggregates, with sizes ranging from 30–338 nm for CuO NPs and 97.0 to 690.4 nm for Ag NPs. The tendency of both NPs to form aggregates while in suspension have previously been established by other authors using these particles, some of which from the same provenience (e.g. Ahamed *et al*., 2010; Choi *et al*., 2010; Griffitt *et al*., 2007; Park and Choi, 2010).

**Table 4.1 –** Characterization of CuO and Ag nanoparticles using different techniques. Values are mean ± std.

| Particle characterization | Method | CuO NPs | Ag NPs |
|---|---|---|---|
| Particle size (nm) | TEM | <50[a] | <100[a] |
| Primary particle size distribution (nm) | TEM | 31 ± 10[b] | – |
| Polydispersity index | DLS | 0.35 ± 0.03[c] | 0.44 ± 0.03[c] |
| Mean particle diameter (nm) | DLS | 284 ± 21[c] | 144.2 ± 39.2[c] |
| Specific surface area ($m^2/g$) | – | 29[a] | 5.0[a] |

[a]Information from the manufacturer Sigma–Aldrich
[b]CuO NPs dispersed in ultrapure water. Average diameter of 250 particles.
[c]CuO and Ag NPs dispersed in natural seawater during a 12 hours cycle.

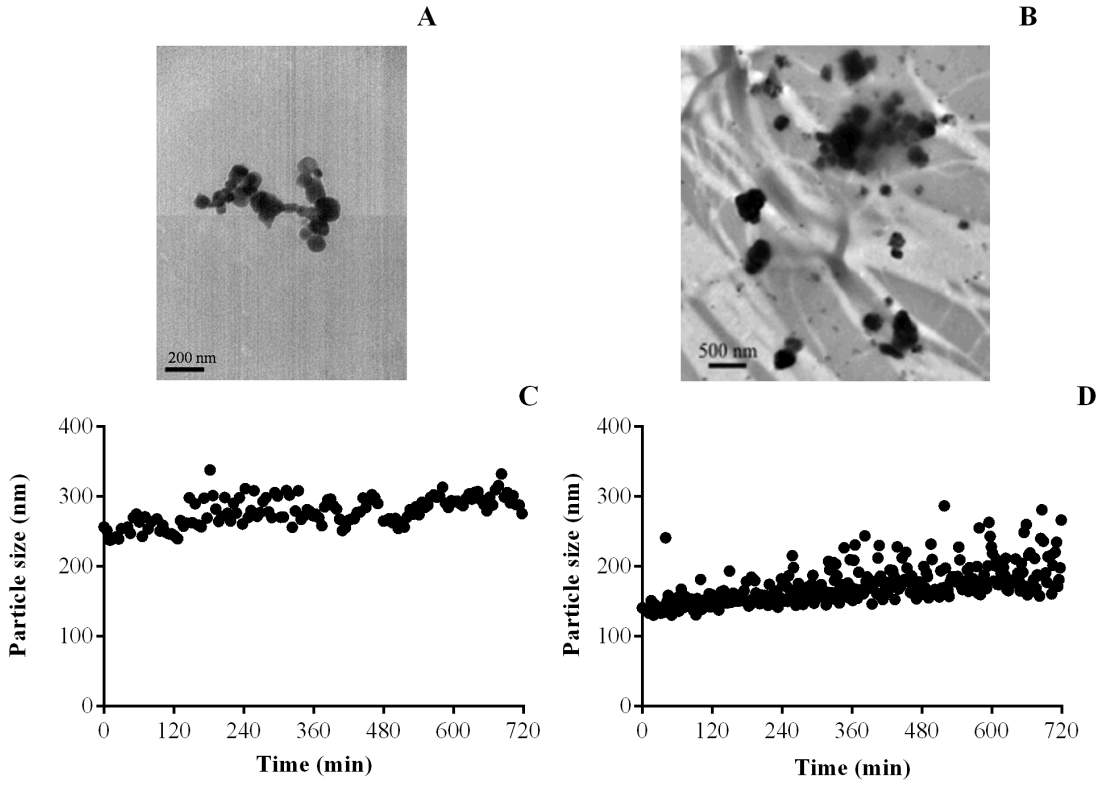


**Figure 4.1 –** Transmission electron microscopic image of CuO NPs (A) and Ag NPs (B) at 32 ppm in Milli–Q water. Particle size distribution (nm) during a 12 h cycle by dynamic light scattering for CuO NPs (C) and Ag NPs (D).

### 4.3.2. Condition Index

No significant changes were obtained in the condition index of unexposed and exposed mussels throughout the exposure period, ranging from 18.4 ± 1.5% to 20.6 ± 3.8% ($p$>0.05) in Cu exposure and 16.0 ± 2.6% to 22.2 ± 4.2% in the Ag exposure ($p$>0.05).

### 4.3.3. Metal concentrations

Copper analysis of water samples from the exposure tanks showed that after 12 hours of exposure (between water renewal) more than 50% of the Cu added in the nano and ionic form was removed from the water column, as already referred in Chapter 2. The dissolution of $Cu^{2+}$ from CuO NPs (<1%) indicate that most of the Cu present is in the nanoparticulate form. As for silver, as already referred in Chapter 3, more than 80% of the nominal concentration of 10μgAg.$L^{-1}$ added in the nano or ionic form was removed from the water column after the 12–hour exposure. Approximately 24% of the initial added Ag NPs dose is present in the dissolved form, indicating that majority of the Ag present in solution is in the nanoparticulate form. The loss of this amount of Cu and Ag may be due either to the presence of the mussels, to metal dissolution or nanoparticles aggregation and sedimentation.

The exposure to both forms of Cu and Ag resulted in a significant Cu and Ag accumulation in mussel tissues throughout the exposure period when compared to unexposed mussels (Fig. 4.2A–B). In CuO NPs exposure, Cu concentrations in mussel tissues significantly increased with time of exposure, from 5.3 ± 1.3 μg.$g^{-1}$ dw to 8.5 ± 1.9 μg.$g^{-1}$ dw, with an accumulation rate of 0.3 μg.$g^{-1}d^{-1}$ (r=0.99, $p$< 0.05, Fig. 4.2A). As for $Cu^{2+}$ exposure, Cu was significantly accumulated in mussel tissues in the first 3 days (7.2 ± 1.7 μg.$g^{-1}$ dw and 6.7 ± 1.1 μg.$g^{-1}$ dw), reaching a steady state during the first week of exposure (7.2 ± 1.7 μg.$g^{-1}$ dw and 6.7 ±1.1 μg.$g^{-1}$ dw) followed by a 1.8–fold decrease by the end of the experiment (Fig. 4.2A). No differences were detected between Cu forms after 3 and 7 days of exposure ($p$>0.05), however by the end of the experiment, Cu concentrations in mussels exposed to CuO NPs continued to increase while those exposed to $Cu^{2+}$ significantly decreased ($p$<0.05).

Mussels exposed to both Ag forms presented a similar trend of accumulation throughout the exposure period (Fig. 4.2B). In the first 3 days of exposure, $Ag^{+}$ exposed mussels' accumulated higher Ag levels than those exposed to Ag NPs (1.6 ± 0.3 μg.$g^{-1}$ dw and 2.6 ± 0.6 μg.$g^{-1}$ dw, respectively), while in the remaining exposure period no significant differences were found ($p$>0.05). After the first week, Ag continued to accumulate in whole soft tissues with a 3.8–fold and 2.7–fold increase, reaching similar levels, followed by a 1.7

and 2.3–fold decrease by the end of the experiment for Ag NPs and $Ag^{+}$ exposed mussels, respectively.

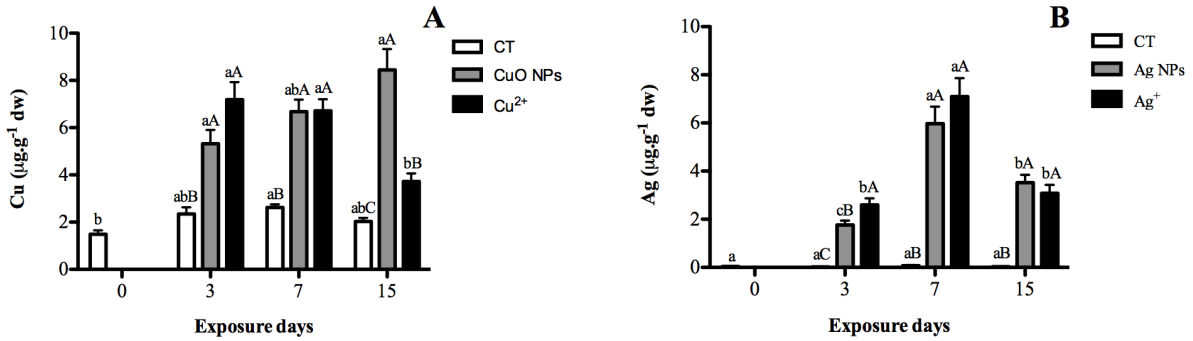


**Figure 4.2 –** A) Copper concentrations (µg.$g^{-1}$ d.w.) and B) Silver concentrations in whole soft tissues of mussels *M. galloprovincialis* from controls (CT) and exposed to CuO and Ag NPs and $Cu^{2+}$ and $Ag^{+}$ for 15 days (average ± Std). Capital and lower letters represent statistical differences between treatments in each exposure day and for each treatment during the exposure duration, respectively ($p$<0.05).

### 4.3.4. DNA Damage

After electrophoresis, the presence of strand breaks (in the form of broken DNA fragments or damaged DNA) will move from the core of the nucleus cells towards to anode, forming a classical comet shape (Singh *et al*., 1988). Some examples of comets in hemocytes of mussels from control and exposed to Cu and Ag are in Figure 4.3. The amount of DNA damage is proportional to the quantity of DNA that migrates into the tail region; quantified in the form of percentage of tail DNA, tail length or the product of these two measurements, the olive tail moment (Fig. 4.4B–D). The olive tail moment (OTM), the % of tail DNA and tail length were the comet parameters chosen to reflect the DNA damage caused by CuO NPs and $Cu^{2+}$ exposure (Fig. 4.4A–C–E) as well as Ag NPs and $Ag^{+}$ in hemolymph cells (Figure 4.4B– D–F).

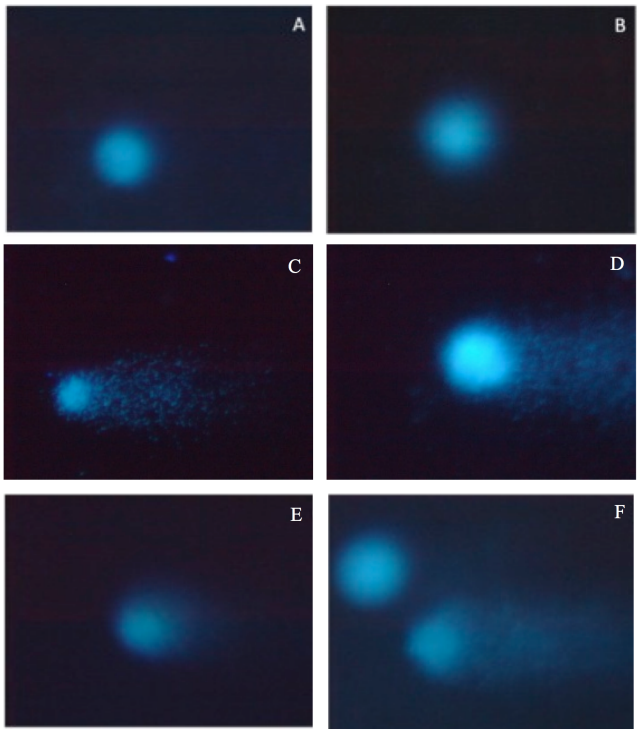


**Figure 4.3 –** Examples of comet assay images, recorded with an optical fluorescence microscope (Axiovert S100) coupled to a camera (Sony) using a total magnification of x400. A–B) control *M. galloprovincialis* hemocytes showing a comet head (nucleoid core) with no DNA migrating into the tail region; C–D) CuO NPs and $Cu^{2+}$ exposure and E–F) Ag NPs and $Ag^{+}$ exposure, respectively, showing a comet head (nucleoid core) with broken DNA fragments or damaged DNA migrating away from the nucleus into the tail region.

In hemocytes from unexposed mussels (either in Cu and Ag experiments) no significant changes were detected in any of the parameters during the course of the experiment ($p$>0.05, Fig. 4.4). The OTM, % of tail DNA and tail length were always higher in Cu–exposed mussels than in unexposed ones, except for the third day of exposure, where no significant changes occurred ($p$>0.05). Additionally, significant differences exist between levels of DNA damage of both nano and ionic copper and silver (at 7 and 15 days), with higher damage in mussels exposed to $Cu^{2+}$ and $Ag^{+}$ ($p$<0.05). Exposure to CuO NPs showed an increase in the OTM (1.8–fold) following 7 days of exposure, that remained unchanged until the end of the experiment (5.1 ± 0.3 a.u.; $p$>0.05, Fig. 4.4A). The same pattern was found for the % of tail DNA and tail length, with a 1.5– and 2.0–fold increase, respectively (Fig. 4.4C and 4.4E), with no significant changes during the remaining period of exposure (9.0 ± 0.3 % and 27.0 ± 1.6 μm, $p$>0.05). Unlike for Cu accumulation, regression analysis showed a linear relationship between time of exposure and DNA damage following exposure to $Cu^{2+}$. OTM

increased linearly (y=0.86x+0.87, $r$=0.99, $p$<0.05) along the course of the experiment ranging from 3.8 ± 0.2 a.u. to 13.9 ± 0.8 a.u ($p$<0.05) (Fig. 4.4A). As for % of tail DNA, a 2.1–fold increase was also detected in exposed mussels from the beginning until the 15$^{th}$ day of exposure (7.1 ± 0.3 % to 14.5 ± 0.6 %; $p$<0.05, Fig. 4.4C). A linear increase was also detected for comet tail length (Fig. 4.4E) during the whole experiment with a rate of 6.0 μm.d$^{-1}$ ($r$=0.99; $p$<0.05).

For Ag, the OTM, % of tail DNA and tail length were always higher in exposed mussels than in unexposed ones, except for the 3$^{th}$ day of exposure where no significant changes occurred in OTM and % of Tail DNA in Ag NPs exposed ones ($p$>0.05). Exposure to Ag NPs showed a linear increase in OTM (Fig. 4.4B) and tail length (Fig. 4.4F) over time, with induction rates of 0.24 au.d$^{-1}$ (r=0.99, $p$<0.05) and 1.17 μm.d$^{-1}$ ($r$=0.99; $p$<0.05), respectively. The % of tail DNA (Fig. 4.4D) also increased with time of exposure, although not linearly, ranging from 8.1 ± 0.3 % to 11.1 ± 0.5 %). Following exposure to $Ag^{+}$, OTM increased linearly (0.67 au.d$^{-1}$, r=0.99, $p$<0.05) along the course of the experiment ranging from 4.5 ± 0.1 a.u. to 12.4 ± 0.8 a.u ($p$<0.05) (Fig. 4.4B). As for % of tail DNA, a 1.4–fold increase was also detected in exposed mussels from the beginning until the 15$^{th}$ day of exposure (9.3 ± 0.3 % to 13.0 ± 0.6 %; $p$<0.05, Fig. 4.4D). A linear increase was also detected for comet tail length (Fig. 4.4F) with increasing time of exposure with a rate of 3.9 μm.d$^{-1}$ ($r$=0.99; $p$<0.05).

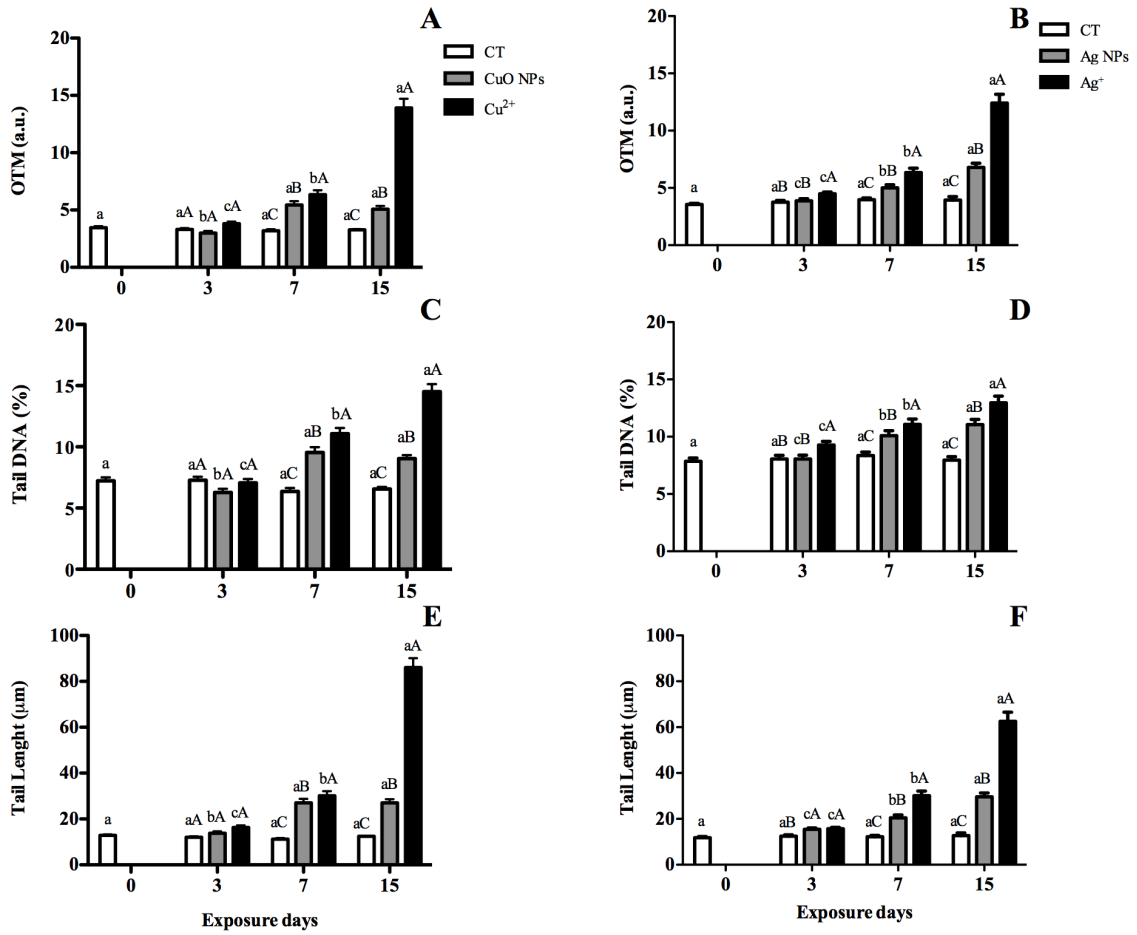


**Figure 4.4 –** DNA damage in hemocytes of mussels *M. galloprovincialis* from control and exposed to CuO NPs and $Cu^{2+}$ and Ag NPs and $Ag^{+}$ for 15 days (average ± SEM, n=500) expressed as Olive Tail Moment (A, B), Tail DNA (C, D) and Tail Length (E, F), respectively. Capital and lower letters represent statistical differences between treatments in each day of exposure and for each treatment during the exposure duration, respectively ($p$<0.05).

Although DNA damage in mussel hemocytes increased with time of exposure, no significant relationship was found between DNA damage, copper and silver concentrations ($p$>0.05).

The percentage of DNA in the tail was used to categorize the grade of damage in unexposed and exposed mussels (Table 4.2). The majority of control cells showed minimal and low grade of damage (>95% of the cells), characterized by zero or minimal DNA migration toward the anode. A small proportion of the control hemocytes exhibited mid damage, 1.6% to 0.1% in Cu and 1.8% to 3.0% in Ag experiment, probably related to some strand breaks occurring in the field (e.g. environmental and/or pollutant stress) or originated during the steps of the comet assay (e.g. cell isolation and/or processing). The results obtained for control mussels are in the same range as those found in mussels collected in the south coast

of Portugal (Almeida *et al*., 2011). As for mussels exposed to CuO NPs and Ag NPs >90% of hemocytes also presented minimal and low DNA damage, while for those exposed to $Cu^{2+}$ and $Ag^{+}$ fewer cells showed minimal (from 73.4% to 38.6%) and low damage (40.4% to 28.2%), with increasing time of exposure, respectively. For both CuO and Ag NPs and respective ionic forms, a significant percentage of cells with mid and high damage increased with time, namely after 15 days of exposure to $Cu^{2+}$ (>30% of cells) and to $Ag^{+}$ (>18% of cells).

**Table 4.2 –** Percentage of cells distributed by grade of DNA damage in hemocytes of mussels *M. galloprovincialis* from controls (CT) and exposed to CuO NPs, $Cu^{2+}$, Ag NPs and $Ag^{+}$ for 15 days (n=500).

| Time of exposure (days) | | DNA damage criteria | | | | |
|---|---|---|---|---|---|---|
| | | Minimal | Low | Mid | High | Extreme |
| 0 | CT | 68.8 | 29.8 | 1.4 | 0 | 0 |
| 3 | CT | 69.8 | 28.6 | 1.6 | 0 | 0 |
| | CuO NPs | 77.6 | 19.6 | 2.8 | 0 | 0 |
| | $Cu^{2+}$ | 73.4 | 24.0 | 2.6 | 0 | 0 |
| 7 | CT | 74.4 | 24.0 | 1.6 | 0 | 0 |
| | CuO NPs | 63.0 | 29.4 | 7.6 | 0 | 0 |
| | $Cu^{2+}$ | 57.4 | 31.2 | 11.0 | 0.4 | 0 |
| 15 | CT | 81.8 | 18.1 | 0.1 | 0 | 0 |
| | CuO NPs | 70.4 | 23.4 | 5.6 | 0.6 | 0 |
| | $Cu^{2+}$ | 38.6 | 28.6 | 29.3 | 3.5 | 0 |
| 0 | CT | 68.0 | 30.2 | 1.8 | 0 | 0 |
| 3 | CT | 68.0 | 29.0 | 3.0 | 0 | 0 |
| | Ag NPs | 66.2 | 30.6 | 3.2 | 0 | 0 |
| | $Ag^{+}$ | 57.6 | 40.4 | 2.0 | 0 | 0 |
| 7 | CT | 64.8 | 32.8 | 2.4 | 0 | 0 |
| | Ag NPs | 61.4 | 29.8 | 8.8 | 0 | 0 |
| | $Ag^{+}$ | 56.3 | 30.6 | 12.6 | 0.5 | 0 |
| 15 | CT | 73.6 | 24.6 | 1.8 | 0 | 0 |
| | Ag NPs | 56.0 | 34.6 | 8.8 | 0.6 | 0 |
| | $Ag^{+}$ | 53.4 | 28.2 | 16.8 | 1.6 | 0 |

## 4.4. Discussion

Nanomaterials have unpredictable genotoxic properties with several mechanisms controlling their capacity to promote DNA damage, making essential to investigate their genotoxic potential. Direct or indirectly, damage can occur not only generated by direct particles influence through their high reactivity and surface area and/or physical and chemical properties, by transition metals comprised or released from the particles (e.g. Cu, Fe, Cd) that have the ability to produce ROS and generate oxidative stress. The main genotoxic effect of nanoparticles comes from the induction of cellular responses or stimulation of target cells that can produce compounds with oxidant or genotoxic capacity, leading to oxidative and inflammatory processes. Additionally, cellular internalization of nanoparticles may promote direct interaction with DNA inside the nucleus or even during mitosis where they can induce several DNA damages (Bhatt and Tripathi, 2011; Handy *et al*., 2008; Karlsson, 2010; Singh *et al*., 2009).

The results obtained from the comet assay showed that CuO NPs are genotoxic to mussels' hemocytes after 7 days of exposure (Fig. 4.4). A time–lag response effect of CuO NPs on DNA damage was evident and resulted in a significant increase in the Olive tail moment, % of tail DNA and tail length when compared to control mussels, except at the first 3 days of exposure. $Cu^{2+}$ presented a similar but higher genotoxic trend as its nano counterpart, shown not only by the significant linear increase in DNA strand breaks with time (demonstrated by the comet parameters) (Fig. 4.4) but also by the significant increase in the percentage of cells with mid and high damage, namely after 15 days of exposure (Table 4.2). These results are the opposite of those reported by other authors, that showed higher cytotoxic and genotoxic capacity of CuO NPs compared to bulk and micrometre CuO and $Cu^{2+}$ (e.g. Griffitt *et al*., 2007; Karlsson *et al*., 2008). The genotoxicity of $Cu^{2+}$ in mussels hemocytes may be related to its involvement in the formation of ROS and subsequent oxidative damage as reported for different aquatic species, namely in the form of DNA strand breaks, oxidation of bases and apoptotic DNA fragmentation (Al–Subiai *et al*., 2011; Bolognesi *et al*., 1999; Steinert, 1995). As for CuO NPs, some information exist on their genotoxic potential to human cells, where DNA damage and oxidative DNA lesions by these particles seem to be mediated through oxidative DNA damage rather than direct interaction with the DNA (Ahamed *et al*., 2010; Karlsson *et al*., 2008; Midander *et al*., 2009).

As for Ag, the present results demonstrate that both Ag forms exert genotoxic effects in mussels' hemocytes (Fig. 4.4), which is in accordance with previous studies on the

genotoxicity of Ag NPs and $Ag^+$ (Ahamed *et al*., 2010; Asharani *et al*., 2009; Choi *et al*., 2010; Hackenberg *et al*., 2011; Park and Choi, 2010). DNA strand breaks (OTM, % Tail DNA and Tail Length) increased with time of exposure in Ag NPs–exposed mussels, even though OTM and % Tail DNA were similar to controls at day 3 (Fig. 4.4). On the other hand, the degree of increase in DNA damage was higher in $Ag^+$–exposed mussels than in those exposed to Ag NPs (and control mussels), reflected not only by the significant increase in comet parameters (Fig. 4.4) but also by the increase in the percentage of cells with mid and high damage (particularly at the end of the experiment) (Table 4.2). There have been contradictory discussions regarding the comparative toxicity of Ag NPs and $Ag^+$, where $Ag^+$ seems to have a higher genotoxic potential than Ag NPs in several cell types (e.g. Asharani *et al*., 2008; Bar–Ilan *et al*., 2009; Park and Choi, 2010). Based on the greater tendency of $Ag^+$ ion to strongly interact with sulfhydryl groups of vital enzymes and phosphorus–containing bases, it is likely that $Ag^+$ can interact with DNA directly of by the formation of ROS, causing damage by covalent binding to DNA (Hossain and Hug, 2002) or by inhibiting DNA synthesis (Hidalgo and Dominguez, 1998), thus preventing cell division and DNA replication (Bar–Ilan *et al*., 2009; Singh et al., 2009). As for Ag NPs, the exact outcome of these NPs in the nucleus is not clear yet, but it is expected to interfere with DNA synthesis, DNA damage, chromosomal morphology and segregation and DNA and cell division. Some studies have reported the genotoxic potential of Ag NPs to different cell types either by direct (direct interaction of NPs with DNA) or indirect mechanisms (oxidative stress and ROS), resulting in oxidative lesions as DNA strand breaks, induction of specific molecular markers (e.g. p53 protein) and DNA repair proteins (e.g. Rad51 protein), chromosomal aberrations and formation of micronuclei (Ahamed *et al*., 2010; Asharani *et al*., 2009; Choi *et al*., 2010; Hackenberg *et al*., 2011; Park and Choi, 2010). The different extent in DNA damaging effects in mussel hemocytes presented by both CuO NPs and Ag NPs and corresponding ionic forms suggest different toxic mechanisms involved in the occurrence of DNA damage or different degrees of reactivity of Cu and Ag that are dependent on the metal form added (nano vs ionic). In fact, different surface chemistry of NPs can result in different effects on genotoxicity (Ahamed *et al*., 2010). If extracellular ions dissolution explained the effects seen, the genotoxic response of both nanometals should be identical to the ones of $Cu^{2+}$ and $Ag^+$ (same mass added). This is in accordance with the results that reported that the cytotoxicity of these NPs is not caused by the soluble fraction alone (e.g. Asharani *et al*., 2008; Griffitt *et al*., 2007, 2009; Midander *et al*., 2009). In fact, most of the CuO and Ag NPs present in solution are in the nanoparticulate form, with less than 1% of the initial added dose

in the dissolved form for CuO NPs (Chapter 2) and about 25% for Ag NPs (Chapter 3). These findings suggest that CuO NPs and Ag NPs exposed hemocytes are exposed to fewer ions than hemocytes exposed with corresponding concentrations of $Cu^{2+}$ and $Ag^{+}$, even considering the potential intracellular release of these ions from the NPs and the inefficient absorption of $Cu^{2+}$ and $Ag^{+}$ ions into the cells due to the efficient barrier capacity of cellular membranes for most ions. Furthermore, reduced amounts of metals ions are entering the nucleus and interacting with DNA. Thus, the genotoxic potential of both NPs cannot be solely explained by the release of metal ions from the particles but also by the effects of the particle properties (e.g. particle size, surface charge processes). It has already been suggested that CuO and Ag NPs may be taken up into cells and generate radicals that will alter or interfere with the metabolic activity of various organelles and inevitably lead to DNA damage (Asharani *et al*., 2009; Bhatt and Tripathi, 2011; Chapters 2 and 3; Karlsson *et al*., 2008). Other mechanisms as the extracellular release of Cu and Ag ions from the particles or even particle surface processes can also be a possible mechanism by which CuO and Ag NPs can indirectly interact with DNA. Additionally, the hypothesis that CuO NPs and Ag NPs can pass through the cell nucleus cannot be excluded, since $Cu^{2+}$ is known to accumulate in the nucleus and bind to DNA to form adducts (Sagripanti *et al*., 1991) and Ag NPs have shown to accumulate in the nuclei of several cell types and lead to genomic damage and instability and chromosomal aberrations (Asharani *et al*., 2008, 2009; Hackenberg *et al*., 2011). On the other hand, Cu and Ag NPs induce mitochondrial dysfunction and induction of oxidative stress, which in turn set off DNA damage (e.g. Asharani *et al*., 2009; Manna *et al*., 2012). Nevertheless, no clear data exists on the exact mechanism by which CuO and Ag NPs promote DNA strand breaks. Based on what is already known on these nanometals toxicity in mussels (Chapters 2 and 3), it is proposed that the DNA damage seen in mussel hemocytes is mediated by oxidative stress.

As filter–feeding organisms, bivalves have the capacity to distribute nanoparticles throughout their organs and respective cells via the seawater filtered, where capture and ingestion are the major routes of internal exposure and potential effects. Once exposed, cells will take up NPs through different mechanisms, as phagocytosis, pinocytosis, endocytosis and direct penetration via disturbance of membrane components (Bhatt and Tripati, 2011; Canesi *et al*., 2012; Handy *et al*., 2008; Moore, 2006; Ward and Kach, 2009). In short–term exposure where most of the nanoparticles are present in the form of aggregates, as in our experimental conditions, NPs agglomerates can be taken up mainly by the digestive system while gills appear to be more sensitive to dissolved metals (Canesi *et al*., 2010, 2012; Chapters 2 and 3;

Ward and Kach, 2009). Nevertheless, evidence exists of a sorting process in the gills, followed by the transport of larger particles and aggregates to the digestive gland. During this passage, aggregates can be broken down in smaller particles, accumulate and even be transferred to the hemolymph and circulating hemocytes (Browne *et al*., 2008; Canesi *et al*., 2010; Moore *et al*., 2009; Ward and Kach, 2009). Hemocytes, as components of the open circulatory system of molluscs, are highly susceptible to NPs uptake and toxicity (e.g. nano carbon black, C60 fullerene) and changes in the immune parameters and ROS production were also reported (Canesi *et al*., 2012 and literature cited therein). Even though bivalve hemocytes can participate in the transport of metals and nanoparticles, particle translocation can be dependent on the particle size or other particle properties (Moore *et al*., 2009; Zuykov *et al*., 2010). In the present case, the existence of large aggregates (as seen by the DLS studies) may explain a lack of CuO and Ag NPs availability and uptake by the hemocytes (that probably are ingested/incorporated by the gills and digestive system), resulting in a lower genotoxic potential of CuO and Ag NPs when compared to its ionic forms. In *M. edulis* exposed to polystyrene microspheres the particle size influenced their capacity to translocate from the gut cavity to the hemolymph (Browne *et al*., 2008). The lack of relationship between Cu and Ag concentrations in mussel whole tissues and DNA damage in hemocytes reinforces the idea that NPs availability between tissues is different (Chapters 2 and 4). Time seems also an important factor in DNA damaging effects, and further work is needed to determine if and how quick particles can translocate from water/organs to the hemolymph and the mechanisms by which these particles are taken up by hemocytes and accumulate in the hemolymph. Further studies using dose–response relationships after exposure to CuO NPs and Ag NPs of different sizes can help to define target cell types and endpoints.

At present little information is available on the bioavailability of nanoparticles to aquatic organisms, route of exposure and uptake mechanisms, as well as their ingestion rates, internal exposure concentrations and cell and tissue distribution. The challenge lies in the development of methods that allow accurate detection and quantification of the uptake of nanoparticles, mode of action, and distribution inside tissues, cells and sub–cellular components of the organisms. Additionally, several constraints arise when using nanoparticles, related not only to their small size and quantity but also to inherent particle properties (Bhatt and Tripathi, 2011; Canesi *et al*., 2012; Ward and Kach, 2009). The current literature suggests nanoparticles uptake in bivalve molluscs (see Canesi *et al*., 2012), but little is known on the cellular uptake of CuO and Ag NPs and their accumulation and effects in bivalve tissues. Our results on bioaccumulation in mussels' tissues showed that both Cu and

Ag are bioavailable to mussels regardless of the form used (NPs or ionic). Exposure to CuO NPs resulted in an increasing rate of Cu accumulation in mussel tissues with time, while for $Cu^{2+}$ by the 15$^{th}$ day of exposure Cu was already eliminated. These results are in line with those observed in mussels gills exposed to the same nanoparticles, where the elimination rate of CuO NPs was slower that its accumulation, in contrast to $Cu^{2+}$ exposure (Chapter 2.1). As for Ag, exposure to both Ag NPs and $Ag^{+}$ resulted in a significant accumulation in the first week of exposure while by the end of the experiment both Ag forms seem to be eliminated from mussels' tissues. Bivalve species have developed several mechanisms of regulation/detoxification to cope with excess of Cu and Ag, as the binding to metallothioneins (Amiard *et al*., 2006; Bolognesi *et al*., 1999; Langston *et al*., 1998), as seems to be the case in mussels exposed to $Cu^{2+}$, Ag NPs and $Ag^{+}$. The increasing DNA damage of CuO NPs, $Cu^{2+}$, Ag NPs and $Ag^{+}$ did not follow metal accumulation in mussels' whole soft tissues. This may be related to different accumulation patterns that reflect distinct physiological and metabolic functions of tissues that when measured in the whole tissues don't allow discriminating responses. Despite the evidences shown (Chapters 2 and 3 and the present Chapter) no clear insights exist on CuO and Ag NPs mediated genotoxicity and accumulation in mussels' hemocytes.

Overall, our results suggest that CuO NPs and Ag NPs are genotoxic towards aquatic organisms, namely filter–feeding bivalves, contributing to the knowledge on aquatic toxicology of two of the most widely used NPs. Both particles possess DNA damaging potential in hemocytes that may be mediated through oxidative stress. The measurement of genotoxic effects of emerging nanomaterials using the comet assay is a useful tool for monitoring toxicity due to nanoparticles in the marine environment.

## 4.5. References

Ahamed, M.; Siddiqui, M.; Akhtar, M.J.; Ahmad, I.; Pant, A.B.; Alhadlaq, H.A. (2010). Genotoxic potential of copper oxide nanoparticles in human lung epithelial cells. *Biochemical and Biophysiological Research Communications*. **396:** 578–583.

Almeida, C.; Pereira, C.; Gomes, T.; Bebianno, M.J.; Cravo, A. (2011). DNA damage as a biomarker of genotoxic contamination in *Mytilus galloprovincialis* from the south coast of Portugal. *Journal of Environmental Monitoring*. **13:** 2559–2567.

Al–Subiai, S.N.; Moody, A.J.; Mustafa, S.A.; Jha, A.N. (2011). A multiple biomarker approach to investigate the effects of copper on the marine bivalve mollusc, *Mytilus edulis*. *Ecotoxicology and Environmental Safety*. **74:** 1913–1920.

Amiard, J.–C.; Amiard–Triquet, C.; Barka, S.; Pellerin, J.; Rainbow, P.S. (2006). Metallothioneins in aquatic invertebrates: Their role in metal detoxification and their use as biomarkers. *Aquatic Toxicology*. **76:** 160–202.

Asharani, P.V.; Wu, Y.L.; Gong, Z.; Valiyaveettil, S. (2008). Toxicity of silver nanoparticles in zebrafish models. *Nanotechnology*. **19:** 255102.

Asharani, P.V.; Mun, G.L.K.; Hande, M.P.; Valiyaveettil, S. (2009). Cytotoxicity and genotoxicity of silver nanoparticles in human cells. *ACS Nano*. **3(2):** 279–290.

Bar–Ilan, O.; Albrecht, R.M.; Fako, V.E.; Furgeson, D.Y. (2009). Toxicity assessments of multisized gold and silver nanoparticles in zebrafish embryos. *Small*. **5(16):** 1897–1910.

Bhatt, I.; Tripathi, B.N. (2011). Interaction of engineered nanoparticles with various components of the environment and possible strategies for their risk assessment. *Chemosphere*. **82(3):** 308–317.

Bolognesi, C.; Landini, E.; Roggieri, P.; Fabbri, R.; Viarengo, A. (1999). Genotoxicity biomarkers in the assessment of heavy metal effects in mussels: experimental studies. *Environmental and Molecular Mutagenesis*. **33:** 287–292.

Browne, M.A.; Dissanayake, A.; Galloway, T.S.; Lowe, D.M.; Thompson, R.C. (2008). Ingested microscopic plastic translocates to the circulatory system of the mussel, *Mytilus edulis* (L.). *Environmental Science and Technology*. **42:** 5026–5031.

Bryan, G.W.; Langston, W.J. (1992). Bioavailability, accumulation and effects of heavy metals in sediments with special reference to United Kingdom estuaries: a review. *Environmental Pollution*. **76:** 89–131.

Canesi, L.; Fabbri, R.; Vallotto, D.; Marcomini, A.; Pojana, G. (2010). Biomarkers in *Mytilus galloprovincialis* exposed to suspensions of selected nanoparticles (Nano carbon black, C60 fullerene, Nano–$TiO_2$, Nano–$SiO_2$). *Aquatic Toxicology*. **100:** 168–177.

Canesi, L.; Ciacci, C.; Fabbri, R.; Marcomini, A.; Pojana, G.; Gallo, G. (2012). Bivalve molluscs as a unique target group for nanoparticle toxicity. *Marine Environmental Research*. **76:** 16–21.

Choi, J.E.; Kim, S.; Ahn, J.H.; Youn, P.; Kang, J.S.; Park, K.; Yi, J.; Ryu, D.–Y. (2010). Induction of oxidative stress and apoptosis by silver nanoparticles in the liver of adult zebrafish. *Aquatic Toxicology*. **100:** 151–159.

Fabrega, J.; Luoma, S.N.; Tyler, C.R.; Galloway, T.M.; Lead, J.R. (2011). Silver nanoparticles: Behaviour and effects in the aquatic environment. *Environmental International*. **37(2):** 517–531.

Fahmy, B.; Cormier, S.A. (2009). Copper oxide nanoparticles induce oxidative stress and cytotoxicity in airway epithelial cells. *Toxicology In Vitro*. **23:** 1365–1371.

Gagné, F.; Auclair, J.; Turcotte, P.; Fournier, M.; Gagnona, C.; Sauvé, S.; Blaise, C. (2008). Ecotoxicity of CdTe quantum dots to freshwater mussels: Impacts on immune system, oxidative stress and genotoxicity. *Aquatic Toxicology*. **86:** 333–340.

Griffitt, R.J.; Weil, R.; Hyndman, K.A.; Denslow, N.D.; Powers, K.; Taylor, D.; Barber, S.D. (2007). Exposure to copper nanoparticles causes gill injury and acute lethality in zebrafish (*Danio rerio*). *Environmental Science and Technology*. **41:** 8178–8186.

Griffitt, R.J.; Hyndman, K.; Denslow, N.D.; Barber, D.S. (2009). Comparison of molecular and histological changes in zebrafish gills exposed to metallic nanoparticles. *Toxicological Sciences*. **107(2):** 404–415.

Hackenberg, S.; Scherzed, A.; Kessler, M.; Hummel, S.; Technau, A.; Froelich, K.; Ginzkey, C.; Koehler, C.; Hagen, R.; Kleinsasser, N. (2011). Silver nanoparticles: Evaluation of DNA damage, toxicity and functional impairment in human mesenchymal stem cells. *Toxicological Letters*. **201:** 27–33.

Halliwell, B.; Gutteridge, J.M.C. (1984). Oxygen toxicity, oxygen radicals, transition metals and disease. *Biochemical Journal*. **219:** 1–14.

Handy, R.D.; Kammer, F.; Lead, J.R.; Hassellöv, M.; Owen, R.; Crane, M. (2008). The ecotoxicology and chemistry of manufactured nanoparticles. *Ecotoxicology*. **17:** 287–314.

Hidalgo, E.; Dominguez, C. (1998). Study of cytotoxicity mechanisms of silver nitrate in human dermal fibroblasts. *Toxicological Letters*. **98:** 169–179.

Hossain, Z.; Huq, F. (2002). Studies on the interaction between $Ag^+$ and DNA. *Journal of Inorganic Biochemistry*. **91:** 398–404.

Kádar, E.; Tarran, G.A.; Jha, A.N.; Al–Subiai, S.N. (2011). Stabilization of engineered zero–valent nanoiron with Na–acrylic copolymer enhances spermiotoxicity. *Environmental Science and Technology*. **45:** 3245–3251.

Karlsson, H.L.; Cronholm, P.; Gustafsson, J.; Möller, L. (2008). Copper oxide nanoparticles are highly toxic: a comparison between metal oxide nanoparticles and carbon nanotubes. *Chemical Research in Toxicology*. **21:** 1726–1732.

Karlsson, H.L. (2010). The comet assay in nanotoxicology research. *Analytical and Bioanalytical Chemistry*. **398:** 651–666.

Langston, W.J.; Bebianno, M.J.; Burt, G.R. (1998). Metal handling strategies in molluscs. In: Langston, W.J.; Bebianno, M.J. (Eds.). Metal Metabolism in Aquatic Environments. Chapman & Hall, London, pp. 219–284.

Luoma, S.N. (2008). Silver Nanotechnologies and the Environment: Old Problems or New Challenges. Project on Emerging Nanotechnologies. Publication 15. Woodrow Wilson International Centre for Scholars and PEW Charitable Trusts, Washington, DC.

Manna, P.; Ghosh, M.; Ghosh, J.; Das, J.; Sil, P.C. (2012). Contribution of nano–copper particles to *in vivo* liver dysfunction and cellular damage: Role of IκBα/NF–κB, MAPKS and mitochondrial signal. *Nanotoxicology*. **6(1):** 1–21.

Midander, K.; Cronholm, P.; Karlsson, H.L.; Elihn, K.; Möller, L.; Leygraf, C.; Wallinder, I.O. (2009). Surface characteristics, copper release, and toxicity of nano– and micrometer–sized copper and copper(II) oxide particles: a cross–disciplinary study. *Small*. **5(3):** 389–399.

Moore, M.N. (2006). Do nanoparticles present ecotoxicological risks for the health of the aquatic environment? *Environmental International*. **32:** 967–976.

Moore, M.N.; Readman, J.A.J.; Readman, J.W.; Lowe, D.M.; Frickers, P.E.; Beesley. A. (2009). Lysosomal cytotoxicity of carbon nanoparticles in cells of the molluscan immune system: An *in vitro* study. *Nanotoxicology*. **3(1):** 40–45.

Park, S.–Y.; Choi, J. (2011). Geno– and ecotoxicity evaluation of silver nanoparticles in freshwater crustacean *Daphnia magna*. *Environmental Engineering Research*. **15(1):** 23–27.

Sagripanti, J.L.; Goering, P.L.; Lamanna, A. (1991). Interaction of copper with DNA and antagonism by other metals. *Toxicology and Applied Pharmacology*. **110:** 477–85.

Singh, N.P.; McCoy, M.T.; Tice, R.R.; Schneider, E.L. (1988). A simple technique for quantitation of low levels of DNA damage in individual cells. *Experimental Cell Research*. **175(1):** 184–191.

Singh, N.; Manshian, B.; Jenkins, G.J.S.; Griffiths, S.M.; Williams, P.M.; Maffeis, T.G.G.; Wrigh, C.J.; Doak, S.H. (2009). NanoGenotoxicology: The DNA damaging potential of engineered nanomaterials. *Biomaterials*. **30:** 3891–3914.

Steinert, S.A. (1995). Contribution of apoptosis to observed DNA damage in mussel cells. *Marine Environmental Research*. **42(1–4):** 253–259.

Valavanidis, A.; Vlahogianni, T.; Dassenakis, M.; Scoullos, M. (2006). Molecular biomarkers of oxidative stress in aquatic organisms in relation to toxic environmental pollutants. *Ecotoxicology and Environmental Safety*. **64:** 178–189.

Ward, J.E.; Kach, D.J. (2009). Marine aggregates facilitate ingestion of nanoparticles by suspension–feeding bivalves. *Marine Environmental Research*. **68:** 137–142.

Zuykov, M.; Pelletier, E.; Demers, S. (2011). Colloidal complexed silver and silver nanoparticles in extrapallial fluid of *Mytilus edulis*. *Marine Environmental Research*. **71(1):** 17–21.

# CHAPTER 5

## Proteomic analysis in mussels *Mytilus galloprovincialis* exposed to CuO NPs and $Cu^{2+}$

# 5.

# PROTEOMIC ANALYSIS IN MUSSELS *MYTILLUS GALLOPROVINCIALIS* EXPOSED TO COPPER OXIDE NANOPARTICLES AND $Cu^{2+}$

*Tânia Gomes, Suze Chora, Catarina G. Pereira, Cátia Cardoso, Maria João Bebianno*
CIMA, Faculty of Science and Technology, University of Algarve, Campus de Gambelas, 8005–139 Faro, Portugal

Submitted to Journal of Proteomics

## Abstract

CuO NPs are one of the most used metal nanomaterials nowadays with several industrial and commercial applications due to their increased thermal and electrical conductivity and antimicrobial capacity. Nevertheless, less is known about the mechanisms by which these particles inflict toxicity in mussels' tissues and to what extent it differs from $Cu^{2+}$. So, the aim of this study was to investigate the proteomic responses in the gills and digestive gland of mussels *Mytilus galloprovincialis* after a 15 days of exposure to CuO NPs and $Cu^{2+}$ (10 $\mu g.L^{-1}$) using two–dimensional gel electrophoresis. These results demonstrate that exposure to CuO NPs and $Cu^{2+}$ induced different responses at the protein expression level in gills and digestive gland. The comparative analysis of protein data sets allowed the discrimination of groups of proteins that varied commonly between the two copper forms. Additionally, unique sets of tissue–specific protein expression signatures were also obtained for each copper form. Fifteen differentially expressed proteins common and specific to CuO NPs and $Cu^{2+}$ were identified using MALDI–TOF–TOF and database search and assigned to eight different categories of biological functions. Proteins involved in cytoskeleton and cell structure (actin, α–tubulin, paramyosin), transcription regulation (zinc–finger BED domain–containing protein, nuclear receptor subfamily 1G), stress response (heat shock cognate 71, putative C1q domain containing protein) and energy metabolism (ATP synthase F0 subunit 6) were assigned to both copper forms. Exposure to CuO NPs altered the expression of three proteins that are involved in apoptosis (caspase 3/7–1), oxidative stress responses (glutathione s–transferase) and proteolysis (cathepsin L), while exposure to $Cu^{2+}$ increased the expression of one protein related to adhesion and cell mobility (precollagen–D). Protein identification showed that CuO NPs exposure not only leads to significant oxidative stress (as do $Cu^{2+}$), but also results in mitochondrial and nucleus stress–induced cell signalling cascades that eventually leads to apoptosis. These results clearly show that the toxicity of CuO NPs is not solely due to $Cu^{2+}$ dissolution and differs from that of $Cu^{2+}$. This study confirms that proteomic analysis of bivalve species is a promising approach for assessing effects of nanoparticles and our experiment provided some insight on the molecular mechanisms underlying CuO NPs exposure. Nevertheless, additional studies are needed to investigate thoroughly the exact mechanism by which CuO NPs interact with cellular components.


Keywords: *Mytilus galloprovincialis*, proteomic analysis, CuO NPs, two–dimensional gel electrophoresis, MALDI–TOF–TOF

## 5.1. Introduction

Copper is an essential metal with a known role as a co–factor in many enzymatic systems and other proteins (e.g. cytochrome oxidase, superoxide dismutase), involved in several biological processes required for growth, development and maintenance of organisms. However, this metal can be extremely toxic if present in high concentrations or if organisms are exposed chronically to low levels in the environment (da Silva and Williams, 2001; Gaetke and Chow, 2003). Its inherent toxicity is a consequence of the propensity of free Cu ions to participate in the formation of reactive oxygen species (ROS). As a redox cycling metal, Cu is capable of directly induce oxidative stress by catalysing the production of superoxide and hydroxyl radicals via Haber–Weiss and Fenton reactions that will potentially damage biological molecules (DNA, proteins, membrane lipids), interfere with cellular transport processes and change metabolites concentrations (Gaetke and Chow, 2003; Halliwell and Gutteridge, 1985). Additionally, Cu has a high affinity to thiol groups being capable to bind to cysteine and lead to protein inactivation. Even though the adverse effects and bioaccumulation of Cu ions in aquatic organisms has been extensively investigated (Maria and Bebianno, 2011; Regoli and Principato, 1995), less is known about the effect of this metal in the form of nanoparticles.

Nanoparticles (NPs) unique and attractive properties have made nanotechnology a rapid growing industry with applications in a variety of different areas such as electronics, medicine, consumer products, food packaging, water treatment technology, fuel cells, catalysts and biosensors (Handy *et al*., 2008; Tiede *et al*., 2009). Although clear benefits are expected from the expansion of nanotechnology products, concern is growing about their impact in the environment and possible interactions with the aquatic biota (Handy *et al*., 2008; Scown *et al*., 2010). The physical and chemical characteristics of NPs (e.g. chemical composition, size, solubility, agglomeration, mobility, density, concentration and charge), behaviour in the environment, mechanisms of biological uptake and toxic effects in aquatic systems can differ considerably from those of corresponding ionic and bulk counterparts (Bhatt and Tripathi, 2011; Scown *et al*., 2010; Tiede *et al*., 2009). Even though the number of studies concerning NPs–induced toxicity on aquatic organisms under laboratory conditions continuous to increase, its mode of action in invertebrate species need further clarification (e.g. Canesi *et al*., 2012; Moore, 2006; Scown *et al*., 2010). Copper oxide nanoparticles (CuO NPs) are one of the most used metal nanomaterials with several industrial and commercial applications (e.g. air and liquid filtration, coatings of integrated circuits and batteries, wood

preservation, inks, skin products and textiles) associated to their antimicrobial properties and elevated thermal and electrical conductivity (Buffet *et al*., 2011 and literature cited therein; Griffitt *et al*., 2009 and literature cited therein). These NPs possess potent redox cycling properties with the capacity to intra– and extra–cellular generation of ROS due not only to the dissolution of $Cu^{2+}$ from the particles but also to the inherent NPs properties (e.g. metal reactivity, surface area) (e.g. Fahmy and Cormier, 2009; Griffitt *et al*., 2009; Heinlaan *et al*., 2011). CuO NPs are accumulated in different tissues of filter–feeding bivalves but the mechanisms by which these particles can induce oxidative stress are still poorly understood (Buffet *et al*., 2011; Chapter 2). When mussels are exposed to CuO NPs for two weeks (10 $\mu g.L^{-1}$; 31 ± 10 nm), the antioxidant defence system failed, lipid peroxidation increase and metallothioneins are induced in both gills and digestive gland, as well as neurotoxic impairment in the gills and DNA damage in hemolymph cells (Chapters 2 and 4).

Conventional biomarkers proved to be sensitive indicators in assessing the toxic effects of NPs (e.g. antioxidant enzymes, lipid peroxidation, metallothionein, DNA damage), nevertheless, it is likely that there are other specific proteins that may be more effective in establishing a nano–specific biological response (Handy *et al*., 2012; Moore, 2006). The responses of classic biomarkers are highly dependent on the route of exposure, bioaccumulation tendency and detoxification mechanisms of chemicals and are influenced by a number of factors (e.g. abiotic). Proteomics–based methods provide a more insightful view on the global changes in protein expression in organisms and provide specific molecular signatures to a type of contaminant without the need to know their toxic mode of action (López–Barea and Gómez–Ariza, 2006; Vioque–Fernández *et al*., 2009). Proteomics applied to nanotoxicology may help understand the major toxic mechanism and modes of action of different types of NPs in aquatic organisms and identify novel and unbiased biomarkers of NPs exposure and effect. In the last years, this technology was applied to mussels for the screening of protein expression signatures (PESs) in response to conventional contaminants, including Cu (Apraiz *et al*., 2006; Shepard and Bradley, 2000; Shepard *et al*., 2000) but also to citrate gold nanoparticles (750 ppb, ~5 nm) (Tedesco *et al*., 2010). Thus, the identification of proteins altered by CuO NPs or $Cu^{2+}$ in mussel tissues will allow a global view of their action at a molecular level, help clarify and differentiate the mechanisms by which both Cu forms inflict toxicity and even provide new biomarkers of exposure and effect.

This study aims to characterize differential protein expression and identify new molecular biomarkers in mussels *Mytilus galloprovincialis* exposed to an environmental relevant

concentration of CuO NPs and $Cu^{2+}$ (10 μgCu.$L^{-1}$) for a period of 15 days using proteomics technology. Two–dimensional gel electrophoresis and mass spectrophotometry procedures were employed to compare protein expression profiles in the gills and digestive gland of mussels exposed to CuO NPs and $Cu^{2+}$ with a control condition. To our knowledge this is the first study to address the effects of CuO NPs at the proteome level.

## 5.2. Materials and methods

### 5.2.1. Preparation and characterization of CuO NPs

CuO NPs (<50 nm) stock solution was prepared in ultrapure water and characterized as previously described in Chapter 2. The size distribution of 250 randomly selected CuO NPs (32 ppm in ultrapure water) was determined by transmission electron microscopy (TEM) using a JEOL JEM–230 TEM equipped with a digital camera model 785 ES1000 W. The hydrodynamic size and polydispersity index of CuO NPs (100 μg.$L^{-1}$ in filtered seawater) during a 12 hours cycle (corresponding to the period between water change and NPs re–dosing) were determined by dynamic light scattering (DLS) using an ALV apparatus with Ar ion lased (515.5 nm). The results of CuO NPs characterization are summarised in Table 5.1.

### 5.2.2. Experimental design

Mussels *M. galloprovincialis* of similar shell length (61.7 ± 8.4 mm) were collected in the Ria Formosa Lagoon (southern coast of Portugal), transported alive to the laboratory and acclimated for 7 days in natural seawater at constant temperature and aeration, as previously described in Chapter 2.1. After acclimation, fifty mussels were placed in 25L tanks filled with 20L of seawater (2.5 mussels/L) in a triplicate design (3 tanks per treatment): 10 μgCu.$L^{-1}$ of CuO NPs, 10 μg.$L^{-1}$ of $Cu^{2+}$, and a control group kept in clean seawater for a period of 15 days. To avoid nanoparticle aggregation, water in tanks was renewed every 12 hours with re–dosing of Cu solutions after each change. Seawater quality was confirmed daily in each tank by measuring temperature, salinity, oxygen saturation and pH (17.8 ± 1.1ºC; 36.3 ± 0.2; 97.8 ± 4.9% and 7.8 ± 0.1, respectively). Mussels were not fed during the experiment and no mortality was registered. After the exposure period, mussels were dissected and gills and digestive glands immediately frozen in liquid nitrogen and stored at –80ºC until further use.

### 5.2.3. Metal analysis

Copper was analysed in water samples collected 12 hours before water renewal and re–dosing from the CuO NPs and $Cu^{2+}$ exposure groups, as previously described in Chapter 2.1. Cu was also determined in dried (80ºC) mussels' gills and digestive gland after wet digestion with $HNO_3$ followed by graphite furnace atomic absorption spectrometry (AAS AAnalyst 800 – Perkin Elmer). Accuracy of the analytical procedure was assured with certified reference material (TORT–II, Lobster Hepatopancreas) from the National Research Council (Canada). The analysed Cu concentration was 106.8 ± 2.5 $\mu g.g^{-1}$ compared to the certified value of 106.0 ± 10.0 $\mu g.g^{-1}$). Metal levels are expressed as $\mu g.g^{-1}$ of dry weight.

### 5.2.4. Cell–free extract preparation and protein assay

Pools of five gills and digestive glands were weighted, suspended in 20% (w/v) HEPES–saccharose buffer (10 mM HEPES and 250 mM saccharose) containing 1 mM DTT, 1 mM EDTA, 1 mM PMSF and 10% protease inhibitor cocktail (Sigma–Aldrich P8340) and homogenized at 4ºC. Cell–free extracts were collected after centrifugation at 15,000 *g* for 2h. Protein content was determined in each tissue using the method developed by Bradford et al. (1976) with bovine serum albumin (BSA) as a standard. Afterwards, 100 µg of protein content of gills and digestive gland were suspended in nine volumes of a precipitation solution (20 mM DTT, 10% trichloroacetic in cold acetone) for 2h at –20ºC, centrifuged at 10,000 *g* for 30 minutes (4ºC) and washed with cold acetone. The residual acetone was removed by air–drying.

### 5.2.5. Two–Dimensional electrophoresis (2–DE)

Proteins were first separated by isoelectric focusing (IEF) followed by SDS–PAGE. Each tissue sample (containing 100 µg of protein) was incubated for 30 min in 300 µL of rehydration buffer (7M urea, 2 M thiourea, 4% CHAPS, 0.8 % pharmalyte, 65 mM DTT and bromophenol blue traces), centrifuged at 14,000 *g* for 10 min (4ºC) and loaded on Immobiline® DryStrip (pH 4–7, 18 cm). After 6h of passive and 6h active (50V) rehydration, IEF was carried out (20ºC, 50 µA/strip) in a Protean IEF Cell (BIORAD, Hercules, CA) using a five–step program: 1,000 V, 1h; 4,000 V 1h; 8000 V, 1h and 8,000 V, to each a total of 50,000 V. Before the second dimension, strips were equilibrated in SDS equilibration buffer (6 M urea, 75 mM Tris–HCl, 4% SDS, 29.3% glycerol, and bromophenol blue traces)

first with 2% DTT and second with 2.5% iodoacetamide. After equilibration, SDS–PAGE was performed in 10% polyacrylamide gels using the Protean Cell XL Cell Format vertical system (20ºC, BIORAD, Hercules, CA) in two steps: 90V, 30 min and 300 V until separation was finished (~5h). Gels were silver stained using a protocol compatible with MS analysis (Blum *et al*., 1987, modified). To ensure the reproducibility of the gels, four replicates of each condition, control and CuO NPs and $Cu^{2+}$, were prepared.

### 5.2.6. Image acquisition and analysis

The gels were scanned using a GS–800 densitometer (BIORAD, Hercules, CA) and analysed using PDQuest software (V8.0, BIORAD, Hercules, CA). All the 2–DE maps were performed with identical background subtraction (floating ball method) after spot detection. A normalized volume for each spot was used for quantitative analyses by dividing its volume by the total volume of the detected spots on the image in order to reduce experimental errors (protein loading and staining). The normalized volumes from the different spots obtained from CuO NPs and $Cu^{2+}$ exposed tissues (gills and digestive gland) were matched against the corresponding spots from control gels. The number of valid protein spots was determined for each gel, as well as the number of proteins matched to every gel, and qualitative and quantitative differences in the protein patterns between unexposed and exposed mussels were determined. The protein intensity of each spot was normalized to the total intensity of each gel image. Only spots expressed in 2/3 of the replicates gels for each group were included in the statistical analysis. Protein spots with 2–fold or higher expression changes in exposed gills and digestive gland (compared to control mussels) were the only ones considered for protein identification.

### 5.2.7. Protein digestion and identification by mass spectrometry

Proteins of interest (total of 40 protein spots) were manually excised from silver stained gels, digested with trypsin as described in Shevchenko *et al*. (2007), and subjected to peptide mass fingerprint (PMF). Mass spectra were acquired using an Ultraflex II MALDI–TOF–TOF (Bruker Daltonics), operating with positive polarity in reflectron mode and spectra were acquired in the range of m/z 900–3500. A total of 3000 spectra were acquired at each spot position at a laser frequency of 50 Hz. For MS/MS experiments peptide ions with a S/N exceeding 25 and a peak intensity higher than 800 were selected for MS/MS. Laser shots

(300 and 1000) were used to acquire the MS/ and MS/MS experiments, respectively. The laser power was 2–5% above ionization threshold. Data acquisition and processing was performed with FlexAnalysis software 3.0 (Bruker Daltonics) with the SNAP peak detection algorithm. The obtained peptide mass list was sent to the MASCOT search engine using the NCBI Database. Searches were performed using the following parameters: taxonomy: other metazoa; proteolytic enzyme: trypsin; peptide tolerance: 100 ppm; fixed modifications: carbamidomethyl (C); variable modification; oxidation (M); peptide charge state: +1; missed cleavages allowed: up to 1. The significance threshold was set to a minimum of 95%. MS BLAST searches (NCBI/Blastp) were performed against a non–redundant protein database for the available sequences for *M. galloprovincialis* (taxid: 29158) using the protein–protein BLAST algorithm (Default Parameters).

### 5.2.8. Statistical analysis

Differences between protein expression obtained in control and exposed mussels (CuO NPs and $Cu^{2+}$) were analyzed using non–parametric Mann–Whitney U–rank. The level of significance was set at 0.05. Data was also submitted to principal component analysis (PCA) using XLStat2009® to extract global information, following the normalization method described by Apraiz *et al*. (2009). Briefly, the volume (%) data was normalized following NVol%=Ln (vol.%+1), where NVol.% is the normalized vol.% obtained for each spot and condition. After normalization of volume data, replicate variability within each exposure condition was reduced using the coefficient of variation (CV) where protein spots with CV<40% where the only taken into account in the PCA.

## 5.3. Results

### 5.3.1. Nanoparticles characterization

The size and shape of CuO NPs were determined by TEM and DLS analysis (Table 5.1) and the characterization is described in detail in Chapter 2.1. The size of CuO NPs reported by the manufacturer was < 50 nm (Table 5.1), which is in agreement with the size obtained by TEM (31 ± 10 nm). The mean particle size was also determined in seawater during a 12 hours cycle by DLS. The hydrodynamic size obtained ranges from approximately 238 nm to 338 nm (Table 5.1, 284 ± 21 nm) that increases with time (Chapter 2.2). A high polydispersity index was also observed by DLS (Table 5.1, 0.35 ± 0.03), suggesting that

under the exposure conditions, CuO NPs tends to aggregate producing suspensions with both small and large aggregates.

**Table 5.1 –** Characterization of CuO nanoparticles using different techniques. Values are mean ± std.

| Particle characterization | Method | CuO NPs |
|---|---|---|
| Particle size (nm) | TEM | <50[a] |
| Primary particle size distribution (nm) | TEM | 31 ± 10[b] |
| Polydispersity index | DLS | 0.35 ± 0.03[c] |
| Mean particle diameter (nm) | DLS | 284 ± 21[c] |
| Specific surface area ($m^2/g$) | – | 29[a] |

[a]Information from the manufacturer Sigma–Aldrich
[b]CuO NPs dispersed in ultrapure water. Average diameter of 250 particles.
[c]CuO NPs dispersed in natural seawater during a 12 hours cycle.

### 5.3.2. Metal analysis

Copper analysis of water samples from the exposure tanks showed that after 12 hours of exposure (between water renewal) more than 50% of the Cu added in the nano and ionic form was removed from the water column, as already referred in Chapter 2.1. The dissolution from $Cu^{2+}$ from CuO NPs <1%, indicating that most of the Cu present is in the nanoparticulate form.

Copper levels of unexposed mussels were similar between tissues ($p$>0.05, Table 5.2). In exposed mussels, Cu accumulated significantly in the gills and digestive glands compared with controls ($p$<0.05), except for $Cu^{2+}$ in gills where no differences were found with controls ($p$>0.05). The accumulation of Cu in the digestive gland was 2–fold higher in CuO NPs exposure when compared with the gills and around 4–fold in $Cu^{2+}$ exposed mussels. The detailed accumulation patterns of both CuO NPs and $Cu^{2+}$ in the gills and digestive gland are described in Chapter 2.

**Table 5.2 –** Copper concentrations (μg.g$^{-1}$ dry weight) in gills and digestive gland of mussels *M. galloprovincialis* from controls and exposed to CuO NPs and $Cu^{2+}$ for 15 days (mean ± Std). Different letters represent statistical differences between treatments within the same tissue and asterisk differences between tissues ($p$<0.05).

| | Gills | | Digestive Gland | |
|---|---|---|---|---|
| | **Day 0** | **Day 15** | **Day 0** | **Day 15** |
| **Controls** | 5.4 ± 1.1$^{b}$ | 7.0 ± 0.6$^{b}$ | 6.9 ± 1.1$^{b}$ | 6.8 ± 0.8$^{b}$ |
| **CuO NPs** | – | 12.51 ± 1.4$^{a*}$ | – | 26.9 ± 3.7$^{a}$ |
| **$Cu^{2+}$** | – | 6.0 ± 0.8$^{b*}$ | – | 22.4 ± 2.8$^{a}$ |

### 5.3.3. 2–DE image patterns

Protein expression profiles (PEPs) were obtained by 2–DE in cell extracts of *M. galloprovincialis* gills and digestive glands, either unexposed or exposed to CuO NPs and $Cu^{2+}$, whose representative proteomes from control mussel tissues are in Figure 5.1. Approximately 1000 proteins were detected on the 2–DE gels but only 430 ± 9 average proteins in the gills and 411 ± 19 average proteins in the digestive gland were matched after data analysis of control proteomes.

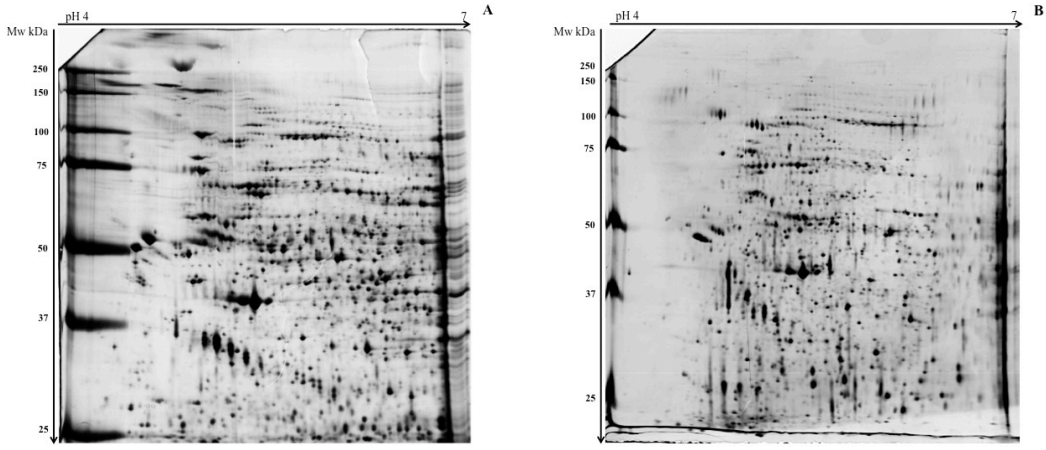


**Figure 5.1 –** *M. galloprovincialis* gills (A) and digestive gland (B) 2–DE representative control gels. One hundred micrograms of protein content was separated on 18 cm IPG strips, in 4–7 pH gradients. The second dimension was performed in 10% SDS–PAGE gels.

PEPs obtained for CuO NPs and $Cu^{2+}$ exposure groups were compared using the PDQuest software, where a master gel was constructed combining the information from the 2–DE gels

from control and from each Cu exposed tissues. New and suppressed proteins and proteins with 2–fold or higher variation were highlighted, discriminating those common to both CuO NPs and $Cu^{2+}$ as well as those specific to each Cu form. Exposure to both Cu forms resulted in different patterns of protein expression and overall quantity of proteins (Table 5.3), that were distributed within p*I* values from 4.7 to 6.9 and Mw ranging from 21.5 to 130.7 kDa. Three hundred and eight and 292 proteins were significantly different in the gills of exposed mussels (CuO NPs and $Cu^{2+}$) compared to controls (Mann–Whitney U–rank test; $p<0.05$), while in the digestive gland 503 and 426 protein spots were significantly different (Mann–Whitney U–rank test; $p<0.05$).

Exposure to CuO NPs resulted in a higher number of new proteins in the gills (28% of total proteins), with approximately 122 proteins when compared to 112 (26% of total proteins) in the $Cu^{2+}$ exposure group (Table 5.3). On the other hand, $Cu^{2+}$ accumulation suppressed more proteins in the gills (109, 25% of total proteins) than CuO NPs (83, 19% of total proteins). In the digestive gland the effects of CuO NPs were higher, with 39% and 34% of total new (244 proteins) and suppressed (140 proteins) proteins, respectively, whereas $Cu^{2+}$ exposure resulted in 208 new and 80 suppressed proteins (30% and 19% of total proteins, respectively) (Table 5.3). A detailed list of these proteins is provided as supplementary material (Tables S1-S12, Annex I).

**Table 5.3 –** Number and % of new, suppressed and 2–fold differentially expressed proteins for each exposure group (CuO NPs and $Cu^{2+}$) compared with controls. N=4 replicate gels for each group.

| Tissue | Cu form | New proteins | | Suppressed proteins | | 2–fold differentially expressed proteins | | | |
|---|---|---|---|---|---|---|---|---|---|
| | | | | | | Common | | Specific | |
| | | Common | Specific | Common | Specific | Up regulated | Down regulated | Up regulated | Down regulated |
| **Gills** | NPs | 44 | 78 | 50 | 33 | 17 | 9 | 69 | 8 |
| | $Cu^{2+}$ | | 68 | | 59 | | | 15 | 30 |
| **Digestive Gland** | NPs | 71 | 173 | 50 | 90 | 41 | 13 | 27 | 38 |
| | $Cu^{2+}$ | | 137 | | 30 | | | 71 | 37 |

Of the total of new proteins induced by both Cu forms, 44 from the gills and 71 from the digestive gland are common to both Cu forms, while 78 and 68 proteins are specific for CuO

NPs and $Cu^{2+}$ in the gills and 173 and 137 in the digestive gland, respectively (Table 5.3). As for the suppressed proteins, 50 are common between CuO NPs and $Cu^{2+}$ in both gills and digestive gland, leaving 33 and 59 proteins specific for CuO NPs and $Cu^{2+}$ effects in the gills and 90 and 30 in the digestive gland, respectively (Table 5.3).

CuO NPs exposure induced changes in 103 and 119 proteins 2–fold or higher compared with unexposed gills and digestive gland, respectively (Table 5.3). On the other hand, $Cu^{2+}$ exposure induced modifications in 119 proteins in the gills and 162 in the digestive gland. Comparing the changes in expression levels, several proteins were common to the two Cu exposure groups where others were specific to CuO NPs or $Cu^{2+}$ (Table 5.3) Venn diagrams are presented in Figure 5.2 showing these changes in both mussel tissues.

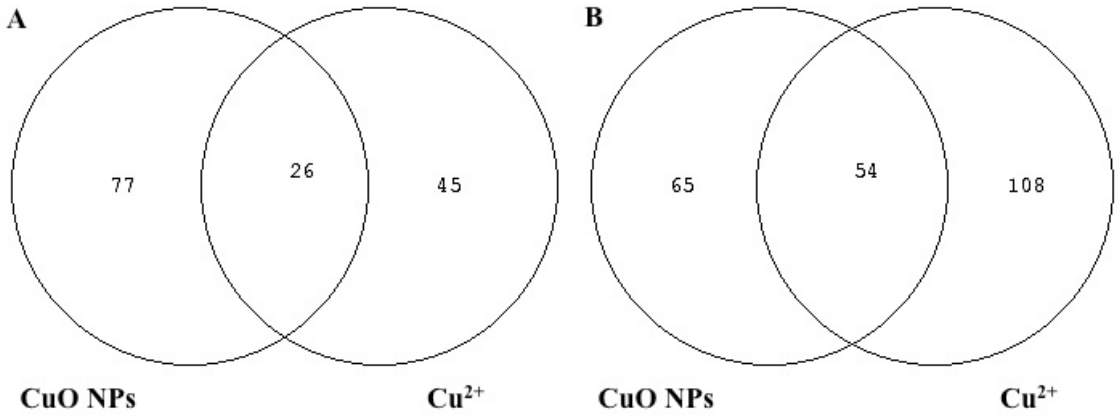


**Figure 5.2 –** Venn diagram representing differentially expressed protein spots (2 fold) between CuO NPs and $Cu^{2+}$ exposure groups. A – Gills; B – Digestive gland.

Among the proteins that altered their expression upon exposure to both CuO NPs and $Cu^{2+}$, 26 were common in the gills (17 up–regulated and 9 down–regulated) and 54 in the digestive gland (41 up–regulated and 13 down–regulated) (Table 5.3, Fig. 5.2). Figure 5.3 shows sets of protein spots differentially expressed in mussels tissues exposed to CuO NPs and $Cu^{2+}$, respectively. In general, higher increase in common protein spots from the gills corresponded to the CuO NPs group, with protein changes up to 5–fold, whereas the down–regulation was more significant in the $Cu^{2+}$ group (up to 10–fold) (Fig. 5.3A). The contrary was observed in the digestive gland, with a higher up–regulation induced by $Cu^{2+}$ (maximum 32–fold), together with a significant down–regulation upon exposure to CuO NPs (up to 37–fold) (Fig. 5.3B). Specific alterations in PEPs upon exposure to CuO NPs showed an overall tendency to

up–regulation in the gills and down–regulation in the digestive gland (Table 5.3, Fig. 5.3). Of the 77 proteins specific to CuO NPs exposure in the gills, 69 were up–regulated (over 10–fold) and only 8 down–regulated (between 2–4 fold) (Table 5.3, Fig. 5.3C). On the other hand, from the 65 specific protein spots in the digestive gland, 27 were up–regulated (up to 8–fold) and 38 down–regulated (up to 15–fold) (Table 5.3, Fig. 5.3D). Exposure to $Cu^{2+}$ showed an inverse tendency compared to CuO NPs, with higher protein down–regulated in the gills and up–regulated in the digestive gland (Table 5.3). A total of 45 specific protein spots changed after exposure to $Cu^{2+}$ in the gills (Table 5.3, Fig. 5.2). Fifteen were up–regulated (over 4–fold) and 30 down–regulated (up to 10–fold) (Table 5.3, Fig. 5.3E). In the digestive gland, 71 of the 108 differentially expressed proteins were up–regulated (maximum 30–fold) in contrast to the 37 that were down–regulated (over 10–fold) (Table 5.3, Fig. 5.3F). A detailed list of these proteins is provided as supplementary material (Tables S13-S18, Annex I).

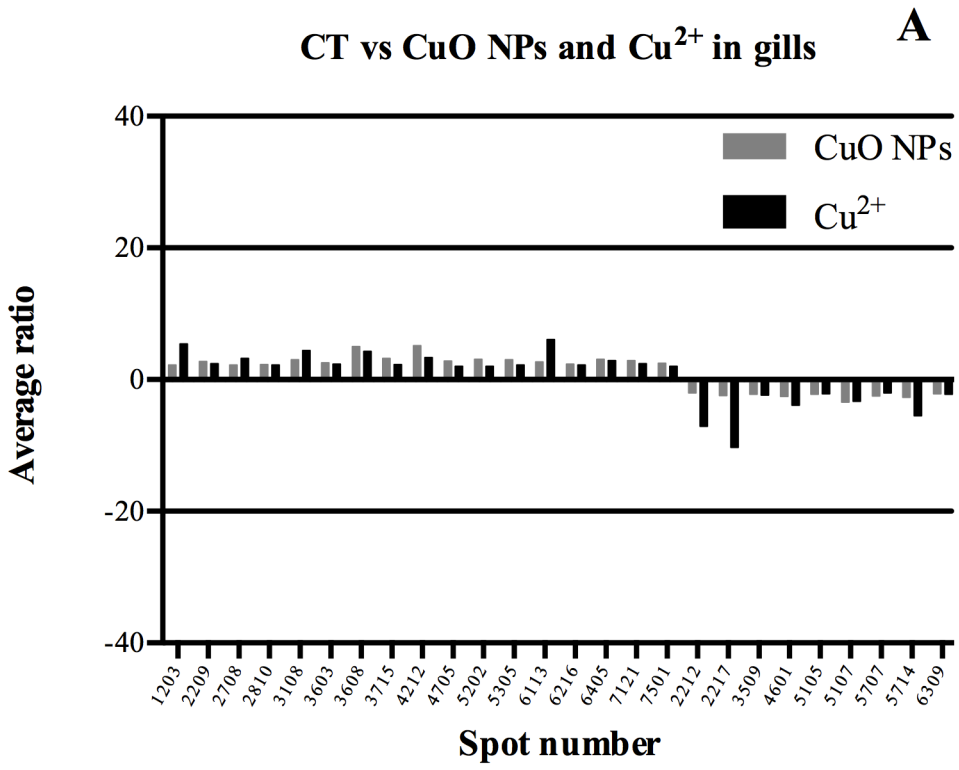
A
CT vs CuO NPs and Cu2+ in gills
CuO NPs
Cu2+
Average ratio
40
20
0
-20
-40
1203
2209
2708
2810
3108
3603
3608
3715
4212
4705
5202
5305
6113
6216
6405
7121
7501
2212
2217
3509
4601
5105
5107
5707
5714
6309
Spot number

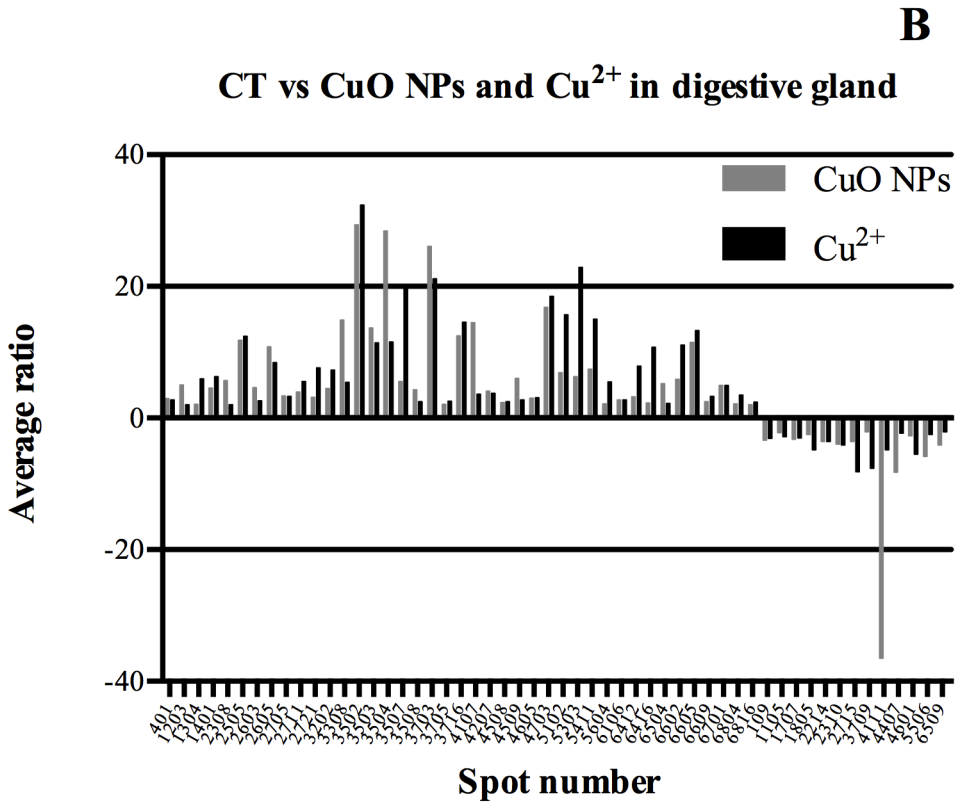
B
CT vs CuO NPs and Cu2+ in digestive gland
CuO NPs
Cu2+
Average ratio
40
20
0
-20
-40
Spot number

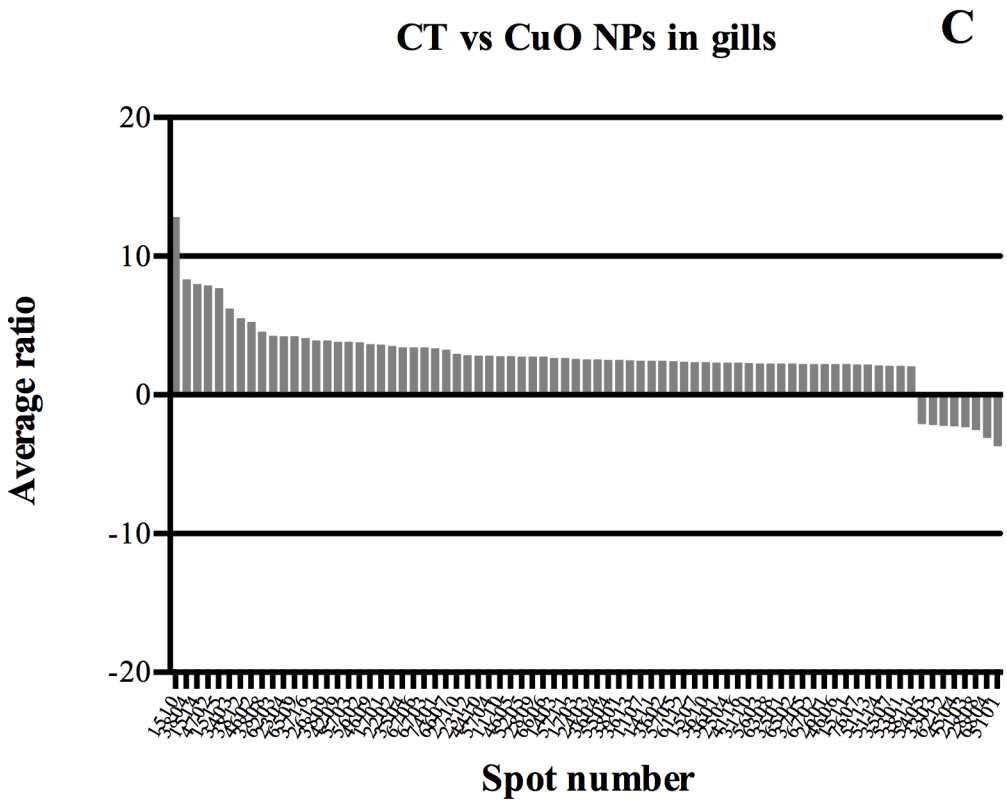
C
CT vs CuO NPs in gills
Average ratio
20
10
0
-10
-20
Spot number

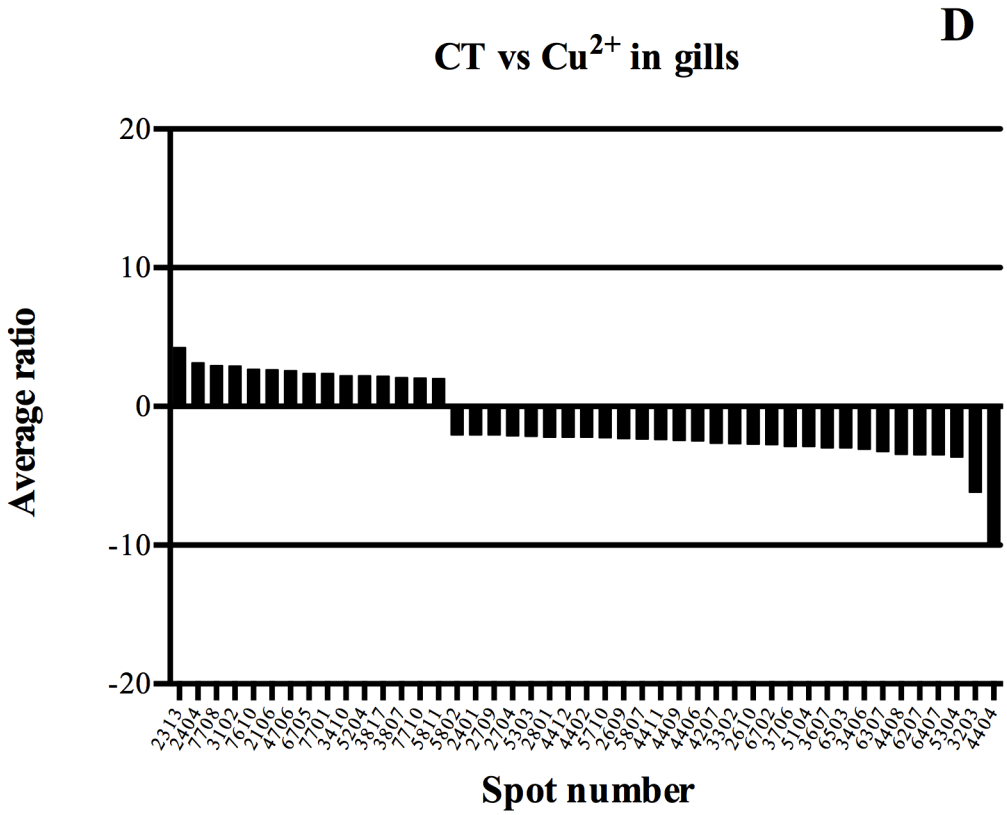
D
CT vs Cu2+ in gills
Average ratio
20
10
0
-10
-20
2313
2404
7708
3102
7610
2106
4706
6705
7701
3410
5204
3817
3807
7710
5811
5802
2401
2709
2704
5303
2801
4412
4402
5710
2609
5807
4411
4409
4406
4207
3302
2610
6702
3706
5104
3607
6503
3406
6307
4408
6207
6407
5304
3203
4404
Spot number

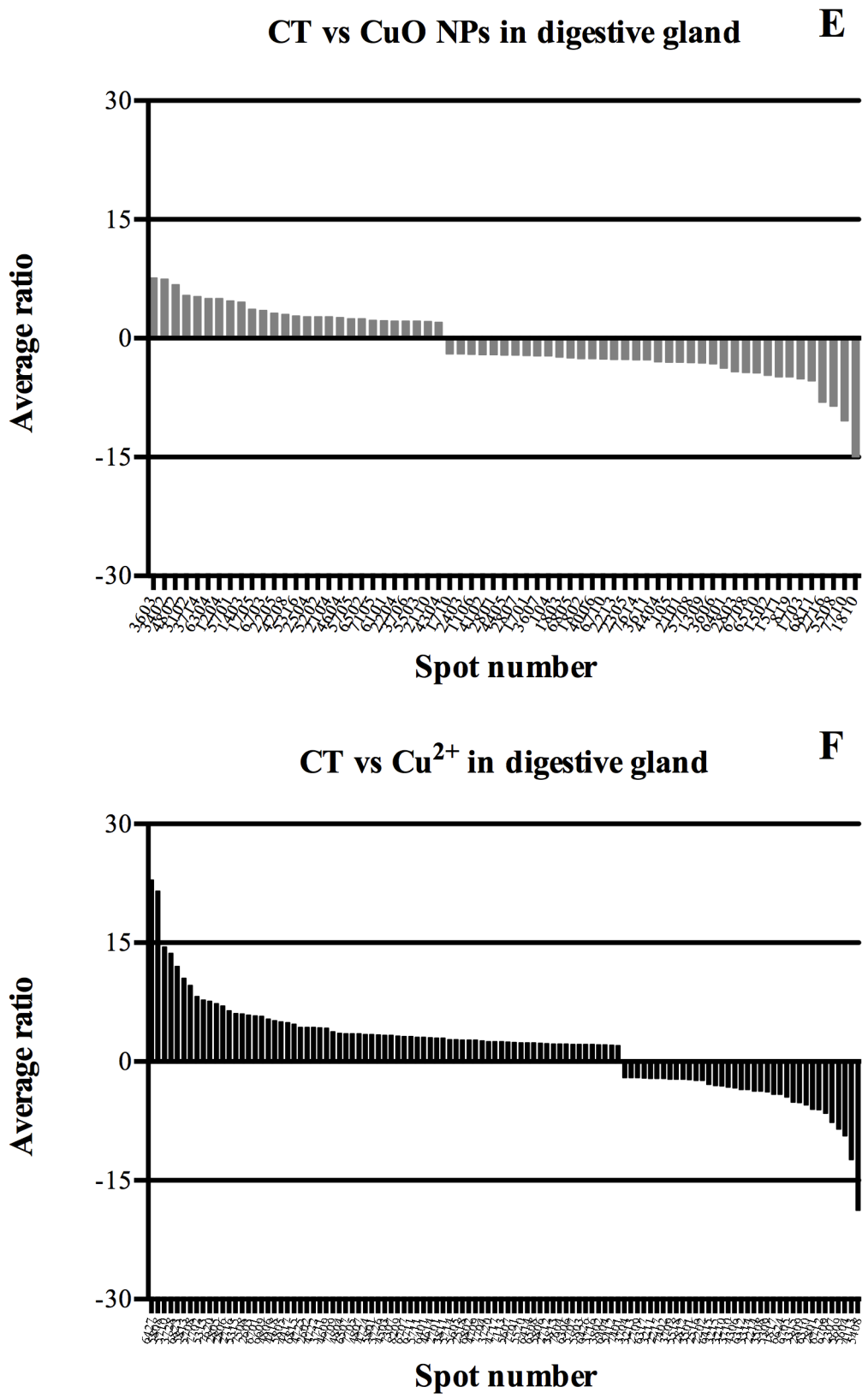


**Figure 5.3 –** Sets of protein spots differentially expressed in mussels' gills and digestive glands exposed to CuO NPs and $Cu^{2+}$. Proteins with the same trend common to both Cu forms in the gills (A) and digestive glands (B); specific to CuO NPs in the gills (C) and

digestive glands (D) and specific to $Cu^{2+}$ in the gills (E) and digestive glands (F) all in comparison to controls. The y–axis corresponds to the average ratio of protein expression, where above the 0 value for the up–regulated protein spots and below the 0 value for the down–regulated ones. In the horizontal axis, the specific up–regulated protein spots are organized with the highest values on the left side and the specific down–regulated ones show the highest values on the right side.

### 5.3.4. Identification of differentially expressed proteins

Of the differentially expressed protein spots (common and specific) in the gills and digestive glands of CuO NPs and $Cu^{2+}$ exposed mussels, 40 with the higher expression changes were analysed by MALDI–TOF–TOF and 15 identified. These proteins are highlighted in Figure 5.4. Since mussels *M. galloprovincialis* are non–model organisms, the majority of its sequences are absent from databases making difficult to match sequence data and the subsequent identification. Homology identity of the proteins using MASCOT was further performed by similarity with available *M. galloprovincialis* sequences using Blastp by NCBI Blast. The identified proteins are listed in Table 5.4.

The identified proteins belong to four functional classes: structural proteins (actin, paramyosin, precollagen D and α–tubulin), metabolic proteins (ATP synthase F0 subunit 6, cytochrome C oxidase subunit III and caspase 3/7–1), stress proteins (heat shock cognate 71, glutathione s–transferase, putative C1q domain containing protein and cathepsine L) and transcription proteins (nuclear receptor family 1G and zinc–finger BED domain–containing protein 1) distributed between copper forms and mussel tissues.

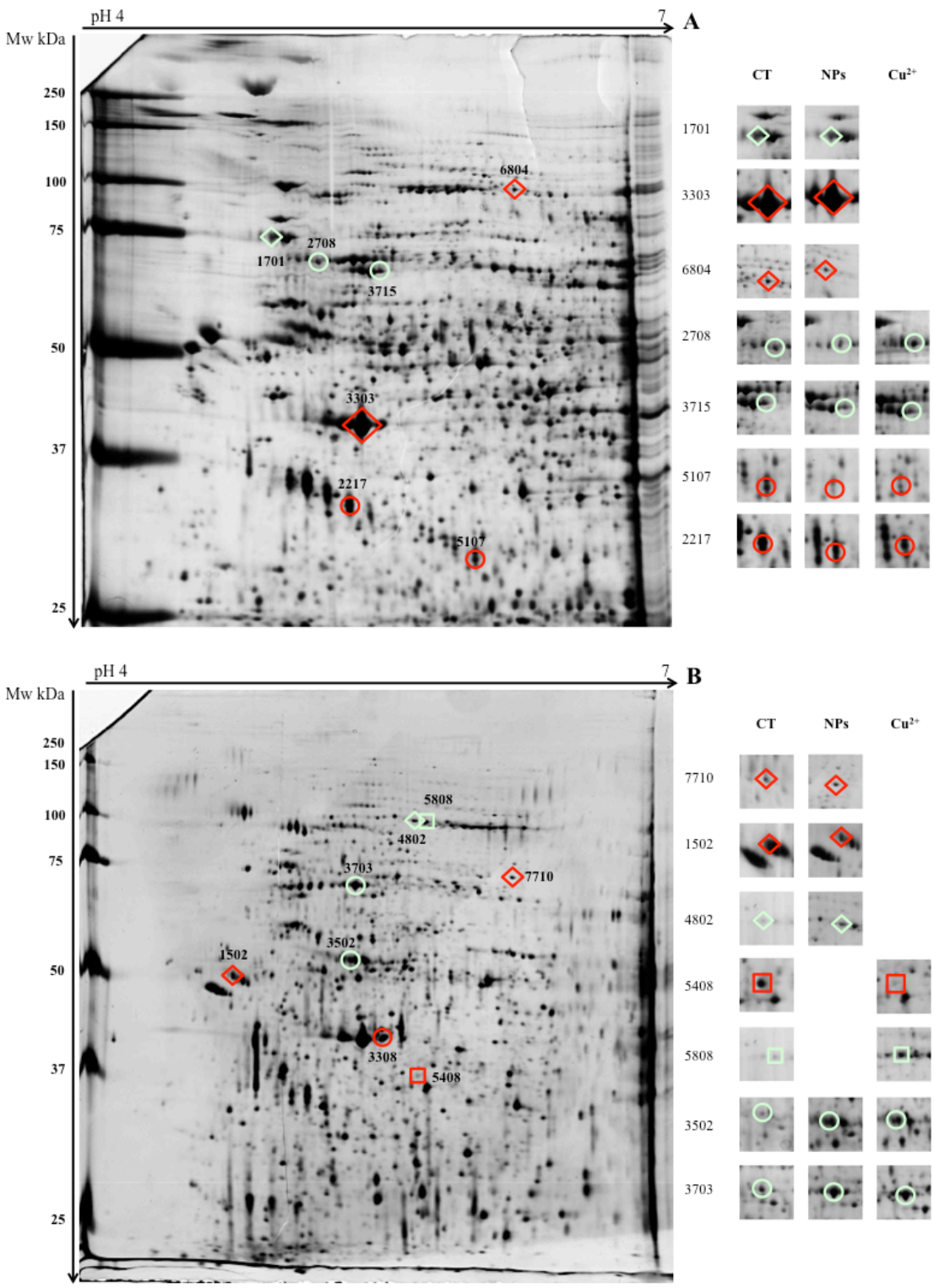


**Figure 5.4 –** *M. galloprovincialis* gills (A) and digestive gland (B) 2–DE representative gels after CuO NPs and $Cu^{2+}$ exposure with identified proteins by MALDI–TOF–TOF. Common proteins 2–fold up (green circle) and 2–fold down–regulated (red circle), specific proteins 2–fold up– (green diamond) and down–regulated (red diamond) after CuO NPs exposure and specific proteins 2–fold up– (green square) and down–regulated (red square) after $Cu^{2+}$ exposure. One hundred micrograms of protein content was separated on 18 cm IPG strips, in 4–7 pH gradients. The second dimension was performed in 10% SDS–PAGE gels.

**Table 5.4 –** Identification of differentially expressed proteins by MALDI–TOF–TOF mass spectrometry in *M. galloprovincialis* exposed to CuO NPs and $Cu^{2+}$.

**A)** Identification performed with peptide mass fingerprint and MASCOT

| Cu form | Spot n°[a] | Name | PDQuest | Accession number | Theor. Mr/pI[b] | MASCOT | | | Species | Function |
|---|---|---|---|---|---|---|---|---|---|---|
| | | | Av. Ratio[b] (CuO NPs/$Cu^{2+}$) | | | Score[c] | % Coverage | N° peptides | | |
| **GILLS** | | | | | | | | | | |
| **CuO NPs** | 3303* | Actin | 2 ↓ | gi\|5114428 | 42.12/5.46 | 91 | – | 4 | *M. galloprovincialis* | Cytoskeleton and cell structure |
| | 6804 | Zinc–finger BED domain–containing protein 1 | 3 ↓ | gi\|307204729 | 8.04/6.92 | 76 | 69 | 4 | *Harpegnathos saltator* | Transcription regulation |
| **Common** | 2708 | Heat shock cognate 71 | 2/3↑ | gi\|76780612 | 71.51/5.28 | 141 | 37 | 19 | *M. galloprovincialis* | Stress response |
| **DIGESTIVE GLAND** | | | | | | | | | | |
| **Common** | 3308 | Actin | 15/5 ↓ | gi\|5114428 | 42.12/5.46 | 91 | – | 4 | *M. galloprovincialis* | Cytoskeleton and cell structure |
| | 3703 | Heat shock cognate 71 | 26/21 ↑ | gi\|76780612 | 71.51/5.28 | 165 | 27 | 17 | *M. galloprovincialis* | Stress response |

**B)** Identification performed with peptide mass fingerprint and BLAST

| Cu form | Spot n°[a] | Name | PDQuest | Accession number | Theor. Mr/pI | BLAST | | | Function |
|---|---|---|---|---|---|---|---|---|---|
| | | | Av. Ratio[b] (CuO NPs/$Cu^{2+}$) | | | Score[d] | % Coverage | E value | |
| **GILLS** | | | | | | | | | |
| **CuO NPs** | 1701 | Glutahione S–tranferase GSTpi1 | 4↑ | gi\|22094809 | 23717.2/5.9 | 23.5 | 5 | 0.027 | Oxidative stress |
| **Common** | 2217 | Nuclear receptor subfamily 1G | 2/10 ↓ | gi\|345971942 | 59.49/5.74 | 22.7 | 12 | 1.1 | Transcription regulation |
| | 3715 | ATP synthase F0 subunit 6 | 3/2 ↑ | gi\|227002086 | 25.79/6.68 | 20 | 31 | 1.9 | Energy metabolism |
| | 5107 | Putative C1q domain containing protein | 4/3 ↓ | gi\|325504419 | 26.18/6.30 | 26.2 | 2 | 0.002 | Stress response |
| **DIGESTIVE GLAND** | | | | | | | | | |
| **CuO NPs** | 7710 | Caspase 3/7–1 | 10 ↓ | gi\|325516443 | 35.41/6.04 | 25 | 19 | 0.26 | Apoptosis |
| | 1502 | Paramyosin | 3 ↓ | gi\|42559342 | 99.57/5.25 | 62 | 53 | $3e^{-12}$ | Cytoskeleton and cell structure |
| | 4802 | Cathepsin L | 7 ↑ | gi\|55710282 | 17.81/5.75 | 43.1 | 40 | $1e^{-7}$ | Proteolysis |
| **$Cu^{2+}$** | 5408 | Cytochrome C oxidase subunit III | 19 ↓ | gi\|306441545 | 31.71/8.07 | 20.4 | 28 | 0.26 | Energy metabolism |
| | 5808 | Precollagen–D | 22 ↑ | gi\|21105303 | 80.75/10.02 | 30.8 | 4 | 0.046 | Adhesion and mobility |
| **Common** | 3502 | α–tubulin | 30/32 ↑ | gi\|302029718 | 41.69/5.11 | 698 | 80 | 0 | Cytoskeleton and cell structure |

[a]Spot number on 2–DE map (Fig. 5.4)

[b]Fold change increase (↑) or decrease (↓) in terms of intensity between control, CuO Nps and $Cu^{2+}$ exposed mussels. Average ratio calculated by PDQuest using four replicates in each group. For all comparisons the *p*–value is <0.05.

[c]Scores of the matches using MASCOT (http://www.matrixscience.com) and percentage of coverage and number of matched peptides in the identified proteins.

[d]Scores of the matches using NCBI/BLAST (http://blast.ncbi.nlm.nih.gov) and percentage of coverage of matched peptides in the identified proteins.

Six proteins distributed between the 4 classes were altered upon exposure to CuO NPs (specific PES), three in the gills and three in the digestive gland. Of the group of structural proteins related to the cytoskeleton, actin (spot nº3303) and paramyosin (spot nº1502) were down–regulated in the gills and digestive gland, respectively. Caspase (spot nº7710) was the only metabolic protein down–regulated (10–fold) in digestive gland with the highest variation upon exposure to CuO NPs. Among the proteins involved in stress response, the antioxidant enzyme glutathione s–transferase (spot nº1701) and the lysosomal enzyme cathepsin L (spot nº4802) were over–expressed (4– and 7–fold) in the gills and digestive gland, respectively. Finally, the DNA–binding zinc–finger BED domain–containing protein 1 was under–expressed 3–fold in the gills. Of the specific PES of $Cu^{2+}$ exposure, only two proteins were identified in the digestive gland, the precollagen–D (spot nº5808) and the cytochrome oxidase subunit III (spot nº5408), the first was 22–fold up–regulated and the second 19–fold down–regulated. Only seven of common differentially expressed proteins (for both CuO NPs and $Cu^{2+}$) were identified, two of which with the highest and lowest expression variation induced by both copper forms. The structural protein α–tubulin (spot nº3502) was the protein with higher increased expression (29– and 32–fold) in the digestive gland while actin (spot nº3308) had the higher decrease (15– and 5–fold). Among the proteins related to metabolic processes, the ATP synthase F0 subunit 6 (spot nº3715) was up–regulated in the gills, with a 3–fold increase in CuO NPs exposure and a 2–fold increase in $Cu^{2+}$. Stress response proteins represented by heat shock cognate 71 proteins (spots nº2708 and 3703) and putative C1q domain containing protein (spot nº5107) were significantly over–expressed in the gills and digestive gland. Lastly, CuO NPs and $Cu^{2+}$ exposure up–regulated one DNA–binding protein in the gills, the nuclear receptor subfamily 1G (spot nº2217).

### 5.3.5. Principal component analysis

A PCA was applied to evaluate significant differences in protein expression between exposure conditions (control, CuO NPs and $Cu^{2+}$) in the gills and digestive gland of mussels. The overall PCAs (Fig. 5.5) show reproducibility between replicate samples within groups in each tissue, as well as a clear separation of each exposure condition, showing distinct protein expression. The two principal components obtained for the 242 proteins in the gills represent 60.5% of total variance (Fig. 5.5A). No clear discrimination of exposure groups is given by the first component (PC1), whereas PC2 clearly separates control (negative side) from the

$Cu^{2+}$ exposure group that occupies the positive side of the y–axis. As for the 282 proteins of the digestive gland, the two principal components represented 67.5% of total variance (Fig. 5.5B). CuO NPs group is clearly separated from the $Cu^{2+}$ group by PC1, while PC2 discriminates the control group in the negative side of the y–axis from the Cu exposure groups plotted in the positive side.

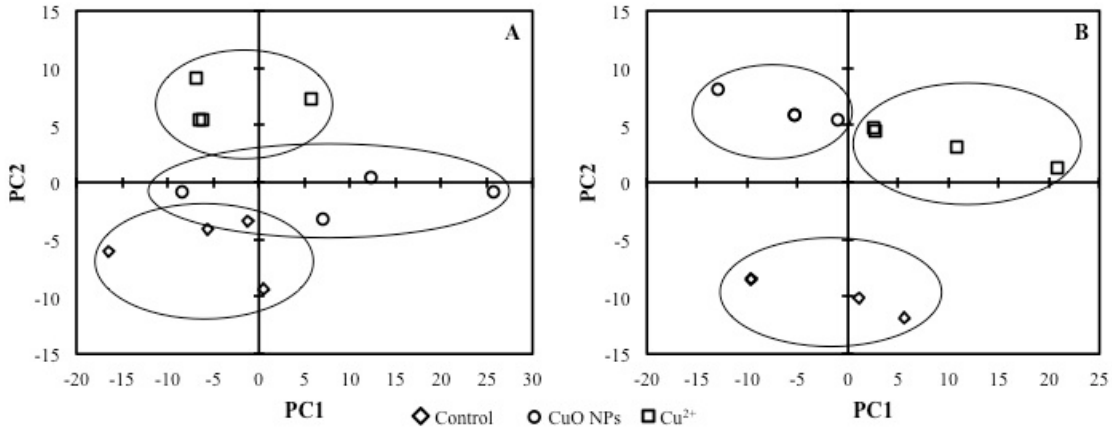


**Figure 5.5 –** PCA obtained after analysis of 242 and 199 variables (spots) and 12 gels in gills (A) and digestive glands (B), respectively, of mussels from control and exposed to CuO NPs and $Cu^{2+}$ for a period of 15 days.

## 5.4. Discussion

It is well established that bivalves represent a target group for NPs uptake with the potential for investigating the underlying mechanisms of toxicity of NPs, even at low concentrations (see Canesi *et al*., 2012). Accordingly, this study aims to investigate changes in protein expression profiles in mussels *M. galloprovincialis* exposed to the same concentration of CuO and $Cu^{2+}$.

Cu was accumulated significantly in the gills and digestive glands compared with controls (Table 5.2), except for $Cu^{2+}$ in gills where no significant differences were found with controls ($p$>0.05). As previously referred in Chapter 2.1, this decrease indicated that Cu in bivalves is easily eliminated, whereas in those exposed to CuO NPs the elimination rate is slower resulting in an increasing accumulation with time of exposure. The digestive gland accumulated more Cu than the gills in both cases, which is in accordance with the role of the digestive gland in copper (CuO NPs and $Cu^{2+}$) accumulation (Chapter 2.1).

CuO NPs and $Cu^{2+}$ exposures induced major changes in protein expression profiles in gills and digestive gland of mussels that were copper and tissue dependent. This was further corroborated by the PCA analysis (Fig. 5.5) that allowed the differentiation of the 3 groups corresponding to controls, CuO NPs and $Cu^{2+}$–exposed mussels within each tissue. These tissue and Cu–dependent responses reflect tissue–specific redox requirements (MacDonagh and Sheehan, 2006) associated with different toxic mechanisms of CuO NPs and $Cu^{2+}$. As the main tissue involved in filtration, gills are in direct contact with water containing CuO NPs and $Cu^{2+}$ being more susceptible to oxidative stress and to Cu accumulation (Chapter 2.1). In gills exposed to CuO NPs a higher up–regulation of proteins (combined with high number of new proteins) was observed when compared to $Cu^{2+}$ that had a tendency to down–regulation and to protein reduction. This could be related to the fact that gills respond differently to both forms of Cu, where $Cu^{2+}$ stimulates a higher degree of peroxidative damage (e.g. lipid peroxidation, DNA damage) (as demonstrated in Chapters 2.1 and 4). The higher protein reduction detected in the digestive gland of CuO NPs–exposed mussels compared to the gills (and $Cu^{2+}$ exposure) may be the result of the higher NPs accumulation and/or slower NPs elimination from this tissue (mainly in the form of aggregates), as previous detected in Chapter 2.2. On the other hand, in $Cu^{2+}$–exposed mussels a higher tendency for up–regulation was detected, probably associated with the importance of digestive gland in $Cu^{2+}$ storage and elimination (e.g. Viarengo *et al*., 1981, 1990). This protective role against Cu toxicity also explains the smallest protein reduction in this tissue. The specific responses in PEPs induced by both Cu forms (Table 5.3, Fig. 5.2) are probably related to the intrinsic nanoparticles properties (e.g. size, surface area, metal reactivity or physical contact). Nevertheless, the comparison of the PEPs obtained for each tissue also allowed the discrimination of a set of 2–fold or higher regulated proteins shared between Cu forms (Table 5.3, Fig. 5.3). The identification of these specific PESs is essential to understand the responses of mussels towards CuO NPs and $Cu^{2+}$ exposure and their modes of action. When working with metal nanoparticles, the release of metal ions from the NPs may occur, which could explain the alteration of similar proteins after CuO NPs and $Cu^{2+}$ exposure. Thus, the effects in CuO NPs–exposed mussels cannot be solely attributed to the nanoparticle effect, and the release of Cu ions from the NPs, even though less than 1%, may also have a significant role. This is in accordance with previous studies that observed that Cu–NP effects were not only caused by the NPs inherent properties (Buffet *et al*., 2011; Fahmy and Cormier, 2009; Heinlaan *et al*., 2011).

The peptide mass fingerprint approach enabled the identification of 15 of the 40 differentially expressed proteins with higher expression changes (Table 5.4). Modifications of proteins involved in cytoskeleton and cell structure, transcription regulation, stress response, oxidative stress, energy metabolism, apoptosis, proteolysis and adhesion and mobility were detected in response to both CuO NPs and $Cu^{2+}$.

Proteins associated with cytoskeleton and cell structure (actin, paramyosin and α–tubulin) were affected upon exposure to both Cu forms in gills and digestive gland. Actin isoforms (spots nº3303 and 3308, Table 5.4, Fig. 5.4) were down–regulated (2–fold) in response to CuO NPs exposure in the gills and in the digestive gland in response to CuO NPs (15–fold) and $Cu^{2+}$ (5–fold). Actin is a ubiquitous cytosolic protein and the fundamental component of the cytoskeleton, with an important role in protein synthesis, phagocytosis, organelle and cell motility, endocytosis, exocytosis, vesicular transport and cellular plasticity (Dalle–Donne *et al*., 2001; McDonagh *et al*., 2005; Rodríguez–Ortega *et al*., 2003). Another cytoskeletal protein affected by CuO NPs in the digestive gland (3–fold down–regulated) was paramyosin (spot nº1502, Table 5.4, Fig. 5.4), that regulates motility and contractile functions in cells (core of thick filaments beneath myosin surface), being responsible for the "catch" mechanism that enables sustained contraction of muscles with very little energy expenditure (Watabe *et al*., 2000; Yamada *et al*., 2000). α–tubulin (spot nº3502, Table 5.4, Fig. 5.4) is another key component of the cytoskeleton that was similarly up–regulated in the digestive gland by CuO NPs (29–fold) and $Cu^{2+}$ (32–fold). Tubulin subunits are responsible for microtubule polymerization (Miura *et al*. 2005) and are involved in several cellular processes as cell transport and motility, cell division and intracellular positioning of organelles (Apraiz *et al*., 2006; Yang *et al*., 2010). Proteins related to the structure and function of the cytoskeleton are the first target of oxidative stress in bivalves, highlighting a direct link between ROS production and cytoskeleton disruption (Dalle–Donne *et al*., 2001; Gómez–Mendikute and Cajaraville, 2003; McDonagh *et al*., 2005; Miura *et al*., 2005). Actin disorganization and its impact on cytoskeletal functions was already been linked to $Cu^{2+}$ exposure in clams *Chamaelea gallina* (0.1-5 $mg.L^{-1}$, 7 days), oysters *Saccrostea glomerata* (5 $\mu g.L^{-1}$, 4 days) and mussels *M. galloprovincialis* ($3.178x10^{5}$–$12.72x10^{5}$ $\mu g.L^{-1}$, 24h) (Goméz–Mendikute and Cajaraville, 2003; Rodríguez–Ortega *et al*., 2003; Thompson *et al*., 2012), while for CuO NPs this study is the first to associate the impact of these NPs on the cytoskeletal activity of mussel tissues. The cytoskeleton alterations in tissues exposed to CuO NPs are possibly due to NPs–induced ROS that altered the cytoskeleton and microtubule

remodelling by redirecting actin cytoskeleton polymerization and contraction. These alterations could be directly mediated by $Cu^{2+}$ (released from CuO NPs) that to cytoskeletal structural proteins, or indirectly by oxidation of sulfhydryl (–SH) groups of cytoskeletal proteins or impairment of calcium ($Ca^{2+}$) homeostasis mediated by ROS, leading to the disorganization of the cytoskeleton and disruption of the cellular membrane (Dalle–Donne *et al*., 2001; Gómez–Mendikute and Cajaraville, 2003; Huang *et al*., 2010a; Matozzo *et al*., 2001). Similar patterns of disruption of the cellular membrane and cytoskeleton damage was already been detected in human cells exposed to Ag NPs (6-20 nm, 100-400 $\mu g.mL^{-1}$, 2h), Au NPs (13-45 nm, 0-189 $\mu g.mL^{-1}$, 6 days) and gelatin NPs (37 ± 0.84 nm, 0.2 $mg.mL^{-1}$, 24h), attributed not only to ROS but also to particle uptake by endocytosis (Asharani *et al*., 2009; Gupta *et al*., 2004; Mironava *et al*., 2010). Endocytosis is one of the possible mechanisms by which CuO NPs can be internalized in mussel tissues, leading to several structural and functional interactions between the cytoskeletal components (Gupta *et al*., 2004; Moore, 2006; Ward and Kach, 2009). Additionally, direct contact between particles and cell membranes may also be a pre–requisite for the manifestation of the effects in cytoskeleton proteins. Accordingly, given the importance of cytoskeleton proteins in the maintenance of several cellular processes, the alteration in the expression of these three proteins by CuO NPs and $Cu^{2+}$ will compromise important cellular and physiological functions as muscle contraction, phagocytic activity, adhesion and motility, cell differentiation and cell death, among others (Matozzo *et al*., 2001; Thompson *et al*., 2012).

The expression of two proteins associated with energy metabolism was also altered upon exposure to Cu. Both CuO NPs and $Cu^{2+}$ up–regulated ATP synthase F0 subunit 6 (spot nº3715) in the gills (3– and 2–fold, respectively), while $Cu^{2+}$ down–regulated (19–fold) cytochrome C oxidase subunit III (spot nº5408) in the digestive gland (Table 5.4, Fig. 5.4). ATP synthase is a ubiquitous protein responsible for the production of ATP in the mitochondria and consequently for the supply of energy to cells. Mitochondria plays an important role on the entire cellular Cu homeostatic mechanisms, and therefore, cellular Cu levels alterations can affect the mitochondrial proteome (Banci *et al*., 2011). Accordingly, an up–regulation of ATP synthase F0 subunit 6 indicates a higher general metabolic rate associated with the presence of high copper levels (both CuO NPs and $Cu^{2+}$) in the cytosol of gill cells (Apraiz *et al*., 2006; Banci *et al*., 2011). Cytochrome c oxidase subunit III is responsible for the electron transport from cytochrome C to $O_2$ (Puerto *et al*., 2011; Yang *et al*., 2010) and is one of the proteins that require $Cu^{2+}$ for a proper assembly, which is

essential for the proper functioning of the mitochondria (Banci *et al*., 2011). So, the down–regulation of this protein is indicative of a decrease in Cu levels in mitochondria or of a direct action of $Cu^{2+}$–induced ROS. This decrease in Cu levels is probably related to the triggering of mussels detoxification mechanisms (e.g. MTs) or to a transfer of Cu ions for the functioning of SOD to counteract ROS originated by $Cu^{2+}$ and protect the mitochondria. In fact, SOD activity increased together with an MT induction and a reduction of Cu levels in mussels' digestive glands after 15 days of exposure to $Cu^{2+}$ (Chapter 2.2). The changes in energy metabolism along with an increase in lipid peroxidation (as seen in Chapter 2) and cytoskeleton disorganization are also indicative of membrane damage. Lipid peroxides originated by lipid peroxidation also affect the mitochondrial metabolism by altering their respiration and oxidative phosphorylation, their $Ca^{2+}$ buffering capacity and the properties of mitochondrial membranes (Huang *et al*., 2010a; Orrenius *et al*., 2007). The ability of CuO NPs and $Cu^{2+}$ to damage mitochondria, compromise the oxidative chain and deplete ATP levels (by increasing ROS levels) may be one of their toxicity mechanisms, than in the long run can enhance apoptosis by creating a cellular oxidative stress.

Among the proteins related to stress response, heat–shock proteins (HSPs) are molecular chaperones essential to the assembly, folding and intracellular transport of proteins, protecting cells from stress–associated cellular damage. Originally identified as proteins up–regulated in response to heat stress, HSPs are also induced by a wide range of other stressors as oxidative stress, hypoxia, pH, salinity, radiation and several contaminants including metals and therefore have been widely used as biomarkers (Dutton and Hofmann, 2009; Kefaloyianni *et al*., 2005; Leung *et al*., 2011; Rodríguez–Ortega *et al*., 2003; Thompson *et al*., 2012). Exposure to both CuO NPs and $Cu^{2+}$ affected HSPs, namely the heat–shock cognate 71 (spots nº2708 and 3703) in gills and digestive glands (Table 5.4, Fig. 5.4). Their induction was probably initiated to protect and/or repair target proteins and attempt to cope with Cu toxicity. The great capacity of both CuO NPs and $Cu^{2+}$ to produce ROS is consistent with the importance of heat–shock cognate 71 in the protection against oxidative stress. Phosphorylation of small heat shock proteins has been described to prevent actin depolarization and to regulate microfilament dynamics following oxidative stress, while phosphorylation of α–tubulin prevents the formation of microtubules under oxidative stress (Dalle–Donne *et al*., 2001; Miura *et al*., 2005). This could explain actin down–regulation, alpha–tubulin and heat–shock up–regulation (>20–fold) in the gills and digestive gland of exposed mussels in response to cytoskeleton disruption.

The putative C1q domain containing protein (spot 5107, Table 5.4, Fig. 5.4) was another protein related to stress response altered upon exposure to both CuO NPs and $Cu^{2+}$ in the gills. The large family of C1q domain proteins is known to participate in several metabolic processes in organisms, namely in tissue homeostasis, protein activation, immune responses, apoptosis, phagocytosis, cell adhesion and cell growth modulation (Gerdol *et al*., 2011; Gestal *et al*., 2010). The down–regulation of this protein by CuO NPs (4–fold) and $Cu^{2+}$ (3–fold) seem to indicate disruption of the immune capacity of exposed mussels probably associated to oxidative stress. In fact, cell–mediated immunity represents a significant target for NPs in bivalve molluscs (Canesi *et al*., 2012).

Two proteins related to transcription regulation were down–regulated following CuO NPs and $Cu^{2+}$ exposure in the gills: zinc–finger BED domain–containing protein 1 (spot nº6804) by CuO NPs and the nuclear receptor subfamily 1G (spot nº2217) by both CuO NPs and $Cu^{2+}$ (Table 5.4, Fig. 5.4). Zinc finger proteins are one of the best–known transcription factors that bind specifically to short DNA–sequences and control the expression of many genes (Yang *et al*., 2010). In addition to transcription factors, different Zn–binding motifs have been discovered at many levels of DNA repair mechanisms (Hartwing, 2001; Yang *et al*., 2010). More than 300 DNA binding proteins contain Zn–finger domains, including the nuclear–receptor subfamily 1G, and various metals (e.g. Cu, Ni, Co, Cd and Fe) are able to replace Zn in these Zn–binding structures leading to reduced DNA–binding activity. As for NPs, the release of $Cu^{2+}$ from CuO NPs (even <1%) may be responsible for the disruption of these proteins by substituting zinc atoms in Zn–finger proteins, generate free radicals and cause DNA damage or lead to decreasing activities in DNA repair enzymes, thus contributing to increased levels of modified DNA forms (Achard–Joris *et al*., 2006; Galaris and Evangelou, 2002; Hartwig, 2001). In NPs with low solubility, as the case of the NPs used, their capacity to originate ROS is normally associated with their genotoxic potential (Chapter 4); nevertheless, other factors (e.g. metal release from the NPs and particle reactivity) need to be considered (Gonzalez *et al*., 2008; Karlsson, 2010). The change in expression of these proteins in exposed mussels indicate that the impairment of signal transduction in DNA–related functions may be one mechanism by which CuO NPs and $Cu^{2+}$ induce genotoxicity. Nevertheless, the interaction between Zn–finger proteins and DNA repair mechanisms needs more investigation, specially associated with nanoparticles toxicity, as well as the exact mechanisms by which CuO NPs inflict genotoxicity to mussels' gills.

CuO NPs exposure resulted in the up–regulation of GST (spot nº1701) in the gills of exposed mussels (Table 5.4, Fig. 5.4). GST is a phase II detoxification enzyme that catalyses the conjugated reactions between reduced glutathione (GSH) and electrophilic compounds leading to their eventual excretion (Fitzpatrick *et al*., 1995; MacDonagh and Sheehan, 2006). GST activity is widely used as a biomarker of exposure and is implicated in the defence against oxidative stress (e.g. Canesi *et al*., 1999; Hoarau *et al*., 2006). Gills are one the main detoxification organ of mussels, where a high number of phase II detoxification enzymes (as GST) are concentrated (Fitzpatrick *et al*., 1995; MacDonagh and Sheehan, 2006). Given the capacity of CuO NPs to alter the antioxidant capacity of cells (inactivation of antioxidant enzymes) and cause oxidative damage (lipid peroxidation) through the formation of ROS in the gills of exposed mussels (Chapter 2.1), the up–regulation of antioxidant defence–related proteins is to be expected. Accordingly, an increase in GST expression act as a cellular compensation mechanism when other antioxidant enzymes activities are low (e.g. CAT activity), as well as reflect an increased utilization of GSH in conjugation reactions involved in the metabolism of lipid hydroperoxides formed by the CuO NPs–induced peroxidation of cellular membranes (Canesi *et al*., 1999; Chapter 2). Several other studies have demonstrated a similar relationship between NPs exposure and GST induction not only in medaka fish *Oryzias latipes* exposed to Ag NPs (1–25 $\mu g.L^{-1}$, 49.6 nm, 1–4 days) but also in clams *Scrobicularia plana* and mussels *M. galloprovincialis* exposed to CuO NPs (10 $\mu g.L^{-1}$, 40-500 nm, 16 days) and $TiO_2$ NPs (0.05–1.5 $mg.mL^{-1}$, 22 nm, 24h), respectively (e.g. Buffet *et al*., 2011; Canesi *et al*., 2010; Chae *et al*., 2009).

Cathepsin L (catL) (spot nº4802) and caspase 3/7–1 (spot nº7710) were two proteins were up– and down–regulated after exposure to CuO NPs in the digestive gland (Table 5.4, Fig. 5.4). CatL is a cysteine protease normally located in lysosomes, where it contributes to lysosomal digestion and detoxification and to the initiation of degradation of exogenous and endogenous proteins (Margiotta–Casaluci and Carnevali, 2009; Yang *et al*., 2010), and is one of the most highly up–regulated genes in mussels exposed to metal or organic mixtures (Venier *et al*. 2006). In the digestive gland, metals (e.g. $Cu^{2+}$) are detoxified in lysosomes where they are captured in insoluble oxide forms (e.g. Cu–thionein and lipofuscin) and eliminated via exocytosis (e.g. Viarengo *et al*., 1981, 1990). However, this does not seem to be the case, and the up–regulation of catL is probably associated with CuO NPs uptake in cells. After entering cells, NPs are sequestered into lysosomes, where proteolytic enzymes as catL will participate in the degradation of ingested particles (e.g. Koehler *et al*. 2008, Moore,

2006). As previously detected in Chapter 2.2, the increasing accumulation of CuO NPs with time of exposure in the digestive gland of mussels demonstrated that the lysosomes are not able to eliminate these particles either bound to MT or to lipid peroxidation products, resulting in a higher retention rate of CuO NPs in this tissue. The digestive gland cells are highly adapted to endocytosis of large particles and this mode of uptake is especially relevant where aggregation of NPs occurs (Koehler *et al*., 2008; Moore, 2006; Ward and Kach, 2009), as in the case of the CuO NPs (Table 5.1). Nanoparticle uptake and accumulation by lysosomes are also be responsible for lysosomal membrane destabilization that will result in organelle clumping, oxidative cell injury, intracellular $Ca^{2+}$ release, mitochondrial depolarization and cell death (see Canesi *et al*., 2012; Xia *et al*., 2008).

The apoptotic process in bivalve molluscs is tightly regulated by the overexpression/ suppression of the caspase genes and is of great importance in the digestive gland (Romero *et al*., 2011). The present results indicate that apoptosis directly reflect the cytotoxicity of CuO NPs in the digestive gland of mussels, highlighted by the down–regulation (14–fold) of the protein caspase 3/7–1 (spot nº7710, Table 5.4, Fig. 5.4). Apoptosis, or programmed cell death, is a complex and highly regulated process during which irreparably damaged cells are eliminated (Garrido *et al*., 2001; Huang *et al*., 2010b). Exposure to NPs (e.g. Cu NPs, ZnO NPs, Ag NPs) seem to cause several metabolic disorders in human cells, as ATP depletion, increased $Ca^{2+}$ levels, ROS/RNS overproduction, DNA damage that eventually lead to cell death, however, it is unclear which pathways are involved (Asharani *et al*., 2009; Huang *et al*., 2010a, b; Karlsson *et al*., 2009; Manna *et al*., 2012; Sarkar *et al*., 2011). Different pathways can lead to apoptosis, which can be mitochondria depended (intrinsic pathway) or independent via death receptors (extrinsic pathway). In the intrinsic pathway, mitochondria play an important role in the initiation of apoptosis (that in response to oxidative stress, genotoxic or other specific apoptotic signals, release cytochrome c into the cytosol (increased permeability of their membranes) that triggers an apoptotic cascade, via caspase family members, ultimately leading to cell death. On the other hand, the extrinsic pathway is activated by extracellular ligands that are recognized by plasma membrane death receptors (implicated mainly in inflammatory and immune responses), resulting in the direct activation of the caspase cascade and/or induction of the mitochondrial apoptotic pathway (Arora *et al*., 2008; Garrido *et al*., 2001; Huang *et al*., 2010b; Romero *et al*., 2011; Sarkar *et al*., 2011). Excessive DNA damage associated with oxidative stress may also trigger apoptosis by numerous and complex pathways associated with the activation of the p53 protein (Karlsson

*et al*., 2009). CuO NPs induce DNA strand breaks in mussels' hemocytes where a role of ROS was suggested (Chapter 4). Another cause of apoptosis related to nanoparticles toxicity is the increase of $Ca^{2+}$ levels in cells. As stated earlier, the interaction of nanoparticles with cellular structures (e.g. cytoskeleton proteins, mitochondria, endoplasmic reticulum) results in the generation of ROS along with an increase of $Ca^{2+}$ in the cytosol that eventually will lead to cell death (Asharani *et al*., 2009; Huang *et al*., 2010a, b; Karlsson e al., 2009; Manna *et al*., 2012; Sarkar *et al*., 2011). In mussels exposed to glass wool (3–7 μm; 0.18–1 μm) a continuous uptake of NPs was detected in the digestive gland over 16 days of exposure, which resulted in large aggregates of lysosomes full of ingested nanoparticles and finally apoptosis (Koehler *et al*., 2008). Lysosomal cysteine proteases are not normally thought to participate in apoptosis, however, under oxidative stress; lysosomal membranes can disintegrate and leak their constituents into the cytosol activating apoptotic events. Once released, catL may act through caspase–dependent or independent mechanisms by either facilitating the release of cytochrome C from mitochondria or directly activating caspase–3 (Cailhier *et al*., 2008; Pratt *et al*., 2009; Yang *et al*., 2010). Nevertheless, the precise mechanisms of catL (or any other cathepsins) in programmed cell death are not clear yet, specially associated with NPs toxicity. In human cells, the mechanism of toxicity of $TiO_2$ NPs is governed by the loss of lysosomal integrity and the consequence release of cathepsin B, initiating apoptotic pathways (Hamilton *et al*., 2009). Although this aspect obviously deserves further research, it is conceivable to hypothesize that the up–regulation of catL in the digestive gland may be determinant for the regulation of CuO NPs–induced apoptosis. Moreover, heat–shock proteins are also among the well–established anti–apoptotic proteins, functioning as potent endogenous modulators of cell death (Garrido *et al*., 2001; Takayama *et al*., 2003). In fact, HSP 70 overexpression can protect cells from stress–induced apoptosis by inhibiting caspase–dependent events along the pathway of caspase cascade activation (Garrido *et al*., 2001; Kefaloyianni *et al*., 2005; Takayama *et al*., 2003). Accordingly, the decrease in caspase 3/–1 in the digestive gland of CuO NPs–exposed mussels may also be related to the observed overexpression of heat–shock cognate 71. Although we did not identify any other specific marker for different modes of apoptosis (except caspase 3/7–1), the observed microtubules and actin disorganization, alterations in the mitochondrial membrane potential, capacity to induce ROS (NPs surface reactivity and/or release $Cu^{2+}$), potency to genotoxicity (already reported for CuO NPs in mussels haemocytes – Chapter 4) and disruption of the membrane systems (lipid peroxidation/ROS) together with

disorganization of intracellular $Ca^{2+}$ homeostasis (cytoskeleton/oxidative stress) seems to point towards multiple ways of CuO NPs to induce cell death.

Lastly, precollagen–D (precol–D, spot nº5808) was up–regulated by $Cu^{2+}$ in the digestive gland (Table 5.4, Fig. 5.4). Precol–D is one of the collagen fibers that are mainly associated with byssus secretion (Lucas *et al*., 2002). In mussels *Perna viridis* (Nicholson and Lam, 2005) and oysters *Saccostrea glomerata* (Thompson *et al*., 2012) alterations in non–gradient byssal precursor proteins were observed in response to $Cu^{2+}$ exposure. Byssal threads are mainly constituted by collagen proteins and contain some metal binding sites that are responsible for the accumulation of several metals. The byssus has an active role in the elimination of metals (including Cu) as they are actively transferred from the soft tissues and concentrated in byssus to be further eliminated (Nicholson and Szefer, 2003; Nicholson and Lam, 2005; Szefer *et al*., 2006). Accordingly, our results suggest that the up–regulation of these proteins may be associated with the detoxification mechanisms of $Cu^{2+}$ in mussels' digestive gland, which are in accordance with the accumulation results observed in Chapter 2.2.

This study revealed for the first time the utility of proteomics to assess differences in protein expression in mussels exposed to CuO NPs and $Cu^{2+}$ and provided additional knowledge of potential CuO NPs effects at biochemical and molecular level. Overall both Cu forms induced major alterations in PEPs in gills and digestive gland showing several tissue and Cu–dependant responses mainly from differences between accumulation and modes of action. Identified proteins indicate common response mechanisms induced by CuO NPs and $Cu^{2+}$, namely in cytoskeleton and cell structure (actin, α–tubulin, paramyosin), stress response (heat shock cognate 71, putative C1q domain containing protein), transcription regulation (zinc–finger BED domain–containing protein 1, nuclear receptor subfamily 1G) and energy metabolism (ATP synthase F0 subunit 6). Additionally, there is an indication that there are different underlying mechanisms of toxicity for CuO NPs and $Cu^{2+}$, mainly depicted by the set of differently expressed proteins obtained in both the gills and digestive gland of exposed mussels. CuO NPs had marked effects on oxidative stress (GST), apoptosis (caspase 3/7–1) and proteolysis (cathepsin L). On the other hand, $Cu^{2+}$ had a marked effect in proteins normally associated with adhesion and mobility, precollagen D. These results clearly show that the toxicity of CuO NPs is not solely due to $Cu^{2+}$ dissolution and is mediated by oxidative stress–induced cell signalling cascades (including signals from mitochondria and nucleus) that eventually lead to apoptosis. Even though the dataset obtained highlights some

of the drawbacks in applying this type of proteomics in bivalve species, as limitations in protein identification by low signal intensities (insufficient amount of peptide) or a poor representation of bivalve species in DNA and protein databases (López *et al*., 2005; Thompson *et al*., 2012), the present study identified a number of traditional (e.g. HSPs, actin, GST, ATP synthase) and potentially novel (caspase 3/7–1, catL, Zn–finger, precol–D) molecular biomarkers for CuO NPs and $Cu^{2+}$ exposure in mussel tissues. Future studies are needed to investigate more thoroughly some of the mechanisms referred and clarify how NPs interact with target sites (e.g. mitochondria, nucleus) and in what form they remain in the cell ($Cu^{2+}$ or NPs).

## 5.5. References

Achard–Joris, M.; Gonzalez, P.; Marie, V.; Baudrimont, M.; Bourdineaud, J.–P. (2006). cDNA cloning and gene expression of ribosoma S9 protein gene in the mollusk *Corbicula fluminea*: A new potential biomarker of metal contamination up–regulated by cadmium and repressed by zinc. *Environmental Toxicology and Chemistry*. **25(2):** 527–533.

Apraiz, I.; Cajaraville, M.P.; Cristobal, S. (2009). Peroxisomal proteomics: Biomonitoring in mussels after the Prestige's oil spill. *Marine Pollution Bulletin*. **58(12):** 1815–1826.

Apraiz, I.; Mi, J.; Cristobal, S. (2006). Identification of proteomic signatures of exposure to marine pollutants in mussels (*Mytilus edulis*). *Molecular and Cellular Proteomics*. **5(7):** 1274–1285.

Arora, S.; Jain, J.; Rajwade, J.M.; Paknikar, K.M. (2008). Cellular responses induced by silver nanoparticles: In vitro studies. *Toxicology Letters*. **179:** 93–100.

Asharani, P.V.; Hande, M.P.; Valiyaveettil, S. (2009). Anti–proliferative activity of silver nanoparticles. *BMC Cell Biology*. **10:** 65.

Banci, L.; Bertini, I.; Ciofi–Baffoni, S.; D'Alessandro, A.; Jaiswal, D.; Marzano, V.; Neri, S.; Ronci, M.; Urbani, A. (2011). Copper exposure effects on yeast mitochondrial proteome. Journal of Proteomics. **74:** 2522–2535.

Bhatt, I.; Tripathi, B.N. (2011). Interaction of engineered nanoparticles with various components of the environment and possible strategies for their risk assessment. *Chemosphere*. **82(3):** 308–317.

Blum, H.; Biere, H.; Gross, H.J. (1987). Improved silver staining of plant proteins, RNA and DNA in polyacrylamide gels. *Electrophoresis.* **8:** 93–99.

Bradford, M. (1976). A rapid and sensitive method for the quantitation of microgram quantities of protein utilizing the principle of protein–dye binding. *Analytical Biochemistry*. **72:** 248–254.

Buffet, P.E.; Tankoua, O.F.; Pan, J.F.; Berhanu, D.; Herrenknecht, C.; Poirier, L.; Amiard–Triquet, C.; Amiard, J.C.; Bérard, J.B.; Risso, C.; Guibbolini, M.; Roméo, M.; Reip, P.; Valsami–Jones, E.; Mouneyrac, C. (2011). Behavioural and biochemical responses of two

marine invertebrates *Scrobicularia plana* and *Hediste diversicolor* to copper oxide nanoparticles. *Chemosphere*. **84:** 166–174.

Cailhier, J.–F.; Sirois, I.; Laplante, P.; Lepage, S.; Raymond, M–.A.; Brassard, N.; Prat, A.; Iozzo, R.V.; Pshezhetsky, A.V.; Hébert, M.J. (2008). Caspase–3 activation triggers extracellular cathepsin L release and endorepellin proteolysis. *The Journal of Biological Chemistry*. **283(40):** 27220–27229.

Canesi, L.; Ciacci, C.; Fabbri, R.; Marcomini, A.; Pojana, G.; Gallo, G. (2012). Bivalve molluscs as a unique target group for nanoparticle toxicity. *Marine Environmental Research*. **76:** 16–21.

Canesi, L.; Fabbri, R.; Vallotto, D.; Marcomini, A.; Pojana, G. (2010). Biomarkers in *Mytilus galloprovincialis* exposed to suspensions of selected nanoparticles (Nano carbon black, C60 fullerene, Nano–$TiO_2$, Nano–$SiO_2$). *Aquatic Toxicology*. **100:** 168–177.

Canesi, L.; Viarengo, A.; Leonzio, C.; Filippelli, M.; Gallo, G. (1999). Heavy metals and glutathione metabolism in mussel tissues. *Aquatic Toxicology*. **46:** 67–76.

Chae, Y.J.; Pham, C.H.; Lee, J.; Bae, E.; Yi, J.; Gu, M.B. (2009). Evaluation of the toxic impact of silver nanoparticles on Japanese medaka (*Oryzias latipes*). *Aquatic toxicology*. **94(4):** 320–327.

da Silva, J.J.R.F.; Williams, R.J.P. (2001). *The Biological Chemistry of the Elements: The Inorganic Chemistry of Live*, 2nd ed.; Oxford University Press: New York.

Dalle–Donne, I.; Rossi, R.; Milzani, A.; Di Simplicio, P.; Colombo, R. (2001). The actin cytoskeleton response to oxidants: from small heat shock protein phosphorylation to changes in the redox state of actin itself. *Free Radical Biology and Medicine*. **31(12):** 1624–1632.

Dutton, J.M.; Hofmann, G.E. (2009). Biogeographic variation in *Mytilus galloprovincialis* heat shock gene expression across the eastern Pacific range. *Journal of Experimental Marine Biology and Ecology*. **376:** 37–42.

Fahmy, B.; Cormier, S.A. (2009). Copper oxide nanoparticles induce oxidative stress and cytotoxicity in airway epithelial cells. *Toxicology In Vitro*. **23:** 1365–1371.

Fitzpatrick, P.J.; Krag, T.O.; Hojrup, P.; Sheehan, D. (1995). Characterization of a glutathione S–transferase and a related glutathione–binding protein from gill of the blue mussel, *Mytilus edulis*. *Biochemical Journal*. **305:** 145–150.

Gaetke, L.M.; Chow, C.K. (2003). Copper toxicity, oxidative stress, and antioxidant nutrients. *Toxicology*. **189:** 147–163.

Galaris, D.; Evangelou, A. (2002). The role of oxidative stress in mechanisms of metal–induced carcinogenesis. *Critical Reviews in Oncology/Hematology*. **42:** 93–103.

Garrido, C.; Gurbuxani, S.; Ravagnan, L.; Kroemer, G. (2001). Heat shock proteins: endogenous modulators of apoptotic cell death. *Biochemical and Biophysical Research Communications*. **286:** 433–442.

Gerdol, M.; Manfrin, C.; De Moro, G.; Figueras, A.; Novoa, B.; Venier, P.; Pallavicini, A. (2011). The C1q domain containing proteins of the Mediterranean mussel *Mytilus galloprovincialis*: A widespread and diverse family of immune–related molecules. *Developmental and Comparative Immunology*. **35:** 635–643.

Gestal, C.; Pallavicini, A.; Venier, P.; Novoa, B.; Figueras, A. (2010). MgC1q, a novel C1q–domain–containing protein involved in the immune response of *Mytilus galloprovincialis*. *Developmental and Comparative Immunology*. **34:** 926–934.

Gómez–Mendikute, A.; Cajaraville, M.P. (2003). Comparative effects of cadmium, copper, paraquat and benzo[a]pyrene on the actin cytoskeleton and production of reactive oxygen species (ROS) in mussel haemocytes. *Toxicology In vitro*. **17:** 539–546.

Gonzalez, L.; Lison, D.; Kirsch–Volders, M. (2008). Genotoxicity of engineered nanomaterials: A critical review. *Nanotoxicology*. **2(4):** 252–273.

Griffitt, R.J.; Hyndman, K.; Denslow, N.D.; Barber, D.S. (2009). Comparison of molecular and histological changes in zebrafish gills exposed to metallic nanoparticles. *Toxicological Sciences*. **107(2):** 404–415.

Gupta, A.K.; Gupta, M.; Yarwood, S.J.; Curtis, A.S.G. (2004). Effect of cellular uptake of gelatin nanoparticles on adhesion, morphology and cytoskeleton organisation of human fibroblasts. *Journal of Controlled Release*. **95:** 197–207.

Halliwell, B.; Gutteridge, J.M.C. (1984). Oxygen toxicity, oxygen radicals, transition metals and disease. *Biochemical Journal*. **219:** 1–14.

Hamilton Jr., R.F.; Wu, N.; Porter, D.; Buford, M.; Wolfarth, M.; Holian, A. (2009). Particle length–dependent titanium dioxide nanomaterials toxicity and bioactivity. *Particle and Fibre Toxicology*. **6**: 35.

Handy, R.D.; Cornelis, G.; Fernandes, T.; Tsyusko, O.; Decho, A.; Sabo–Attwood, T.; Metcalfe, C.; Steevens, J.A.; Klaine, S.J.; Koelmans, A.A.; Horn, N. (2012). Ecotoxicity test methods for engineered nanomaterials: Practical experiences and recommendations from the bench. *Environmental Toxicology and Chemistry*. **31(1):** 15–31.

Handy, R.D.; Kammer, F.; Lead, J.R.; Hassellöv, M.; Owen, R.; Crane, M. (2008). The ecotoxicology and chemistry of manufactured nanoparticles. *Ecotoxicology*. **17:** 287–314.

Hartwig, A. (2001). Zinc finger proteins as potential targets for toxic metal ions: Differential effects on structure and function. *Antioxidants and redox signaling*. **3(4):** 625–634.

Heinlaan, M.; Kahru, A.; Kasemets, K.; Arbeille, B.; Prensier, G.; Dubourgier, H.–C. (2011). Changes in the *Daphnia magna* midgut upon ingestion of copper oxide nanoparticles: A transmission electron microscopy study. *Water Research*. **45:** 179–190.

Hoarau, P.; Damiens, G.; Roméo, M.; Gnassia–Barelli, M.; Bebianno, M.J. (2006). Cloning and expression of a GST–pi gene in *Mytilus galloprovincialis*. Attempt to use the GST–pi transcript as a biomarker of pollution. *Comparative Biochemistry and Physiology, Part C*. **143:** 196–203.

Huang, C.–C.; Aronstam, R.S.; Chen, D.–R.; Huang, Y.–W. (2010a). Oxidative stress, calcium homeostasis, and altered gene expression in human lung epithelial cells exposed to ZnO nanoparticles. *Toxicology in Vitro*. **24:** 45–55.

Huang, Y.–C.; Wu, C.–h.; Aronstam, R.S. (2010b). Toxicity of transition metal oxide nanoparticles: Recent insights from *in vitro* studies. *Materials*. **3:** 4842–4859.

Karlsson, H.L. (2010). The comet assay in nanotoxicology research. *Analytical and Bioanalytical Chemistry*. **398:** 651–666.

Karlsson, H.L.; Gustafsson, J.; Cronholm, P.; Möller, L. (2009). Size-dependent toxicity of metal oxide particles – A comparison between nano– and micrometer size. *Toxicology Letters*. **188:** 112–118.

Kefaloyianni, E.; Gourgou, E.; Ferle, V.; Kotsakis, E.; Gaitanaki, C.; Isidoros Beis, I. (2005). Acute thermal stress and various heavy metals induce tissue–specific pro– or anti– apoptotic events *via* the p38–MAPK signal transduction pathway in *Mytilus galloprovincialis* (Lam.). *The Journal of Experimental Biology*. **208:** 4427–4436.

Koehler, A.; Marx, U.; Broeg, K.; Bahns, S.; Bressling, J. (2008). Effects of nanoparticles in *Mytilus edulis* gills and hepatopancreas – a new threat to marine life? *Marine Environmental Research*. **66(1):** 12–14.

Leung, P.T.Y.; Wang, Y.; Mak, S.S.T.; Ng, W.C.; Leung, K.M.Y. (2011). Differential proteomic responses in hepatopancreas and adductor muscles of the green–lipped mussel *Perna viridis* to stresses induced by cadmium and hydrogen peroxide. *Aquatic Toxicology.* **105:** 49–61.

López–Barea, J.; Gómez–Ariza, J.L. (2006). Environmental proteomics and metallomics. *Proteomics*. **6:** S51–S62.

López, J.L. (2005). Role of proteomics in taxonomy: the *Mytilus* complex as a model of study. *Journal of Chromatography B*. **815:** 261–274.

Lucas, J.M.; Vaccaro, E.; Waite, J.H. (2002). A molecular, morphometric and mechanical comparison of the structural elements of byssus from *Mytilus edulis* and *Mytilus galloprovincialis*. *The Journal of Experimental Biology*. **205:** 1807–1817.

Manna, P.; Ghosh, M.; Shosh, J., Das, J.; Sil, P.C. (2012). Contribution of nano–copper particles to in vivo liver dysfunction and cellular damage: Role of IκBα/NF–κB, MAPKs and mitochondrial signal. *Nanotoxicology*. **6(1):** 1–21.

Margiotta–Casaluci, L.; Carnevali, O. (2009). Can estrogenic compounds enhance the activity of cathepsin D and cathepsin L in the mussel, *Mytilus galloprovincialis*? *Chemistry and Ecology.* **25(1):** 49–60.

Maria, V.L.; Bebianno, M.J. (2011). Antioxidant and lipid peroxidation responses in *Mytilus galloprovincialis* exposed to mixtures of benzo(a)pyrene and copper. *Comparative Biochemistry and Physiology Part C: Toxicology and Pharmacology*. **154(1):** 56–63.

Matozzo, V.; Ballarin, L.; Pamparin, D.M.; Marin, M.G. (2001). Effects of copper and cadmium exposure on functional responses of hemocytes in the clam, *Tapes philippinarum*. *Archives in Environmental Contamination and Toxicology*. **41:** 163–170.

McDonagh, B.; Sheehan, D. (2006). Redox proteomics in the blue mussel *Mytilus edulis*: Carbonylation is not a pre–requisite for ubiquitination in acute free radical–mediated oxidative stress. *Aquatic Toxicology*. **79(4):** 325–333.

McDonagh, B.; Tyther, R.; Sheehan, D. (2005). Carbonylation and glutathionylation of proteins in the blue mussel *Mytilus edulis* detected by proteomic analysis and Western blotting: Actin as a target for oxidative stress. *Aquatic Toxicology*. **73:** 315–326.

Mironava, T.; Hadjiargyrou, M.; Simon, M.; Jurukovski, V.; Rafailovich, M.H. (2010). Gold nanoparticles cellular toxicity and recovery: Effect of size, concentration and exposure time. *Nanotoxicology*. **4(1):** 120–137.

Miura, Y.; Kano, M.; Abe1, K.; Urano, S.; Suzuki, S.; Toda, T. (2005). Age–dependent variations of cell response to oxidative stress: Proteomic approach to protein expression and phosphorylation. *Electrophoresis.* **26:** 2786–2796.

Moore, M.N. (2006). Do nanoparticles present ecotoxicological risks for the health of the aquatic environment? *Environmental International*. **32:** 967–976.

Nicholson, S.; Lam, P.K.S. (2005). Pollution monitoring in Southeast Asia using biomarkers in the mytilid *mussel Perna viridis* (Mytilidae: Bivalvia). *Environment International*. **31:** 121–132.

Nicholson, S.; Szefer, P. (2003). Accumulation of metals in the soft tissues, byssus and shell of the mytilid mussel *Perna viridis* (Bivalvia: Mytilidae) from polluted and uncontaminated locations in Hong Kong coastal waters. *Marine Pollution Bulletin*. 46: 1035–1048.

Orrenius, S.; Gogvadze, A.; Zhivotovsky. B. (2007). Mitochondrial oxidative stress: Implications for cell death. *Annual Review of Pharmacology and Toxicology*. **47:** 143–183.

Pratt, M.R.; Sekedat, M.D.; Chiang, K.P.; Muir, T.W. (2009). Direct measurement of cathepsin B activity in the cytosol of apoptotic cells by an activity–based probe. *Chemistry and Biology*. **16:** 1001–1012.

Puerto, M.; Campos, A.; Prieto, A.; Cameán, A.; de Almeida, A.M.; Coelho, A.V.; Vasconcelos, V. (2011). Differential protein expression in two bivalve species; *Mytilus galloprovincialis* and *Corbicula fluminea*; exposed to *Cylindrospermopsis raciborskii* cells. *Aquatic Toxicology*. **101:** 109–116.

Regoli, F.; Principato, G. (1995). Glutathione, glutathione–dependent and antioxidant enzymes in mussel, *Mytilus galloprovincialis*, exposed to metals under field and laboratory conditions: implications for the use of biochemical biomarkers. *Aquatic Toxicology*. **31:** 143–164.

Rodríguez–Ortega, M.J.; Grøsvik, B.E.; Rodríguez–Ariza, A.; Goksøyr, A.; López–Barea, J. (2003). Changes in protein expression profiles in bivalve molluscs (*Chamaelea gallina*) exposed to four model environmental pollutants. *Proteomics*. **3:** 1535–1543.

Romero, A.; Estévez–Calvar, N.; Dios, S.; Figueras, A.; Novoa, B. (2011). New insights into the apoptotic process in mollusks: Characterization of caspase genes in *Mytilus galloprovincialis*. *PLoS ONE*. **6(2):** e17003.

Sarkar, A.; Das, J.; Manna, P.; Sil, P.C. (2011). Nano–copper induces oxidative stress and apoptosis in kidney via both extrinsic and intrinsic pathways. *Toxicology*. **290:** 208–217.

Scown, T.M.; Aerle, R.V.; Tyler, C.R. (2010). Review: do engineered nanoparticles pose a significant threat to the aquatic environment? *Critical Reviews in Toxicology*. **40(7):** 653–670.

Shepard, J.L.; Bradley, B.P. (2000). Protein expression signatures and lysosomal stability in *Mytilus edulis* exposed to graded copper concentrations. *Marine Environmental Research*. **50:** 457–463.

Shepard, J.L.; Olsson, B.; Tedengren, M.; Bradley, B.P. (2000). Protein expression signatures identified in *Mytilus edulis* exposed to PCBs, copper and salinity stress. *Marine Environmental Research*. **50:** 337–340.

Shevchenko, A.; Tomas, H.; Havlis, J.; Olsen, J.V.; Mann, M. (2007). In–gel digestion for mass spectrometric characterization of proteins and proteomes. *Nature Protocols.* **1(6):** 2856–2860.

Szefer, P.; Fowler, S.W.; Ikuta, K.; Osuna, F.P.; Ali, A.A.; Kim, B.–S.; Fernandes, H.M.; Belzunce, M.–J.; Guterstam, B.; Kunzendorf, H.; Wo1owicz, M.; Hummel, H.; Deslous–Paoli, M. (2006). A comparative assessment of heavy metal accumulation in soft parts and byssus of mussels from subarctic, temperate, subtropical and tropical marine environments. *Environmental Pollution*. **139:** 70–78.

Takayama, S.; Reed, J.C.; Homma, S. (2003). Heat–shock proteins as regulators of apoptosis. *Oncogene*. **22:** 9041–9047.

Tedesco, S.; Doyle, H.; Blasco, J.; Redmond, G.; Sheehan, D. (2010). Oxidative stress and toxicity of gold nanoparticles in *Mytilus edulis*. *Aquatic Toxicology*. **100:** 178–186.

Thompson, E.L.; Taylor, D.A.; Nair, S.V.; Birch, G.; Haynes, P.A.; Raftos, D.A. (2012). Proteomic discovery of biomarkers of metal contamination in Sydney Rock oysters (*Saccostrea glomerata*). *Aquatic Toxicology*. **109:** 202–212.

Tiede, K.; Hassellöv, M.; Breitbarth, E.; Chaudhry, Q.; Boxall, A.B.A. (2009). Considerations for environmental fate and ecotoxicity testing to support environmental risk assessments for engineered nanoparticles. *Journal of Chromatography A*. **1216(3):** 503–509.

Venier, P.; De Pittà, C.; Pallavicini, A.; Marsano, F.; Varotto, L.; Romualdi, C.; Dondero, F.; Viarengo, A.; Lanfranchi, G. (2006). Development of mussel mRNA profiling: Can gene expression trends reveal coastal water pollution? *Mutation Research*. **602:** 121–134.

Viarengo, A.; Canesi, L.; Pertica, M.; Poli, G.; Moore, M.N.; Orunesu, M. (1990). Heavy metal effects on lipid peroxidation in the tissues of *Mytilus galloprovincialis* Lam. *Comparative Biochemistry and Physiology Part C: Comparative Pharmacology*. **97(1):** 37–42.

Viarengo, A.; Zanicchi, G.; Moore, M.N.; Orunesu, M. (1981). Accumulation and detoxification of copper by the mussel *Mytilus galloprovincialis* Lam: a study of subcellular distribution in the digestive gland cells. *Aquatic Toxicology*. **1:** 147–157.

Vioque-Fernández, A. de Almeida, E.A.; López-Barea, J. (2009). Assessment of Doñana National Park contamination in *Procambarus clarkii*: Integration of conventional biomarkers and proteomic approaches. *Science of the Total Environment*. **407:** 1784-1797.

Ward, J.E.; Kach, D.J. (2009). Marine aggregates facilitate ingestion of nanoparticles by suspension–feeding bivalves. *Marine Environmental Research.* **68:** 137–142.

Watabe, S.; Iwasaki, K.; Funabara, D.; Hirayama, Y.; Nakaya, M.; Kikuchi, K. (2000). Complete amino acid sequence of *Mytilus* anterior byssus retractor paramyosin and its putative phosphorylation site. *Journal of Experimental Zoology*. **286:** 24–35.

Xia, T.; Kovochich, M.; Liong, M.; Mädler, L.; Gilbert, B.; Shi, H.; Yeh, J.I.; Zink, J.I.; Nel, A.E. (2008). Comparison of the mechanism of toxicity of zinc oxide and cerium oxide nanoparticles based on dissolution and oxidative stress properties. *ACS Nano*. **10(2):** 2121–2134.

Yamada, A.; Yoshio, M.; Oiwa, K.; Nyitray, L. (2000). Catchin, a novel protein in molluscan catch muscles, is produced by alternative splicing from the myosin heavy chain gene. *Journal of Molecular Biology*. **295:** 169–178.

Yang, Z.; Wu, H.; Li, Y. (2010). Toxic Effect on Tissues and Differentially Expressed Genes in Hepatopancreas Identified by Suppression Subtractive Hybridization of Freshwater Pearl Mussel (*Hyriopsis cumingii*) Following Microcystin–LR Challenge. *Environmental Toxicology*. **27(7):** 393–403.

# CHAPTER 6

## Differential protein expression in mussels *Mytilus galloprovincialis* exposed to nano and ionic Ag

# 6.

# DIFFERENTIAL PROTEIN EXPRESSION IN MUSSELS *MYTILLUS GALLOPROVINCIALIS* EXPOSED TO NANO AND IONIC Ag

*Tânia Gomes, Catarina G. Pereira, Cátia Cardoso, Maria João Bebianno*

CIMA, Faculty of Science and Technology, University of Algarve, Campus de Gambelas, 8005–139 Faro, Portugal

Submitted to Aquatic Toxicology

## Abstract

Ag NPs is one of the most commonly used NPs in nanotechnology whose environmental impacts are to date unknown and the information about bioavailability, mechanisms of biological uptake and toxic implications in organisms is scarce. So, the main objective of this study was to investigate differences in protein expression profiles in gills and digestive gland of mussels *M. galloprovincialis* exposed to Ag NPs and $Ag^{+}$ (10 $\mu g.L^{-1}$) for a period of 15 days. Protein expression profiles of exposed gills and digestive gland were compared from those of control mussels using two–dimensional electrophoresis to discriminate differentially expressed proteins. Different patterns of protein expression were obtained for exposed mussels, dependent not only on the different redox requirements of each tissue but also to the Ag form used. Unique sets of differentially expressed proteins were affected by each silver form in addition to proteins that were affected by both Ag NPs and $Ag^{+}$. Fifteen of these proteins were subsequently identified by MALDI–TOF–TOF and database search. Ag NPs affected similar cellular pathways as $Ag^{+}$, with common response mechanisms in cytoskeleton and cell structure (catchin, myosin heavy chain), stress response (heat shock protein 70), oxidative stress (glutathione s–transferase), transcription regulation (nuclear receptor subfamily 1G), adhesion and mobility (precollagen–P) and energy metabolism (ATP synthase F0 subunit 6 and NADH dehydrogenase subunit 2). Exposure to Ag NPs altered the expression of two proteins associated with stress response (major vault protein and ras partial) and one protein involved in cytoskeleton and cell structure (paramyosin), while exposure to $Ag^{+}$ had a strong influence in one protein related to stress response (putative c1q domain containing protein) and two proteins involved in cytoskeleton and cell structure (actin and $\alpha$–tubulin). Protein identification showed that Ag NPs toxicity is mediated by oxidative stress–induced cell signalling cascades (including mitochondria and nucleus) that can lead to cell death. This toxicity represents the cumulative effect of $Ag^{+}$ released from the particles and other properties as particle size and surface reactivity. This study helped to unravel the molecular mechanisms that can be associated with Ag NPs toxicity; nevertheless, some additional studies are required to investigate the exact interaction between these NPs and cellular components.


Keywords: *Mytilus galloprovincialis*, proteomic analysis, Ag NPs, two–dimensional gel electrophoresis, MALDI–TOF–TOF

## 6.1. Introduction

Nanoparticles (NPs) are defined as particles with dimensions between 1–100 nm whose unique properties (e.g. small size, high surface–area) are distinguishable from their micro–sized equivalents. The exploration of the properties and applications of NPs have made nanotechnology an expanding industry that covers a high range of areas as medicine, cosmetics, electronics, food products and environmental remediation (Handy *et al*., 2008; Tiede *et al*., 2009). The rapid development and use of nanomaterials have led to a growing concern of their potential inputs and risks to ecosystems and consequently unpredictable health or environmental hazards. Whether NPs are released during their lifecycle (e.g. erosion of the materials or introduction during remediation), production facilities, wastewater treatment plants or leaching from NPs–containing products (e.g. household products) they can end up in the environment in significant quantities (Borm *et al*., 2006; Handy *et al*., 2008; Klaine *et al*., 2008). Nevertheless, it is still unknown at what amounts NPs can be found in the environment, their fate, potential bioavailability and subsequent hazardous effects to biological systems.

From the variety of NPs that are currently being developed in nanotechnology, Ag NPs are one of the most used particles in consumer products. Ag NPs have unique physico–chemical properties, including a high electrical and thermal conductivity, catalytic activity and chemical stability (Fabrega *et al*., 2011; Luoma, 2008). Nevertheless, it is their antibacterial activity that makes them of common use in textiles, eating utensils, food storage, cosmetics and personal hygiene and household appliances (e.g. washing machines, vacuum cleaners) (www.nanoproject.org). The rapid devolvement of these nano–products containing Ag NPs increase their probability to end up in the environment and interact to aquatic organisms, as bivalve molluscs.

Ionic silver ($Ag^{+}$) is a known environmental stressor due to its persistence and accumulation in the environment (water, sediments and organisms) as well as elevated toxicity towards aquatic organisms, even at low levels ($\mu g.L^{-1}$ range) (Fabrega *et al*., 2011; Luoma, 2008; Wang and Rainbow, 2005). In aquatic organisms (e.g. fish) its effects are well documented but less is known about the mechanism by which Ag in the nano form exerts toxicity to organisms, namely invertebrate species. Accumulation and adverse effects of Ag NPs (e.g. ROS–derived oxidative stress, genotoxicity, reduction metabolic activity) were reported in aquatic organisms as *Daphnia magna* (0–5 $\mu g.L^{-1}$, <50 nm, 24h), fish *Oryzias latipes* (1–25 $\mu g.L^{-1}$, 49.6 nm, 1–4 days) and oysters *Crassostrea virginica* (1.6–0.0016 $\mu g.L^{-1}$, 16 ± 6 nm,

48h), but their mechanisms of toxicity at cellular and molecular levels need to be addressed more in depth (e.g Chae *et al*., 2009; Park and Choi, 2010; Ringwood *et al*., 2010). Given the capacity of Ag NPs to release $Ag^{+}$ ions (Navarro *et al*., 2008) it seems inevitable that these particles (as well as $Ag^{+}$ ions) can easily enter cells, bind to –SH groups and modify proteins leading to the dysfunction of target structures, in addition to the effects caused by the NPs inherent properties (Bar–Ilan *et al*., 2009 and literature cited therein; Lapresta–Fernández *et al*., 2012 and literature cited therein). In this context, it seems critical to expand the information about Ag NPs presence and behaviour in the marine environment as well as their consequences in marine organisms. Mussels are particularly susceptive to NPs due to their sessile nature, filter feeding habits and capacity to bioaccumulate and concentrate xenobiotics, making them appropriate candidates for biomonitoring and ecotoxicology experiments, including nanotoxicology (Baun *et al*., 2008; Moore, 2006).

Integrated approaches have been used in nanotoxicology studies combining several biomarkers; nevertheless, many of these toxic responses (e.g. oxidative stress, enzymatic activation/inhibition, genotoxicity) are common to several contaminants, including NPs or ionic/bulk form (Handy *et al*., 2012). The use of conventional biomarkers present some disadvantages, as they can be influenced by confounding factors, require a deep knowledge of the toxic mechanisms of contaminants and prevent a more comprehensive view of toxicity by focusing in only few proteins (López–Barea and Gómez–Ariza, 2006; Vioque–Férnandez *et al*., 2009). Accordingly, there is a need to develop nano–specific biological measurements that could be used to differentiate nano–specific biological responses and mechanisms of action from their similar ionic/bulk counterparts. Proteomics–based approaches can provide a suite of responses indicative of NPs exposure or effect by looking for specific protein expression alterations. These protein expression signatures (PES) can be quantified, identified and used as unbiased biomarkers of NPs exposure (Shepard and Bradley, 2000; Shepard *et al*., 2000). These approaches were used previously to detect new biomarkers in mussels in response to conventional contaminants, as metals (e.g. Apraiz *et al*., 2006; Shepard and Bradley, 2000) and citrate gold nanoparticles (750 ppb, ~5 nm) (Tedesco *et al*., 2010). Thus, changes of PES as a result of Ag NPs or $Ag^{+}$ exposure in mussel tissues will help to identify protein pathways affected by NPs, clarify and differentiate the modes of action by which both Ag forms inflict toxicity.

The main objective of this study was to compare differential protein expression signatures in mussels *Mytilus galloprovincialis* exposed to an environmental relevant concentration of Ag NPs and $Ag^{+}$ (10 $\mu gAg.L^{-1}$) for a period of 15 days. Additionally, characterize PES and key

protein signatures specific and common for each silver form and suggest possible biomarkers for NPs exposure. Two–dimensional gel electrophoresis and mass spectrophotometry procedures were employed in proteomic analysis of gills and digestive gland of mussels to compare the exposure to Ag NPs and $Ag^{+}$.

## 6.2. Materials and methods

### 6.2.1. Preparation and characterization of Ag NPs

Silver nanoparticles (<100 nm) stock solution was prepared in ultrapure water and characterized as previously described in Chapter 3. The size (z–average hydrodynamic diameter) and surface charge (zeta potential) of Ag NPs were determined by dynamic light scattering (DLS) and electrophoretic light scattering (ELS), respectively, using a Zetasizer Nano ZS analyzer (Malvern Instruments Inc., UK). The hydrodynamic size, polydispersity index and intensity of Ag NPs in natural seawater during 12 hours (period between water renewals) were also determined using an ALV apparatus with Ar Ion Lased (514.5 nm) by DLS. The results obtained of Ag NPs characterization are summarised in Table 6.1.

### 6.2.2. Experimental design

Mussels *M. galloprovincialis* (61.7 ± 8.4 mm) were collected in the Ria Formosa Lagoon (southern coast of Portugal), transported alive to the laboratory and acclimated for 7 days in natural seawater at constant temperature and aeration. After acclimation, fifty mussels were placed in 25L tanks filled with 20L of seawater (2.5 mussels/L) in a triplicate design (3 tanks per treatment): 10 $\mu gAg.L^{-1}$ of Ag NPs, 10 $\mu g.L^{-1}$ of $Ag^{+}$, and a control group kept in clean seawater for a period of 15 days. To avoid nanoparticle aggregation, water in tanks was renewed every 12 hours with redosing of Ag solutions after each change. During the experimental period, seawater quality was confirmed daily in each tank by measuring temperature, salinity, oxygen saturation and pH (17.6 ± 0.3ºC; 36.3 ± 0.1; 96.9 ± 3.3% and 7.8 ± 0.1, respectively). Mussels were not fed during the experiment to minimize the risk of Ag NPs absorbing to food or faecal material and to help maintain water quality. No mortality was registered. Five mussels were collected from each treatment after the 15 days of exposure, dissected and gills and digestive gland immediately frozen in liquid nitrogen and stored at –80ºC until further use.

### 6.2.3. Metal analysis

Silver was analysed in water samples from control and exposure groups collected immediately after addition of Ag NPs and $Ag^{+}$ stock solution and 12 hours after water renewal and re–dosing from the Ag–exposure groups. Total silver concentrations were determined after nitric acid (2%) digestion and dissolved silver from the nanoparticle exposure group was determined after water filtration (0.02 μm filter, Anotop 25, Whatman) and acid digestion (Griffitt *et al*., 2009). Ag was also determined in dried (80ºC) mussels' gills and digestive gland (control and exposed to Ag NPs and $Ag^{+}$) after wet digestion with $HNO_3$ followed by graphite furnace atomic absorption spectrometry (AAS AAnalyst 800 – Perkin Elmer).

### 6.2.4. Cell–free extract preparation and protein assay

Pools of five gills and digestive glands were weighted, suspended in 20% (w/v) HEPES–saccharose buffer (10 mM HEPES, 250 mM saccharose, 1 mM DTT, 1 mM EDTA, 1 mM PMSF and 10% protease inhibitor cocktail), homogenized at 4ºC and centrifuged at 15,000 *g* for 2h. Protein content was determined in each tissue using the method developed by Bradford *et al*. (1976) with bovine serum albumin (BSA) as a standard. Afterwards, 100 μg of protein content of gills and digestive gland were precipitated at –20ºC for 2 hours with 20 mM DTT and 10% trichloroacetic in cold acetone, centrifuged at 10,000 *g* for 30 minutes (4ºC) and washed with cold acetone.

### 6.2.5. Two–Dimensional electrophoresis (2–DE)

100 μg of each tissue sample was incubated for 30 min in 300 μL of rehydration buffer (7M urea, 2 M thiourea, 4% CHAPS, 0.8 % pharmalyte, 65 mM DTT and bromophenol blue traces), centrifuged at 14,000 *g* for 10 min (4ºC) and applied onto 18 cm Immobiline® DryStrip, pH 4–7. Afterwards, strips were equilibrated in a SDS equilibration buffer (6 M urea, 75 mM Tris–HCl, 4% SDS, 29.3% glycerol, and bromophenol blue traces) first with 2% DTT and second with 2.5% iodoacetamide. Isoelectric focusing was performed on a IEF Cell (BIORAD, Hercules, CA) at 20ºC using the following program: 6 h of passive rehydration and 6 h of active rehydration (50V), IEF was carried out (50 μA/strip), step 1: 1,000 V for 1h, step 2: 4000 V for 1h, step 3: 8,000 V for 1h and step 4: 8,000 V until 50,000 Vh were reached. The second dimension, SDS–PAGE, was carried out on 10% polyacrylamide gels

using the Protean Cell XL Cell Format vertical system (20ºC, BIORAD, Hercules, CA) in two steps: 90V, 30 min and 300 V until separation was finished (~5h). Gels were silver stained using a protocol compatible with MS analysis (Blum *et al*., 1987, modified). To ensure the reproducibility of the gels, four replicates of each condition (control, Ag NPs and $Ag^{+}$) were prepared.

### 6.2.6. Image acquisition and analysis

The gels were scanned using a GS–800 densitometer (BIORAD, Hercules, CA) and data analysed including spot detection, quantification and normalization, matching and statistical analysis using the PDQuest software (V8.0, BIORAD, Hercules, CA). All the 2–DE maps were performed with identical background subtraction (floating ball method) after spot detection. A normalized volume for each spot was used for quantitative analyses by dividing its volume by the total volume of the detected spots on the image in order to reduce experimental errors (protein loading and staining). The normalized volumes of the different spots from Ag NPs and $Ag^{+}$ exposed tissues (gills and digestive gland) were matched against the corresponding ones from control gels. The number of valid protein spots was determined for each gel, as well as the number of proteins matched to every gel, and qualitative and quantitative differences in the protein patterns between unexposed and Ag exposed (NPs and ionic) mussels were determined. The protein intensity of each spot was normalized to the total intensity of each gel image. Only spots expressed in 2/3 of the replicates gels for each group were included in the statistical analysis. Only spots with 2–fold or higher change in protein expression in exposed gills and digestive gland (compared to controls) where considered for protein identification.

### 6.2.7. Protein digestion and identification by mass spectrometry

Proteins from the gills and digestive gland of Ag NPs and $Ag^{+}$ exposed mussels with the higher changes in protein expression (when compared to control mussels) were manually excised from silver stained gels and digested with trypsine, as described elsewhere (Shevchenko *et al*., 2007). Proteins were subjected to peptide mass fingerprint (PMF) and mass spectra were acquired using an Ultraflex II MALDI–TOF–TOF (Bruker Daltonics) operating with positive polarity in reflectron mode and spectra were acquired in the range of m/z 900–3500. A total of 3000 spectra were acquired at each spot position at a laser

frequency of 50 Hz. For MS/MS experiments a peptide ions with a S/N exceeding 25 and a peak intensity higher than 800 were selected for MS/MS. Laser shots (300 and 1000) were used to acquire the MS/ and MS/MS experiments, respectively. The laser power was 2–5% above ionization threshold. Data acquisition and processing was performed with FlexAnalysis software 3.0 (Bruker Daltonics) with the SNAP peak detection algorithm. The obtained peptide mass list was sent to the MASCOT search engine using the NCBI Database. Searches were performed using the following parameters: taxonomy: other metazoa; proteolytic enzyme: trypsin; peptide tolerance: 100 ppm; fixed modifications: carbamidomethyl (C); variable modification; oxidation (M); peptide charge state: +1; missed cleavages allowed: up to 1. The significance threshold was set to a minimum of 95%. MS BLAST searches (NCBI/Blastp) were performed against a non–redundant protein database for the available sequences for *M. galloprovincialis* (taxid: 29158) using the protein–protein BLAST algorithm (Default Parameters).

## 6.3. Results

### 6.3.1. Nanoparticles characterization

As described in Chapter 3, the size, shape and zeta potential of the Ag NPs particles were characterized by TEM and DLS analysis (Table 6.1). Ag NPs are mainly spherical in shape and polysdiperse (Fig. 6.1A). The size of Ag NPs reported by the manufacturer (< 100nm) is broadly in agreement with the sizes obtained by TEM but lower than the ones obtained by DLS. On the other hand, when suspended in seawater, Ag NPs tend to aggregate displaying higher sizes than those reported by the manufacturer. Zeta potential measurements of Ag NPs in both ultrapure water and natural seawater suggest that these NPs have a propensity to aggregate, corroborating the results obtained by the hydrodynamic diameter of particles. A typical XRD pattern of Ag nanoparticles is shown in Figure 6.1B from which the intensities and positions of the diffraction peaks of the NPs are in good agreement with the reported values (JCPDS #01–087–0718) and no peaks of impurities are found. During a period of 12h (between water renewal and redosing), the mean particle size of Ag NPs increases, showing a wide size distribution ranging from approximately 97.0 to 690.4 nm (Table 6.1, 144.2 ± 39.2 nm). On the other hand, Ag NPs intensity decreases during the 12–hour period, indicative of particles dissolution or settlement with time. A high polydispersity index was also observed by DLS (0.44 ± 0.03), suggesting that under the exposure conditions, Ag NPs tends to aggregate producing suspensions with the presence of both small and large aggregates.

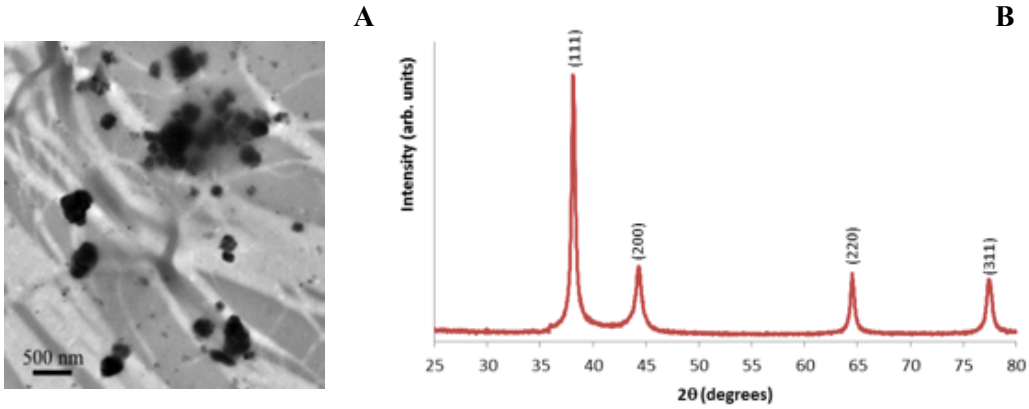


**Figure 6.1 –** Characterization of Ag NPs. (A) Transmission electron microscopic image of Ag nanoparticles at 32 ppm in Milli–Q water. (B) XRD patterns of Ag NPs.

**Table 6.1 –** Characterization of Ag nanoparticles using different techniques. Values are mean ± std.

| Particle characterization | Method | Manufacturer specifications | Ultrapure water | Natural seawater |
|---|---|---|---|---|
| Particle size (nm) | TEM | <100 | – | – |
| Specific surface area ($m^2.g^{-1}$) | – | 5.0 | – | – |
| Density ($g.cm^{-3}$) | – | 10.49 | | |
| Z–average (nm)[a] | DLS | – | 141.1 ± 3.2 | 895.5 ± 83.9 |
| Zeta potential (mV)[a] | ELS | – | –42.5 ± 1.3 | –10.2 ± 1.2 |
| Mean particle diameter (nm)[b] | DLS | – | – | 144.2 ± 39.2 |
| Polydispersity index | DLS | – | – | 0.44 ± 0.03 |

[a] 100 $mg.L^{-1}$ of Ag NPs dispersed in ultrapure and natural seawater.
[b] 100 $\mu g.L^{-1}$ of Ag NPs dispersed in natural seawater during a 12 hours cycle.

### 6.3.2. Metal analysis

Silver analysis of water samples showed that Ag concentrations were below the detection limit (<1 $\mu g.L^{-1}$). Immediately after dosing, the actual Ag concentrations in the exposure tanks were 41.3% and 39.4% lower than the nominal concentration of 10$\mu g Ag.L^{-1}$ for Ag

NPs and $Ag^+$, respectively. After the 12h period between water change and redosing, more than 80% of the initial added dose of 10μgAg.$L^{-1}$ added in the nano or ionic form was removed from the water column (84.2% for Ag NPs and 89.1% for $Ag^+$). Of the total Ag concentrations obtained from the Ag NPs exposure (4.13 ± 0.1 μg.$L^{-1}$), around 24.5% of the initial added dose is present in the dissolved form, indicating that most of the Ag present in solution is in the nanoparticulate form. The percentage of total dissolved Ag from the Ag NPs increased to 44.2 % after 12 hours indicating that these particles tend to dissolve in seawater with increasing time of exposure.

Silver concentrations in mussel tissues significantly increased in gills and digestive glands of Ag exposed mussels compared with controls (Table 6.2) ($p$<0.05). Upon 15 days of exposure, Ag in the gills increased by 14–fold for Ag NPs and 20–fold for $Ag^+$ (but similar among conditions, $p$>0.05), whereas in the digestive gland, mussels exposed to Ag NPs accumulated higher (2–fold) Ag levels (27.7 ± 4.7 μg.$g^{-1}$ dw) than those exposed to $Ag^+$ (13.8 ± 2.1 μg.$g^{-1}$ dw). The accumulation of Ag in the digestive gland was 5–fold higher in Ag NPs exposure when compared with the gills and around 2–fold in $Ag^+$ exposed mussels. The accumulation patterns of both Ag NPs and $Ag^+$ along the 15 days of exposure are described in detail in Chapter 3.

**Table 6.2 –** Silver concentrations (μg.$g^{-1}$ dry weight) in gills and digestive gland of mussels *M. galloprovincialis* from controls and exposed to Ag NPs and $Ag^+$ for 15 days (mean ± Std). Different letters represent statistical differences between treatments for each tissue and asterisk differences between tissues ($p$<0.05).

| | **Gills** | | **Digestive Gland** | |
|---|---|---|---|---|
| | **0** | **15** | **0** | **15** |
| **CT** | $0.3 \pm 0.1^{b}$ | $0.4 \pm 0.1^{b}$ | $0.1 \pm 0.0^{c}$ | $0.1 \pm 0.0^{c}$ |
| **Ag NPs** | – | $5.9 \pm 1.4^{a*}$ | – | $27.7 \pm 4.7^{a}$ |
| **$Ag^+$** | – | $8.5 \pm 2.0^{a*}$ | – | $13.8 \pm 2.1^{b}$ |

### 6.3.3. 2–DE image patterns

Protein expression profiles (PEPs) were obtained after 2–DE for the gills and digestive gland of *M. galloprovincialis* unexposed or exposed to Ag NPs and $Ag^+$ after two weeks, whose representative proteomes from control mussels are in Figure 6.2. Data analysis of the control

group allowed the detection of 531 ± 20 average proteins for the gills and 340 ± 46 in the digestive gland in a total of approximately 1000 detected proteins.

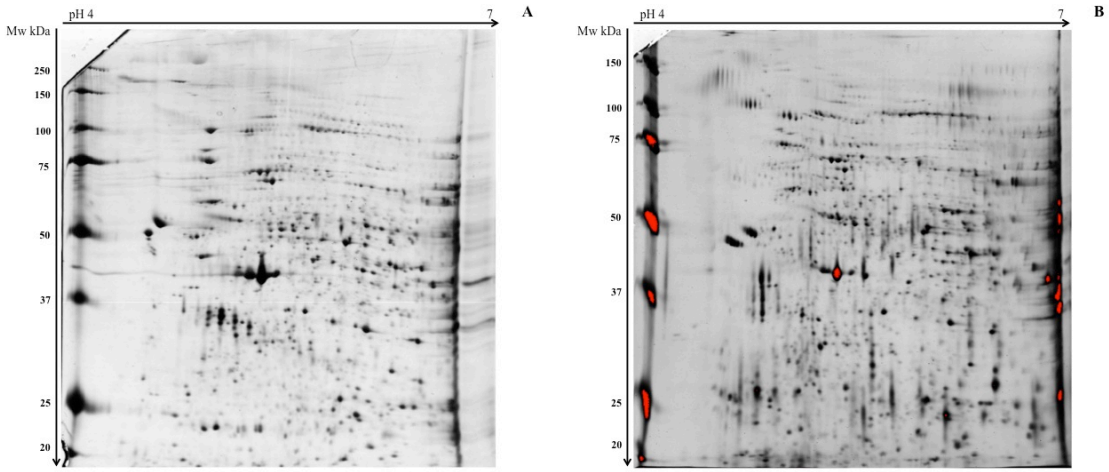


**Figure 6.2 –** *M. galloprovincialis* gills (A) and digestive gland (B) 2–DE representative control gels. One hundred micrograms of protein content was separated on 18 cm IPG strips, in 4–7 pH gradients. The second dimension was performed in 10% SDS–PAGE gels.

A master gel was constructed combining the information from PEPs obtained for Ag NPs and $Ag^+$ exposure groups (upon comparison with controls), where new and suppressed proteins and proteins with 2–fold or higher variation were highlighted, discriminating those common to both Ag NPs and $Ag^+$ as well as those specific to each Ag form. Exposure to Ag NPs and $Ag^+$ changed the pattern of protein expression in both tissues, as well as the overall quantity of proteins (Table 6.3), with proteins distributed between p*I* values from 4.4 to 7 and Mw ranging from 22.8 to 112.7 kDa in gills of exposed mussels. Three hundred and forty seven and 482 significantly different proteins spots were detected in the gills of Ag NPs and $Ag^+$ exposed mussels, respectively (Mann–Whitney U–rank test; $p<0.05$), while in the digestive gland of exposed mussels, 248 and 138 proteins were discriminated (Mann–Whitney U–rank test; $p<0.05$).

Exposure to Ag NPs resulted in 88 new proteins in the gills (27% of total proteins) and 138 proteins in the digestive gland (30% of total protein), while in the $Ag^+$ exposure a lower number of new protein spots were detected (26% and 34% of total proteins) (Table 6.3). Ag NPs accumulation also induced more suppressed proteins in the gills (135, 18% of total

proteins), whereas in the digestive gland the effect of both Ag forms was similar with 17% of total proteins disappearing after exposure (Table 6.3).

**Table 6. 3 –** Number of new, suppressed and 2–fold differentially expressed proteins for each group (Ag NPs and $Ag^+$) compared with control. N=4 replicate gels for each group.

| Tissue | Ag form | New proteins | | Suppressed proteins | | 2–fold differentially expressed proteins | | | |
|---|---|---|---|---|---|---|---|---|---|
| | | | | | | Common | | Specific | |
| | | Common | Specific | Common | Specific | Up regulated | Down regulated | Up regulated | Down regulated |
| Gills | NPs | 40 | 48 | 85 | 50 | 39 | 9 | 65 | 16 |
| | $Ag^+$ | | 36 | | 38 | | | 38 | 20 |
| Digestive Gland | NPs | 59 | 79 | 31 | 27 | 17 | 2 | 43 | 21 |
| | $Ag^+$ | | 28 | | 28 | | | 14 | 15 |

Of the total of new proteins induced by Ag NPs and $Ag^+$, 40 proteins from the gills and 59 from the digestive gland are common, leaving 48 and 36 specific proteins for Ag NPs and $Ag^+$ in the gills and 79 and 28 in the digestive gland, respectively (Table 6.3). Eighty–five and thirty–one suppressed proteins are common between Ag NPs and $Ag^+$ in both gills and digestive gland, respectively, leaving 50 and 38 specific proteins for Ag NPs and $Ag^+$ in the gills and 27 and 28 in the digestive gland, respectively (Table 6.3). A detailed list of these proteins is provided as supplementary material (Tables S1-S12, Annex II).

One hundred and twenty nine and eighty–three differentially expressed proteins with 2–fold or higher changes compared with controls were detected in mussels' gills and digestive gland exposed to Ag NPs, respectively (Table 6.3). On the other hand, $Ag^+$ exposure generated lower protein modifications, with 106 in the gills and 48 in the digestive gland (Table 6.3). Comparing the changes in expression levels, several proteins were common in the two Ag groups in the gills and digestive gland, respectively, where several others were specific of the Ag form with a general tendency to up–regulation (Table 6.3). Venn diagrams are presented in Figure 6.3 showing these changes in both mussel tissues.

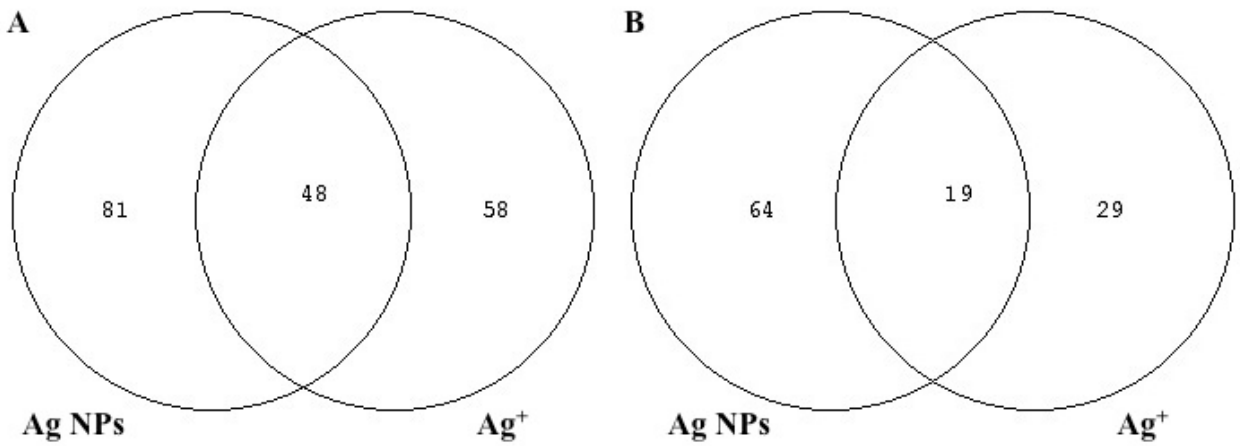


**Figure 6.3 –** Venn diagram representing differentially expressed proteins (2 fold) between Ag NPs and $Ag^+$ exposure groups. A – Gills; B – Digestive gland.

Of the differential proteins whose expression was altered upon exposure to both nano and ionic Ag, 48 were common in the gills (39 up–regulated and 9 down–regulated) and 19 in the digestive gland (17 up–regulated and only 2 down–regulated) (Table 6.3, Fig. 6.3). Sets of proteins spots differentially expressed in mussels' gills and digestive glands exposed to Ag NPs and $Ag^+$ are in Figure 6.4. In general, there is a higher up–regulation and down–regulation in common proteins from the $Ag^+$ exposure group in the gills (up to 14–fold) (Fig. 6.4A), whereas in the digestive gland, a higher up–regulation was detected in Ag NPs exposed mussels (maximum 7–fold) (Fig. 6.4B). Of the 81 specific differentially expressed proteins spots detected in Ag NPs exposed gills, 65 were up–regulated (up to 28–fold) and 16 down–regulated (up to 5–fold) (Table 6.3, Fig. 6.4C). On the other hand, in the digestive gland a total of 64 specific proteins were detected, corresponding to 43 up–regulated and 21 down–regulated (up to 9–fold) (Table 6.3, Fig. 6.4D). As for $Ag^+$ in the gills, 38 specific proteins were up–regulated in contrast to 20 down–regulated (over 4–fold) (Table 6.3, Fig. 6.4E). In the digestive gland, 14 specific differentially expressed proteins were up–regulated (up to 4–fold) and 15 proteins were down–regulated (up to 9–fold) (Table 6.3, Fig. 6.4F). A detailed list of these proteins is provided as supplementary material (Tables S13-S18, Annex II).

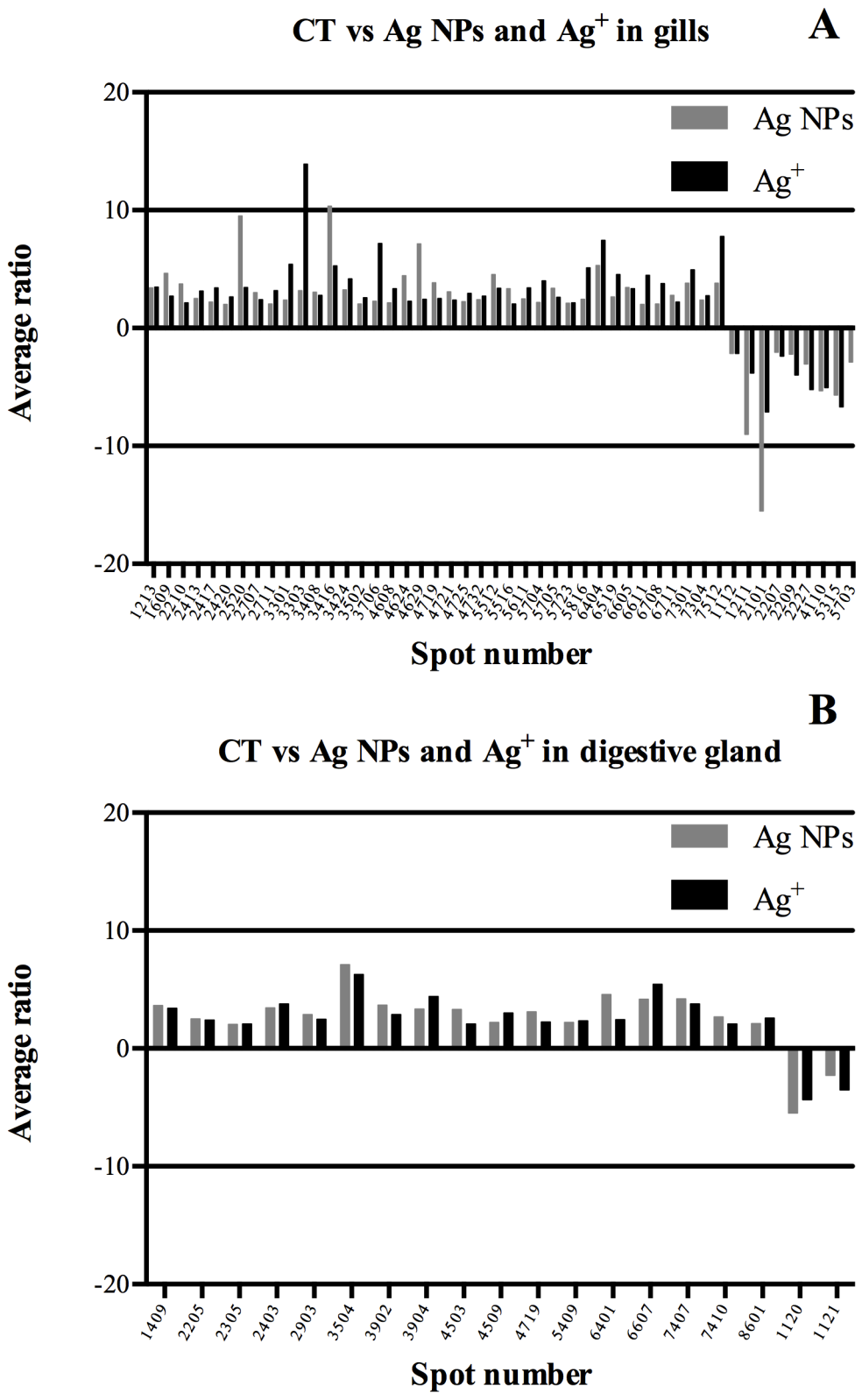
CT vs Ag NPs and Ag+ in gills
A
Ag NPs
Ag+
Average ratio
20
10
0
-10
-20
1213
1609
2210
2413
2417
2420
2520
2707
2711
3301
3303
3408
3416
3424
3502
3706
4608
4624
4629
4719
4721
4725
4732
5312
5516
5611
5704
5705
5723
5816
6404
6519
6605
6611
6708
6711
7301
7304
7512
1172
1211
2101
2207
2209
2222
4110
5315
5703
Spot number
B
CT vs Ag NPs and Ag+ in digestive gland
Ag NPs
Ag+
Average ratio
20
10
0
-10
-20
1409
2205
2305
2403
2903
3504
3902
3904
4503
4509
4719
5409
6401
6607
7407
7410
8601
1120
1121
Spot number

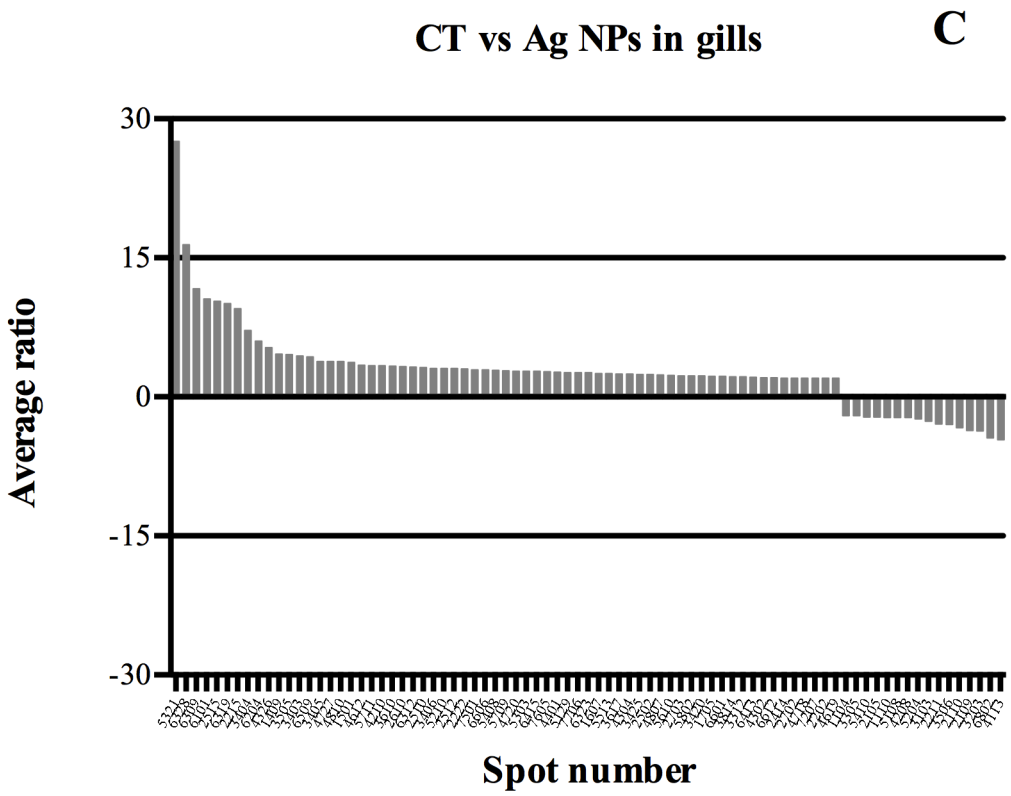
C
CT vs Ag NPs in gills
30
15
0
-15
-30
Average ratio
Spot number

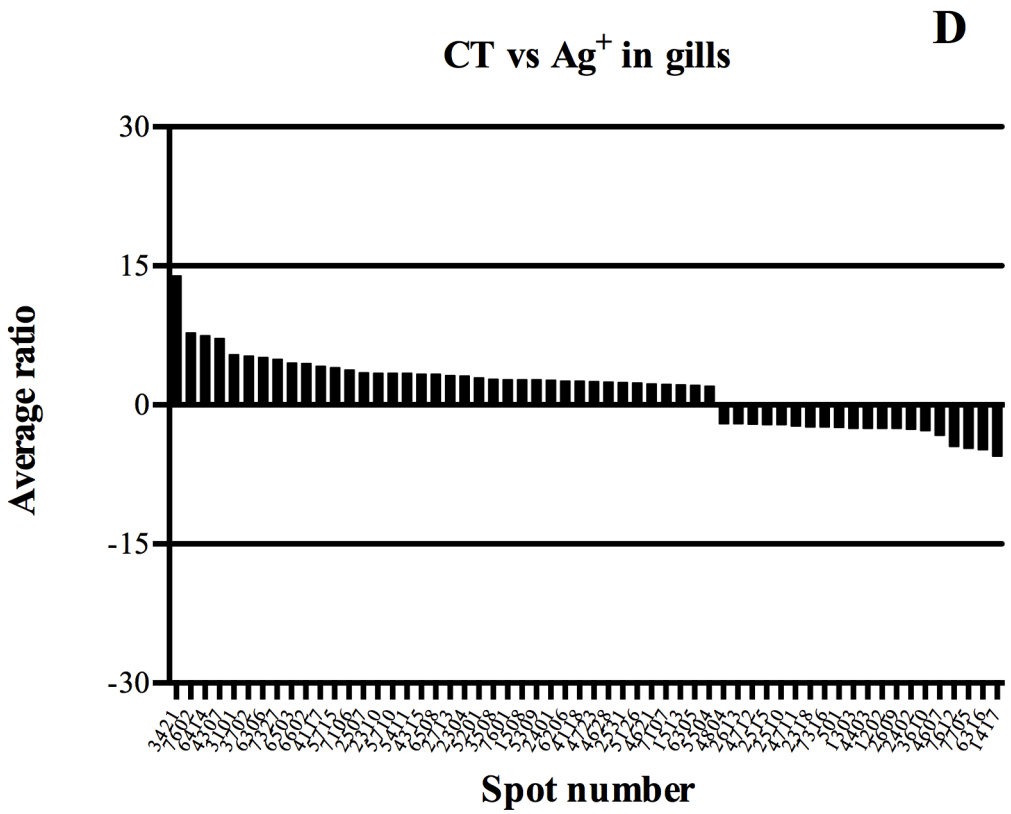
D
CT vs Ag+ in gills
30
15
0
-15
-30
Average ratio
Spot number

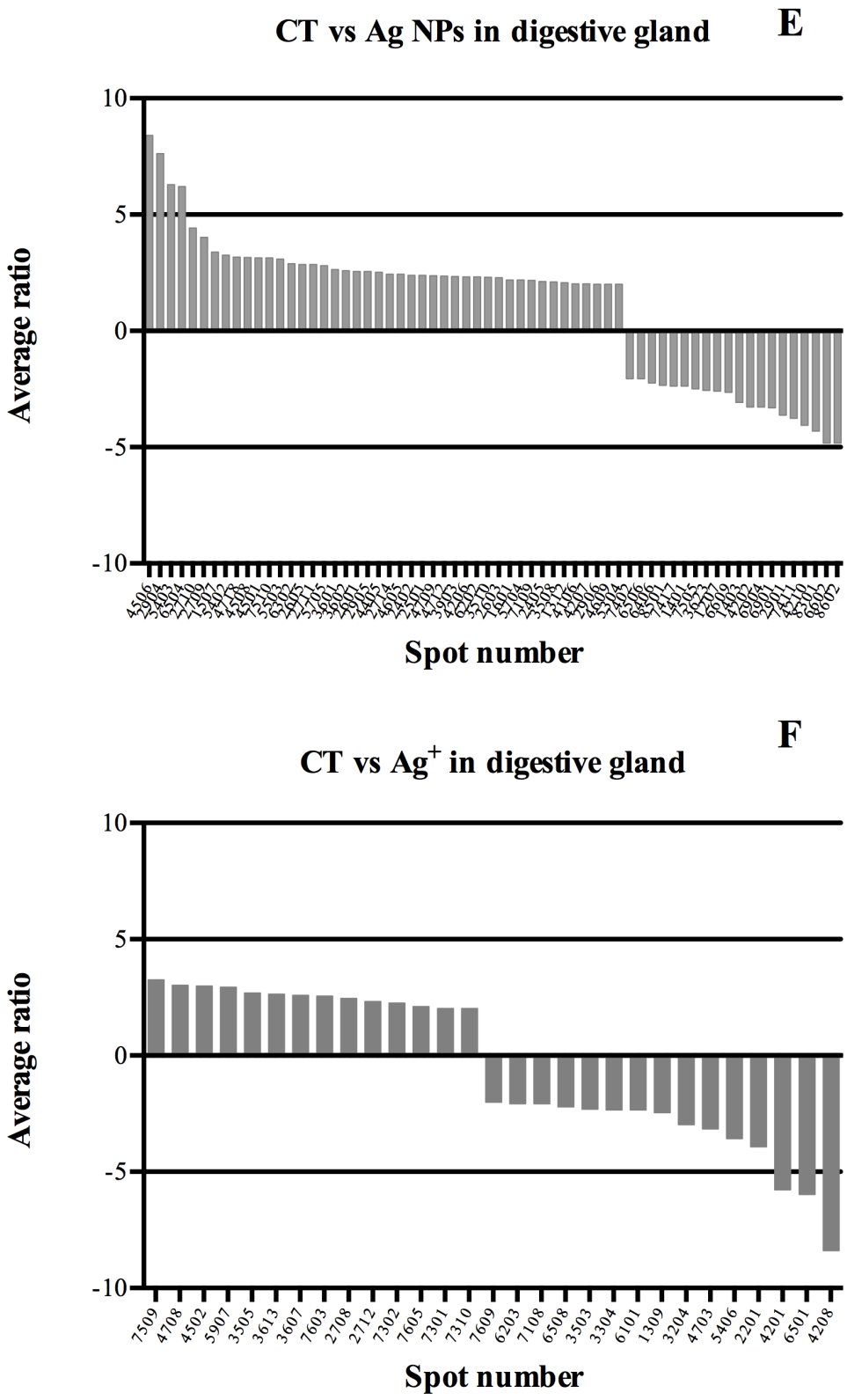


**Figure 6.4 –** Sets of protein spots differentially expressed in mussels' gills and digestive glands exposed to Ag NPs and $Ag^{+}$. Proteins with the same trend common to both Ag forms in the gills (A) and digestive glands (B); specific to Ag NPs in the gills (C) and digestive glands (D) and specific to $Ag^{+}$ in the gills (E) and digestive glands (F) all in comparison to control. The y–axis corresponds to the average ratio of protein expression, where above the 0

value for the up–regulated protein spots and below the 0 value for the down–regulated ones. In the horizontal axis, the specific up–regulated protein spots are organized with the highest values on the left side and the specific down–regulated ones show the highest values on the right side.

### 6.3.4. Identification of differentially expressed proteins

Of the common and specific differentially expressed proteins (2–fold and higher) obtained in the gills and digestive gland after exposure to both Ag forms, 40 proteins with the higher change in expression were analysed by MALDI–TOF–TOF and 15 putatively identified (Fig. 6.5). Since mussels *M. galloprovincialis* are non–model organisms, the majority of its sequences are absent from databases making the identification difficult. Homology identity of the proteins using MASCOT was further performed by similarity with available *M. galloprovincialis* sequences using Blastp by NCBI Blast (Table 6.4).

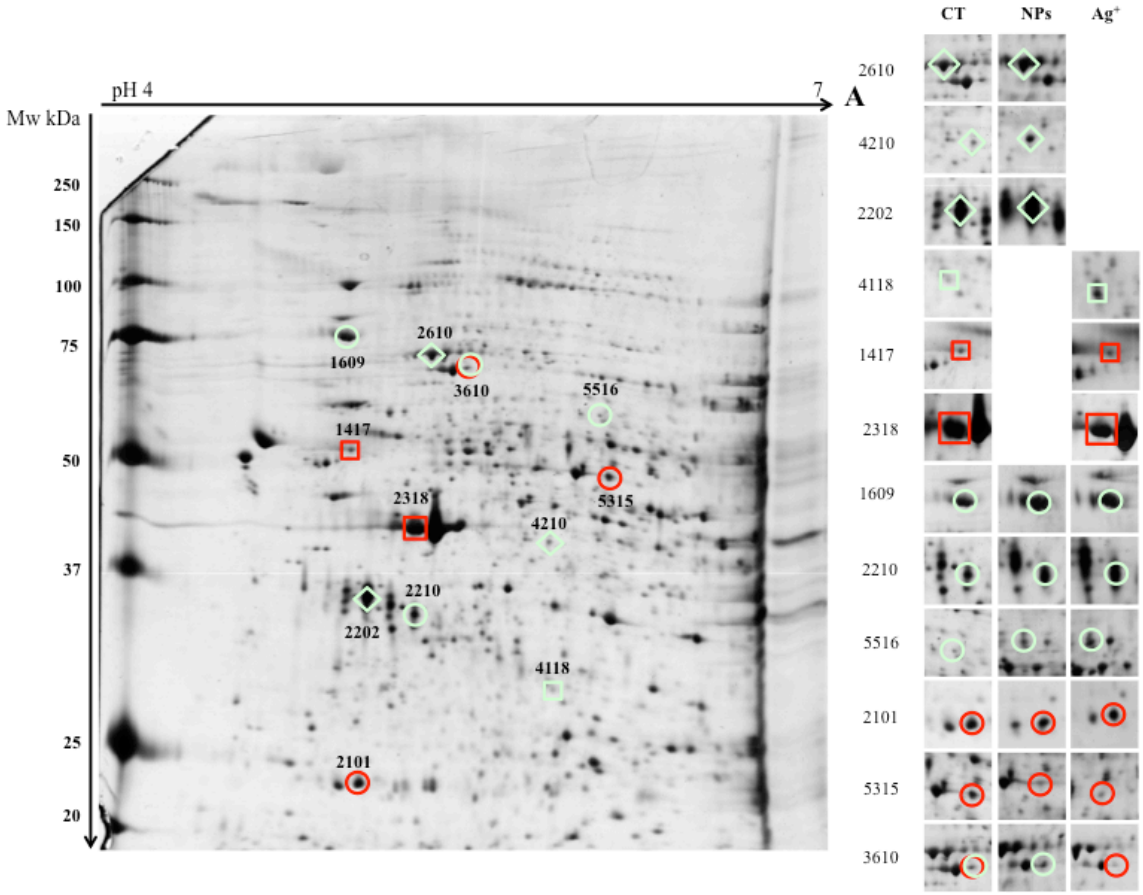

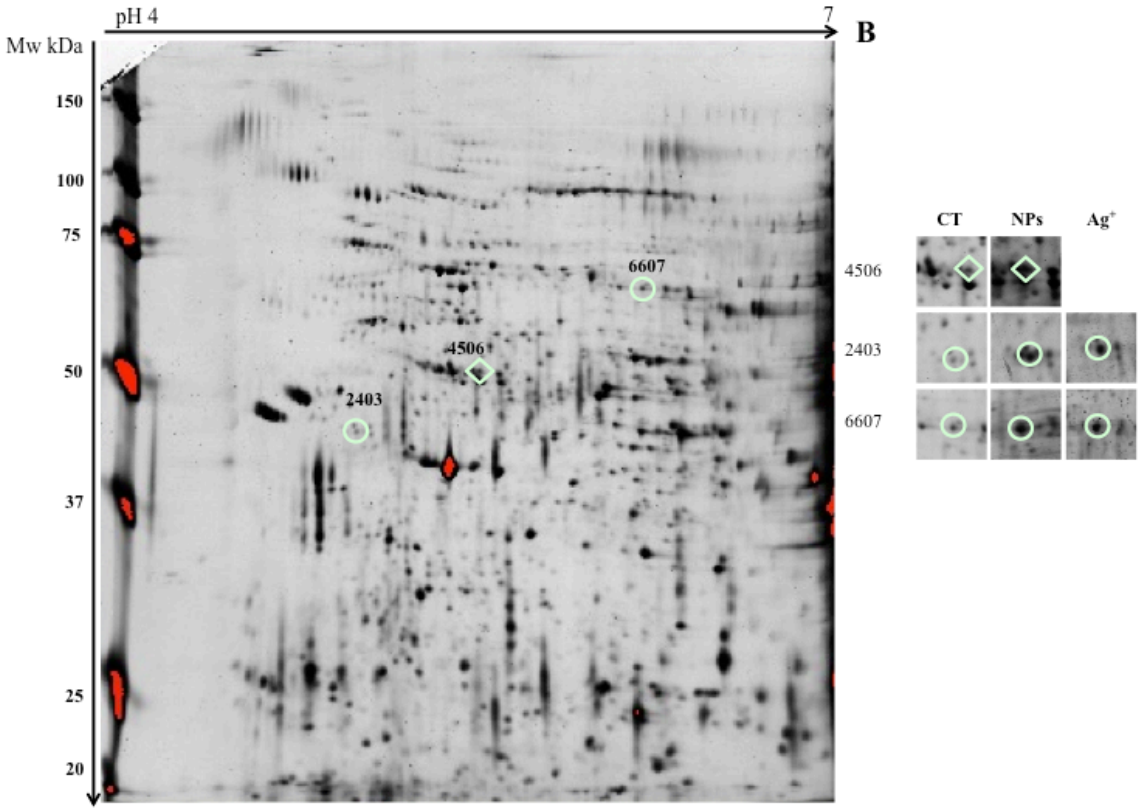


**Figure 6.5 –** *M. galloprovincialis* gills (A) and digestive gland (B) 2–DE representative gels after Ag NPs and $Ag^{+}$ exposure with identified proteins by MALDI–TOF–TOF. Common proteins 2–fold up (green circle) and 2–fold down–regulated (red circle), specific proteins 2–fold up– (green diamond) and down–regulated (red diamond) after Ag NPs exposure and specific proteins 2–fold up– (green square) and down–regulated (red square) after $Ag^{+}$ exposure. One hundred micrograms of protein content was separated on 18 cm IPG strips, in 4–7 pH gradients. The second dimension was performed in 10% SDS–PAGE gels.

**Table 6.4 –** Identification of differentially expressed proteins by MALDI–TOF–TOF mass spectrometry in *M. galloprovincialis* exposed to Ag NPs and $Ag^{+}$.

**A)** Identification performed with peptide mass fingerprint and MASCOT

| Ag form | Spot n°[a] | Name | PDQuest | Acession number | Theor. Mr/pI | MASCOT | | | Species | Function |
|---|---|---|---|---|---|---|---|---|---|---|
| | | | Av. Ratio[b] | | | Score[c] | % Coverage | N° peptides | | |
| **GILLS** | | | | | | | | | | |
| **Ag NPs** | 2610 | Major vault protein | 3↑ | gi\|118151639 | 31.81/5.69 | 146 | 36 | 12 | *M. galloprovincialis* | Stress response |
| **$Ag^{+}$** | 2318 | Actin | 2↓ | gi\|5114428 | 42.12/5.46 | 91 | – | 4 | *M. galloprovincialis* | Cytoskeleton and cell structure |

**B)** Identification performed with peptide mass fingerprint and BLAST

| Ag form | Spot n°[a] | Name | PDQuest Av. Ratio[b] (Ag NPs/$Ag^+$) | Acession n° | Theor. Mr/pI | BLAST Score[d] | BLAST % Coverage | BLAST E value | Function |
|---|---|---|---|---|---|---|---|---|---|
| | | | | **GILLS** | | | | | |
| **Ag NPs** | 4210 | Paramyosin | 3↑ | gi\|42559342 | 99.57/5.25 | 320 | 53 | $3.0e^{-13}$ | Cytoskeleton and cell structure |
| | 2202 | Catchin protein | 2↑ | gi\|6682323 | 112.56/5.22 | 121 | 35 | $6.0e^{-08}$ | Cytoskeleton and cell structure |
| **$Ag^+$** | 1417 | α–tubulin | 6↓ | gi\|302029718 | 41.69/5.11 | 260 | 84 | $2.0e^{-86}$ | Cytoskeleton and cell structure |
| | 4118 | putative C1q domain containing protein | 3↑ | gi\|325504419 | 26.18/6.30 | 26.2 | 2 | 0.002 | Stress response |
| **Common** | 1609 | Glutahione s–transferase (GST) | 5/3↑ | gi\|22094809 | 23717.2/5.9 | 23.5 | 5 | 0.03 | Oxidative stress |
| | 5516 | Precollagen–P | 3/2↑ | gi\|21105301 | 78.25/11.31 | 23.5 | 7 | 1 | Adhesion and mobility |
| | 3610 | ATP synthase F0 subunit 6 | 3↑/3↓ | gi\|227002086 | 25.79/6.68 | 20 | 31 | 1.9 | Energy metabolism |
| | 2210 | Nuclear receptor subfamily 1G | 4/2↑ | gi\|345971942 | 59.49/5.74 | 22.7 | 12 | 1.1 | Transcription regulation |
| | 5315 | Catchin protein | 6/7↓ | gi\|6682323 | 112.56/5.22 | 23.5 | 48 | 0.2 | Cytoskeleton and cell structure |
| | 2101 | HSP70 | 16/7↓ | gi\|57635269 | 71.21/5.33 | 24.6 | 3 | 1.6 | Stress response |
| | | | | **DIGESTIVE GLAND** | | | | | |
| **Ag NPs** | 4506 | Ras, partial | 8↑ | gi\|83777078 | 197.16/5.44 | 81.3 | 89 | $5.0^{e-22}$ | Stress response |
| **Common** | 2403 | NADH dehydrogenase subunit 2 | 4/4↑ | gi\|34328770 | 34.47/8.55 | 25.8 | 4 | 0.6 | Energy metabolism |
| | 6607 | Myosin heavy chain | 4/6↑ | gi\|6682319 | 197.16/5.44 | 20 | 38 | 1.7 | Cytoskeleton and cell structure |

[a]Spot number on 2–DE map (Fig. 6.4)

[b]Fold change increase (↑) or decrease (↓) in terms of intensity between control, Ag Nps and $Ag^+$ exposed mussels. Average ratio calculated by PDQuest using four replicates in each group. For all comparisons the *p*–value is <0.05.

[c]Scores of the matches using MASCOT (http://www.matrixscience.com) and percentage of coverage and number of matched peptides in the identified proteins.

[d]Scores of the matches using NCBI/BLAST (http://blast.ncbi.nlm.nih.gov) and percentage of coverage of matched peptides in the identified proteins.

The identified proteins belong to four functional classes: structural proteins (actin, paramyosin, catchin protein, α–tubulin, precollagen P and myosin heavy chain), metabolic proteins (ATP synthase F0 subunit 6, NADH dehydrogenase subunit 2), stress response proteins (major vault protein, glutathione s–transferase, putative C1q domain containing protein, heat shock protein 70 and ras, partial) and transcription proteins (nuclear receptor family 1G) distributed between Ag forms and mussel tissues. Figure 6.5 shows close–up views of the identified proteins.

Some of identified proteins corresponded to PESs common to both silver forms, six in the gills and two in the digestive gland. The stress response protein HSP70 (spot nº2101) was the protein with highest decrease in the gills (16–fold and 7–fold after Ag NPs and $Ag^+$ exposures, respectively), followed by the structural protein catchin (spot nº5315) with a 6–fold decrease by Ag NPs and 7–fold decrease by $Ag^+$. The ATP synthase F0 subunit 6 (spot nº3610) was the only protein that was up–regulated by Ag NPs exposure and down–regulated by $Ag^+$, with a 3–fold increase and the same decrease. The remaining proteins were over–expressed following exposure to Ag NPs and $Ag^+$, the antioxidant enzyme GST (spot nº1609), the nuclear receptor subfamily 1G (spot nº2210) and the precollagen–P protein (spot nº5516). Finally, the structural protein myosin (spot nº6607) and the NADH dehydrogenase subunit 2 were (spot nº2403) up–regulated in the digestive gland, with higher expression after exposure to $Ag^+$ (6–fold and 4–fold) when compared to Ag NPs (4–fold each). Four identified proteins were over–expressed after exposure to Ag NPs (specific PESs), three of which in the gills and one in the digestive gland. Of the PES whose expression was altered in the gills, two correspond to the structural proteins paramyosin (spot nº4210) and catchin protein (spot nº2202) with 3– and 2–fold increase, respectively and one to the stress response major vault protein (spot nº2610) with a 3–fold increase. Ras partial (spot nº4506) was the only protein up–regulated in the digestive gland that corresponded to the highest variation upon exposure to these NPs (8–fold). Of the PES specific of $Ag^+$ exposure, only three proteins were identified in the gills of exposed mussels, the stress response protein putative C1q domain containing protein (spot nº4118) and the cytoskeleton proteins α–tubulin (spot nº1417) and actin (spot nº2318), the first 3–fold up–regulated, the second and the third 6–fold and 2–fold down–regulated.

## 6.4. Discussion

The environmental impact of Ag NPs is to date unknown and information about their bioavailability, mechanisms of uptake and toxic implications in organisms is scarce. So, the main objective of this study was to investigate changes in PEPs in the gills and digestive gland of mussels *M. galloprovincialis* exposed to Ag NPs and $Ag^+$.

The exposure to these forms of Ag resulted in a significant Ag accumulation ($p<0.05$) in mussel tissues (Table 6.2). In the gills Ag accumulation in NP and ionic forms was similar. This is explained by a similar bioavailability of $Ag^+$ mainly due to the ions solubility from the Ag NPs. Upon 15 days of exposure, the digestive gland accumulated more Ag than the gills in both Ag forms ($p>0.05$), indicative of the role of digestive gland in Ag accumulation and storage (Chapter 3).

Significant differences observed on the PEPs of the gills and digestive gland of mussels exposed to Ag NPs and $Ag^+$ were Ag form and tissue dependent. Differential uptake, tissue–specific functions and redox requirements associated with different modes of action can explain the differences between Ag forms. Exposure to Ag NPs induced a higher up–regulation combined with a high number of new and suppressed protein spots in the gills, while in those exposed to $Ag^+$ a lower number of new and suppressed protein spots were detected (Table 6.3). Mussel gills is the first organ in contact with surrounding water being more vulnerable to metal release from the particles as well as particle interaction and accumulation (as seen in Chapter 3). The higher number of new protein spots also detected in the digestive gland of Ag NPs–exposed mussels compared to the gills and to $Ag^+$ exposure may be related to the higher Ag NPs accumulation and a low elimination rate. The digestive gland is targeted mainly by particle ingestion in the form of aggregates (Chapter 3), which could explain the importance of Ag NPs accumulation in this tissue. Accordingly, the similar number of suppressed proteins between Ag NPs and $Ag^+$ in the digestive gland (lower than the gills) revealed the importance of the digestive gland in the protection against Ag toxicity (previously detected in Chapter 3). The size of Ag NPs (single particles or aggregates) has different properties from Ag ions largely due to their relatively large surface area and higher reactivity, which accounted for the specific PEPs responses in both tissues (Table 6.3; Fig. 6.3 and 6.5). Nevertheless, some similarities exist between Ag forms since a set of 2–fold or higher regulated common proteins are discriminated (Table 6.3; Fig. 6.3 and 6.4), which could be explained by the tendency of these particles to dissolve with time (Chapter 3). It is

therefore essential to identify these proteins in order to discriminate the effects of Ag NPs and $Ag^+$ and unravel the possible biological mechanisms of Ag NPs.

Fifteen of the 40 differentially expressed proteins with higher expression changes were identified by peptide mass fingerprint (Table 6.4, Fig. 6.5). Changes in proteins involved in cytoskeleton and cell structure, stress response, oxidative stress, transcription regulation, adhesion and mobility, and energy metabolism were detected in response to both Ag NPs and $Ag^+$. Proteomic analysis using *E. coli* was also used to discriminate the effects of both Ag NPs and $Ag^+$ that showed similar alterations in cellular functions (Hwang *et al*., 2008; Lok *et al*., 2006). On the other hand, this is the first study to address the effects of Ag NPs and $Ag^+$ in the proteome of mussels.

Two proteins involved in cytoskeleton and cell structure altered their expression after exposure to both Ag NPs and $Ag^+$, catchin (spot nº5315) was down–regulated (6– and 7–fold, respectively) in the gills and myosin heavy chain (spot nº6607) up–regulated in the digestive gland (4– and 6–fold, respectively) (Table 6.4, Fig. 6.5). Additionally, paramyosin (spot nº4210) and catchin (spot nº2202) were two cytoskeleton proteins up–regulated only by Ag NPs exposure (3– and 2–fold, respectively), while in mussels exposed to $Ag^+$ actin (spots nº2318, 2–fold) and α-tubulin (spot nº1417, 6–fold) were down-regulated in the gills (Table 6.4, Fig. 6.5). Paramyosin, catchin and myosin (heavy chain) are proteins responsible for generating muscle contraction in molluscs (Watabe *et al*., 2000; Yamada *et al*., 2000). Actin is a ubiquitous protein that combined with microtubules (formed by α–tubulin polymerization) and intermediate filaments represent the fundamental components of the cytoskeleton (Apraiz *et al*., 2006; Dalle–Donne *et al*., 2001; Rodríguez–Ortega *et al*., 2003). In non–muscle cells, actin microfilaments interact with myosin (heavy and light chains) and paramyosin to produce a sliding effect, which is the basis of muscular contraction, and many aspects of cell motility and organelle transport (Grøsvik *et al*., 2006; Watabe *et al*., 2000; Yamada *et al*., 2000). One of the most common explanations for the alterations of these proteins is oxidative stress, which induces cytoskeleton disorganization (Gómez–Mendikute and Cajaraville, 2003; Rodríguez–Ortega *et al*., 2003). In fact, the disturbance of cytoskeleton proteins associated with muscle contraction was already detected in clams *Chamaelea gallina* and oysters *Saccrostea glomerata* exposed to Cu (0.1-5 $mg.L^{-1}$ and 5 $\mu g.L^{-1}$) for 7 and 4 days, respectively, and mussels *Perna viridis* exposed to Cd (0.5 $mg.L^{-1}$, 14 days), whereas for Ag NPs this is the first time that the impact of these NPs was linked to the cytoskeletal activity of mussel tissues (Leung *et al*., 2011; Rodríguez–Ortega *et al*., 2003;

Thompson *et al*., 2012). The interference of Ag NPs in the structure and function of mussels' cytoskeleton is possibly associated with ROS formation, as already detected in human cells exposed to Ag NPs (6-20 nm, 100-400 μg.mL$^{-1}$, 2h) and gelatin NPs (37 ± 0.84 nm, 0.2 mg.mL$^{-1}$, 24h) (Asharani *et al*., 2009a; Gupta *et al*., 2004), as well as in mussels exposed to CuO NPs (Chapter 5). $Ag^{+}$ released from the NPs (e.g. surface oxidation in contact with proteins) could directly bind to cytoskeleton structural proteins promoting their denaturation, or indirectly interact with sulfhydryl groups of proteins (e.g. $Ca^{2+}$–ATPases) and disrupt calcium ($Ca^{2+}$) homeostasis through ROS formation (Asharani *et al*., 2009a; Vijayavel *et al*., 2007). The fluctuation in intracellular $Ca^{2+}$ levels affects the "catch" contraction (tension of muscles with little energy consumption) by direct binding to myosin thus disrupting cell motility and organelle transport (Watabe *et al*., 2000; Yamada *et al*., 2000). This could also explain the changes of catchin isoforms (spots 2202 and 5315) with contrasting responses in the gills upon exposure to Ag NPs, which could be associated with post–translational modifications (e.g. glutathionylation) in response to oxidative stress (Rodríguez–Ortega *et al*., 2003). Similar patterns of disorganization of the cytoskeleton and disruption of the cellular membrane was already detected in human cells exposed to Ag NPs (6-20 nm, 100-400 μg.mL$^{-1}$, 2-48h), linking oxidative stress, $Ca^{2+}$ disruption, ATP depletion and particle uptake (diffusion or endocytosis) (Asharani *et al*., 2009a, b). The alterations in the expression of these proteins have major adverse consequences in cells, as they are involved in the maintenance of several key physiological processes, namely muscle contraction, protein synthesis, cell adhesion and motility, intracellular organization and transport, cell differentiation and death (Matozzo *et al*., 2001; Thompson *et al*., 2012).

A protein associated with adhesion and mobility was altered after exposure to Ag NPs and $Ag^{+}$ in the gills. Precollagen–P (spot nº5516, Table 6.4, Fig. 6.5) is one of the main structural components of byssal threads that have some potential metal binding sites responsible for scavenging metals (Lucas *et al*., 2002; Szefer *et al*., 2006). The increase in expression of this protein suggests that the byssus serves as an important pathway for Ag elimination in mussel gills in response to Ag NPs (mainly $Ag^{+}$ released from the particles) and $Ag^{+}$ exposure, which is in accordance with the accumulation patterns described in Chapter 3. As byssus is known to play a role in the detoxification of metals from mussels, it is likely that certain metals are actively transferred from the soft tissues and concentrated in the byssal threads to be further eliminated (Nicholson and Lam, 2005; Nicholson and Szefer, 2003; Szefer *et al*., 2006). Alterations in byssal precursors proteins in response to metal exposure (e.g. $Cu^{2+}$

(Chapter 5), Co, Ni, Cr, Mn, Pb and Fe) were also detected in mussels *Perna viridis* (Nicholson and Szefer, 2003), *M. galloprovincialis* (precollagen–D) and oysters *Saccostrea glomerata* (Thompson *et al*., 2012).

Exposure to Ag NPs and $Ag^{+}$ also affected two proteins involved in energy metabolism. ATP synthase F0 subunit 6 (spot nº3610) was affected in the gills, whilst changes in NADH dehydrogenase subunit 2 (spot nº2403) only occurred in the digestive gland (Table 6.4, Fig. 6.5). ATP synthase F0 subunit 6 is a constituent of the ATP synthase complex, responsible for the production of ATP in the mitochondria through oxidative phosphorylation and consequently the supply of energy to cells (Puerto *et al*., 2011; Yang *et al*., 2010). NADH dehydrogenase is the first enzyme located in the electron transport chain that catalysis the transfer of electrons from NADH to ubiquinone, establishing a proton motive force required for ATP synthesis (Yang *et al*., 2010). The increase in ATP synthase F0 subunit 6 expression (3–fold) after exposure to Ag NPs lead to an increase in oxidative phosphorylation (and ATP production) reflecting a higher metabolic rate associated with the presence of these NPs in the cytosol of gill cells that can lead to an additional ROS production (Apraiz *et al*., 2006; Banci *et al*., 2011). Mechanical injury caused by Ag NPs localization/accumulation in mitochondria may be another reason for mitochondrial damage, where Ag induce major changes in membrane permeability, disrupt the respiratory chain and contribute to oxidative stress (Asharani *et al*., 2009b; Yeo and Pak, 2008). On the other hand, the down–regulation (2–fold) of this protein by $Ag^{+}$ exposure indicates a decreased mitochondrial activity leading to the reduction in electron transfer and ATP depletion in cells by inhibition of thiol–containing proteins on the surface of plasma membranes (Lapresta–Férnandez *et al*., 2012). The significant difference in this protein expression between mussels exposed to Ag–NPs and $Ag^{+}$ demonstrate different toxic modes of action in this tissue. An up–regulation of ATP synthase F0 subunit 6 has also been detected after exposure to CuO NPs in the gills (Chapter 5), confirming the close relationship between NPs–induced oxidative stress and mitochondria function. The up–regulation of NADH dehydrogenase (4–fold for both Ag forms) is also indicative of an increase in ROS production by both Ag NPs and $Ag^{+}$ in mussels' digestive gland. NADH dehydrogenase complex produce ROS (e.g. superoxide anions and hydrogen peroxide) in its extra–membranous portion (Murphy, 2009), and is associated with Pb exposure in oysters *Saccostrea glomerata* (100 $\mu g.L^{-1}$, 4 days) (Muralidharan *et al*., 2012). These changes in energy metabolism along with cytoskeleton disorganization and lipid peroxidation (as seen in Chapter 3) promote physical changes in the membrane, altering the

respiratory, oxidative and $Ca^{2+}$ buffering capacity of the mitochondria (Huang et al., 2010; Orrenius et al., 2007; Vijayavel *et al*., 2004). Ag NPs–mediated damage to the mitochondria by reducing mitochondrial membrane potential and increasing ROS production is a possible mechanism by which these particles can initiate cytotoxic pathways that ultimately lead to cell death.

Similarly to what was found in mussels exposed to CuO NPs and $Cu^{2+}$ (Chapter 5), the nuclear receptor subfamily 1G (spot nº2210, Table 6.4, Fig. 6.5) was up–regulated following Ag NPs and $Ag^{+}$ exposure in the gills, indicating that both Ag forms have the capacity to interfere with signal transduction in DNA–related functions and induce genotoxicity. Nuclear receptors belong to a class of proteins that regulate the transcription of specific target genes, thereby controlling the development, homeostasis and metabolism of organisms. These receptors possess a highly conserved DNA–binding domain that recognizes specific sequences via a Zinc–finger, which primarily role is to bind to DNA and regulate a variety of cellular activities at the transcriptional level, such as development, differentiation, and tumour suppression (Huang *et al*., 2011; Nieto *et al*., 2010; Yang *et al*., 2010). The release of $Ag^{+}$ from Ag NPs may be responsible for the disruption of these proteins and consequently cause DNA damage by either replacing zinc atoms in Zn–finger proteins or by generating free radicals (Achard–Joris *et al*., 2006; Hartwig, 2001). In fact, Ag NPs (as well as $Ag^{+}$) induce DNA strand breaks in mussel hemocytes where a role of ROS–induced oxidative stress was suggested (Chapter 3). The disruption of the mitochondrial respiratory chain by Ag NPs is also a possible inducer of genotoxicity that ultimately result in apoptosis (Asharani *et al*., 2009b). Additionally, the direct interaction of Ag NPs with DNA may also lead to genomic damage and instability (Asharani *et al*., 2008). Nevertheless, the exact outcome of these NPs in the nucleus is not yet clear, but it is expected to interfere with DNA synthesis, DNA damage, chromosomal morphology and segregation and DNA and cell division (Asharani *et al*., 2008, 2009b; Hackenberg *et al*., 2011).

Four proteins associated with stress response were altered after exposure to Ag NPs and $Ag^{+}$, the major vault protein (MVP), ras partial, heat shock protein 70 (HSP70) and putative C1q domain containing protein (MgC1q60). The major vault protein (spot nº2610) is the main component of the ubiquitous vault particles, large cytoplasmatic ribonucleoproteins highly conserved in both morphology and protein composition (Grøsvik *et al*., 2006; Tomanek *et al*., 2010). Even though the exact function of the MVP is still unclear, it is implicated in the cellular response to abiotic factors (e.g. temperature, salinity and oxygen), xenobiotics and

metals (e.g. Cu) by direct binding and excretion of conjugated metabolites, thus preventing their accumulation and toxic effects (Berger *et al*., 2009; Dondero *et al*., 2006; Luedeking and Koehler, 2004). The MVP is localized in the cytoplasm close to cytoskeleton elements while a small fraction is consistently associated with the nucleus (in particular the nuclear membrane and nuclear pore complex). This subcellular localization led to the hypothesis that vaults have a major role in intracellular cytoskeleton–mediated transport, particularly between the cytoplasm and the nucleus (Mossink *et al*., 2003; van Zon *et al*., 2006). In addition, these proteins also bind to stress–induced signalling cascades as apoptosis (Berger *et al*., 2009). The up–regulation (3–fold) of the MVP (spot 2610, Table 6.4, Fig. 6.5) in mussels exposed to Ag NPs represent a specific response to counteract the toxic effects of these NPs, specifically its genotoxic potential (as demonstrated by the up-regulation of nuclear receptor subfamily 1G and the DNA strand breaks in Chapter 4), due to their accumulation in the gills (Chapter 3). Ras partial (spot nº4506, Table 6.4, Fig. 6.5), has a central role in cell growth, differentiation and apoptotic signalling cascades, was up–regulated (8–fold) by Ag NPs in the digestive gland. Carcinogenesis in mammals and fish reported activated mutant forms of the ras gene involved in aberrant cell proliferation, altered cell checkpoint control and cell differentiation. A number of *Mytilus* sp. cancer genes, including the ras gene, were recently characterized, nevertheless, the expression of these tumour–regulating genes still need to be elucidated in mussels (Ciocan and Rotchell, 2005; Di *et al*., 2011; Lima *et al*., 2008). The ras gene encodes a GTP/GDP binding protein that is responsible for the transduction of mitogenic signals from the cellular membrane to the nucleus. GTP–binding proteins are responsible for cytoskeleton organization (namely actin reorganization) and induced by a wide range of extracellular factors by mediating membrane ruffling, pinocytosis, cell contractility and the formation of stress fibres (Di *et al*., 2011; Gupta *et al*., 2004; Rotchell *et al*., 2001). The induction of this protein may be related to the disruption of the cellular membrane and cytoskeleton disorganization that combined with the alterations obtained in the cytoskeleton proteins myosin heavy chain are indicative of Ag NPs uptake in mussel digestive gland. Apart from alteration of ras expression reflecting their functional change in cells, the mutation and post–transcriptional modification of this gene was also linked to DNA damage, functioning in association with DNA repair and apoptosis processes (Di *et al*., 2011 and literature cited therein). Accordingly, given the genotoxic potential of these NPs (Chapter 4) and the up–regulation of both MVP and the nuclear

receptor subfamily 1G, the association between ras expression and DNA damage inflicted by these NPs cannot be ruled out.

Heat shock proteins (HSPs) are molecular chaperones that assist in the modulation of stress response and protection against stress–associated cellular damages, including co– and post–translational protein folding and unfolding, intracellular trafficking and triggering and control of apoptosis. Though originally identified as proteins induced by heat stress, these proteins are up–regulated by a range of other stressors including oxidative stress, radiation, pH, salinity and xenobiotics (Creagh *et al*., 2000; Kefaloyianni *et al*., 2005; Leung *et al*., 2011). Because of their sensitivity to environmental pollutants such as metals, the HSP70 are used as conventional biomarkers (Rodríguez–Ortega *et al*., 2003; Thompson *et al*., 2012). Exposure to Ag NPs and $Ag^{+}$ affected HSP70 expression (spot nº2101, Table 6.4, Fig. 6.5) causing a significant down–regulation (16– and 7–fold, respectively) in mussel gills. The oxidative stress induced by Ag NPs and $Ag^{+}$ result in a decrease of the metabolic capacity of mussels either by disturbing the normal folding or by causing indirect damage to proteins. Ag NPs was more effective in down–regulating HSP70 probably due to a high ROS formation in this tissue, as suggested in Chapter 3. Moreover, HSPs are also known to protect cells from apoptosis by preventing the activation of caspases, the execution proteases in programmed cell death (Garrido *et al*., 2001; Takayama *et al*., 2003), and apoptosis is one of the mechanisms by which Ag NPs induce toxicity (Ahamed *et al*., 2010; Choi *et al*., 2010). So, the down–regulation of HSP70 by both Ag forms is related to the induction of a specific form of apoptosis or programmed cell death that is caspase–independent. In tumour cells, the depletion of this protein results in lysosomal destabilization, release of lysosomal constituents into the cytosol and a caspase–independent cell death (Dudeja *et al*., 2009; Frese *et al*., 2003; Jäättela *et al*., 2004; Nylandsted *et al*., 2000). Even though no specific markers of carcinogenesis or apoptosis were detected in this study, the differential expression of MVP, ras partial and HSP70 seems to support the idea of the activation of an alternative HSP70–controlled death pathway by Ag NPs that is probably tumour–specific. Nevertheless, this type of cell death needs further evaluation. Additionally, the alterations in mitochondrial membrane potential, capacity to induce ROS ($Ag^{+}$ release), cytoskeleton disruption, genotoxic capacity (Chapter 4), disruption of membrane systems (lipid peroxidation, Chapter 3) combined with fluctuations in $Ca^{2+}$ suggest other cytotoxic pathways by which Ag NPs can induce cell death.

A protein associated with oxidative stress was also up-regulated (5– and 3–fold, respectively) after exposure to Ag NOs and $Ag^+$ in the gills, GST (spot nº1609, Table 6.4, Fig. 6.5). GSTs are phase II detoxification enzymes that are involved in the conjugated reactions between reduced glutathione and lipophilic contaminants that lead to their detoxification. As one of the main mussel detoxification tissues, gills have a high number of phase II detoxification enzymes, as GST (Fitzpatrick *et al*., 1995; McDonagh and Sheehan, 2006). These proteins are also known for their role in the antioxidant defence system of bivalves including ROS metabolism where its activity is modulated by metals (e.g. Canesi *et al*., 1999; Hoarau *et al*. 2006). Ag NPs and $Ag^+$ have the capacity to cause oxidative damage through ROS, consequently altering the antioxidant capacity of mussel tissues by enzymatic induction or reduction (Chapter 3). So the up–regulation of this enzyme is not surprising. The expression of GST after exposure to Ag NPs plays an important role in the defence against these NPs (Chae *et al*., 2009), which is also in accordance with the results obtained for mussels CuO NPs exposure (Chapter 5). Additionally, GST has the capacity to metabolize reactive products produced during the lipid peroxidation process (Canesi *et al*., 1999), which is an oxidative damage for both Ag NPs and $Ag^+$ in mussels' gills (Chapter 3).

Finally, exposure to $Ag^+$ resulted in the up–regulation (3–fold) of the MgC1q60 (spot nº4118) in mussel gills (Table 6.4, Fig. 6.5). The protein family with a C1q domain are responsible for numerous biological processes as tissue homeostasis, protein activation, immune responses, apoptosis, phagocytosis, cell adhesion, and cell growth modulation (Gerdol *et al*., 2011; Gestal *et al*., 2010). So, $Ag^+$ exposure has detrimental consequences on the immune function of mussels probably related to the oxidative stress capacity of this metal (previously detected in Chapter 3). In *Mya arenaria*, the effects of $Ag^+$ ($10^{-9}$–$10^{-3}$ M, 18h) on immune function were already identified, where lysosomal membrane stability, lysozyme release and phagocytosis are some of the immune parameters disturbed (Brousseau *et al*., 2000). Additionally, this protein was also detected upon exposure of CuO NPs and $Cu^{2+}$ in mussels' gills (Chapter 5), reinforcing the disruption of the immune capacity of mussels associated with oxidative stress. However, the investigation of invertebrate C1q proteins remains deficient, specially associated with metal toxicity. Moreover, the down–regulation of the cytoskeleton proteins actin (spot nº2318), α–tubulin (spot nº1417) and catchin (spot nº5315) by $Ag^+$ exposure in the gills also points out to the decline of the condition state of mussels associated with oxidative stress and $Ca^{2+}$ homeostasis (Chora *et al*., 2009; Gómez–Mendikute and Cajaraville, 2003).

Overall, this study validates the use of proteomic analysis to assess the protein expression changes in mussel tissues exposed to Ag NPs and $Ag^+$ even with the limitations imposed by a low representativeness of mussel proteins in protein databases. These results not only confirmed the role of Ag NPs and $Ag^+$ in inducing oxidative stress, but also helped to elucidate their underlying modes of toxic action. Most of the identified proteins showed that exposure to Ag NPs affected similar cellular pathways as $Ag^+$, with common response mechanisms in cytoskeleton and cell structure (catchin protein, myosin heavy chain), stress response (HSP70), oxidative stress (GST), transcription regulation (nuclear receptor subfamily 1G), adhesion and mobility (precol–P), and energy metabolism (ATP synthase F0 subunit 6 and NADH dehydrogenase subunit 2). Nevertheless, different mechanisms seem to be involved in their toxicity as different sets of proteins were differentially expressed in both gills and digestive gland of exposed mussels. Exposure to Ag NPs significantly affected MVP, paramyosin and ras, partial, whereas $Ag^+$ had a strong influence in MGC1q60, actin and α–tubulin. These results indicated that $Ag^+$ ions released from the NPs are not the only factor responsible for the different expressions detected in exposed mussels and is mediated by oxidative stress signal transduction pathways that can lead to apoptosis. The differential expression patterns for Ag NPs and $Ag^+$ exposures helped to identify classical biomarkers (HSP70, GST, actin), as well as new putative candidate molecular biomarkers to assess Ag NPs (MVP, ras partial and precol–P) and $Ag^+$ toxicity (MgC1q60 and precol–P). Nevertheless, additional information is required to validate the utility of these putative new biomarkers in nanotoxicology. More research efforts are needed to characterize the modes of action of Ag NPs and clarify their interaction with different cellular targets.

## 6.5. References

Achard–Joris, M.; Gonzalez, P.; Marie, V.; Baudrimont, M.; Bourdineaud, J.–P. (2006). cDNA cloning and gene expression of ribosoma S9 protein gene in the mollusk *Corbicula fluminea*: A new potential biomarker of metal contamination up–regulated by cadmium and repressed by zinc. *Environmental Toxicology and Chemistry*. **25(2):** 527–533.

Ahamed, M.; Posgai, R.; Gorey, T.J.; Nielsen, M.; Hussain, S.M.; Ro–we, J.J. (2010). Silver nanoparticles induced heat shock protein 70, oxidative stress and apoptosis in *Drosophila melanogaster*. *Toxicology and Applied Pharmacology*. **242:** 263–269.

Apraiz, I.; Mi, J.; Cristobal, S. (2006). Identification of proteomic signatures of exposure to marine pollutants in mussels (*Mytilus edulis*). *Molecular and Cellular Proteomics*. **5(7):** 1274–1285.

Asharani, P.V.; Wu, Y.L.; Gong, Z.; Valiyaveettil, S. (2008). Toxicity of silver nanoparticles in zebrafish models. *Nanotechnology*. **19:** 255102.

Asharani, P.V.; Hande, M.P.; Valiyaveettil, S. (2009a). Anti–proliferative activity of silver nanoparticles. *BMC Cell Biology*. **10:** 65.

Asharani, P.V.; Mun, G.L.K.; Hande, M.P.; Valiyaveettil, S. (2009b). Cytotoxicity and genotoxicity of silver nanoparticles in human cells. *ACS Nano*. **3(2):** 279–290.

Banci, L.; Bertini, I.; Ciofi–Baffoni, S.; D'Alessandro, A.; Jaiswal, D.; Marzano, V.; Neri, S.; Ronci, M.; Urbani, A. (2011). Copper exposure effects on yeast mitochondrial proteome. Journal of Proteomics. **74:** 2522–2535.

Bar–Ilan, O.; Albrecht, R.M.; Fako, V.E.; Furgeson, D.Y. (2009). Toxicity assessments of multisized gold and silver nanoparticles in zebrafish embryos. *Small*. **5(16):** 1897–1910.

Baun, A.; Hartmann, N.B.; Grieger, K.; Kusk, K.O. (2008). Ecotoxicity of engineered nanoparticles to aquatic invertebrates: a brief review and recommendations for future toxicity testing. *Ecotoxicology*. **17:** 387–395.

Berger, W.; Steiner, E.; Grusch, M.; Elbling, L.; Micksche, M. (2009). Vaults and the major vault protein: novel roles in signal pathway regulation and immunity. *Cellular and Molecular Life Sciences*. **66**: 43–61.

Blum, H.; Biere, H.; Gross, H.J. (1987). Improved silver staining of plant proteins, RNA and DNA in polyacrylamide gels. *Electrophoresis.* **8:** 93–99.

Borm, P. J. A.; Robbins, D.; Haubold, S.; Kuhlbusch, T., Fissan, H., Donaldson, K.; Schins, R.; Stone, V.; Kreyling, W.; Lademann, J.; Krutmann, J., Warheit, D.; Oberdorster, E. (2006). The potential risks of nanomaterials: a review carried out for ECETOC. *Particle and Fibre Toxicology*. **3:**11

Bradford, M. (1976). A rapid and sensitive method for the quantitation of microgram quantities of protein utilizing the principle of protein–dye binding. *Analytical Biochemistry*. **72:** 248–254.

Brousseau, P.; Pellerin, J.; Morin, Y.; Cyr, D.; Blakley, B.; Boermans, H.; Fournier, M. (2000). Flow cytometry as a tool to monitor the disturbance of phagocytosis in the clam *Mya arenaria* hemocytes following in vitro exposure to heavy metals. *Toxicology*. **142:** 145–156.

Canesi, L.; Viarengo, A.; Leonzio, C.; Filippelli, M.; Gallo, G. (1999). Heavy metals and glutathione metabolism in mussel tissues. *Aquatic Toxicology*. **46:** 67–76.

Chae, Y.J.; Pham, C.H.; Lee, J.; Bae, E.; Yi, J.; Gu, M.B. (2009). Evaluation of the toxic impact of silver nanoparticles on Japanese medaka (*Oryzias latipes*). *Aquatic toxicology*. **94(4):** 320–327.

Choi, J.E.; Kim, S.; Ahn, J.H.; Youn, P.; Kang, J.S.; Park, K.; Yi, J.; Ryu, D.–Y. (2010). Induction of oxidative stress and apoptosis by silver nanoparticles in the liver of adult zebrafish. *Aquatic Toxicology*. **100:** 151–159.

Chora, S.; Starita–Geribaldi, M.; Guigonis, J.–M.; Samson, M.; Roméo, M.; Bebianno, M.J. (2009). Effect of cadmium in the clam *Ruditapes decussatus* assessed by proteomic analysis. *Aquatic Toxicology*. **94:** 300–308.

Ciocan, C.M.; Rotchell, J.M. (2005). Conservation of cancer genes in the marine invertebrate *Mytilus edulis*. *Environmental Science and Technology*. **39(9):** 3029–3033.

Creagh, E.M.; Sheehan, D.; Cotter, T.G. (2000). Heat shock proteins—modulators of apoptosis in tumour cells. *Leukemia*. **14:** 1161–73.

Dalle–Donne, I.; Rossi, R.; Milzani, A.; Di Simplicio, P.; Colombo, R. (2001). The actin cytoskeleton response to oxidants: from small heat shock protein phosphorylation to changes in the redox state of actin itself. *Free Radical Biology and Medicine*. **31(12):** 1624–1632.

Di, Y.; Schroeder, D.C.; Highfield, A.; Readman, J.w.; Jha, A.N. (2011). Tissue–specific expression of p53 and ras genes in response to the environmental genotoxicant benzo(a)pyrene in marine mussels. *Environmental Science and Technology*. **45:** 8974–8981.

Dondero, F.; Dagnino, A.; Jonsson, H.; Caprì, F.; Gastaldi, L.; Viarengo, A. (2006). Assessing the occurrence of a stress syndrome in mussels (*Mytilus edulis*) using a combined biomarker/gene expression approach. *Aquatic Toxicology*. **78S:** S13–S24.

Dudeja, V.; Mujumdar, N.; Phillips, P.; Chugh, R.; Borja–Cacho, D.; Dawra, R. K.; Vickers, S.M.; Saluja, A.K. (2009). Heat shock protein 70 inhibits apoptosis in cancer cells through simultaneous and independent mechanisms. *Gastroenterology*. **136:** 1772–1782.

Fabrega, J.; Luoma, S.N.; Tyler, C.R.; Galloway, T.M.; Lead, J.R. (2011). Silver nanoparticles: Behaviour and effects in the aquatic environment. *Environmental International*. **37(2):** 517–531.

Fitzpatrick, P.J.; Krag, T.O.; Hojrup, P.; Sheehan, D. (1995). Characterization of a glutathione S–transferase and a related glutathione–binding protein from gill of the blue mussel, *Mytilus edulis*. *Biochemical Journal*. **305:** 145–150.

Frese, S.; Schaper, M.; Kuster, J.–R.; Miescher, D.; Jäätelä, M.; Buehler, T.; Schmid, R.A. (2003). Cell death induced by down–regulation of heat shock protein 70 in lung cancer cell lines is p53–independent and does not require DNA cleavage. *The Journal of Thoracic and Cardiovascular Surgery*. **126:** 748–754.

Garrido, C.; Gurbuxani, S.; Ravagnan, L.; Kroemer, G. (2001). Heat shock proteins: endogenous modulators of apoptotic cell death. *Biochemical and Biophysical Research Communications*. **286:** 433–442.

Gerdol, M.; Manfrin, C.; De Moro, G.; Figueras, A.; Novoa, B.; Venier, P.; Pallavicini, A. (2011). The C1q domain containing proteins of the Mediterranean mussel *Mytilus galloprovincialis*: A widespread and diverse family of immune–related molecules. *Developmental and Comparative Immunology*. **35:** 635–643.

Gestal, C.; Pallavicini, A.; Venier, P.; Novoa, B.; Figueras, A. (2010). MgC1q, a novel C1q–domain–containing protein involved in the immune response of *Mytilus galloprovincialis*. *Developmental and Comparative Immunology*. **34:** 926–934.

Gómez–Mendikute, A.; Cajaraville, M.P. (2003). Comparative effects of cadmium, copper, paraquat and benzo[a]pyrene on the actin cytoskeleton and production of reactive oxygen species (ROS) in mussel haemocytes. *Toxicology In Vitro*. **17:** 539–546.

Griffitt, R.J.; Hyndman, K.; Denslow, N.D.; Barber, D.S. (2009). Comparison of molecular and histological changes in zebrafish gills exposed to metallic nanoparticles. *Toxicological Sciences*. **107(2):** 404–415.

Grøsvik, B.E.; Jonsson, H.; Rodriguez–Ortega, M.J.; Roepstorff, P.; Goksøyr, A. (2006). CYP1A–immunopositive proteins in bivalves identified as cytoskeletal and major vault proteins. *Aquatic Toxicology*. **79:** 334–340.

Gupta, A.K.; Gupta, M.; Yarwood, S.J.; Curtis, A.S.G. (2004). Effect of cellular uptake of gelatin nanoparticles on adhesion, morphology and cytoskeleton organisation of human fibroblasts. *Journal of Controlled Release*. **95:** 197–207.

Hackenberg, S.; Scherzed, A.; Kessler, M.; Hummel, S.; Technau, A.; Froelich, K.; Ginzkey, C.; Koehler, C.; Hagen, R.; Kleinsasser, N. (2011). Silver nanoparticles: Evaluation of DNA damage, toxicity and functional impairment in human mesenchymal stem cells. *Toxicological Letters*. **201:** 27–33.

Handy, R.D.; Kammer, F.; Lead, J.R.; Hassellöv, M.; Owen, R.; Crane, M. (2008). The ecotoxicology and chemistry of manufactured nanoparticles. *Ecotoxicology*. **17:** 287–314.

Handy, R.D.; Cornelis, G.; Fernandes, T.; Tsyusko, O.; Decho, A.; Sabo–Attwood, T.; Metcalfe, C.; Steevens, J.A.; Klaine, S.J.; Koelmans, A.A.; Horn, N. (2012). Ecotoxicity test methods for engineered nanomaterials: Practical experiences and recommendations from the bench. *Environmental Toxicology and Chemistry*. **31(1):** 15–31.

Hartwig, A. (2001). Zinc finger proteins as potential targets for toxic metal ions: Differential effects on structure and function. *Antioxidants and redox signaling*. **3(4):** 625–634.

Hoarau, P.; Damiens, G.; Roméo, M.; Gnassia–Barelli, M.; Bebianno, M.J. (2006). Cloning and expression of a GST–pi gene in *Mytilus galloprovincialis*. Attempt to use the GST–pi transcript as a biomarker of pollution. *Comparative Biochemistry and Physiology, Part C*. **143:** 196–203.

Huang, C.–C.; Aronstam, R.S.; Chen, D.–R.; Huang, Y.–W. (2010). Oxidative stress, calcium homeostasis, and altered gene expression in human lung epithelial cells exposed to ZnO nanoparticles. *Toxicology in Vitro*. **24:** 45–55.

Huang. X.; Fang, C.–W.; Guo, Y.–W.; Huang, H.–Q. (2011). Differential protein expression of kidney tissue in the scallop *Patinopecten yessoensis* under acute cadmium stress. *Ecotoxicology and Environmental Safety*. **74:** 1232–1237

Hwang, E.T.; Lee, J.H.; Chae, Y.J.; Kim, Y.S.; Kim, B.C.; Sang, B.I.; Gu, M.B. (2008). Analysis of the toxic mode of action of silver nanoparticles using stress–specific bioluminescent bacteria. *Small*. **4:** 746–750.

Jäätelä, M. (2004). Multiple cell death pathways as regulators of tumour initiation and progression. *Oncogene*. **23:** 2746–2756.

Kefaloyianni, E.; Gourgou, E.; Ferle, V.; Kotsakis, E.; Gaitanaki, C.; Isidoros Beis, I. (2005). Acute thermal stress and various heavy metals induce tissue–specific pro– or anti– apoptotic events *via* the p38–MAPK signal transduction pathway in *Mytilus galloprovincialis* (Lam.). *The Journal of Experimental Biology*. **208:** 4427–4436.

Klaine, S. J.; Alvarez, P. J. J.; Batley, G. E.; Fernandes, T. F.; Handy, R. D.; Lyon, D. Y.; Mahendra, S.; McLaughlin, M. J.; Lead, J. R. (2008). Nanomaterials in the environment: behavior, fate, bioavailability and effects. *Environmental Toxicology and Chemistry*. **27(9):** 1825–1851

Lapresta–Fernández, A.; Fernández, A.; Blasco, J. (2012). Nanoecotoxicity effects of engineered silver and gold nanoparticles in aquatic organisms. *Trends of Analytical Chemistry*. **32:** 40–59.

Leung, P.T.Y.; Wang, Y.; Mak, S.S.T.; Ng, W.C.; Leung, K.M.Y. (2011). Differential proteomic responses in hepatopancreas and adductor muscles of the green–lipped mussel *Perna viridis* to stresses induced by cadmium and hydrogen peroxide. *Aquatic Toxicology.* **105:** 49–61.

Lima, I.; Peck, M.R.; Osten, J.R.–V.; Soares, A.M.V.M.; Guilhermino, L.; Rotchell, J.M. (2008). Ras gene in marine mussels: A molecular level response to petrochemical exposure. *Marine Pollution Bulletin*. **56:** 633–640.

Lok, C. M.; Ho, C. M.; Chen, R.; He, Q. Y.; Yu W. Y.; Sun, H.; Tam, P. K. H.; Chiu, J. F.; Che, F. M. (2006). Proteomic Analysis of the Mode of Antibacterial Action of Silver Nanoparticles. *Journal of Proteome Analysis*. **5:** 916–924

López–Barea, J.; Gómez–Ariza, J.L. (2006). Environmental proteomics and metallomics. *Proteomics*. **6:** S51–S62.

Lucas, J.M.; Vaccaro, E.; Waite, J.H. (2002). A molecular, morphometric and mechanical comparison of the structural elements of byssus from *Mytilus edulis* and *Mytilus galloprovincialis*. *The Journal of Experimental Biology*. **205:** 1807–1817.

Luedeking, A.; Koehler, A. (2004). Regulation of expression of multixenobiotic resistance (MXR) genes by environmental factors in the blue mussel *Mytilus edulis*. *Aquatic Toxicology*. **69:** 1–10.

Luoma, S.N. (2008). Silver Nanotechnologies and the Environment: Old Problems or New Challenges. Project on Emerging Nanotechnologies. Publication 15. Woodrow Wilson International Centre for Scholars and PEW Charitable Trusts, Washington, DC.

Matozzo, V.; Ballarin, L.; Pamparin, D.M.; Marin, M.G. (2001). Effects of copper and cadmium exposure on functional responses of hemocytes in the clam, *Tapes philippinarum*. *Archives in Environmental Contamination and Toxicology*. **41:** 163–170.

McDonagh, B.; Sheehan, D. (2006). Redox proteomics in the blue mussel *Mytilus edulis*: Carbonylation is not a pre–requisite for ubiquitination in acute free radical–mediated oxidative stress. *Aquatic Toxicology*. **79(4):** 325–333.

Moore, M.N. (2006). Do nanoparticles present ecotoxicological risks for the health of the aquatic environment? *Environmental International*. **32:** 967–976.

Mossink, M.; van Zon, A.; Scheper, R.J.; Sonneveld, P.; Wiemer, E.A.C. (2003). Vaults: a ribonucleoprotein involved in drug resistance? *Oncogene*. **22:** 7458–7467.

Muralidharan, S.; Thompson, E.; Raftos, D.; Birch, G.; Haynes, P.A. (2012). Quantitative proteomics of heavy metal stress responses in Sydney rock oysters. *Proteomics*. **12(6):** 906–921.

Murphy, M.P. (2009). How mitochondria produce reactive oxygen species. *Biochemical Journal*. **417(1):** 1–13.

Navarro, E.; Baun, A.; Behra, R.; Hartmann, N.B.; Filser, J.; Miao, A.; Quigg, A.; Santschi, P.H.; Sigg, L. (2008). Environmental behavior and ecotoxicity of engineered nanoparticles to algae, plants and fungi. *Ecotoxicology*. **17:** 372–386.

Nicholson, S.; Lam, P.K.S. (2005). Pollution monitoring in Southeast Asia using biomarkers in the mytilid *mussel Perna viridis* (Mytilidae: Bivalvia). *Environment International*. **31:** 121–132.

Nicholson, S.; Szefer, P. (2003). Accumulation of metals in the soft tissues, byssus and shell of the mytilid mussel *Perna viridis* (Bivalvia: Mytilidae) from polluted and uncontaminated locations in Hong Kong coastal waters. *Marine Pollution Bulletin*. 46: 1035–1048.

Nieto, R.M.; García–Barrera, T.; Gómez–Ariza, J.–L.; López–Barea, J.; (2010). Environmental monitoring of Domingo Rubio stream (Huelva Estuary, SW Spain) by

combining conventional biomarkers and proteomic analysis in *Carcinus maenas*. *Environmental Pollution*. **158:** 401–408.

Nylandsted, J.; Gyrd–Hansen, M.; Danielewicz, A.; Fehrenbacher, N.; Lademann, U.; Høyer–Hansen, M.; Weber, E.; Multhoff, G.; Rohde, M.; Jäättelä, M. (2004). Heat shock protein 70 promotes cell survival by inhibiting lysosomal membrane permeabilization. *The Journal of Experimental Medicine*. **200(4):** 425–435.

Orrenius, S.; Gogvadze, A.; Zhivotovsky. B. (2007). Mitochondrial oxidative stress: Implications for cell death. *Annual Review of Pharmacology and Toxicology*. **47:** 143–183.

Park, S.–Y.; Choi, J. (2011). Geno– and ecotoxicity evaluation of silver nanoparticles in freshwater crustacean *Daphnia magna*. *Environmental Engineering Research*. **15(1):** 23–27.

Puerto, M.; Campos, A.; Prieto, A.; Cameán, A.; de Almeida, A.M.; Coelho, A.V.; Vasconcelos, V. (2011). Differential protein expression in two bivalve species; *Mytilus galloprovincialis* and *Corbicula fluminea*; exposed to *Cylindrospermopsis raciborskii* cells. *Aquatic Toxicology*. **101:** 109–116.

Ringwood, A.H.; McCarthy, M.; Bates, T.C.; Carroll, D.L. (2010). The effects of silver nanoparticles on oyster embryos. *Marine Environmental Research*. **69(1):** 549–551.

Rodríguez–Ortega, M.J.; Grøsvik, B.E.; Rodríguez–Ariza, A.; Goksøyr, A.; López–Barea, J. (2003). Changes in protein expression profiles in bivalve molluscs (*Chamaelea gallina*) exposed to four model environmental pollutants. *Proteomics*. **3:** 1535–1543.

Rotchell, J.M.; Lee, J.–S.; Chipman, J.K.; Ostrander, G.K. (2001). Structure, expression and activation of fish ras genes. *Aquatic Toxicology*. **55:** 1–21.

Shepard, J.L.; Bradley, B.P. (2000). Protein expression signatures and lysosomal stability in *Mytilus edulis* exposed to graded copper concentrations. *Marine Environmental Research*. **50:** 457–463.

Shepard, J.L.; Olsson, B.; Tedengren, M.; Bradley, B.P. (2000). Protein expression signatures identified in *Mytilus edulis* exposed to PCBs, copper and salinity stress. *Marine Environmental Research*. **50:** 337–340.

Shevchenko, A.; Tomas, H.; Havlis, J.; Olsen, J.V.; Mann, M. (2007). In–gel digestion for mass spectrometric characterization of proteins and proteomes. *Nature Protocols.* **1(6):** 2856–2860.

Szefer, P.; Fowler, S.W.; Ikuta, K.; Osuna, F.P.; Ali, A.A.; Kim, B.–S.; Fernandes, H.M.; Belzunce, M.–J.; Guterstam, B.; Kunzendorf, H.; Wo1owicz, M.; Hummel, H.; Deslous–Paoli, M. (2006). A comparative assessment of heavy metal accumulation in soft parts and byssus of mussels from subarctic, temperate, subtropical and tropical marine environments. *Environmental Pollution*. **139:** 70–78.

Takayama, S.; Reed, J.C.; Homma, S. (2003). Heat–shock proteins as regulators of apoptosis. *Oncogene*. **22:** 9041–9047.

Tedesco, S.; Doyle, H.; Blasco, J.; Redmond, G.; Sheehan, D. (2010). Oxidative stress and toxicity of gold nanoparticles in *Mytilus edulis*. *Aquatic Toxicology*. **100:** 178–186.

Thompson, E.L.; Taylor, D.A.; Nair, S.V.; Birch, G.; Haynes, P.A.; Raftos, D.A. (2012). Proteomic discovery of biomarkers of metal contamination in Sydney Rock oysters (*Saccostrea glomerata*). *Aquatic Toxicology*. **109:** 202–212.

Tiede, K.; Hassellöv, M.; Breitbarth, E.; Chaudhry, Q.; Boxall, A.B.A. (2009). Considerations for environmental fate and ecotoxicity testing to support environmental risk assessments for engineered nanoparticles. *Journal of Chromatography A*. **1216(3):** 503–509.

Tomanek L.; Zuzow, M.J. (2010). The proteomic response of the mussel congeners *Mytilus galloprovincialis* and *M. trossulus* to acute heat stress: implications for thermal tolerance limits and metabolic costs of thermal stress. *The Journal of Experimental Biology*. **213:** 3559–3574.

Van Zon, A.; Mossink, M.H.; Houtsmuller, A.B.; Schoester, M.; Scheffer, G.L.; Cheper, R.J.; Sonneveld, P.; Wiemer, E.A.C. (2006). Vault mobility depends in part on microtubules and vaults can be recruited to the nuclear envelope. *Experimental Cell Research*. **312:** 245 – 255.

Vijayavel, K.; Gopalakrishnan, S.; Balasubramanian, M.P. (2007). Sublethal effect of silver and chromium in the green mussel *Perna viridis* with reference to alterations in oxygen uptake, filtration rate and membrane bound ATPase system as biomarkers. *Chemosphere*. **69:** 979–986.

Vioque–Fernández, A. de Almeida, E.A.; López–Barea, J. (2009). Assessment of Doñana National Park contamination in *Procambarus clarkii*: Integration of conventional biomarkers and proteomic approaches. *Science of the Total Environment*. **407:** 1784–1797.

Wang, W.–X.; Rainbow, P.S. (2005). Influence of metal exposure history on trace metal uptake and accumulation by marine invertebrates. *Ecotoxicology and Environmental Safety*. **61:** 145–159.

Watabe, S.; Iwasaki, K.; Funabara, D.; Hirayama, Y.; Nakaya, M.; Kikuchi, K. (2000). Complete amino acid sequence of *Mytilus* anterior byssus retractor paramyosin and its putative phosphorylation site. *Journal of Experimental Zoology*. **286:** 24–35.

Yamada, A.; Yoshio, M.; Oiwa, K.; Nyitray, L. (2000). Catchin, a novel protein in molluscan catch muscles, is produced by alternative splicing from the myosin heavy chain gene. *Journal of Molecular Biology*. **295:** 169–178.

Yang, Z.; Wu, H.; Li, Y. (2010). Toxic Effect on Tissues and Differentially Expressed Genes in Hepatopancreas Identified by Suppression Subtractive Hybridization of Freshwater Pearl Mussel (*Hyriopsis cumingii*) Following Microcystin–LR Challenge. *Environmental Toxicology*. **27(7):** 393–403.

Yeo, M.–K.; Pak, S.–W. (2008). Exposing zebrafish to silver nanoparticles during caudal fin regeneration disrupts caudal fin growth and p53 signaling. *Molecular and Cellular Toxicology*. **4(4):** 311–317.

# CHAPTER 7

## General Discussion

# 7. General discussion

In recent years, nanotechnology has attracted increasing attention due to the capacity to alter the properties of conventional materials and to apply them in different areas such as electronic, biomedical, pharmaceutical, cosmetic, energy, environmental, catalytic and material applications (Tiede *et al*., 2009). Such a large-scale production and increasing applications in several industries underscore the rapid threat for discharge and environmental exposure. Inevitably, these nanomaterials and their by-products will find their way to the aquatic environment. Perhaps the greatest risk of nanotechnology is the fate and interaction of these nanomaterials with the environment and its biological components, which are largely unknown and difficult to predict at present (Bhatt and Tripathi, 2011; Moore, 2006). As the ultimate sink for most conventional contaminants, the aquatic environment is highly susceptible to NPs and aquatic organisms (e.g. filter-feeding molluscs) represent a target group for their effects. Key questions surrounding the environmental risk analysis of nanotechnology include the fate, transport, and behaviour of nanomaterials with its various including biota, tissue distribution, and the response to such exposure (Canesi *et al*., 2012; Moore, 2006; Scown *et al*., 2010). Although knowledge on the toxicology of NMs in aquatic organisms is increasing, there is lack of knowledge regarding exposure concentrations and bioaccumulation of NPs in various tissues, as well as the toxicity at environmentally realistic levels (Baun *et al*., 2008). The present thesis emerges in this context, focusing on the uptake and effects of two important metal NPs (CuO NPs and Ag NPs) in mussels *M. galloprovincialis* using traditional biomarkers and a proteomic approach and comparing their effects to their ionic counterparts ($Cu^{2+}$ and $Ag^{+}$). CuO NPs are one of the most used metal NPs nowadays, with a wide range of industrial and commercial applications (e.g. electronic circuits and batteries, gas sensors, polymers) mainly due to its bactericide properties, and thermal and electrical conductive efficiency (Buffet *et al*., 2011; Griffitt *et al*., 2009). Ag NPs are one of the most commonly used NPs in a broad range of products such as medical equipment, consumer products and household appliances due to their antibacterial properties (www.nanoproject.org). In this chapter, the general conclusions are summarised along with some suggestions for future research.

## 7.1. Nanoparticles characterization

It is often expected that the smaller the particle, the stronger the toxicity, nevertheless, the relationship between the particles inherent properties and their toxicity is more complex that just surface chemistry. Several factors influence the behaviour of NPs in the aquatic environment, namely their physico-chemical properties (e.g. solubility, agglomeration, concentration) the most important ones for determining their fate and ecotoxicity. Considering the properties of these particles, adequate preparation, dosing, maintenance and characterization within the test medium should be taken into account prior to the assessment of ecotoxicological effects (Bhatt and Tripathi, 2011; Scown *et al*., 2010; Tiede *et al*., 2009). In fact, a combination of NPs properties and the behaviour merged with the characteristics of the exposure media should be considered in a NP exposure scenario. In this context, it was necessary to accurately prepare, dose and characterize CuO NPs and Ag NPs in the exposure media (natural seawater) (Chapter 2 and 3) to fully understand and interpret their effects. At the beginning of this thesis little was known about the levels and behaviour of NPs in the marine environment, therefore it was difficult to truly sense what where the emission and load of these NPs in the environment to ensure what were the environmentally relevant concentrations that should de used. Accordingly, the concentrations selected were based on environmentally realist concentrations of their ionic counterparts (Cu and Ag, 10 $\mu g.L^{-1}$), along with data from modelling studies (Chapter 1).

Nanoparticles characterization was accomplished by exploiting particle shape, size (hydrodynamic diameter), surface charge (zeta potential), polydispersity index and intensity using transmission electron microscopy (TEM) and dynamic light scattering (DLS) using NPs suspended in both ultrapure and natural seawater. Results from TEM and DLS for both CuO NPs and Ag NPs (Figure 2.1.1; Chapter 2 and Figure 3.1; Chapter 3, respectively) show spherical shapes and sizes within and higher than those specified by the manufacturer (<50 and <100nm, respectively). CuO NPs and Ag NPs stock solutions were prepared in ultrapure water without the addition of chemical dispersants to eliminate the possibility of additional toxic effects caused by dispersants. Stock solutions were sonicated and kept in constant shake prior to dispersion in the exposure media to ensure the breakdown of NPs aggregates and keep the particles in suspension. As a result, a rapid aggregation of the particles in seawater occurred with sizes increasing with time of exposure (12 hours cycle between water renewal) and the presence of both small and large aggregates (Figure 2.2.1; Chapter 2.2 and Figure 3.1; Chapter 3), leading to the rapid settling of the large aggregates. Furthermore, metal

concentrations in water (collected from the exposure tanks immediately after dosing) gradually decreased over the 12-hour period between water change and redosing. In fact, 53% and 84.2 % of the initial mass of CuO NPs and Ag NPs, respectively, was removed from the water column after the 12-hour exposure. The lost of this amount of both Cu and Ag suggest aggregation, sedimentation and dissolution of the particles in the exposure media that resulted in a lower NPs concentration in the water column and thus a reduced bioavailability of NPs to mussels. Solubility is another important factor, since the release of ions from metal NPs may be determinant for their toxicity. CuO NPs showed a lower solubility (less with 1% of the initial dose), whereas Ag NPs solubility was higher (24.5% of the initial dose, that increases with time). The release of free metal ions from NPs and NPs agglomeration contribute to a higher toxicity towards aquatic organisms and consequently is a major concern in ecotoxicology.

## 7.2. Accumulation of NPs in mussels *M. galloprovincialis* tissues

Little information is available on the route of exposure, bioavailability and uptake mechanisms of NPs to aquatic organisms, as well as their ingestion rates, tissue distribution and internal dose. The challenge lies in the development of methods that allow accurate detection and quantification of the uptake of nanoparticles, mode of action, tissue distribution, and partitioning within cells and sub-cellular components of the organisms. The uptake and mediating toxic responses of these NPs were evaluated and compared to their ionic counterparts.

Even though aggregation and decrease of Cu and Ag concentrations in the water column was observed (12 h cycle), uptake in the gills and digestive gland of mussels occurred, suggesting that Cu and Ag in the water column (NP or ionic form release from the NPs) were available to mussels. Exposure to CuO NPs resulted in an accumulation increased of Cu in mussel gills and digestive gland with time of exposure (Figures 2.1.2 and 2.2.2; Chapter 2). The accumulation pathway of CuO NPs was different from their ionic counterpart, whose accumulation was higher accumulation in the first week and decreased at the end of the exposure period indicating an easier removal of Cu ions. In the case of exposure to Ag NPs and $Ag^{+}$, both Ag forms were accumulated similarly in the gills (Figure 3.2; Chapter 3), decreasing by the end of the exposure period indicating of elimination of Ag from NPs (released from the particles) and $Ag^{+}$. On the other hand, in the digestive gland, Ag NPs accumulation increased with time of exposure, whereas for $Ag^{+}$ a similar pattern of the gills

occurred, with Ag ions eliminated at the end of exposure period (Figure 3.2; Chapter 3). These results suggest that the accumulation of Ag NPs in the digestive gland is, in contrast to that of $Ag^{+}$, time dependent with a similarly pattern to that of CuO NPs in mussel tissues (Chapter 2). Regarding tissue distribution, the digestive gland is the preferential site for CuO and Ag NPs storage (2– to 5–fold higher than the gills), reflecting the key role of this tissue in the metal bioaccumulation and detoxification (Figures 2.2.2 and 3.2; Chapters 2 and 3). The translocation and extent of NPs uptake is size and tissue dependent and in these experimental conditions, the presence of aggregates in suspension (Figure 2.2.1, Chapter 2; Figure 3.1 and Table 3.1; Chapter 3) and particles solubility occurrence increases CuO NPs and Ag NPs bioavailability to mussels, enhancing their uptake and internal distribution. Mussels can incorporate NPs either in the form of aggregates in suspension or dissolved particles across the gills (Canesi *et al*., 2010; Ward and Kach, 2009) where a selective handling of NPs occurs, with NPs aggregates sorted and broken down into smaller particles followed by their transport to the digestive system where they can be stored, eliminated or transferred to other tissues. This is consistent with the results of Ward and Kach (2009) that demonstrated that in mussels exposed to polystyrene NPs ($1.3x10^{4}$ particles.$mL^{-1}$, 100 nm), the presence of aggregates promotes the transport of NPs to the digestive gland where they are taken up by digestive cells possibly via endocytosis with longer gut retention times. Aggregation and solubility although being key factors in exposure and uptake of NPs in aquatic organisms, are also determinants in NPs toxicity (Canesi *et al*., 2010; Ward and Kach, 2009). Overall, NPs are easily taken up by cells especially in the of aggregates/agglomerates form and even though gills seem to be the primary target for NPs toxicity, the digestive gland is the main tissue for their storage.

## 7.3. Effects of CuO NPs in mussels *M. galloprovincialis*

Based on the toxicity of Cu ions towards aquatic organisms namely through the induction of reactive oxygen species (ROS) and oxidative stress (Bebianno *et al*., 2004; Maria and Bebianno, 2011; Regoli and Principato, 1995), the understanding of the effects of Cu in a nano form is of extreme importance. Therefore, Chapters 2, 4 and 5 report for the first time the *in vivo* effects of CuO NPs in *M. galloprovincialis* tissues. For this purpose, biomarkers of oxidative stress (SOD, CAT and GPX), damage (LPO), metal exposure (MT) and neurotoxicity (AChE) were measured in mussel tissues exposed to CuO NPs previously characterized and to their ionic counterpart. Gills and digestive gland are differently affected

by CuO NPs and $Cu^{2+}$, reflecting the distinct physiological and metabolic functions of the two tissues. These two forms of Cu have the capacity to generate ROS by altering the antioxidant capacity of mussels, but these alterations are tissue, time and copper form dependent. In gills, all the antioxidant enzymes increased in the first week following exposure to CuO NPs (Figure 2.1.2; Chapter 2), but at the end of the experiment, both SOD and CAT activities decreased, whereas GPX activities increased. In the gills of mussels exposed to $Cu^{2+}$ all enzymatic activities were activated during the whole exposure period, particularly SOD, while CAT and GPX remained unchanged after the first 3 days of exposure (Figure 2.1.2; Chapter 2.1). In the digestive gland, contrarily to the gills, antioxidant defence system was induced only after a week of exposure to CuO NPs (compared to controls). By the end of exposure, SOD activity remained unchanged, CAT activity decreased (to levels similar to controls) and GPX activity increased (Figure 2.2.3; Chapter 2). As for $Cu^{2+}$, SOD activity was induced after 3 days of exposure, and even though remained unaltered in the following exposure period, the activities were higher than controls and CuO NPs exposed mussels. CAT and GPX activities were only triggered after 7 days of exposure (comparatively to controls) and were in general similar to that of CuO NPs exposed mussels. These findings are in line with data in human cells ($40 g.L^{-1}$, 25-70 nm, 4h) and clams *S. plana* ($10 \mu g.L^{-1}$, 40-500 nm, 16 days) that show that CuO NPs toxicity is mediated by altering the antioxidant capacity of cells against ROS and consequently enzymatic activation or inhibition (e.g. Buffet *et al*., 2011; Fahmy and Cormier, 2009).

In mussels exposed to CuO NPs, MT was induced with time of exposure in both tissues (Figures 2.1.3 and 2.2.4; Chapter 2), reflecting not only the role of this protein in Cu homeostasis and detoxification, but also a possible involvement in the antioxidant defence system by capturing harmful oxidant radicals (e.g. superoxide and hydroxyl radicals) in response to unaltered or inhibited enzymes activities (Viarengo *et al*., 1999). Even though MT induction was directly related to Cu accumulation, no clear signs of CuO NPs elimination (via formation of Cu-MT complexes) were detected in both tissues. These results are similar to others that suggested an important role of MT in oxidative stress originated by NPs, namely in clams *S. plana* exposed to CuO NPs ($10 \mu g.L^{-1}$, 40-500 nm, 16 days) (Buffet *et al*., 2011), the clam *C. fluminea* exposed to Au NPs ($1.6x10^3$-$1.6x10^5$ Au NP/cell, $10 \pm 0.5$ nm, 7 days) (Renault *et al*., 2008) and the freshwater mussel *E. complanata* exposed to CdTe quantum dots (0-8 $mg.L^{-1}$, 24h) (Peyrot *et al*., 2009). MT plays an important role in controlling $Cu^{2+}$ availability and detoxification in mussel tissues (Langston *et al*., 1998; Maria and Bebianno, 2011), so it is not surprising that a relationship exist between Cu

concentrations and MT levels were detected in gills and digestive gland of mussels exposed to $Cu^{2+}$. In the gills, MT levels increased in the first week of exposure (lower induction rate than CuO NPs), decreasing afterwards until the end of the experiment (Figure 2.1.3; Chapter 2). Contrarily, in the digestive gland MT was only induced at the end of the exposure period (Figure 2.2.4; Chapter 2.1), which is in accordance with the Cu accumulation pattern (Figure 2.2.2, Chapter 2.2), corroborating the active role of MT in Cu homeostasis and detoxification as well as in scavenger activities (Langston *et al*., 1998; Maria and Bebianno, 2011). Similar results were detected in *R. decussatus* (Serafim *et al*. 2009) and *Crassostrea gigas* (Damiens *et al*., 2006) exposed to 50 $\mu gCu.L^{-1}$ and 0.5-5 $\mu gCu.L^{-1}$, respectively.

Antioxidant protection in mussel tissues was unable to prevent ROS mediated oxidative damage, as LPO increased linearly with time in mussel gills exposed to CuO NPs and $Cu^{2+}$ (Figure 2.1.3; Chapter 2), with a higher induction in the latter. In the digestive gland, LPO was only detected after one week in mussels exposed to both forms of copper (CuO NPs and $Cu^{2+}$). The cell defence mechanisms (enzymatic activities and MT levels) only proved efficient in the first three days of CuO NPs exposure in both tissues and in $Cu^{2+}$ in the digestive gland, where LPO remained unchanged. These results confirm the hypothesis that one of CuO NPs main toxic mechanism is mediated by oxidative stress leading to significant oxidative damage in the cells that changes over time. This was also observed in human cell cultures (80 $\mu g.cm^2$, 30 nm) and in *E. coli* exposed to CuO NPs (40$g.L^{-1}$, 25-70 nm) (e.g. Fahmy and Cormier, 2009; Ivask *et al*., 2010), as well as in *M. galloprovincialis* exposed to $Cu^{2+}$ (5-60 $\mu g.L^{-1}$) (Bebianno *et al*., 2004; Maria and Bebianno, 2011; Regoli *et al*., 1995).

Regarding neurotoxic effects, AChE activity was inhibited only at the end of the exposure period (Figure 2.1.3; Chapter) in mussels exposed to both CuO NPs and $Cu^{2+}$, with a higher inhibition in the latter. These results confirm the specificity of AChE response to Cu exposure, either in the nano or ionic form, as established in bivalve species exposed to $Cu^{2+}$, e.g. *R. decussatus* exposed to 75 $\mu gCu.L^{-1}$ for 5 days (Bebianno *et al*., 2004) and mussels exposed to 40 $\mu g.L^{-1}$ and 60 $\mu g.L^{-1}$, 1 for 3 weeks (Lehtonen and Leiniö, 2003; Regoli and Principato, 1995) and upon exposure to several types of NPs, specially CuO NPs (100-800 $mg.L^{-1}$ , ~25 nm) (Wang *et al*., 2009).

Given the capacity of CuO NPs to generate oxidative stress and induce oxidative damage, as demonstrated in Chapter 2, it becomes imperative to address the genotoxic potential of these particles, principally in bivalve species. Accordingly, the genotoxic effects of CuO NPs in mussels *M. galloprovincialis* were further assessed (Chapter 4) in mussels exposed to the same CuO NPs concentration and for the same time. Genotoxicity was evaluated by DNA

strand breaks in mussel hemocytes. The exposure to CuO NPs and $Cu^{2+}$ caused different DNA damaging effects, suggesting different modes of action or different degrees of reactivity of Cu dependent on the metal form (nano vs ionic). Exposure to CuO NPs resulted in a significant DNA damage, characterized by an increase in the Comet assay parameters (Olive tail moment, % of tail DNA and tail length), except at the first 3 days of exposure (Figure 4.4, Chapter 4). Contrasting to what exists in the literature, $Cu^{2+}$ is more genotoxic than CuO NPs, as shown by the significant increase in DNA strand breaks with time (Figure 4.4, Chapter 4). These findings suggest that reduced amounts of $Cu^{2+}$ ions are entering the nucleus and interacting with DNA in hemocytes exposed to CuO NPs. Additionally, the presence of aggregates result in the lack of CuO NPs availability and uptake by the hemocytes and their genotoxic potential is most likely mediated by oxidative stress rather than direct interaction with the DNA (Ahamed *et al*., 2010; Karlsson *et al*., 2008). The increased genotoxicity of $Cu^{2+}$ in mussels' hemocytes are be related to its involvement in the formation of ROS and subsequent oxidative damage (Al-Subiai *et al*., 2011; Bolognesi *et al*., 1999).

Overall, these results (Chapters 2 and 4) suggest that oxidative stress is a significant mechanism of CuO NPs toxicity, with a distinct mode of action from $Cu^{2+}$. The levels of free Cu ions are determinant to the dissimilar antioxidant capacity, as well as MT induction, LPO, AChE inhibition and DNA damage. Nevertheless, other factors than the solubility of $Cu^{2+}$ from NPs (poor in the exposure media) seem to contribute to the toxicity of CuO NPs like the tendency to form large particles aggregates that increase with increasing time of exposure, the significant accumulation with time and high retention rate, and the mechanisms inherent to the NPs effects (e.g. extracellular ROS formation, direct contact between particles and cellular membranes or other surface processes). A Trojan horse type mechanism also account for the disruption of Cu homeostasis and ROS production by enabling the transport of Cu ions into the cells (Karlsson *et al*., 2008; Studer *et al*., 2010). Even though all the results (Chapters 2 and 4) have shed a light at the possible mechanisms of action of CuO NPs, further research is required to understand not only the mechanisms inherent to CuO NPs-related oxidative stress but also their uptake pathways, target cell types and endpoints and subsequent detoxification mechanisms among tissues.

With this in mind, a proteomic approach was applied to improve the understanding of the underlying mechanisms of CuO NPs exposure and compare it to that of $Cu^{2+}$. The identification of proteins altered by CuO NPs and $Cu^{2+}$ allowed a global view of their action at the molecular level, helped to clarify and differentiate the mechanisms by which both

forms inflict toxicity and even provide novel and unbiased biomarkers of exposure and effect. Accordingly, in Chapter 5 it is reported for the first time the differential PEPs and the identification of possible new biomarkers in mussels *M. galloprovincialis* exposed to CuO NPs and $Cu^{2+}$ (10 $\mu gCu.L^{-1}$) after 15 days. PEPs from gills and digestive glands were compared between them and to controls. Both CuO NPs and $Cu^{2+}$ induced major changes in PEPs in gills and digestive gland that were tissue and Cu form dependent. These differences reflect the distinct role of these mussel tissues, as well as tissue-specific redox requirements associated with differences in CuO NPs and $Cu^{2+}$ toxic mechanisms. CuO NPs showed a higher tendency to up-regulate proteins in the gills (combined with higher number of new protein spots) while a higher protein reduction was detected in the digestive gland (Table 5.3, Chapter 5). On the other hand, $Cu^{2+}$ that had a tendency to down-regulate and reduce protein spots in the gills and a higher tendency for up-regulate proteins in the digestive gland (Table 5.3, Chapter 5). Gills respond differently to both forms of Cu, where $Cu^{2+}$ stimulates a higher degree of peroxidative damage (e.g. lipid peroxidation, DNA damage) (as seen in Chapter 2 and 4). On the other hand, the digestive gland is the main tissue for $Cu^{2+}$ storage and elimination, as well as NPs storage (mainly in the form of aggregates) allied with a slower NPs elimination (Chapter 2). Apart from specific responses for each Cu form, a set of 2-fold or higher differentially expressed proteins were common between the two Cu forms (Table 5.3 and Figure 5.2, Chapter 5). Fifteen of these proteins were identified by peptide mass fingerprint (Table 5.4 and Figure 5.4, Chapter 5). Identified proteins indicate common response mechanisms induced by CuO NPs and $Cu^{2+}$, namely in cytoskeleton and cell structure (actin, α-tubulin, paramyosin), stress response (heat shock cognate 71, putative C1q domain containing protein), transcription regulation (zinc-finger BED domain-containing protein 1, nuclear receptor subfamily 1G) and energy metabolism (ATP synthase F0 subunit 6). Proteins related to the structure and function of the cytoskeleton (down-regulation of actin and paramyosin and up-regulation of α-tubulin) are the first targets of oxidative stress in bivalves, highlighting a direct link between ROS production and cytoskeleton disruption in mussels exposed to both Cu forms. The induction of heat-shock cognate 71 and C1q domain containing protein was probably initiated in response to oxidative stress, cytoskeleton disruption and apoptosis to protect and repair target proteins and attempt to cope with Cu toxicity (CuO NPs and $Cu^{2+}$). Changes in the expression of zinc-finger BED domain-containing protein 1, nuclear receptor subfamily 1G indicate that the impairment of signal transduction in DNA-related functions is a mechanism by which CuO NPs and $Cu^{2+}$ induce

genotoxicity (as previously seen in Chapter 4). Apart from cytoskeleton, both Cu forms affect the electron transport system by up-regulating ATP synthase F0 subunit 6 in the gills, while $Cu^{2+}$ also down-regulate cytochrome C oxidase subunit III in the digestive gland. Mitochondria plays an important role on the entire cellular Cu homeostasis mechanisms, so, it is not surprising that alterations in cellular Cu levels (Chapter 2) together with Cu-induced ROS affected the mitochondrial proteome and consequently ATP production. Besides the proteins that changed after exposure to both Cu forms, CuO NPs had a marked effect on other biological processes, namely oxidative stress (GST), proteolysis (cathepsin L) and apoptosis (caspase 3/7-1). The up-regulation of GST in the gills is representative of a cellular compensation mechanism when other antioxidant enzymes activities are low (e.g. CAT activity, as seen in Chapter 2.1) to protect against ROS-induced damage. Cathepsin L is a cysteine protease whose up-regulation in the digestive gland is probably associated with CuO NPs uptake in cells and accumulation in lysosomes that upon oxidative stress is determinant for the regulation of CuO NPs-induced apoptosis. The down-regulation of caspase 3/7-1 (main precursor in cell death) shows that apoptosis directly reflect the cytotoxicity of CuO NPs in the digestive gland. On the other hand, $Cu^{2+}$ affects a protein associated with adhesion and mobility, precollagen-D (up-regulated in the digestive gland), that is associated with the detoxification mechanism of $Cu^{2+}$ in mussel digestive gland, and in agreement with the accumulation pattern in this tissue (Figure 2.2.2, Chapter 2.2). The identified proteins clearly show that the toxicity of CuO NPs is not solely due to $Cu^{2+}$ dissolution and mediated by oxidative stress-induced cell signalling cascades (including signals from mitochondria and nucleus) that eventually lead to apoptosis. The present study identified some traditional biomarkers (e.g. heat shock proteins, actin, GST, ATP synthase) along with putative novel ones for CuO NPs (caspase 3/7-1, catL, Zn-finger) and $Cu^{2+}$ (precol-D) exposure in mussel tissues.

### 7.4 Effects of Ag NPs in mussels *M. galloprovincialis*

Ionic Ag is one of the most toxic metals to both freshwater and marine organisms, being highly persistent in the environment with a great capacity to accumulate in sediments and organisms (e.g. Luoma, 2008; Wang and Rainbow, 2005). In aquatic organisms (as fish) its effects are well document but less is known about the mechanisms by which Ag NPs exert toxicity to invertebrates. Accordingly, there is a pressing need to unravel the *in vivo* effects of Ag NPs in *M. galloprovincialis*. Chapter 3 describes and compares the potential of both Ag

NPs and $Ag^{+}$ to induce cellular oxidative stress in the gills and digestive gland of *M. galloprovincialis* exposed to 10μgAg.$L^{-1}$ for 15 days. Like for Cu, traditional biomarkers of oxidative stress (SOD, CAT and GPX), damage (LPO) and metal exposure (MT) were followed in mussel tissues. Similarly to what was observed for CuO NPs and $Cu^{2+}$ exposures, the effects of Ag NPs and $Ag^{+}$ in *M. galloprovincialis* are tissue, time and metal form dependent (ionic vs nano). Ag NPs induced an overall increase in the antioxidant enzymes in the gills, whereas in $Ag^{+}$ exposed mussels enzymatic activities tend to decrease with time of exposure (Figure 3.3, Chapter 3). Therefore, exposure to Ag NPs is likely to enhance the production of superoxide radical and hydrogen peroxide in the gills that consequently enhance the activity of SOD, CAT and GPX and reduce the possibility of oxidative damage to occur. Contrarily, a higher production of free ROS levels (superoxide anions and hydroxyl radicals) originated by $Ag^{+}$ and the reduction of SOD lead to the catalytic impairment (decrease in enzymatic activities) of CAT and GPX (Figure 3.3, Chapter 3) by interaction with thiol-groups (Bar-Ilan *et al*., 2009; Lapresta-Fernández *et al*., 2012). Contrarily to what was found in the gills, in the digestive gland Ag NPs enhanced all enzymatic activities at the beginning of the experiment as a result of ROS formation. However, the alterations in SOD and GPX activities were only transitory, while CAT was inhibited suggesting an increase of $H_2O_2$ formation. As for $Ag^{+}$, a reduction on SOD activity was also observed with time of exposure. Nevertheless, CAT and GPX activities remained (in general) unchanged with time and where lower than Ag NPs. These results suggest differential and less pronounced responses in the digestive gland compared to the gills, especially for Ag NPs exposed mussels, suggesting a lower damaging effect of ROS in this tissue. No data is available concerning either the effect of $Ag^{+}$ or Ag NPs in mussel antioxidant system. However different and transitory responses of antioxidant activities and consequent oxidative stress were already reported for Ag NPs in *D. rerio* (2-120 mg.$L^{-1}$, 5-20 nm), *Drosophila melanogaster* (50-100 μg.$mL^{-1}$, 10 nm) and human cells (0.76-50 μg.$mL^{-1}$, 7-20 nm) (Ahamed *et al*., 2010; Asharani *et al*., 2009; Choi *et al*., 2010).

The role of MT in Ag homeostasis and detoxification (Amiard *et al*., 2006; Lansgton *et al*., 1998) was confirmed by the exposure of mussels' gills to Ag NPs and $Ag^{+}$ (Figure 3.4; Chapter 3), with a significant induction of MT along the exposure period (especially by $Ag^{+}$ at day 15). This result is further corroborated by Ag accumulation patterns for both Ag forms in this tissue (Figure 3.2; Chapter 3). So, it seems that Ag NPs and $Ag^{+}$ released from the NPs are able to bind to MTs to regulate Ag bioavailability, detoxify Ag ions or scavenge ROS generated by these particles. These results are in accordance with those obtained for Ag NPs

in *C. virginica* (1.6-0.0016 μg.$L^{-1}$, 15 ± 6 nm), *D. rerio* (30-120 mg.$L^{-1}$, 5-20 nm) and *O. latipes* (1-25 μg.$L^{-1}$, 49.6 nm) (Chae *et al*., 2009; Choi *et al*., 2010; Ringwood *et al*., 2010). On the other hand, in the digestive gland MT levels remained unchanged after a significant induction in the first 3 days of exposure to both Ag forms (NPs and $Ag^{+}$) (Figure 3.4; Chapter 3). The induction of MT is related to the decrease in $Ag^{+}$ in the end of exposure, whereas for Ag NPs the presence of other mechanisms of detoxification (small fraction of Ag associated with MT) may explain the absence of any signs of detoxification in this tissue. This is in agreement with previous results that show that in the digestive gland of bivalves $Ag^{+}$ is mainly associated with sulphides in lysosomes forming stable insoluble Ag-complex that are able to detoxify Ag in this tissue (Berthet *et al*., 1992; Geffard *et al*., 2004). Nevertheless, this complex is not easily eliminated by mussels especially in the case of Ag NPs (Figure 3.2; Chapter 3). The mechanism of storage of Ag NPs as non-toxic, insoluble silver-sulphide precipitates could inhibit the potentially deleterious effects of these NPs.

Given the capacity of Ag NPs and $Ag^{+}$ to generate ROS (e.g. Bar-Ilan *et al*., 2009; Lapresta-Férnandez *et al*., 2012) and cause membrane damage by increasing LPO (Ahamed *et al*., 2010; Choi *et al*., 2010), it is not surprising that Ag NPs and $Ag^{+}$ exposure cause LPO in the gills of exposed mussels (Figure 3.4; Chapter 3). These results suggest that the antioxidant defence system (antioxidant enzymes plus MT) were unable to efficiently detoxify ROS production and prevent oxidative damage, especially in the case of mussels exposed to Ag NPs while in those exposed to $Ag^{+}$ this only occurred at the beginning of the experiment. In the digestive gland, $Ag^{+}$ presented a similar trend to the gills, whereas for Ag NPs no LPO was detected (Figure 3.4; Chapter 3). The lack of LPO in the digestive gland of mussels exposed to Ag NPs (despite the accumulation of Ag – Chapter 3) could result from an intensification of the antioxidant defence system of mussels (including MT) or to the induction of other components of the antioxidant defence system (e.g. GR, GST). These results strongly suggests a higher ROS formation by Ag NPs exposure than $Ag^{+}$, probably related to a higher availability of free Ag ions released from the particles combined with the intrinsic effect of Ag NPs. As for CuO NPs, the potential of Ag NPs to originate oxidative stress and oxidative damage (see Chapter 3) led to further analysis on the possible genotoxic effects of these particles (Chapter 4). Exposure to Ag NPs and $Ag^{+}$ caused different degrees of DNA damage in mussel hemocytes that are time and Ag form dependent, suggesting different modes of action involved in DNA damage. DNA strand breaks increased with time of exposure in mussels exposed to Ag NPs but the increase was higher in $Ag^{+}$-exposed mussels (Figure 4.4, Chapter 4). These results are in accordance with previous studies that

showed that $Ag^+$ has a higher genotoxic potential than Ag NPs, namely through direct interaction with DNA by the formation of ROS (e.g. Bar-Ilan *et al*., 2009; Singh *et al*., 2009). Commonly to what was found for CuO NPs, reduced amounts of $Ag^+$ ions are entering the nucleus and interacting with DNA in hemocytes exposed to Ag NPs (compared to $Ag^+$), probably resulting from a lack of NPs availability and uptake by hemocytes due to the formation of aggregates/agglomerates (Figure 3.2, Chapter 3). Thus, their genotoxic potential are most likely due to direct (direct interaction of NPs with DNA) or indirect interactions (oxidative stress and ROS) that result in oxidative lesions as DNA strand breaks, among others (e.g. Ahamed *et al*., 2010; Asharani *et al*., 2009; Choi *et al*., 2010).

Overall, these results (Chapters 3 and 4) show that the different antioxidant capacity, MT induction, LPO and DNA damage obtained of Ag NPs exposed mussels confirm the hypothesis that oxidative stress mediates these NPs toxicity, with a different mode of action to $Ag^+$, with ROS mostly generated by free Ag ions. This different capacity of the two forms of Ag to originate ROS is also related to the presence of Ag NPs mainly in the form of aggregates/agglomerates and the significant Ag NPs accumulation with time of exposure, namely in the digestive gland. In addition to the release of $Ag^+$ ions from NPs (increased solubility with time of exposure), other mechanisms by which these NPs can originate toxicity at the cellular level cannot be discharged. If not taken up by cells Ag NPs could mediate toxicity by attacking the cellular membrane surface and release $Ag^+$ compromising cell integrity and permeability or originate extracellular ROS and oxidative stress by surface processes due to the nanoparticle effect (Farkas *et al*., 2010; Navarro *et al*., 2008). A Trojan horse-type mechanism that enable the transport of metal ions into cells (Limbach *et al*., 2007) or surface oxidation of Ag NPs after contact with proteins in the cytoplasm that liberates $Ag^+$ ions, can also amplify Ag NPs toxicity (Asharani *et al*., 2009).

As for CuO NPs, a proteomic analysis was undertaken in mussels exposed to both Ag NPs and $Ag^+$ to clarify the Ag NPs-induced oxidative stress, identify other protein pathways due to NPs exposure or detect new biomarkers. Accordingly, Chapter 6 reports for the first time the differential protein expression signatures and the identification of putative new biomarkers in mussels *M. galloprovincialis* exposed to 10 $\mu gAg.L^{-1}$ of Ag NPs and $Ag^+$ for 15 days. The 2-DE proteomes of gills and digestive glands of mussels exposed to both Ag forms were compared between them and to controls. As for CuO NPs (Chapter 5), the effects of Ag NPs and $Ag^+$ in PEPs are tissue and Ag form dependent. Higher up-regulation combined with new and suppressed protein spots were observed in the gills of Ag NPs exposed mussels, while in $Ag^+$ exposure this number was lower (Table 6.3; Chapter 6). The

fact that gills are more vulnerable to metal release from the particles, as well as particle interaction may result in oxidative stress (Chapter 3). On the other hand, Ag NPs induced a higher number of new proteins in the digestive gland (compared to the gills and to $Ag^{+}$) (Table 6.3; Chapter 6) that may be related to the higher Ag NPs accumulation (in the form of aggregates) (Chapter 3). Furthermore, the similar number of suppressed proteins between Ag NPs and $Ag^{+}$ (lower than gills) also account for the importance of the digestive gland in the accumulation and detoxification of Ag (Chapter 3). Different mechanisms are involved in the toxicity of Ag NPs and $Ag^{+}$ as different sets of differentially expressed proteins were detected in both tissues (Table 6.3, Figure 6.3, Chapter 6). Nevertheless, the release of $Ag^{+}$ from the particles may also account for the similarity of PEPs of exposed mussels, characterized by a common set of 2-fold or higher regulated proteins (Table 6.3, Figure 6.3, Chapter 6). Fifteen of the differentially expressed proteins from both tissues (common and specific to Ag NPs and $Ag^{+}$) were identified (Table 6.4, Figure 6.5, Chapter 6). The proteins common to Ag NPs and $Ag^{+}$ are related to cytoskeleton and cell structure (catchin protein, myosin heavy chain), stress response (heat-shock protein 70), oxidative stress (GST), transcription regulation (nuclear receptor subfamily 1G), adhesion and mobility (precollagen-P), and energy metabolism (ATP synthase F0 subunit 6 and NADH dehydrogenase subunit 2). As in Chapter 5, one of the explanations for the alteration in proteins associated with the structure and function of the cytoskeleton (down-regulation of catchin in gills and up-regulation of myosin in digestive gland) is oxidative stress that is related with the production of ROS by both Ag NPs and $Ag^{+}$ with cytoskeleton disorganization. The down-regulation of heat shock protein 70 in response to Ag NPs and $Ag^{+}$ in the gills is not surprising, as these proteins have key roles in cell protection and repair from damage induced by oxidative stress. Nevertheless, this alteration is also associated with the induction of apoptosis in mussel gills. GST plays a role in the antioxidant defence system of bivalves including ROS metabolism, so the up-regulation of this enzyme in the gills account for a cellular compensation mechanism to protect cells against ROS-induced damage (e.g. Chapter 3). Furthermore, the up-regulation of the nuclear receptor subfamily 1G in the gills indicates that both Ag forms have the capacity to interfere with signal transduction in DNA-related functions and induce genotoxicity, confirming the genotoxic potential of both Ag NPs and $Ag^{+}$, as seen in Chapter 4. The up-regulation of precollagen-P seems to be associated with Ag elimination in mussel gills in response to Ag NPs increased solubility with time of exposure ($Ag^{+}$ released from the particles) and $Ag^{+}$ exposure, which is in agreement with the accumulation patterns obtained for this tissue (Figure 3.2, Chapter 3). Both Ag forms also affected ATP synthase F0 subunit

6 (up-regulated by Ag NPs and down-regulated by $Ag^+$) and NADH dehydrogenase subunit 2 (up-regulated) in the gills and digestive gland, respectively, altering the normal mitochondrial electron transport system and consequently the production of ATP and ROS. Apart from affecting proteins related to cytoskeleton (paramyosin), exposure to Ag NPs also affects two proteins involved in stress response (major vault protein and and ras partial). The up-regulation of major vault protein in the gills and ras partial in the digestive gland represent a specific response against the genotoxic potential of these particles (seen in Chapter 4). Additionally, the induction of ras partial is also associated with the uptake of Ag NPs in the digestive gland (and consequent cytoskeleton disruption). $Ag^+$ had a strong influence in the up-regulation of the stress protein putative c1q domain containing protein in the gills, representative of disruption of the immune function of mussels associated with oxidative stress. Furthermore, the oxidative stress capacity of $Ag^+$ also resulted in the down-regulation of two cytoskeleton proteins (actin and $\alpha$-tubulin) in the gills. Overall, these results show that $Ag^+$ released from the NPs is not the only factor responsible for the different patterns of expression detected in exposed mussels and commonly to what was found for CuO NPs, is mediated by oxidative stress signal transduction pathways that can lead to apoptosis, even if by different pathways. Some classical biomarkers (heat shock protein 70, GST, actin) were identified, as well as new biomarkers proposed to assess Ag NPs (major vault protein, and ras partial) and $Ag^+$ (precol-P and putative C1q domain containing protein) toxicity in mussel tissues. These results along with those for CuO NPs show that proteomic is a valuable approach to assess NPs exposure and effect and can help differentiate nano-specific biological responses and mechanisms of action between NPs and their similar ionic/bulk counterpart. However, the absence of the mussel genome prevents the identification of other proteins that might be relevant to clarify the mode of action of these NPs in this species.

All of the oxidative and genotoxic changes induced by CuO NPs and Ag NPs suggest that oxidative stress is the major NP-induced toxicity, nevertheless, with different mechanisms and oxidative stress potential. Both NPs toxicity in mussel tissues is mediated by altering the antioxidant capacity of cells against ROS and consequently enzymatic activation or inhibition. Nevertheless, gills seem to be more susceptible to CuO NPs, as inhibition of antioxidants enzymes was more pronounced. Both CuO NPs and Ag NPs induced MT in gills, confirming its role in metal homeostasis and detoxification and in the capture of harmful oxidant radicals. Additionally, despite different antioxidant efficiency, both NPs were also responsible for inducing LPO, confirming the capacity of these NPs to inflict

oxidative damage. Mussels were more efficient in eliminating Ag NPs from this tissue (reflected by the accumulation patterns), probably due to a higher propensity of these particles to dissolve with time compared to CuO NPs (<1%), evidencing a higher effect of the CuO NPs themselves rather than dissolved $Cu^{2+}$, thus leading to higher ROS formation. On the other hand, significant differences were obtained between NPs mode of action in the digestive gland. Even though this tissue is the main storage tissue for CuO NPs and Ag NPs (namely aggregates), less pronounced antioxidant responses were obtained than that of gills (generally increased or unchanged), suggesting a lower effect of ROS in this tissue by both NPs. The results obtained for MT diverged between NPs, reflecting different/additional mechanism of storage associated with the NP/metal type. Similarly to the gills, in mussels exposed to CuO NPs MT was induced with time of exposure, while in Ag NPs exposure, the storage of Ag NPs as non-toxic, insoluble Ag-sulphide precipitates left a little role for MT. The presence of these stable Ag-sulphide complexes is also responsible for the absence of LPO in mussels exposed to Ag NPs, contrarily to what was found in CuO NPs exposure. Oxidative stress was also responsible for the genotoxicity results in mussel hemocytes, where both particles presented similar time response effects. However, no clear insights exist on the mechanisms by which these NPs inflict DNA strand breaks.

Commonly to what was concluded from the biomarker responses, protein identification revealed that NPs toxicity is mediated by oxidative stress-induced signalling pathways mediated by the mitochondria and nucleus that can lead to apoptosis, even if by different pathways. Most of the identified proteins for CuO NPs and Ag NPs belong to the same biological functions, with responses in cytoskeleton and cell structure (paramyosin), stress response (HSPs), oxidative stress (GST), transcription regulation (nuclear receptor 1G) and energy metabolism (ATP synthase F0 subunit6). In general, cytoskeleton disorganization (particle uptake), alterations in the mitochondrial membrane potential (ATP and ROS production), capacity to induce ROS (NPs surface reactivity and/or release $Cu^{2+}$ and $Ag^{+}$), potency to genotoxicity and disruption of the membrane systems (lipid peroxidation/ROS) together with disorganization of intracellular $Ca^{2+}$ homeostasis (cytoskeleton/oxidative stress) seems to point towards multiple ways of these NPs to induce cell death. Nevertheless, some of the identified PESs specific for CuO NPs and Ag NPs allowed the differentiation of the mechanisms by which they inflict apoptosis in mussels. CuO NPs affected proteins involved in apoptosis (caspase 3/7-1) and proteolysis (cathepsin L) that combined with the over-expression of heat-shock cognate 71 where essential do unravel that the most likely apoptotic pathway followed by these particles is caspase dependent. On the other hand, no specific

markers of apoptosis were detected in Ag NPs exposure, but the differential expression of MVP, ras partial and HSP70 seems to support the idea of the activation of an alternative HSP70-controlled apoptotic pathway that is most likely tumour-specific and caspase independent. Additionally, Ag NPs higher dissolution with time (compared to CuO NPs) also promoted the alteration of precollagen P, a protein involved in the detoxification of metals in mussels' tissues, highlighting the importance of particle solubility in NP behaviour and toxicity. Taken together, these results show that even though oxidative stress and apoptosis are similar outcomes for NP toxicity, particle composition, size and distribution, solubility, agglomeration and chemistry are key elements for determining their modes of action.

## 7.5. Conclusions

In this thesis, the use of traditional biomarkers of oxidative stress, damage, metal exposure and neurotoxicity were combined with proteomic methods to evaluate the effects of CuO and Ag NPs exposure in mussels *M. galloprovincialis*. A proper NP characterization in experimental media was also undertaken to link NPs properties and behaviour to toxic responses. The final conclusions of this dissertation on the effects of nanoparticles in the mussel *M. galloprovincialis* are summarized as follows:

- Filter-feeding organisms as *M. galloprovincialis* are significant targets for NP exposure thus being appropriate species to evaluate nano-ecotoxicology in the aquatic environment.
- Aggregation and solubility are key factors in exposure, uptake and toxicity of NPs in aquatic organisms. In fact, a relationship between the formation of aggregates/ agglomerates and particle solubility in exposure media and biomarkers responses with time of exposure seems to exist.
- NPs uptake and distribution in mussels are type, time and tissue dependent, where the presence of aggregates/agglomerates in suspension and NP solubility increases NP bioavailability, enhancing their uptake and internal distribution.
- Mussel gills are more susceptible to metal dissociation from NPs than its internalization, as evidenced by a stronger oxidative response, whereas the digestive gland is the main tissue for their storage, namely in the form of aggregates.
- Oxidative stress is a significant mechanism of toxicity of CuO and Ag NPs in mussel tissues, suggested by the alteration on the antioxidant capacity of cells against ROS formation and consequently enzymatic activation/ inhibition, along with increases in

LPO and DNA damage with time of exposure, whose mode of action depends on the particle type and tissue (more pronounced in the gills).

- MTs have an important role in Cu and Ag detoxification, either by binding specifically to NPs to regulate metal homeostasis, detoxifying metal ions released from the particles or scavenging ROS generated by these particles. The same do not apply for the digestive gland in mussels exposed to Ag, as other mechanisms of storage and elimination seem to exist, namely by the formation of insoluble Ag-sulphite precipitates.
- Antioxidant enzymes activities (SOD, CAT and GPX), MTs induction, LPO and DNA damage are valuable tools to assess the oxidative status of mussel tissues exposed to both types of NPs (CuO and Ag NPs). Additionally, AChE is also an efficient biomarker to assess the neurotoxic potential of CuO NPs.
- Proteomic data show that CuO NPs and Ag NPs toxicity are not solely due to $Cu^{2+}$ and $Ag^{+}$ dissolution and is mediated by oxidative stress-induced cell signaling cascades (including signals from mitochondria and nucleus) that eventually lead to apoptosis but by different mechanisms.
- CuO NPs and $Cu^{2+}$, as well as Ag NPs and $Ag^{+}$ induced major alterations in PEPs in mussel tissues showing several tissue and metal-dependant responses (ionic vs nano). The obtained PESs obtained were useful for detecting the effects of these NPs in organisms and for suggesting new putative biomarkers.
- Both CuO NPs and $Cu^{2+}$ induce changes in proteins involved in cytoskeleton and cell structure (actin, α-tubulin, paramyosin) stress response (heat shock cognate 71, putative C1q domain containing protein), transcription regulation (Zn-finger BED containing protein 1, nuclear receptor family 1G) and energy metabolism (ATP synthase F0 subunit 6). CuO NPs alone affect proteins related to oxidative stress (GST), apoptosis (caspase 3/7-1) and proteolysis (cathepsin L), whereas $Cu^{2+}$ has a marked effect in a protein normally associated with adhesion and mobility (precollagen D).
- Ag NPs affected the same type of cellular pathways as $Ag^{+}$, namely cytoskeleton and cell structure (catchin protein, myosin heavy chain), stress response (heat shock protein 70), oxidative stress (GST), transcription regulation (nuclear receptor family 1G), adhesion and mobility (precollagen D), and energy metabolism (ATP synthase F0 subunit 6 and NADH dehydrogenase subunit 2). Exposure to Ag NPs alone

significantly affect proteins involved in stress response (major vault protein and ras, partial) and cytoskeleton and cell structure (paramyosin), whereas $Ag^{+}$ had a strong influence in two proteins involved in cytoskeleton and cell structure (actin and α-tubulin) and one protein responsible for stress response (putative C1q domain containing protein).

- Zinc-finger protein is proposed as a potential new biomarker for CuO NPs and $Cu^{2+}$ exposure; caspase 3/7-1 and cathepsin L as potential biomarkers for CuO NPs exposure, while precollagen D molecular a new biomarker for $Cu^{2+}$ exposure in mussel tissues.
- Precollagen P is proposed as a potential new biomarker for Ag NPs and $Ag^{+}$ exposure; ras partial and main vault protein Ag NPs exposure; while putative C1q domain containing protein a new biomarker for $Ag^{+}$ exposure in mussel tissues.
- While the absence of the mussel genome precluded the identification of other proteins relevant to clarify the effects of these NPs, proteomics analysis allowed the identification of protein expression changes in mussel tissues exposed to NPs and provided additional knowledge of potential CuO NPs and Ag NPs effects at biochemical level.

## 7.6. Future perspectives

Having in mind these thesis results, some key points are suggested for future research to better understand the mechanisms associated with NPs toxicity:

- Unravel NPs uptake pathways in mussels and determine if and how quick NPs can translocate from water to the hemolymph and to other tissues and accumulate.
- Dose-dependent studies using CuO and Ag NPs of different size to help define target cell types and endpoints, as well as the importance of size in the toxicity of these particles.
- The detoxification mechanisms by which mussels eliminate CuO and Ag NPs, and the involvement of MTs, whether they differ between nano and ionic form, how and how long after exposure they are triggered and in what form are these metals eliminated.
- Validate the utility of the putative new biomarkers suggested for future use in nanotoxicology. Proper characterization of the toxic mechanisms of CuO NPs and Ag NPs, and clarification of their interaction with different cellular targets (e.g. mitochondria, nucleus) and in what form they remain in the cell (ionic or NP).

- Application of other 'omics' tools, e.g. genomic and metallomics to complement the information obtained at the gene expression level and metal binding to better understand the mechanisms of toxicity of these two NPs.

## 7.7. References

Ahamed, M.; Siddiqui, M.A.; Akhtar, M.J.; Ahmad, I.; Pant, A.B. (2010). Genotoxic potential of copper oxide nanoparticles in human lung epithelial cells. *Biochemical and Biophysical Research Communications*. **396:** 578-583.

Al-Subiai, S.N.; Moody, A.J.; Mustafa, S.A.; Jha, A.N. (2011). A multiple biomarker approach to investigate the effects of copper on the marine bivalve mollusc, *Mytilus edulis*. *Ecotoxicology and Environmental Safety*. **74:** 1913-1920.

Amiard, J.-C.; Amiard-Triquet, C.; Barka, S.; Pellerin, J.; Rainbow, P.S. (2006). Metallothioneins in aquatic invertebrates: Their role in metal detoxification and their use as biomarkers. *Aquatic Toxicology*. **76:** 160-202.

Asharani, P.V.; Mun, G.L.K.; Hande, M.P.; Valiyaveettil, S. (2009). Cytotoxicity and genotoxicity of silver nanoparticles in human cells. *ACS Nano*. **3(2):** 279-290.

Bar-Ilan, O.; Albrecht, R.M.; Fako, V.E.; Furgeson, D.Y. (2009). Toxicity assessments of multisized gold and silver nanoparticles in zebrafish embryos. *Small*. **5(16):** 1897-1910.

Baun, A.; Hartmann, N.B.; Grieger, K.; Kusk, K.O. (2008). Ecotoxicity of engineered nanoparticles to aquatic invertebrates: a brief review and recommendations for future toxicity testing. *Ecotoxicology*. **17:** 387-395.

Bebianno, M.J.; Géret, F.; Hoarau, P.; Serafim, M.A.; Coelho, M.R.; Gnassia-Barelli, M.; Roméo, M. (2004). Biomarkers in *Ruditapes decussatus*: a potential biondicator species. *Biomarkers*. ***9*(4-5):** 305-330.

Berthet, B.; Amiard, J.C.; Amiard-Triquet, C.; Martoja, M.; Jeantet, A.Y. (1992) Bioaccumulation, toxicity and physico-chemical speciation of silver in bivalve molluscs: ecotoxicological and health consequences. *Science of the Total Environment*. **125:** 97–122.

Bhatt, I.; Tripathi, B.N. (2011). Interaction of engineered nanoparticles with various components of the environment and possible strategies for their risk assessment. *Chemosphere*. **82(3):** 308–317.

Bolognesi, C.; Landini, E.; Roggieri, P.; Fabbri, R.; Viarengo, A. (1999). Genotoxicity biomarkers in the assessment of heavy metal effects in mussels: experimental studies. *Environmental and Molecular Mutagenesis*. **33:** 287-292.

Buffet, P.E.; Tankoua, O.F.; Pan, J.F.; Berhanu, D.; Herrenknecht, C.; Poirier, L.; Amiard-Triquet, C.; Amiard, J.C.; Bérard, J.B.; Risso, C.; Guibbolini, M.; Roméo, M.; Reip, P.; Valsami-Jones, E.; Mouneyrac, C. (2011). Behavioural and biochemical responses of two marine invertebrates *Scrobicularia plana* and *Hediste diversicolor* to copper oxide nanoparticles. *Chemosphere*. **84:** 166–174.

Canesi, L.; Ciacci, C.; Fabbri, R.; Marcomini, A.; Pojana, G.; Gallo, G. (2012). Bivalve molluscs as a unique target group for nanoparticle toxicity. *Marine Environmental Research*. **76:** 16-21.

Canesi, L.; Fabbri, R.; Vallotto, D.; Marcomini, A.; Pojana, G. (2010). Biomarkers in *Mytilus galloprovincialis* exposed to suspensions of selected nanoparticles (Nano carbon black, C60 fullerene, Nano–$TiO_2$, Nano–$SiO_2$). *Aquatic Toxicology*. **100:** 168–177.

Chae, Y.J.; Pham, C.H.; Lee, J.; Bae, E.; Yi, J.; Gu, M.B. (2009). Evaluation of the toxic impact of silver nanoparticles on Japanese medaka (*Oryzias latipes*). *Aquatic toxicology*. **94(4):** 320–327.

Choi, J.E.; Kim, S.; Ahn, J.H.; Youn, P.; Kang, J.S.; Park, K.; Yi, J.; Ryu, D.-Y. (2010). Induction of oxidative stress and apoptosis by silver nanoparticles in the liver of adult zebrafish. *Aquatic Toxicology*. **100:** 151–159.

Damiens, G.; Mouneyrac, C.; Quiniou, F.; His, E.; Gnassia-Barelli, M.; Roméo, M. (2006). Metal bioaccumulation and metallothionein concentrations in larvae of *Crassostrea gigas*. *Environmental Pollution*. **140:** 492-499.

Fahmy, B.; Cormier, S.A. (2009). Copper oxide nanoparticles induce oxidative stress and cytotoxicity in airway epithelial cells. *Toxicology In Vitro*. **23:** 1365–1371.

Farkas, J.; Christian, P.; Urrea, J.A.G.; Roos, N.; Hassellöv, M.; Tollefsen, K.E.; Thomas, K.V. (2010). Effects of silver and gold nanoparticles on rainbow trout (*Oncorhynchus mykiss*) hepatocytes. *Aquatic toxicology*. **96(1):** 44–52.

Geffard, A.; Jeantet, A.Y.; Amiard, J.C.; Pennec, M.L.; Ballan-Dufrançais, C.; Amiard-Triquet, C. (2004). Comparative study of metal handling strategies in bivalves *Mytilus edulis* and *Crassostrea gigas*: a multidisciplinary approach. *Journal of Marine Biological Association of the United Kingdom*. **84:** 641–650.

Griffitt, R.J.; Hyndman, K.; Denslow, N.D.; Barber, D.S. (2009). Comparison of molecular and histological changes in zebrafish gills exposed to metallic nanoparticles. *Toxicological Sciences*. **107(2):** 404–415.

http://www.nanotechproject.org The project on emerging nanotechnologies (2012). Woodrow Wilson International Center for Scholars, Washington, DC, USA. Accessed March 2012.

Ivask, A.; Bondarenko, O.; Jepihhina, N.; Kahru, A. (2010). Profiling of the reactive oxygen species-related ecotoxicity of CuO, ZnO, $TiO_2$, silver and fullerene nanoparticles using a set of recombinant luminescent *Escherichia coli* strains: differentiating the impact of particles and solubilised metals. *Analytical and Bioanalytical Chemistry*. **398:** 701–716.

Karlsson, H.L.; Cronholm, P.; Gustafsson, J.; Möller, L. (2008). Copper oxide nanoparticles are highly toxic: a comparison between metal oxide nanoparticles and carbon nanotubes. *Chemical Research in Toxicology*. **21:** 1726-1732.

Langston, W.J.; Bebianno, M.J.; Burt, G.R. (1998). Metal handling strategies in molluscs. In: Langston, W.J.; Bebianno, M.J. (Eds.). Metal Metabolism in Aquatic Environments. Chapman and Hall, London, pp. 219–283.

Lapresta-Fernández, A.; Fernández, A.; Blasco, J. (2012). Nanoecotoxicity effects of engineered silver and gold nanoparticles in aquatic organisms. *Trends of Analytical Chemistry*. **32:** 40–59.

Lehtonen, K.K.; Leiniö, S. (2003). Effects of exposure to copper and malathion on metallothionein levels and acetylcholinesterase activity of the mussel *Mytilus edulis* and the clam *Macoma balthica* from the Northern Baltic Sea. *Bulletin of Environmental Contamination and Toxicology*. **71:** 489-496.

Limbach, L.K.; Wick, P.; Manser, P.; Grass, R.N.; Bruinink, A.; Stark, W.J. (2007). Exposure of engineered nanoparticles to human lung epithelial cells: influence of chemical composition and catalytic activity on oxidative stress. *Environmental Science and Technology*. **41:** 4158-4163.

Luoma, S.N. (2008). Silver Nanotechnologies and the Environment: Old Problems or New Challenges. Project on Emerging Nanotechnologies. Publication 15. Woodrow Wilson International Centre for Scholars and PEW Charitable Trusts, Washington, DC.

Maria, V.L.; Bebianno, M.J. (2011). Antioxidant and lipid peroxidation responses in *Mytilus galloprovincialis* exposed to mixtures of benzo(a)pyrene and copper. *Comparative Biochemistry and Physiology Part C: Toxicology and Pharmacology*. **154(1):** 56–63.

Moore, M.N. (2006). Do nanoparticles present ecotoxicological risks for the health of the aquatic environment? *Environmental International*. **32:** 967–976.

Navarro, E.; Baun, A.; Behra, R.; Hartmann, N.B.; Filser, J.; Miao, A.; Quigg, A.; Santschi, P.H.; Sigg, L. (2008). Environmental behavior and ecotoxicity of engineered nanoparticles to algae, plants and fungi. *Ecotoxicology*. **17:** 372-386.

Peyrot, C.; Gagnon, C.; Gagné, F.; Willkinson, K. J.; Turcotte, P.; Sauvé, S. (2009). Effects of cadmium telluride quantum dots on cadmium bioaccumulation and metallothionein production to the freshwater mussel, *Elliptio complanata*. *Comparative Biochemistry and Physioogy C*. **150:** 246-251.

Regoli, F.; Principato, G. (1995). Glutathione, glutathione-dependent and antioxidant enzymes in mussel, *Mytilus galloprovincialis*, exposed to metals under field and laboratory conditions: implications for the use of biochemical biomarkers. *Aquatic Toxicology*. **31:** 143-164.

Renault, S.; Baudrimont, M.; Mesmer- Dudons, N.; Gonzalez, P.; Mornet, S.; Brisson, A. (2008). Impacts of gold nanoparticle exposure on two freshwater species: a phytoplanktonic alga (*Scenedesmus subspicatus*) and a benthic bivalve (*Corbicula fluminea*). *Gold Bulletin*. **41(2):** 116-126.

Ringwood, A.H.; McCarthy, M.; Bates, T.C.; Carroll, D.L. (2010). The effects of silver nanoparticles on oyster embryos. *Marine Environmental Research*. **69(1):** 549-551.

Scown, T.M.; Aerle, R.V.; Tyler, C.R. (2010). Review: do engineered nanoparticles pose a significant threat to the aquatic environment? *Critical Reviews in Toxicology*. **40(7):** 653–670.

Serafim, A.; Bebianno, M.J. (2009). Metallothionein role in the kinetic model of copper accumulation and elimination in the clam *Ruditapes decussatus*. *Environmental Research*. **109:** 390-399.

Singh, N.; Manshian, B.; Jenkins, G.J.S.; Griffiths, S.M.; Williams, P.M.; Maffeis, T.G.G.; Wrigh, C.J.; Doak, S.H. (2009). NanoGenotoxicology: The DNA damaging potential of engineered nanomaterials. *Biomaterials*. **30:** 3891-3914.

Studer, A.M.; Limbach, L.K.; Duc, L.V.; Krumeich, F.; Athanassiou, E.K.; Gerber, L.C.; Moch, H.; Stark, W.J. (2010). Nanoparticle cytotoxicity depends on intracellular solubility: Comparison of stabilized copper metal and degradable copper oxide nanoparticles. *Toxicological Letters*. **197:** 169-174.

Tiede, K.; Hassellöv, M.; Breitbarth, E.; Chaudhry, Q.; Boxall, A.B.A. (2009). Considerations for environmental fate and ecotoxicity testing to support environmental risk assessments for engineered nanoparticles. *Journal of Chromatography A*. **1216(3):** 503–509.

Viarengo, A.; Burlando, B.; Cavaletto, M.; Marchi, B.; Ponzano, E.; Blasco, J. (1999). Role of metallothionein against oxidative stress in the mussel *Mytilus galloprovincialis*. *American Journal of Physiology: Regulatory, Integrative and Comparative Physiology*. **277:** R1612–R1619.

Wang, W.-X.; Rainbow, P.S. (2005). Influence of metal exposure history on trace metal uptake and accumulation by marine invertebrates. *Ecotoxicology and Environmental Safety*. **61:** 145–159.

Wang, Z.; Zhao, J.; Li, F.; Gao, D.; Xing, B. (2009). Adsoprtion and inhibition of acetylcholinesterase by different nanoparticles. *Chemosphere.* **77(1):** 67-73.

Ward, J.E.; Kach, D.J. (2009). Marine aggregates facilitate ingestion of nanoparticles by suspension–feeding bivalves. *Marine Environmental Research.* **68:** 137–142.

# APPENDIX I

## Supplementary tables for Chapter 5:

## "Proteomic analysis in mussels *Mytilus galloprovincialis* exposed to CuO NPs and $Cu^{2+}$"

# APPENDIX I.

# SUPPLEMENTARY TABLES FOR CHAPTER 5

**Table S1 –** List of new common spots for CuO NPs and $Cu^{2+}$ exposure in the gills.

| Spot number | Obs. Mr (kDa) | Obs. pI | NPs | $Cu^{2+}$ |
|---|---|---|---|---|
| 1204 | 34.68 | 4.91 | 445.58 | 141.00 |
| 1205 | 33.93 | 4.91 | 270.25 | 107.93 |
| 1305 | 37.87 | 4.77 | 7.53 | 9.30 |
| 1307 | 39.49 | 4.94 | 12.10 | 8.23 |
| 2220 | 33.60 | 5.14 | 322.33 | 128.38 |
| 2221 | 33.00 | 5.20 | 119.78 | 43.85 |
| 2225 | 32.82 | 5.15 | 54.48 | 29.45 |
| 2616 | 59.47 | 5.13 | 75.83 | 47.40 |
| 3106 | 31.57 | 5.33 | 52.30 | 39.95 |
| 3107 | 29.96 | 5.43 | 45.18 | 29.88 |
| 3207 | 37.67 | 5.33 | 36.75 | 11.08 |
| 3617 | 55.41 | 5.42 | 33.33 | 15.95 |
| 3620 | 59.74 | 5.34 | 89.15 | 14.50 |
| 3717 | 74.91 | 5.38 | 36.98 | 4.38 |
| 3720 | 66.31 | 5.34 | 68.68 | 28.80 |
| 3813 | 98.60 | 5.35 | 8.03 | 2.55 |
| 3818 | 130.09 | 5.41 | 13.35 | 11.25 |
| 3819 | 130.71 | 5.40 | 13.85 | 10.65 |
| 4121 | 25.43 | 5.49 | 40.10 | 36.88 |
| 4122 | 23.37 | 5.46 | 50.88 | 30.28 |
| 4214 | 30.76 | 5.43 | 66.60 | 56.55 |
| 4514 | 50.56 | 5.44 | 84.38 | 41.78 |
| 4612 | 52.61 | 5.42 | 25.23 | 3.98 |
| 4717 | 89.29 | 5.42 | 17.78 | 3.55 |
| 4723 | 67.75 | 5.50 | 20.70 | 8.43 |
| 4810 | 113.46 | 5.44 | 13.80 | 5.23 |
| 4811 | 129.16 | 5.42 | 8.03 | 5.38 |
| 4812 | 113.95 | 5.45 | 4.08 | 4.73 |
| 5413 | 43.28 | 5.74 | 32.68 | 9.55 |
| 5512 | 48.36 | 5.75 | 76.53 | 42.80 |
| 5722 | 77.33 | 5.82 | 27.18 | 16.00 |
| 5723 | 74.26 | 5.84 | 13.53 | 2.73 |
| 5812 | 107.70 | 5.76 | 26.73 | 12.75 |
| 5813 | 93.83 | 5.73 | 27.45 | 12.05 |
| 6316 | 41.30 | 6.31 | 34.30 | 40.55 |
| 6417 | 44.01 | 5.97 | 71.25 | 40.45 |
| 6508 | 49.82 | 6.43 | 51.90 | 24.80 |
| 6611 | 59.74 | 5.97 | 29.50 | 4.70 |
| 6612 | 54.05 | 6.42 | 21.70 | 3.88 |
| 6615 | 59.83 | 5.94 | 7.75 | 6.88 |
| 6616 | 52.20 | 5.93 | 67.78 | 16.18 |
| 6802 | 91.26 | 5.96 | 8.38 | 3.53 |
| 6805 | 96.94 | 5.98 | 23.28 | 4.73 |
| 6806 | 97.96 | 5.92 | 9.75 | 5.18 |

**Table S2 –** List of new specific spots for CuO NPs exposure in the gills.

| Spot number | Obs. Mr (KDa) | Obs. pI | NPs | Spot number | Obs. Mr (KDa) | Obs. pI | NPs |
|---|---|---|---|---|---|---|---|
| 1206 | 35.42 | 4.90 | 495.25 | 5412 | 43.68 | 5.73 | 155.23 |
| 1208 | 33.05 | 5.10 | 101.15 | 5414 | 43.49 | 5.76 | 66.93 |
| 1210 | 34.44 | 4.85 | 113.03 | 5509 | 48.52 | 5.72 | 163.10 |
| 1306 | 37.37 | 4.88 | 35.95 | 5511 | 50.22 | 5.72 | 369.15 |
| 2222 | 32.96 | 5.13 | 256.78 | 5608 | 54.02 | 5.77 | 145.55 |
| 2615 | 56.16 | 5.25 | 80.13 | 5609 | 58.99 | 5.76 | 51.25 |
| 2617 | 56.13 | 5.20 | 27.93 | 5716 | 65.35 | 5.91 | 522.55 |
| 2618 | 62.24 | 5.26 | 67.60 | 5717 | 65.74 | 5.78 | 127.98 |
| 2811 | 74.18 | 5.11 | 438.88 | 5718 | 73.75 | 5.66 | 27.05 |
| 2812 | 90.29 | 5.32 | 169.13 | 5719 | 73.06 | 5.71 | 30.43 |
| 3112 | 28.78 | 5.30 | 64.80 | 5720 | 67.99 | 5.73 | 78.78 |
| 3210 | 33.70 | 5.33 | 423.70 | 5815 | 107.88 | 5.73 | 183.40 |
| 3212 | 31.54 | 5.30 | 306.13 | 5816 | 109.82 | 5.72 | 121.68 |
| 3510 | 52.18 | 5.41 | 222.95 | 5817 | 110.63 | 5.70 | 68.63 |
| 3511 | 49.74 | 5.35 | 169.73 | 6111 | 25.87 | 5.95 | 243.43 |
| 3615 | 54.01 | 5.34 | 297.38 | 6114 | 22.26 | 5.91 | 410.08 |
| 3618 | 61.95 | 5.41 | 66.10 | 6217 | 36.53 | 5.98 | 68.80 |
| 3619 | 60.76 | 5.38 | 51.35 | 6320 | 37.02 | 6.28 | 117.93 |
| 3718 | 74.93 | 5.34 | 61.55 | 6321 | 36.85 | 5.90 | 167.00 |
| 3719 | 77.57 | 5.41 | 266.65 | 6415 | 44.81 | 6.54 | 649.98 |
| 3810 | 92.14 | 5.38 | 267.00 | 6418 | 45.22 | 5.91 | 143.50 |
| 3814 | 90.06 | 5.41 | 50.35 | 6419 | 46.00 | 5.96 | 68.15 |
| 4117 | 26.47 | 5.44 | 89.25 | 6507 | 52.29 | 5.98 | 366.95 |
| 4120 | 29.20 | 5.46 | 181.70 | 6510 | 51.86 | 6.42 | 94.90 |
| 4414 | 43.16 | 5.45 | 70.78 | 6613 | 59.91 | 6.27 | 116.75 |
| 4515 | 48.43 | 5.47 | 82.68 | 6614 | 55.91 | 5.96 | 166.33 |
| 4516 | 47.91 | 5.49 | 79.03 | 6712 | 68.14 | 5.85 | 24.63 |
| 4610 | 64.55 | 5.43 | 57.30 | 6807 | 88.67 | 5.96 | 27.65 |
| 4611 | 54.91 | 5.47 | 107.28 | 7312 | 38.36 | 6.57 | 96.95 |
| 4613 | 58.80 | 5.43 | 185.40 | 7313 | 38.54 | 6.60 | 62.35 |
| 4719 | 74.22 | 5.45 | 76.70 | 7314 | 41.72 | 6.50 | 202.48 |
| 4720 | 70.51 | 5.43 | 108.80 | 7515 | 49.12 | 6.55 | 77.58 |
| 4721 | 68.31 | 5.44 | 103.08 | 7614 | 56.87 | 6.51 | 324.68 |
| 4722 | 69.72 | 5.50 | 88.00 | 7616 | 57.51 | 6.58 | 469.00 |
| 4809 | 113.86 | 5.43 | 88.25 | 7805 | 94.03 | 6.42 | 51.23 |
| 5125 | 28.43 | 5.71 | 84.93 | 7806 | 94.44 | 6.50 | 54.43 |
| 5128 | 25.34 | 5.83 | 161.80 | | | | |
| 5306 | 42.02 | 5.77 | 201.63 | | | | |
| 5307 | 42.58 | 5.90 | 194.38 | | | | |
| 5313 | 41.47 | 5.73 | 211.13 | | | | |
| 5410 | 46.19 | 5.74 | 67.00 | | | | |
| 5411 | 47.43 | 5.79 | 180.85 | | | | |

**Table S3 –** List of new specific spots for $Cu^{2+}$ exposure in the gills.

| Spot number | Obs. Mr (KDa) | Obs. pI | $Cu^{2+}$ |
|---|---|---|---|
| 601 | 53.57 | 4.74 | 150.00 |
| 1113 | 23.55 | 4.83 | 140.93 |
| 2115 | 22.47 | 5.23 | 812.93 |
| 2116 | 22.91 | 5.18 | 246.68 |
| 2226 | 34.73 | 5.20 | 1118.83 |
| 2227 | 33.75 | 5.29 | 587.33 |
| 2619 | 58.03 | 5.12 | 136.83 |
| 2620 | 52.95 | 5.19 | 528.53 |
| 2712 | 69.33 | 5.11 | 59.75 |
| 2814 | 95.18 | 5.14 | 55.58 |
| 3012 | 22.71 | 5.30 | 485.48 |
| 3214 | 32.45 | 5.30 | 501.75 |
| 3621 | 54.08 | 5.41 | 60.78 |
| 3820 | 124.34 | 5.41 | 80.50 |
| 3821 | 123.88 | 5.42 | 44.45 |
| 3822 | 93.02 | 5.40 | 52.58 |
| 4008 | 22.29 | 5.48 | 293.80 |
| 4215 | 31.62 | 5.42 | 83.85 |
| 4517 | 50.62 | 5.46 | 211.33 |
| 4518 | 50.55 | 5.43 | 286.35 |
| 4614 | 55.96 | 5.47 | 70.83 |
| 5116 | 21.74 | 5.80 | 760.20 |
| 5120 | 26.92 | 5.73 | 75.08 |
| 5129 | 29.23 | 5.77 | 86.23 |
| 5130 | 27.89 | 5.74 | 82.63 |
| 5209 | 34.88 | 5.74 | 109.00 |
| 5311 | 39.84 | 5.74 | 33.88 |
| 5314 | 38.93 | 5.71 | 480.95 |
| 6001 | 21.55 | 5.88 | 213.10 |
| 6115 | 23.67 | 5.95 | 761.35 |
| 6116 | 23.01 | 5.98 | 280.13 |
| 6117 | 22.93 | 5.85 | 210.08 |
| 6118 | 30.46 | 5.82 | 46.23 |
| 6119 | 28.40 | 5.92 | 78.10 |
| 6120 | 28.17 | 5.98 | 121.38 |
| 6121 | 27.86 | 5.81 | 89.38 |
| 6220 | 31.97 | 6.26 | 138.43 |
| 6323 | 40.27 | 5.80 | 58.63 |
| 6421 | 42.41 | 5.89 | 80.55 |
| 6422 | 44.10 | 5.89 | 214.73 |
| 6617 | 51.61 | 5.94 | 107.33 |
| 6711 | 69.28 | 5.92 | 22.83 |
| 6808 | 94.09 | 5.86 | 110.08 |
| 6809 | 95.83 | 5.82 | 216.90 |
| 6810 | 83.27 | 5.94 | 111.43 |
| 6811 | 104.46 | 6.28 | 53.68 |
| 7002 | 22.84 | 6.58 | 196.58 |
| 7003 | 22.59 | 6.55 | 167.18 |
| 7124 | 25.94 | 6.64 | 81.75 |
| 7125 | 24.34 | 6.70 | 223.60 |
| 7207 | 32.27 | 6.44 | 151.13 |
| 7208 | 32.29 | 6.76 | 120.85 |
| 7315 | 41.15 | 6.57 | 228.00 |
| 7516 | 48.44 | 6.48 | 58.65 |
| 7615 | 53.18 | 6.49 | 24.80 |
| 7712 | 66.59 | 6.72 | 184.30 |

**Table S4 –** List of new common spots for CuO NPs and $Cu^{2+}$ exposure in the digestive gland.

| Spot number | Obs. Mr (KDa) | Obs. pI | NPs | $Cu^{2+}$ | Spot number | Obs. Mr (KDa) | Obs. pI | NPs | $Cu^{2+}$ |
|---|---|---|---|---|---|---|---|---|---|
| 1107 | 28.59 | 4.87 | 137.98 | 64.50 | 4506 | 51.48 | 5.57 | 98.40 | 85.80 |
| 1205 | 29.86 | 4.93 | 54.45 | 91.93 | 4514 | 51.09 | 5.68 | 50.53 | 39.40 |
| 1306 | 39.86 | 4.82 | 112.55 | 45.93 | 4517 | 51.70 | 5.77 | 68.55 | 249.55 |
| 1402 | 45.96 | 4.86 | 63.18 | 103.13 | 4608 | 56.47 | 5.77 | 67.20 | 21.23 |
| 1602 | 58.90 | 4.88 | 112.40 | 204.73 | 4706 | 67.58 | 5.59 | 29.93 | 27.78 |
| 1604 | 58.58 | 4.91 | 376.55 | 493.90 | 4805 | 91.18 | 5.69 | 165.50 | 70.38 |
| 1605 | 58.53 | 4.93 | 295.28 | 374.88 | 5104 | 26.72 | 5.87 | 105.93 | 177.83 |
| 1614 | 56.25 | 4.90 | 42.50 | 85.83 | 5105 | 27.77 | 5.95 | 153.85 | 178.43 |
| 2203 | 32.94 | 5.00 | 127.20 | 177.23 | 5109 | 27.78 | 6.01 | 54.85 | 121.88 |
| 2211 | 30.72 | 5.19 | 109.60 | 906.88 | 5204 | 32.13 | 5.87 | 22.20 | 50.13 |
| 2301 | 38.33 | 4.99 | 79.45 | 35.48 | 5304 | 36.26 | 5.99 | 21.58 | 39.20 |
| 2307 | 37.51 | 5.19 | 42.90 | 204.98 | 5305 | 43.64 | 6.03 | 20.80 | 71.13 |
| 2404 | 46.80 | 5.17 | 35.80 | 62.53 | 5702 | 67.42 | 5.83 | 25.78 | 27.40 |
| 2416 | 47.04 | 4.95 | 23.35 | 32.20 | 5707 | 66.91 | 5.94 | 18.95 | 12.60 |
| 2501 | 49.56 | 5.02 | 153.05 | 46.00 | 6104 | 25.28 | 6.26 | 79.25 | 252.28 |
| 2502 | 49.48 | 5.05 | 96.75 | 61.28 | 6107 | 24.95 | 6.45 | 350.43 | 751.45 |
| 2503 | 49.27 | 5.08 | 435.53 | 273.85 | 6212 | 30.20 | 6.00 | 54.80 | 155.25 |
| 2507 | 48.50 | 5.20 | 168.40 | 386.90 | 6302 | 42.00 | 6.22 | 66.25 | 241.68 |
| 2508 | 51.21 | 5.21 | 280.03 | 154.53 | 6305 | 42.46 | 6.38 | 39.93 | 158.33 |
| 2601 | 58.58 | 4.96 | 55.83 | 49.45 | 6306 | 42.61 | 6.52 | 49.33 | 260.25 |
| 2602 | 57.84 | 4.98 | 84.45 | 102.48 | 6308 | 36.80 | 6.55 | 97.13 | 82.30 |
| 2805 | 87.87 | 5.08 | 30.88 | 73.60 | 6316 | 42.11 | 6.05 | 19.70 | 29.00 |
| 2806 | 87.69 | 5.10 | 28.00 | 73.08 | 6402 | 46.45 | 6.15 | 42.10 | 35.23 |
| 3302 | 37.00 | 5.27 | 110.03 | 200.65 | 6405 | 46.77 | 6.18 | 48.63 | 161.95 |
| 3309 | 42.86 | 5.43 | 73.33 | 63.28 | 6406 | 47.79 | 6.24 | 58.73 | 245.98 |
| 3602 | 53.48 | 5.29 | 22.35 | 103.63 | 6411 | 46.13 | 6.46 | 232.83 | 780.95 |
| 3613 | 52.45 | 5.44 | 18.58 | 53.83 | 6506 | 48.14 | 6.39 | 51.48 | 33.03 |
| 3712 | 69.30 | 5.37 | 58.28 | 404.43 | 6702 | 68.07 | 6.19 | 18.78 | 31.45 |
| 3806 | 88.38 | 5.30 | 59.50 | 64.33 | 6718 | 65.82 | 6.23 | 27.48 | 96.20 |
| 3807 | 99.48 | 5.33 | 66.70 | 122.48 | 7302 | 43.40 | 6.66 | 120.95 | 69.98 |
| 4201 | 30.37 | 5.49 | 169.63 | 190.25 | 7303 | 40.70 | 6.69 | 40.90 | 194.28 |
| 4210 | 32.24 | 5.62 | 45.93 | 68.00 | 7403 | 45.33 | 6.68 | 54.90 | 333.65 |
| 4211 | 30.67 | 5.62 | 217.55 | 249.20 | 7404 | 44.64 | 6.71 | 33.15 | 291.05 |
| 4220 | 35.55 | 5.62 | 31.40 | 29.98 | 7701 | 66.93 | 6.77 | 17.28 | 54.53 |
| 4222 | 30.69 | 5.39 | 16.68 | 49.40 | | | | | |
| 4502 | 50.04 | 5.49 | 23.63 | 124.65 | | | | | |
| 4504 | 49.98 | 5.54 | 222.55 | 292.40 | | | | | |

**Table S5 –** List of new specific spots for CuO NPs exposure in the digestive gland.

| Spot number | Obs. Mr (KDa) | Obs. pI | NPs | Spot number | Obs. Mr (KDa) | Obs. pI | NPs |
|---|---|---|---|---|---|---|---|
| 108 | 26.99 | 4.40 | 626.65 | 4306 | 36.28 | 5.63 | 97.58 |
| 201 | 30.61 | 4.49 | 310.10 | 4412 | 46.19 | 5.41 | 131.53 |
| 504 | 51.91 | 4.55 | 146.88 | 4415 | 47.68 | 5.43 | 87.38 |
| 505 | 49.93 | 4.42 | 132.65 | 4501 | 47.89 | 5.49 | 207.45 |
| 506 | 49.97 | 4.44 | 178.63 | 4507 | 49.28 | 5.58 | 695.75 |
| 602 | 53.92 | 4.58 | 189.50 | 4512 | 48.64 | 5.63 | 214.45 |
| 1015 | 23.46 | 4.71 | 654.93 | 4515 | 50.21 | 5.70 | 213.03 |
| 1016 | 23.47 | 4.78 | 551.63 | 4516 | 49.27 | 5.76 | 455.73 |
| 1104 | 24.65 | 4.79 | 390.48 | 4602 | 56.73 | 5.56 | 264.60 |
| 1202 | 34.28 | 4.83 | 296.10 | 4607 | 55.42 | 5.71 | 102.80 |
| 1213 | 33.42 | 4.84 | 145.85 | 4702 | 67.69 | 5.49 | 166.43 |
| 1216 | 30.07 | 4.71 | 183.70 | 4709 | 67.09 | 5.74 | 65.58 |
| 1217 | 29.83 | 4.74 | 132.75 | 4710 | 68.63 | 5.78 | 515.60 |
| 1218 | 29.60 | 4.82 | 372.50 | 4716 | 73.22 | 5.51 | 66.10 |
| 1307 | 35.98 | 4.86 | 2050.25 | 4806 | 90.24 | 5.76 | 175.00 |
| 1308 | 36.70 | 4.87 | 3460.30 | 4810 | 77.20 | 5.52 | 81.15 |
| 1312 | 36.02 | 4.79 | 403.10 | 4814 | 119.56 | 5.39 | 38.45 |
| 1313 | 39.70 | 4.88 | 127.95 | 5004 | 23.58 | 6.03 | 650.73 |
| 1404 | 47.19 | 4.88 | 155.28 | 5007 | 23.20 | 5.93 | 129.48 |
| 1405 | 44.57 | 4.93 | 346.88 | 5114 | 29.16 | 5.99 | 2531.03 |
| 1416 | 45.21 | 4.92 | 325.63 | 5201 | 29.97 | 5.80 | 314.40 |
| 1420 | 46.58 | 4.87 | 177.75 | 5203 | 32.59 | 5.83 | 351.55 |
| 1421 | 45.42 | 4.84 | 176.88 | 5212 | 30.75 | 5.97 | 237.58 |
| 1505 | 48.34 | 4.70 | 730.70 | 5213 | 31.83 | 5.72 | 185.93 |
| 1506 | 49.40 | 4.82 | 612.38 | 5301 | 36.97 | 5.87 | 224.95 |
| 1509 | 48.76 | 4.74 | 84.75 | 5302 | 36.90 | 5.92 | 317.25 |
| 1608 | 56.61 | 4.85 | 261.23 | 5306 | 36.17 | 6.03 | 194.78 |
| 1609 | 62.30 | 4.70 | 123.85 | 5402 | 44.31 | 5.85 | 188.33 |
| 1610 | 60.86 | 4.70 | 57.88 | 5404 | 44.77 | 5.85 | 337.48 |
| 1612 | 55.99 | 4.83 | 76.35 | 5405 | 45.65 | 5.87 | 260.68 |
| 1704 | 74.17 | 4.87 | 1467.00 | 5410 | 45.36 | 6.02 | 175.00 |
| 1718 | 69.41 | 4.90 | 99.05 | 5502 | 48.53 | 5.82 | 116.10 |
| 1806 | 75.61 | 4.80 | 108.73 | 5505 | 47.88 | 5.88 | 422.50 |
| 2001 | 23.65 | 4.96 | 173.40 | 5507 | 48.21 | 5.93 | 202.40 |
| 2008 | 23.10 | 4.97 | 453.85 | 5602 | 58.13 | 5.82 | 160.48 |
| 2119 | 28.62 | 5.17 | 647.68 | 5607 | 52.88 | 6.00 | 139.75 |
| 2209 | 30.67 | 5.13 | 504.23 | 5703 | 66.58 | 5.89 | 219.60 |
| 2215 | 32.75 | 5.23 | 439.43 | 5704 | 68.83 | 5.89 | 428.43 |
| 2221 | 32.04 | 5.01 | 203.48 | 5709 | 66.64 | 6.03 | 1645.30 |
| 2222 | 32.51 | 5.10 | 413.20 | 5711 | 65.03 | 6.05 | 378.80 |
| 2319 | 38.02 | 4.95 | 151.13 | 5712 | 68.90 | 6.07 | 90.85 |
| 2402 | 44.05 | 4.99 | 624.75 | 5801 | 91.19 | 5.80 | 180.68 |
| 2405 | 46.16 | 5.19 | 237.03 | 5803 | 90.04 | 5.88 | 72.60 |
| 2406 | 47.46 | 5.20 | 580.63 | 5807 | 90.15 | 5.98 | 85.10 |
| 2411 | 45.10 | 5.07 | 219.58 | 5808 | 91.04 | 5.99 | 478.45 |
| 2412 | 44.21 | 5.07 | 117.98 | 5819 | 102.30 | 5.70 | 30.58 |
| 2413 | 46.12 | 5.08 | 152.80 | 6009 | 23.17 | 6.12 | 432.10 |
| 2414 | 45.07 | 5.15 | 128.08 | 6201 | 34.87 | 6.10 | 124.10 |
| 2511 | 51.84 | 5.03 | 207.15 | 6202 | 34.29 | 6.15 | 110.75 |
| 2619 | 57.12 | 5.00 | 278.03 | 6203 | 33.22 | 6.23 | 373.80 |
| 2708 | 67.71 | 5.07 | 795.23 | 6206 | 32.60 | 6.50 | 587.15 |
| 2713 | 67.63 | 5.21 | 1220.68 | 6207 | 34.87 | 6.52 | 588.18 |
| 2726 | 72.60 | 4.97 | 105.18 | 6307 | 42.84 | 6.55 | 268.28 |
| 2802 | 87.09 | 5.01 | 109.93 | 6317 | 36.82 | 6.06 | 325.85 |
| 2804 | 88.67 | 5.05 | 234.53 | 6410 | 43.96 | 6.45 | 171.38 |
| 2817 | 93.44 | 5.15 | 177.48 | 6413 | 45.51 | 6.55 | 323.93 |

| | | | |
|---|---|---|---|
| 2818 | 74.36 | 5.05 | 81.78 |
| 3110 | 24.92 | 5.35 | 218.48 |
| 3206 | 34.10 | 5.35 | 234.48 |
| 3304 | 39.21 | 5.30 | 174.18 |
| 3306 | 42.14 | 5.35 | 426.23 |
| 3307 | 43.03 | 5.39 | 1095.00 |
| 3311 | 38.21 | 5.21 | 224.75 |
| 3401 | 45.27 | 5.28 | 338.45 |
| 3403 | 44.50 | 5.45 | 793.90 |
| 3501 | 49.77 | 5.25 | 182.35 |
| 3505 | 49.62 | 5.32 | 831.25 |
| 3510 | 49.96 | 5.40 | 197.63 |
| 3601 | 57.44 | 5.27 | 155.95 |
| 3604 | 60.84 | 5.30 | 182.50 |
| 3707 | 69.61 | 5.32 | 247.43 |
| 3715 | 76.12 | 5.40 | 51.80 |
| 3810 | 92.80 | 5.37 | 113.38 |
| 3811 | 85.94 | 5.39 | 107.60 |
| 3813 | 84.41 | 5.45 | 123.58 |
| 3814 | 79.89 | 5.45 | 167.83 |
| 3821 | 120.66 | 5.32 | 76.78 |
| 3822 | 133.39 | 5.30 | 27.28 |
| 4101 | 28.23 | 5.47 | 557.23 |
| 4104 | 25.06 | 5.62 | 591.98 |
| 4109 | 25.01 | 5.70 | 950.33 |
| 4110 | 27.72 | 5.74 | 820.23 |
| 4112 | 26.12 | 5.52 | 600.25 |
| 4113 | 27.51 | 5.62 | 536.48 |
| 4114 | 26.99 | 5.50 | 156.15 |
| 4203 | 35.84 | 5.52 | 210.53 |
| 4206 | 32.56 | 5.58 | 188.48 |
| 4221 | 35.14 | 5.39 | 350.05 |
| 4223 | 29.68 | 5.50 | 102.35 |
| 4225 | 33.02 | 5.53 | 115.30 |
| 6419 | 46.27 | 6.22 | 193.00 |
| 6503 | 48.22 | 6.24 | 409.53 |
| 6507 | 49.87 | 6.45 | 409.58 |
| 6603 | 52.82 | 6.17 | 277.30 |
| 6606 | 52.89 | 6.30 | 256.45 |
| 6610 | 62.40 | 6.53 | 303.88 |
| 6619 | 59.00 | 6.08 | 39.63 |
| 6806 | 92.48 | 6.28 | 473.28 |
| 7103 | 24.95 | 6.64 | 473.03 |
| 7109 | 24.75 | 6.84 | 1037.60 |
| 7115 | 28.56 | 6.49 | 461.65 |
| 7118 | 25.08 | 6.51 | 249.50 |
| 7202 | 32.92 | 6.75 | 425.73 |
| 7203 | 30.93 | 6.79 | 524.23 |
| 7211 | 30.00 | 6.25 | 177.73 |
| 7214 | 29.72 | 6.35 | 72.20 |
| 7304 | 43.18 | 6.79 | 412.35 |
| 7314 | 39.03 | 6.46 | 124.08 |
| 7315 | 38.48 | 6.39 | 147.10 |
| 7319 | 36.56 | 6.51 | 153.23 |
| 7415 | 45.96 | 6.27 | 486.60 |
| 7501 | 50.01 | 6.59 | 249.65 |
| 7505 | 47.93 | 6.64 | 775.43 |
| 7617 | 54.75 | 6.53 | 96.55 |
| 7707 | 65.77 | 6.53 | 89.60 |
| 7708 | 64.36 | 6.54 | 125.43 |

**Table S6 –** List of new specific spots for $Cu^{2+}$ exposure in the digestive gland.

| Spot number | Obs. Mr (KDa) | Obs. pI | $Cu^{2+}$ | Spot number | Obs. Mr (KDa) | Obs. pI | $Cu^{2+}$ |
|---|---|---|---|---|---|---|---|
| 1215 | 26.32 | 4.57 | 811.93 | 5720 | 64.54 | 5.81 | 128.18 |
| 1509 | 46.41 | 4.72 | 150.38 | 5721 | 65.46 | 5.66 | 90.98 |
| 2116 | 25.51 | 4.76 | 525.60 | 5723 | 66.33 | 5.54 | 152.58 |
| 2223 | 31.04 | 4.93 | 76.23 | 5724 | 67.27 | 5.63 | 133.58 |
| 2313 | 34.90 | 4.97 | 152.53 | 5725 | 59.20 | 5.73 | 82.33 |
| 2314 | 31.42 | 4.95 | 155.10 | 5816 | 95.73 | 5.70 | 503.30 |
| 2315 | 32.45 | 4.85 | 86.50 | 6117 | 25.37 | 5.96 | 636.00 |
| 2429 | 39.54 | 4.78 | 366.60 | 6217 | 26.37 | 5.94 | 272.28 |
| 2431 | 37.65 | 5.00 | 113.08 | 6418 | 41.13 | 6.21 | 173.08 |
| 2521 | 46.38 | 4.76 | 98.85 | 6419 | 42.32 | 6.03 | 194.95 |
| 2522 | 45.55 | 4.82 | 101.75 | 6420 | 41.80 | 5.98 | 197.23 |
| 2611 | 56.72 | 4.86 | 214.73 | 6424 | 42.53 | 5.87 | 109.68 |
| 2612 | 55.62 | 4.82 | 173.33 | 6425 | 40.19 | 6.15 | 134.53 |
| 2613 | 48.81 | 4.75 | 160.85 | 6516 | 48.12 | 5.85 | 128.93 |
| 2814 | 80.34 | 4.84 | 105.63 | 6517 | 47.73 | 5.82 | 176.08 |
| 2815 | 77.73 | 4.89 | 131.08 | 6521 | 48.27 | 6.23 | 850.85 |
| 2816 | 77.44 | 4.91 | 94.80 | 6524 | 46.41 | 5.91 | 141.98 |
| 2817 | 78.02 | 4.93 | 115.40 | 6628 | 54.83 | 6.07 | 285.95 |
| 3220 | 28.51 | 5.10 | 358.13 | 6629 | 54.40 | 6.11 | 142.50 |
| 3221 | 27.61 | 5.15 | 222.48 | 6630 | 55.29 | 6.12 | 154.03 |
| 3222 | 30.09 | 5.02 | 60.73 | 6631 | 54.61 | 6.14 | 146.98 |
| 3327 | 35.62 | 5.08 | 109.43 | 6632 | 56.46 | 5.98 | 204.63 |
| 3329 | 31.12 | 5.20 | 2496.63 | 6634 | 49.40 | 6.10 | 296.18 |
| 3523 | 45.37 | 5.15 | 78.45 | 6716 | 68.13 | 5.86 | 151.68 |
| 3524 | 48.41 | 5.01 | 102.33 | 6718 | 65.71 | 5.85 | 38.35 |
| 3610 | 54.61 | 5.20 | 73.83 | 6719 | 63.03 | 6.09 | 375.10 |
| 3611 | 53.44 | 5.20 | 77.35 | 6720 | 63.12 | 6.04 | 131.78 |
| 3612 | 57.59 | 5.20 | 148.55 | 6722 | 60.31 | 6.03 | 49.83 |
| 3613 | 57.44 | 5.20 | 184.85 | 6824 | 90.29 | 6.24 | 660.98 |
| 3614 | 50.21 | 5.10 | 326.45 | 6826 | 68.61 | 6.10 | 101.10 |
| 3814 | 70.68 | 5.21 | 329.05 | 6829 | 73.61 | 5.91 | 92.35 |
| 3815 | 71.64 | 5.11 | 45.25 | 7226 | 29.09 | 6.32 | 233.25 |
| 3818 | 89.41 | 5.07 | 283.03 | 7311 | 36.75 | 6.59 | 167.70 |
| 3821 | 87.77 | 5.16 | 200.33 | 7313 | 36.60 | 6.35 | 229.23 |
| 3822 | 87.38 | 5.20 | 122.13 | 7314 | 36.35 | 6.32 | 52.65 |
| 3823 | 101.84 | 5.26 | 287.98 | 7315 | 35.34 | 6.23 | 109.38 |
| 4210 | 29.48 | 5.48 | 436.18 | 7412 | 41.69 | 6.31 | 191.03 |
| 4313 | 31.23 | 5.27 | 122.60 | 7413 | 39.81 | 6.35 | 549.40 |
| 4416 | 38.17 | 5.26 | 529.28 | 7414 | 39.89 | 6.40 | 293.00 |
| 4514 | 47.70 | 5.45 | 266.63 | 7415 | 37.54 | 6.40 | 237.80 |
| 4515 | 48.01 | 5.39 | 131.70 | 7416 | 43.27 | 6.55 | 585.23 |
| 4620 | 51.73 | 5.43 | 327.93 | 7417 | 40.25 | 6.50 | 205.90 |
| 4621 | 51.19 | 5.44 | 325.75 | 7419 | 36.94 | 6.52 | 190.88 |
| 4622 | 51.15 | 5.46 | 249.53 | 7420 | 38.73 | 6.30 | 184.43 |
| 4625 | 55.02 | 5.39 | 231.25 | 7421 | 37.17 | 6.30 | 129.73 |
| 4626 | 55.36 | 5.44 | 243.45 | 7526 | 48.12 | 6.50 | 1879.48 |
| 4627 | 53.63 | 5.41 | 103.93 | 7527 | 48.20 | 6.61 | 553.13 |
| 4733 | 61.61 | 5.40 | 67.53 | 7532 | 44.61 | 6.38 | 374.23 |
| 4736 | 67.23 | 5.34 | 558.68 | 7533 | 44.36 | 6.54 | 444.15 |
| 4737 | 69.10 | 5.28 | 634.08 | 7625 | 50.00 | 6.49 | 68.25 |
| 4812 | 86.86 | 5.39 | 150.68 | 7626 | 49.34 | 6.27 | 129.13 |
| 4814 | 101.85 | 5.34 | 443.18 | 7627 | 49.98 | 6.30 | 125.38 |
| 4815 | 101.77 | 5.39 | 205.13 | 7714 | 64.02 | 6.32 | 361.30 |
| 5314 | 35.06 | 5.80 | 716.18 | 7715 | 61.77 | 6.37 | 98.65 |
| 5318 | 32.86 | 5.66 | 146.88 | 7717 | 63.52 | 6.16 | 108.50 |
| 5319 | 33.51 | 5.71 | 67.85 | 7718 | 58.85 | 6.15 | 36.98 |

| | | | | | | | |
|---|---|---|---|---|---|---|---|
| 5416 | 37.20 | 5.78 | 334.28 | 7719 | 56.90 | 6.20 | 60.70 |
| 5417 | 40.30 | 5.60 | 103.95 | 7720 | 56.07 | 6.24 | 49.73 |
| 5418 | 38.15 | 5.63 | 95.08 | 7721 | 57.74 | 6.26 | 209.48 |
| 5521 | 47.82 | 5.74 | 263.48 | 7813 | 68.81 | 6.13 | 91.05 |
| 5617 | 49.96 | 5.65 | 652.83 | 8423 | 40.03 | 6.66 | 325.10 |
| 5618 | 56.35 | 5.70 | 58.88 | 8514 | 46.10 | 6.69 | 742.60 |
| 5620 | 51.39 | 5.54 | 257.10 | 8515 | 47.87 | 6.67 | 555.10 |
| 5622 | 48.80 | 5.51 | 1067.28 | 8715 | 62.40 | 6.64 | 651.95 |
| 5623 | 56.37 | 5.56 | 188.95 | 8717 | 65.49 | 6.62 | 178.93 |
| 5624 | 52.45 | 5.62 | 112.88 | 8718 | 62.58 | 6.58 | 217.08 |
| 5626 | 49.44 | 5.62 | 398.03 | 8719 | 58.93 | 6.54 | 968.85 |
| 5717 | 58.75 | 5.54 | 123.80 | 8720 | 60.33 | 6.64 | 192.95 |
| 5719 | 65.12 | 5.76 | 115.60 | | | | |

**Table S7 –** List of suppressed common spots for CuO NPs and $Cu^{2+}$ exposure in the gills.

| Spot number | Obs. Mr (KDa) | Obs. pI | CT |
|---|---|---|---|
| 1304 | 42.56 | 5.10 | 11.58 |
| 1505 | 51.16 | 4.83 | 84.80 |
| 1508 | 51.15 | 4.85 | 42.65 |
| 1513 | 51.76 | 4.92 | 63.45 |
| 2108 | 22.87 | 5.25 | 71.73 |
| 2301 | 42.35 | 5.14 | 44.75 |
| 2309 | 37.07 | 5.11 | 2.08 |
| 2310 | 36.85 | 5.14 | 3.18 |
| 2311 | 36.74 | 5.17 | 3.25 |
| 2508 | 51.48 | 5.27 | 12.40 |
| 2605 | 54.24 | 5.12 | 55.38 |
| 3104 | 22.63 | 5.31 | 86.45 |
| 3111 | 22.61 | 5.42 | 28.13 |
| 3204 | 31.90 | 5.38 | 60.03 |
| 3609 | 54.60 | 5.34 | 7.25 |
| 3612 | 59.50 | 5.40 | 7.20 |
| 3704 | 74.47 | 5.36 | 8.28 |
| 4007 | 21.50 | 5.44 | 28.53 |
| 4105 | 30.39 | 5.48 | 28.68 |
| 4305 | 42.05 | 5.44 | 7.43 |
| 4413 | 47.82 | 5.71 | 14.88 |
| 4510 | 48.63 | 5.49 | 6.35 |
| 4802 | 94.61 | 5.46 | 7.75 |
| 5123 | 27.50 | 5.93 | 11.95 |
| 5502 | 48.78 | 5.74 | 22.05 |
| 5507 | 49.03 | 5.92 | 17.78 |
| 5510 | 51.57 | 5.75 | 4.98 |
| 5605 | 53.86 | 5.84 | 11.73 |
| 5715 | 77.69 | 5.91 | 7.85 |
| 6201 | 33.60 | 5.98 | 37.88 |
| 6204 | 35.28 | 6.26 | 7.45 |
| 6211 | 31.87 | 6.47 | 20.00 |
| 6318 | 39.01 | 6.27 | 5.88 |
| 6402 | 44.87 | 5.95 | 12.38 |
| 6406 | 44.29 | 6.36 | 55.95 |
| 6411 | 44.31 | 6.44 | 19.68 |
| 6412 | 47.55 | 6.45 | 6.20 |
| 6605 | 54.78 | 6.32 | 7.33 |
| 6608 | 64.11 | 6.43 | 14.33 |
| 6704 | 71.52 | 6.43 | 3.85 |
| 7301 | 39.01 | 6.53 | 8.95 |
| 7306 | 39.22 | 6.68 | 31.85 |
| 7403 | 45.50 | 6.60 | 10.43 |
| 7405 | 45.12 | 6.85 | 21.30 |
| 7505 | 48.95 | 6.89 | 60.13 |
| 7602 | 60.94 | 6.55 | 28.93 |
| 7609 | 53.65 | 6.90 | 127.50 |
| 7612 | 64.68 | 6.56 | 3.88 |
| 7711 | 69.76 | 6.60 | 2.85 |
| 8701 | 66.34 | 6.97 | 84.13 |

**Table S8 –** List of suppressed specific spots for CuO NPs exposure in the gills.

| Spot number | Obs. Mr (KDa) | Obs. pI | CT |
|---|---|---|---|
| 2205 | 35.76 | 5.12 | 167.13 |
| 2305 | 42.59 | 5.22 | 983.23 |
| 2313 | 37.81 | 5.25 | 24.45 |
| 2315 | 40.79 | 5.24 | 78.50 |
| 2606 | 53.88 | 5.14 | 608.53 |
| 2609 | 53.58 | 5.16 | 846.25 |
| 2803 | 97.98 | 5.11 | 2264.33 |
| 3102 | 22.62 | 5.33 | 477.23 |
| 3203 | 32.39 | 5.37 | 746.50 |
| 3208 | 35.86 | 5.41 | 47.10 |
| 3505 | 50.93 | 5.41 | 661.68 |
| 3701 | 69.21 | 5.30 | 883.35 |
| 3708 | 74.97 | 5.41 | 50.83 |
| 3713 | 74.15 | 5.42 | 95.58 |
| 3817 | 93.62 | 5.37 | 44.75 |
| 4406 | 44.27 | 5.46 | 161.63 |
| 5115 | 22.58 | 5.93 | 336.63 |
| 5713 | 68.02 | 5.87 | 152.40 |
| 6208 | 35.54 | 6.43 | 91.63 |
| 6503 | 48.45 | 6.14 | 156.70 |
| 6803 | 108.66 | 5.90 | 34.45 |
| 7105 | 22.79 | 6.73 | 183.93 |
| 7107 | 22.86 | 6.76 | 188.93 |
| 7205 | 32.97 | 6.85 | 363.85 |
| 7311 | 42.49 | 6.90 | 2308.15 |
| 7610 | 60.87 | 6.90 | 731.40 |
| 7701 | 81.64 | 6.61 | 41.38 |
| 7702 | 66.57 | 6.66 | 72.68 |
| 7703 | 66.63 | 6.81 | 730.03 |
| 7704 | 79.20 | 6.82 | 375.30 |
| 7708 | 66.38 | 6.90 | 1020.45 |
| 7709 | 78.90 | 6.92 | 594.43 |
| 7710 | 66.13 | 6.94 | 492.53 |

**Table S9 –** List of suppressed specific spots for $Cu^{2+}$ exposure in the gills.

| Spot number | Obs. Mr (KDa) | Obs. pI | CT |
|---|---|---|---|
| 1109 | 29.38 | 5.05 | 55.63 |
| 1110 | 27.77 | 4.93 | 73.03 |
| 1201 | 37.78 | 4.81 | 61.40 |
| 1408 | 44.90 | 4.95 | 802.68 |
| 1511 | 48.62 | 4.87 | 77.53 |
| 1514 | 49.14 | 4.93 | 107.58 |
| 1701 | 74.92 | 4.93 | 321.33 |
| 2101 | 30.30 | 5.10 | 93.05 |
| 2202 | 35.19 | 5.05 | 2122.10 |
| 2302 | 41.34 | 5.18 | 209.75 |
| 2304 | 42.21 | 5.21 | 417.55 |
| 2312 | 36.78 | 5.24 | 31.78 |
| 2503 | 49.53 | 5.16 | 179.73 |
| 2504 | 52.23 | 5.17 | 127.05 |
| 2809 | 90.05 | 5.28 | 115.43 |
| 3201 | 33.08 | 5.37 | 403.63 |
| 3602 | 61.70 | 5.30 | 79.53 |
| 3604 | 58.81 | 5.34 | 372.23 |
| 3610 | 62.80 | 5.35 | 46.75 |
| 3611 | 56.04 | 5.40 | 134.75 |
| 3714 | 66.15 | 5.42 | 83.70 |
| 4101 | 31.11 | 5.43 | 412.85 |
| 4103 | 22.37 | 5.46 | 265.18 |
| 4107 | 30.70 | 5.50 | 320.25 |
| 4203 | 35.40 | 5.44 | 122.35 |
| 4209 | 32.09 | 5.43 | 83.33 |
| 4508 | 50.71 | 5.48 | 104.58 |
| 4609 | 53.21 | 5.46 | 53.93 |
| 4702 | 74.15 | 5.43 | 55.80 |
| 4709 | 74.32 | 5.45 | 60.03 |
| 4712 | 68.46 | 5.48 | 33.38 |
| 4716 | 74.91 | 5.71 | 67.30 |
| 5101 | 29.58 | 5.72 | 358.13 |
| 5111 | 21.52 | 5.81 | 326.63 |
| 5121 | 28.99 | 5.96 | 26.38 |
| 5309 | 37.87 | 5.84 | 23.55 |
| 5504 | 53.05 | 5.79 | 102.33 |
| 5602 | 58.50 | 5.73 | 70.83 |
| 5606 | 57.06 | 5.90 | 63.70 |
| 5711 | 77.62 | 5.77 | 45.23 |
| 6112 | 28.78 | 6.00 | 118.58 |
| 6206 | 36.53 | 6.32 | 80.55 |
| 6212 | 34.37 | 6.47 | 194.43 |
| 6303 | 41.93 | 5.97 | 183.75 |
| 6308 | 41.15 | 6.36 | 148.68 |
| 6310 | 42.09 | 6.46 | 90.40 |
| 6313 | 40.86 | 6.51 | 119.40 |
| 6401 | 44.17 | 5.95 | 227.83 |
| 6416 | 46.23 | 5.96 | 73.98 |
| 6502 | 48.82 | 6.06 | 125.40 |
| 6505 | 49.74 | 6.46 | 153.23 |
| 6509 | 51.53 | 6.31 | 88.28 |
| 6601 | 53.25 | 5.99 | 372.15 |
| 6603 | 56.42 | 6.28 | 262.15 |
| 6604 | 55.56 | 6.31 | 168.78 |
| 6609 | 62.48 | 6.49 | 58.03 |
| 7120 | 25.14 | 6.73 | 111.75 |
| 7201 | 35.74 | 6.54 | 185.15 |
| 7605 | 60.99 | 6.59 | 293.38 |

**Table S10 –** List of suppressed common spots for CuO NPs and $Cu^{2+}$ exposure in the digestive gland.

| Spot number | Obs. Mr (KDa) | Obs. pI | CT |
|---|---|---|---|
| 303 | 42.73 | 4.54 | 200.78 |
| 305 | 42.97 | 4.51 | 63.40 |
| 403 | 44.70 | 4.66 | 172.03 |
| 1210 | 35.03 | 4.81 | 69.40 |
| 1220 | 35.35 | 4.76 | 43.90 |
| 1310 | 36.12 | 4.75 | 116.30 |
| 1407 | 47.71 | 4.90 | 67.98 |
| 1410 | 47.97 | 4.82 | 50.35 |
| 1512 | 48.90 | 4.83 | 56.68 |
| 1711 | 67.06 | 4.85 | 46.40 |
| 2106 | 26.81 | 5.21 | 183.20 |
| 2216 | 29.92 | 5.04 | 111.63 |
| 2313 | 42.65 | 4.93 | 32.23 |
| 2315 | 39.48 | 5.04 | 137.65 |
| 2409 | 45.10 | 5.20 | 109.30 |
| 2615 | 53.43 | 5.16 | 39.78 |
| 2617 | 60.60 | 4.97 | 27.10 |
| 2718 | 71.86 | 5.03 | 45.75 |
| 3005 | 23.57 | 5.30 | 922.63 |
| 3106 | 24.27 | 5.24 | 76.40 |
| 3107 | 27.58 | 5.24 | 32.23 |
| 3310 | 38.60 | 5.34 | 45.88 |
| 3619 | 55.10 | 5.24 | 25.00 |
| 3719 | 66.01 | 5.32 | 52.45 |
| 3726 | 66.05 | 5.27 | 68.15 |
| 4009 | 23.78 | 5.61 | 20.08 |
| 4010 | 23.38 | 5.58 | 174.20 |
| 4214 | 34.72 | 5.43 | 343.05 |
| 4218 | 36.11 | 5.45 | 87.88 |
| 4219 | 34.79 | 5.46 | 54.00 |
| 4411 | 45.43 | 5.55 | 15.70 |
| 4713 | 71.96 | 5.44 | 15.73 |
| 4721 | 66.38 | 5.49 | 12.68 |
| 4808 | 78.78 | 5.64 | 32.15 |
| 5208 | 33.43 | 5.92 | 69.38 |
| 5210 | 32.86 | 5.92 | 28.68 |
| 5414 | 47.39 | 5.71 | 101.13 |
| 5510 | 48.92 | 5.70 | 323.03 |
| 5609 | 57.78 | 5.89 | 29.75 |
| 5812 | 80.07 | 5.90 | 25.35 |
| 5814 | 79.51 | 5.96 | 39.55 |
| 6112 | 24.00 | 6.12 | 71.60 |
| 6310 | 36.27 | 6.15 | 320.03 |
| 6313 | 38.37 | 6.07 | 53.75 |
| 6807 | 119.30 | 6.37 | 252.40 |
| 6810 | 121.14 | 6.45 | 230.60 |
| 6812 | 80.53 | 6.17 | 60.93 |
| 6813 | 80.19 | 6.09 | 59.80 |
| 6818 | 78.83 | 6.17 | 26.88 |
| 7705 | 72.49 | 6.54 | 25.03 |

**Table S11 –** List of suppressed specific spots for CuO NPs exposure in the digestive gland.

| Spot number | Obs. Mr (KDa) | Obs. pI | CT | Spot number | Obs. Mr (KDa) | Obs. pI | CT |
|---|---|---|---|---|---|---|---|
| 111 | 27.01 | 4.43 | 220.05 | 4216 | 30.2 | 5.6 | 567.65 |
| 204 | 35.57 | 4.6 | 269.4 | 4217 | 30.94 | 5.54 | 291.675 |
| 1117 | 29.92 | 4.76 | 436.425 | 4410 | 47.47 | 5.5 | 96.725 |
| 1118 | 29.31 | 4.76 | 274 | 4414 | 46.37 | 5.4 | 250.675 |
| 1208 | 35.91 | 4.57 | 500.05 | 4518 | 48.46 | 5.57 | 514.25 |
| 1211 | 35.27 | 4.86 | 69.05 | 4609 | 56.24 | 5.49 | 124.325 |
| 1221 | 30.81 | 4.84 | 444.45 | 4611 | 60.3 | 5.48 | 79.425 |
| 1222 | 35.04 | 4.91 | 144.575 | 4612 | 58.77 | 5.42 | 52.2 |
| 1408 | 48.06 | 4.71 | 153.1 | 4615 | 64.4 | 5.4 | 61.425 |
| 1409 | 43.91 | 4.67 | 255.475 | 4712 | 67.03 | 5.45 | 62.625 |
| 1411 | 44.57 | 4.79 | 110 | 4720 | 67.17 | 5.55 | 81.3 |
| 1422 | 43.97 | 4.92 | 73.85 | 5113 | 27.65 | 5.79 | 323.05 |
| 1712 | 66.37 | 4.89 | 143.525 | 5209 | 32.72 | 5.71 | 148.975 |
| 1715 | 68.7 | 4.77 | 56.275 | 5211 | 35.87 | 5.91 | 190.725 |
| 1722 | 75.71 | 4.8 | 59.125 | 5307 | 43.38 | 5.79 | 2719.625 |
| 1723 | 68.53 | 4.8 | 39.075 | 5308 | 41 | 5.79 | 140.3 |
| 2107 | 26.06 | 5.19 | 584.55 | 5311 | 38.74 | 5.96 | 95.9 |
| 2111 | 28.45 | 5.12 | 188.675 | 5412 | 48.28 | 5.76 | 1267.3 |
| 2217 | 30.13 | 5.09 | 264.675 | 5413 | 48.21 | 5.7 | 1007.475 |
| 2314 | 36.16 | 5.04 | 90.225 | 5415 | 47.2 | 5.76 | 561.725 |
| 2407 | 45.44 | 5.07 | 1015.575 | 5511 | 51.27 | 5.9 | 131.35 |
| 2408 | 44.52 | 5.07 | 698.875 | 5713 | 74.1 | 5.92 | 53.35 |
| 2516 | 55.71 | 5.05 | 51.275 | 5717 | 73.8 | 5.85 | 197.95 |
| 2610 | 62.67 | 4.97 | 269.925 | 5820 | 90.23 | 5.91 | 82.05 |
| 2611 | 61.86 | 5.03 | 247.75 | 5821 | 89.27 | 5.84 | 94.4 |
| 2612 | 59.7 | 5.03 | 151.55 | 6208 | 33.11 | 6.19 | 519 |
| 2613 | 63.56 | 4.93 | 178.625 | 6417 | 45.35 | 6.05 | 191.6 |
| 2717 | 70.68 | 5.05 | 155.375 | 6513 | 51.69 | 6.37 | 315.175 |
| 3104 | 24.32 | 5.35 | 2603.6 | 6516 | 52.81 | 6.08 | 212.725 |
| 3105 | 27.27 | 5.31 | 327.5 | 6612 | 61.33 | 6.12 | 1337.6 |
| 3208 | 31.74 | 5.24 | 485.9 | 6613 | 61.74 | 6.22 | 1142 |
| 3209 | 36.02 | 5.4 | 255.425 | 6615 | 60.07 | 6.27 | 70.05 |
| 3404 | 47.68 | 5.24 | 58.35 | 6704 | 68.84 | 6.03 | 1822.2 |
| 3406 | 46.49 | 5.36 | 125.625 | 6705 | 68.24 | 6.09 | 1221.85 |
| 3515 | 51.4 | 5.3 | 183.1 | 6709 | 72.54 | 6.26 | 149.325 |
| 3614 | 63 | 5.39 | 145.075 | 6711 | 67.84 | 6.11 | 95.225 |
| 3615 | 59.22 | 5.29 | 168.4 | 6808 | 97.93 | 6.31 | 769.45 |
| 3616 | 55.02 | 5.38 | 151.175 | 6809 | 86.74 | 6.4 | 539.125 |
| 3718 | 66.53 | 5.21 | 288.7 | 6814 | 79.5 | 6.01 | 177.625 |
| 3720 | 68.57 | 5.24 | 109.8 | 7206 | 31.48 | 6.53 | 909.325 |
| 3721 | 72.74 | 5.3 | 83.675 | 7312 | 36.45 | 6.48 | 398.225 |
| 3722 | 71.94 | 5.4 | 84.7 | 7514 | 51.15 | 6.62 | 345.65 |
| 3725 | 72.38 | 5.35 | 39.575 | 7515 | 49.44 | 6.62 | 424 |
| 4213 | 35.8 | 5.6 | 2331.975 | 7704 | 74.5 | 6.53 | 184.025 |
| 4215 | 32.31 | 5.42 | 421.1 | 7706 | 64.28 | 6.52 | 318.8 |

**Table S12 –** List of suppressed specific spots for $Cu^{2+}$ exposure in the digestive gland.

| Spot number | Obs. Mr (KDa) | Obs. pI | CT |
|---|---|---|---|
| 1109 | 29.38 | 5.05 | 55.63 |
| 1110 | 27.77 | 4.93 | 73.03 |
| 1201 | 37.78 | 4.81 | 61.40 |
| 1408 | 44.90 | 4.95 | 802.68 |
| 1511 | 48.62 | 4.87 | 77.53 |
| 1514 | 49.14 | 4.93 | 107.58 |
| 1701 | 74.92 | 4.93 | 321.33 |
| 2101 | 30.30 | 5.10 | 93.05 |
| 2202 | 35.19 | 5.05 | 2122.10 |
| 2302 | 41.34 | 5.18 | 209.75 |
| 2304 | 42.21 | 5.21 | 417.55 |
| 2312 | 36.78 | 5.24 | 31.78 |
| 2503 | 49.53 | 5.16 | 179.73 |
| 2504 | 52.23 | 5.17 | 127.05 |
| 2809 | 90.05 | 5.28 | 115.43 |
| 3201 | 33.08 | 5.37 | 403.63 |
| 3602 | 61.70 | 5.30 | 79.53 |
| 3604 | 58.81 | 5.34 | 372.23 |
| 3610 | 62.80 | 5.35 | 46.75 |
| 3611 | 56.04 | 5.40 | 134.75 |
| 3714 | 66.15 | 5.42 | 83.70 |
| 4101 | 31.11 | 5.43 | 412.85 |
| 4103 | 22.37 | 5.46 | 265.18 |
| 4107 | 30.70 | 5.50 | 320.25 |
| 4203 | 35.40 | 5.44 | 122.35 |
| 4209 | 32.09 | 5.43 | 83.33 |
| 4508 | 50.71 | 5.48 | 104.58 |
| 4609 | 53.21 | 5.46 | 53.93 |
| 4702 | 74.15 | 5.43 | 55.80 |
| 4709 | 74.32 | 5.45 | 60.03 |
| 4712 | 68.46 | 5.48 | 33.38 |
| 4716 | 74.91 | 5.71 | 67.30 |
| 5101 | 29.58 | 5.72 | 358.13 |
| 5111 | 21.52 | 5.81 | 326.63 |
| 5121 | 28.99 | 5.96 | 26.38 |
| 5309 | 37.87 | 5.84 | 23.55 |
| 5504 | 53.05 | 5.79 | 102.33 |
| 5602 | 58.50 | 5.73 | 70.83 |
| 5606 | 57.06 | 5.90 | 63.70 |
| 5711 | 77.62 | 5.77 | 45.23 |
| 6112 | 28.78 | 6.00 | 118.58 |
| 6206 | 36.53 | 6.32 | 80.55 |
| 6212 | 34.37 | 6.47 | 194.43 |
| 6303 | 41.93 | 5.97 | 183.75 |
| 6308 | 41.15 | 6.36 | 148.68 |
| 6310 | 42.09 | 6.46 | 90.40 |
| 6313 | 40.86 | 6.51 | 119.40 |
| 6401 | 44.17 | 5.95 | 227.83 |
| 6416 | 46.23 | 5.96 | 73.98 |
| 6502 | 48.82 | 6.06 | 125.40 |
| 6505 | 49.74 | 6.46 | 153.23 |
| 6509 | 51.53 | 6.31 | 88.28 |
| 6601 | 53.25 | 5.99 | 372.15 |
| 6603 | 56.42 | 6.28 | 262.15 |
| 6604 | 55.56 | 6.31 | 168.78 |
| 6609 | 62.48 | 6.49 | 58.03 |
| 7120 | 25.14 | 6.73 | 111.75 |
| 7201 | 35.74 | 6.54 | 185.15 |
| 7605 | 60.99 | 6.59 | 293.38 |

**Table S13 –** List of proteins 2-fold common to CuO NPs and $Cu^{2+}$ exposure in the gills.

| Spot number | Obs. Mr (KDa) | Obs. pI | Average ratios | |
|---|---|---|---|---|
| | | | CuO NPs | $Cu^{2+}$ |
| 1203 | 34.68 | 5.04 | 2.20 ↑ | 5.41 ↑ |
| 2209 | 33.89 | 5.17 | 2.79 ↑ | 2.40 ↑ |
| 2708 | 68.98 | 5.19 | 2.22 ↑ | 3.25 ↑ |
| 2810 | 94.02 | 5.29 | 2.29 ↑ | 2.23 ↑ |
| 3108 | 30.90 | 5.40 | 3.00 ↑ | 4.43 ↑ |
| 3603 | 63.03 | 5.32 | 2.58 ↑ | 2.34 ↑ |
| 3608 | 54.32 | 5.31 | 5.00 ↑ | 4.27 ↑ |
| 3715 | 65.72 | 5.42 | 3.24 ↑ | 2.28 ↑ |
| 4212 | 33.24 | 5.46 | 5.17 ↑ | 3.38 ↑ |
| 4705 | 88.41 | 5.44 | 2.83 ↑ | 2.03 ↑ |
| 5202 | 37.61 | 5.74 | 3.07 ↑ | 2.04 ↑ |
| 5305 | 43.09 | 5.87 | 3.02 ↑ | 2.23 ↑ |
| 6113 | 27.64 | 6.31 | 2.69 ↑ | 6.12 ↑ |
| 6216 | 32.64 | 6.34 | 2.34 ↑ | 2.23 ↑ |
| 6405 | 44.20 | 6.34 | 3.12 ↑ | 2.91 ↑ |
| 7121 | 24.22 | 6.80 | 2.93 ↑ | 2.41 ↑ |
| 7501 | 48.98 | 6.53 | 2.50 ↑ | 2.06 ↑ |
| 2212 | 34.00 | 5.20 | 2.05 ↓ | 7.12 ↓ |
| 2217 | 33.24 | 5.29 | 2.40 ↓ | 10.32 ↓ |
| 3509 | 50.51 | 5.43 | 2.23 ↓ | 2.35 ↓ |
| 4601 | 55.20 | 5.44 | 2.54 ↓ | 3.93 ↓ |
| 5105 | 29.39 | 5.73 | 2.24 ↓ | 2.14 ↓ |
| 5107 | 28.40 | 5.80 | 3.45 ↓ | 3.32 ↓ |
| 5707 | 69.23 | 5.75 | 2.51 ↓ | 2.04 ↓ |
| 5714 | 65.61 | 5.90 | 2.72 ↓ | 5.53 ↓ |
| 6309 | 43.72 | 6.39 | 2.19 ↓ | 2.20 ↓ |

**Table S14 –** List of proteins 2-fold specific for CuO NPs exposure in the gills.

| Spot number | Obs. Mr (kDa) | Obs. pI | Average ratio |
|---|---|---|---|
| 1107 | 25.84 | 4.85 | 2.43 ↑ |
| 1110 | 27.77 | 4.93 | 2.76 ↑ |
| 1403 | 44.83 | 4.62 | 2.62 ↑ |
| 1411 | 44.44 | 4.64 | 2.42 ↑ |
| 1507 | 48.97 | 4.83 | 2.31 ↑ |
| 1510 | 48.95 | 4.86 | 12.78 ↑ |
| 1511 | 48.62 | 4.87 | 2.17 ↑ |
| 1514 | 49.14 | 4.93 | 7.95 ↑ |
| 1515 | 51.26 | 4.98 | 7.66 ↑ |
| 1701 | 74.92 | 4.93 | 3.57 ↑ |
| 1703 | 80.90 | 5.00 | 2.55 ↑ |
| 2202 | 35.19 | 5.05 | 3.49 ↑ |
| 2304 | 42.21 | 5.21 | 4.19 ↑ |
| 2312 | 36.78 | 5.24 | 2.82 ↑ |
| 2403 | 47.62 | 5.28 | 2.50 ↑ |
| 2504 | 52.23 | 5.17 | 2.28 ↑ |
| 2601 | 59.26 | 5.05 | 2.18 ↑ |
| 2613 | 56.92 | 5.25 | 3.89 ↑ |
| 2710 | 68.89 | 5.28 | 2.91 ↑ |
| 2809 | 90.05 | 5.28 | 2.71 ↑ |
| 3110 | 28.64 | 5.43 | 2.26 ↑ |
| 3403 | 45.43 | 5.36 | 6.19 ↑ |
| 3501 | 52.33 | 5.30 | 2.21 ↑ |
| 3504 | 49.46 | 5.41 | 3.40 ↑ |
| 3507 | 50.46 | 5.42 | 2.04 ↑ |
| 3601 | 59.03 | 5.30 | 2.29 ↑ |
| 3602 | 61.70 | 5.30 | 2.41 ↑ |
| 3604 | 58.81 | 5.34 | 2.50 ↑ |
| 3610 | 62.80 | 5.35 | 2.31 ↑ |
| 3613 | 55.41 | 5.41 | 2.46 ↑ |
| 3705 | 66.17 | 5.37 | 2.19 ↑ |
| 3716 | 76.56 | 5.42 | 4.05 ↑ |
| 3801 | 90.02 | 5.30 | 2.47 ↑ |
| 3804 | 93.70 | 5.34 | 8.30 ↑ |
| 3808 | 98.78 | 5.41 | 4.53 ↑ |
| 3809 | 107.7 | 5.41 | 3.88 ↑ |
| 3811 | 98.96 | 5.40 | 2.03 ↑ |
| 3812 | 98.33 | 5.42 | 5.49 ↑ |
| 4116 | 28.45 | 5.48 | 2.28 ↑ |
| 4209 | 32.09 | 5.43 | 3.78 ↑ |
| 4410 | 46.87 | 5.64 | 2.80 ↑ |
| 4602 | 58.77 | 5.45 | 5.22 ↑ |
| 4605 | 53.84 | 5.54 | 2.74 ↑ |
| 4606 | 58.46 | 5.65 | 2.18 ↑ |
| 4609 | 53.21 | 5.46 | 3.62 ↑ |
| 4702 | 74.15 | 5.43 | 7.86 ↑ |
| 5113 | 30.06 | 5.89 | 2.14 ↑ |
| 5114 | 25.17 | 5.92 | 2.09 ↑ |
| 5205 | 36.42 | 5.80 | 2.73 ↑ |
| 5301 | 40.63 | 5.73 | 2.04 ↑ |
| 5504 | 53.05 | 5.79 | 2.49 ↑ |
| 5602 | 58.5 | 5.73 | 3.75 ↑ |
| 5603 | 53.73 | 5.73 | 2.22 ↑ |
| 5703 | 65.87 | 5.73 | 3.78 ↑ |
| 5704 | 76.6 | 5.74 | 2.77 ↑ |
| 5705 | 74.46 | 5.74 | 2.39 ↑ |
| 5711 | 77.62 | 5.77 | 2.61 ↑ |
| 6112 | 28.78 | 6.00 | 2.36 ↑ |
| 6203 | 36.60 | 6.19 | 4.22 ↑ |
| 6308 | 41.15 | 6.36 | 2.22 ↑ |
| 6502 | 48.82 | 6.06 | 2.2 ↑ |
| 6509 | 51.53 | 6.31 | 4.17 ↑ |
| 6606 | 64.53 | 6.37 | 2.7 ↑ |
| 6607 | 55.34 | 6.39 | 3.23 ↑ |
| 6702 | 65.02 | 5.96 | 2.19 ↑ |
| 6703 | 64.90 | 6.49 | 3.37 ↑ |
| 6706 | 71.95 | 6.30 | 3.39 ↑ |
| 7401 | 44.68 | 6.54 | 3.33 ↑ |
| 7607 | 60.89 | 6.76 | 2.15 ↑ |
| 2103 | 23.70 | 5.14 | 2.29 ↓ |
| 2808 | 93.73 | 5.26 | 2.48 ↓ |
| 3303 | 41.90 | 5.30 | 2.13 ↓ |
| 4504 | 49.44 | 5.45 | 2.20 ↓ |
| 5101 | 29.58 | 5.72 | 3.64 ↓ |
| 5405 | 44.21 | 5.79 | 2.05 ↓ |
| 6212 | 34.37 | 6.47 | 2.17 ↓ |
| 6804 | 97.27 | 6.20 | 3.04 ↓ |
| 2103 | 23.70 | 5.14 | 2.29 ↓ |
| 2808 | 93.73 | 5.26 | 2.48 ↓ |

**Table S15 –** List of proteins 2-fold specific for $Cu^{2+}$ expsure in the gills.

| Spot number | Obs. Mr (kDa) | Obs. pI | Average ratio |
|---|---|---|---|
| 2106 | 22.84 | 5.22 | 2.65 ↑ |
| 2313 | 37.81 | 5.25 | 4.24 ↑ |
| 2404 | 47.24 | 5.12 | 3.15 ↑ |
| 3102 | 22.62 | 5.33 | 2.91 ↑ |
| 3410 | 45.84 | 5.30 | 2.21 ↑ |
| 3807 | 107.67 | 5.40 | 2.08 ↑ |
| 3817 | 93.62 | 5.37 | 2.19 ↑ |
| 4706 | 74.72 | 5.44 | 2.58 ↑ |
| 5204 | 34.09 | 5.8 | 2.21↑ |
| 5811 | 102.89 | 5.93 | 2.01 ↑ |
| 6705 | 71.85 | 6.34 | 2.40 ↑ |
| 7610 | 60.87 | 6.90 | 2.69 ↑ |
| 7701 | 81.64 | 6.61 | 2.39 ↑ |
| 7708 | 66.38 | 6.90 | 2.95 ↑ |
| 7710 | 66.13 | 6.94 | 2.05 ↑ |
| 2401 | 45.09 | 5.24 | 2.05 ↓ |
| 2609 | 53.58 | 5.16 | 2.32 ↓ |
| 2610 | 53.38 | 5.18 | 2.70 ↓ |
| 2704 | 69.39 | 5.13 | 2.11 ↓ |
| 2709 | 69.26 | 5.25 | 2.06 ↓ |
| 2801 | 98.46 | 5.05 | 2.21 ↓ |
| 3203 | 32.39 | 5.37 | 6.20 ↓ |
| 3302 | 38.58 | 5.33 | 2.69 ↓ |
| 3406 | 46.54 | 5.41 | 3.09 ↓ |
| 3607 | 61.51 | 5.35 | 2.98 ↓ |
| 3706 | 68.70 | 5.40 | 2.89 ↓ |
| 4207 | 36.79 | 5.48 | 2.65 ↓ |
| 4402 | 47.37 | 5.44 | 2.23 ↓ |
| 4404 | 46.24 | 5.46 | 9.89 ↓ |
| 4406 | 44.27 | 5.46 | 2.5 ↓ |
| 4408 | 44.24 | 5.54 | 3.46 ↓ |
| 4409 | 47.44 | 5.55 | 2.45 ↓ |
| 4411 | 46.13 | 5.70 | 2.38 ↓ |
| 4412 | 44.18 | 5.71 | 2.21 ↓ |
| 5104 | 30.03 | 5.73 | 2.90 ↓ |
| 5303 | 40.40 | 5.77 | 2.16 ↓ |
| 5304 | 40.91 | 5.78 | 3.64 ↓ |
| 5710 | 74.62 | 5.77 | 2.24 ↓ |
| 5802 | 93.85 | 5.74 | 2.04 ↓ |
| 5807 | 94.53 | 5.81 | 2.35 ↓ |
| 6207 | 37.88 | 6.37 | 3.50 ↓ |
| 6307 | 42.84 | 6.32 | 3.26 ↓ |
| 6407 | 46.98 | 6.37 | 3.50 ↓ |
| 6503 | 48.45 | 6.14 | 2.98 ↓ |
| 6702 | 65.02 | 5.96 | 2.74 ↓ |

**Table S16 –** List of proteins 2-fold common for CuO NPs and $Cu^{2+}$ exposure in the digestive gland.

| Spot number | Obs. Mr (KDa) | Obs. pI | Average ratios | |
|---|---|---|---|---|
| | | | CuO NPs | $Cu^{2+}$ |
| 401 | 47.39 | 4.55 | 2.98 ↑ | 2.78 ↑ |
| 1203 | 33.63 | 4.91 | 5.01 ↑ | 2.01 ↑ |
| 1304 | 40.05 | 4.79 | 2.09 ↑ | 5.94 ↑ |
| 1401 | 47.16 | 4.60 | 4.57 ↑ | 6.30 ↑ |
| 2308 | 42.12 | 5.21 | 5.71 ↑ | 2.02 ↑ |
| 2505 | 51.06 | 5.19 | 11.81 ↑ | 12.46 ↑ |
| 2603 | 56.48 | 5.07 | 4.62 ↑ | 2.66 ↑ |
| 2605 | 52.21 | 5.11 | 10.85 ↑ | 8.46 ↑ |
| 2705 | 67.51 | 5.01 | 3.34 ↑ | 3.33 ↑ |
| 2711 | 67.60 | 5.20 | 3.99 ↑ | 5.59 ↑ |
| 2721 | 70.32 | 5.19 | 3.16 ↑ | 7.63 ↑ |
| 3202 | 31.91 | 5.31 | 4.51 ↑ | 7.28 ↑ |
| 3308 | 42.10 | 5.40 | 14.89 ↑ | 5.42 ↑ |
| 3502 | 50.94 | 5.27 | 29.39 ↑ | 32.38 ↑ |
| 3503 | 48.33 | 5.29 | 13.71 ↑ | 11.43 ↑ |
| 3504 | 50.56 | 5.32 | 28.45 ↑ | 11.55 ↑ |
| 3507 | 49.27 | 5.35 | 5.58 ↑ | 20.05 ↑ |
| 3508 | 50.47 | 5.36 | 4.29 ↑ | 2.47 ↑ |
| 3703 | 67.13 | 5.27 | 26.13 ↑ | 21.14 ↑ |
| 3705 | 64.90 | 5.31 | 2.08 ↑ | 2.60 ↑ |
| 3716 | 69.10 | 5.41 | 12.50 ↑ | 14.60 ↑ |
| 4107 | 26.33 | 5.66 | 14.50 ↑ | 3.66 ↑ |
| 4207 | 34.60 | 5.58 | 4.11 ↑ | 3.74 ↑ |
| 4508 | 47.91 | 5.59 | 2.38 ↑ | 2.47 ↑ |
| 4509 | 50.39 | 5.59 | 6.02 ↑ | 2.78 ↑ |
| 4605 | 56.49 | 5.68 | 3.04 ↑ | 3.07 ↑ |
| 4703 | 68.83 | 5.49 | 16.81 ↑ | 18.53 ↑ |
| 5102 | 24.71 | 5.80 | 6.87 ↑ | 15.69 ↑ |
| 5303 | 39.82 | 5.93 | 6.32 ↑ | 22.91 ↑ |
| 5411 | 47.63 | 6.05 | 7.46 ↑ | 15.01 ↑ |
| 5604 | 56.91 | 5.87 | 2.14 ↑ | 5.52 ↑ |
| 6106 | 25.26 | 6.37 | 2.75 ↑ | 2.77 ↑ |
| 6412 | 45.55 | 6.52 | 3.23 ↑ | 7.90 ↑ |
| 6416 | 45.54 | 6.36 | 2.28 ↑ | 10.78 ↑ |
| 6504 | 48.74 | 6.35 | 5.22 ↑ | 2.26 ↑ |
| 6602 | 52.75 | 6.13 | 5.91 ↑ | 11.11 ↑ |
| 6605 | 52.81 | 6.24 | 11.47 ↑ | 13.30 ↑ |
| 6609 | 53.23 | 6.52 | 2.51 ↑ | 3.27 ↑ |
| 6701 | 65.00 | 6.16 | 4.99 ↑ | 4.95 ↑ |
| 6804 | 91.29 | 6.14 | 2.16 ↑ | 3.47 ↑ |
| 6816 | 97.26 | 6.11 | 2.03 ↑ | 2.44 ↑ |
| 109 | 27.67 | 4.63 | 3.36 ↓ | 3.13 ↓ |
| 1105 | 25.33 | 4.79 | 2.25 ↓ | 2.83 ↓ |
| 1707 | 72.92 | 4.88 | 3.22 ↓ | 3.06 ↓ |
| 1805 | 91.35 | 4.86 | 2.50 ↓ | 4.85 ↓ |
| 2214 | 32.38 | 5.22 | 3.57 ↓ | 3.56 ↓ |
| 2310 | 40.50 | 5.19 | 3.97 ↓ | 4.07 ↓ |
| 2715 | 72.23 | 4.95 | 3.60 ↓ | 8.15 ↓ |
| 3709 | 67.26 | 5.35 | 2.10 ↓ | 7.62 ↓ |
| 4111 | 27.02 | 5.59 | 36.47 ↓ | 4.84 ↓ |
| 4407 | 46.45 | 5.55 | 8.23 ↓ | 2.32 ↓ |
| 4601 | 54.33 | 5.49 | 2.69 ↓ | 5.48 ↓ |
| 5506 | 48.30 | 5.90 | 5.83 ↓ | 2.50 ↓ |
| 6509 | 48.22 | 6.49 | 4.12 ↓ | 2.11 ↓ |

**Table S17 –** List of proteins 2-fold specific for CuO NPs exposure in the digestive gland.

| Spot number | Obs. Mr (kDa) | Obs. pI | Average ratio |
|---|---|---|---|
| 1204 | 34.34 | 4.91 | 5.01 ↑ |
| 1403 | 45.24 | 4.87 | 4.57 ↑ |
| 1705 | 68.37 | 4.87 | 3.69 ↑ |
| 2104 | 26.29 | 5.10 | 2.70 ↑ |
| 2110 | 27.43 | 5.20 | 2.13 ↑ |
| 2204 | 34.67 | 5.00 | 2.19 ↑ |
| 2205 | 32.98 | 5.09 | 3.16 ↑ |
| 2504 | 51.77 | 5.13 | 2.72 ↑ |
| 3102 | 27.43 | 5.36 | 5.41 ↑ |
| 3402 | 44.30 | 5.30 | 7.48 ↑ |
| 3603 | 55.36 | 5.30 | 7.64 ↑ |
| 3706 | 67.29 | 5.32 | 2.17 ↑ |
| 3714 | 65.07 | 5.40 | 5.26 ↑ |
| 4208 | 29.78 | 5.59 | 3.01 ↑ |
| 4304 | 40.12 | 5.52 | 2.01 ↑ |
| 4604 | 56.65 | 5.63 | 2.63 ↑ |
| 4802 | 92.22 | 5.60 | 6.76 ↑ |
| 5202 | 29.75 | 5.82 | 2.72 ↑ |
| 5316 | 36.59 | 5.75 | 2.82 ↑ |
| 5503 | 49.24 | 5.87 | 2.16 ↑ |
| 5701 | 67.67 | 5.80 | 4.71 ↑ |
| 5705 | 67.81 | 5.90 | 2.49 ↑ |
| 6101 | 24.94 | 6.11 | 2.21 ↑ |
| 6304 | 36.58 | 6.28 | 5.05 ↑ |
| 6502 | 48.91 | 6.23 | 2.48 ↑ |
| 6703 | 65.43 | 6.27 | 3.52 ↑ |
| 7105 | 27.91 | 6.72 | 2.30 ↑ |

| Spot number | Obs. Mr (kDa) | Obs. pI | Average ratio |
|---|---|---|---|
| 104 | 25.30 | 4.57 | 2.24 ↓ |
| 105 | 26.17 | 4.48 | 3.01 ↓ |
| 819 | 102.64 | 4.56 | 4.90 ↓ |
| 1106 | 25.84 | 4.81 | 2.01 ↓ |
| 1309 | 42.16 | 4.72 | 3.12 ↓ |
| 1502 | 48.78 | 4.64 | 4.69 ↓ |
| 1511 | 51.13 | 4.91 | 4.87 ↓ |
| 1701 | 68.51 | 4.83 | 2.17 ↓ |
| 1703 | 68.35 | 4.85 | 5.15 ↓ |
| 1710 | 73.22 | 4.92 | 2.00 ↓ |
| 1802 | 99.74 | 4.72 | 2.57 ↓ |
| 1803 | 91.06 | 4.89 | 2.36 ↓ |
| 1810 | 99.43 | 4.62 | 14.98 ↓ |
| 2101 | 25.65 | 4.95 | 3.04 ↓ |
| 2213 | 31.54 | 5.21 | 2.66 ↓ |
| 2305 | 35.99 | 5.15 | 2.69 ↓ |
| 2403 | 47.62 | 5.04 | 2.00 ↓ |
| 2716 | 71.82 | 4.99 | 8.07 ↓ |
| 2801 | 87.12 | 4.97 | 2.09 ↓ |
| 2803 | 88.93 | 5.03 | 4.21 ↓ |
| 2807 | 89.59 | 5.18 | 2.14 ↓ |
| 3606 | 60.39 | 5.33 | 3.24 ↓ |
| 3607 | 58.85 | 5.35 | 2.22 ↓ |
| 3611 | 60.26 | 5.40 | 2.75 ↓ |
| 4006 | 23.21 | 5.51 | 2.58 ↓ |
| 4102 | 26.23 | 5.58 | 2.08 ↓ |
| 4404 | 44.57 | 5.69 | 2.95 ↓ |
| 4405 | 46.27 | 5.70 | 2.12 ↓ |
| 5508 | 49.08 | 5.97 | 8.56 ↓ |
| 5708 | 67.72 | 6.01 | 3.07 ↓ |
| 6401 | 45.33 | 6.15 | 3.77 ↓ |
| 6510 | 48.95 | 6.49 | 4.38 ↓ |
| 6708 | 68.06 | 6.13 | 4.32 ↓ |
| 6710 | 73.21 | 6.43 | 2.62 ↓ |
| 6805 | 91.48 | 6.18 | 2.46 ↓ |
| 6811 | 81.57 | 6.15 | 5.36 ↓ |
| 7614 | 56.13 | 6.64 | 2.71 ↓ |
| 7710 | 76.13 | 6.30 | 10.44 ↓ |

**Table S18 –** List of proteins 2-fold specific for $Cu^{2+}$ exposure in the digestive gland.

| Spot number | Obs. Mr (kDa) | Obs. pI | Average ratio |
|---|---|---|---|
| 2518 | 43.37 | 4.94 | 2.73 ↑ |
| 2602 | 48.19 | 4.71 | 4.32 ↑ |
| 2603 | 49.00 | 4.80 | 5.88 ↑ |
| 2701 | 67.00 | 4.76 | 2.96 ↑ |
| 2712 | 64.80 | 4.96 | 2.28 ↑ |
| 2716 | 66.86 | 4.78 | 6.43 ↑ |
| 2805 | 73.97 | 4.79 | 7.34 ↑ |
| 2806 | 73.00 | 4.83 | 7.03 ↑ |
| 3711 | 69.64 | 5.05 | 4.30 ↑ |
| 3716 | 66.92 | 5.11 | 2.15 ↑ |
| 3720 | 61.84 | 5.20 | 2.55 ↑ |
| 3726 | 61.59 | 5.22 | 3.39 ↑ |
| 3728 | 68.45 | 5.22 | 13.65 ↑ |
| 3802 | 71.74 | 4.98 | 2.14 ↑ |
| 3811 | 91.27 | 5.20 | 2.96 ↑ |
| 3813 | 91.51 | 5.21 | 2.24 ↑ |
| 4417 | 37.27 | 5.26 | 4.94 ↑ |
| 4418 | 34.92 | 5.41 | 5.18 ↑ |
| 4503 | 41.90 | 5.30 | 3.34 ↑ |
| 4804 | 72.18 | 5.37 | 3.58 ↑ |
| 4806 | 72.89 | 5.43 | 5.38 ↑ |
| 4807 | 71.99 | 5.43 | 3.50 ↑ |
| 5313 | 30.64 | 5.75 | 7.79 ↑ |
| 5315 | 32.95 | 5.58 | 6.06 ↑ |
| 5412 | 35.20 | 5.66 | 2.09 ↑ |
| 5520 | 45.89 | 5.79 | 2.38 ↑ |
| 5605 | 48.22 | 5.56 | 2.77 ↑ |
| 5607 | 55.21 | 5.58 | 2.46 ↑ |
| 5707 | 66.64 | 5.60 | 2.18 ↑ |
| 5708 | 56.15 | 5.64 | 9.64 ↑ |
| 5710 | 66.84 | 5.71 | 14.45 ↑ |
| 5711 | 56.69 | 5.72 | 3.07 ↑ |
| 5714 | 58.56 | 5.78 | 2.79 ↑ |
| 5801 | 72.76 | 5.50 | 3.41 ↑ |
| 5803 | 73.56 | 5.55 | 2.17 ↑ |
| 5805 | 96.14 | 5.57 | 5.03 ↑ |
| 5806 | 73.23 | 5.58 | 2.35 ↑ |
| 5808 | 95.79 | 5.63 | 21.53 ↑ |
| 5813 | 95.00 | 5.77 | 10.50 ↑ |
| 6306 | 34.30 | 5.90 | 2.22 ↑ |
| 6401 | 37.16 | 5.82 | 3.07 ↑ |
| 6404 | 40.83 | 5.85 | 2.13 ↑ |
| 6414 | 36.97 | 6.22 | 2.38 ↑ |
| 6426 | 36.94 | 5.97 | 2.16 ↑ |
| 6427 | 39.30 | 5.84 | 22.91 ↑ |
| 6507 | 46.65 | 5.98 | 3.55 ↑ |
| 4609 | 49.38 | 5.40 | 4.23 ↑ |
| 4614 | 49.41 | 5.45 | 3.05 ↑ |
| 4709 | 61.51 | 5.29 | 2.71 ↑ |
| 4717 | 64.40 | 5.40 | 2.52 ↑ |
| 4722 | 64.42 | 5.44 | 4.32 ↑ |
| 4724 | 58.78 | 5.45 | 3.44 ↑ |
| 4725 | 67.10 | 5.46 | 4.35 ↑ |
| 7401 | 40.65 | 6.26 | 2.02 ↑ |
| 7508 | 45.22 | 6.36 | 6.00 ↑ |
| 7604 | 53.29 | 6.32 | 2.23 ↑ |
| 7620 | 51.76 | 6.57 | 7.61 ↑ |
| 7701 | 59.54 | 6.25 | 2.40 ↑ |
| 7702 | 63.93 | 6.27 | 8.21 ↑ |
| 7704 | 56.96 | 6.33 | 2.61 ↑ |
| 6508 | 45.78 | 5.98 | 2.37 ↑ |
| 6609 | 50.31 | 5.90 | 5.70 ↑ |
| 6701 | 67.58 | 5.80 | 5.78 ↑ |
| 6707 | 66.70 | 5.91 | 3.17 ↑ |
| 6711 | 66.76 | 6.06 | 3.17 ↑ |
| 6802 | 73.65 | 5.82 | 2.73 ↑ |
| 6815 | 103.69 | 6.03 | 4.72 ↑ |
| 6823 | 95.00 | 5.83 | 12.00 ↑ |
| 7113 | 25.28 | 6.62 | 2.5 ↑ |
| 7307 | 30.00 | 6.50 | 3.33 ↑ |
| 7705 | 63.97 | 6.36 | 3.55 ↑ |
| 7709 | 64.90 | 6.50 | 3.80 ↑ |
| 8209 | 29.27 | 6.69 | 3.22 ↑ |
| 1817 | 106.09 | 4.64 | 4.12 ↓ |
| 2202 | 26.88 | 4.70 | 2.39 ↓ |
| 2214 | 26.19 | 4.88 | 3.71 ↓ |
| 2217 | 27.95 | 4.80 | 2.13 ↓ |
| 2307 | 31.24 | 4.87 | 7.68 ↓ |
| 2516 | 44.72 | 4.90 | 2.35 ↓ |
| 2709 | 62.72 | 4.90 | 2.05 ↓ |
| 2801 | 104.05 | 4.69 | 6.02 ↓ |
| 2809 | 91.20 | 4.88 | 5.19 ↓ |
| 2812 | 89.66 | 4.94 | 2.24 ↓ |
| 3210 | 28.22 | 5.10 | 3.06 ↓ |
| 3211 | 26.91 | 5.13 | 2.10 ↓ |
| 3213 | 28.00 | 5.20 | 2.04 ↓ |
| 3215 | 26.73 | 5.20 | 3.03 ↓ |
| 3314 | 34.44 | 5.11 | 3.53 ↓ |
| 3315 | 33.91 | 5.11 | 5.14↓ |
| 3501 | 47.46 | 4.99 | 2.30 ↓ |
| 3508 | 44.06 | 5.10 | 3.71 ↓ |
| 3704 | 61.82 | 5.00 | 2.01 ↓ |
| 3709 | 61.62 | 5.05 | 2.23 ↓ |
| 3710 | 59.59 | 5.05 | 3.23 ↓ |
| 4113 | 25.28 | 5.40 | 12.37 ↓ |
| 4306 | 32.18 | 5.40 | 3.32 ↓ |
| 5309 | 30.43 | 5.66 | 3.83 ↓ |
| 5408 | 36.52 | 5.59 | 18.79 ↓ |
| 5518 | 43.53 | 5.72 | 2.23 ↓ |
| 5604 | 48.83 | 5.55 | 9.37 ↓ |
| 5609 | 48.54 | 5.65 | 8.55 ↓ |
| 6310 | 33.99 | 6.16 | 5.50 ↓ |
| 6312 | 29.68 | 6.23 | 3.52 ↓ |
| 6317 | 35.69 | 6.07 | 2.09 ↓ |
| 6415 | 39.63 | 6.23 | 2.90 ↓ |
| 6624 | 50.00 | 6.21 | 4.14 ↓ |
| 6705 | 67.85 | 5.91 | 4.46 ↓ |
| 6709 | 67.16 | 6.02 | 6.53 ↓ |
| 6712 | 60.94 | 6.08 | 6.08 ↓ |
| 7402 | 37.09 | 6.38 | 2.13 ↓ |

# APPENDIX II

## Supplementary tables for Chapter 6: "Differential protein expression in mussels *Mytilus galloprovincialis* exposed to nano and ionic Ag"

# APPENDIX II.

# SUPPLEMENTARY TABLES FOR CHAPTER 6

**Table S1 –** List of new common spots for Ag NPs and $Ag^{+}$ exposure in the gills.

| Spot number | Obs. Mr (kDa) | Obs. pI | NPs | $Ag^{+}$ |
|---|---|---|---|---|
| 1111 | 22.81 | 4.87 | 1518.95 | 1136.13 |
| 2220 | 32.11 | 5.34 | 201.58 | 582.80 |
| 2525 | 58.59 | 5.23 | 419.45 | 229.28 |
| 2528 | 58.41 | 5.26 | 231.30 | 184.23 |
| 2529 | 54.54 | 5.20 | 157.28 | 89.33 |
| 2530 | 60.09 | 4.97 | 359.08 | 279.05 |
| 2717 | 75.52 | 5.28 | 196.23 | 64.43 |
| 3111 | 30.17 | 5.55 | 785.50 | 346.85 |
| 3310 | 44.84 | 5.58 | 172.80 | 114.33 |
| 3520 | 59.36 | 5.50 | 264.08 | 157.78 |
| 3521 | 58.90 | 5.43 | 221.18 | 203.55 |
| 3820 | 108.61 | 5.57 | 55.85 | 52.18 |
| 4128 | 29.16 | 5.79 | 436.00 | 869.18 |
| 4130 | 29.89 | 5.73 | 102.20 | 306.18 |
| 4131 | 29.92 | 5.68 | 904.55 | 1292.53 |
| 4318 | 44.40 | 5.77 | 113.98 | 325.08 |
| 5518 | 56.71 | 6.12 | 103.53 | 141.35 |
| 5617 | 69.07 | 6.13 | 30.15 | 46.05 |
| 5725 | 97.58 | 5.96 | 135.48 | 115.38 |
| 6331 | 45.66 | 6.35 | 102.45 | 344.25 |
| 6417 | 49.49 | 6.37 | 112.18 | 131.45 |
| 6521 | 58.12 | 6.22 | 251.45 | 306.00 |
| 6614 | 68.43 | 6.53 | 189.38 | 48.35 |
| 6615 | 66.89 | 6.51 | 132.15 | 74.18 |
| 7415 | 53.29 | 6.61 | 405.53 | 512.95 |
| 7715 | 86.79 | 6.67 | 1771.60 | 122.30 |
| 1709 | 79.28 | 4.80 | 416.00 | 660.13 |
| 3630 | 73.90 | 5.52 | 123.57 | 38.23 |
| 3821 | 112.68 | 5.43 | 62.77 | 36.80 |
| 5122 | 28.73 | 6.20 | 51.77 | 235.00 |
| 6418 | 48.59 | 6.27 | 43.03 | 80.65 |
| 1117 | 24.65 | 4.70 | 36.33 | 300.10 |
| 2231 | 30.87 | 5.14 | 60.55 | 111.77 |
| 2423 | 51.12 | 5.13 | 85.93 | 99.30 |
| 3313 | 43.25 | 5.44 | 167.85 | 117.47 |
| 3314 | 42.14 | 5.50 | 455.80 | 213.67 |
| 3819 | 108.34 | 5.64 | 101.40 | 40.07 |
| 4512 | 53.92 | 5.90 | 310.20 | 314.80 |
| 5131 | 29.56 | 5.89 | 94.60 | 138.73 |
| 5412 | 53.22 | 6.15 | 253.98 | 68.20 |

**Table S2 –** List of new specific spots for Ag NPs exposure in the gills.

| Spot number | Obs. Mr (kDa) | Obs. pI | NPs |
|---|---|---|---|
| 1118 | 24.01 | 4.74 | 62.25 |
| 1309 | 43.48 | 4.92 | 320.30 |
| 1310 | 41.61 | 4.89 | 37.90 |
| 2119 | 27.08 | 5.06 | 945.85 |
| 2123 | 29.11 | 5.24 | 36.68 |
| 2232 | 36.50 | 5.06 | 40.68 |
| 2320 | 41.31 | 4.94 | 40.55 |
| 2321 | 38.72 | 5.16 | 69.18 |
| 2425 | 51.10 | 5.28 | 244.35 |
| 3315 | 39.12 | 5.50 | 90.23 |
| 3523 | 62.29 | 5.67 | 93.70 |
| 4125 | 29.41 | 5.92 | 508.00 |
| 4127 | 29.69 | 5.80 | 250.30 |
| 4129 | 26.36 | 5.83 | 58.90 |
| 4317 | 45.38 | 5.89 | 172.03 |
| 4327 | 42.09 | 5.86 | 52.25 |
| 4416 | 49.22 | 5.68 | 432.00 |
| 4625 | 65.84 | 5.89 | 115.45 |
| 4626 | 66.41 | 5.87 | 51.15 |
| 4627 | 74.33 | 5.74 | 48.13 |
| 4735 | 74.02 | 5.70 | 51.73 |
| 5132 | 27.67 | 5.97 | 79.00 |
| 5325 | 42.60 | 6.12 | 103.48 |
| 5326 | 44.93 | 6.11 | 40.68 |
| 5327 | 39.80 | 5.91 | 46.58 |
| 5413 | 52.79 | 6.02 | 73.03 |
| 5517 | 56.53 | 6.14 | 140.60 |
| 5521 | 58.65 | 6.17 | 218.25 |
| 5722 | 83.07 | 6.21 | 462.48 |
| 5726 | 84.97 | 6.07 | 209.63 |
| 5727 | 80.03 | 5.94 | 253.28 |
| 5728 | 75.27 | 5.90 | 97.83 |
| 5729 | 80.44 | 5.90 | 40.35 |
| 5731 | 74.92 | 6.04 | 69.20 |
| 6212 | 32.35 | 6.36 | 177.55 |
| 6327 | 43.65 | 6.56 | 186.33 |
| 6523 | 52.83 | 6.40 | 265.73 |
| 6524 | 55.65 | 6.42 | 48.50 |
| 6810 | 103.62 | 6.24 | 132.95 |
| 6811 | 102.37 | 6.29 | 82.33 |
| 6814 | 103.23 | 6.20 | 66.85 |
| 7123 | 24.57 | 6.69 | 172.00 |
| 7226 | 36.83 | 6.67 | 336.25 |
| 7323 | 44.94 | 6.83 | 3927.03 |
| 7528 | 56.91 | 6.64 | 67.85 |
| 7616 | 63.33 | 6.55 | 529.28 |
| 7714 | 83.31 | 6.44 | 662.75 |
| 7716 | 86.56 | 6.56 | 62.60 |

**Table S3 –** List of new specific spots for $Ag^+$ exposure in the gills.

| Spot number | Obs. Mr (kDa) | Obs. pI | $Ag^+$ |
|---|---|---|---|
| 303 | 46.57 | 4.52 | 392.88 |
| 304 | 46.06 | 4.52 | 185.98 |
| 409 | 48.43 | 4.47 | 717.33 |
| 1215 | 34.17 | 4.73 | 499.80 |
| 1216 | 33.59 | 4.91 | 140.80 |
| 1217 | 33.49 | 4.73 | 289.83 |
| 1220 | 34.49 | 4.78 | 1700.08 |
| 1221 | 33.79 | 4.78 | 963.93 |
| 1222 | 33.77 | 4.83 | 302.33 |
| 1223 | 33.13 | 4.82 | 192.08 |
| 2122 | 30.11 | 5.24 | 65.03 |
| 2219 | 32.82 | 4.94 | 142.53 |
| 2419 | 50.33 | 5.31 | 247.35 |
| 2526 | 56.03 | 5.33 | 138.30 |
| 2527 | 60.68 | 5.27 | 140.35 |
| 2532 | 55.82 | 5.23 | 108.63 |
| 2617 | 69.28 | 5.12 | 77.28 |
| 4213 | 32.38 | 5.59 | 57.33 |
| 4316 | 41.55 | 5.70 | 361.60 |
| 4415 | 49.22 | 5.77 | 55.68 |
| 4733 | 77.52 | 5.69 | 68.55 |
| 5123 | 28.07 | 6.03 | 178.05 |
| 5134 | 24.22 | 6.03 | 306.93 |
| 5323 | 45.03 | 6.06 | 139.35 |
| 5519 | 56.39 | 6.09 | 48.10 |
| 5615 | 65.48 | 6.01 | 199.93 |
| 5616 | 66.33 | 6.16 | 171.48 |
| 5721 | 77.53 | 5.99 | 60.48 |
| 5724 | 77.53 | 5.91 | 135.70 |
| 6123 | 28.10 | 6.29 | 1026.50 |
| 6330 | 39.94 | 6.20 | 80.65 |
| 6713 | 95.69 | 6.39 | 77.35 |
| 7125 | 25.16 | 6.58 | 135.60 |
| 7325 | 39.94 | 6.57 | 273.15 |
| 7719 | 72.39 | 6.66 | 85.33 |
| 8718 | 81.81 | 6.98 | 1759.83 |

**Table S4 –** List of new common spots for Ag NPs and $Ag^+$ exposure in the digestive gland.

| Spot number | Obs. Mr (kDa) | Obs. pI | NPs | $Ag^+$ | Spot number | Obs. Mr (kDa) | Obs. pI | NPs | $Ag^+$ |
|---|---|---|---|---|---|---|---|---|---|
| 1211 | 25.99 | 4.58 | 1824.00 | 2220.00 | 7323 | 34.45 | 6.38 | 456.40 | 243.33 |
| 1213 | 26.86 | 4.69 | 751.40 | 1540.78 | 7324 | 34.09 | 6.42 | 98.20 | 117.50 |
| 2214 | 32.90 | 5.12 | 283.25 | 324.90 | 7413 | 46.54 | 6.61 | 221.95 | 444.90 |
| 2408 | 44.58 | 4.91 | 465.60 | 276.47 | 7414 | 46.05 | 6.47 | 363.23 | 270.30 |
| 2503 | 48.37 | 5.10 | 197.70 | 202.93 | 7415 | 42.58 | 6.38 | 216.05 | 302.03 |
| 2611 | 61.16 | 4.99 | 450.00 | 205.18 | 7419 | 46.64 | 6.27 | 224.40 | 463.48 |
| 2618 | 54.85 | 4.89 | 460.20 | 270.00 | 7513 | 49.08 | 6.50 | 333.30 | 131.00 |
| 2619 | 55.73 | 4.94 | 310.10 | 67.17 | 7514 | 48.94 | 6.56 | 129.60 | 192.33 |
| 2907 | 89.49 | 5.11 | 175.05 | 100.93 | 7515 | 49.66 | 6.28 | 229.25 | 154.30 |
| 2908 | 88.51 | 5.19 | 213.75 | 131.78 | 7516 | 46.86 | 6.47 | 379.35 | 426.28 |
| 3218 | 31.80 | 5.30 | 145.35 | 226.27 | 7517 | 47.23 | 6.37 | 154.55 | 164.20 |
| 3307 | 36.40 | 5.19 | 220.95 | 151.70 | 7518 | 49.30 | 6.45 | 416.65 | 198.57 |
| 3618 | 55.42 | 5.30 | 52.65 | 308.90 | 7611 | 63.09 | 6.48 | 213.65 | 237.43 |
| 3910 | 91.06 | 5.24 | 880.00 | 296.10 | 7612 | 61.62 | 6.33 | 86.53 | 92.13 |
| 4115 | 24.50 | 5.52 | 430.55 | 384.63 | 7613 | 59.55 | 6.44 | 326.35 | 323.45 |
| 4221 | 30.55 | 5.51 | 456.40 | 302.33 | 7614 | 55.71 | 6.59 | 152.95 | 113.20 |
| 4516 | 48.84 | 5.54 | 129.75 | 153.80 | 7615 | 59.59 | 6.31 | 177.45 | 196.87 |
| 4720 | 66.96 | 5.56 | 351.80 | 353.23 | 7616 | 63.49 | 6.40 | 240.35 | 108.95 |
| 4721 | 68.62 | 5.56 | 241.70 | 242.20 | 7703 | 65.49 | 6.59 | 319.60 | 399.33 |
| 5211 | 25.28 | 5.89 | 3093.50 | 1950.83 | 7704 | 65.94 | 6.42 | 357.55 | 66.38 |
| 5414 | 43.61 | 5.59 | 573.23 | 84.13 | 7705 | 75.86 | 6.35 | 138.10 | 113.47 |
| 5609 | 55.48 | 5.71 | 109.15 | 204.83 | 7706 | 81.24 | 6.55 | 149.60 | 187.00 |
| 5710 | 66.09 | 5.81 | 275.35 | 167.08 | 7710 | 65.04 | 6.47 | 188.30 | 179.35 |
| 6208 | 25.97 | 5.99 | 1745.40 | 1140.75 | 8112 | 22.92 | 6.60 | 725.30 | 347.60 |
| 7311 | 36.93 | 6.61 | 455.65 | 1790.38 | 8323 | 36.39 | 6.62 | 277.90 | 601.08 |
| 7313 | 37.82 | 6.45 | 330.95 | 396.53 | 8406 | 44.15 | 6.71 | 455.25 | 194.17 |
| 7314 | 37.08 | 6.45 | 124.75 | 486.17 | 8407 | 45.22 | 6.70 | 369.15 | 530.65 |
| 7315 | 36.43 | 6.46 | 285.85 | 431.07 | 8618 | 55.87 | 6.56 | 248.05 | 173.80 |
| 7321 | 40.67 | 6.46 | 98.65 | 233.43 | 8714 | 68.40 | 6.78 | 986.35 | 989.70 |
| | | | | | 8716 | 66.23 | 6.69 | 190.80 | 215.63 |

**Table S5 –** List of new specific spots for Ag NPs exposure in the digestive gland.

| Spot number | Obs. Mr (kDa) | Obs. pI | NPs | Spot number | Obs. Mr (kDa) | Obs. pI | NPs |
|---|---|---|---|---|---|---|---|
| 201 | 25.76 | 4.41 | 458.68 | 4116 | 23.36 | 5.52 | 513.25 |
| 202 | 26.14 | 4.41 | 395.35 | 4217 | 31.52 | 5.41 | 195.75 |
| 1125 | 23.91 | 4.81 | 133.35 | 4307 | 34.42 | 5.55 | 369.90 |
| 1209 | 29.05 | 4.46 | 261.70 | 4308 | 33.59 | 5.51 | 306.30 |
| 1412 | 44.22 | 4.84 | 406.70 | 4309 | 33.84 | 5.41 | 226.20 |
| 1602 | 56.86 | 4.84 | 92.45 | 4512 | 47.48 | 5.58 | 1193.65 |
| 2215 | 25.38 | 4.90 | 426.20 | 4513 | 47.60 | 5.51 | 434.30 |
| 2216 | 30.62 | 5.11 | 420.10 | 4514 | 47.63 | 5.32 | 402.53 |
| 2217 | 29.26 | 5.15 | 184.85 | 4515 | 47.36 | 5.45 | 160.15 |
| 2218 | 29.08 | 4.97 | 311.65 | 4517 | 46.86 | 5.50 | 73.85 |
| 2219 | 27.70 | 5.09 | 163.45 | 4614 | 59.57 | 5.48 | 152.90 |
| 2307 | 37.31 | 4.93 | 208.50 | 4615 | 56.76 | 5.50 | 101.55 |
| 2410 | 44.23 | 4.88 | 353.05 | 4616 | 59.65 | 5.32 | 79.55 |
| 2504 | 50.78 | 5.11 | 326.50 | 4617 | 54.39 | 5.56 | 232.00 |
| 2505 | 49.98 | 5.12 | 488.05 | 4722 | 64.59 | 5.42 | 217.65 |
| 2506 | 49.09 | 5.10 | 82.48 | 4723 | 67.20 | 5.40 | 74.70 |
| 2612 | 50.56 | 5.08 | 382.45 | 4724 | 75.11 | 5.46 | 133.40 |
| 2613 | 56.01 | 4.98 | 192.10 | 4725 | 69.47 | 5.53 | 118.20 |
| 2716 | 77.51 | 5.09 | 219.90 | 4726 | 67.47 | 5.44 | 125.45 |
| 2909 | 90.61 | 5.06 | 104.38 | 4727 | 71.15 | 5.44 | 121.00 |
| 3214 | 32.12 | 5.29 | 208.50 | 4728 | 67.56 | 5.50 | 225.60 |
| 3215 | 32.16 | 5.19 | 210.95 | 5206 | 32.95 | 5.59 | 454.15 |
| 3216 | 30.89 | 5.26 | 237.88 | 5207 | 30.12 | 5.64 | 196.80 |
| 3219 | 31.33 | 5.19 | 93.30 | 5208 | 31.60 | 5.63 | 136.85 |
| 3308 | 34.52 | 5.30 | 231.60 | 5308 | 35.23 | 5.91 | 483.05 |
| 3309 | 34.88 | 5.17 | 105.45 | 5415 | 44.63 | 5.80 | 820.60 |
| 3404 | 44.84 | 5.30 | 443.55 | 5416 | 44.75 | 5.91 | 186.70 |
| 3512 | 46.87 | 5.25 | 342.90 | 5417 | 43.67 | 5.70 | 657.25 |
| 3513 | 48.46 | 5.30 | 956.08 | 5711 | 69.19 | 5.62 | 100.45 |
| 3614 | 60.29 | 5.23 | 135.45 | 5918 | 90.64 | 5.75 | 300.30 |
| 3615 | 57.79 | 5.23 | 210.10 | 6209 | 27.30 | 6.03 | 223.15 |
| 3616 | 52.18 | 5.23 | 124.80 | 6516 | 47.51 | 6.12 | 287.50 |
| 3617 | 60.10 | 5.30 | 105.25 | 6517 | 48.45 | 6.09 | 194.80 |
| 3619 | 57.01 | 5.23 | 188.15 | 6611 | 50.54 | 6.03 | 296.90 |
| 3621 | 59.53 | 5.30 | 203.45 | 6708 | 73.09 | 6.07 | 94.85 |
| 3622 | 55.51 | 5.31 | 189.05 | 6911 | 91.21 | 5.98 | 223.70 |
| 3709 | 68.19 | 5.24 | 169.10 | 7416 | 44.59 | 6.42 | 218.40 |
| 3710 | 76.24 | 5.30 | 102.60 | 8322 | 36.35 | 6.64 | 428.15 |
| 3911 | 88.30 | 5.22 | 309.95 | 8409 | 42.73 | 6.72 | 176.20 |
| | | | | 8617 | 52.01 | 6.78 | 433.08 |

**Table S6 –** List of new specific spots for $Ag^+$ exposure in the digestive gland.

| Spot number | Obs. Mr (kDa) | Obs. pI | $Ag^+$ |
|---|---|---|---|
| 1124 | 23.93 | 4.58 | 471.75 |
| 1210 | 26.85 | 4.81 | 492.95 |
| 2212 | 26.82 | 4.95 | 654.73 |
| 2308 | 34.47 | 4.97 | 315.68 |
| 2614 | 62.28 | 4.88 | 59.13 |
| 2615 | 61.95 | 4.92 | 148.35 |
| 2616 | 61.15 | 5.05 | 242.88 |
| 2617 | 59.05 | 5.05 | 120.18 |
| 2717 | 68.27 | 4.93 | 98.90 |
| 2718 | 67.73 | 4.99 | 83.13 |
| 2719 | 67.81 | 5.07 | 108.83 |
| 4905 | 92.04 | 5.56 | 180.08 |
| 5209 | 26.02 | 5.78 | 186.60 |
| 5511 | 49.53 | 5.89 | 304.30 |
| 5608 | 51.24 | 5.82 | 389.40 |
| 5709 | 67.08 | 5.77 | 417.70 |
| 6210 | 27.03 | 6.08 | 114.58 |
| 6610 | 54.40 | 6.22 | 268.73 |
| 6612 | 54.87 | 6.11 | 261.65 |
| 6706 | 64.89 | 6.04 | 249.03 |
| 6707 | 67.77 | 5.98 | 175.88 |
| 6907 | 89.29 | 6.01 | 159.15 |
| 6909 | 89.44 | 5.96 | 72.53 |
| 7418 | 46.61 | 6.19 | 194.05 |
| 7512 | 47.29 | 6.53 | 349.95 |
| 7709 | 66.65 | 6.42 | 131.60 |
| 8321 | 37.00 | 6.67 | 440.30 |
| 8717 | 64.96 | 6.49 | 148.03 |

**Table S7 –** List of suppressed common spots for Ag NPs and $Ag^{+}$ exposure in the gills.

| Spot number | Obs. Mr (kDa) | Obs. pI | CT |
|---|---|---|---|
| 117 | 26.28 | 4.59 | 49.95 |
| 203 | 31.47 | 4.60 | 77.70 |
| 205 | 36.15 | 4.56 | 141.65 |
| 302 | 47.78 | 4.60 | 188.93 |
| 408 | 49.79 | 4.56 | 1110.48 |
| 1101 | 24.31 | 4.72 | 507.43 |
| 1107 | 30.33 | 4.88 | 338.90 |
| 1113 | 26.21 | 4.62 | 54.50 |
| 1116 | 28.24 | 4.86 | 49.83 |
| 1204 | 40.71 | 4.76 | 61.08 |
| 1208 | 35.86 | 4.84 | 774.00 |
| 1218 | 36.78 | 4.90 | 438.55 |
| 1605 | 68.65 | 4.84 | 135.40 |
| 1606 | 68.12 | 4.87 | 132.35 |
| 2102 | 24.68 | 5.01 | 154.65 |
| 2121 | 28.77 | 4.95 | 51.03 |
| 2205 | 33.60 | 5.12 | 1703.60 |
| 2214 | 37.57 | 5.29 | 95.18 |
| 2225 | 35.63 | 4.95 | 670.93 |
| 2226 | 37.02 | 4.95 | 80.50 |
| 2308 | 47.15 | 5.16 | 187.70 |
| 2411 | 48.59 | 5.19 | 56.85 |
| 2418 | 52.02 | 5.37 | 476.80 |
| 2421 | 47.43 | 5.10 | 24.05 |
| 2501 | 58.68 | 4.93 | 199.95 |
| 2516 | 62.63 | 5.16 | 22.53 |
| 2521 | 54.46 | 5.31 | 168.35 |
| 2602 | 67.96 | 5.15 | 92.10 |
| 2616 | 67.29 | 5.33 | 48.75 |
| 2715 | 93.99 | 5.35 | 67.45 |
| 3108 | 24.50 | 5.56 | 220.95 |
| 3201 | 37.54 | 5.39 | 46.88 |
| 3208 | 32.60 | 5.51 | 131.73 |
| 3210 | 32.81 | 5.57 | 267.23 |
| 3212 | 31.24 | 5.60 | 284.48 |
| 3214 | 34.81 | 5.39 | 89.68 |
| 3215 | 32.99 | 5.40 | 83.85 |
| 3216 | 32.56 | 5.40 | 71.20 |
| 3419 | 50.88 | 5.56 | 192.83 |
| 3507 | 54.54 | 5.39 | 124.45 |
| 3509 | 58.48 | 5.40 | 55.73 |
| 3511 | 58.18 | 5.50 | 141.28 |
| 3525 | 53.40 | 5.49 | 217.40 |
| 3605 | 70.45 | 5.40 | 104.70 |
| 3629 | 69.86 | 5.67 | 141.73 |
| 3704 | 79.74 | 5.39 | 53.20 |
| 3815 | 105.55 | 5.50 | 26.30 |
| 4102 | 27.64 | 5.70 | 121.73 |
| 4104 | 25.87 | 5.70 | 161.00 |
| 4111 | 30.21 | 5.76 | 359.35 |
| 4120 | 24.46 | 5.95 | 606.55 |
| 4203 | 39.80 | 5.76 | 76.40 |
| 4207 | 36.80 | 5.79 | 151.05 |
| 4211 | 33.37 | 5.84 | 59.35 |
| 4308 | 46.57 | 5.77 | 73.88 |
| 4310 | 43.58 | 5.78 | 68.15 |

**Table S8 –** List of suppressed specific spots for Ag NPs exposure in the gills.

| Spot number | Obs. Mr (kDa) | Obs. pI | CT |
|---|---|---|---|
| 1202 | 38.04 | 4.74 | 117.38 |
| 1203 | 35.78 | 4.76 | 1492.55 |
| 1207 | 34.73 | 4.84 | 268.65 |
| 1301 | 43.14 | 4.71 | 147.83 |
| 1515 | 60.54 | 4.88 | 1156.53 |
| 2103 | 28.43 | 5.11 | 242.58 |
| 2118 | 29.89 | 5.37 | 95.90 |
| 2208 | 36.13 | 5.15 | 46.90 |
| 2218 | 32.67 | 5.34 | 469.23 |
| 2224 | 37.17 | 5.15 | 86.88 |
| 2304 | 41.46 | 5.09 | 35.43 |
| 2422 | 47.01 | 5.27 | 142.38 |
| 2507 | 59.18 | 4.99 | 166.73 |
| 2524 | 64.15 | 5.35 | 368.35 |
| 2609 | 65.02 | 5.26 | 199.73 |
| 2613 | 65.03 | 5.32 | 816.85 |
| 2705 | 90.76 | 5.16 | 150.68 |
| 2712 | 97.12 | 5.27 | 47.88 |
| 2713 | 91.41 | 5.27 | 160.53 |
| 3101 | 31.08 | 5.38 | 166.43 |
| 3213 | 36.40 | 5.63 | 100.08 |
| 3306 | 42.45 | 5.52 | 267.35 |
| 3307 | 46.85 | 5.55 | 63.75 |
| 3421 | 51.63 | 5.62 | 122.58 |
| 3501 | 56.44 | 5.37 | 227.90 |
| 3503 | 58.35 | 5.38 | 65.08 |
| 3510 | 55.55 | 5.47 | 369.45 |
| 3512 | 54.90 | 5.54 | 237.23 |
| 3607 | 73.67 | 5.40 | 120.68 |
| 4115 | 24.88 | 5.84 | 181.08 |
| 4118 | 28.50 | 5.91 | 157.55 |
| 4305 | 47.99 | 5.72 | 168.15 |
| 4307 | 44.52 | 5.74 | 244.98 |
| 4319 | 38.50 | 5.86 | 56.30 |
| 4403 | 50.78 | 5.70 | 545.73 |
| 4407 | 51.58 | 5.76 | 593.00 |
| 4604 | 75.01 | 5.72 | 44.75 |
| 4605 | 66.60 | 5.72 | 78.55 |
| 4616 | 69.72 | 5.82 | 288.85 |
| 4617 | 68.81 | 5.83 | 116.88 |
| 5127 | 27.92 | 6.02 | 94.63 |
| 5201 | 36.61 | 5.97 | 134.08 |
| 5306 | 46.59 | 6.10 | 96.90 |
| 5409 | 50.32 | 6.20 | 546.13 |
| 5814 | 117.78 | 6.10 | 22.60 |
| 5822 | 106.11 | 6.20 | 65.53 |
| 5826 | 105.79 | 6.22 | 95.08 |
| 6308 | 44.59 | 6.32 | 110.53 |
| 6314 | 45.52 | 6.44 | 367.85 |
| 7306 | 47.15 | 6.61 | 277.05 |

**Table S9 –** List of suppressed specific spots for $Ag^{+}$ exposure in the gills.

| Spot number | Obs. Mr (kDa) | Obs. pI | CT |
|---|---|---|---|
| 111 | 27.50 | 4.54 | 467.95 |
| 1104 | 26.39 | 4.79 | 456.35 |
| 1109 | 30.33 | 4.91 | 79.05 |
| 1110 | 31.16 | 4.93 | 118.40 |
| 1201 | 38.07 | 4.71 | 55.85 |
| 1401 | 51.65 | 4.76 | 267.43 |
| 1409 | 53.49 | 4.82 | 324.15 |
| 1414 | 52.36 | 4.87 | 821.85 |
| 1418 | 50.80 | 4.90 | 126.18 |
| 1501 | 56.09 | 4.65 | 144.73 |
| 2303 | 43.62 | 5.01 | 1454.58 |
| 2307 | 45.68 | 5.14 | 104.50 |
| 2412 | 52.90 | 5.20 | 138.18 |
| 2517 | 62.47 | 5.18 | 71.48 |
| 3305 | 44.59 | 5.50 | 142.08 |
| 3312 | 39.47 | 5.56 | 44.00 |
| 3406 | 51.77 | 5.40 | 117.35 |
| 3420 | 53.34 | 5.58 | 383.53 |
| 3425 | 48.86 | 5.41 | 822.20 |
| 3817 | 112.55 | 5.51 | 55.63 |
| 4311 | 45.60 | 5.78 | 429.33 |
| 4326 | 45.01 | 5.70 | 55.30 |
| 4406 | 53.78 | 5.76 | 556.23 |
| 5129 | 25.86 | 5.91 | 100.03 |
| 5202 | 32.98 | 6.13 | 465.30 |
| 5501 | 57.30 | 5.99 | 72.98 |
| 5503 | 61.93 | 6.03 | 136.93 |
| 5510 | 61.20 | 6.16 | 81.98 |
| 5602 | 70.03 | 5.99 | 30.23 |
| 5713 | 94.99 | 6.15 | 41.78 |
| 6319 | 45.57 | 6.48 | 144.68 |
| 6512 | 63.42 | 6.48 | 227.53 |
| 6601 | 66.12 | 6.25 | 53.30 |
| 6804 | 105.45 | 6.31 | 68.58 |
| 7111 | 24.53 | 6.73 | 256.50 |
| 7116 | 26.16 | 6.78 | 396.20 |
| 7124 | 26.41 | 6.69 | 185.03 |
| 7204 | 39.91 | 6.61 | 288.05 |

**Table S10 –** List of suppressed common spots for Ag NPs and $Ag^{+}$ exposure in the digestive gland.

| Spot number | Obs. Mr (kDa) | Obs. pI | CT |
|---|---|---|---|
| 1701 | 66.42 | 4.81 | 80.68 |
| 1906 | 97.24 | 4.62 | 784.90 |
| 1907 | 96.82 | 4.65 | 2359.60 |
| 1908 | 97.07 | 4.68 | 1197.68 |
| 1909 | 104.16 | 4.77 | 41.48 |
| 2207 | 25.93 | 5.05 | 267.75 |
| 2401 | 46.26 | 4.84 | 182.65 |
| 2409 | 46.53 | 4.90 | 105.18 |
| 2701 | 74.65 | 4.82 | 180.15 |
| 3203 | 27.12 | 5.16 | 1899.25 |
| 3221 | 32.38 | 5.30 | 98.70 |
| 3907 | 98.71 | 5.30 | 90.70 |
| 3909 | 98.37 | 5.31 | 180.90 |
| 4113 | 24.56 | 5.58 | 968.68 |
| 4204 | 31.14 | 5.50 | 316.50 |
| 4218 | 31.95 | 5.42 | 223.73 |
| 4301 | 36.10 | 5.37 | 169.05 |
| 4504 | 48.43 | 5.42 | 1590.18 |
| 4511 | 47.30 | 5.54 | 312.73 |
| 4901 | 98.23 | 5.32 | 80.13 |
| 5104 | 24.31 | 5.69 | 1926.20 |
| 5201 | 29.98 | 5.68 | 231.68 |
| 5407 | 43.63 | 5.75 | 342.15 |
| 5506 | 48.33 | 5.83 | 249.08 |
| 5701 | 87.65 | 5.59 | 113.88 |
| 6405 | 43.74 | 6.08 | 78.25 |
| 7204 | 30.15 | 6.31 | 448.08 |
| 7210 | 27.12 | 6.25 | 572.08 |
| 7403 | 42.87 | 6.30 | 79.08 |
| 7412 | 44.20 | 6.53 | 539.98 |
| 7707 | 75.90 | 6.34 | 232.70 |

**Table S11 –** List of suppressed specific spots for Ag NPs exposure in the digestive gland.

| Spot number | Obs. Mr (kDa) | Obs. pI | CT |
|---|---|---|---|
| 1301 | 33.37 | 4.66 | 558.70 |
| 1311 | 38.76 | 4.77 | 1625.00 |
| 2201 | 28.20 | 4.89 | 1185.45 |
| 2203 | 29.77 | 4.91 | 130.00 |
| 2404 | 43.92 | 4.92 | 171.53 |
| 2706 | 75.09 | 4.85 | 1018.38 |
| 2713 | 65.32 | 4.97 | 108.25 |
| 3213 | 30.11 | 5.31 | 261.18 |
| 3503 | 49.40 | 5.20 | 664.20 |
| 4201 | 25.63 | 5.33 | 2616.73 |
| 4208 | 26.78 | 5.54 | 1606.10 |
| 4211 | 28.97 | 5.54 | 793.98 |
| 4502 | 48.77 | 5.34 | 289.30 |
| 4708 | 86.15 | 5.40 | 56.83 |
| 5303 | 35.87 | 5.77 | 136.85 |
| 5406 | 42.55 | 5.69 | 3710.38 |
| 5501 | 48.33 | 5.60 | 280.43 |
| 5502 | 47.19 | 5.63 | 568.18 |
| 6304 | 37.78 | 6.07 | 279.73 |
| 6306 | 40.35 | 6.09 | 119.88 |
| 6501 | 46.94 | 5.95 | 1419.18 |
| 7202 | 30.02 | 6.28 | 675.80 |
| 7302 | 34.83 | 6.28 | 337.65 |
| 7308 | 42.07 | 6.47 | 705.95 |
| 7401 | 42.71 | 6.23 | 245.25 |
| 7609 | 59.45 | 6.52 | 1269.70 |
| 7708 | 75.51 | 6.42 | 397.20 |

**Table S12 –** List of suppressed specific spots for $Ag^{+}$ exposure in the digestive gland.

| Spot number | Obs. Mr (kDa) | Obs. pI | CT |
|---|---|---|---|
| 1201 | 25.20 | 4.46 | 827.80 |
| 2209 | 27.24 | 5.09 | 378.25 |
| 2211 | 29.32 | 4.94 | 262.68 |
| 2301 | 33.82 | 4.83 | 474.55 |
| 2709 | 74.91 | 4.90 | 366.80 |
| 2904 | 88.97 | 4.99 | 133.93 |
| 3220 | 31.85 | 5.30 | 128.05 |
| 3511 | 48.26 | 5.30 | 530.25 |
| 3601 | 56.04 | 5.15 | 130.28 |
| 3705 | 74.83 | 5.30 | 164.28 |
| 4106 | 23.58 | 5.49 | 1517.28 |
| 4206 | 29.03 | 5.53 | 564.48 |
| 4210 | 27.84 | 5.54 | 2143.88 |
| 4402 | 45.78 | 5.41 | 578.55 |
| 4506 | 49.01 | 5.42 | 295.10 |
| 4508 | 48.74 | 5.50 | 514.93 |
| 4606 | 57.35 | 5.41 | 249.63 |
| 4702 | 67.67 | 5.32 | 513.15 |
| 4704 | 68.19 | 5.36 | 252.88 |
| 4715 | 86.57 | 5.49 | 125.93 |
| 4716 | 75.01 | 5.50 | 58.98 |
| 5703 | 67.28 | 5.70 | 113.65 |
| 6110 | 23.39 | 6.07 | 7455.23 |
| 6202 | 32.52 | 6.02 | 190.98 |
| 6904 | 91.30 | 6.03 | 488.43 |
| 7606 | 55.95 | 6.41 | 555.20 |
| 7701 | 72.85 | 6.26 | 94.93 |
| 8602 | 59.30 | 6.62 | 686.75 |

**Table S13 –** List of proteins 2-fold common to Ag NPs and $Ag^+$ exposure in the gills.

| Spot number | Obs. Mr (KDa) | Obs. pI | Average ratios | |
|---|---|---|---|---|
| | | | Ag NPs | $Ag^+$ |
| 1213 | 35.20 | 4.90 | 3.42 ↑ | 3.47 ↑ |
| 1609 | 75.31 | 4.90 | 4.64 ↑ | 2.71 ↑ |
| 2210 | 32.50 | 5.21 | 3.74 ↑ | 2.16 ↑ |
| 2413 | 52.05 | 5.28 | 2.52 ↑ | 3.14 ↑ |
| 2417 | 51.59 | 5.36 | 2.23 ↑ | 3.43 ↑ |
| 2420 | 52.95 | 5.17 | 2.00 ↑ | 2.66 ↑ |
| 2520 | 54.27 | 5.29 | 9.51 ↑ | 3.45 ↑ |
| 2707 | 90.31 | 5.18 | 3.01 ↑ | 2.41 ↑ |
| 2711 | 92.06 | 5.23 | 2.05 ↑ | 3.19 ↑ |
| 3301 | 47.03 | 5.39 | 2.40 ↑ | 5.43 ↑ |
| 3303 | 47.81 | 5.40 | 3.19 ↑ | 13.93 ↑ |
| 3408 | 51.70 | 5.41 | 3.06 ↑ | 2.80 ↑ |
| 3416 | 51.40 | 5.52 | 10.34 ↑ | 5.29 ↑ |
| 3424 | 52.79 | 5.58 | 3.25 ↑ | 4.18 ↑ |
| 3502 | 55.44 | 5.38 | 2.04 ↑ | 2.59 ↑ |
| 3706 | 96.21 | 5.40 | 2.29 ↑ | 7.17 ↑ |
| 4608 | 68.60 | 5.74 | 2.16 ↑ | 3.35 ↑ |
| 4624 | 68.23 | 5.96 | 4.44 ↑ | 2.28 ↑ |
| 4629 | 68.33 | 5.62 | 7.16 ↑ | 2.45 ↑ |
| 4719 | 77.68 | 5.85 | 3.85 ↑ | 2.51 ↑ |
| 4721 | 93.38 | 5.85 | 3.09 ↑ | 2.37 ↑ |
| 4725 | 94.09 | 5.88 | 2.25 ↑ | 2.94 ↑ |
| 4732 | 94.28 | 5.96 | 2.41 ↑ | 2.71 ↑ |
| 5512 | 57.39 | 6.16 | 4.56 ↑ | 3.40 ↑ |
| 5516 | 57.40 | 6.23 | 3.34 ↑ | 2.04 ↑ |
| 5611 | 65.93 | 6.20 | 2.49 ↑ | 3.42 ↑ |
| 5704 | 94.46 | 6.01 | 2.19 ↑ | 4.03 ↑ |
| 5705 | 98.09 | 6.02 | 3.38 ↑ | 2.60 ↑ |
| 5723 | 78.97 | 5.93 | 2.10 ↑ | 2.14 ↑ |
| 5816 | 102.89 | 6.11 | 2.46 ↑ | 5.13 ↑ |
| 6404 | 49.97 | 6.33 | 5.31 ↑ | 7.46 ↑ |
| 6519 | 57.87 | 6.31 | 2.65 ↑ | 4.55 ↑ |
| 6605 | 73.47 | 6.31 | 3.44 ↑ | 3.34 ↑ |
| 6611 | 64.84 | 6.44 | 2.00 ↑ | 4.48 ↑ |
| 6708 | 95.00 | 6.45 | 2.04 ↑ | 3.78 ↑ |
| 6711 | 95.66 | 6.55 | 2.80 ↑ | 2.21 ↑ |
| 7301 | 43.40 | 6.59 | 3.81 ↑ | 4.94 ↑ |
| 7304 | 41.80 | 6.61 | 2.38 ↑ | 2.74 ↑ |
| 7512 | 54.01 | 6.67 | 3.81 ↑ | 7.77 ↑ |
| 1112 | 22.70 | 4.80 | 2.14 ↓ | 2.16 ↓ |
| 1211 | 35.93 | 4.90 | 9.02 ↓ | 3.82 ↓ |
| 2101 | 23.85 | 4.97 | 15.53 ↓ | 7.12 ↓ |
| 2207 | 32.36 | 5.12 | 2.06 ↓ | 2.38 ↓ |
| 2209 | 33.28 | 5.16 | 2.22 ↓ | 4.00 ↓ |
| 2227 | 35.18 | 5.08 | 3.04 ↓ | 5.21 ↓ |
| 4110 | 30.76 | 5.74 | 5.32 ↓ | 5.04 ↓ |
| 5315 | 48.33 | 6.19 | 5.67 ↓ | 6.70 ↓ |
| 5703 | 78.61 | 6.01 | 2.87 ↓ | 2.15 ↓ |

**Table S14 –** List of proteins 2-fold specific for Ag NPs exposure in the gills.

| Spot number | Obs. Mr (kDa) | Obs. pI | Average ratio | Spot number | Obs. Mr (kDa) | Obs. pI | Average ratio |
|---|---|---|---|---|---|---|---|
| 1409 | 53.49 | 4.82 | 4.64 ↑ | 5321 | 45.68 | 6.08 | 27.56 ↑ |
| 1501 | 56.09 | 4.65 | 3.74 ↑ | 5408 | 49.67 | 6.20 | 2.87 ↑ |
| 1607 | 76.22 | 4.88 | 2.52 ↑ | 5513 | 54.24 | 6.17 | 2.52 ↑ |
| 1705 | 83.64 | 4.88 | 2.23 ↑ | 5610 | 73.25 | 6.20 | 2.31 ↑ |
| 2202 | 33.38 | 5.07 | 2.00 ↑ | 5709 | 95.11 | 6.09 | 2.84 ↑ |
| 2215 | 32.32 | 5.31 | 9.51 ↑ | 5711 | 92.06 | 6.11 | 3.39 ↑ |
| 2222 | 34.10 | 5.00 | 3.01 ↑ | 5802 | 104.78 | 5.98 | 2.27 ↑ |
| 2414 | 52.88 | 5.32 | 2.05 ↑ | 6101 | 26.06 | 6.25 | 10.56 ↑ |
| 2502 | 60.35 | 4.94 | 2.40 ↑ | 6204 | 32.89 | 6.36 | 6.00 ↑ |
| 2510 | 54.14 | 5.06 | 3.19 ↑ | 6309 | 44.85 | 6.33 | 11.69 ↑ |
| 2512 | 58.60 | 5.10 | 3.06 ↑ | 6312 | 42.77 | 6.39 | 3.21 ↑ |
| 2515 | 58.44 | 5.15 | 10.34 ↑ | 6319 | 45.57 | 6.48 | 10.07 ↑ |
| 2610 | 68.25 | 5.27 | 3.25 ↑ | 6323 | 47.12 | 6.51 | 2.62 ↑ |
| 2702 | 94.02 | 5.12 | 2.04 ↑ | 6328 | 44.30 | 6.49 | 16.42 ↑ |
| 2703 | 93.19 | 5.15 | 2.29 ↑ | 6413 | 50.79 | 6.54 | 2.14 ↑ |
| 3312 | 39.47 | 5.56 | 2.16 ↑ | 6415 | 52.00 | 6.55 | 2.76 ↑ |
| 3403 | 49.68 | 5.39 | 4.44 ↑ | 6509 | 64.04 | 6.43 | 4.34 ↑ |
| 3404 | 49.02 | 5.39 | 7.16 ↑ | 6601 | 66.12 | 6.25 | 2.20 ↑ |
| 3405 | 52.87 | 5.40 | 3.85 ↑ | 6606 | 74.62 | 6.33 | 2.91 ↑ |
| 3406 | 51.77 | 5.40 | 3.09 ↑ | 6612 | 65.58 | 6.44 | 2.08 ↑ |
| 3420 | 53.34 | 5.58 | 2.25 ↑ | 7207 | 40.95 | 6.68 | 2.04 ↑ |
| 3425 | 48.86 | 5.41 | 2.41 ↑ | 7501 | 64.15 | 6.59 | 2.93 ↑ |
| 3505 | 64.70 | 5.39 | 4.56 ↑ | 7605 | 69.57 | 6.68 | 2.74 ↑ |
| 3610 | 65.18 | 5.40 | 3.34 ↑ | 7706 | 86.55 | 6.79 | 2.64 ↑ |
| 3617 | 73.31 | 5.47 | 2.49 ↑ | 1104 | 26.39 | 4.79 | 2.04 ↓ |
| 3814 | 112.59 | 5.49 | 2.19 ↑ | 1110 | 31.16 | 4.93 | 2.22 ↓ |
| 4210 | 38.14 | 5.73 | 3.38 ↑ | 2105 | 29.35 | 5.13 | 2.17 ↓ |
| 4302 | 48.08 | 5.70 | 2.10 ↑ | 2109 | 28.10 | 5.16 | 3.65 ↓ |
| 4304 | 46.77 | 5.71 | 2.46 ↑ | 2110 | 31.19 | 5.28 | 3.31 ↓ |
| 4326 | 45.01 | 5.70 | 5.31 ↑ | 2211 | 33.58 | 5.21 | 2.92 ↓ |
| 4401 | 52.67 | 5.68 | 2.65 ↑ | 3103 | 31.16 | 5.44 | 2.61 ↓ |
| 4612 | 66.31 | 5.79 | 3.44 ↑ | 3203 | 31.40 | 5.40 | 3.66 ↓ |
| 4619 | 68.19 | 5.84 | 2.00 ↑ | 3305 | 44.59 | 5.50 | 2.04 ↓ |
| 4718 | 79.25 | 5.84 | 2.04 ↑ | 3506 | 62.75 | 5.39 | 2.98 ↓ |
| 4720 | 94.45 | 5.85 | 2.80 ↑ | 4113 | 29.62 | 5.77 | 4.60 ↓ |
| 4727 | 94.17 | 5.92 | 3.81 ↑ | 4208 | 39.90 | 5.87 | 2.23 ↓ |
| 4807 | 104.86 | 5.84 | 2.38 ↑ | 5108 | 29.69 | 6.09 | 2.22 ↓ |
| 4810 | 104.90 | 5.92 | 3.81 ↑ | 5204 | 36.64 | 6.20 | 2.38 ↓ |
| 5129 | 25.86 | 5.91 | 2.64 ↑ | 5410 | 53.21 | 6.22 | 2.16 ↓ |
| 5210 | 32.30 | 6.22 | 3.09 ↑ | 6802 | 105.77 | 6.27 | 4.43 ↓ |
| 5303 | 43.98 | 5.98 | 2.78 ↑ | | | | |

**Table S15 –** List of proteins 2-fold specific for $Ag^{+}$ exposure in the gills.

| Spot number | Obs. Mr (kDa) | Obs. pI | Average ratio | Spot number | Obs. Mr (kDa) | Obs. pI | Average ratio |
|---|---|---|---|---|---|---|---|
| 1508 | 59.04 | 4.87 | 2.71 ↑ | 501 | 53.89 | 4.62 | 2.41 ↓ |
| 1513 | 60.33 | 4.91 | 2.16 ↑ | 1202 | 38.04 | 4.74 | 2.54 ↓ |
| 2304 | 41.46 | 5.09 | 3.14 ↑ | 1303 | 46.75 | 4.84 | 2.51 ↓ |
| 2310 | 45.92 | 5.28 | 3.43 ↑ | 1417 | 51.76 | 4.90 | 5.53 ↓ |
| 2401 | 53.69 | 4.94 | 2.66 ↑ | 2318 | 42.20 | 5.20 | 2.36 ↓ |
| 2507 | 59.18 | 4.99 | 3.45 ↑ | 2402 | 51.22 | 4.96 | 2.62 ↓ |
| 2531 | 52.85 | 5.25 | 2.41 ↑ | 2510 | 54.14 | 5.06 | 2.14 ↓ |
| 2713 | 91.41 | 5.27 | 3.19 ↑ | 2515 | 58.44 | 5.15 | 2.13 ↓ |
| 3101 | 31.08 | 5.38 | 5.43 ↑ | 2609 | 65.02 | 5.26 | 2.54 ↓ |
| 3421 | 51.63 | 5.62 | 13.93 ↑ | 2613 | 65.03 | 5.32 | 2.05 ↓ |
| 3508 | 54.64 | 5.40 | 2.80 ↑ | 3610 | 65.18 | 5.40 | 2.76 ↓ |
| 3702 | 89.26 | 5.39 | 5.29 ↑ | 4403 | 50.78 | 5.70 | 2.53 ↓ |
| 4117 | 28.80 | 5.90 | 4.18 ↑ | 4607 | 69.77 | 5.74 | 3.29 ↓ |
| 4118 | 28.50 | 5.91 | 2.59 ↑ | 4711 | 95.48 | 5.75 | 2.29 ↓ |
| 4307 | 44.52 | 5.74 | 7.17 ↑ | 4712 | 77.54 | 5.78 | 2.08 ↓ |
| 4315 | 43.53 | 5.95 | 3.35 ↑ | 4804 | 106.76 | 5.75 | 2.01 ↓ |
| 4621 | 69.89 | 5.93 | 2.28 ↑ | 6316 | 46.26 | 6.45 | 4.83 ↓ |
| 4628 | 67.10 | 5.83 | 2.45 ↑ | 7316 | 41.45 | 6.80 | 2.39 ↓ |
| 4723 | 77.71 | 5.86 | 2.51 ↑ | 7612 | 69.89 | 6.78 | 4.47 ↓ |
| 5126 | 27.27 | 6.07 | 2.37 ↑ | 7705 | 86.41 | 6.75 | 4.69 ↓ |
| 5201 | 36.61 | 5.97 | 2.94 ↑ | | | | |
| 5309 | 42.14 | 6.14 | 2.71 ↑ | | | | |
| 5411 | 50.09 | 6.23 | 3.40 ↑ | | | | |
| 5504 | 54.21 | 6.04 | 2.04 ↑ | | | | |
| 5710 | 97.84 | 6.10 | 3.42 ↑ | | | | |
| 5715 | 97.36 | 6.17 | 4.03 ↑ | | | | |
| 6206 | 34.80 | 6.39 | 2.60 ↑ | | | | |
| 6305 | 43.10 | 6.28 | 2.14 ↑ | | | | |
| 6306 | 45.18 | 6.30 | 5.13 ↑ | | | | |
| 6414 | 51.47 | 6.54 | 7.46 ↑ | | | | |
| 6503 | 55.18 | 6.33 | 4.55 ↑ | | | | |
| 6508 | 63.08 | 6.43 | 3.34 ↑ | | | | |
| 6602 | 73.32 | 6.25 | 4.48 ↑ | | | | |
| 7106 | 27.97 | 6.62 | 3.78 ↑ | | | | |
| 7107 | 27.25 | 6.63 | 2.21 ↑ | | | | |
| 7327 | 42.68 | 6.57 | 4.94 ↑ | | | | |
| 7601 | 69.12 | 6.59 | 2.74 ↑ | | | | |
| 7602 | 67.66 | 6.60 | 7.77 ↑ | | | | |

**Table S16 –** List of proteins 2-fold common for Ag NPs and $Ag^+$ exposure in the digestive gland.

| Spot number | Obs. Mr (KDa) | Obs. pI | Average ratios | |
|---|---|---|---|---|
| | | | Ag NPs | $Ag^+$ |
| 1409 | 46.57 | 4.68 | 3.66 ↑ | 3.41 ↑ |
| 2205 | 25.36 | 4.97 | 2.53 ↑ | 2.43 ↑ |
| 2305 | 33.90 | 5.00 | 2.05 ↑ | 2.09 ↑ |
| 2403 | 44.14 | 4.86 | 3.46 ↑ | 3.79 ↑ |
| 2903 | 88.33 | 4.95 | 2.90 ↑ | 2.49 ↑ |
| 3504 | 49.76 | 5.22 | 7.13 ↑ | 6.29 ↑ |
| 3902 | 89.07 | 5.16 | 3.69 ↑ | 2.89 ↑ |
| 3904 | 89.81 | 5.26 | 3.36 ↑ | 4.43 ↑ |
| 4503 | 49.01 | 5.40 | 3.33 ↑ | 2.07 ↑ |
| 4509 | 48.05 | 5.51 | 2.22 ↑ | 3.01 ↑ |
| 4719 | 74.76 | 5.56 | 3.10 ↑ | 2.26 ↑ |
| 5409 | 46.72 | 5.79 | 2.20 ↑ | 2.34 ↑ |
| 6401 | 44.70 | 5.99 | 4.57 ↑ | 2.44 ↑ |
| 6607 | 64.21 | 6.09 | 4.17 ↑ | 5.45 ↑ |
| 7407 | 43.93 | 6.42 | 4.20 ↑ | 3.77 ↑ |
| 7410 | 43.32 | 6.51 | 2.69 ↑ | 2.07 ↑ |
| 8601 | 60.49 | 6.62 | 2.13 ↑ | 2.57 ↑ |
| 1120 | 24.06 | 4.77 | 5.50 ↓ | 4.35 ↓ |
| 1121 | 24.59 | 4.77 | 2.27 ↓ | 3.51 ↓ |

**Table S17 –** List of proteins 2-fold specific for Ag NPs exposure in the digestive gland.

| Spot number | Obs. Mr (kDa) | Obs. pI | Average ratio |
|---|---|---|---|
| 1312 | 36.85 | 4.81 | 2.07 ↑ |
| 1507 | 47.14 | 4.63 | 3.4 0↑ |
| 1601 | 53.59 | 4.81 | 2.20 ↑ |
| 2402 | 44.62 | 4.85 | 2.40 ↑ |
| 2405 | 43.82 | 5.09 | 2.13 ↑ |
| 2501 | 48.64 | 5.02 | 2.39 ↑ |
| 2601 | 55.11 | 4.85 | 2.56 ↑ |
| 2603 | 57.15 | 4.90 | 2.29 ↑ |
| 2605 | 57.42 | 4.93 | 2.86 ↑ |
| 2709 | 74.91 | 4.90 | 4.03 ↑ |
| 2710 | 80.29 | 4.9 | 4.42 ↑ |
| 2711 | 64.9 | 4.93 | 2.85 ↑ |
| 2714 | 74.29 | 4.99 | 2.45 ↑ |
| 2904 | 88.97 | 4.99 | 7.63 ↑ |
| 2905 | 91.13 | 5.04 | 2.56 ↑ |
| 2906 | 90.09 | 5.08 | 2.01 ↑ |
| 3508 | 47.17 | 5.30 | 2.10 ↑ |
| 3510 | 48.88 | 5.3 | 2.31 ↑ |
| 3601 | 56.04 | 5.15 | 2.65 ↑ |
| 3602 | 61.57 | 5.19 | 2.59 ↑ |
| 3903 | 90.95 | 5.19 | 2.34 ↑ |
| 4106 | 23.58 | 5.49 | 2.02 ↑ |
| 4206 | 29.03 | 5.53 | 2.33 ↑ |
| 4207 | 31.74 | 5.53 | 2.02 ↑ |
| 4405 | 46.7 | 5.54 | 2.53 ↑ |
| 4501 | 48.02 | 5.32 | 3.15 ↑ |
| 4506 | 49.01 | 5.42 | 8.41 ↑ |
| 4508 | 48.74 | 5.50 | 3.16 ↑ |
| 4605 | 64.33 | 5.41 | 2.45 ↑ |
| 4609 | 51.42 | 5.47 | 2.01 ↑ |
| 4709 | 78.12 | 5.41 | 2.38 ↑ |
| 4712 | 74.05 | 5.45 | 2.36 ↑ |
| 4718 | 75.04 | 5.53 | 3.18 ↑ |
| 5304 | 35.94 | 5.83 | 2.00 ↑ |
| 5402 | 45.47 | 5.6 | 3.26 ↑ |
| 5403 | 46.47 | 5.64 | 6.30 ↑ |
| 5503 | 49.68 | 5.66 | 3.09 ↑ |
| 5705 | 67.31 | 5.82 | 2.80 ↑ |
| 6202 | 32.52 | 6.02 | 2.32 ↑ |
| 6302 | 40.12 | 6.02 | 2.90 ↑ |
| 6504 | 49.51 | 5.99 | 6.20 ↑ |
| 7109 | 24.34 | 6.42 | 2.18 ↑ |
| 7510 | 47.60 | 6.42 | 3.14 ↑ |

| Spot number | Obs. Mr (kDa) | Obs. pI | Average ratio |
|---|---|---|---|
| 1207 | 32.61 | 4.72 | 2.60 ↓ |
| 1401 | 45.90 | 4.50 | 2.38 ↓ |
| 1403 | 45.40 | 4.54 | 3.08 ↓ |
| 2901 | 90.22 | 4.86 | 3.62 ↓ |
| 3623 | 52.41 | 5.32 | 2.55 ↓ |
| 4202 | 29.93 | 5.34 | 3.27 ↓ |
| 4210 | 27.84 | 5.54 | 4.05 ↓ |
| 5704 | 68.60 | 5.8 | 2.19 ↓ |
| 6406 | 44.15 | 6.08 | 2.24 ↓ |
| 6506 | 46.82 | 6.06 | 2.06 ↓ |
| 6602 | 51.05 | 5.97 | 4.83 ↓ |
| 6609 | 64.08 | 6.22 | 2.64 ↓ |
| 6901 | 91.03 | 5.95 | 3.31 ↓ |
| 6904 | 91.30 | 6.03 | 3.28 ↓ |
| 7402 | 44.60 | 6.26 | 2.05 ↓ |
| 7411 | 46.21 | 6.52 | 3.76 ↓ |
| 7417 | 44.45 | 6.36 | 2.37 ↓ |
| 7505 | 49.93 | 6.31 | 2.49 ↓ |
| 8301 | 37.08 | 6.63 | 4.30 ↓ |
| 8501 | 48.77 | 6.62 | 2.35 ↓ |
| 8602 | 59.30 | 6.62 | 4.83 ↓ |

**Table S18 –** List of proteins 2-fold specific for $Ag^{+}$ exposure in the digestive gland.

| Spot number | Obs. Mr (kDa) | Obs. pI | Average ratio |
|---|---|---|---|
| 2708 | 74.85 | 4.88 | 2.46 ↑ |
| 2712 | 74.44 | 4.94 | 2.32 ↑ |
| 3505 | 49.34 | 5.26 | 2.69 ↑ |
| 3607 | 57.63 | 5.30 | 2.59 ↑ |
| 3613 | 60.75 | 5.32 | 2.65 ↑ |
| 4502 | 48.77 | 5.34 | 2.99 ↑ |
| 4708 | 86.15 | 5.40 | 3.03 ↑ |
| 5907 | 90.55 | 5.84 | 2.94 ↑ |
| 7301 | 34.24 | 6.24 | 2.03 ↑ |
| 7302 | 34.83 | 6.28 | 2.26 ↑ |
| 7310 | 41.06 | 6.56 | 2.03 ↑ |
| 7509 | 48.07 | 6.41 | 3.26 ↑ |
| 7603 | 56.95 | 6.33 | 2.55 ↑ |
| 7605 | 62.41 | 6.34 | 2.10 ↑ |
| 1309 | 35.14 | 4.73 | 2.46 ↓ |
| 2201 | 28.20 | 4.89 | 3.92 ↓ |
| 3204 | 32.70 | 5.18 | 2.98 ↓ |
| 3304 | 36.17 | 5.30 | 2.35 ↓ |
| 3503 | 49.40 | 5.20 | 2.30 ↓ |
| 4201 | 25.63 | 5.33 | 5.78 ↓ |
| 4208 | 26.78 | 5.54 | 8.40 ↓ |
| 4703 | 69.88 | 5.36 | 3.16 ↓ |
| 5406 | 42.55 | 5.69 | 3.57 ↓ |
| 6101 | 24.63 | 5.95 | 2.35 ↓ |
| 6203 | 24.88 | 6.06 | 2.07 ↓ |
| 6501 | 46.94 | 5.95 | 5.98 ↓ |
| 6508 | 48.52 | 6.07 | 2.21 ↓ |
| 7108 | 23.35 | 6.41 | 2.08 ↓ |
| 7609 | 59.45 | 6.52 | 2.01 ↓ |